

TK
9152
A2
V.1
1976
HC

CONF-7608:
UC-



Proceedings of the Fourteenth ERDA Air Cleaning Conference

Editor
Ivin W. First

Volume 1
February 1977

Held at
Sun Valley, Idaho
2-4 August, 1977

Sponsored by
**Energy Research & Development
Administration**
**Harvard Air Cleaning
Laboratory**

PROGRAM COMMITTEE:

W. L. ANDERSON
R. R. BELLAMY
C. A. BURCHSTED
J. T. COLLINS
J. C. DEMPSEY
D. C. DREHMEL
H. L. ETTINGER
H. GILBERT
J. L. KOVACH
D. W. MOELLER
D. PENCE
R. D. RIVERS
C. E. STEVENSON
M. W. FIRST, CHAIRMAN

LOCAL ARRANGEMENTS

GEORGE WEHMANN
SHARLEEN WHITE, ASSISTANT
IDAHO OPERATIONS OFFICE
U.S. ENERGY RESEARCH AND DEVELOPMENT
ADMINISTRATION

14th ERDA AIR CLEANING CONFERENCE

TABLE OF CONTENTS

VOLUME I

WELCOME AND OBJECTIVES OF THE CONFERENCE

Session I - Monday, August 2, 1976

CHAIRMAN: M. W. First

Harvard Air Cleaning Laboratory

WELCOME by M. W. First, Harvard Air Cleaning Laboratory.....	2
WELCOME by W. H. Hannum, Idaho Operations Office, ERDA.....	4
OBJECTIVES OF THE CONFERENCE by M. B. Biles, Division of Operational Safety, ERDA.....	6

WASTE TREATMENT: VOLUME REDUCTION AND PREPARATION FOR STORAGE

Session II - Monday, August 2, 1976

CHAIRMAN: R. W. Ramsey, Jr.

ERDA

OPENING REMARKS OF SESSION CHAIRMAN.....	8
VOLUME REDUCTION OF CONTAMINATED FILTER WASTES by O. I. Buttedahl and K. Terada, Atomics International Division.....	9
DISCUSSION.....	15
MOLTEN SALT COMBUSTION OF RADIOACTIVE WASTES by L. F. Grantham, D. E. McKenzie, W. L. Richards, and R. D. Oldenkamp, Atomics International Division.....	17
DISCUSSION.....	34
CONTROLLED-AIR INCINERATION OF TRANSURANIC-CONTAMINATED SOLID WASTE by L. C. Borduin, W. E. Draper, R. A. Koenig, A. S. Neuls, and C. L. Warner, Los Alamos Scientific Laboratory.....	36
DISCUSSION.....	50
AN INCINERATOR FOR POWER REACTOR LOW-LEVEL RADIOACTIVE WASTE by T. S. Drolet and J. A. Sovka, Ontario Hydro.....	51
DISCUSSION.....	69
FLUIDIZED BED INCINERATOR DEVELOPMENT by D. L. Ziegler and A. L. Johnson, Atomics International Division.....	70
PARTICULATE COLLECTION IN A LOW LEVEL RADIOACTIVE WASTE INCINERATOR by S. N. Rudnick, D. H. Leith, and M. W. First, Harvard Air Cleaning Laboratory.....	80

14th ERDA AIR CLEANING CONFERENCE

DISCUSSION..... 101

DESIGN OF OFF-GAS CLEANING SYSTEMS FOR HIGH-LEVEL WASTE VITRIFICATION
by M. S. Hanson and J. D. Kaser, Pacific Northwest Labora-
tories..... 102

DISCUSSION..... 117

⁸⁵Kr STORAGE BY ZEOLITE ENCAPSULATION by R. A. Brown, M. Hoza, and
D. A. Knecht, Allied Chemical Corporation..... 118

DISCUSSION..... 131

CLOSING REMARKS OF SESSION CHAIRMAN..... 131

SYSTEM PROTECTION FROM FIRE, EXPLOSION, AND NATURAL DISASTERS

Session III - Monday, August 2, 1976

CHAIRMAN: B. P. Brown
ERDA

PRELIMINARY RESULTS OF HEPA-FILTER SMOKE PLUGGING TESTS USING THE
LLL FULL-SCALE FIRE-TEST FACILITY by J. R. Gaskill, N. J. Alvares,
D. G. Beason, H. W. Ford, Jr., Lawrence Livermore Labora-
tories..... 134

DISCUSSION..... 170

TORNADO DEPRESSURIZATION AND AIR CLEANING SYSTEMS by W. S. Gregory,
K. H. Duerre, P. R. Smith, and R. W. Andrae, Los Alamos Scien-
tific Laboratory..... 171

DISCUSSION..... 193

DESIGN AND ANALYSIS OF THE SANDIA LABORATORIES HOT CELL FACILITY
SAFETY VENTILATION SYSTEM by E. A. Bernard and H. B. Burress,
Sandia Laboratories..... 194

DISCUSSION..... 209

EFFECTS OF EXPLOSION-GENERATED SHOCK WAVES IN DUCTS by M. R. Busby,
J. E. Kahn, and J. P. Belk, Tennessee State University and Oak
Ridge National Laboratory..... 210

DISCUSSION..... 220

CLOSING REMARKS OF SESSION CHAIRMAN..... 220

RADIOIODINE REMOVAL AND RETENTION

Session IV - Monday, August 2, 1976

CO-CHAIRMEN: R. D. Rivers,
American Air Filter Co.,
J. G. Wilhelm,
Laboratorium fur Aerosolphysik and
und Filtertechnik, Karlsruhe

14th ERDA AIR CLEANING CONFERENCE

OPENING REMARKS OF SESSION CHAIRMAN (J. G. Wilhelm).....	222
IODINE EVAPORATION FROM IRRADIATED AQUEOUS SOLUTIONS CONTAINING THIOSULFATE ADDITIVE by A. H. Dexter, A. G. Evans, and L. R. Jones, Savannah River Laboratory.....	224
DISCUSSION.....	232
DEPENDENCE OF GAS PENETRATION OF CHARCOAL BEDS ON RESIDENCE TIME AND LINEAR VELOCITY by V. R. Deitz, C. H. Blachly, Naval Research Laboratories, and L. A. Jonas, Edgewood Arsenal.....	233
DISCUSSION.....	249
EFFECT OF SERVICE AGING ON IODINE RETENTION OF ACTIVATED CHARCOAL by A. G. Evans, Savannah River Laboratory.....	251
DISCUSSION.....	265
A METHOD FOR CORRELATING WEATHERING DATA ON ADSORBENTS USED FOR THE REMOVAL OF CH_3I by H. C. Parish and R. C. Muhlenhaupt, CVI Corporation.....	266
DISCUSSION.....	286
IODINE REMOVAL ADSORBENT HISTORIES, AGING AND REGENERATION by J. R. Hunt, E. Rankovic, R. Lubbers, and J. L. Kovach, Nuclear Consulting Services.....	287
DISCUSSION.....	293
NEW CHARCOAL IMPREGNANTS FOR TRAPPING METHYL IODIDE	
I. Salts of the Iodine Oxyacids with Iodide or Iodine and Hexamethylenetetraamine by V. R. Deitz and C. H. Blachly, Naval Research Laboratories.....	294
II. Applications to a Variety of Base Charcoals by A. G. Evans, Savannah River Laboratory.....	310
DISCUSSION.....	322
THE BEHAVIOR OF HIGHLY RADIOACTIVE IODINE ON CHARCOAL IN MOIST AIR by R. A. Lorenz, S. R. Manning, and W. J. Martin, Oak Ridge National Laboratory.....	323
DISCUSSION.....	352
REMARKS ON TESTING THE RELIABILITY OF IODINE ADSORPTION IN ION-EXCHANGING CHARCOAL-FILTERS WITH RESPECT TO SOLVENT LOADINGS by H. J. Strauss and K. Winter, Ceagfilter und Entstaubung Technik.....	353
DISCUSSION.....	361
AIRBORNE ELEMENTAL IODINE LOADING CAPACITIES OF METAL ZEOLITES AND A DRY METHOD FOR RECYCLING SILVER ZEOLITE by B. A. Staples, L. P. Murphy, and T. R. Thomas, Idaho National Engineering Laboratory.....	363

14th ERDA AIR CLEANING CONFERENCE

DISCUSSION..... 380

AIR FILTRATION PLANTS OF WALL-TYPE FOR SEPARATION OF FISSION IODINE
IN NUCLEAR REACTORS by H. H. Stiehl, M. Neumann, and D. Sinhuber,
Delbag-Luftfilter..... 381

DISCUSSION..... 388

AN AIRBORNE RADIOIODINE SPECIES SAMPLER AND ITS APPLICATION FOR
MEASURING REMOVAL EFFICIENCIES OF LARGE CHARCOAL ADSORBERS FOR
VENTILATION EXHAUST AIR by W. A. Emel, D. C. Hetzer, C. A.
Pelletier, E. D. Barefoot, and J. E. Cline, Allied Chemical
Corporation..... 389

DISCUSSION..... 431

OPERATING EXPERIENCE WITH THE TESTING OF IODINE ADSORBERS ON THE AIR
CLEAN UP SYSTEMS OF THE BELGIAN PWR POWER PLANTS by B. Deckers,
Association Vincotte, P. Sigli, and L. Trehen, Commissariat a
L'Energie Atomique..... 432

DISCUSSION..... 446

HEAD-END IODINE REMOVAL FROM A REPROCESSING PLANT WITH A SOLID SOR-
BENT by J. G. Wilhelm and J. Furrer, Laboratorium fur Aerosolphysik
und Filtertechnik, E. Schultes, Gesellschaft zur Wiederaufarbeitung
von Kernbrennstoffen..... 447

DISCUSSION..... 477

REPORT OF THE GOVERNMENT-INDUSTRY COMMITTEE ON ADSORBERS AND ADSORP-
TION MEDIA by C. A. Burchsted, Oak Ridge National Laboratory... 478

CLOSING REMARKS OF SESSION CHAIRMAN (R. D. Rivers)..... 486

SAMPLING AND MONITORING
Session V - Tuesday, August 3, 1976
CHAIRMAN: H. Ettinger,
Los Alamos Scientific Laboratory

OPENING REMARKS OF SESSION CHAIRMAN..... 489

SELECTIVE SAMPLING OF HYPOIODOUS ACID by M. J. Kabat, Ontario
Hydro..... 490

DISCUSSION..... 506

AN ANALYSIS FORMAT AND EVALUATION METHODS FOR EFFLUENT PARTICLE
SAMPLING SYSTEMS IN NUCLEAR FACILITIES by L. C. Schwendiman and
J. A. Glissmeyer, Pacific Northwest Laboratories..... 507

THE USE OF A SINGLE PARTICLE INTRA-CAVITY LASER PARTICLE SPECTROMETER
FOR MEASUREMENTS OF HEPA FILTERS AND FILTER SYSTEMS by B. G. Schuster
and D. J. Osetek, Los Alamos Scientific Laboratory..... 528

DISCUSSION..... 540

14th ERDA AIR CLEANING CONFERENCE

VOLUME II

PARTICLE COLLECTION

Session VI - Tuesday, August 3, 1976

CO-CHAIRMEN: H. Gilbert,
Consultant
C. A. Burchsted.
Oak Ridge National Laboratory

THE SRP SAND FILTER: MORE THAN A PILE OF SAND by D. A. Orth, G. H. Sykes, Savannah River Plant, and G. A. Schurr, Engineering Service Division.....	542
DISCUSSION.....	556
DUST FILTRATION ON A PANEL BED OF SAND by W. R. A. Goossens, A. Francesconi, G. Dumont, and R. Harnie, S.C.K./C.E.N.....	557
DISCUSSION.....	563
INHOMOGENEOUS ELECTRIC FIELD AIR CLEANER by B. G. Schuster, Los Alamos Scientific Laboratory.....	564
DISCUSSION.....	577
THE ELECTROSTATIC CAPTURE OF SUBMICRON PARTICLES IN FIBER BEDS by D. L. Reid and L. W. Brown, Pacific Northwest Laboratories...	578
DISCUSSION.....	600
AIR FILTRATION ENHANCEMENT USING ELECTRONIC TECHNIQUES by G. O. Nelson, C. P. Richards, A. H. Biermann, R. D. Taylor, and H. H. Miller, Lawrence Livermore Laboratory.....	602
DISCUSSION.....	611
TESTING OF AIR FILTERS UNDER QUALITY CONTROL SAFETY PROGRAM by C. D. Skaats, Rocky Flats Plant.....	612
DISCUSSION.....	629
HEPA FILTER PERFORMANCE COMPARATIVE STUDY by C. A. Gunn and D. M. Eaton, Mine Safety Appliances Co.	630
DISCUSSION.....	661
PENETRATION OF HEPA FILTERS BY ALPHA RECOIL AEROSOLS by W. J. McDowell, F. G. Seeley, Oak Ridge National Laboratory, and M. T. Ryan, University of Lowell.....	662
DISCUSSION.....	675
EXHAUST FILTRATION ON GLOVEBOXES USED FOR AQUEOUS PROCESSING OF PLUTONIUM by R. W. Woodard, K. J. Grossaint, and T. L. McFeeters, Rocky Flats Plant, N.C.	677

14th ERDA AIR CLEANING CONFERENCE

ENTRAINMENT SEPARATOR PERFORMANCE by M. W. First and D. Leith, Harvard Air Cleaning Laboratory..... 694

DISCUSSION..... 710

GOVERNMENT-INDUSTRY MEETING ON FILTERS, MEDIA, AND MEDIA TESTING by W. L. Anderson, Naval Surface Weapons Center..... 711

CLOSING REMARKS OF SESSION CHAIRMAN (C. A. Burchsted)..... 716

LUNCHEON MEETING

Session VII - Tuesday, August 3, 1976

CHAIRMAN: G. Wehmann,
Idaho Operations Office, USERDA

CONTINUING CHALLENGES IN NUCLEAR AIR CLEANING by D. W. Moeller, Harvard Air Cleaning Laboratory..... 718

SYSTEM DESIGN FOR NUCLEAR FACILITIES

Session VIII - Tuesday, August 3, 1976

CHAIRMAN: J. Murrow,
Bechtel Corporation

OPENING REMARKS OF SESSION CHAIRMAN..... 736

THE REMOVAL OF RADIOACTIVE AEROSOLS FROM THE POST ACCIDENT ATMOSPHERE OF AN LWR-CONTAINMENT by G. Haury, W. Schoeck, Lab. for Aerosol Physics and Filter Technology..... 737

GAS CLEAN-UP SYSTEM FOR VENTED CONTAINMENT by J. L. Kovach, Nuclear Consulting Services..... 749

DISCUSSION..... 759

STANDARDIZATION OF AIR CLEANUP SYSTEMS FOR NUCLEAR POWER PLANTS by E. Nicolaysen, K. E. Carey, and J. J. Wolak, Gibbs and Hill.. 761

DISCUSSION..... 782

CONTROL ROOM VENTILATION INTAKE SELECTION FOR THE FLOATING NUCLEAR POWER PLANT by D. H. Walker, R. N. Nassano and M. A. Capo, Offshore Power Systems..... 784

DISCUSSION..... 810

EVALUATION OF CONTROL ROOM RADIATION EXPOSURE by T. Y. Byoun and J. N. Conway, Burns and Roe..... 811

DISCUSSION..... 828

14th ERDA AIR CLEANING CONFERENCE

OPEN END

Session IX - Tuesday, August 3, 1976

CHAIRMAN: M. W. First,
Harvard Air Cleaning Laboratory

OPENING REMARKS OF SESSION CHAIRMAN..... 829

COORDINATION OF FIRE TERMINOLOGY IN ASTM by J. R. Gaskill, Lawrence Livermore Laboratory..... 830

DISCUSSION..... 833

ULTRAHIGH EFFICIENCY SPARKPROOF ELECTROSTATIC PRECIPITATION by J. K. Thompson, R. C. Clark, and G. H. Fielding, Naval Research Laboratory..... 834

DISCUSSION..... 835

EFFECT OF EXPOSURE TIME IN THE PREHUMIDIFICATION OF CHARCOALS FOR METHYL IODIDE TRAPPING by V. R. Deitz and C. H. Blachly, Naval Research Laboratory..... 836

DISCUSSION..... 842

IODINE EMISSION DURING A PROGRAMMED HEATING OF IMPREGNATED CHARCOALS IN CARRIER AIR by V. R. Deitz and J. B. Romans, Naval Research Laboratory..... 844

DISCUSSION..... 849

AN EXPERIMENTAL INVESTIGATION OF THE RELATIONSHIP BETWEEN BED PACKING AND FLOW DISTRIBUTION by H. C. Parish, R. C. Muhlenhaup, and W. W. Vogelhuber, CVI Corporation..... 852

DISCUSSION..... 867

A CONTAINMENT AND RECOVERY SYSTEM FOR FUEL-REPROCESSING PLANTS by T. R. Galloway, Lawrence Livermore Laboratory..... 870

REDUCING AIR CLEANUP SYSTEM COSTS by H. R. Reedquist, Jr., CTI-Nuclear..... 878

ABSOLUTE FILTERS: EFFECTIVE FILTERING MEDIA by G. H. Cadwell, Jr., Flanders Filters..... 882

DISCUSSION..... 883

LMFBR AIR CLEANING SYSTEMS

Session X - Wednesday, August 4, 1976

CHAIRMAN: C. Newton,
USERDA

OPENING REMARKS OF SESSION CHAIRMAN..... 884

14th ERDA AIR CLEANING CONFERENCE

THE AEROSOL BEHAVIOR IN LMFBR ACCIDENTS: RESULTS OF TUNA EXPERIMENTAL PROGRAM AND COMPARISON WITH PARDISEKO CODE by W. O. Schikarski, Laboratory for Aerosol Physics and Filter Technology..... 885

DISCUSSION..... 897

AN EVALUATION OF ALTERNATIVE AIR CLEANING SYSTEMS FOR EMERGENCY USE IN LMFBR PLANTS by J. D. McCormack, R. K. Hilliard, A. K. Postma, and L. D. Muhlestein, Hanford Engineering Development Laboratory..... 898

DISCUSSION..... 925

EVALUATION OF IN-VESSEL AIR CLEANING SYSTEMS FOR AN LMFBR by W. C. Hinds, E. F. Mallove, and M. W. First, Harvard Air Cleaning Laboratory..... 927

DISCUSSION..... 943

CLOSING REMARKS OF SESSION CHAIRMAN..... 944

REMOVAL OF NOBLE GASES, TRITIUM, AND ¹⁴CARBON
Session XI - Wednesday, August 4, 1976

CHAIRMAN: J. A. Buckham,
Allied Chemical Corporation

OPENING REMARKS OF SESSION CHAIRMAN..... 945

THE DELAY OF XENON ON CHARCOAL BEDS by G. Collard, M. Put, J. Broothaerts, and W. R. A. Goossens, S.C.K./C.E.N..... 947

DISCUSSION..... 955

THE RELEASE OF ADSORBED KRYPTON AND XENON FROM SPILLED CHARCOAL by D. W. Underhill, Harvard Air Cleaning Laboratory..... 957

DISCUSSION..... 963

DEVELOPMENT OF THE CRYOGENIC SELECTIVE ADSORPTION-DESORPTION PROCESS ON REMOVAL OF RADIOACTIVE NOBLE GASES by T. Kanazawa, M. Soya, H. Tanabe, B. An, Kobe Steel, Y. Yuasa, M. Ohta, A. Watanabe, H. Nagao, A. Tani, Nippon Atomic Industry Group, and H. Miharada, Tokyo Shibaura Electric..... 964

DISCUSSION..... 1001

SEPARATION OF THE FISSION PRODUCT NOBLE GASES KRYPTON AND XENON FROM DISSOLVER OFF-GAS IN REPROCESSING HTGR-FUEL by J. Bohnenstigl, S. H. Djoa, M. Laser, St. Mastera, E. Merz, P. Morschl, Institute for Chemical Technology..... 1002

DEVELOPMENT OF THE FASTER PROCESS FOR REMOVING KRYPTON-84, CARBON-14, AND OTHER CONTAMINANTS FROM THE OFF-GAS OF FUEL REPROCESSING PLANTS by M. J. Stephenson, R. S. Eby, Union Carbide Corporation.... 1017

14th ERDA AIR CLEANING CONFERENCE

DISCUSSION..... 1032

HTGR-REPROCESSING OFF-GAS CLEANING BY THE AKUT-PROCESS by H. Barnert-
Wiemer, H. Beaujean, M. Laser, E. Merz, H. Vygen, Institute for
Chemical Technology..... 1034

DISCUSSION..... 1043

EXPERIMENTAL STUDIES ON THE KRYPTON ADSORPTION OF LIQUID CO₂ (FALC)
PROCESS by R. W. Glass, Oak Ridge National Laboratory, H. W. R.
Beaujean, V. L. Fowler, Institute for Chemical Technology, T. M.
Gilliam, D. J. Inman, Oak Ridge National Laboratory, D. M. Levins,
Australian Atomic Energy Commission..... 1044

EXPERIMENTAL DETERMINATION OF REACTION RATES OF WATER-HYDROGEN EXCHANGE
OF TRITIUM WITH HYDROPHOBIC CATALYSTS by J. C. Bixel, B. W. Hartzell,
and W. K. Park, Mound Laboratory..... 1065

DISCUSSION..... 1074

SEPARATION OF KRYPTON FROM CARBON DIOXIDE AND OXYGEN WITH MOLECULAR
SIEVES by C. W. Forsberg, Oak Ridge National Laboratory..... 1076

DISCUSSION..... 1087

CLOSING REMARKS OF SESSION CHAIRMAN..... 1087

REGULATION

Session XII - Wednesday, August 4, 1976

CHAIRMAN: J. T. Collins,
Nuclear Regulatory Commission

OPENING REMARKS OF SESSION CHAIRMAN..... 1088

USE OF ANSI N-509 IN DESIGN AND LICENSING OF NUCLEAR AIR CLEANING
SYSTEMS by C. A. Thompson, Bechtel Power Corporation..... 1089

DISCUSSION..... 1103

RECENT DEVELOPMENTS IN NRC GUIDELINES FOR ATMOSPHERE CLEANUP SYSTEMS
by R. R. Bellamy, USNRC..... 1104

DISCUSSION..... 1111

THE IMPACT OF APPENDIX 1 TO 10 CFR 50 ON ATMOSPHERE CLEANUP SYSTEMS
by J. T. Collins, USNRC..... 1113

DISCUSSION..... 1121

INTERNATIONAL SYMPOSIUM ON THE MANAGEMENT OF WASTES
FROM THE NUCLEAR FUEL CYCLE

Session XIII - Wednesday, August 4, 1976

CHAIRMAN: R. W. Ramsey,
USERDA

14th ERDA AIR CLEANING CONFERENCE

OVERVIEW OF SYMPOSIUM AND EXPLANATION OF TECHNICAL ALTERNATIVES
DOCUMENT (TAD) by R. W. Ramsey, USERDA..... 1122

TECHNICAL OVERVIEW OF AIR CLEANING ASPECTS OF SYMPOSIUM AND TAD by
R. A. Brown, Allied Chemical, INEL..... 1127

SUMMARIES OF AVAILABLE TECHNOLOGY ON GASEOUS EFFLUENT CONTROL OF
KRYPTON, IODINE, TRITIUM, ¹⁴CARBON, RUTHENIUM, NO_x, HCl, AND
PARTICULATES by D. A. Knecht, T. R. Thomas, L. L. Burger, C. M.
Slansky, J. D. Christian, C. A. Burchsted..... 1129

DISCUSSION..... 1133



14th ERDA AIR CLEANING CONFERENCE

SESSION I

WELCOME AND OBJECTIVES OF THE CONFERENCE

Monday, August 2, 1976
CHAIRMAN: M. W. First

WELCOME	M. W. First
WELCOME	W. H. Hannum
OBJECTIVES OF THE CONFERENCE	M. B. Biles

14th ERDA AIR CLEANING CONFERENCE

WELCOME

Melvin W. First
Harvard Air Cleaning Laboratory
Harvard School of Public Health
Boston, Massachusetts

I am Melvin First, Conference Chairman, and it is my privilege and my pleasure to open the 14th ERDA Air Cleaning Conference. On behalf of the Harvard Air Cleaning Laboratory, co-sponsors of this Conference with the United States Energy Research and Development Administration, I bid you welcome. I would like to extend a special welcome to our speakers and delegates who came from countries outside the U.S. These countries include, Canada, Germany, Belgium, France, England, Sweden, Switzerland, Denmark, Holland, Japan and Spain. Although this is a U.S. Government sponsored meeting, those of you from other countries who have attended previously know that you are considered full participants as well as guests.

It has been two years since we last met and many important things have happened during this interval. You will hear about most of the technical matters of importance that have occurred over the past two years during the three days of this Conference. Therefore, I would like to speak very briefly about a non-technical matter that troubles me greatly and that I am sure troubles you, also. It is the negative attitude of the public regarding the safety of nuclear power. The fact that the California nuclear initiative (Proposition 15) was voted down by a better than 2 to 1 majority should not make us complaisant. The mere presence of a nuclear initiative on the California ballot indicates the public's deep interest and concern in this energy area. It seems to me that the nuclear industry and its advocates must respond, and respond vigorously. Not only with multimillion dollar government-sponsored safety studies, important as they are, but by every involved individual exercising the same diligence and unflagging enthusiasm and self sacrifice that the "antis" exhibit in their eagerness to speak to and find converts among every available lay group.

How many of us make a practice of appearing before all the community groups that will listen; in order to bring the message of nuclear power's safety record and its potential for universal human benefit? I don't intend to take a poll among us, but, if I did, I think I would find a pitifully small number who take this obligation to heart and then act upon it. As a consequence, I fear we are leaving the education of the public to the antinuclear zealots who devote their total resources to reaching citizen groups and persuading them to join their cause. Those of you who have attended public hearings on nuclear power and nuclear waste disposal, have heard these sincere, well-meaning individuals express their fears and utter the antinuclear party line.

Until recently, violent opposition to nuclear power was largely a U.S. phenomenon but the rest of the world is catching up rapidly. We note the rapid growth of a vigorous antinuclear group in France

14th ERDA AIR CLEANING CONFERENCE

during the past year or so and growing hostility elsewhere.

As genuine experts on many important phases of nuclear safety, this group has, I believe, a heavy obligation to become involved, personally and passionately, in the education of the public on matters of nuclear safety at every possible opportunity. I suggest such groups as science classes at schools, scout groups, service clubs, church groups, etc.

I do not believe we can leave delivery of this important message solely up to the Federal Government. Rather, we must all pitch in and express our convictions by constructive activities that reach the public. If this makes sense to you, please act on it, and carry the message to your colleagues who are not here.

14th ERDA AIR CLEANING CONFERENCE

WELCOME

W. H. Hannum
Idaho Operations
U.S. Energy Research and Development Administration
Idaho Falls, Idaho

Your program states that Wayne Bills would welcome you on behalf of the Idaho Operations Office. We couldn't quite leave you with "Bills and Biles" as the welcome team, so I came instead.

It is a pleasure to welcome you here, not only personally, but on behalf of the Idaho Operations Office and our contractor operations at the Idaho National Engineering Laboratory (INEL). We have approximately 6,500 people employed here in Idaho working for ERDA and its prime contractors. It's appropriate that this air cleaning conference be held here for a variety of reasons. First, of course, here in Idaho, we do believe in clean air and we're happy to see people working to preserve clean air, not only for Idaho, but for the entire country and the world.

As far as the nuclear aspect of air cleaning is concerned, at the Idaho National Engineering Laboratory, we do have almost the full range of the nuclear fuel cycle. We operate reactors and we have to worry about the effluents from them. We have a major chemical processing operation and we have to worry about the effluent from that. We have waste storage and we have to worry about any effluent there might be from that. Except for the fuel supply and the enrichment process, we are involved in the entire fuel cycle.

Also, at INEL, Allied Chemical Corporation, one of our major contractors, has just recently completed their assignment as task leader for the Volatile Radioisotope Recovery and Off-Gas Treatment section of the alternatives for Managing Wastes from Reactors and Postfission Operations in the LWR Fuel Cycle. That's the so-called Technical Alternatives Documented for Commercial Wastes.

Allied will continue to be involved in this and has been assigned as a Task leader for the off-gas section of the Generic Environmental Statement for Managing Radioactive Wastes from Commercial Reactors and Postfission Operations in the LWR Fuel Cycle.

One other item I ought to note, lest there be unnecessary confusion: the last time this particular conference was held in Idaho (in 1959) it was sponsored by the Atomic Energy Commission. The current conference is sponsored by ERDA. These are not quite the same things. Many of you at that time visited the National Reactor Testing Station. Many of you this time will visit the Idaho National Engineering Laboratory; the same geography but not quite the same operation.

This meeting comes in reasonable proximity to a meeting in Denver: the International Symposium on Waste Management. This meeting is immediately followed by the ANS-AIChE meeting on air cleaning. I trust there will be adequate overlap among these meetings. There

14th ERDA AIR CLEANING CONFERENCE

are special sessions devoted to trying to exchange information from the various symposiums.

I suspect after five days on air cleaning, many of you may feel sort of like the 12 year old who read a 500-page book on frogs. His entire book report read, "I now really know more about frogs than I ever wanted to know."

Let me make one other comment here as we begin. This is the 14th Air Cleaning Conference. To be honest with you, I worry when I seen the 14th meeting on a particular specialty topic. I trust this is not simply a continuing club; people getting together to exchange friendships. That's beneficial, but I hope also we're making some progress. As I review, following the meeting, the results of this conference, I will be looking for results. I'll be looking for conclusions. I'll be looking for things that we may have accomplished in the past 14 meetings. I hope to be able to find some.

Another comment I'd like to make: previous conferences in this series have been sponsored by the American Nuclear Society. Air cleaning is a very serious matter in the nuclear fuel cycle. For one particular reactor type, I made an estimate a few years ago that, in our analysis of the potential environmental impact of the one particular reactor type, we were choosing to not take credit for a safety margin factor of somewhere between 10^6 and 10^{22} . As we all know, there is considerable public concern over nuclear power. If we're failing to take credit for factors between 10^6 and 10^{22} , maybe we'd better start looking for them so that in our representations to the public, we can show that not only are reactors safe by current conservative evaluations, but when looked at rationally, this really is a good way to supply the energy needs of our country.

I hope this conference also marks a turning point, in the sense that ERDA is not the same as the AEC. ERDA is involved with the full range of energy development. We must be concerned in any form of energy generation, that what we develop is satisfactory from an environmental point of view.

I hope this meeting does reflect, at least to some extent, that we are worried not only about the nuclear aspect of air cleaning, but air cleaning in its broader context of energy supply.

Again, our welcome. We're happy to have you here. I'm sure you will enjoy Sun Valley and I hope you learn something. I hope we all learn something from this conference. Thank you.

14th ERDA AIR CLEANING CONFERENCE

ERDA WELCOME

Dr. Martin B. Biles, Director
Division of Safety, Standards, and Compliance
U.S. Energy Research and Development Administration

On behalf of the U.S. Energy Research and Development Administration, it is my pleasure to welcome you at this 14th Air Cleaning Conference. In extending this welcome, I would like to make special note of the many foreign guests present and wish them a particularly warm personal welcome. It is gratifying to see this large turnout, which exemplifies the importance of your activities.

These air cleaning conferences began at Harvard University in June 1951 under the auspices of the AEC. Since the last air cleaning conference in August 1974 in San Francisco, the AEC has been abolished and two new agencies were established--the Nuclear Regulatory Commission and the Energy Research and Development Administration. ERDA was formed to bring together and to direct Federal activities in the research and development of all energy sources, non-nuclear as well as nuclear. This is, therefore, the first air cleaning conference sponsored by ERDA.

Since their inception, these air cleaning conferences have served as a forum for exchange of new developments in air cleaning, with the published proceedings representing the most up-to-date literature available on the subject. The accomplishments in air cleaning during this period are far too numerous to mention, but are well reflected in the proceedings. The unique characteristic of the air cleaning conferences was to address the reported research considered most essential to nuclear facilities and their related support activities. Certainly, there are still problems remaining in nuclear air cleaning, but I think we should now begin to consider the needs of the non-nuclear energy technologies in view of the broad responsibilities of ERDA.

In the non-nuclear area the problem of air cleaning of present coal and oil fired plants is with us now, particularly with regard to scrubbers. I am not sure that we even know the magnitude of the air cleaning problems facing us with sources such as coal gasification and oil shale development. How to handle the carcinogenic compounds in the coal gasification products is an interesting challenge. Also, some of the geothermal fields produce sulphurous gases that require control. These problems will test our engineering ingenuity and research technology. The engineering knowledge developed under nuclear air cleaning may be relevant and applicable to the air cleaning needs of the non-nuclear field. I invite Dr. First and you to include air cleaning related to non-nuclear activities in future air cleaning conferences.

14th ERDA AIR CLEANING CONFERENCE

In the nuclear area, the success of the commercialization of the LMFBR will depend heavily on the performance and reliability of the air cleaning systems in the demonstration CRFBR now under design, as well as the success of ongoing laboratory research. The capture and the storage of noble gases, particularly krypton 85, when necessary will be a challenge. In the long term, as fusion is developed, the containment and control of tritium will be challenging.

As in the past, the basic objective of this conference is the exchange of information. What is to be discussed here are the accomplishments and developments since our last air cleaning conference. The program is full and interesting. The meeting should be a certain success.

In closing, I would like to express our appreciation for the efforts of Dr. First and those who have helped him to organize this meeting, including the program committee and the Idaho Operations Office. Thank you.

SESSION II

WASTE TREATMENT: VOLUME REDUCTION AND PREPARATION FOR STORAGE

Monday, August 2, 1976
CHAIRMAN: R. W. Ramsey, Jr.

VOLUME REDUCTION OF CONTAMINATED FILTER WASTES

O. I. Buttedahl, K. Terada

MOLTEN SALT COMBUSTION OF RADIOACTIVE WASTES

L. F. Grantham, D. E. McKenzie,
W. L. Richards, R. D. Oldenkamp

CONTROLLED-AIR INCINERATION OF TRANSURANIC-CONTAMINATED SOLID WASTE

L. C. Borduin, W. E. Draper,
R. A. Koenig, A. S. Neuls,
C. L. Warner

AN INCINERATOR FOR POWER REACTOR LOW-LEVEL RADIOACTIVE WASTE

T. S. Drolet, J. A. Sovka

FLUIDIZED BED INCINERATOR DEVELOPMENT

D. L. Ziegler, A. L. Johnson

PARTICULATE COLLECTION IN A LOW LEVEL RADIOACTIVE WASTE INCINERATOR

S. N. Rudnick, D. H. Leith,
M. W. First

DESIGN OF OFF-GAS CLEANING SYSTEMS FOR HIGH-LEVEL WASTE VITRIFICATION

M. S. Hanson, J. D. Kaser

⁸⁵Kr STORAGE BY ZEOLITE ENCAPSULATION

R. A. Brown, M. Hoza, D. A. Knecht

OPENING REMARKS OF SESSION CHAIRMAN:

The processing of waste to achieve volume reduction and passivate or stabilize material for storage or disposal is an important frontier of research and development for waste management in general and for air cleaning in particular. The removal of radioactive material from effluents of air and water are major sources of waste material that must be managed. Therefore, processes to reduce the volume of these residues are receiving major attention in the ERDA Waste Management R & D Program. Several of the processes under development are described in papers at this Conference along with the many other significant contributions to this technology.

VOLUME REDUCTION OF CONTAMINATED FILTER WASTES

O. I. Buttedahl and K. Terada
Rockwell International
Atomics International Division
Rocky Flats Plant
Golden, Colorado

Abstract

Reported are details of a pilot project to design and construct a compactor to reduce the handling of high efficiency particulate air (HEPA) filters used in air filtration systems at facilities where radioactive materials are processed. In such systems at Rocky Flats Plant, filters require frequent change and removal. Large quantities are used and will be increased for future operations. With the completion of the pilot model, it has been demonstrated that volume reductions of more than 80 percent can be achieved and cost savings will be realized also.

I. Introduction

A highly efficient air filtration system is essential in plant operations to safeguard personnel and the environment. The high efficiency particulate filters (HEPA) used in the system must be replaced frequently because of exposure from radioactive materials being processed in various areas.

Currently, some 3000 (2 by 2 by 1-foot) filters are handled per year and future operations will require use of about 10,000 filters. Replacement and handling procedures from procurement through retrievable storage will cost about \$415.00 for each HEPA filter. To reduce space consumption and handling problems of the volume of filters, a pilot compactor was designed and constructed to demonstrate its feasibility.

II. Description of Compactor

The constructed pilot model consisted of a hydraulically operated punch, rams, and an extruding die. The function of the model was to separate the filter components from the frame and to extrude them through the die. The HEPA filters were 8 by 8 by 6 inches.

In the model, a standard 5000 pounds per square inch (psi) pump is connected through a series of valves to four cylinders which can be operated and controlled independently (see Figure 1). A ram is attached to the piston rod of each cylinder. The main cylinder has a capacity of 25 tons of force and is used to extrude the filter media through the pelletizing die. Although different configurations of

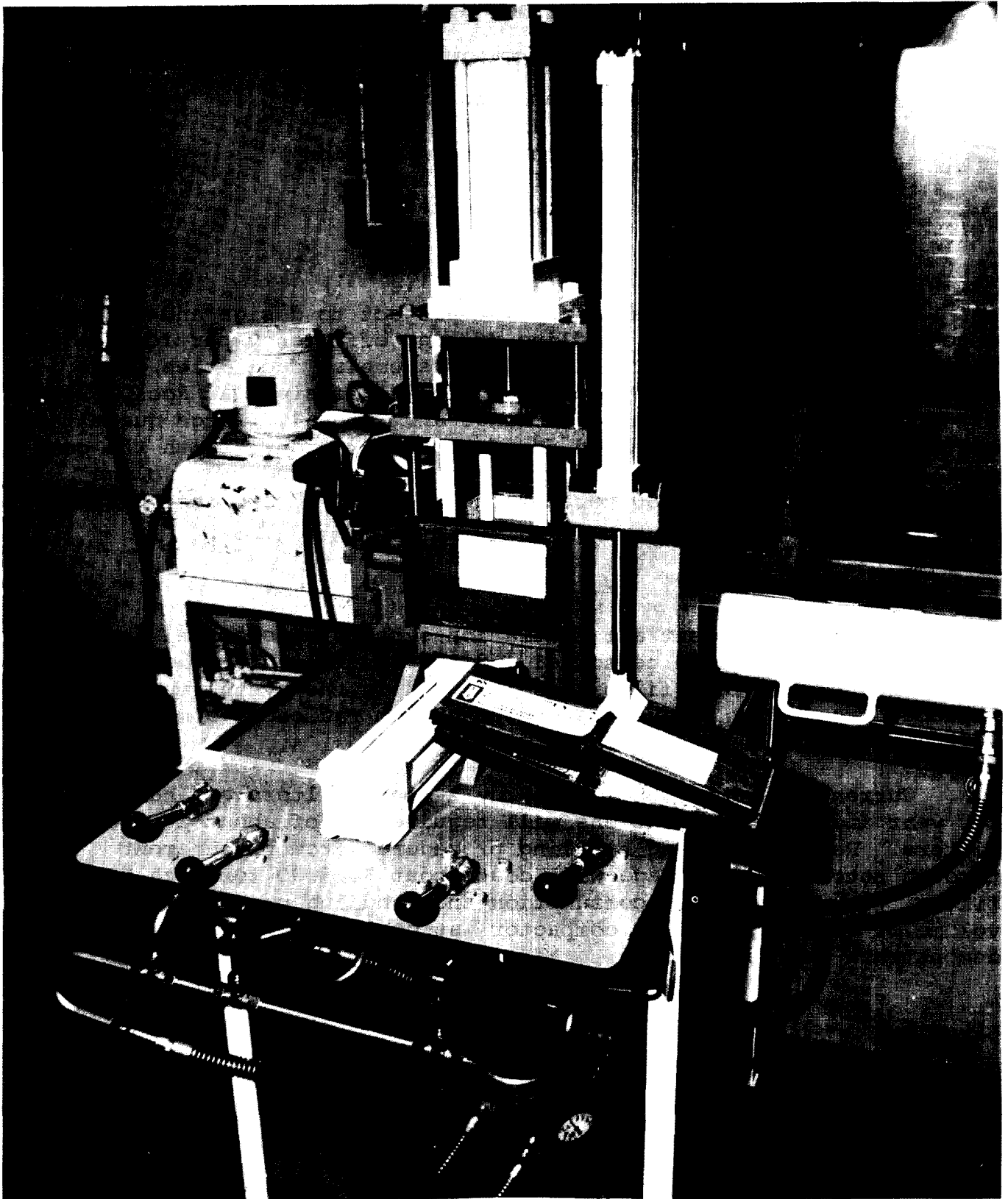


Figure 1. Filter-Media Compactor

dies were tested, one that produced pellets with a square cross section proved the most satisfactory (see Figure 2).

The overall dimension of the inside of the die is 4 inches and is divided into four equal sections. The leading edge of the divider comes to a knife edge where the filter media is sheared. Each of the four sections is 2 inches square at the knife edge. These openings are tapered down to 1.75 inches square, 1 inch into the 2-inch thick die. Because of poor flow characteristics of the filter media, the dividers and the taper provide sufficient resistance to the ram to compact the media being extruded. Attempts to produce cylindrical pellets failed because the die openings were too severely tapered for the filter media to be extruded. By moderating the taper, undoubtedly, pellets of different shapes could be produced.

The original concept involved punching the media out of the frame and shredding them before pelletizing. However, because the flow characteristics of filter media were poor, it was decided to use a shear die and eliminate the shredding operation. For the 8 by 8 by 6-inch filter, it took a force of about 2000 pounds to separate the media from the frame. About 20,000 pounds are required to compact and extrude the media through the die.

With the current system, the filter is soaked with water before compaction, otherwise, the extruded pellets tend to re-expand. Pellets resulting from soaked media expand by about 20 percent as they come out of the die. The lubricating properties of water appear to be minimal. The water serves to make the filter components pliable so that the compacted material retains its shape and size. The use of water as a rinse to partially wash off contamination will be considered in the future.

The pressure exerted on the wet media squeezes out most of the liquid and no free liquid exudes from the compacted pellet. In the current laboratory atmosphere, the exterior of the pellet is visibly dry within 24 hours. The frame of the filter can be crushed in preparation for combustion in the incinerator being planned for Rocky Flats (see Figure 3). An 83 percent volume reduction of the media and separator is obtained.

III. Benefits of Compaction

The current system of packaging the 2 by 2 by 1-foot contaminated filters for disposal consists of crushing the filters in a press and packing them in 4 by 4 by 7-foot fiberglass reinforced polyester coated plywood boxes. Each box costs about \$320.00. Approximately 20 to 27 of the filters are presently packed in a box.

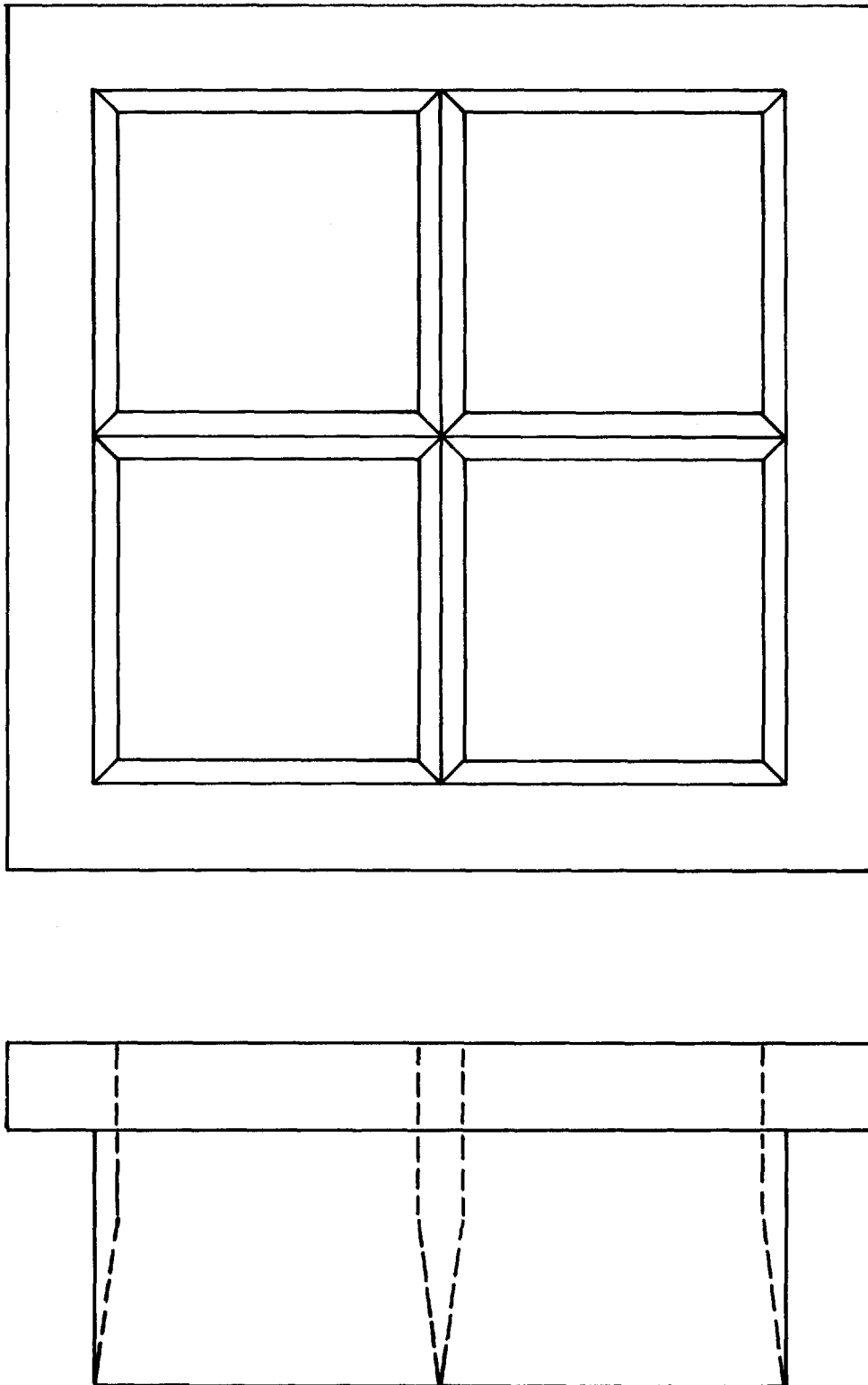


Figure 2. Pelletizing Die.

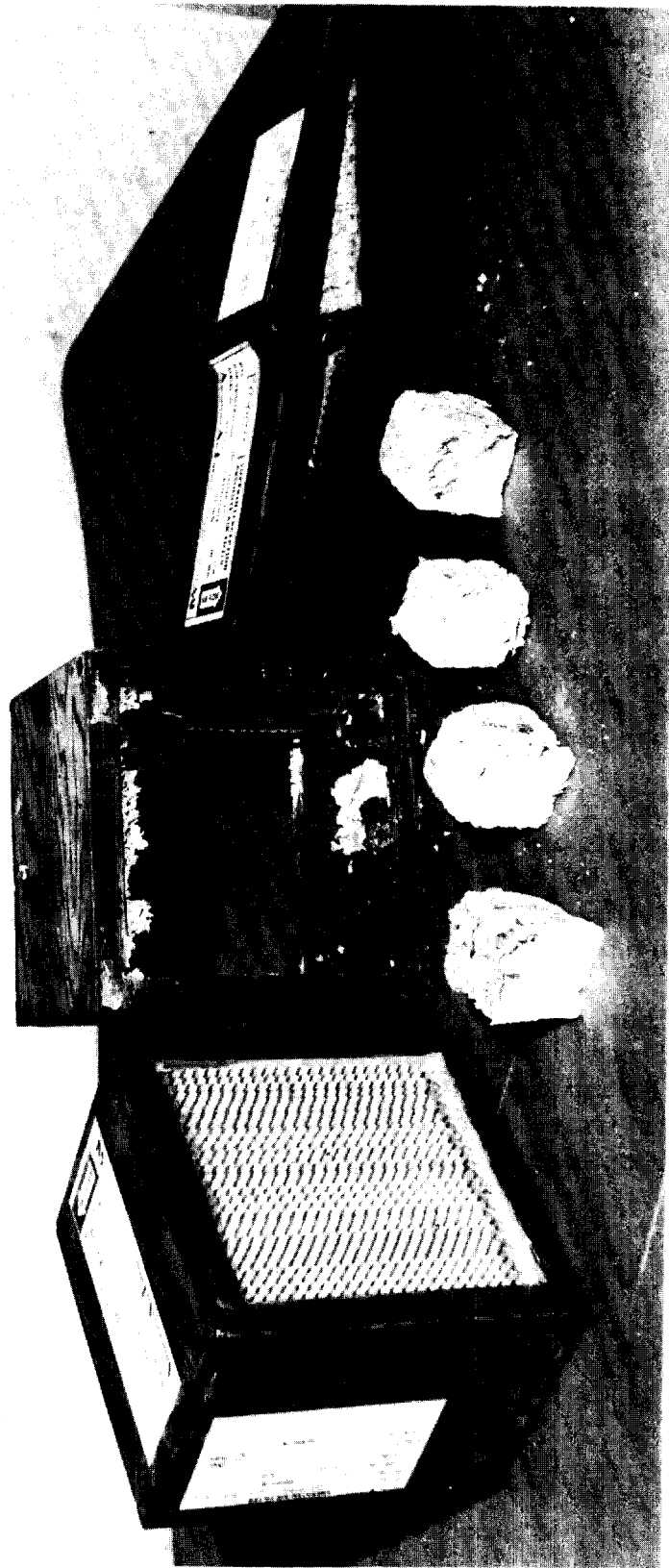


Figure 3. Pelletized 8 by 8 by 6-inch HEPA Filter Media

In packaging the pellets for waste shipment, the possibility is being explored of placing them in unused space of plywood boxes which are already filled with other types of waste. Thus a savings would occur in the number of boxes shipped. Waste Management personnel are interested in the procedure and do not envision any major problems. At Rocky Flats, excess weight would not be a problem since the average weight of the crate shipped is about 4000 pounds and the maximum allowable is 5000 pounds.

Preliminary discussion with Nuclear Safety has not revealed any insurmountable criticality problems associated with the compacting and proposed packing of contaminated filter media.

At Rocky Flats, we currently discard about 3000 2 by 2 by 1-foot filters a year. (This requires approximately 120 waste boxes at a cost of about \$600.00 each, including shipping.) A potential savings of \$72,000.00 a year could be achieved at the present level of usage. This does not include the cost of retrievable or permanent storage (or both) which has been quoted as high as \$30.00 per cubic foot. Also, when the new plutonium recovery facility comes on stream, the volume of contaminated filter waste will increase.

IV. Future Plans

Design is in progress for a new scaled-up compactor to handle the 2 by 2 by 1-foot HEPA filters. Tests show that pressures of about 20,000 pounds of force are required to punch the media from the frame of the large filters.

After development and testing, it is planned to enclose the new unit and test it in actual use with contaminated filters. The system will be automated with the addition of flow control and sequencing valves so that it can be operated remotely. The compactor is expected to be in operation by 1979.

DISCUSSION

MOELLER: I had two questions. How much of the activity from the filter media is carried off by the water and, secondly, is this whole process conducted in an airtight room or with exhaust ventilation and so forth?

BUTTEDAHL: At the present time, we are operating this pilot model strictly with uncontaminated filters for development purposes. We haven't done any work with contaminated filters yet.

OLSON: What is being done to reclaim plutonium from the filter before it is crushed, if anything?

BUTTEDAHL: At this point we have come up with a relatively new thing. Our group has not been concerned about plutonium recovery but, hopefully, when we wet these filters (we will spray them and rinse them off) we expect some of the Pu contamination will rinse off with the dirt. The chemical operations group surveys each filter and recovers the Pu when economically feasible.

PITTMAN: You mentioned the current costs of shipping packages and the potential costs of the long range management of the packages. Have you made any cost estimates for doing what you are planning to do; namely, for the equipment, the operation, and the recovery, obviously, of some waste from the operation itself? In other words, have you been able, yet, to make a cost analysis?

BUTTEDAHL: No, we have just started engineering on the scaled-up model and at this point we don't have figures.

BURCHSTED: Is it necessary to reduce this to a cube in two directions or could you reduce it to just a leaf and simplify the process, i.e., a layer of materials that, in this case, would be 23- x 23-in.?

BUTTEDAHL: You mean, rather than pelletizing it, just flatten it?

BURCHSTED: Right.

BUTTEDAHL: Yes, that is possible. We went the way we did because we could get smaller pellets that would better fill the voids in waste boxes. You can always get a few more pellets in a waste box that is technically full.

GRADY: You said originally you had looked at the concept of taking the entire filter and putting it through a shredder and then compacting the resulting material. You indicated that you had problems with this. Could you elaborate on what these problems were and why you went through the separate concept of dividing it into two parts?

BUTTEDAHL: We never considered shredding the frame. We had always planned to incinerate the frame. We were only operating with

14th ERDA AIR CLEANING CONFERENCE

the media, and the media just didn't flow properly on the design of the die that we had. So, rather than go with the shredding operation, we decided that if we could get it through this particular die we are using, we would eliminate the shredding operation. It is just one less operation.

GASKILL: Since the filter frames are usually made out of wood, have you given any consideration to cleaning up the effluent from incineration and if so, what?

BUTTEDAHL: Not at this point. We aren't far enough into the program to be concerned with that. Don Ziegler has a paper later this morning on incineration, and, hopefully, we can run them through such a device.

KAHN: Since you have liquid waste, what about dissolving the filter media? Have you looked into the possibility of dissolving the filter media rather than pelletizing?

BUTTEDAHL: No.

W. C. BROWN: I was wondering if this method of compaction was limited to filters without separators.

BUTTEDAHL: No, these are standard HEPA filters that have asbestos separators.

DEITZ: The authors mention soaking the filter with water before compaction. It is suggested that an alkali or CaO be added so as to harden the final pellets due to slow formation of a cement-like silicate. The hardened product should be easier to handle without abrading.

BUTTEDAHL: Good suggestion. It certainly will be considered.

14th ERDA AIR CLEANING CONFERENCE

MOLTEN SALT COMBUSTION OF RADIOACTIVE WASTES*

L. F. Grantham, D. E. McKenzie,
W. L. Richards, and R. D. Oldenkamp
Atomics International Division
Rockwell International
Canoga Park, California 91304

Abstract

The Atomics International Molten Salt Combustion Process reduces the weight and volume of combustible β - γ contaminated transuranic waste by utilizing air in a molten salt medium to combust organic materials, to trap particulates, and to react chemically with any acidic gases produced during combustion.

Typically, incomplete combustion products such as hydrocarbons and carbon monoxide are below detection limits (i.e., <30 ppm and <0.05%, respectively). Hydrogen chloride in the off-gas, when pure polyvinyl chloride is burned, is also below detection limits (<5 ppm). Particulate concentration in the off-gas (typically 0.2 mg/m³) is directly related to the sodium chloride vapor pressure of the melt; >80% of the particulate is sodium chloride. Essentially all metal oxides (combustion ash) are retained in the melt, e.g., >99.9% of the plutonium, >99.6% of the europium, and >99.9% of the ruthenium are retained in the melt.

Both bench-scale radioactive and pilot scale (50 kg/hr) non-radioactive combustion tests have been completed with essentially the same results. Design of three combustors for industrial applications are underway.

I. Introduction

Atomics International has been investigating the use of molten carbonate salts for industrial applications for over two decades. These processes vary from utilization of the molten salt as a chemical scrubber^(1,2) for acid gases to the use of the molten salt as a reaction media for in-situ combustion.^(3,4) By feeding less than the stoichiometric requirements of air, molten carbonates are also being utilized to gasify coal,⁽⁵⁾ organic wastes,⁽⁶⁾ high sulfur oil, etc., to produce a source of clean combustible gas.

Since 1974, application of this combustion process to reduce the weight and volume of solid transuranic (TRU) fuel cycle wastes has been under development.^(3,4) In this application, the molten salt medium is utilized to combust the organic materials, to trap inorganic (noncombustible) particulates, and to react chemically with acidic gases (such as HCl, or SO₂,) produced during combustion. Subsequently (in a company funded program), this process has also been applied to other nuclear fuel cycle wastes such as β - γ contaminated solid wastes.

*Supported in part by ERDA Contract AT(04-3)-701

Following the combustion step, there are two options available: Option 1 direct fused casting of the spent salt into disposal containers or Option 2 processing the spent salt to recover the salt and transuranics. Option 1 has been studied on a bench-scale with both uncontaminated waste tests (Figure 1) and radioactive waste tests (Figure 2) and on a pilot-scale (Figure 3) with uncontaminated waste tests (50 kg/hr feed - 1000 kg casts of fused salt). Salt and transuranic recovery (Option 2) has been studied only on a bench-scale (0.5 kg/hr feed) with uncontaminated and contaminated melt-ash mixtures. Salt recovery tests have been performed on a pilot scale in related combustion applications. Following a brief process description, results of various development tests are presented particularly as they relate to control of air pollution during volume reduction of these wastes.

II. Process Description

In the Molten Salt Combustion Process, the shredded waste is fed, with air, to the molten salt combustor. Initially, the molten salt consists of sodium carbonate, an inexpensive natural mineral, and about 10 wt % sodium sulfate. Rapid and complete combustion of the organic material (>99.999%) occurs in the melt producing steam and carbon dioxide. As the combustion products rise through the melt and are scrubbed by it, the melt reacts chemically with any acidic pollutants such as hydrogen chloride, sulfur oxides, and phosphorus oxides to form sodium chloride, sulfate and phosphate. The noncombustible inorganic matter, such as oxides of aluminum, silicon, iron, and transuranics, is trapped in the melt. The molten salt completely oxidizes the waste; no incomplete combustion products such as hydrogen, hydrocarbons, or carbon monoxides are observed as long as excess air is fed with the combustible waste.

Inorganic combustion products can build up to different levels before the physical and chemical properties of the melt are altered significantly. Ash, such as aluminum or iron oxides, can build up to 20 wt %. If the melt becomes viscous due to too high a buildup of insoluble materials, the hydraulics become impaired and the melt must be changed, more salt must be added, or the temperature must be increased. Soluble products, such as sodium chloride, can build up to about 85 wt %. About 5 wt % sodium carbonate and sulfate must remain in the melt to assure complete combustion and removal of acidic gases from the off-gas.

To control the amount of noncombustible substances in the melt, a portion of the molten salt is periodically drained from the combustor. The product salt-ash mixture can be cast directly into a metal canister for retrievable storage (Option 1; Figure 4). Alternatively, it is possible to process the salt-ash mixture to separate ash for disposal, to recover the salt for recycle, and to recover fissile materials (Option 2; Figure 5). Either option results in the rapid, complete, and nonpolluting destruction of the combustible waste. No liquid wastes are produced. With typical TRU solid waste, a volume reduction factor of 47 is obtained if the salt is not processed for recycling (Option 1) and a volume reduction of 57 is obtained if the salt is recycled and the insoluble ash sent to waste disposal (Option 2).

III. Bench Scale Combustion Tests With Nonradioactive WasteA. Test Description

A diagram of the bench scale combustion apparatus⁽³⁾ is given in Figure 6. The combustor consisted of a 6" dia alumina tube inside a thick-walled Type 321SS vessel in a clam-shell tube furnace. The waste was placed in the feed-hopper and then fed (by a screw feeder) into the combustion air stream which conveyed the waste down the central alumina tube into the molten salt bed. Combustion took place in the bed. The combustion products passed up through the melt and out of the combustor, past ports where off-gas and particulate samples were taken. The off-gas was monitored continuously for carbon dioxide, carbon monoxide, nitrogen oxide, and hydrocarbon content, and periodically (by gas chromatography) for oxygen, nitrogen, and trace components that might be present. Isokinetic particulate samples were also taken and analyzed. Downstream of the particulate filter, aqueous hydroxide scrubbers were used to verify that no acidic gaseous components escaped from the melt.

The simulated radioactive waste consisted of 50 wt % paper, 32 wt % polyethylene, 8 wt % polyvinyl chloride, and 10 wt % rubber (mixed surgeon gloves and black rubber) and was reduced to <3 mm size in a Wiley mill before feeding. This mixture had essentially the same heating value, ash content, ash composition, and chloride content as typical TRU waste. This material was fed with a 1/2" or 5/8" dia x 6" variable speed screw feeder.

Two different ash-melt mixtures were used in these combustion tests (16 wt % ash-16 wt % NaCl-10 wt % Na₂SO₄-58 wt % Na₂CO₃ and 20 wt % ash-20 wt % NaCl-10 wt % Na₂SO₄-50 wt % Na₂CO₃). The two mixtures are the concentration extremes anticipated in actual rad-waste combustion.

B. Off-Gas Analysis

Typically in combustion tests nitrogen oxide emissions were ~20 ppm, and carbon monoxide and hydrocarbon emissions were less than the detection limits of the instruments, i.e., <0.05% and <10 ppm, respectively. As shown in Table I no HCl could be detected in the off-gas (i.e., <5 ppm).

Particulates in the off-gas were greater than 80 wt % sodium chloride and varied with temperature (Figure 7). It was found that the particulate loading depended on the sodium chloride vapor pressure at the combustion conditions (Figure 7) and was essentially independent of the carbon dioxide content of the off-gas. At about 800°C the particulate loading is ~0.2 mg/m³ (0.1 gr/scf) which is the allowable particulate loading for new combustion sources.

C. Retention of Specific Elements in the Melt

In several combustion tests the waste was contaminated with known amounts of (non-radioactive) specific elements such as cesium, strontium, europium, ruthenium, and iodine, by adding an aqueous solution (nitrate, chloride, or sodium) containing these elements to the waste. The particulates, off-gas scrubbers, and melt were then

14th ERDA AIR CLEANING CONFERENCE

analyzed for these elements to determine the melt retention of specific elements. In general, none of the cations (Ce^+ , Sr^{++} , Eu^{+++} , Ru^{+++} , were detected downstream of the melt, indicating that essentially all (>99.5%) of these cations were retained in the melt (see Table II)).

Iodine was detected downstream of the melt and the amount was related to the sodium iodide vapor pressure above the melt (as might be expected). Under combustion conditions about 99% of the iodine was retained in the melt.

IV. Bench Scale Combustion of TRU Wastes

A bench-scale combustor (see Figure 2), was incorporated in a glove-box in Atomics International's Plutonium Facility to study combustion of transuranic (TRU) contaminated wastes.⁽⁴⁾ A diagram of this combustor is shown in Figure 8. Except for safety features (water trap, heat exchangers, prefilters, and HEPA filters) this combustor was essentially the same as described previously, except it was smaller i.e., a 4" dia alumina combustor tube was used instead of a 6" tube.

Typical combustion conditions used in the plutonium ($PuCl_4$, $Pu(NO_3)_4$ and $Pu(SO_4)_2$) contaminated combustion tests of the paper-plastic-rubber waste (described previously) and the off-gas composition are given in Table III. The disposition of plutonium in the system after the tests is given in Table IV. These results show that waste combustion is complete in the molten salt and that essentially all (>99.9%) of the plutonium is retained in the melt. A similar test with uranium indicated that uranium and plutonium behave identically during combustion, i.e., >99.9% of the uranium was also retained in the melt.

V. Pilot Scale Combustion Tests

Large scale combustion tests of typical paper-plastic-rubber wastes were performed in Atomics International's Molten Salt Test Facility (MSTF) shown in Figure 3.⁽⁴⁾ A schematic diagram of this combustor is shown in Figure 9. This system consists of a 4' dia steel vessel lined with alumina blocks (Monofrax A)^(7,8), an industrial sized hammermill, rotary valve feeder, venturi scrubber, and HEPA filters. Approximately 1000 kg of salt are contained in the MSTF during combustion. The multipurpose system can be operated at reduced pressure (for radioactive containment) or positive pressure (for coal gasification) and is designed to readily by-pass or modify various components in the system. In these tests, all components were used and the system was operated at reduced pressure.

Typical combustion parameters observed in these tests are given in Tables V and VI. Again, combustion was complete and particulate loading was ~ 0.2 mg/m³ during 800°C combustion temperature. No HCl could be detected in the off-gas even when pure polyvinyl chloride was burned. In some of these tests magazines were used to increase the ash content of the waste. The magazines had colored dyes containing nitrogen which accounted for the high nitric oxide content of the off-gas (up to 500 ppm) observed for part of the test.⁽⁹⁾

VI. Salt and Plutonium Recovery

In some applications, it may be desirable to recycle the salt and transuranics from the melt-ash mixture. A scheme for accomplishing this has been developed and tested on a bench scale; large scale salt recovery tests are underway in other molten salt applications.

Salt recovery is accomplished using technology developed to recover minerals from dry lake beds. Briefly the salt is recovered by dissolving the salt in water and selectively crystalizing sodium carbonate-sulfate mixtures for recycle and sodium chloride for disposal. Although crystal purity has not been optimized to date, typical results are given in Table VII. Typically, the sodium carbonate crystals contain about 8% sodium chloride and the chloride crystals contain about 6% sodium carbonate and sulfate. Since these contaminants in the various crystal fractions do not detract from the process, studies to improve the crystal purity have not been made. Weight and volume reductions found for the two process options (with and without salt recycle) are given in Table VIII. Without salt recycle (Option 1) a volume reduction of 47 was found; with salt recycle (Option 2) a volume reduction of 57 was obtained.

Although the specific plutonium recovery procedure has not been selected, initial tests indicate that essentially all of the plutonium can be recovered. Plutonium remains with the insoluble ash when the salt is dissolved; only about one percent of the plutonium is dissolved in concentrated salt solutions. (This dissolved plutonium crystalizes with the sodium carbonate and is recycled to the combustor; it is not lost from the system). The plutonium remaining with the ash fraction is leached with acid (HCl or HNO₃). About 99% of the plutonium in the ash is dissolved in a single acid leach and about 99.6% is dissolved in two acid leaches. The plutonium is readily recovered from these solutions by existing ion-exchange or solvent extraction technology.

VII. Development Status

Development of molten salt combustion technology has progressed to the point where large systems are being designed. Conceptual design of a combustion unit for hazardous organic chemicals has been completed by AI and Title I design is underway; this design and required safeguards are very similar to a TRU waste combustion unit. Furthermore, AI is presently designing a 1000 kg/hr molten salt coal gasification unit, with many features similar to the TRU waste combustor. Design of a 50 kg/hr radwaste combustion system for INEL began July 1, 1976; this unit should be operational in early 1978.

VIII. References

1. S. J. Yosim, et al, "The Chemistry of the Molten Carbonate Process for Sulfur Oxide Removal from Stack Gases," in Advances in Chemistry Series No. 127, American Chemical Society, Washington, D.C., 174 (1973)
2. W. V. Botts and D. C. Gehri, "Regenerative Aqueous Carbonate Process for Utility and Industrial Sulfur Dioxide Removal," Advances in Chemistry Series No. 139, American Chemical Society, Washington, D.C., 164 (1974)
3. D. E. McKenzie, et al, "Disposal of Transuranic Solid Waste Using Atomics International Molten Salt Combustion Process," AI-ERDA-13151 (May 1975)
4. L. F. Grantham, et al, "Disposal of Transuranic Solid Waste Using Atomics International's Molten Salt Combustion Process, II," AI-ERDA-13169 (March 1976)
5. C. A. Trilling, "Coal Gasification by the Atomics International Rockgas Process," Paper Presented at the November 1974 ASME Meeting
6. S. J. Yosim and K. M. Barclay, "Gasification of Wastes Using Molten Salts," Fuel from Waste Symposium Preprints, Div. of Fuel Chemistry, American Chemical Society, Washington, D.C., (1976)
7. Monofrax-A is a fused-cast high-purity alumina product of Carborundum Company, Falconer, N.Y.
8. L. F. Grantham and P. B. Ferry, "Corrosion in Alkali-Metal Carbonate Based Melts," in Proceedings of the 1976 International Molten Salt Symposium to be published by the Electrochem. Soc.
9. R. J. Roberts, et al, "An Attempt to Reduce NO_x Emissions from Pulverized Coal Furnaces," J. Air Pollut. Control Assoc., 9, 859 (1975)

14th ERDA AIR CLEANING CONFERENCE

Table I Typical offgas analyses found in nonradioactive bench-scale combustion tests.

<u>Component</u>		<u>Typical Amount in Offgas</u>
Hydrocarbons	(HC)	<10 ppm*
Hydrogen Chloride	(HCl)	<5 ppm*
Nitrogen Oxides	(NO _x)	15-30 ppm**
Carbon Monoxide	(CO)	<0.05%
Oxygen	(O ₂)	4-12
Carbon Dioxide	(CO ₂)	6-15%
Nitrogen	(N ₂)	balance

*Detection limit

**Varied with nitrogen content of feed material and was essentially all nitric oxide (NO)

Table II Retention of specific elements in the melt.

<u>Element</u>	<u>Compound</u>	<u>Disposition in Combustion System (wt %)*</u>		
		<u>Scrubber</u>	<u>Particulates</u>	<u>Melt</u>
Ce	CeNO ₃	(ND) 0.01	<0.5	>99.5
Sr	Sr(NO ₃) ₂	(ND) 0.01	<0.2	>99.7
Ru	HRuCl ₄	(ND) 0.01	(ND) <0.05	>99.9
Eu	Eu(NO ₃) ₃	(ND) 0.01	(ND) <0.1	>99.8
I	NaI	0.01	~1	~99

* (ND) = Not detected; in most tests no Ce, Sr, Ru, or Eu was detected in the particulates; values reported are maximum amounts found in any of the tests downstream of the scrubber or the maximum amounts that could have been present based on the analytical detection limit

Table III Test parameters for plutonium waste combustion tests.

<u>Test No.</u>	<u>Pu Concentration in Waste Feed (wt %)</u>	<u>Feed Rate (g/hr)</u>	<u>Average Combustion Temperature (°C)</u>	<u>Off-Gas Analysis</u>			
				<u>CO₂ (%)</u>	<u>CO (%)</u>	<u>HC (ppm)</u>	<u>O₂ (%)</u>
1	9 x 10 ⁻³	190	895	7	0.1	5	12.0
2	1.1 x 10 ⁻¹	180	892	6.3	0.1	5	12.0
3	9 x 10 ⁻³	170	880	6.0	0.02	5	13.0

14th ERDA AIR CLEANING CONFERENCE

Table IV Disposition of plutonium in bench-scale radwaste combustion tests.

Plutonium Found in Various Components (wt %)

Test No.	HEPA Filters	Pre-Filter	Condensate	Water Trap	Combustor Offgas Line	Melt*
1	<10 ⁻⁴	0.07	<10 ⁻⁴	--	--	(99.9)
2	<10 ⁻⁴	0.01	<10 ⁻⁴	--	--	(99.9)
3	<10 ⁻⁴	0.02	<10 ⁻⁴	0.01	0.009	(99.9)

*By difference, melt analysis indicated that 99.0 ±1.3% of the plutonium was in the melt

Table V Particulate loading for combustion of simulated TRU waste in the MSTF pilot plant.

Sample No.	Feed Material	Feed Rate (kg/hr)	Average Melt Temp. (°C)	Particulate Loading (g/m ³)		
				Before Venturi	After Venturi	After HEPA Filter*
1	PVC	16	975	0.31	0.014	(ND; <10 ⁻⁶)
2	Radwaste** +40% PVC	50	1020	0.62	0.043	(ND; <10 ⁻⁶)
3	Radwaste** +40% PVC	50	845	0.11	0.016	(ND; <10 ⁻⁶)
4	Radwaste** +45% PVC	43	790	0.10	0.014	(ND; <10 ⁻⁶)

*(ND) = not detected

**Radwaste consisted of 33 wt % high ash paper, 20 wt % Kimwipes, 32 wt % polyethylene, 8 wt % PVC, and 7 wt % rubber

Table VI Typical offgas analysis for simulated TRU waste combustion in the molten salt test facility.

Component	Amount in Offgas*
N ₂	76-78%
O ₂	5-12%
CO ₂	10-15%
HC	(ND) (< 5 ppm)
SO ₂	(ND) (< 2 ppm)
CO	(ND) (< 0.1%)
HC	(ND) (< 0.1%)
NO _x	30-500 ppm**

*(ND) = not detected

**Depended on nitrogen content of feed material

14th ERDA AIR CLEANING CONFERENCE

Table VII Comparison of salt compositions from flowsheet and experimental results.*

<u>Process Product</u>	<u>Flowsheet Calculations (kg)</u>	<u>Experimental Results (kg)</u>
Ash Disposal	16 Ash	18 Ash + Na ₂ O
Furnace Recycle	40 Na ₂ CO ₃ 8 Na ₂ SO ₄	40 Na ₂ CO ₃ 8 Na ₂ SO ₄ 4.3 NaCl 1.6 Ash
NaCl Disposal	16 NaCl	16 NaCl 1 Na ₂ CO ₃ -Na ₂ SO ₄
Recycle Solution	15 NaCl 14 Na ₂ CO ₃ 1 Na ₂ SO ₄	15.2 NaCl 13.6 Na ₂ CO ₃ 0.7 Na ₂ SO ₄ 0.4 Ash

*Assumes 200 Kg of typical waste with 8 wt % ash and 4.9 wt % chloride content.

Table VIII Weight and Volume Reductions for Various Processing Options.*

	<u>Weight Reduction</u>		<u>Volume Reduction</u>	
	<u>Kg</u>	<u>Factor</u>	<u>m³</u>	<u>Factor</u>
Original Waste	200		1.79	
Option 1 (No Processing)	80	2.5	0.036**	47
Option 2 (Theoretical Maximum w/Disposal of Chloride + Ash)	32	6.2	0.029**	62
Option 2 Experimental	35	5.7	0.031 [†]	57

*The reduction factors are process estimates; they do not take into account the waste generated by normal operation of the facility and the air cleaning train. Some of these wastes would probably also be processed through the salt.

**Assumes 200 Kg of waste containing 8 wt % ash and a bulk density of 112 Kg/m³.

[†]Fused cast salt product (Option 1) has a density of (2200 Kg/m³) while the product filtered and crystalized from aqueous solution (Option 2) has a density of 1120 Kg/m³.

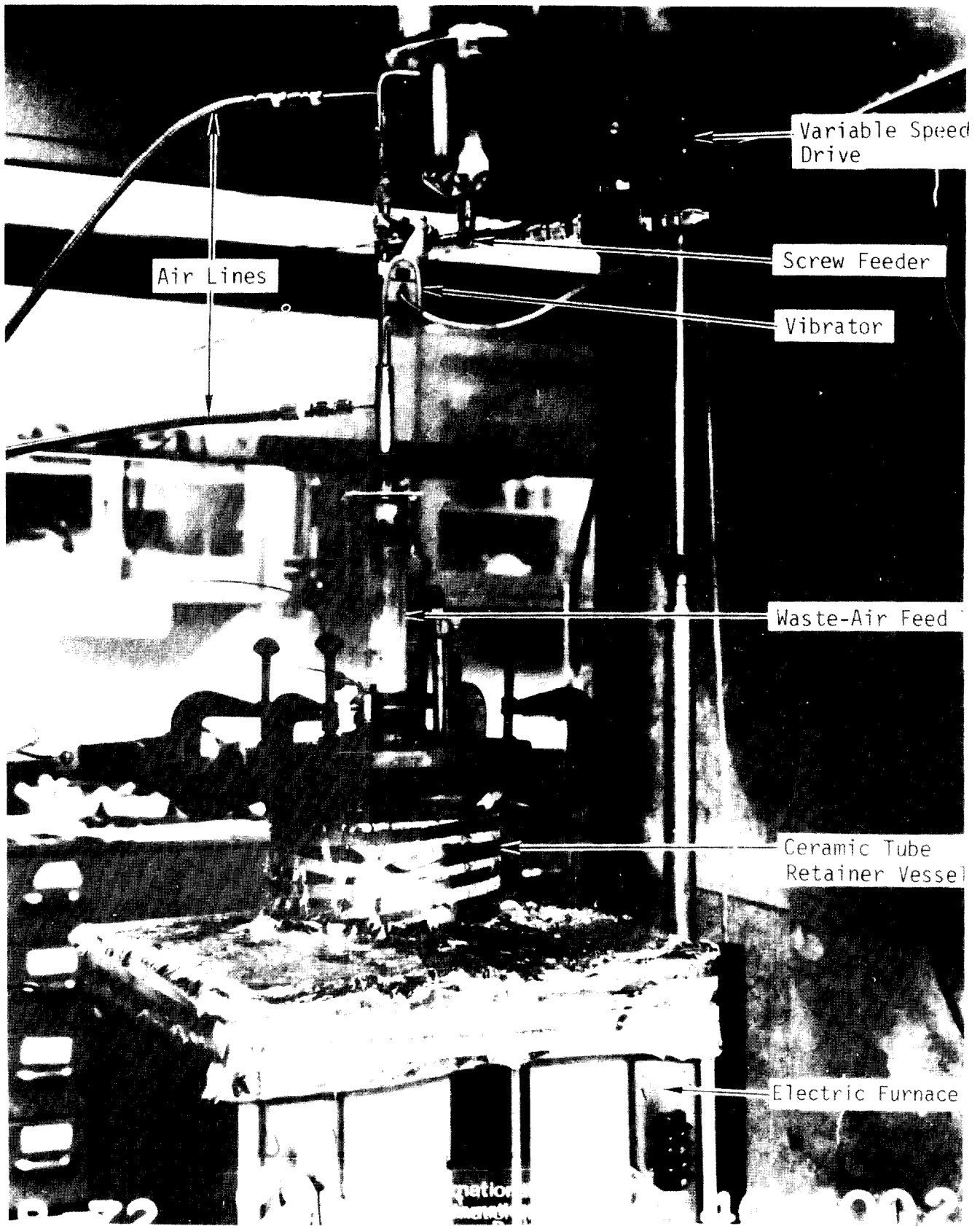


Figure 1. Continuous solid feeding components of bench-scale combustor.

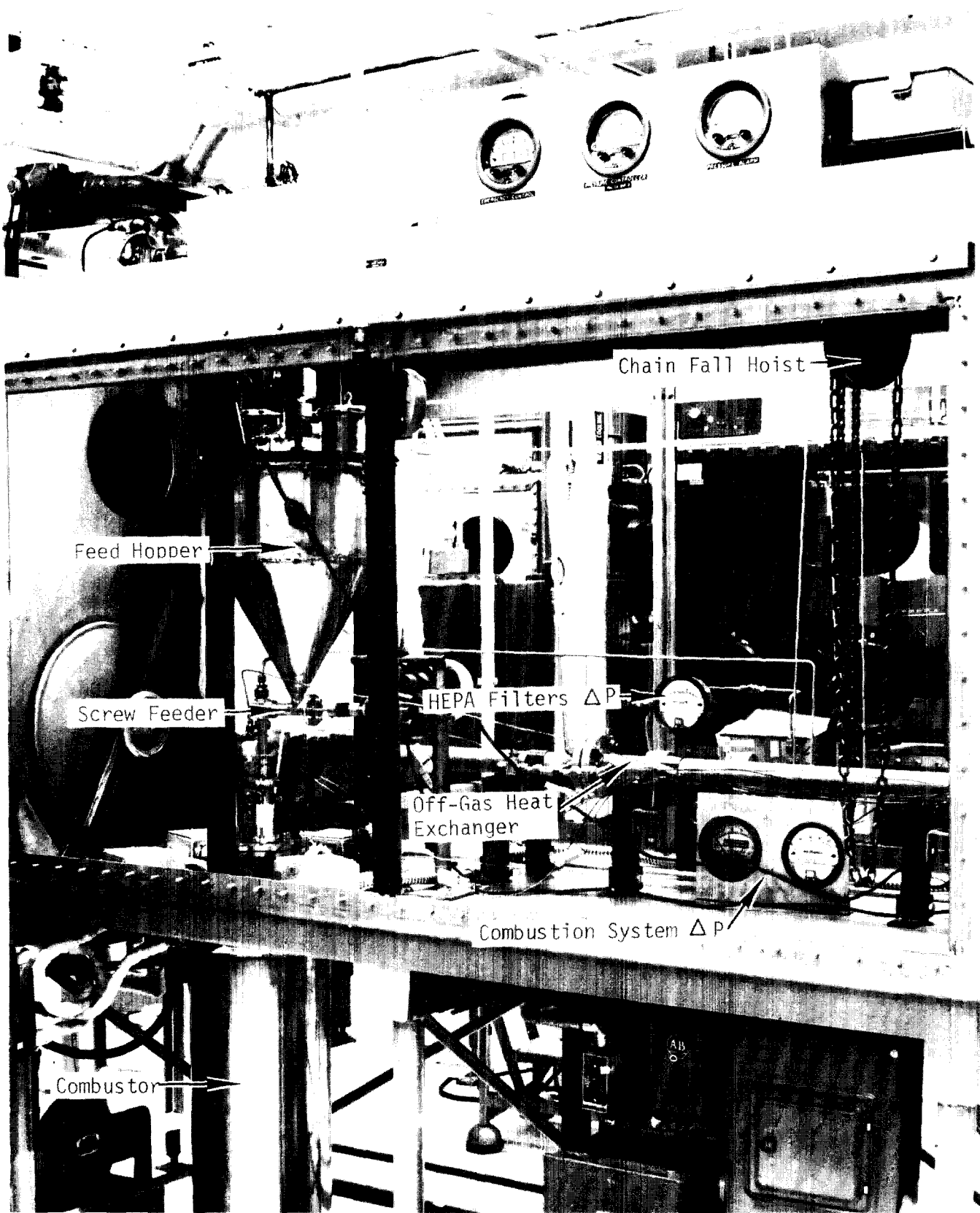


Figure 2. Bench scale radwaste combustion system.

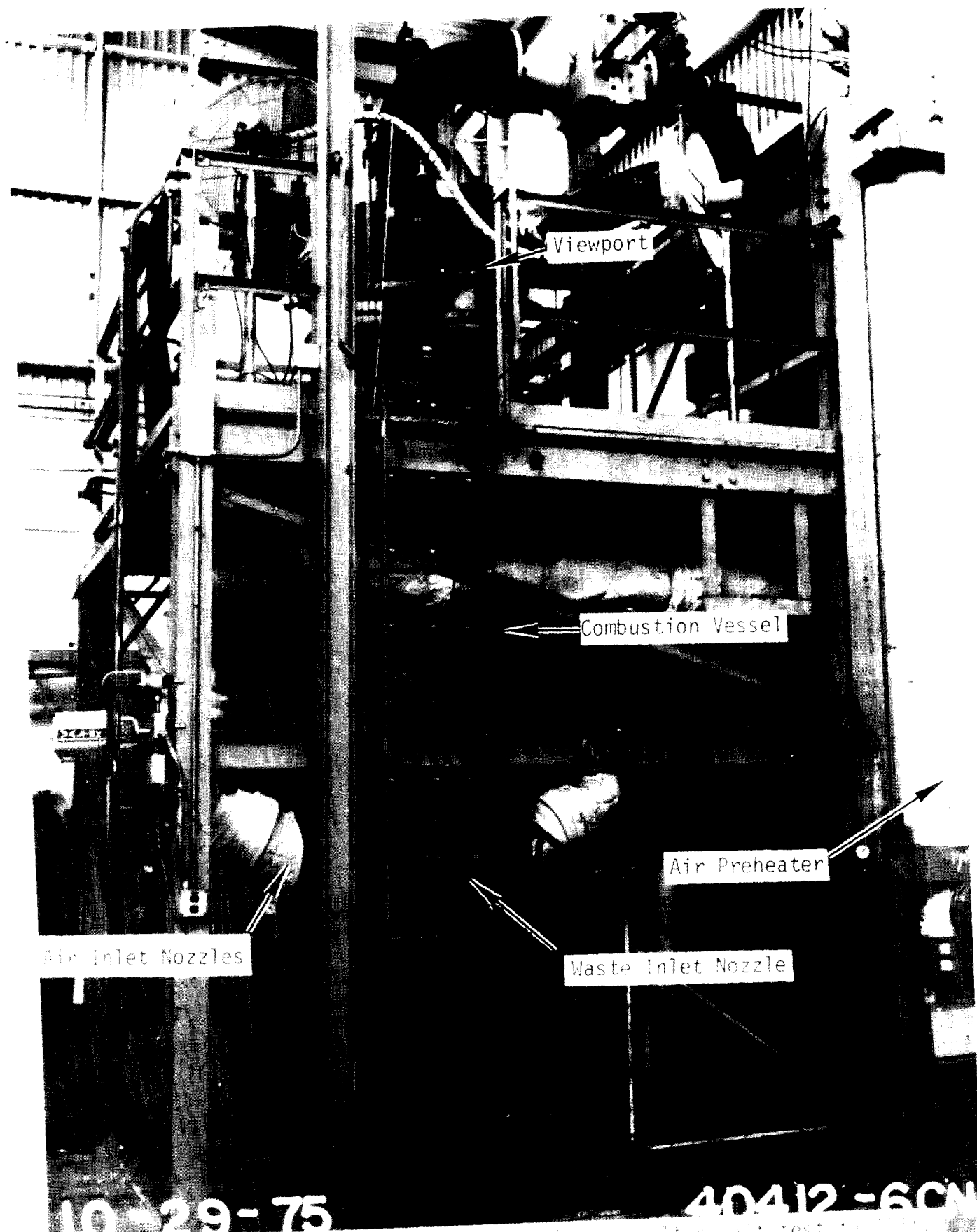
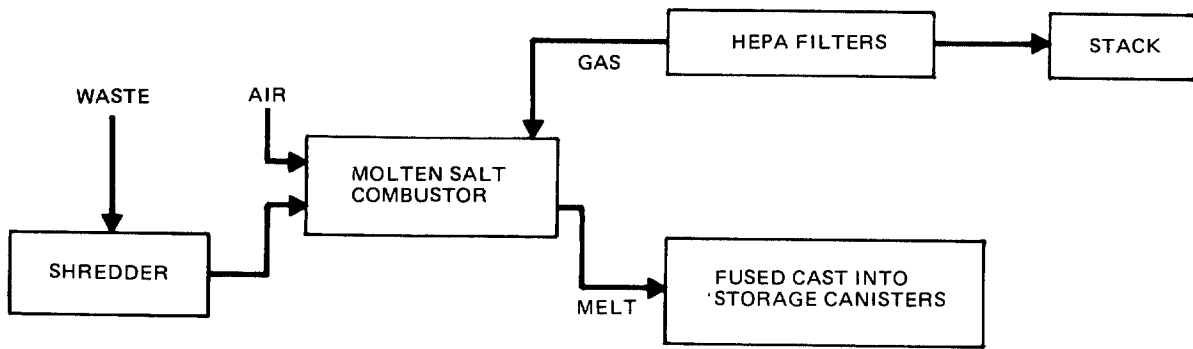
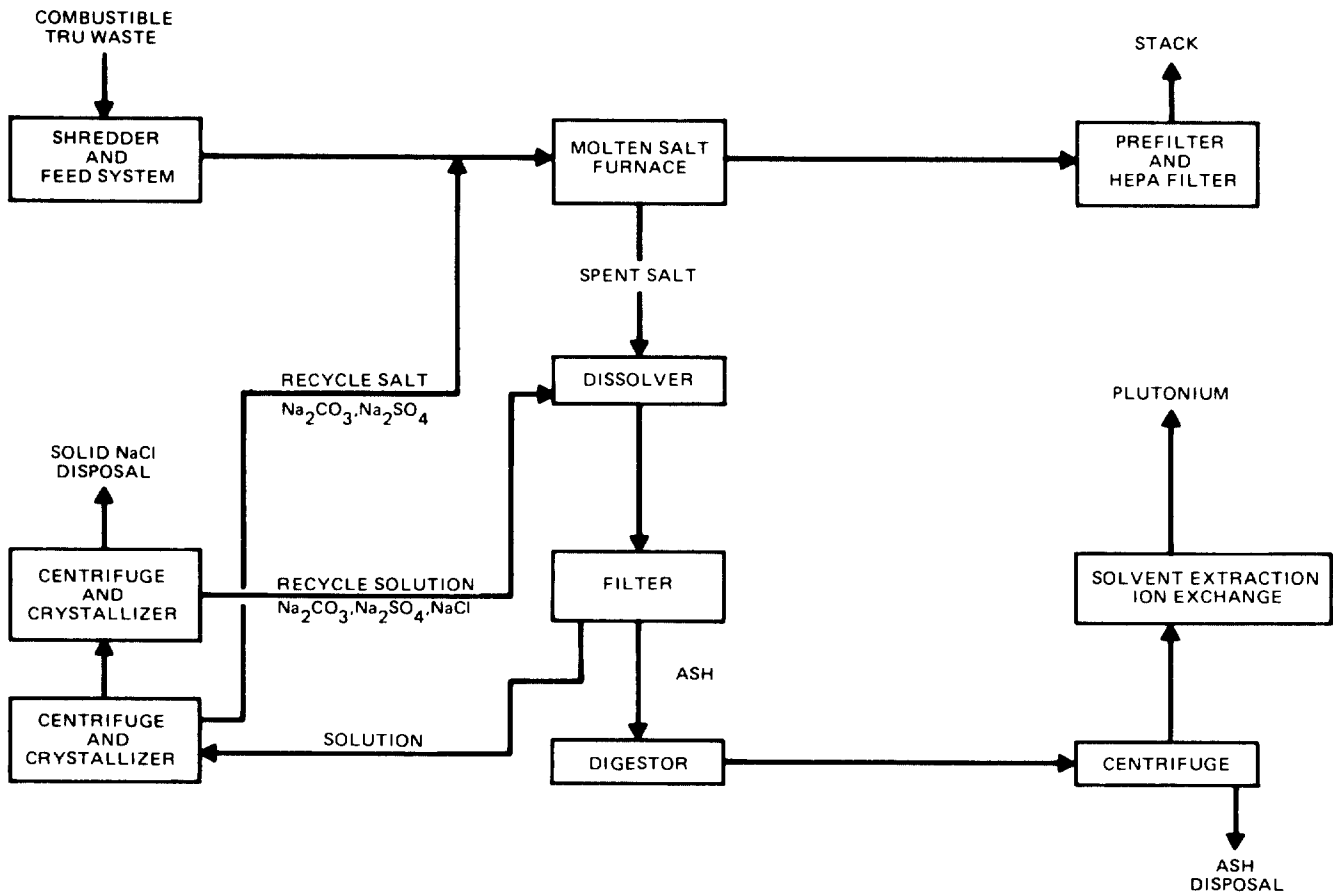


Figure 3. Pilot-scale combustor in the metal air test facility.



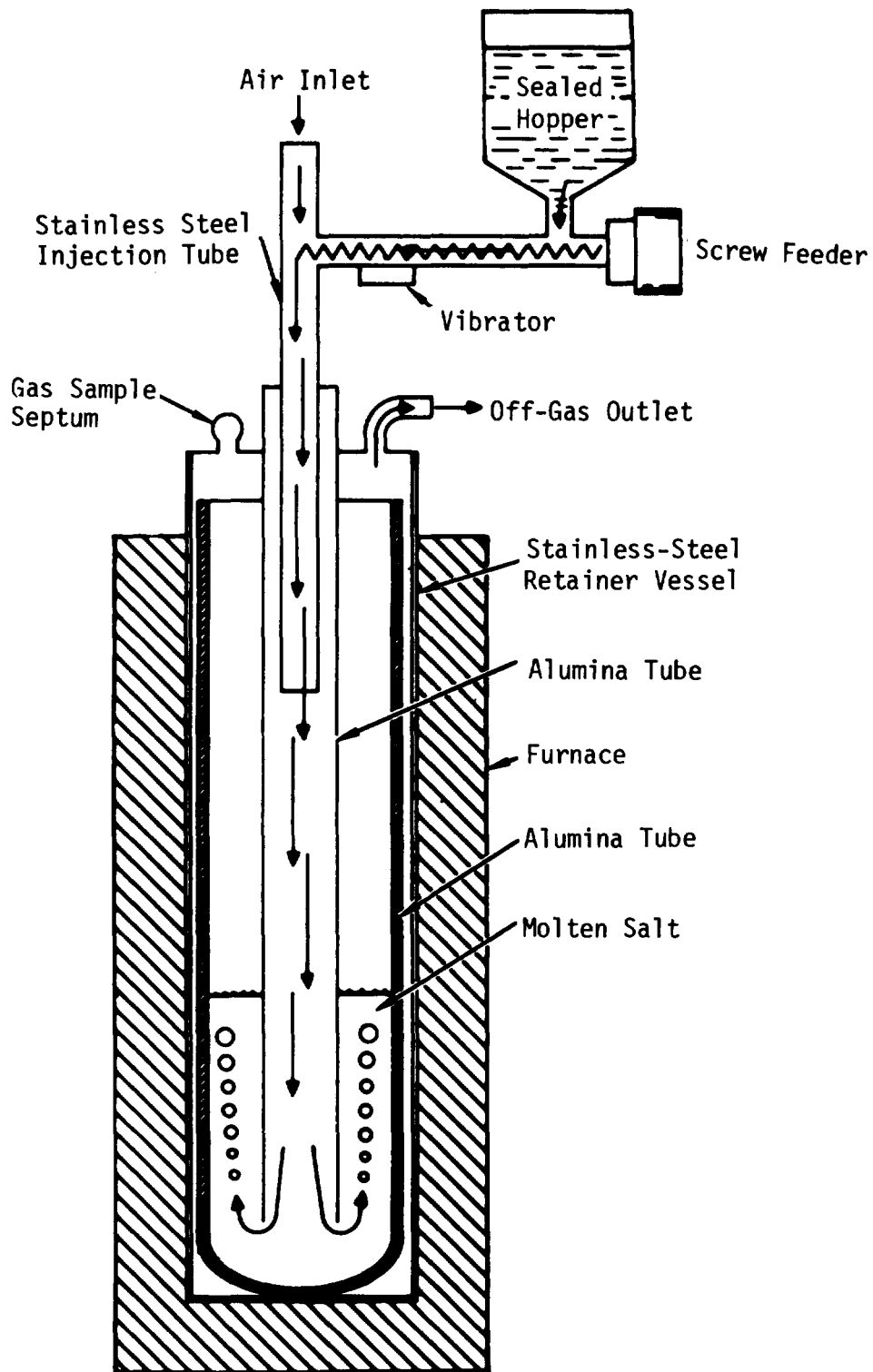
9063-4009

Figure 4. Flow diagram of molten salt combustion process without salt recovery (Option 1)



9063-4009

Figure 5. Alternate molten salt combustion process flow diagram with plutonium and salt recovery (Option 2)



42400-1016

Figure 6. Bench-scale molten salt combustion unit.

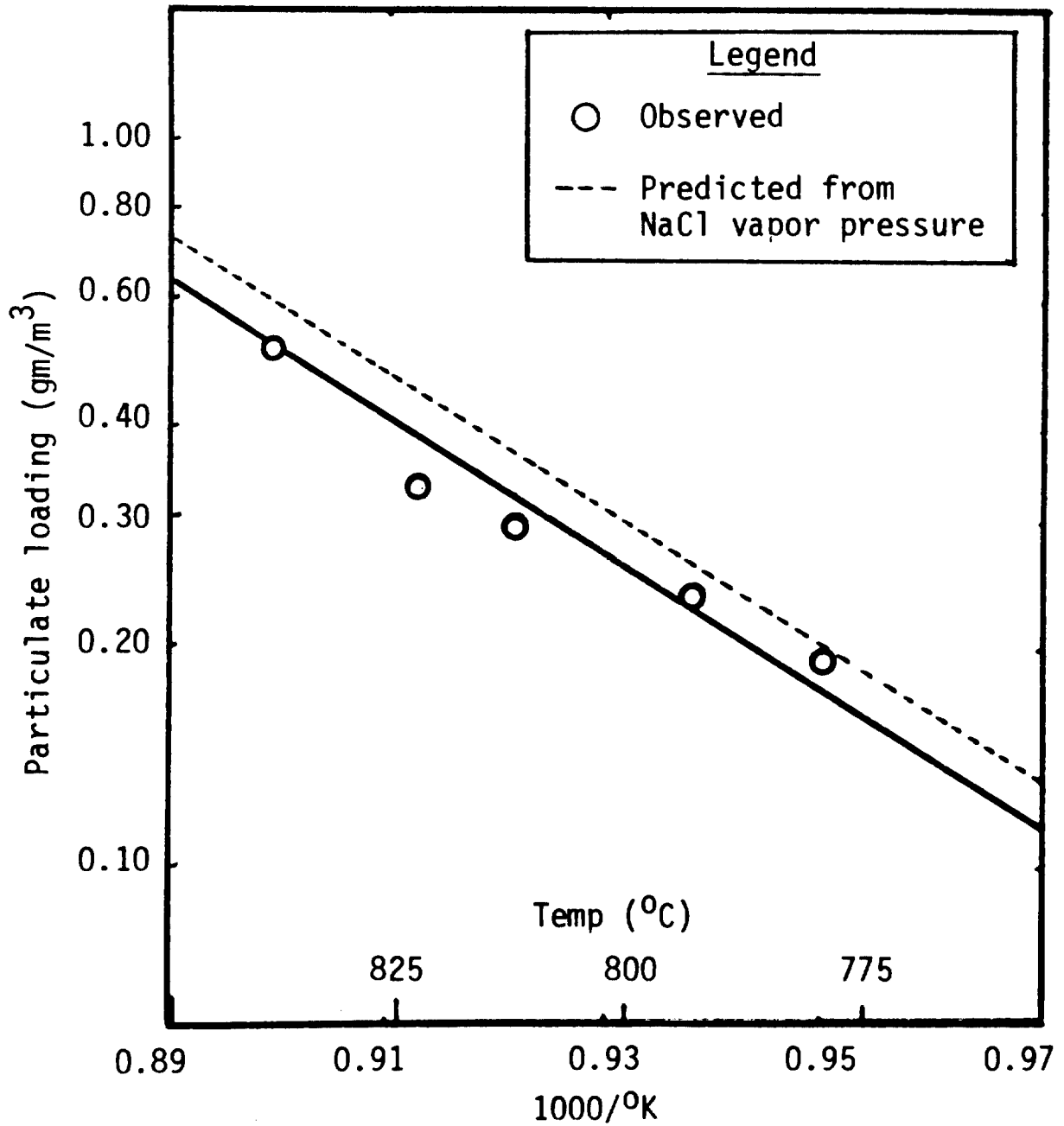


Figure 7. Relationship between observed particulate loading of the off-gas and sodium chloride vapor pressure.

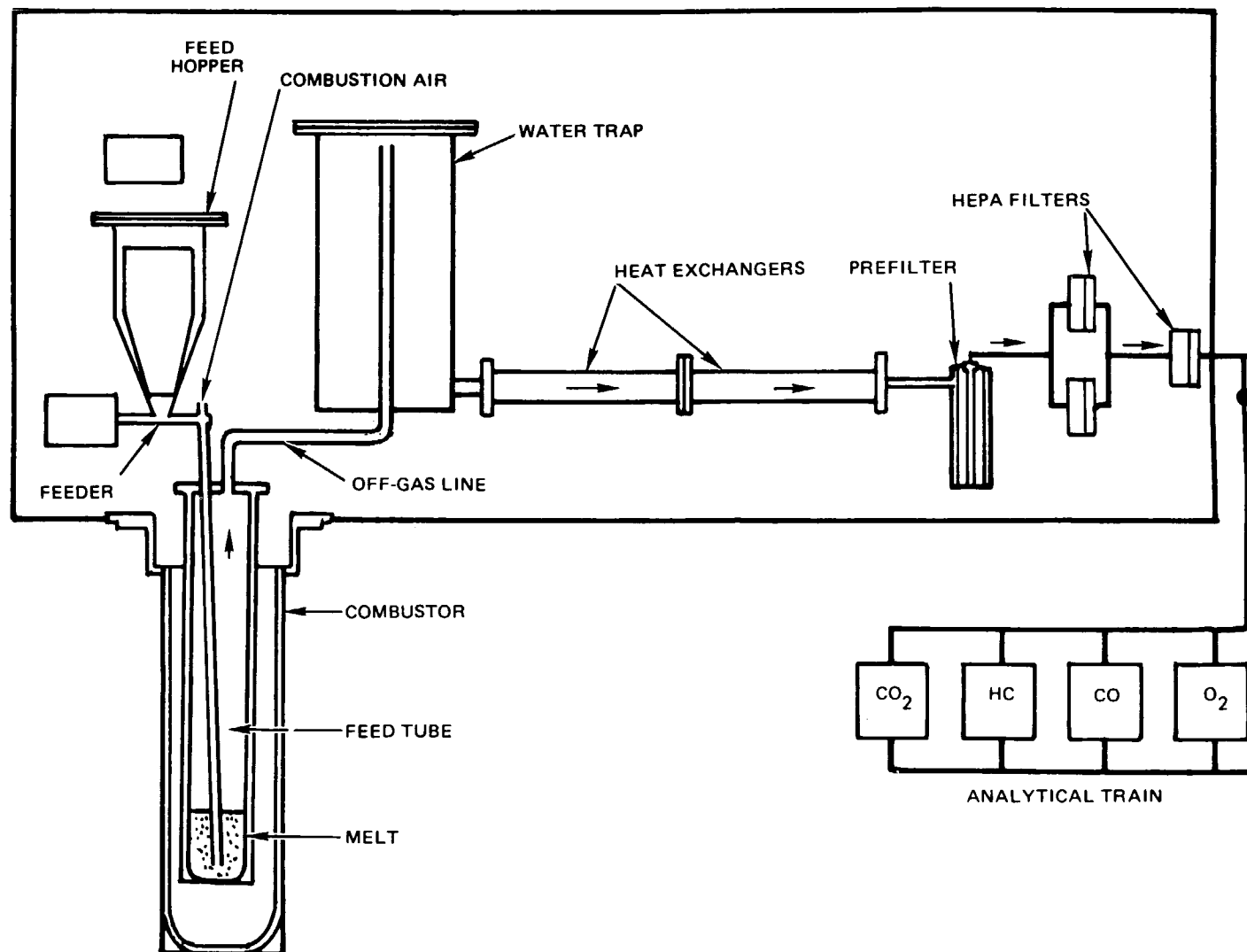


Figure 8. Bench-scale radwaste combustor flow diagram.

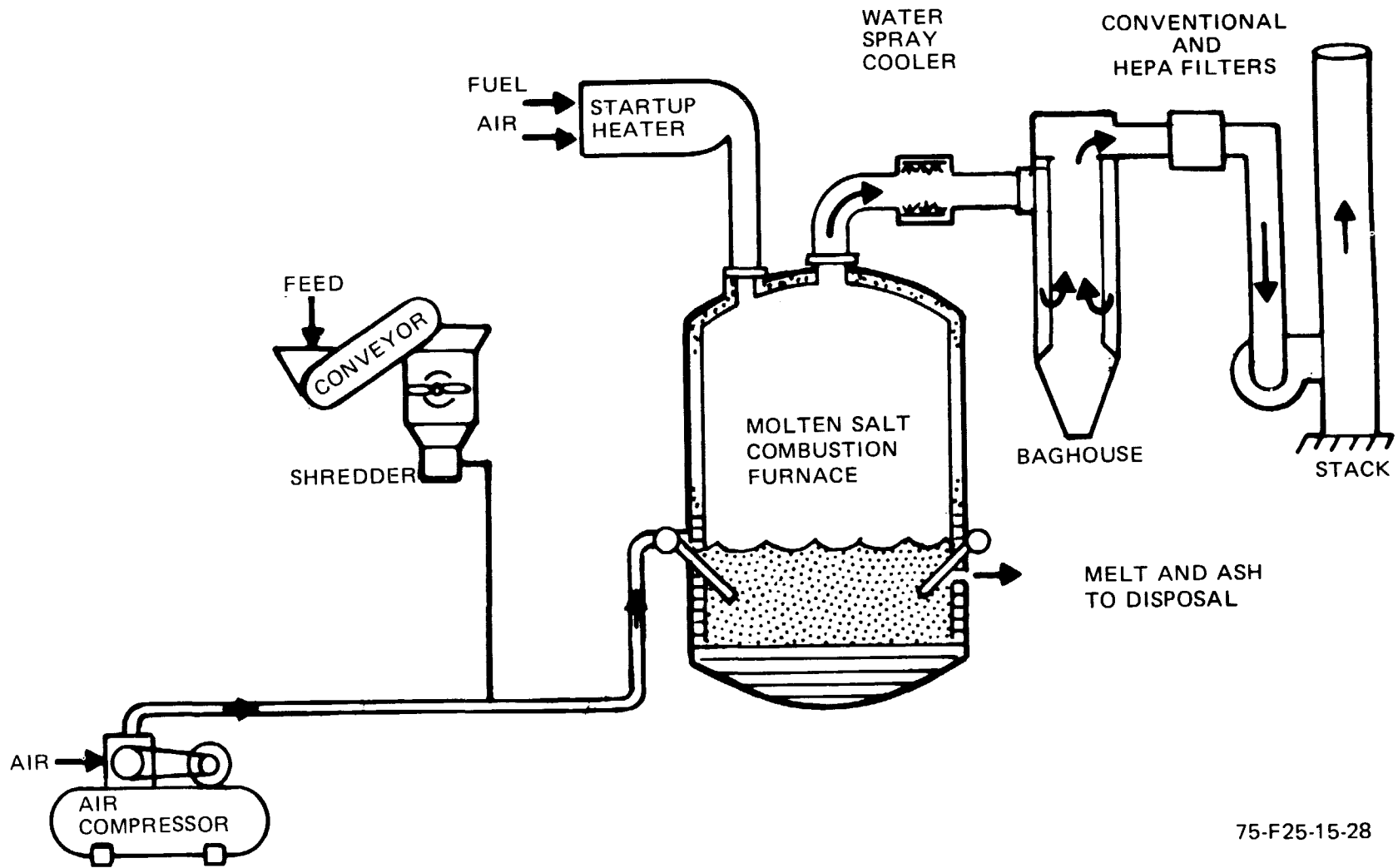


Figure 9. Schematic of a molten salt test facility.

75-F25-15-28

DISCUSSION

RAMSEY: I think this group might be interested in your comments on the feedbacks of the cycling of wastes through this system. Specifically, you have HEPA filters on the outlet. Would these HEPA filters be suitable as components to feed to the system?

GRANTHAM: Yes. The HEPA filters contain asbestos, silica and combustible materials. These can be shredded and fed directly to the molten salt. The silica will dissolve and some of the asbestos will also dissolve. The net result will be an increase in the ash content of the salt so that the HEPA filters themselves can be fed right back into the system.

B. P. BROWN: I was wondering if you can recover fissionable material such as plutonium?

GRANTHAM: Yes. We developed a technique to recover plutonium from the molten salt. This has been tested on a bench scale unit. We can recover about 99.5 per cent of the plutonium from the salt. The plutonium is quite soluble in dilute acid. It is not a refractory plutonium.

SCHURR: My question is in regard to your shredder or pre-treatment hammer mill. Are you going to be looking at potential maintenance of this item? This looks to me like a real critical weak point because most shredders or hammer mills will be high maintenance items with the need for changing blades or hammers.

GRANTHAM: We certainly agree with your concern. Our experience with the hammer mill has required little maintenance on materials we have fed during the past three years. Right now, we are using a hammer mill primarily because it was available, not because we think it is the best system. We are investigating knife shredders as well.

MCDOWELL: Have you noticed the formation of a slag on top of the molten salt from any of the material that you incinerate?

GRANTHAM: Perhaps we would if we let the molten salt settle, but the molten salt is being agitated by air that is injected with the combustible material. The ash is very evenly distributed in the molten salt when we drain the molten salt from the combustor. We have noticed no settling in the vessel during combustion.

CLAIRBORNE: You mentioned the retention of the transuranics but you only mentioned plutonium. How about americium and curium?

GRANTHAM: We haven't looked at americium and curium. We have looked at plutonium and uranium and both of these are retained in the molten salt.

BRODERSEN: I would like to know how long a time you expect your alumina to last in your big furnace. There will probably be some corrosion.

14th ERDA AIR CLEANING CONFERENCE

GRANTHAM: The alumina is protected by the formation of a sodium aluminate film and the corrosion rate after this film is formed is in the neighborhood of a few mills per year. The alumina lining in our large scale molten salt vessel is six inches. This will last for years.

FREEMAN: What is your estimated capital cost for this 50 kg per hour unit?

GRANTHAM: We are designing a unit for INEL now and the cost, including engineering design and testing to support the design, equipment, installation, training, and start-up, is one million dollars. I don't have the exact breakdown.

14th ERDA AIR CLEANING CONFERENCE

CONTROLLED-AIR INCINERATION OF TRANSURANIC-CONTAMINATED SOLID WASTE

L. C. Borduin, W. E. Draper
R. A. Koenig, A. S. Neuls, and C. L. Warner
Los Alamos Scientific Laboratory,
University of California
Los Alamos, New Mexico*

Abstract

A controlled-air incinerator and an associated high-energy aqueous off-gas cleaning system are being installed at the Los Alamos Scientific Laboratory (LASL) Transuranic Waste Treatment Development Facility (TDF) for evaluation as a low-level transuranic-contaminated (TRU) solid waste volume reduction process. Program objectives are: 1) assembly and operation of a production scale (45 kg/hr operation of "off-the-shelf" components representative of current incineration and pollution control technology; 2) process development and modification to meet radioactive health and safety standards, and 3) evaluation of the process to define the advantages and limitations of conventional technology. The results of the program will be the design specifications and operating procedures necessary for successful incineration of TRU waste. Testing, with nonradioactive waste, will begin in October 1976. This discussion covers commercially available incinerator and off-gas cleaning components, the modifications required for radioactive service, process components performance expectations, and a description of the LASL experimental program.

I. Introduction

The Energy Research and Development Administration (ERDA) has directed LASL to establish a study program for the evaluation and development of production-level TRU solid waste treatment processes. This laboratory and other ERDA-contractor installation routinely handle large quantities of radioactive contaminated materials. The bulk of the waste generated by various operations at these sites is low-level activity and, as such, is currently either stored retrievably ($>10\text{nCi/g}$) or buried ($<10\text{nCi/g}$) at controlled disposal areas. However, estimates of future solid waste volumes strongly indicate the need for improved solid waste disposal techniques. Volume reduction, for example, combined with guaranteed control of long-lived isotopes, is a prime consideration for all facilities routinely handling large quantities of transuranic materials. Occupancy of the LASL TDF began in May 1976. This facility will be used to evaluate alternate production-scale (45-90 kgs/hr) processes for reducing the volume of combustible waste contaminated with transuranic isotopes. Candidate processes will be designed to accept waste generated by typical ERDA-site operations.

*Work performed under the auspices of the USERDA, Contract W-7405-ENG. 36 and funded specifically through the Division of Nuclear Fuel Cycle and Production.

14th ERDA AIR CLEANING CONFERENCE

Controlled-air incineration was the first process to be evaluated in the TDF. Although incineration is a well established method of volume reduction in industry, previous attempts to treat radioactive solid waste by this technique have met with only limited success. Problems encountered included equipment sealing, corrosion, and off-gas cleanup. As these are technical problems rather than basic process faults, a development program based on conventional incineration is warranted.

The specific incinerator design selected for the TDF was constrained by the need to implement a contaminated waste treatment study program without undue delay. Recognizing that several promising alternate processes exist or are under development, each system was evaluated in terms of the time required to allow proper engineering of a production-scale (45 kg/hr) plant. Of those systems meeting this criterion, the controlled-air concept was selected on the basis of operational flexibility, ease of combustion rate control, minimum particulate emission due to low turbulence in the primary combustion chamber, combustion efficiency, and availability of commercial equipment.

Proven technology guidelines were likewise followed in the selection of the off-gas cleanup system. The presence of transuranic-contaminated particulates, as well as inorganic acids, primarily HCl, in the incinerator off-gas requires a high-efficiency cleanup system. Thus a high-energy aqueous scrub system, with a variable-orifice venturi and packed-column scrubber as the primary components, was specified.

This paper discusses the incinerator and off-gas cleaning system only. The LASL Waste Management Research and Development Program and TDF, and design features of the feed preparation system are detailed in the references noted.

II. Process Objectives

Processes selected for TDF installation will be oriented toward handling low-level wastes resulting from transuranic operations typical of ERDA-contractor sites. These wastes vary widely between individual facilities but may be categorized on the basis of origin, i.e. laboratory, line or process, and construction. Table I indicates the range of waste compositions expected in these categories, based on a 1973 LASL survey.

Table I. Typical waste composition.

<u>Material</u>	<u>Laboratory</u>	<u>Process</u>	<u>Construction</u>
Paper & Rags	10-60 wt. %	10-40 wt. %	5-20 wt. %
Plastics	5-60	30-40	5-30
Rubber	5-30	10-45	5-20
Lumber	-----	-----	5-30
Dirt & Concrete	-----	-----	5-60
Metallics & Glass	5-50	30-40	10-50

14th ERDA AIR CLEANING CONFERENCE

Laboratory wastes are defined to include wastes from support areas in the immediate vicinity of, as well as, specific-laboratory refuse. Process wastes typically result from glovebox production operations; construction wastes originate with the disassembly of de-commissioned facilities. The bulk of routine, low alpha-activity waste is expected to originate in the laboratory areas.

Depending on the waste reduction process selected, a design feed can be defined by inclusion of those constituents treatable by that process. Waste materials not effectively reduced by, or incompatible with, the candidate process would be sorted out for disposal by other means. For conventional incineration, the "Design Basis" feed was defined as shown in Table II. Heat and material balances required for equipment sizing were based on this waste composition. The controlled-air incinerator can handle 100% of any of the given waste components at a 45 kg/hr feed rate. The off-gas cleaning system is designed to scrub the mineral acids and particulates generated while burning up to 100% of any component including PVC.

Table II. Design basis incineration feed.

<u>Component</u>	<u>Weight %</u>
Paper & Rags	35
Plastics	
Polyethylene	23
PVC	12
Rubber	<u>30</u>
	100

Following preliminary runs with nonradioactive waste, the first TRU wastes processed in the TDF experimental program will have activity concentrations around 10 nCi/g. Higher concentrations will be used as the program progresses. A production facility would be expected to process wastes containing concentrations equal to, or less than, the levels recoverable by current technology (normally 0.5 g/kg).

One criterion for candidate processes is a large volume reduction ratio (ratio of contaminated waste input volume to total contaminated waste output volume). Witness that the cost benefits of a treatment process (packaging, handling, transportation, and storage charges) would be reduced by a high volume reduction ratio, as would be the amount of land required for storage/disposal of waste. Another prime criterion is that related technologies have qualified the system for production-level operations. A survey of six ERDA sites determined that processing rates in the 45 to 90* kgs/hr range were needed to meet current needs. Projected future needs increased the

*The basis for hourly capacity is a 10 month, 5 day/wk, 24 hr/day operation of a production incinerator (217 days/yr). Two months was assumed as adequate maintenance and modification time.

14th ERDA AIR CLEANING CONFERENCE

probable upper limit to 230 kg/hr. The nominal throughput rate of the initial TDF process was set at 45 kg/hr following review of scale-up factors, commercially available equipment sizes, and program testing and development goals.

III. Process Description

Wastes to be processed at the facility are sealed in plastic bags contained in sealed 0.3 X 0.3 X 0.6-m (1 X 1 X 2,ft) cardboard boxes and are transported to the site in 0.14-m³ (30-gal) DOT drums. The drums are loaded individually into the introductory box of the feed preparation line. Packages are assayed for transuranic isotope content (4) and x-rayed (5) for incompatible materials; if necessary, packages are opened to remove non-combustible material. From the sorting glove box, (6) packages are transported to the storage glove box, which provides adequate material storage for approximately eight hours of operation. The storage box is connected to the ram feeder, which charges waste, batch-wise, to the dual-chamber incinerator.

Incinerator

The incinerator is a conventional dual-chamber design, manufactured by Environmental Control Products, Inc. (ECP) (see Figure 1). Similar models are currently in use for disposal of municipal, industrial, and pathological solid wastes. Underfire air is used in the lower (ignition) chamber to incinerate the solid wastes under sub-stoichiometric conditions. This "controlled-air" operation reduces the magnitude of temperature fluctuations and the emissions rates from those normally associated with "free-air" incineration. Unburned volatile components, as well as entrained particulates, exit the lower chamber via an interconnecting port. Excess air and supplemental heat are supplied in this turbulent region to promote complete combustion. The secondary chamber provides additional residence time for completion of combustion reactions. Normal operating temperatures, 650°C to 870°C in the lower chamber and 870°C to 1100°C in the upper chamber, are maintained by two low-intensity, natural-gas fired burner. Air introduction rates and nominal chamber temperatures are varied dependent on waste composition.

The incinerator chamber shells and other primary structural components are carbon steel. The two combustion chambers and the exhaust duct immediately downstream of the upper chamber are lined with 13-cm of high-density plastic refractory, 5-cm of mineral wool block, and 0.6-cm of mastic stack coating. The 2000°C-tolerance plastic refractory is more easily repaired and more resistant to thermal shock than castable-type refractories. The mastic provides diffusion barrier protection for the carbon steel shells, preventing corrosive attack by combustion product acid vapors such as HCl and SO₃. This quantity of refractory is greater than normally specified for³ industrial incinerators, but is required to reduce the heat load on the secondary-containment ventilation system.

The incinerator represents conventional industrial technology. The following design modifications were incorporated in the purchase

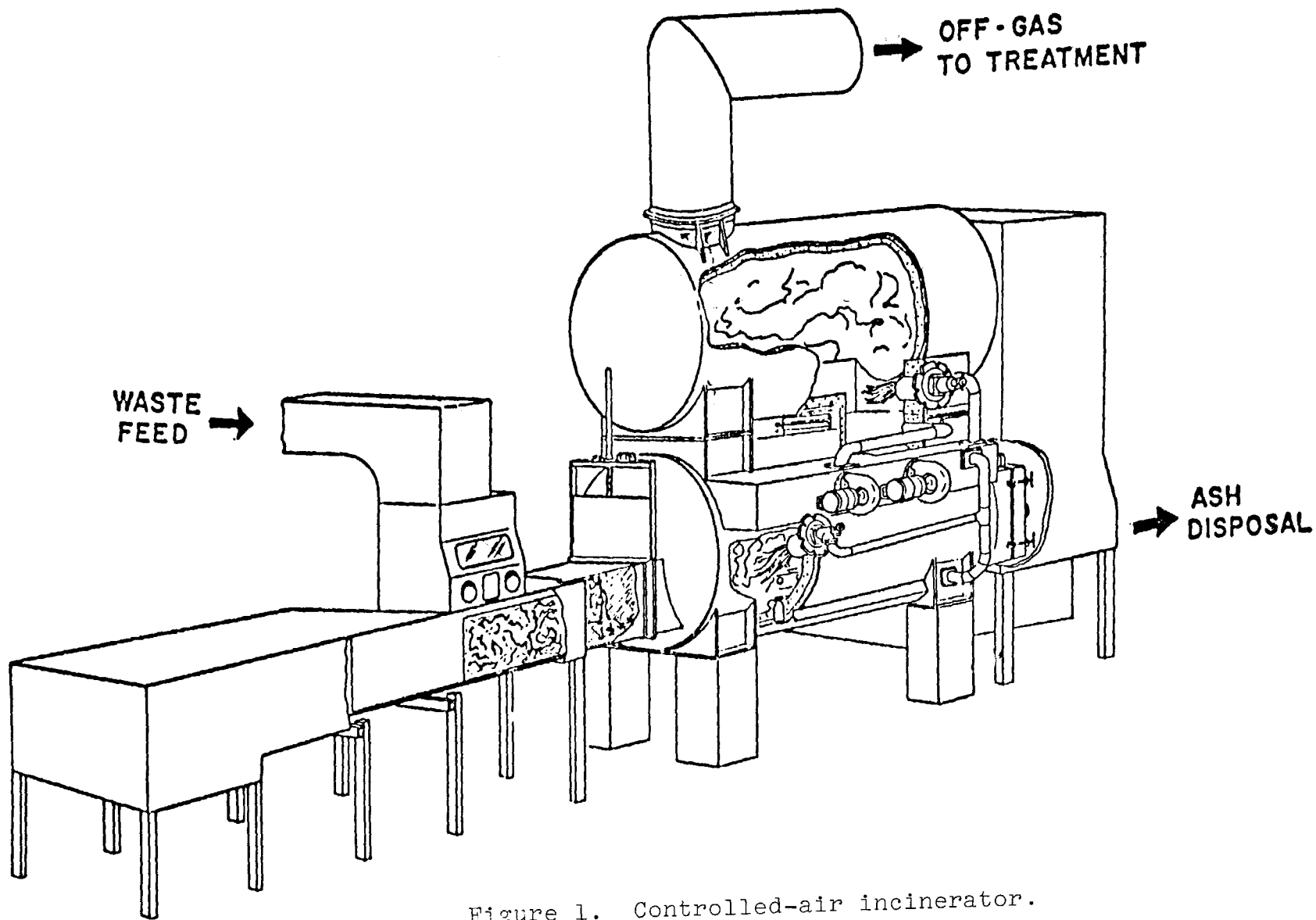


Figure 1. Controlled-air incinerator.

14th ERDA AIR CLEANING CONFERENCE

specification to meet the needs of the development program and radioactive service requirements.

1. Oversize doors were provided in each chamber to ensure ample access for remote removal of ash and partially burned charges.
2. Sight ports with protective blast gates were installed in each chamber to permit observation during operation.
3. Gas sampling ports were provided between the two chambers and at the exit from the upper chamber.
4. Dimensions of the ash dropout door were increased to the floor width to provide improved ash removal efficiency when the ram feeder is in use.

Auxiliary equipment purchased with the incinerator includes a ram feeder assembly, complete with safety interlocks and flashback suppression system, an ash drop-out port, and a modular vacuum ash-removal system.

The incinerator system has been modified to ensure containment of radioactive materials and to permit maintenance of mechanical process equipment. Modifications include: a combustion gas supply glovebox, an ash removal glovebox, full enclosure of the ram feeding system, and secondary seals for all flanges.

Particulate loadings of 1.25 and 1.46 g/std m³ at 12% CO₂ were demonstrated in EPA certification tests in a similar unit burning 225 kgs/hr of Public Health Service standard waste. (8) This loading is well below the Federal standard of 4.5 g/std m³ at 12% CO₂. Public Health Service standard waste is essentially a mixture of cellulose with very little plastics or rubber. Particulate loadings for the LASL incinerator off-gas are expected to be less than 2.3 g/std m³ at 12% CO₂ while burning LASL design basis waste. This low particulate loading will ease some of the operational requirements of the wet off-gas cleaning system.

Off-gas Cleaning Components

Effluents from the incinerator pass through the high efficiency off-gas cleanup train shown in Figure 2. High-temperature combustion gases are cooled to saturation conditions by multiple water sprays in the quench chamber. Particulate removal is primarily effected by the venturi scrubber. Mineral acids are removed in the packed column by counter-current contact with water. A condenser removes the bulk of water vapor from the scrubbed gas stream to reduce volumetric off-gas rates prior to filtration. Reheat of the gases downstream of the condenser prevents condensation of the HEPA filter media and the induced-draft fans. The quench chamber, venturi scrubber, and packed column scrubber were designed and fabricated by the John Zink Company, of fiberglass-reinforced plastic (FRP).

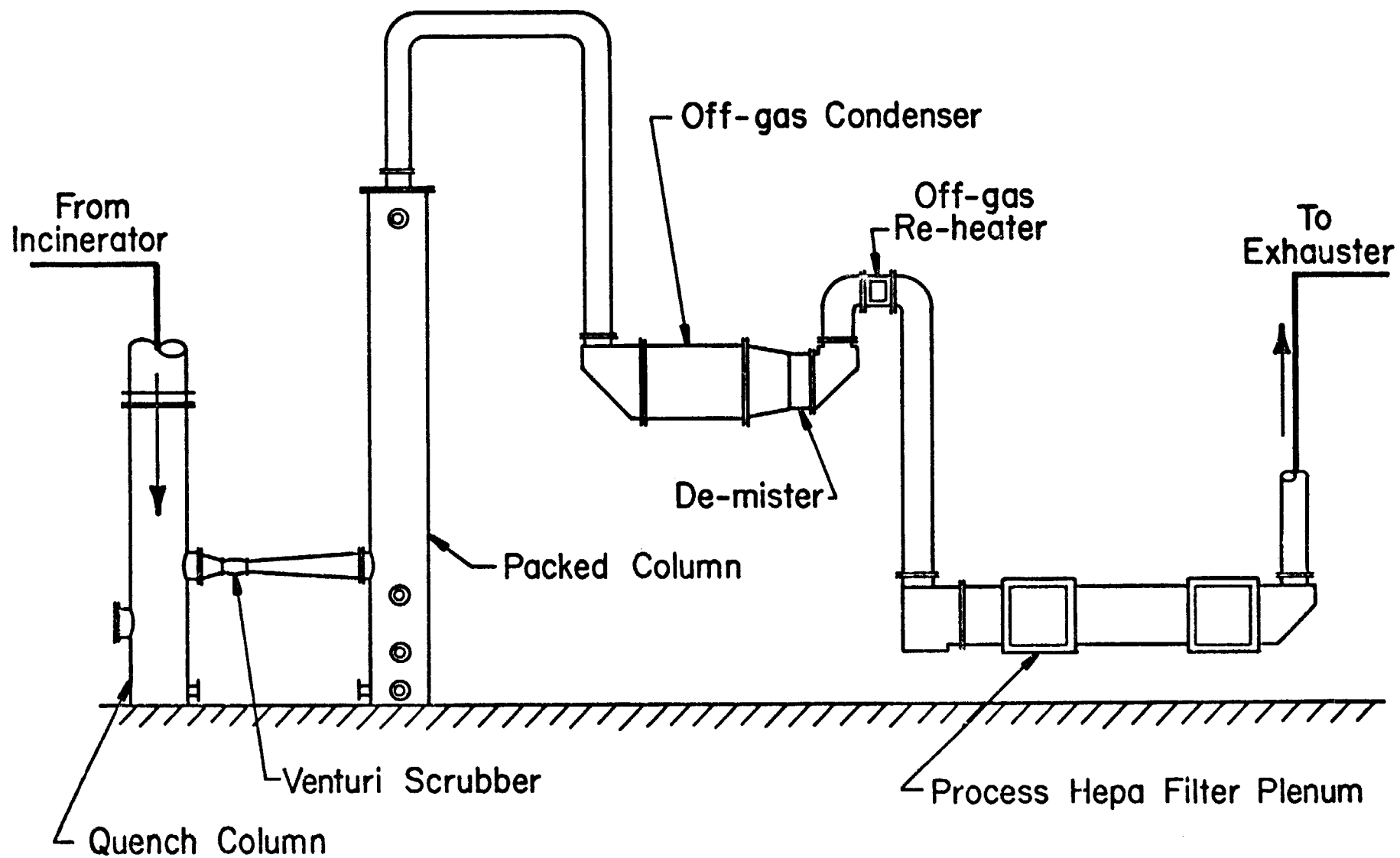


Figure 2. Off-gas cleaning system.

14th ERDA AIR CLEANING CONFERENCE

The quench column, shown in Figure 3, is designed to cool combustion gases from 1100°C to 75°C by direct evaporation of recycled scrubbing solution. The column is divided into a contacting section and a separator. Approximately eight times the amount of scrub solution required for evaporative cooling is injected into the contacting section. Excess solution collects in the separator.

The contacting section consists of a 50-cm i.d. by 150-cm FRP pipe, refractory lined with a weir, three spray lances, and an exit nozzle. The weir is designed to keep the refractory wall fully wetted. Three spray lances, located below the weir, are used to atomize scrub solution for better gas-liquid contact. The weir, spray lances, and nozzles were fabricated from Hastelloy C-276 for corrosion resistance. The 20-cm i.d. FRP exit nozzle serves to 1) re-entrain the quench solution that runs down the refractory wall; 2) promote gas-liquid contact by creating a high velocity, high turbulence area; and 3) aid in separation by imparting a high downward kinetic energy to the liquid droplets.

The separator is a disengaging section to de-entrain the quench liquid. The high inlet velocity caused by the contactor exit nozzle aids in separation. Since the venturi inlet is located at approximately the same level as the contactor exit nozzle, the gas flow must reverse direction. De-entrainment is caused by the combination of the gas-phase flow reversal and the high kinetic energy of the liquid drops. The variable-throat venturi scrubber is located between the quench column and packed column. It is designed to remove up to 99% by weight of the assumed particulate distribution shown in Table III.

Table III. Particulate size distribution.

<u>Particle Diameter, μm</u>	<u>WT. %</u>
Greater than 10	10
5-10	20
2-5	40
1-2	20
0.5-1	10
Specific Gravity	1.5
Particulate Loading	1.7 g/std m ³

The venturi has a 33-cm long converging cone and a 125-cm long diverging cone both constructed with FRP. The throat is a 10-cm diameter, Teflon-lined, clamp valve, which allows the pressure drop to be varied between 28 and 150-mm Hg. Scrub solution is injected through a nozzle located upstream of the throat.

The packed column scrubber, shown in Figure 4, is designed to reduce the gas-phase HCl from 24,400 ppm to a maximum of 25-ppm (99.9% removal) by counter-current contact with condensate and/or fresh water. Polypropylene supports hold a 300-cm deep polypropylene Pall ring packing. Condensate and fresh water is introduced at the top through a polypropylene distributor.

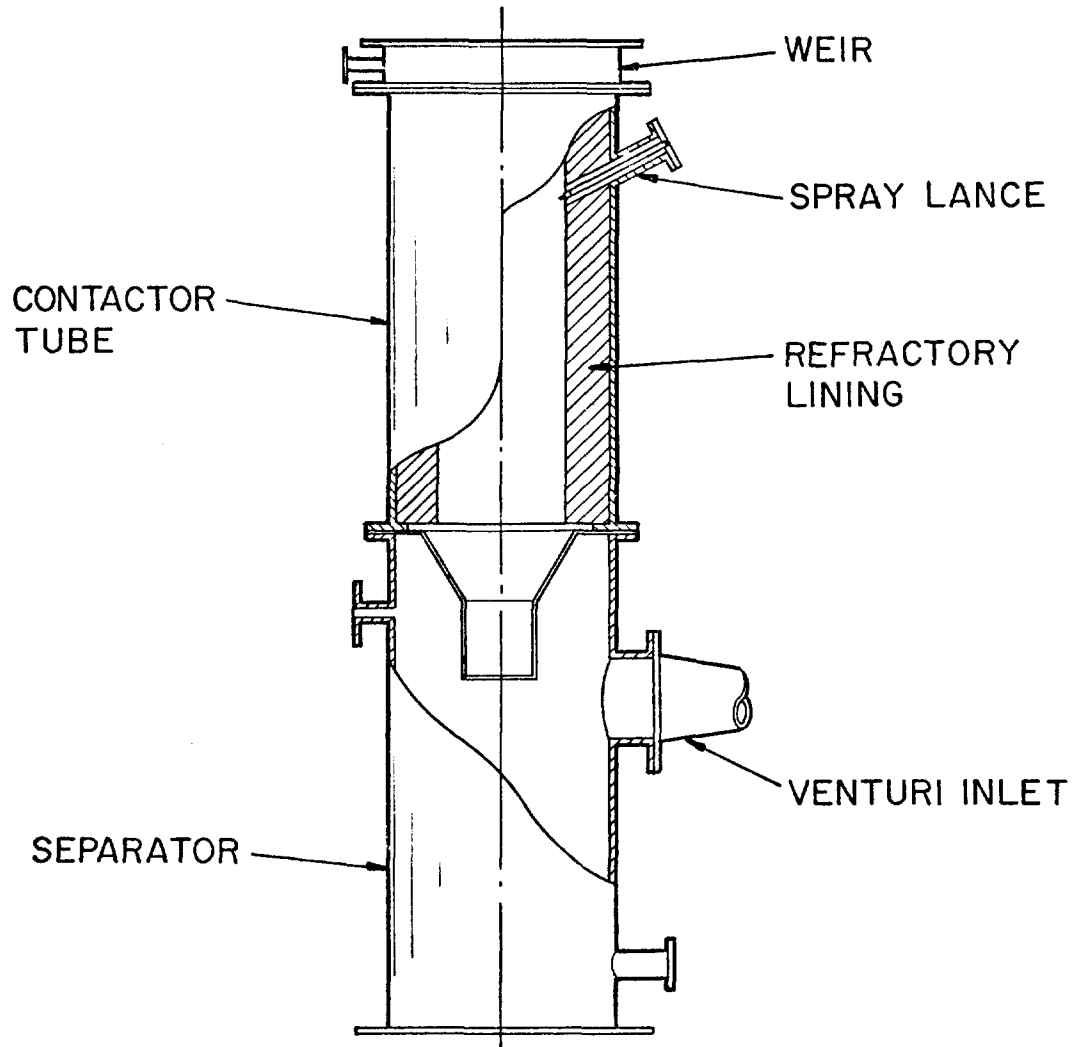


Figure 3. Quench column.

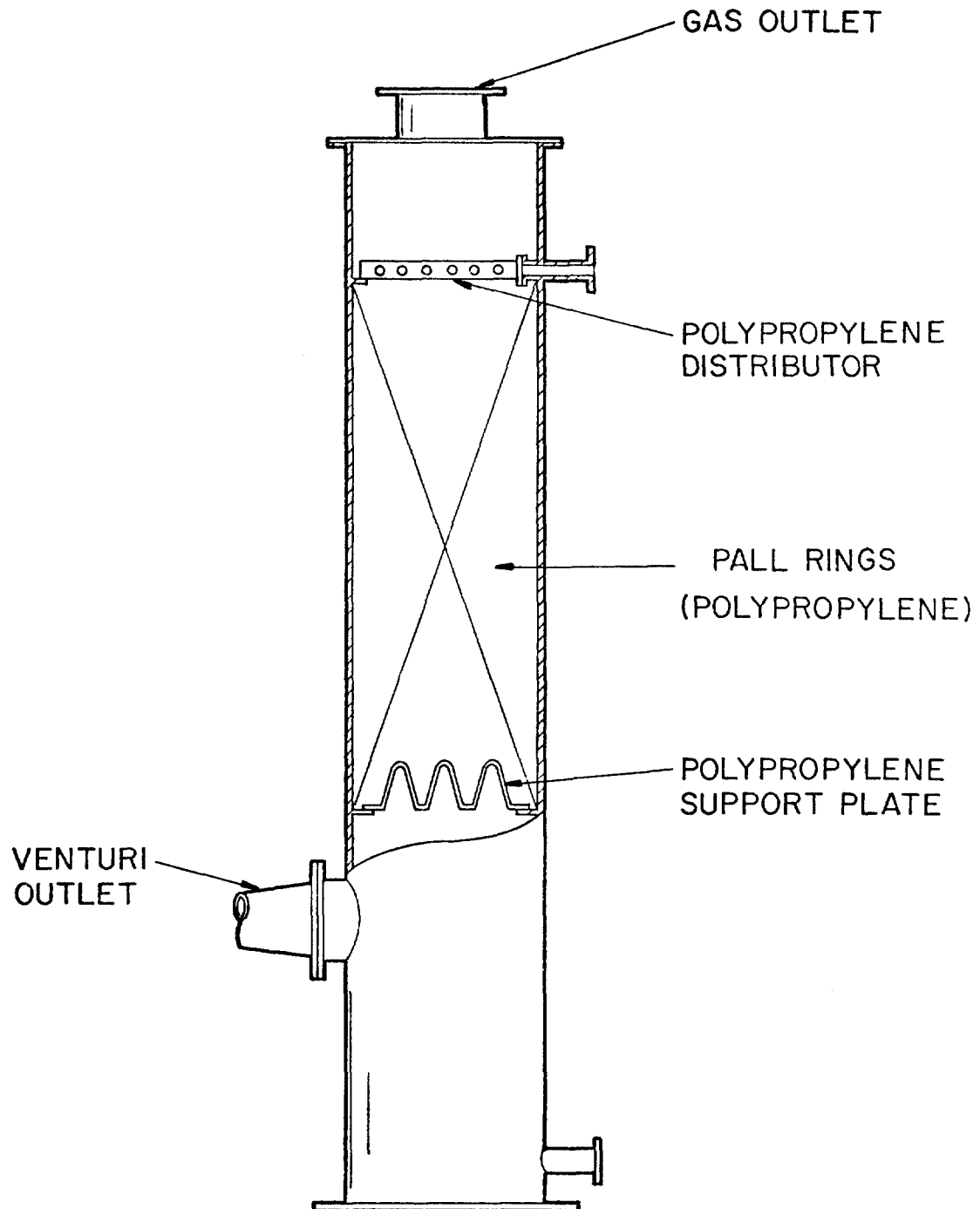


Figure 4. Packed column scrubber.

14th ERDA AIR CLEANING CONFERENCE

The condenser, mist eliminator, re-heater, and HEPA filter frames were purchased from commercial suppliers. However, as these components were not designed to withstand the 160-mm Hg (3psi) vacuum of this process, special enclosures were designed by the LASL to meet the pressure requirements. These enclosures were designed to provide access for maintenance or replacement of contaminated components as dictated by process test results.

The condenser lowers the off-gas temperature from 66°C to 49°C. As the stream is saturated before reaching the condenser, it is necessary to remove approximately 12 l/min of condensate. The condenser core contains two coils consisting of several rows of finned tubes, which are coated with a baked phenolic to prevent chloride corrosion. The total capacity of the two coils is 278 kW. The mist eliminator is located downstream from the condenser. The epoxy-fiberglass frame supports ABS plastic elements.

The re-heater superheats the off-gas approximately 12°C above the saturation temperature to assure that neither condensation nor attendant corrosion will occur downstream in the HEPA filters or off-gas blowers. It is a 12 element unit with a 12 kW capacity. The heater housing is located above the centerlines of the condenser/mist eliminator module and the HEPA filter module to prevent radiant heating of the adjacent modules.

Redundant HEPA filtration is provided for final removal of particulates. The filter module houses two frames in series. The first frame uses a 122 X 61 X 15-cm prefilter and two 61 X 61 X 29-cm HEPA filters. The second frame is similar, but does not have prefilter provisions. Both frames are rated for 56.6 m³/min at 1.9 mm-Hg, and are supplied with bag-out doors. The support module is fitted with hatches to access the bag-out doors and with in-place dioctylphthalate (DOP) filter testing ports. Since there is little possibility of condensate reaching the HEPA filter module, it is fabricated of carbon steel.

The induced-draft blower produces 423 mm-Hg static pressure 53.8 m³/min with a discharge pressure of 580 mm-Hg (elevation at LASL is approximately 3540 m). If blower performance proves adequate, an identical backup blower will be installed. Redundant blowers are required before contaminated waste can be introduced into the process.

Scrubbing Solution Recycle System

A scrubbing solution recycle system is used to minimize liquid blowdown from the aqueous gas-scrubbing system. The system uses full-flow liquid filters, a graphite heat exchanger, two evaporative cooling towers, a scrubbing solution receiver tank, a condensate receiver tank, and a caustic makeup tank. The solution drains from the bottom of the quench column to the packed column. Solution from the packed column sump is pumped through a full-flow filter and heat exchanger to the scrubbing solution receiver tank, where it is stirred to suspend small particulate that is not removed by the full-flow filter. The scrubbing solution is then pumped from the tank to the venturi and quench column. Solution returning to the weir is

filtered a second time to remove a smaller size fraction of particulates.

The blowdown rate from the 2600 l fiberglass scrubbing solution receiver tank is controlled by level and specific gravity. If the specific gravity of the scrubbing solution exceeds a specified value (currently set at 1.05), or if the tank level exceeds 80%, the blowdown rate is increased. Neutralized blowdown is sent to the LASL liquid waste treatment plant for cleanup.

Condensate from the condenser/mist eliminator module drains into a 750-l stainless-steel condensate receiver tank. The level in this tank is maintained at 80% by the addition of fresh water. This solution, being low in acid content, is pumped to the top of the packed column scrubber at a determined rate.

To control the scrubbing solution acidity, 20% caustic solution is added just upstream of the packed column sump pump. The addition rate is controlled by a pH sensor on the outlet of the scrubbing solution receiver tank. The caustic solution is held in a 850-l stainless-steel tank.

Full-flow filters were obtained for removal of suspended particulates. The fluorocarbon-coated housings use polypropylene cartridge-type filters and are enclosed in a glovebox to control contamination during filter changes. The cartridges are bagged-out and incinerated. Cold testing will determine the cartridge porosity requirements for each stream.

The scrubbing solution heat exchanger, a shell and tube model with graphite tubes, is designed to cool solution from 82°C to 49°C. The process (tube) side is operated at least 260 mm-Hg below the coolant side to guarantee in-leakage. Coolant is circulated through two ABS plastic evaporative towers.

IV. Future Plans

Start-up of the controlled-air incineration process will occur in two distinct stages: nonradioactive operations and radioactive operations. Testing of the primary system components with nonradioactive waste is scheduled to begin in October 1976. Objectives of these initial experiments will be to identify specific process design and component deficiencies. The addition, substitution, or modification of components will be greatly facilitated by the complete absence of contamination during these initial tests. Following attainment of satisfactory nonradioactive process performance, final provisions for transuranic containment and process ventilation will be completed in preparation for the introduction of radioactive wastes.

Testing of the process train with transuranic-contaminated wastes is presently scheduled for mid-1977. Challenge-level, i.e., ~ 10 -nCi/g wastes, will be used initially to assess the integrity of the containment systems and adequacy of the process enclosure ventilation system. Contamination levels in the charged wastes will gradually be increased to determine isotope distribution within the system. Major emphasis in the evaluation of controlled-air incin-

14th ERDA AIR CLEANING CONFERENCE

eration will be in determining the effectiveness and reliability of each system component. Because this system relies heavily on existing, proven technology, development efforts will be limited to identified deficiencies related to the adaptation to radioactive service. Materials and design reliability, as well as containment adequacy, will receive primary attention. One exception to this approach is the scrub solution blowdown evaporator. No clear cut system has yet been identified for evaporation-to-dryness of this liquid effluent. Development efforts in this area will be toward reducing all process effluents to solid form.

Program output for this initial waste treatment process will contain design specifications and recommended operating procedures for the system essentially as described. Basic design modifications, e.g. a non-aqueous off-gas system, or a radically different incinerator configuration will be reserved for future development efforts beyond completion of this initial study.

14th ERDA AIR CLEANING CONFERENCE

References

1. General Manager's Task Force, "Incineration of radioactive solid wastes," USAEC report WASH-1168 (August 1970).
2. "Transuranic solid waste management programs, July-December 1974," Los Alamos Scientific Laboratory Report LA-6100-PR (October 1975).
3. "Treatment development facility, conceptual design report," Los Alamos Scientific Laboratory Report LASL-ENG-9-RP-54 (September 1973).
4. D. F. Jones, L. R. Cowder, E. R. Martin, "Computerized low-level waste assay systems, Operational Manual," Los Alamos Scientific Laboratory Report LA-2602-M (February 1976).
5. "AS&E micro-dose x-ray inspection system (model 222) for narcotics, weapons, and contraband detection," American Science and Engineering, Inc., Report ASE-3490 (April 1974).
6. R. A. Hildner, L. C. Borduin, W. E. Draper, and C. L. Warner, "Transuranic solid waste treatment studies at Los Alamos," Proc. 23rd Conf. on Remote System Technology, San Francisco, 1975, pp. 279-277.
7. "Transuranic waste research and development program," Los Alamos Scientific Laboratory Report LA-5281-MS (May 1973).
8. "Specification for incinerator testing at federal facilities," U. S. Dept. of Health, Education, and Welfare, Public Health Service, Bureau of Disease Prevention and Environmental Control, National Center for Air Pollution Control, Abatement Program, Durham, North Carolina.

DISCUSSION

GRADY: The first question concerns the pressure through the unit involving the high energy Venturi and columns. Is your ΔP around 50 or 60 inches of water?

NEULS: The maximum is a little higher than that. It is designed for approximately 3 psi. The variable-throat Venturi varies between 15 and 80 inches of water ΔP .

GRADY: The second question refers to the treatment of waste prior to entering the incinerator. Do you have to shred it or sort it? What handling procedures are required?

NEULS: By the nature of the RAM feeder, it is not required to shred the waste. However, we do go through a feed preparation glovebox line that includes an assay and an x-ray system. The x-ray system spots things like bottles and metal parts. Most of the waste boxes are incinerated without being opened. The glovebox is described in other references that are given in the paper.

C. R. ALLEN: Can you tell me what mass of material is introduced with each cycle of the ram feeding device?

NEULS: The mass per cycle is a variable. It will be determined as part of the development of operating procedures. Obviously, a feed rate of 45 kg/hr is the only parameter we are trying to meet. The feed cycle time could vary over a substantial range.

ORTH: You mentioned that you were going to try to contain it sometime later. Containment isn't an easy thing. Have you designed this thing from the beginning to worry about containment or have you already completed design on how you will contain it?

NEULS: There are two answers. First, this is a process that was assembled from commercially available equipment. Therefore, the design was not made for the specific process to be contained. However, we have nearly completed the design for all the gloveboxes and containment equipment that is required. To simplify checking out the components during nonradioactive testing, we are not going to complete containment until after we are satisfied with the performance.

FREEMAN: How do you plan to repair or replace the contaminated refractory?

NEULS: First, we don't expect to repair or replace it. Refractories have come a long way in the last ten years. We expect that, by using proper operating procedures for the refractory, there will be little problem. It is industry standard to use refractory. The refractory lifetime should be approximately 5 years, or longer than the development program. This particular unit, I might add, will be dismantled and buried. It will not be used for production.

14th ERDA AIR CLEANING CONFERENCE

AN INCINERATOR FOR POWER REACTOR
LOW-LEVEL RADIOACTIVE WASTE

T.S. Drolet and J.A. Sovka
Ontario Hydro
Toronto, Canada

1.0 Introduction

Ontario is presently operating 2200 MWe of CANDU* reactors (Table 1). A further 11000 MWe of CANDU is under design or construction.

Table 1

Ontario Hydro Nuclear Generating Sites

Name	Size	Number of Units	In Service Date	Location
Operating				
1. Nuclear Power Demonstration (NPD)	20 MWe	1 x 20	1962	Ottawa River
2. Douglas Point (DPGS)	200 MWe	1 x 200	1968	Bruce Site
3. Pickering 'A' (PGS 'A')	2000 MWe	4 x 500	1970	Pickering 18 Miles east of Toronto
Under Construction				
4. Bruce 'A' (BGS 'A')	3000 MWe	4 x 750	1976 (1st Unit)	Bruce Site
5. Pickering 'B' (PGS 'B')	2000 MWe	4 x 500	1980 (1st Unit)	Pickering
Under Design				
6. Bruce 'B' (BGS 'B')	3000 MWe	4 x 750	1983	Bruce Site
7. Darlington 'A'	3400 MWe	4 x 850	1984	60 Miles east of Toronto

By 1980, the nuclear portion of the Ontario Hydro system will be producing 2000 m³/yr of low-level combustible waste. To date, low and medium level radioactive waste produced from Ontario Hydro's Nuclear Stations has been stored in sophisticated, capital intensive, engineered structures. There is, therefore, an economic incentive to reduce the volume of this waste to a minimum as well as the safety criteria of preparing waste for storage in a non-combustible

*CANDU - Canadian Deuterium Uranium: Heavy Water Moderated and Cooled Pressurized Reactors

14th ERDA AIR CLEANING CONFERENCE

form for the long term. The technique chosen for volume reduction of combustible waste is incineration by a propane-fired unit. Non-combustible material (relatively high activity, metal content, etc) will be compacted into 200 litre drums (Fig 10). The Waste Volume Reduction Facility is located at the Bruce Nuclear Power Development Site on Lake Huron.

Figure 1, 2 - shows the building and its environment.
 Figure 3 - shows the material flow in the radioactive portion of the WVRF.

2.0 Waste Description

2.1 Physical Composition

In order to segregate combustible waste from non-combustible waste a program of segregation of wastes at the producing nuclear stations has been instituted prior to in-service of the incinerator. The segregated combustible polyethylene bags of waste will contain: disposable coveralls, cotton coveralls, cotton and rubber gloves, cotton towels, rags, cardboard, paper, wood pieces, plastics (suits, bottles, syringes), vermiculites, mopheads, floor cleaning materials and other miscellaneous items. The use of clear PE bags allow a final visual inspection prior to loading. Metal and activity detectors complete the pre-incinerator inspection program. Other physical and chemical waste factors include:

Wt % Moisture	5 - 20
Wt % Ash	10
Wt % Combustible	90
Average Density lb/ft ³	7 - 9
Average Btu/lb	7500 - 8500
Wt % Plastics	10 - 20
Wt % Halogenated	1/2% as PVC
Average Bag volume	1-1/2 - 2 ft ³
Average bag weight	12 lb

2.2 Anticipated Waste Radioactivity Composition

Sampling of waste bags collected over several years have shown the average radiation field at contact to be approximately 2 mR/hr. Approximately 5% of bags have fields in the 5 - 20 mR/hr range.

Table 2 gives the relative number of times various radionuclides have appeared in bags of waste as measured at the nuclear stations.

Table 2

Relative Radionuclide Appearance in Waste

90% of bags	70% of bags	30% of bags	<10% of bags
Cs-134	Ru-106	Co-58	Sb-124 Ba-140
Cs-137	Mn-54	Cr-51	Cs-136 Mo-99
Ce-144	Zn-65	La-140	Cs-138 I-132
Nb-95	Fe-59	I-131	No-24 I-134
Co-60	Ru-103	Xe-133	Np-239 Rb-88
	Ce-141	Kr-88	Np-238

Table 3 gives the relative isotopic composition of a typical bag of solid waste.

Table 3

Relative Isotopic Composition of a
Typical Bag of Solid Waste

Isotope	Half Life (days)	Percent of Total Activity due to Isotope
Co-60	1920	19
Cs-137	10950	17
Cs-134	730	6.7
Zr, Nb-95	66	17
Ce-144	284	17
Ce-141	33	2.3
Fe-59	45	0.8
Zn-65	245	3.4
Mn-54	300	0.5
Ru-106	368	12
Ru-103	40	1.6
I-131	8	0.4
Cr-51	28	1.7
Co-58	71	0.1
La-140	12	0.1
Total		99.6

There will be a normal delay period between waste collection at the stations to actual incinerator burn of 1 - 2 months.

3.0 Incinerator Description

The Waste Volume Reduction Facility contains five (5) areas:

- (a) Administration Wing
- (b) Non Radioactive Waste Incinerator
- (c) Radioactive Waste Incinerator
- (d) Service Area
- (e) Ventilation Equipment Area

Area (c) will be the subject of this paper.

Figures 4 and 5 show the equipment layout and Incinerator Schematic.

3.1 Process Description

The system is based on batch type, controlled air incineration with secondary clean up equipment to reduce radioactivity release to the atmosphere.

The controlled air concept in incineration starves the air quantity in the 310 stainless steel primary chamber to obtain a partially oxidized effluent (800 to 1100°F) consisting of CO, CO₂, H₂, N₂, and Water Vapour. This is accomplished by limiting the air

flow to 30% of the air required for complete oxidization. This design with a gentle air flow pyrolyzes the waste and leaves most of the ash (which has completely oxidized by the end of the cycle) in the primary chamber.

With the ignition of the waste, the pyrolysis reaction proceeds gradually throughout the waste bed. First, the moisture and volatile matter (partially oxidized) are driven from the waste, leaving the fixed carbon in the waste for complete oxidation in the latter stages of the burning cycle.

The greatest volume change occurs in the initial stages when the volatiles are being driven off and partially oxidized. Half way through the cycle a 75% volume reduction has occurred with general waste as described above. The balance of the burn cycle is used to oxidize the fixed carbon content of the waste leaving radioactive ash.

Waste active oil can be burned in this facility. It will be injected into the unit approximately 4 hours into the cycle after the waste level has receded several feet below the liquid waste injection point. The waste oil is injected for three hours at a rate of 5 Imp gal/hr. The waste is injected as droplets (not finely atomized) through the starved air atmosphere to the hot waste bed. The liquid quickly vaporizes and then the fixed carbon residue is oxidized along with the fixed carbon in the solid waste. This disposal method is different to the normal concept of burning liquid droplets in suspension. An air purge is maintained on the liquid waste nozzle (when liquid is not being injected) to keep the nozzle from plugging with residual oil or overheating.

The partially oxidized effluent with small amounts of particulate is completely burned in a stainless steel afterburner where additional air (with an excess of 100%) and fuel is introduced to complete the oxidization. The afterburner temperature is 1600 to 1800°F.

Controlled air burning with a proper afterburner produces an effluent with particulates in the range of .05 grains per standard cubic foot (110 ppb) in the afterburner exhaust. This is sufficient to meet most environmental regulations considering only particulate emission. However, the particulates from radioactive waste usually contain a level of radioactivity that warrants further clean up. Besides handling the normal refuse, the system can also handle 15 gallons of oil based liquid waste each cycle.

Due to the maximum operating temperature level for the fabric filters, the effluent from the afterburner is cooled to 400°F by a shell and tube air cooled heat exchanger. Then the gases proceed through a precoated baghouse for additional particulate clean-up, and then release via the stack to atmosphere.

3.2 Primary Incinerator Assembly

The primary chamber is a vertical cylindrical unit with a cone on the bottom. The unit is a double shell design with a stainless steel inner shell to prevent build up of radioactivity.

14th ERDA AIR CLEANING CONFERENCE

The area between the inner shell and outer shell provides an annulus through which air flow maintains the inner shell temperature above the dew point of the controlled oxidation products and below serious scaling and oxidation temperature of the inner shell.

The cone section at the bottom is replaceable.

The waste (2270 kg/5000 lbs) is loaded directly into the 500 cu ft primary chamber of the incinerator. The unit is only loaded when the incinerator is not burning. During the burning of the waste the loading chamber is under negative pressure direct to the baghouse. During loading the incinerator is under negative pressure. The top loading door is not opened until the sliding gate valve (used to dump the waste into the incinerator) is closed.

After loading, the waste is ignited with three burners equally spaced around the circumference of the primary chamber. Three burners are used to equalize the heat distribution which causes expansion on the inner shell.

The air for the primary incinerator is supplied through the bottom dump plate through nozzles which are self cleaning when the bottom dump plate (which also acts as a valve) is rotated 90°. This plate is also used to dump the ashes into a hopper below the incinerator.

The waste is gravity loaded and the ash gravity dumped.

Below the bottom dump plate and above the ash hopper, there is a sliding gate valve which remains closed except when dumping the ashes into the ash hopper after the cool down portion of the cycle.

The seals on the top sliding gate valve can be replaced from the top of the valve, and the seals on the bottom sliding gate valve can be replaced from the bottom of the valve.

3.3 Afterburner

The afterburner section is designed to ignite and burn the partially oxidized effluent from the primary chamber at a temperature of 1800°F for 1/2 second. The auxiliary burner is sized for 1×10^6 Btu/hr required at start-up and is modulated by a temperature controller to maintain the 1800°F outlet temperature. Normally the auxiliary burner will be running at approximately 200,000 Btu/hr. Additional oxygen is introduced into the afterburner to complete the combustion of the waste. The secondary air comes from the annulus air exhaust from the primary chamber.

3.4 Cooling Heat Exchanger

Due to the temperature limitations of the cloth filter in the baghouse for off gas clean-up a heat exchanger is required to reduce the 1800°F effluent from the afterburner to 400°F. The temperature of 400°F is selected to keep the effluent temperature above the dew temperature.

14th ERDA AIR CLEANING CONFERENCE

The heat exchanger is a shell and tube design with the effluent being cooled by forced ambient air. The air exhaust from the heat exchanger is directed through the system stack, when it is not used for heating the primary chamber inner shell. The tubes and inlet tube sheet are 304L SS because of the high effluent inlet temperature.

3.5 Baghouse Filter

The baghouse filter removes particulate matter from the exhaust gases at better than 99% efficiency by weight according to the American Filter Institute (AFI) weight method. (The efficiency of the filter represents the amount by weight that the filter removes).

The filter media is Nomex which has a temperature rating of 232°C (450°F). There are 96 bags in the baghouse, each bag being 0.15 m (6 in) in diameter, and 3.2 m (10.5 ft) in effective length. Normally the bag life for this application is approximately 5 years.

The filter is initially precoated with 91 kg (200 lb) of short asbestos fibres to achieve a high initial efficiency. The efficiency improves as the fly ash accumulates on the bags. The initial pressure drop is about 0.05 m (2 in) of water. At 0.13 m (5 in) of water pressure drop, the bags are to be shaken to remove the accumulated ash. At this time the bags must again be precoated before putting the filter back into service. The estimated time between shaking must be determined by operating experience, but is estimated to be approximately one year.

The failure of one filter bag could reduce the overall efficiency. Any failures may be detected by visual inspection. Significant leakage would be detected by the stack radioactivity monitor.

3.6 Induced Draft Fan and Stack

An induced draft fan is required by the system to maintain a slight negative pressure at the primary chamber outlet. This is controlled by a pressure indicating controller positioning an inlet damper on the induced fan which exhausts into a 75 foot carbon steel stack. The stack exhausts 25 feet above the top of the building.

3.7 Cycle

The incineration system operates on a timed sequence with safety interlocks to assure proper operation. The unit is operated essentially from a master control panel with the main flows, temperatures, pressures, pressure drops and valve positions tied into the interlock and the annunciator system. The main points of this cycle are:

- | | |
|---|-------------|
| 1. Waste Loading (Estimated) | 1 hr 0 min |
| 2. Pre-purge (after loading)
induced draft fan is started
-burner fans are on | 0 hr 12 min |

14th ERDA AIR CLEANING CONFERENCE

Table 5

Maximum Permissible Concentrations in Air of Biologically Significant Radionuclides
Maximum Permissible Concentration
MPC_a (Ci/m³)

Radionuclide	External Irradiation	Inhalation	Food Chain (Milk)
(1) Noble Gases	6.4×10^{-8} γ Ci-MeV/m ³	NA	NA
(2) I-131		3×10^{-11} *	6×10^{-13}
(3) H-3		3×10^{-7}	NA***
(4) Particulates:			
Cs-137		1.5×10^{-9}	5×10^{-11}
Cs-134		1×10^{-9}	1.5×10^{-11}
Sr-90		4×10^{-11}	1.5×10^{-12}
Sr-89		2×10^{-10}	1.5×10^{-11}
Co-60		9×10^{-11}	NA
Ru-106		4×10^{-11}	NA
Unidentified Particulates**	4×10^{-11}	1.5×10^{-12}	

* Assumes 50% of the dose is from the shorter-lived radioiodines accompanying I-131.

** The lowest MPC_a value under "particulates" is used as the MPC_a for unidentified particulates. Measurement of unidentified particulates activity in the stack effluent will be based on the counting efficiency for Cs-137, which approximates closely the counting efficiency of a typical radionuclide mixture.

***Tritium is not considered to be a food chain hazard.

Table 6

Derived Release Limits for Both Direct and Indirect Exposure Paths

Radionuclide	Indirect Intake Path (Food Chain)		Direct Exposure Path (Inhalation or External Irradiation)	
	MPC _a (Ci/m ³)	Release limit (Ci/7 days)	MPC _a (Ci/m ³)	Release limit (Ci/7 days)
I-131	6×10^{-13}	0.72	3×10^{-11}	14
H-3	—	—	3×10^{-7}	1.4×10^5
Particulates:				
Cs-137	5×10^{-11}	61	1.5×10^{-9}	700
Cs-134	1.5×10^{-11}	18	1×10^{-9}	470
Sr-90	1.5×10^{-12}	1.8	4×10^{-11}	19
Sr-89	1.5×10^{-11}	18	2×10^{-10}	93
Co-60	—	—	9×10^{-11}	42
Ru-106	—	—	4×10^{-11}	19
Unidentified particulates	1.5×10^{-12}	1.8	4×10^{-11}	19

14th ERDA AIR CLEANING CONFERENCE

3. Afterburner Warm-up -start afterburner in secondary chamber	0 hr 30 min
4. Burn Cycle -ignition burners start -afterburner operates on modulating temperature control	11 hr 0 min
5. Cooldown Cycle -all burners are shut off -induced draft fan continues to run	5 hr 0 min
6. Ash Removal (Estimated) -induced draft fan is operated during ash removal to avoid spread of ash	2 hr 0 min
Total Incinerator Cycle Time	19 hr 42 min

4.0 Dose Limits to the Public

The annual dose limits for individual members of the public, as recommended by the ICRP and endorsed by the Atomic Energy Control Board in Canada, are summarized in Table 4. In addition, the AECB also limits the population exposure to personnel in the surrounding area to the BNPD site by stipulating the following limits:

- 10^4 man-rem per year whole-body exposure
- 10^4 man-rem per year thyroid exposure

The dose integration must extend over all areas, outside of the site exclusion boundary, in which the individual dose could exceed 1% of the dose at the boundary. The annual dose limits are maximum limits which must not be exceeded.

The dose to the individual member of the public at the boundary, and not the integrated population dose, limits the releases of radionuclides from the BNPD Radioactive Waste Operations Site No 2.

Table 4
Dose Limits for Members of the Public

Organs	Annual Dose Limit
Whole-body Gonads Red bon-marrow	0.5 rem
Skin, bone	3.0 rem
Thyroid	3.0 rem (Adults) 1.5 rem (Children up to age 16 years)
Other single organs or tissues	1.5 rem
Extremities	7.5 rem

5.0 Derived Release Limits for Airborne Effluents

The maximum permissible concentrations in air (MPCa) of the biologically significant radionuclides for continuous exposure of the public have been calculated (1) and are summarized in Table 5. The derived release limits for the continuous release of the specific radionuclides are calculated using the following relationship:

$$\text{Continuous release rate, } Q \text{ (Ci/sec)} = \frac{\text{MPCa}}{K_a}$$

where K_a is the average or weighted mean dilution factor for continuous releases reported by Bryant (2) and is a function of distance from the source and effective height of release.

The incinerator will be the only potential source of radioactive airborne effluents from the waste operations site under normal operating conditions. The height of the stack will be approximately 15 m. Since this will not be 2-1/2 times the height of adjacent buildings, the effective height of release will be less than 15 m due to downdraught. An effective stack height of 10 m is assumed. This is a conservative value as additional lift will result from the buoyancy of the hot gases and the velocity of discharge from the stack.

5.1 Continuous Releases of Specific Radionuclides

A dilution factor, K_a , of $1.3 \times 10^{-6} \text{ sec/m}^3$ is used for a distance of 1 km from the point of release for direct exposure by inhalation. The combustible materials ashed in the incinerator will not contain significant quantities of noble gases so that release limits for this group of radionuclides are not calculated. Since the nearest grazing land is about 2 km from the site, a dilution factor of $5 \times 10^{-7} \text{ sec/m}^3$ for the indirect exposure path is used.

The derived release limits for both the direct and indirect exposure paths for the various radionuclides are listed in Table 6. The limits are stated in units of Curies per seven day period. This approach has been adopted to accommodate transient releases of a somewhat higher level than those normally envisaged but still acceptable from the basic dose limitation standpoint.

The derived release limits for the airborne releases from the radioactive waste operations site are summarized in Table 7 with the most restrictive limit of the direct and indirect exposure paths for each radionuclide being applied.

14th ERDA AIR CLEANING CONFERENCE

Table 7

**Derived Release Limits for
Airborne Effluents from the BNPD
Waste Operations Site**

Radionuclide	Release Limit (Ci/7 Days)
I-131	0.72
H-3	1.4×10^5
Particulates:	
Cs-137	61
Cs-134	18
Sr-90	1.8
Sr-89	18
Co-60	42
Ru-106	19
Unidentified Particulates	1.8

5.2 Continuous Releases of More Than One Radionuclide

The calculated permissible releases of single radionuclides may be modified in practice to take into account releases of several radionuclides. It is necessary to ensure the dose limit for any organ is not exceeded. This requirement will normally be realized if the following summations are observed:

$$\frac{Q(\text{Sr-89})}{18} + \frac{Q(\text{Sr-90})}{1.8} \leq 1 \quad (\text{Critical organ - bone})$$

and,

$$\frac{Q(\text{H-3})}{1.4 \times 10^5} + \frac{Q(\text{Cs-137})}{61} + \frac{Q(\text{Cs-134})}{18} \leq 1 \quad (\text{Critical organ whole body})$$

where Q is the actual seven-day release of a radionuclide in Curies.

Operating procedures for the active incinerator will be established to ensure that the routine airborne releases, as measured by the stack monitoring, comply with the above summations.

5.3 Derived Release Limit: Design Target

In limiting the release of radioactivity from its nuclear sites to levels as low as practicable, Ontario Hydro has established a design target of 1% of the DRL limit (Table 7) per nuclear facility on a site.

6.0 Anticipated Releases from the Active Incinerator

From the measured relative mix of radionuclides listed in Section 2.2, it is anticipated that approximately 150 m Ci of mixed activated corrosion and fission products will be contained in one average batch load. Assuming a maximum particulate carryover of

14th ERDA AIR CLEANING CONFERENCE

0.2% to the baghouse with a further reduction of 98% by the baghouse filters then 6 μCi of mixed activity will be released per burn. With 5 burns per week, a total of 30 $\mu\text{Ci}/7$ days may be released up the stack.

The most restrictive DRL is for I^{131} . With a built in delay of at least 1 - 2 months, the quantity of I^{131} in the waste, as it is burned, is expected to be very low.

Using the 100% DRL for unidentified particulates (1.8Ci/7 days), the most restrictive category other than I^{131} , it is anticipated that releases could be in the order of:

$$\frac{30}{1.8} \times 10^{-6} \times 10^2 = \underline{0.0016\% \text{ DRL}}$$

References

- (1) "Basis for the Derived Limits for the Release of Radionuclides in Gaseous and Liquid Effluents from Ontario Hydro's Nuclear Stations", K.Y. Wong, Ontario Hydro, August 1974.
- (2) "Methods of Estimation of the Dispersion of Windborne Material and Data to Assist in their Application", P.M. Bryant, 1964.

Acknowledgement

The authors wish to thank all the Design, Health Physics and Operating Personnel in Ontario Hydro who helped to a great extent in supplying a large part of the information contained in this paper. Particular appreciation is extended to Messrs. G. Robb, D.A. Lee and C.J. Bromley of Ontario Hydro. The kind aid of Mr. C.E. Chase of Trecan Co Ltd (Incinerator Supplier) and Dr. D.H. Charlesworth of Chalk River Nuclear Laboratories is acknowledged.

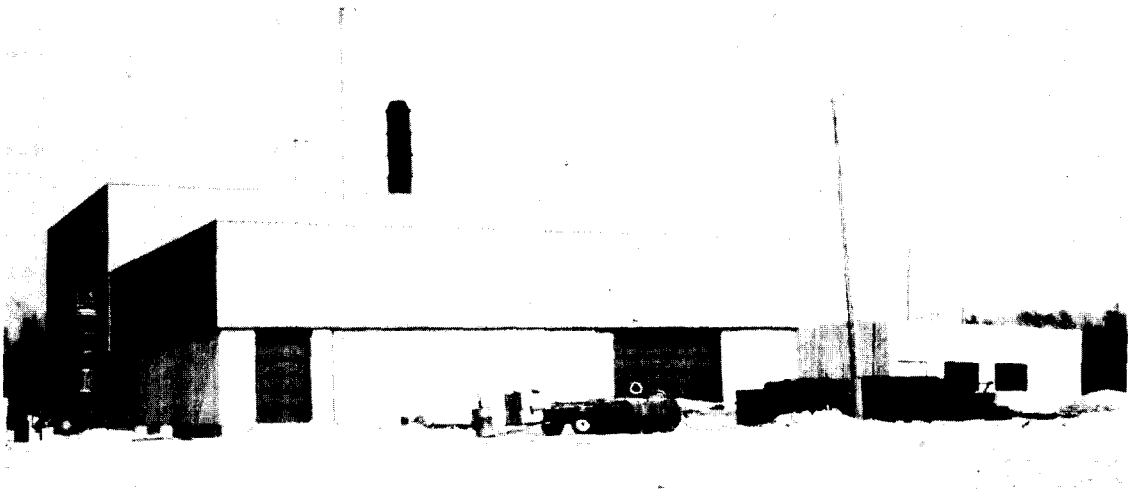


FIGURE 1 THE BNPDS RADIOACTIVE WASTE VOLUME REDUCTION FACILITY VIEWED FROM THE SOUTHWEST

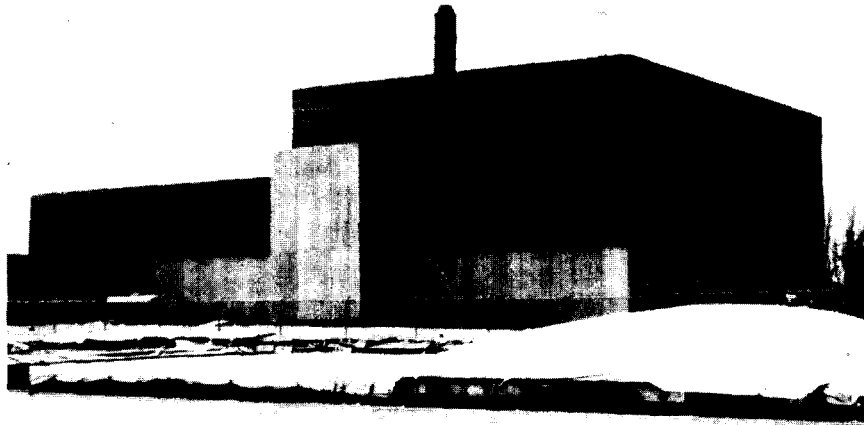


FIGURE 2 THE BNPDS RADIOACTIVE WASTE VOLUME REDUCTION FACILITY VIEWED FROM THE NORTHEAST

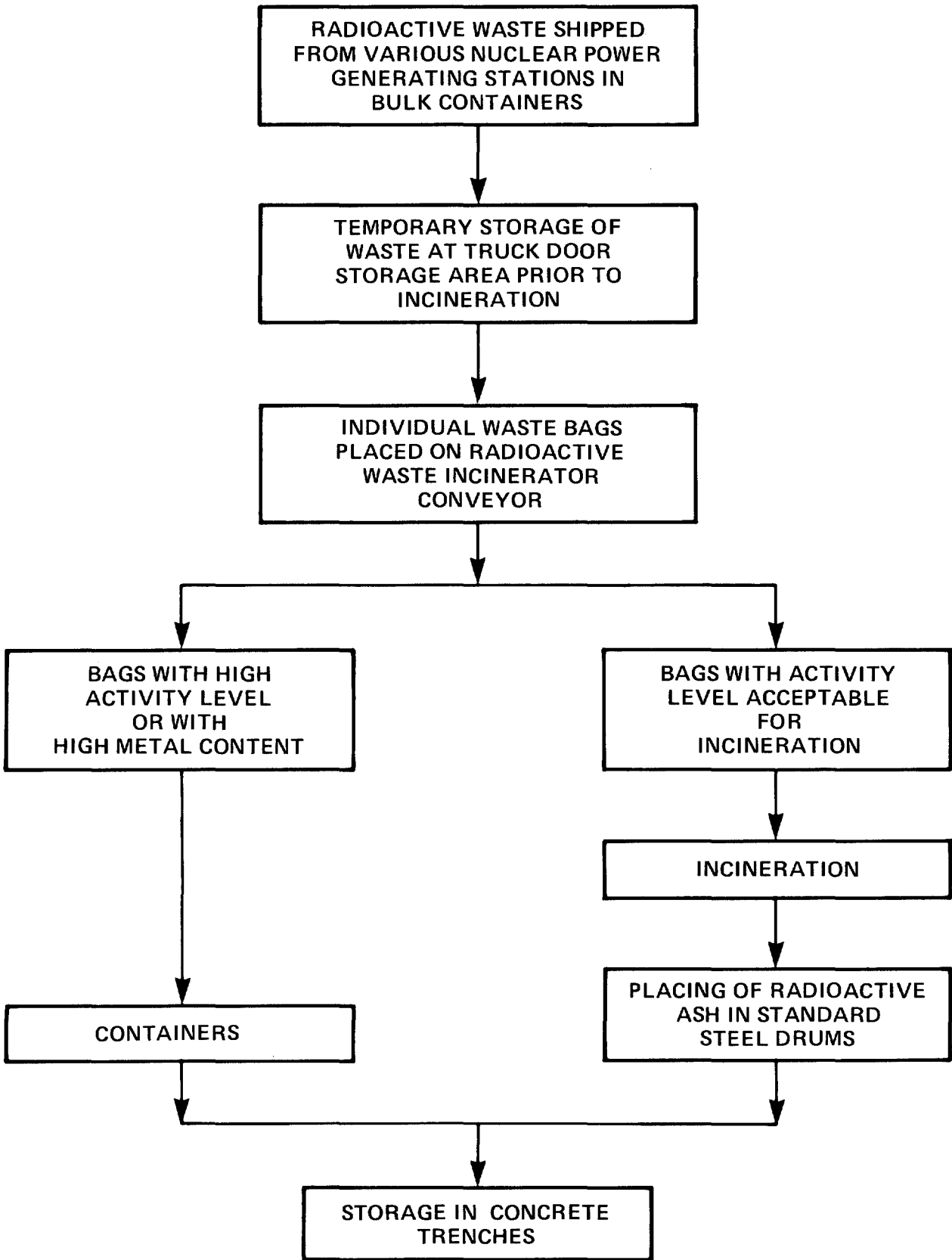


FIGURE 3 RADIOACTIVE WASTE PROCESS FLOW DIAGRAM

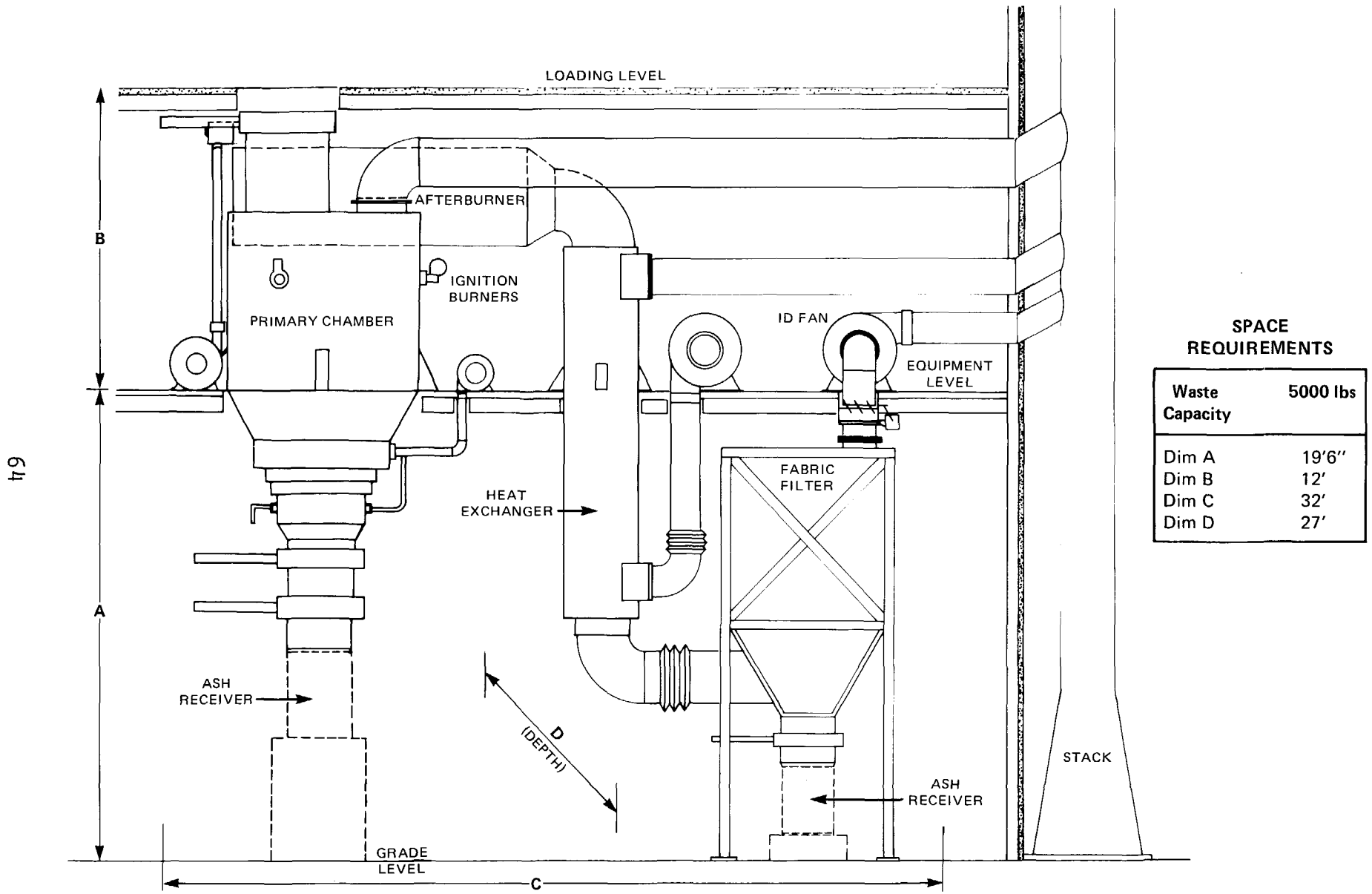


FIGURE 4 INCINERATOR EQUIPMENT LAYOUT

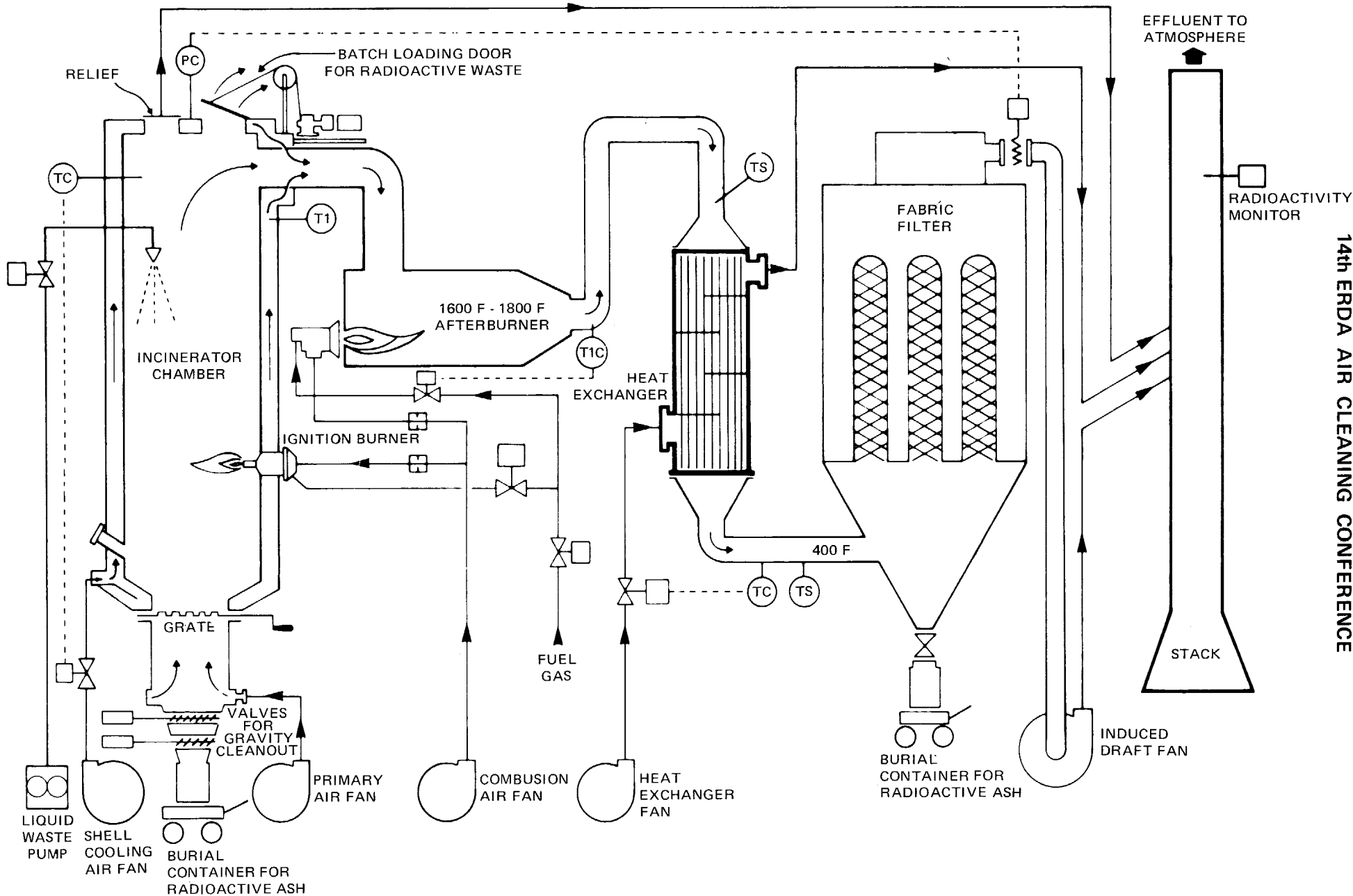


FIGURE 5 INCINERATOR SCHEMATIC

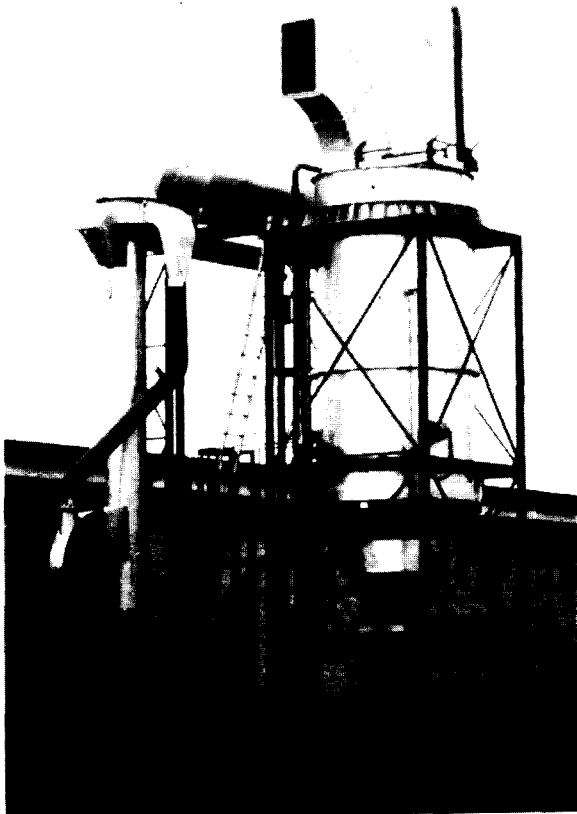


FIGURE 6 THE BNPDS RADIOACTIVE WASTE INCINERATOR SHOWING THE PRECONSTRUCTION ASSEMBLY

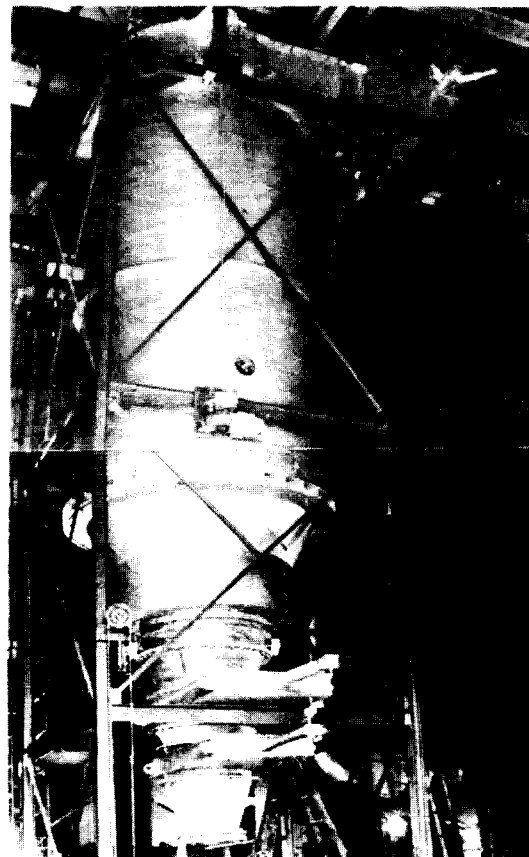


FIGURE 7 THE BNPDS RADIOACTIVE WASTE INCINERATOR DURING CONSTRUCTION

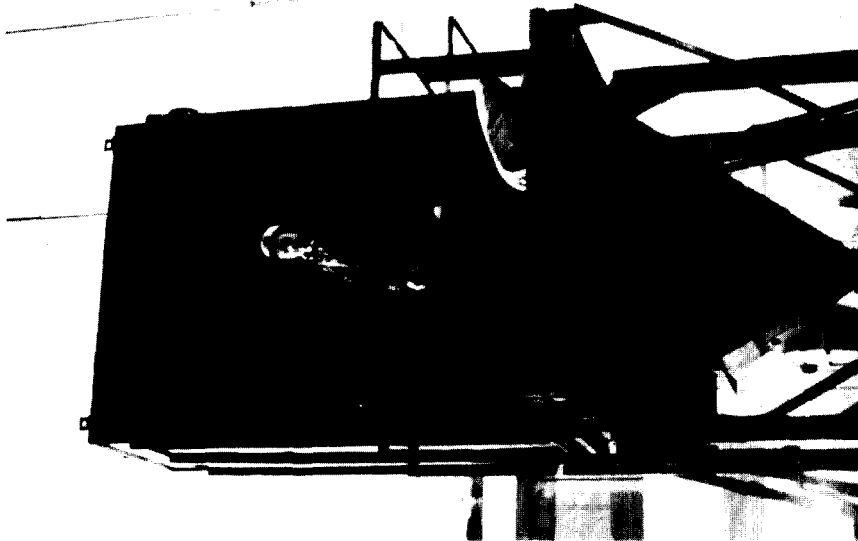


FIGURE 9 BAG HOUSE FILTER



FIGURE 8 THE BNPDS RADIOACTIVE WASTE
INCINERATOR EXHAUST GAS
FILTER BAG-HOUSE

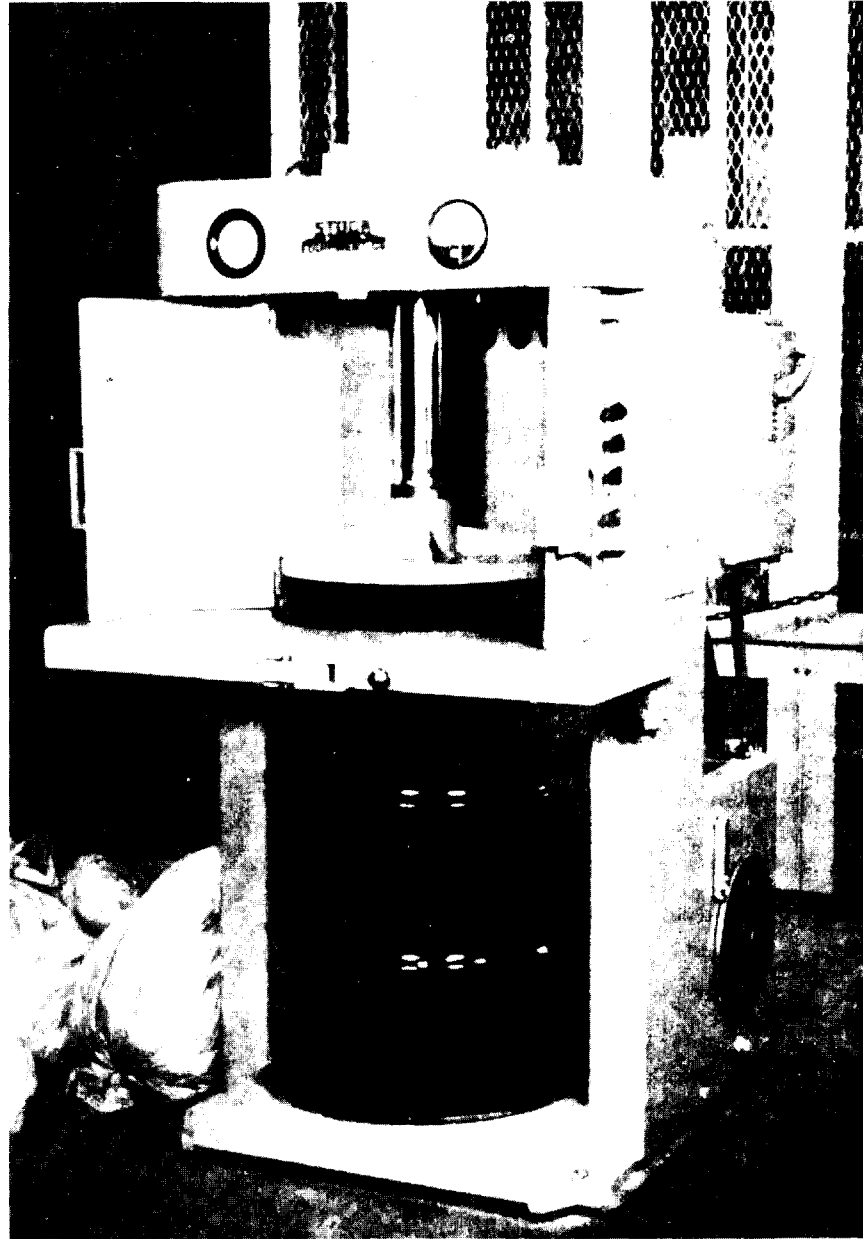


FIGURE 10 THE RADIOACTIVE WASTE COMPACTOR

DISCUSSION

BURCHSTED: Is the efficiency of the bag filters mass efficiency or number efficiency?

DROLET: Mass efficiency.

ETTINGER: My first question is somewhat similar. Is it correct that your paper indicated that you use the American Air Institute efficiency test, which is a mass efficiency for relatively large particles?

DROLET: Yes.

ETTINGER: What do you think the efficiency of the bag house with Nomex filters will be for submicron aerosols? The AFI test is heavily weighted, because of the test aerosol they use and the weight measurement method, to do well against large particles but relatively poorly for small particles. Do you have information on efficiency for some of the particles which are likely to be the source of contaminants coming out of the incineration?

The second question is: Do you think your dilution factor of 10^6 is fairly realistic and consistent with the Canadian regulatory requirements and ERDA or NRC regulatory requirements?

DROLET: To answer the second part first; yes, it is in line with accepted Canadian regulatory requirements and with Canadian experience to date, which we have gathered from the operating nuclear stations and from original R & D work at the Chalk River Nuclear Laboratories.

The first part of the question, no. We have no aerosol information to date. This incinerator is not yet on line. We have no research data to back it up. We will be measuring it after start-up and report it to you as soon as we can.

FREEMAN: Figure 3 shows the flow of bags with activity level acceptable for incineration going to incineration and high activity level being drummed for burial. What is the acceptable level?

DROLET: At Ontario Hydro we do it in terms of radiation doses on contact with each container. For concrete storage of these containers, our operating limit is 15 R.

FREEMAN: How is the waste checked to assure that this level is met?

DROLET: Individual monitoring of each container.

FREEMAN: It must be very low, as you stated later that even if the baghouse is breached, very little activity would be released.

DROLET: It is very low.

14th ERDA AIR CLEANING CONFERENCE

FLUIDIZED BED INCINERATOR DEVELOPMENT

Donald L. Ziegler and Andrew J. Johnson
Rockwell International
Atomics International Division
Rocky Flats Plant
Golden, Colorado

Abstract

A fluidized bed incinerator is being developed for burning rad contaminated solid and liquid waste materials. In situ neutralization of acid gases by the bed material, catalytic afterburning, and gas filtration are used to produce a clean flue gas without the use of aqueous scrubbing.

Introduction

The processing of radioactive materials generates waste, such as polyvinyl chloride (PVC) bags, polyethylene bags, surgeon gloves, paper wipes, and rubber drybox gloves. These waste materials must be processed for recovery of radioactive nuclides, such as plutonium. Conventional incineration, at temperatures of 800 to 1000°C, produces a refractory type of plutonium oxide which is difficult to dissolve. The combustion of chloride-containing waste in conventional incineration results in corrosion of the incinerator shell and of the flue gas scrubbing equipment. Recovery of plutonium from used refractory and the short life of refractory linings are major disadvantages of conventional incineration for this application.

To overcome some of the problems with conventional incineration, a project was initiated to develop a fluidized bed incinerator.⁽¹⁾ The major objectives of this incinerator system are as follows:

1. To produce a non-refractory plutonium oxide in the ash through the use of lower (550°C) operating temperatures.
2. To provide a system in which the corrosion of the incinerator and off-gas handling equipment is minimized with the use of in situ neutralization of acid gases generated by combustion of halogen-containing waste materials.
3. To provide a system which would minimize the complexity of the off-gas cleaning equipment through the use of in situ neutralization of the hydrogen chloride (HCl) and the use of catalytic afterburning of the flue gas.
4. To provide a system which would not require the use of refractory lined equipment because of lower operating temperatures in the reactor (550°C) and in the catalytic afterburner (525-650°C).

Discussion

Equipment

The pilot plant incinerator was designed for a 9 kg/hr capacity.

14th ERDA AIR CLEANING CONFERENCE

A flow diagram is given in Figures 1 and 2. The bagged solid waste is brought into a large sorting glovebox, bags cut open, and visible scrap metal removed before the waste is fed into a thick-bladed (16 mm) cutter type shredder. Coarse shredded waste drops onto a conveyor belt and is carried to an air classifier. Heavy particles fall into a collection glovebox, while the lighter fraction is air conveyed to a cyclone positioned over a second shredder. The cyclone-separated waste is ground in this thin-bladed (6 mm) shredder and falls into the incinerator feed screw hopper, while the air stream is recirculated back through the air classifier.

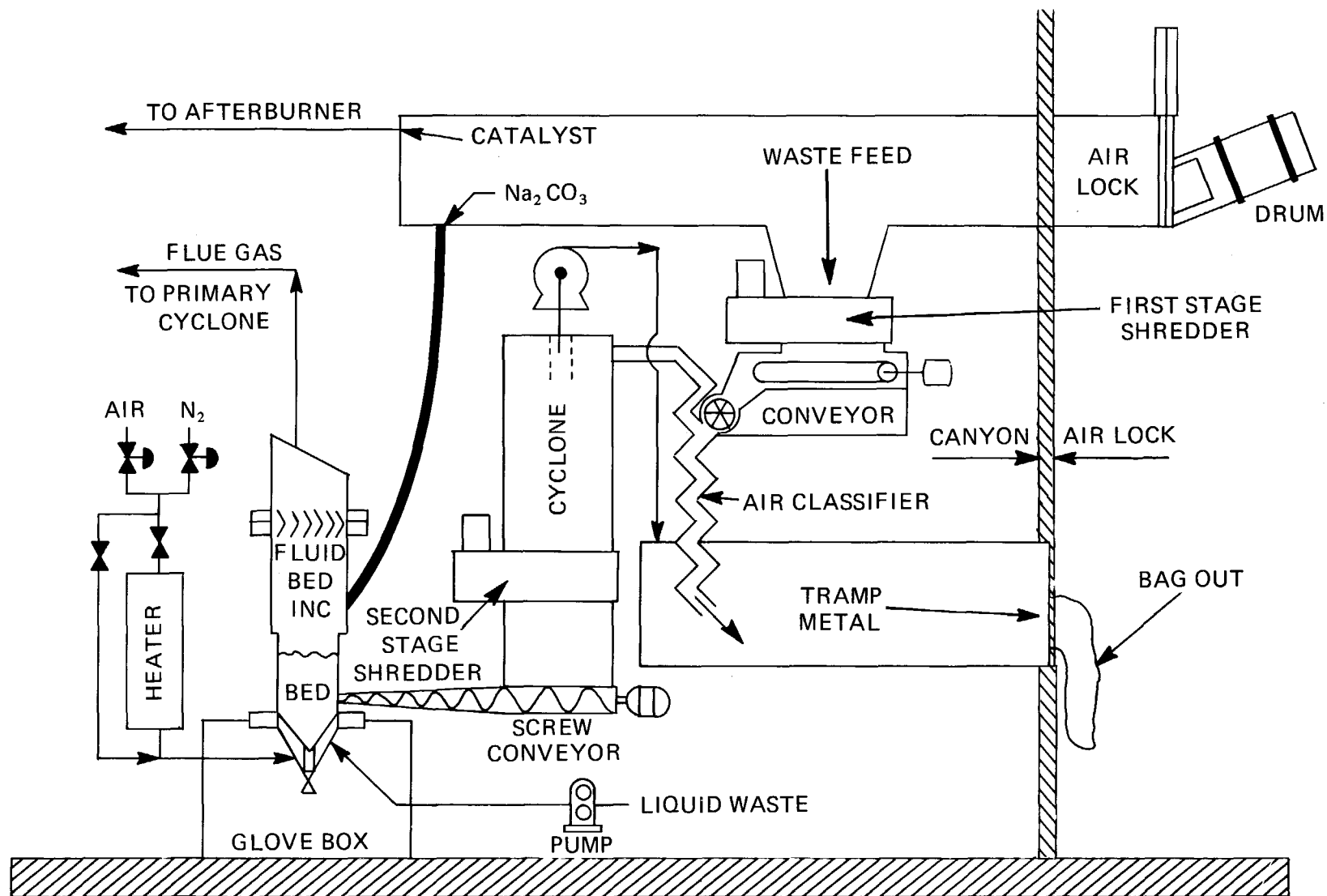
Shredded waste is fed by a tapered screw conveyor into a bed of sodium carbonate (Na_2CO_3) which is fluidized by air or an air-nitrogen mixture introduced through a distributor plate and passing through the bed of granular solids. At a temperature of about 550°C the waste is burned or decomposed and the HCl produced by decomposition of waste PVC reacts with the bed material to form sodium chloride (NaCl).

The flue gas exiting the primary bed passes through a cyclone; this is the major point of residue removal. After most of the elutriated solids are removed by the cyclone, the flue gas passes through a fluidized bed of oxidation catalyst for complete combustion of the contained flammable gases.

The flue gas exits the reactor through a cyclone and sintered metal filters for the final removal of elutriated solids. Gas flow through each of the five filters can be stopped and the dust removed by reverse flow. From the filters the gas passes through an air jet ejector which provides motive force for gas flow through the incinerator. The entire incinerator system operates under a negative pressure to prevent leakage of hazardous materials. The process offgas is blended with $64 \text{ m}^3/\text{min}$ of room air to produce a gas temperature below 70°C before it passes through four stages of high efficiency filtration for release to the atmosphere. Normal operating conditions and material compositions are presented in Table I.

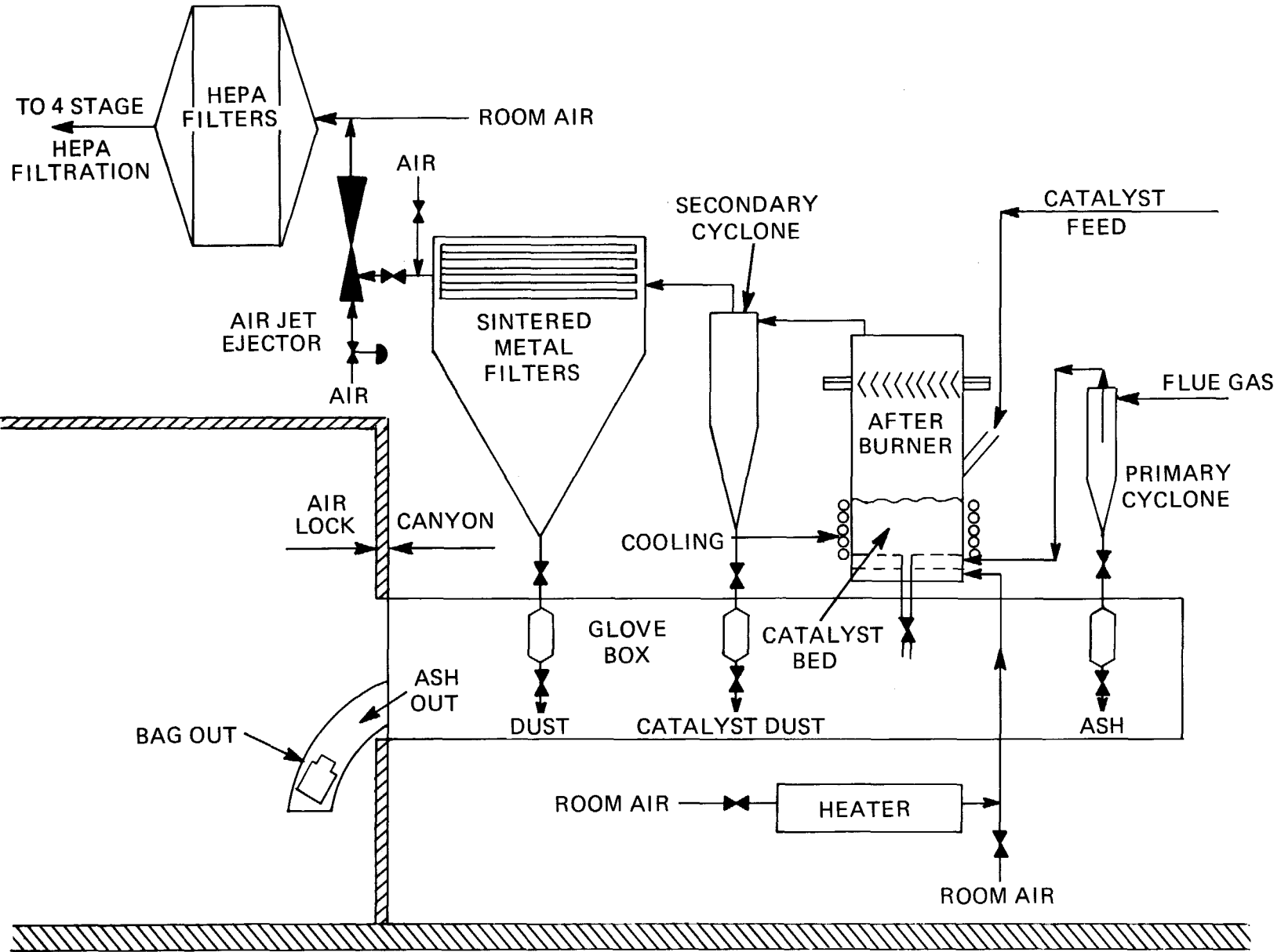
Table I. Operating conditions and materials for solid combustible waste incineration.

	<u>Incinerator</u>	<u>Afterburner</u>
Temperature, $^\circ\text{C}$	525-575	525-650
Gas Velocity, m/sec	0.35-1.0	0.35-1.0
Feed Rate, kg/hr	9	
Bed Depth, m	0.45	0.4
Construction Materials	Hastelloy C276 [®] stainless steel	and 304
Bed Materials	Sodium carbonate, 500-1000 micron	
Catalyst	23% chromic oxide on alumina 500-1000 micron	



FLOW DIAGRAM FOR PILOT PLANT FLUIDIZED BED INCINERATOR

FIGURE 1 - FEED END



FLOW DIAGRAM FOR PILOT PLANT FLUIDIZED BED INCINERATOR

FIGURE 2 - ASH END

14th ERDA AIR CLEANING CONFERENCE

Feed Preparation

The waste fed into any type of incinerator requires preliminary handling that includes sorting and getting the waste in the proper form for adding to the incinerator. For the fluidized bed incinerator, the preparation includes sorting, shredding, and air classification to remove tramp metal.

The shredders now in use were selected after testing shredders proposed by five different manufacturers. Two drums of waste materials, including all materials normally found in Rocky Flats Plant (RFP) waste such as surgeon gloves, plastic bags, wood, and high efficiency air filters, were shipped to each manufacturer. These materials were shredded in a vertical shaft hammer mill with ring type hammers, a horizontal shaft hammer mill with fixed hammers, a rubber chopper, and two low speed cutter type shredders. At the time these were tested, the Shred-Pax, [®] low speed cutter type shredder was found to offer the best combination of product size, minimum space requirement, and cost. It was equipped with an over-torque device to protect the equipment from damage due to tramp metal introduced with the waste material. Two of these units equipped with a hydraulic drive system have been installed in series to prepare feed for the pilot plant incinerator.

Incineration of Liquid Wastes

The fluidized bed incinerator (FBI) is now provided with tankage and an associated pumping system for the incineration of liquids. Two pencil tanks with critically safe dimensions are filled from inside an airlock. The liquid is circulated through a loop for thorough mixing and a controlled amount injected, with admixed air, into a primary bed of oxidation catalyst. If the mixed waste being burned contains some halogenated hydrocarbons, a mixed primary bed of Na_2CO_3 and catalyst is used for acid gas neutralization.

The two pencil tanks are provided with an automatic nitrogen pad that fills the void space as liquid is withdrawn from the tanks. This prevents the buildup of an explosive vapor mixture above the liquid surface. Injection rate and the selection of which tank is being circulated and/or filled is controlled from the master control panel. Level controls provide for automatic shut off when the tanks are full, along with warning lights on the control panel when a tank is near empty.

A dual system allows for the injection, at the same time, of two different liquids at individually controlled rates. This is advantageous for the destruction of a waste such as hydrazine. The hydrazine is noncombustible, but when injected into the incinerator while burning a waste naphtha mixture, the hydrazine is destroyed.

The enclosing of the FBI in a canyon, with residue removal isolated by a glovebox, allowed the incineration of alpha contaminated wastes. A large number of drummed contaminated flammable liquids, mostly from maintenance activities, had collected with no viable method of disposal. The disposal operation was started by pumping the liquid from the storage drums into drums fitted with bottom drains. At this time, as much water as possible was separated from

the organic fraction; the special drums filled with the organic were then sampled for analysis and connected to the incinerator tankage system. The analysis was made to determine if any especially hazardous or halogenated hydrocarbon materials were present.

Analytical data compiled from these typical runs are given in Table II.

Table II. Liquid waste incineration.

Run Number	kg Burned	Rate kg/hr	Residue, wt, kg.	Weight Reduction %
2	326	4.2	11.2	95.8
12	342	6.1	19.9	94.2
14	590	5.8	20.4	96.5

The increased burning rate in Runs 12 and 14 were attainable after the redesigned air ejector was installed. A greater amount of gas could be handled; this allowed the adding of more combustion air and the exhausting of the increased volume of flue gas produced.

Chloride Reaction with Bed Material

One of the major objectives of this process is to neutralize the HCl at the point of generation so as to eliminate the need for flue gas scrubbing to remove acid gases. To accomplish this, the chloride-containing waste is burned in a bed of sodium carbonate which reacts with the HCl to produce sodium chloride. The chloride is thus removed from the system without the complexity of a scrubbing system and with a minimum of chloride corrosion of the equipment.

The efficiency of chloride removal or reaction as a function of the efficiency of sodium carbonate usage has been evaluated in several experimental runs on the pilot unit. Presented in Figure 3 are the results of neutralization efficiency for experiments conducted with continuous waste feeding to a single bed of Na_2CO_3 . For these tests, fresh Na_2CO_3 was continuously fed and bed material continuously discharged from the fluidized bed. Essentially 100% efficiency of HCl reaction was obtained up to a level of about 26% Na_2CO_3 utilization; the chloride reaction efficiency decreases and significant quantities of HCl are released with the flue gas after this point.

The data were generated with 500-1000 micron size sodium carbonate bed material. Analysis, by x-ray microscopy, of the used bed material, indicates that the particle is composed of a dense shell of high concentration NaCl surrounding a core of unreacted Na_2CO_3 . This finding seems to indicate that using smaller particles would tend to improve the neutralization efficiency at higher levels of Na_2CO_3 utilization. This also suggests that abrasion of the NaCl shell to expose the core Na_2CO_3 may improve the Na_2CO_3 utilization.

Presented in Figure 4 are data generated with batch operation of the bed material and continuous feeding of the waste. That is, no Na_2CO_3 was fed and no bed material discharged during the test. All the data represented by the lower line were generated without

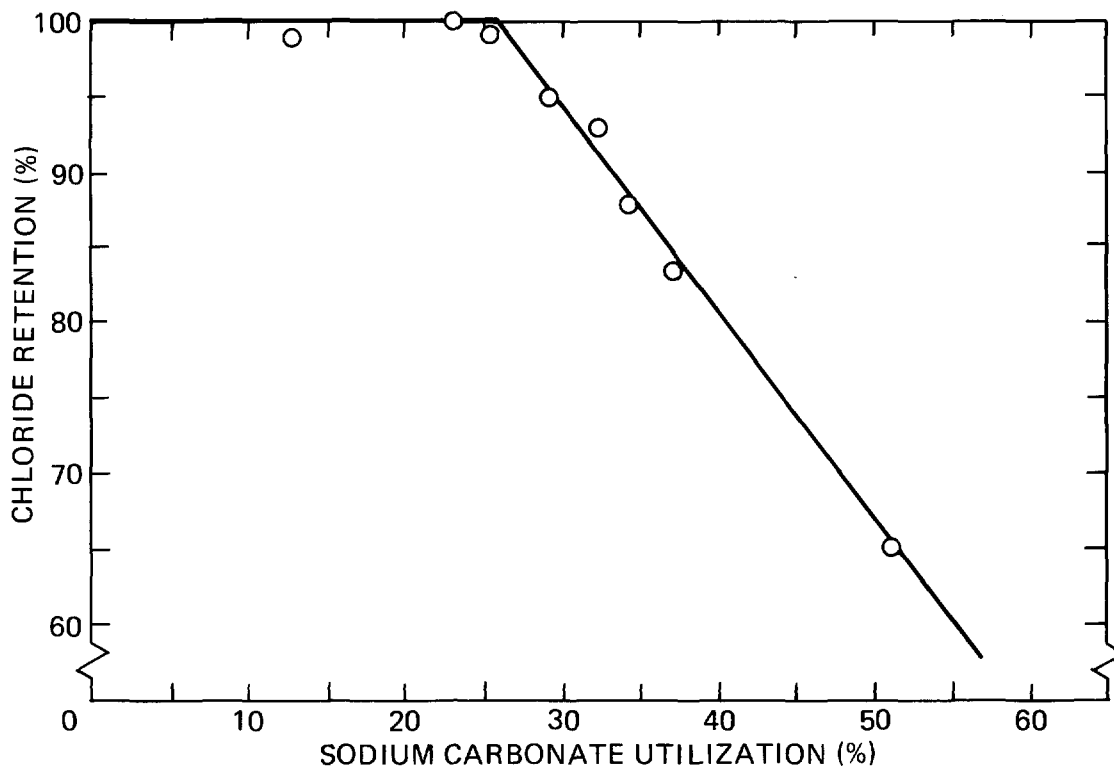


FIGURE 3
HCl REACTION EFFICIENCY FOR CONTINUOUSLY OPERATED FLUIDIZED BED

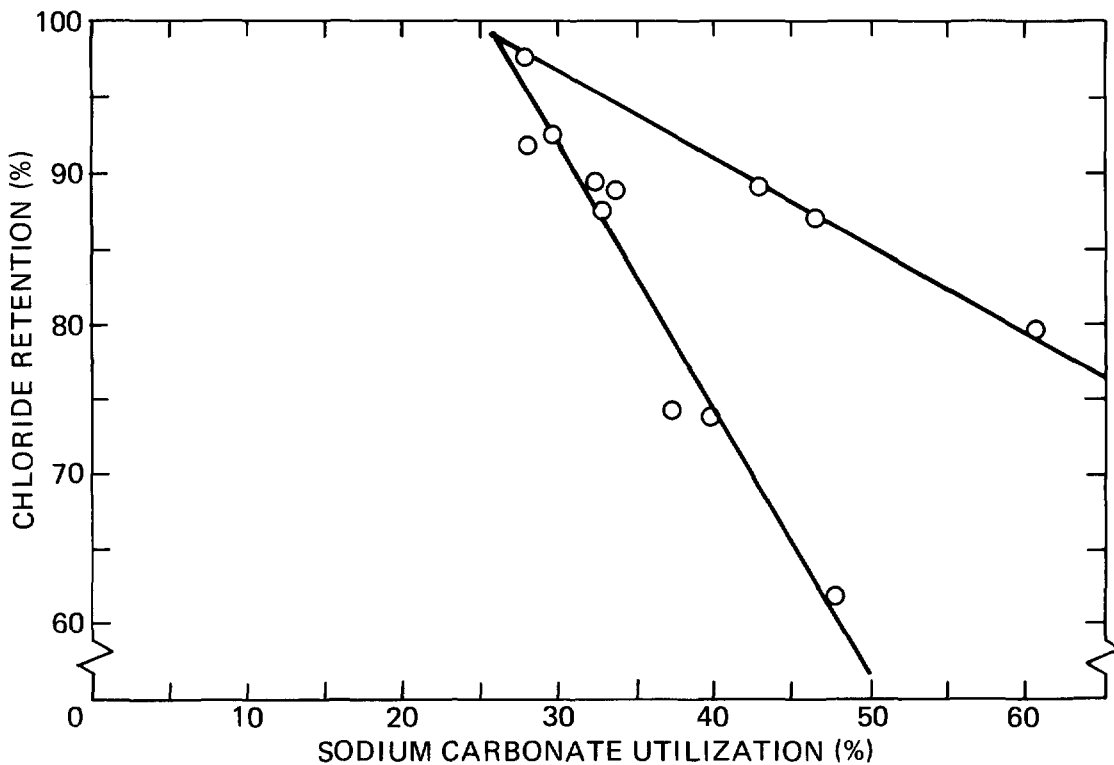


FIGURE 4
HCl REACTION EFFICIENCY FOR BATCH OPERATED FLUIDIZED BED

interruption of the tests. The data represented by the other line were generated by runs which were interrupted during the test. For these runs, the bed material was reacted to an intermediate level of Na_2CO_3 utilization, the bed material cooled to room temperature, and then reheated and carried to completion of the test. This intermediate cooling and reheating tends to increase the neutralization efficiency at equivalent utilization levels. This could be caused by thermal stress cracking of the sodium chloride shell and partial exposure of the core Na_2CO_3 . Both of these lines intersect the 100% chloride retention level at about 26% Na_2CO_3 utilization.

The fluidized bed depth did not have a significant effect on neutralization efficiency. Data from both deep and shallow bed experiments are included in Figures 3 and 4. This suggests that the HCl is generated and reacted shortly after the waste is introduced. Several tests were made using a secondary bed of Na_2CO_3 . The secondary bed did not improve the neutralization efficiency at comparable Na_2CO_3 utilization levels, again supporting the theory of rapid HCl generation and neutralization.

Over a year of operational tests of the pilot plant with plutonium contaminated RFP generated waste has proven that excellent chloride retention can be obtained with Na_2CO_3 utilization levels up to about 70 percent. These improved results during week-long incineration runs burning actual waste were obtained with a waste stream containing a lower PVC content than feed material used in previous tests. This, in effect, provided increased grinding time per unit addition of chloride to remove the sodium chloride shell formed on the outside of bed particle.

Flue Gas Afterburning

When the gas was filtered prior to the afterburner to remove elutriated bed material, the sintered metal filters became plugged with condensing hydrocarbons or tars. Because of this filtration problem, tests were conducted with the filters installed downstream of the fluidized bed catalytic afterburner. This allows the particulate to percolate through the catalyst bed and the filtration to be performed on a gas stream free of significant concentrations of hydrocarbons.

Catalytic oxidation provides several important features for this process. The catalyst is effective at lower temperatures than are required for open flame afterburning. Therefore, the elutriated bed material will not be melted and coated on reactor walls which could occur in conventional open flame afterburning. The low temperature operation of the catalyst also eliminates the need for refractory lined equipment. The catalyst is effective in producing a high quality flue gas. A typical flue gas composition for the fluidized bed afterburner operation is presented in Table III.

14th ERDA AIR CLEANING CONFERENCE

Table III. Typical flue gas composition exiting afterburner.

	<u>Fluidized Bed</u>
Oxygen (%)	7.8
Carbon Dioxide (%)	8.3
Carbon Monoxide (ppm)	400
Total Hydrocarbons (ppm)	100

Particulate Elutriation

The majority of the ash generated is elutriated from the bed and collected in cyclone and filtration system. Most of the tests resulted in 70 to 80% of the ash being elutriated from the bed. The remaining 20 to 30% of the ash was removed with the bed material.

With the fluidized catalytic bed afterburner, some of the catalyst is elutriated from the reactor. The rate of catalyst loss is dependent on gas fluidizing velocity and the mesh size of the catalyst used. These data are presented in Figure 5. This type of information is needed to properly size the fluidized bed afterburner to minimize catalyst usage.

Conclusions

1. The operating temperatures in the incinerator and the afterburner are low enough to eliminate the use of refractories.
2. The performance of waste shredding and feeding of shredded material has been demonstrated to be satisfactory.
3. Efficient HCl neutralization has been accomplished up to a level of about 70% Na_2CO_3 utilization. This eliminates the need for an aqueous scrubbing system.
4. Catalytic afterburning produces a flue gas with minimal levels of unburned hydrocarbons.

Reference

1. D. L. Ziegler, A. J. Johnson, L. J. Meile, and E. L. Shamhart, "Pilot Plant Development of a Fluidized Bed Incineration Process," USAEC RFP-2271, Rocky Flats Division, Dow Chemical U.S.A., Golden, Colorado, October 1974.

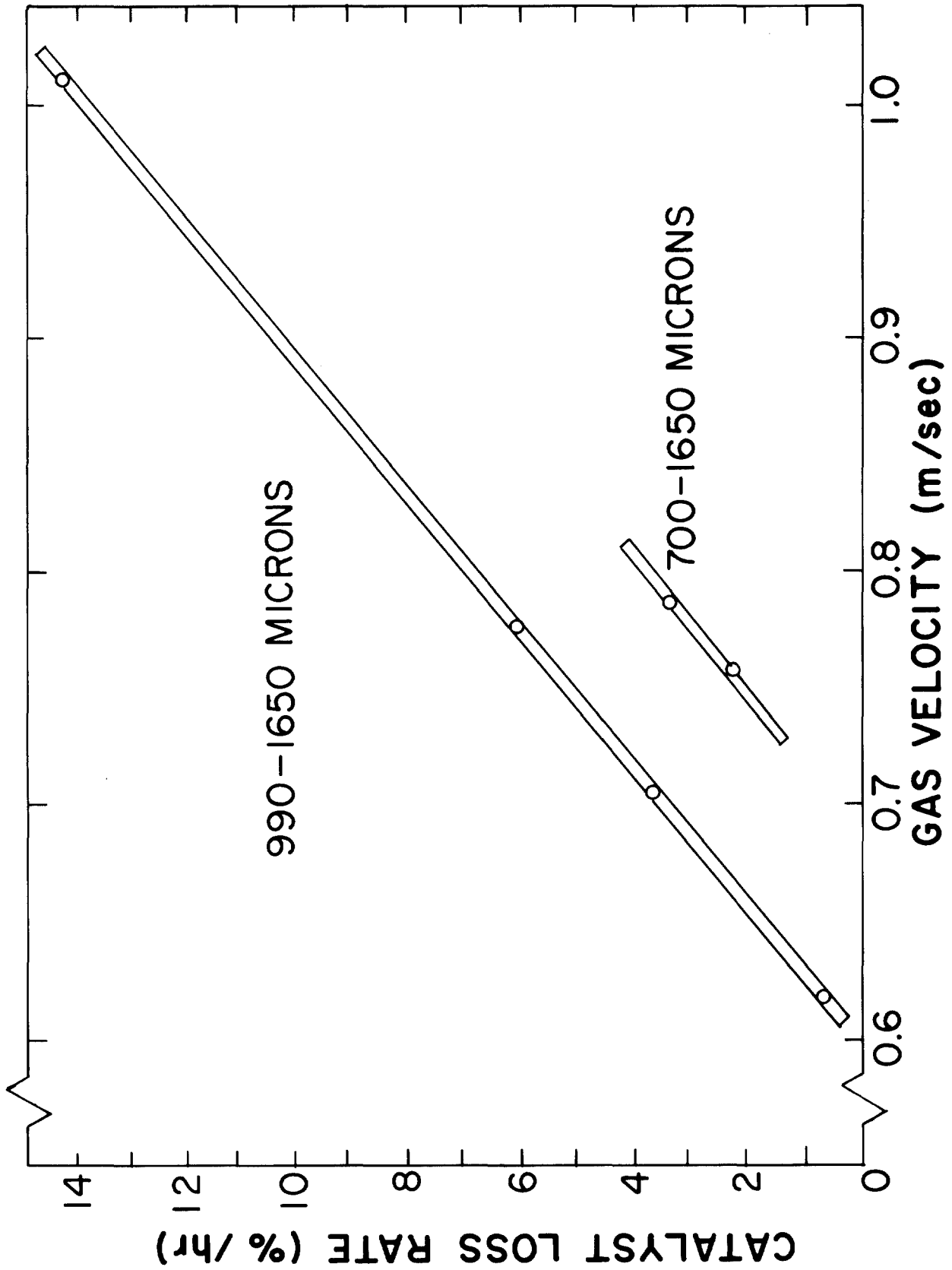


FIGURE 5

14th ERDA AIR CLEANING CONFERENCE

PARTICULATE COLLECTION IN A LOW LEVEL RADIOACTIVE WASTE INCINERATOR

S.N. Rudnick, D. Leith, M.W. First
Harvard Air Cleaning Laboratory
Boston, Massachusetts

Abstract

As designed, sintered stainless steel filters will clean the gas from the secondary cyclone at a low level radioactive waste incinerator. Using bench scale apparatus, asbestos floats and diatomaceous earth were evaluated as filter aids to prevent clogging of the sintered metal interstices and to decrease filter penetration. Both precoats prevented irreversible pressure drop increase, and decreased cold DOP penetration from 80% to less than 1%. To collect the same quantity of fly ash, less diatomaceous earth was needed than asbestos floats.

A back-up study evaluated a moving bed of sodium carbonate pellets in lieu of the sintered metal filters. Since identical sodium carbonate pellets are used to neutralize hydrogen chloride in the incinerator, their use in a moving bed has the advantages of trouble free disposal and cost free replacement. Co, counter, and cross-current beds were studied and gave fly ash penetrations less than 0.1% at moderate pressure drop.

I. Introduction

Volume reduction of solid wastes contaminated with radioactive materials, such as plutonium, in high temperature fixed hearth incinerators has been practiced for about 25 years. These incinerators have experienced rapid deterioration and have required frequent expensive maintenance and repair services because of high combustion temperatures and the presence of corrosive gases from the decomposition of halogen-containing substances, such as PVC. To overcome these problems, a program was undertaken at the Rocky Flats Plant to develop a low temperature (550°C) fluidized bed incinerator utilizing sodium carbonate pellets to react with acid gases and minimize corrosion of the gas incinerator and offgas system.⁽¹⁾ The primary flue gas cleaning system of the pilot scale incinerator consisted of a cyclone collector followed by a bank of sintered metal filters. After some hours of incinerator operation, the air flow resistance of the sintered metal filters increased substantially, and they could not be restored to a serviceable condition by chemical or physical cleaning methods nor by high temperature exposure for prolonged periods. The exact cause of the permanent plugging of the sintered metal filters could not be determined with certainty, but remedial measures were required as these filters are very costly.

Two methods of overcoming the plugging problems experienced with sintered metal incinerator flue gas filters were investigated:

(1) the use of filter aids to protect the sintered metal filter surfaces from direct contact with the particulate matter in the incinerator offgases and (2) substitution of a high temperature granular moving bed filter for the sintered metal filters.

II. Filter Aids for Sintered Metal Filters

When fine particles enter and become wedged into the comparatively large pores of sintered metal filters, they may become fixed in place and impossible to remove. This leads to irreversible increase in pressure drop and premature filter replacement. To prolong filter life, the use of filter aids to shield the sintered metal surface, and enhance collection efficiency, was investigated. To satisfy all design criteria and operate successfully, it was required that the filter aid selected (1) separate easily and uniformly from the sintered metal surface during cleaning (2) form a layer with low pressure drop but high collection efficiency for the incinerator dust (3) coat the filter well with a small amount of filter aid relative to the amount of incinerator dust collected to minimize the disposal of radioactive waste (4) withstand 500°C, the temperature of the incinerator exhaust gases (5) disperse easily into the filter inlet air stream and (6) be easy and safe to handle. Several filter aids were reviewed against these criteria. Two of these, asbestos floats and diatomaceous earth, were low in cost, easily obtainable, and appeared to satisfy most requirements. They were selected for further testing.

Equipment

Three sintered stainless steel filter tubes, each 1 1/2 in. O.D. and 5 3/4" long, were used for evaluation. The filter tubes were mounted in parallel within a stainless steel housing and so arranged that gas flow passed through the filters from the outside to the inside, allowing filter aid and dust to collect on the outside surfaces. Filtered air passed through solenoid valves to an exhaust manifold, and then in turn to an orifice flowmeter, flow control valve, blower, and to the laboratory air exhaust system. Pulses of back-flow cleaning air were admitted by closing solenoid valves connected to the exhaust manifold and then opening solenoid valves connected to a compressed air reservoir. The three filters were operated and cleaned simultaneously. Measured quantities of filter precoat and test dust were fed in to the filter housing by a dust feeder. (2)

Diatomaceous earth has been widely used as a precoat for liquid filters and asbestos floats have been used as a precoat for fabric filters controlling low concentrations of toxic dusts, such as beryllium, which must be collected with exceptionally high efficiency. Cumulative size distributions by count for the diatomaceous earth and asbestos floats precoat materials used in this study are given in Figure 1. Both materials have a count median diameter about 1 micrometer and similar size distributions.

Measurements

A series of tests was performed to determine cleanability of these precoat materials from the sintered metal surface. Air at room temperature was passed through the filters at a face velocity of 20 feet per minute and sufficient precoat added to raise filter pressure drop from 6.5 to 10.5 in. w.g. Cottrell-precipitated fly ash having the size distribution shown in Figure 1 was then added to the pre-coated filters until system pressure drop reached 20 in. w.g.

Filter aid and dust were then removed from the sintered metal filter surface by a one second pulse of 15 psig air directed from inside the filter tubes toward the outside. No decrease in residual pressure drop was found when the length of the cleaning pulse was increased from 1 to 15 seconds.

Twenty repetitions of the loading and cleaning cycle were carried out with asbestos floats and with diatomaceous earth as a precoat. Figure 2 is a plot of pressure drop after cleaning, against cycle number for each filter aid. The residual pressure drop for filters pre-coated with diatomaceous earth was about one in. w.g. higher than for asbestos floats. For both asbestos floats and diatomaceous earth, residual pressure drop appears to have remained stable over twenty cycles, demonstrating that the filter aid plus fly ash can be cleaned effectively from the sintered metal surface.

A second set of experiments was performed to determine the loadability, (i.e. fly ash to precoat mass ratio) of each filter aid and to indicate its ability to prevent fly ash from entering the sintered metal pores. First, cold DOP, generated with a single Laskin nozzle and having a mass median diameter of 0.8 micrometers and standard geometric deviation of 1.65⁽³⁾ was fed to the cleaned filters. Penetration was read directly using a total light scattering photometer. Next, precoat was added, in gram increments, to the filter surface until system pressure drop increased by 4 in. w.g. and then a second DOP test was performed. Finally, fly ash was added, in gram increments, until total system pressure drop reached 20 in. w.g. and a third DOP test was performed. Figure 3 shows pressure drop vs pounds per square foot of filter aid (areal density) when pre-coated with asbestos floats or diatomaceous earth. The pressure drop loading characteristics of both filter aids are almost identical while precoat is being fed, but when fly ash is added, pressure drop builds up much more slowly on the filters pre-coated with diatomaceous earth.

With a precoat of asbestos floats, 35% of the total filter aid-fly ash mixture cleaned from the filters was asbestos whereas with diatomaceous earth, only 15% of the total mass was precoat. Therefore, filters using asbestos floats would have to be cleaned and re-coated more than three times as often as filters using diatomaceous earth, and over three times as much asbestos would have to be used and disposed of.

The results of the DOP penetration tests are shown in Table 1. Clean sintered metal filters show a DOP penetration close to 100% and are inefficient filters for submicrometer particles without the

presence of a filter cake. Additions of both asbestos floats and diatomaceous earth, as precoats, decreased penetration to 0.3 - 0.4%. After loading with fly ash, DOP penetration decreased to less than 0.01% with the asbestos floats precoat, but to only 0.1% with diatomaceous earth.

Discussion of Results

The differences in loadability and DOP penetration of sintered metal filters between filter aids can be explained by differences in the properties of the cake that is formed on the clean filter. Asbestos floats contain a significant fraction of small diameter fibers that are excellent collectors of small fly ash and DOP particles. As a result, when using asbestos floats, most fly ash collection takes place upon the upstream surface of the deposit. The fly ash filter cake that develops rapidly at the precoat surface is a very efficient fly ash collector but has a rapid pressure drop rise. Diatomaceous earth is composed, instead, of cubic and spiny round particles with very few fibers. As a result, fly ash may penetrate below the surface of the diatomaceous earth precoat and deposit within the interstices of the diatomaceous earth cake, thereby delaying the formation of a fly ash filter cake at the precoat surface. Although penetration is not as low as when the fly ash cake forms immediately on the surface of asbestos floats, pressure drop across the filter system increases much more slowly, at least until a homogeneous fly ash cake is established on the surface of the diatomaceous earth. After the fly ash filter cake is fully established, pressure drop should increase at a rate that is independent of the nature of the filter aid. One criterion of the effectiveness of a filter aid is how well the pressure drop increase can be delayed. The data presented here suggest that diatomaceous earth is effective than asbestos floats in this regard.

Both asbestos floats and diatomaceous earth can be used to protect sintered stainless steel filters from irreversible plugging without causing an increase in cleaned filter pressure drop over many cleaning cycles. Although a deposit of diatomaceous earth and fly ash gives greater DOP penetration than one of asbestos floats and fly ash, loadability of the diatomaceous earth coated filter is much better.

III. Moving Bed Granular Filter

The feasibility of using a moving bed granular filter containing sodium carbonate pellets, as an alternative to the use of sintered metal filters to clean the offgases from a fluidized bed incinerator burning low level radioactive wastes, was also studied. Sodium carbonate pellets were selected for the granular filter because they are being utilized in the incinerator to neutralize hydrogen chloride formed during the combustion of chlorine-containing wastes and it was considered possible that the sodium carbonate pellets from the filter could be cycled back to the incinerator, thereby eliminating one radioactive waste stream.

Two types of pellets, in use in a prototype incinerator built at Rocky Flats, Colorado, were tested as candidates for a granular filter. The larger pellets are isometric and close to monodisperse, i.e., they have a geometric mean diameter by count of 1.2 mm and a geometric standard deviation (GSD) of 1.2. The smaller pellets are cylindrical and have a geometric mean length equal to 0.21 mm by count (GSD = 2.0) and geometric mean diameter equal to 0.12 mm (GSD = 1.7).

Granular Bed Configurations

Filtration in fixed granular beds, used for the initial studies, is a non-steady-state process inasmuch as both pressure drop and collection efficiency will vary with time and the bulk of the collected dust will be concentrated on or near the upstream face of the filter whereas a moving bed granular filter is a steady-state unit once equilibrium has been reached. Moving granular beds, often referred to as gravity beds, are used for catalytic cracking units, pebble heaters, shaft furnaces, and blast furnaces. Gas flow through a moving granular bed may be cocurrent, countercurrent, or perpendicular (cross-flow) to the direction of movement of the solids. For cocurrent and countercurrent arrangements, gas flow can accelerate or impede the flow of solids. In either case, the porosity of the flowing granular medium will be the same as the loosest possible packing in a fixed bed. (4)

A cocurrent arrangement is advantageous as a particulate filter because dirty gas initially contacts clean pellets that have low collection efficiency, but as the gas travels deeper into the bed it meets granules that are more heavily laden with collected particles and hence have higher dust collection efficiency. This arrangement is analogous to a deep bed filter using successively finer and more efficient filtering media and makes it possible to distribute the collected material throughout the entire depth of the bed. Cocurrent flow also eliminates the possibility of bed fluidization, a major hazard of a countercurrent flow granular filter. Fluidization occurs when the pressure drop associated with the upward flow of gas is sufficient to overcome the weight of the granular medium, i.e., when

$$\frac{\Delta P}{L} = \rho_B g \quad (1)$$

where $\Delta P/L$ is the pressure drop per unit height of bed, ρ_B is the bulk density of the bed, and g is the acceleration of gravity. For a moving bed of granules, the weight of collected dust will not significantly increase bulk density but will have a profound effect on the pressure drop. For both small and large sodium carbonate pellets, the maximum pressure drop attained per length of bed before fluidization occurs is equal to about 1.0 in. w.g. per inch of bed height. Because this condition can be reached easily, a countercurrent granular bed filter is not desirable.

One disadvantage of cocurrent (and countercurrent) flow is the need for large length-to-diameter bed ratios to assure plug flow of the granules. This is generally not a problem with cross-flow operations.

Fixed Granular Bed Filter

Sodium carbonate pellets supported on a screen in a two-inch diameter column were gently tapped until their volume was minimized. The pressure drop across this bed vs gas velocity for various bed depths is shown in Figures 4 and 5 for large and small pellets, respectively. For the larger pellets, the experimental data were compared to the Ergun equation⁽⁵⁾, a relationship commonly used to predict pressure drop in porous media, i.e.:

$$\Delta P/L = 4.17\mu VS^2(1-\epsilon)^2/\epsilon^3 + 0.292\rho V^2S(1-\epsilon)/\epsilon^3 \quad (2)$$

where ΔP is pressure drop, L is bed depth, μ is gas viscosity, V is superficial gas velocity, S is external specific surface area of the granular medium, ϵ is interpellet porosity of the bed, and ρ is gas density. Using the method of Chalkly, et al.⁽⁶⁾, the external specific surface of the larger pellets was determined to be 7.6 mm^{-1} from photographs of bed cross-sections. Interpellet porosity was evaluated from bed cross-sections and found to be 0.33. The internal specific surface and intrapellet porosity of the porous pellets have an insignificant effect on the flow and do not influence these measurements.

For air at ambient conditions, equation (2) reduces to

$$\frac{\Delta P}{L} = 2.91 \times 10^{-2}V + 1.35 \times 10^{-4}V^2 \quad (3)$$

where ΔP is in inches of water, L is in inches, and V is in fpm. Equation (3) is plotted in Figure 4 and is in excellent agreement with our experimental data.

Cold DOP aerosol was used to determine the collection efficiency of small and large sodium carbonate pellets and the results are shown in Figures 6 and 7 as a function of superficial velocity. For the large pellets, a maximum penetration was detected at about 20 fpm. No maximum was evident for the small pellets in the range of velocities studied.

Cocurrent Moving Bed Granular Filter

The experimental bench scale, cocurrent moving bed granular filter is shown schematically in Figure 8. Sodium carbonate pellets moved downward by gravity through a two-inch diameter glass column. Dirty gas entered the filter at the top of the bed and flowed cocurrent with the pellets. A large funnel served as a pellet feed hopper. The length of the funnel stem protruding into the column was adjustable to give various bed heights. Another funnel served as a gas-pellet separation section. Spent pellets were discharged to a hopper and pellet flow rate was controlled by a rotating drum located in the spent pellet hopper. The distance between the drum and the pellet outlet port and the speed of the drum motor determined the pellet flow rate.

To minimize end effects, the cross-section of the feed hopper

outlet was small compared to the column cross-section and the separation section cross-section was large compared to that of the glass column. Because of its unique geometry, the bottom of the bed was a combination of cocurrent, countercurrent, and cross-flow.

The moving bed granular filter was operated at a superficial gas velocity of 20 fpm, a pellet velocity of 0.016 fpm, and an inlet fly ash concentration of 18 grains/ft³. The size distribution of the fly ash is shown in Figure 1. Pressure drop and DOP penetration as a function of time of operation are shown in Figure 9. The pressure drop increased from an initial value of 1.0 to 10 in. w.g. in about 25 minutes, after which it remained essentially constant. For plug flow of the pellets, steady-state conditions should be reached after 21 minutes (i.e., bed length divided by pellet velocity).

A relatively high pellet velocity (0.016 fpm) was required to attain steady-state conditions in a short period of time and it became necessary to use a very high inlet fly ash loading (18 grains/ft³) to provide an adequate steady-state collection efficiency. At steady-state conditions, the percentage of fly ash in the pellet bed, which depends only on the fly ash feed rate and pellet velocity, was 5.2 wt.%. If the same steady-state value were obtained at lower inlet fly ash concentration and lower pellet velocity, the steady-state efficiency and pressure drop would remain essentially unchanged assuming the effect of dust loading on collection efficiency is minimal.

The fly ash penetration was extremely low for the entire run. (≤ 0.02 wt. %) Inasmuch as pulverized coal fly ash contains many large particles that are relatively easy to collect, the penetration of weight would be expected to be low. DOP penetration, which provides a more severe test of filter efficiency, gave considerably higher penetration values, as shown in Figure 9. DOP penetration decreased from an initial value of 55% for a clean pellet bed to 2% after the pellet bed reached steady-state conditions.

Cross-Flow Moving Bed Filter

A schematic diagram of an experimental cross-flow moving bed granular filter is shown in Figure 10. The filter consisted of a rectangular "cross" in which the pellet bed moved downward by gravity and the gas flowed horizontally. The upper portion of the "cross" served as a pellet feed hopper. A shielded glass window installed in the vertical section of the "cross" permitted a view of the motion of the pellets. Pellet flow was controlled by a motor-driven rotating drum. This cross-flow moving bed granular filter was operated at a superficial gas velocity of 20 fpm, a pellet velocity of 0.006 fpm, and a fly ash concentration of 9 grains/ft³.

Neither pressure drop across the filter nor DOP penetration equilibrated with time because an air pocket formed in the pellet bed after about 10 minutes. The pocket was first detected at the base of the upstream side of the filter (labeled "A" in Figure 10) but, with time, the pocket grew until it reached across the entire filter and the pellets above the plane labeled "B" in Figure 10 no longer flowed downward. Nevertheless, pellets continued to be

14th ERDA AIR CLEANING CONFERENCE

removed at a steady rate by the rotating drum and a fly ash filter cake was clearly visible at the boundary of the air pocket. It was found that when the unit was operated at the same gas flow rate but with dust free air, the pellets moved steadily, with no gas pocket formation. At first, it was believed that the fly ash cemented the pellets together, preventing further motion, but this is incorrect because the pellets fall and fill the air pocket when air flow is discontinued. Therefore, it was concluded that the pressure drop across the fly ash cake is sufficiently large to support the pellets.

Because the pellets flowed freely when clean air was passed through the filter a test was made using lower fly ash concentrations but reducing the fly ash concentration to 1 grain/ft³ had little beneficial effect. Oven dried pellets gave similar results.

As it seemed likely that the pressure drop across the dirty pellets was sufficiently large to support the pellets, the apparatus was modified so that the gas entered the filter at a higher elevation than it exits but an air pocket still formed in the pellet bed. A heavy-duty vibrator was strapped to the pellet bed housing, but it, too, yielded no improvement. Apparently the dirty pellets arranged themselves in such manner that an upward component of the pressure drop still supported part of the pellet bed. Similar results were obtained for both large and small pellets.

Discussion

Air pockets form in that portion of a cross-flow granular bed in which fly ash has deposited and the pellets no longer flow. When pellets move cocurrent with air flow, fly ash deposition on the pellets will not inhibit their movement, but scale-up of a unit to operating size (3500 ACFM) would be difficult. If the volumetric flow rate were to be increased by increasing the cross-sectional area of the bed, the length to diameter ratio would become very small and when the L/D ratio becomes very much less than one, "ratholing" occurs, whereby the pellets do not move in plug flow fashion. Also, pellet addition to and removal from a cocurrent pellet bed becomes particularly troublesome. Our bench scale moving bed filter has a L/D ratio of two and a volumetric flow rate of about 0.5 ACFM. It is unlikely that this ratio can be decreased very much without degrading the operation of the filter. If the length of the bed is significantly increased to compensate for an increase in diameter, the pressure drop even for a clean pellet bed would become excessive. Hence, it would be necessary to modify the cocurrent moving bed filter shown in figure 8 if a full scale unit were constructed.

IV. Summary and Conclusions

Laboratory studies of filter aids for sintered metal filters have demonstrated their ability to protect the porous metal structure from permanent plugging with products contained in incinerator off-gases. In addition, they have shown that the use of appropriate filter aids can greatly reduce penetration of particulate matter through sintered metal filters and, thereby, provide added protection for heat exchangers and absolute filters downstream of the sintered metal filters.

14th ERDA AIR CLEANING CONFERENCE

Moving bed granular filters have excellent characteristics for incinerator offgas treatment, i.e., they operate at constant gas flow resistance, have high temperature tolerance, can store large amounts of dust in the pores of the bed with low pressure drop increase, and are capable of high collection efficiency. For all of these reasons, they have good potential for use in conventional high temperature incinerators as well as for low temperature fluidized bed units.

Acknowledgement

This work was supported by Contract E(11-1)-3049 from the Energy Research and Development Administration.

Table I. Cold DOP Penetration.

<u>Filter Aid</u>	<u>Sintered Metal Filter Condition</u>		
	<u>After Cleaning</u>	<u>After Filter Aid Additions*</u>	<u>After Filter Aid Plus Fly Ash Additions**</u>
Asbestos Floats	90%	0.4%	0.01%
Diatomaceous Earth	80%	0.3%	0.10%

*Filter aid added until pressure drop of clean sintered metal filters increased 4 in. w.g.

**Cottrell-precipitated pulverized coal fly ash added on top of the filter aid until total pressure drop reached 20 in. w.g.

14th ERDA AIR CLEANING CONFERENCE

References

1. D.L. Ziegler, A.J. Johnson, L.J. Meile, A.L. Johnson, and E.L. Shamhart, Pilot Plant Development of a Fluidized Bed Incinerator Process, RFP-2271, Dow Chemical U.S.A., Rocky Flats Div., Golden, Colorado, (Oct. 14, 1974).
2. L. Silverman and C.E. Billings, "Methods of Generating Solid Aerosols," J. Air Poll. Control Assn. 6:76 (1956).
3. H.H. Ettinger, J.D. DeField, D.A. Bevis, and R.N. Mitchell, "HEPA Filter Efficiencies Using Thermal and Air Jet Generated Dioctyl Phthalate," Amer. Ind. Hyg. Assn. J. 30:20 (1969).
4. J. Happel, "Pressure Drop Due to Vapor Flow Through Moving Beds," I & E.C., 41:1161 (1949).
5. R.B. Bird, W.E. Stewart, and E.N. Lightfoot, Transport Phenomena, John Wiley & Sons, New York (1960), p. 200.
6. H.W. Chalkey, J. Cornfield, H. Park, "A Method for Estimating Volume-Surface Ratios," Science 110:295, (1949).

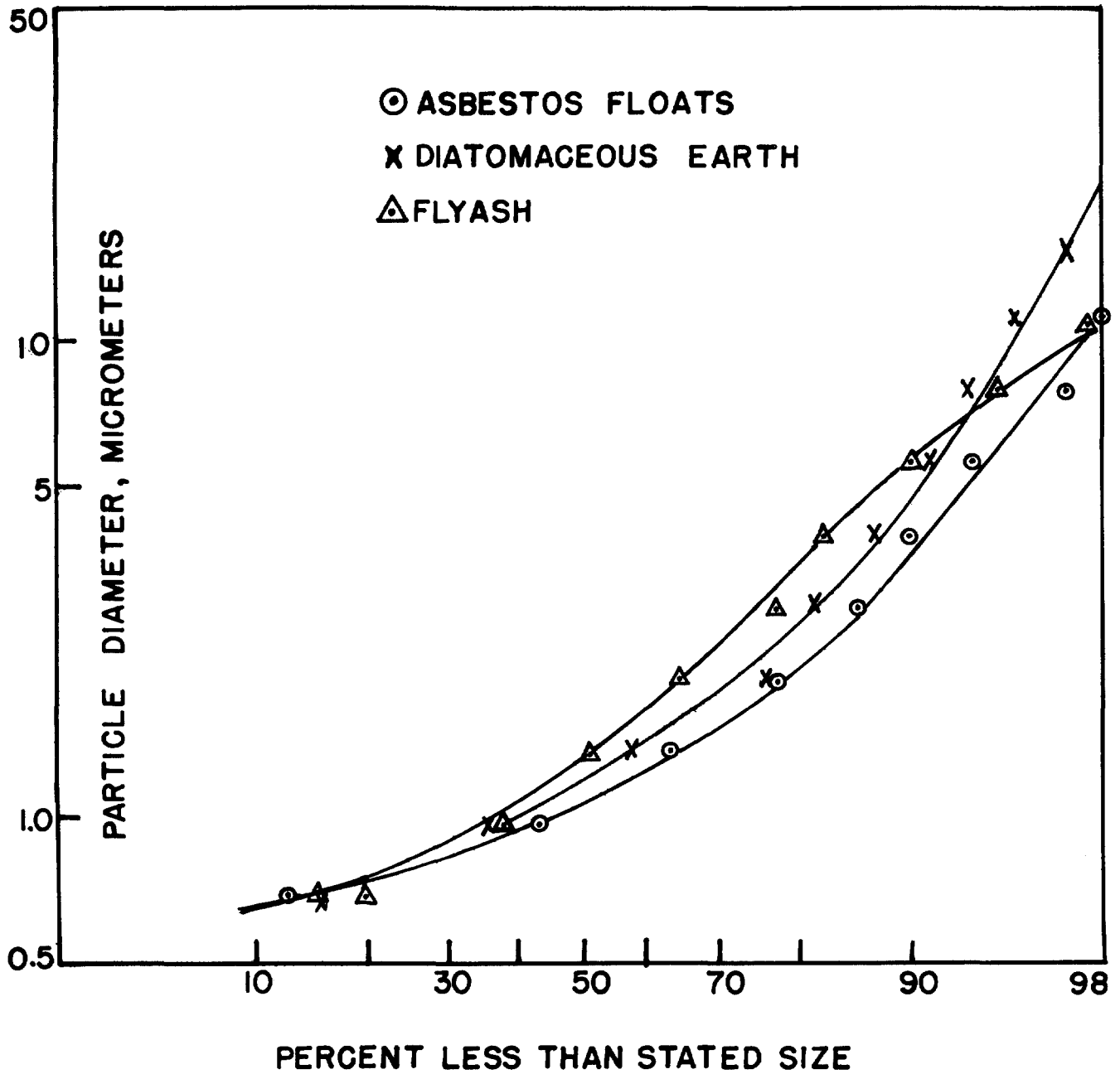
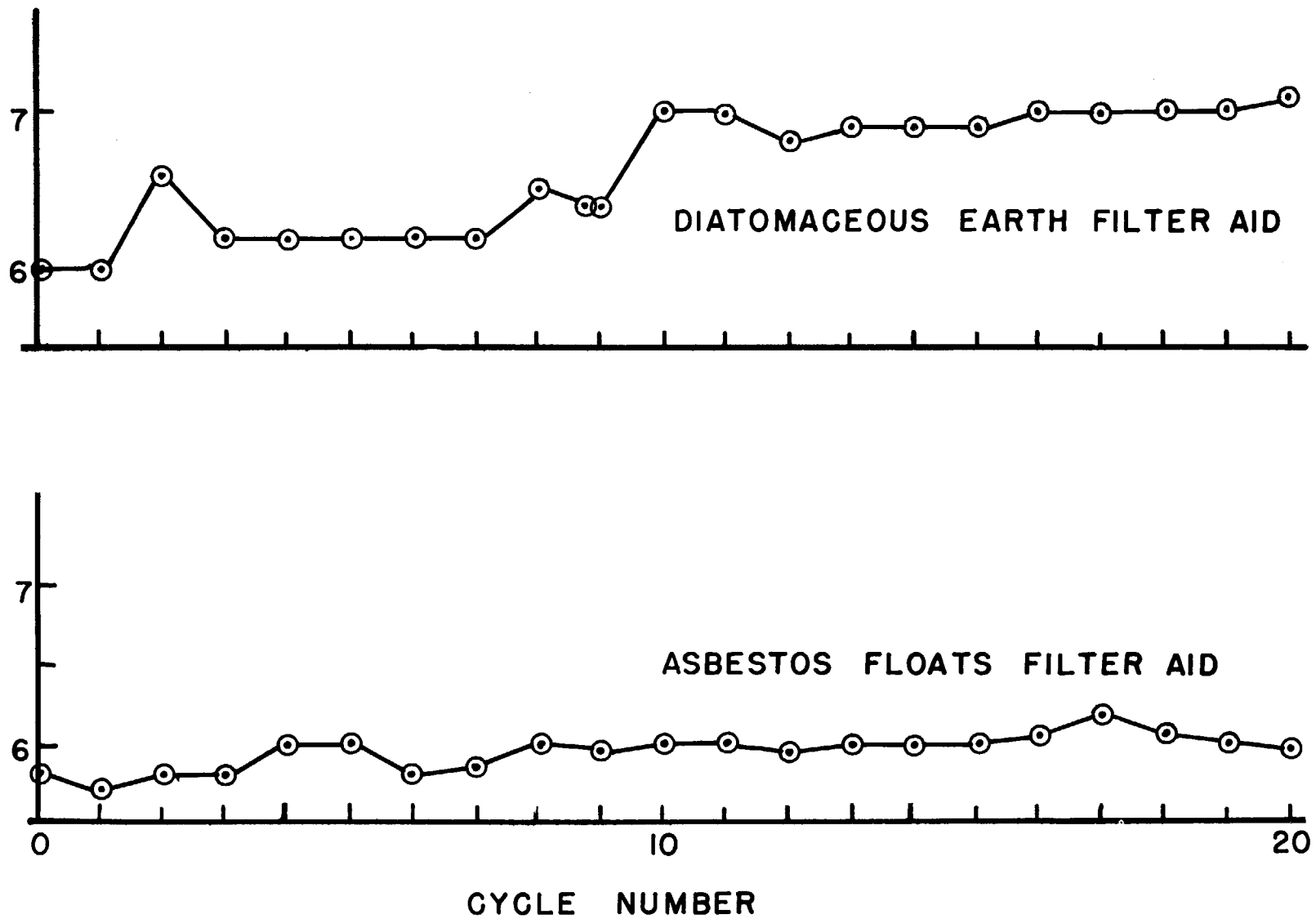


FIGURE 1 CUMULATIVE SIZE DISTRIBUTIONS BY COUNT FOR ASBESTOS FLOATS, DIATOMACEOUS EARTH AND FLY ASH.

RESIDUAL PRESSURE DROP, INCHES OF WATER GAUGE

FIGURE 2 RESIDUAL PRESSURE DROP AFTER CLEANING, DIATOMACEOUS EARTH FILTER AID (ABOVE) ASBESTOS FLOATS FILTER AID (BELOW)



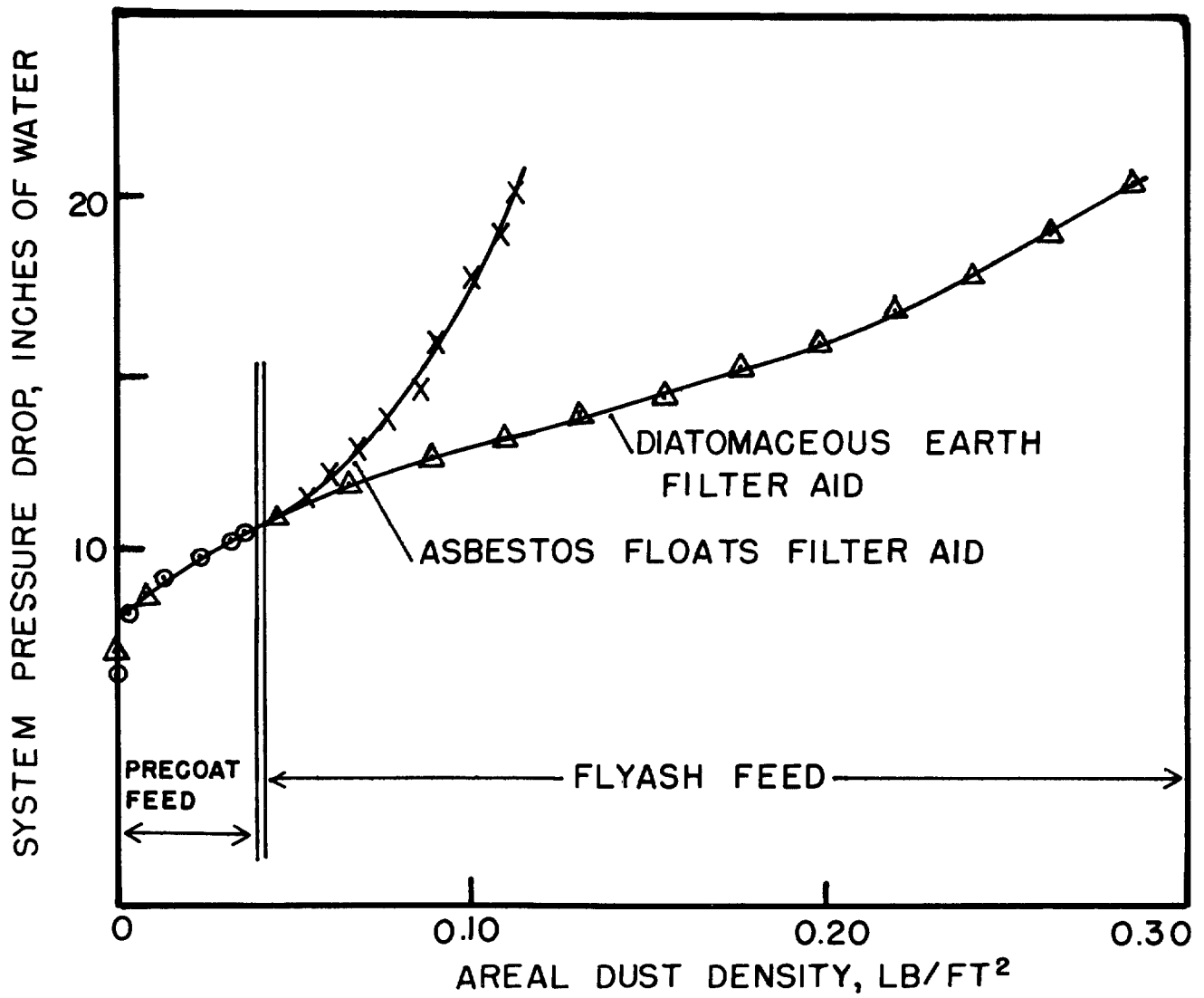


FIGURE 3 PRESSURE DROP VS AREAL DENSITY FOR FILTERS PRECOATED WITH ASBESTOS FLOATS AND DIATOMACEOUS EARTH.

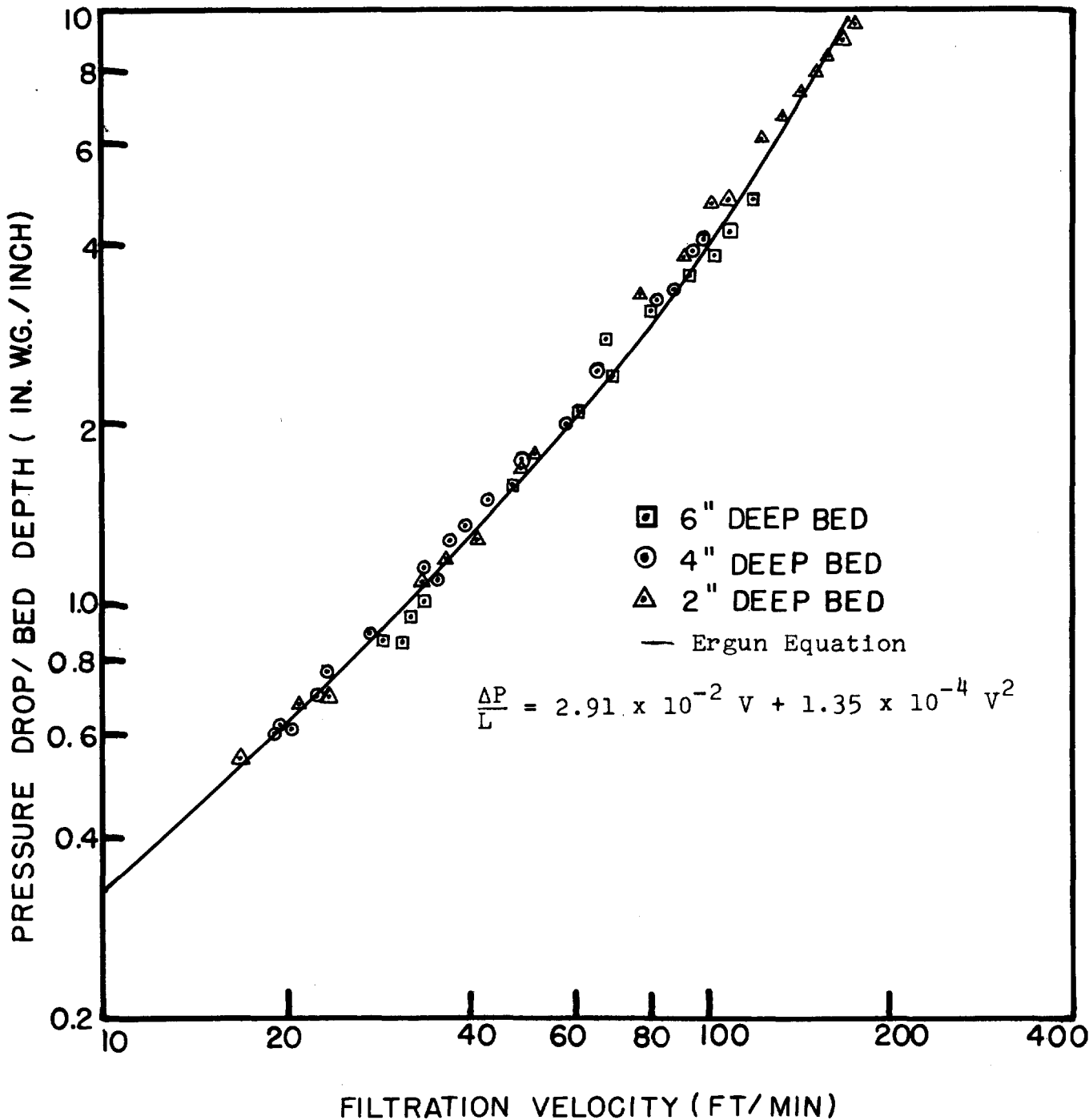


FIGURE 4 PRESSURE DROP PER UNIT BED DEPTH VS FILTRATION VELOCITY, LARGER Na_2CO_3 PELLETS, FIXED BED.

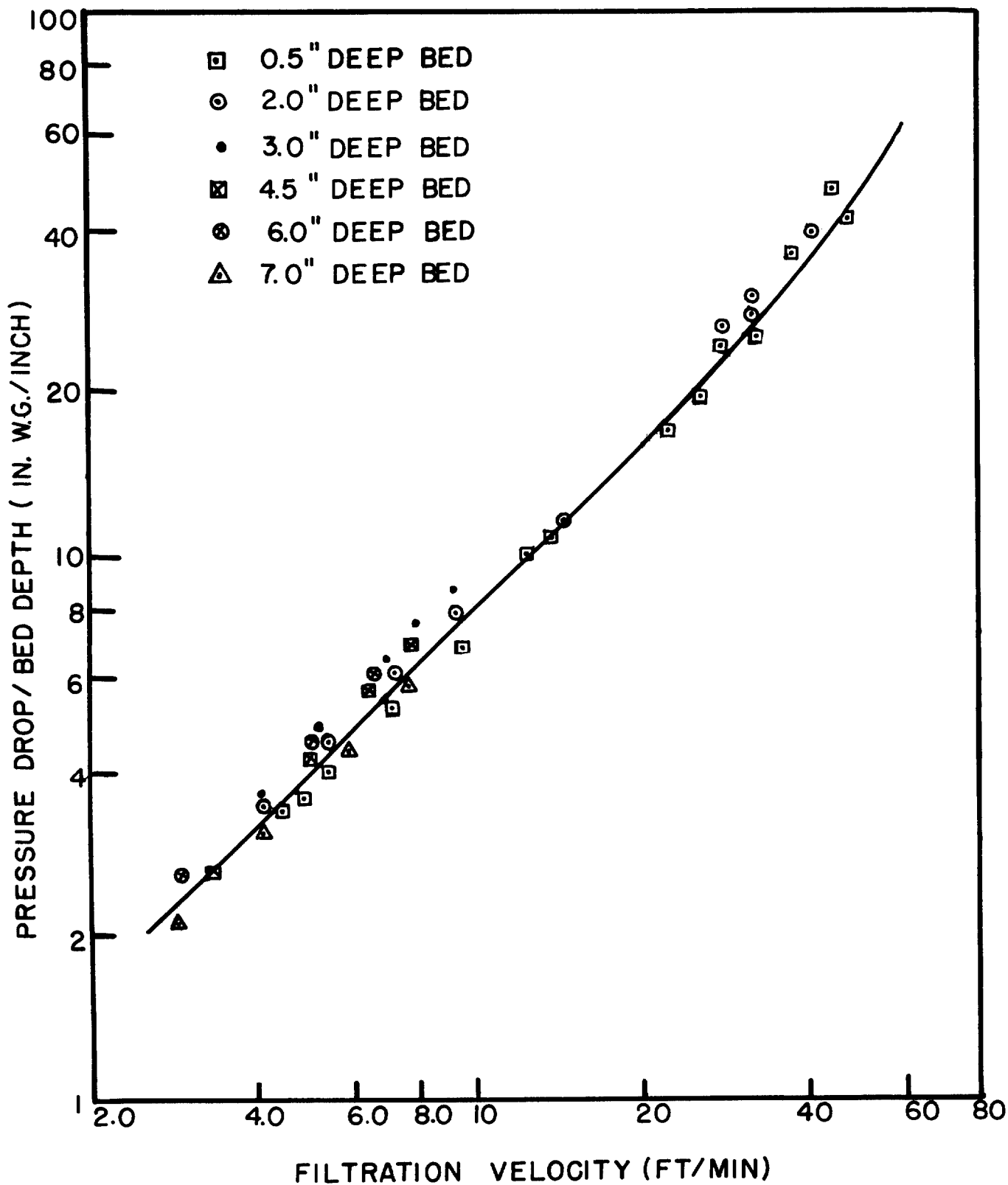


FIGURE 5 PRESSURE DROP PER UNIT BED DEPTH VS FILTRATION VELOCITY, SMALLER Na_2CO_3 PELLETS, FIXED BED.

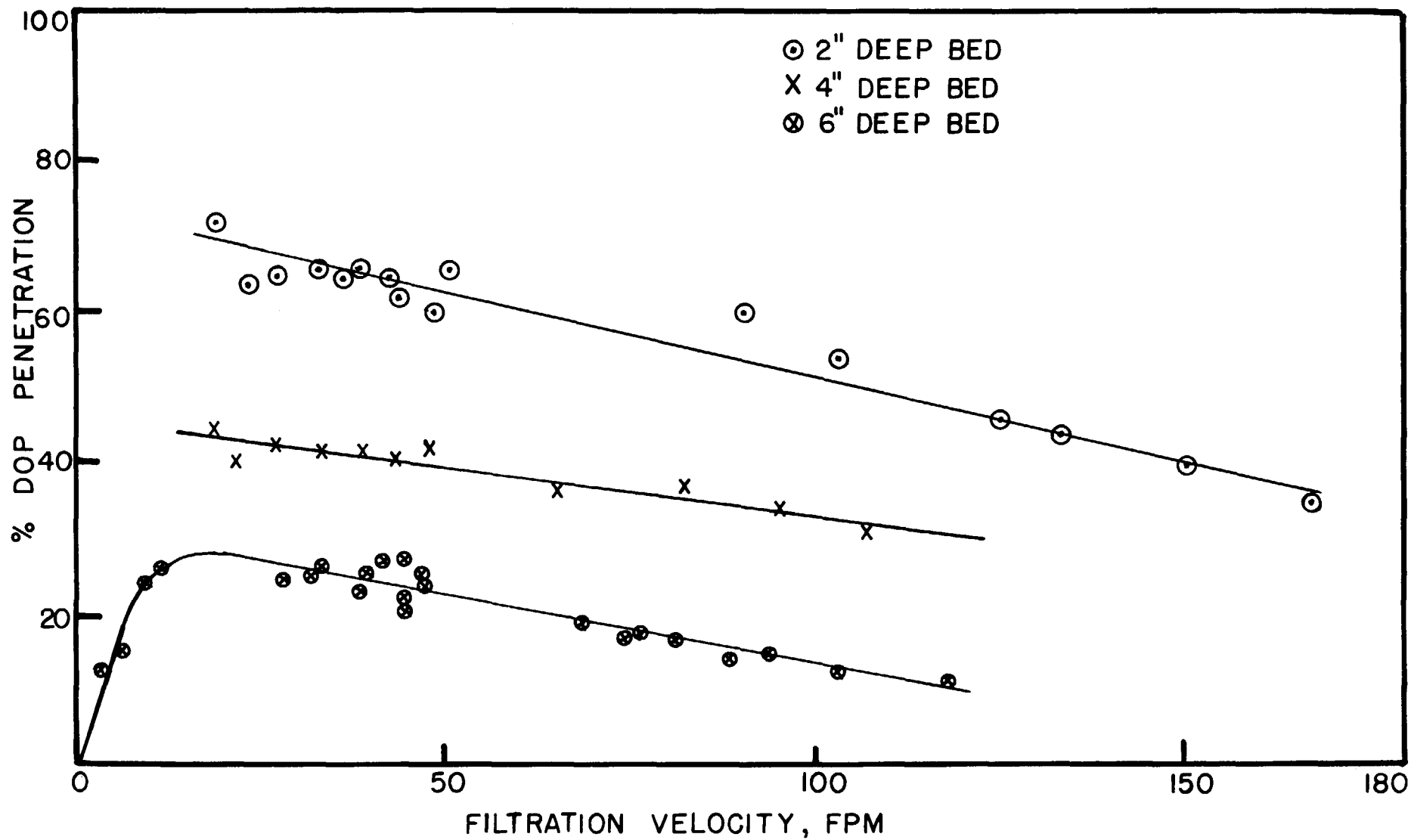


FIGURE 6 COLD DOP PENETRATION VS FILTRATION VELOCITY, BEDS OF LARGER Na_2CO_3 PELLETS.

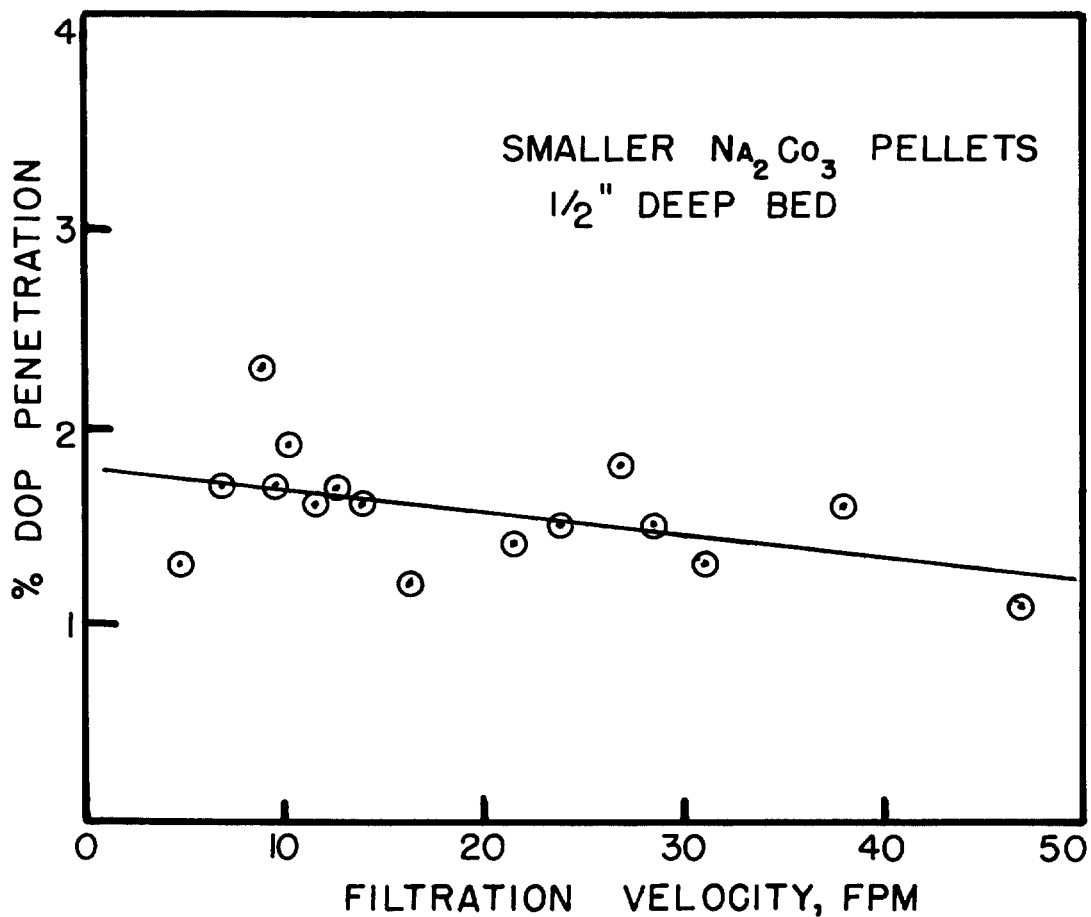


FIGURE 7 COLD DOP PENETRATION VS FILTRATION VELOCITY, BED OF SMALLER Na_2CO_3 PELLETS.

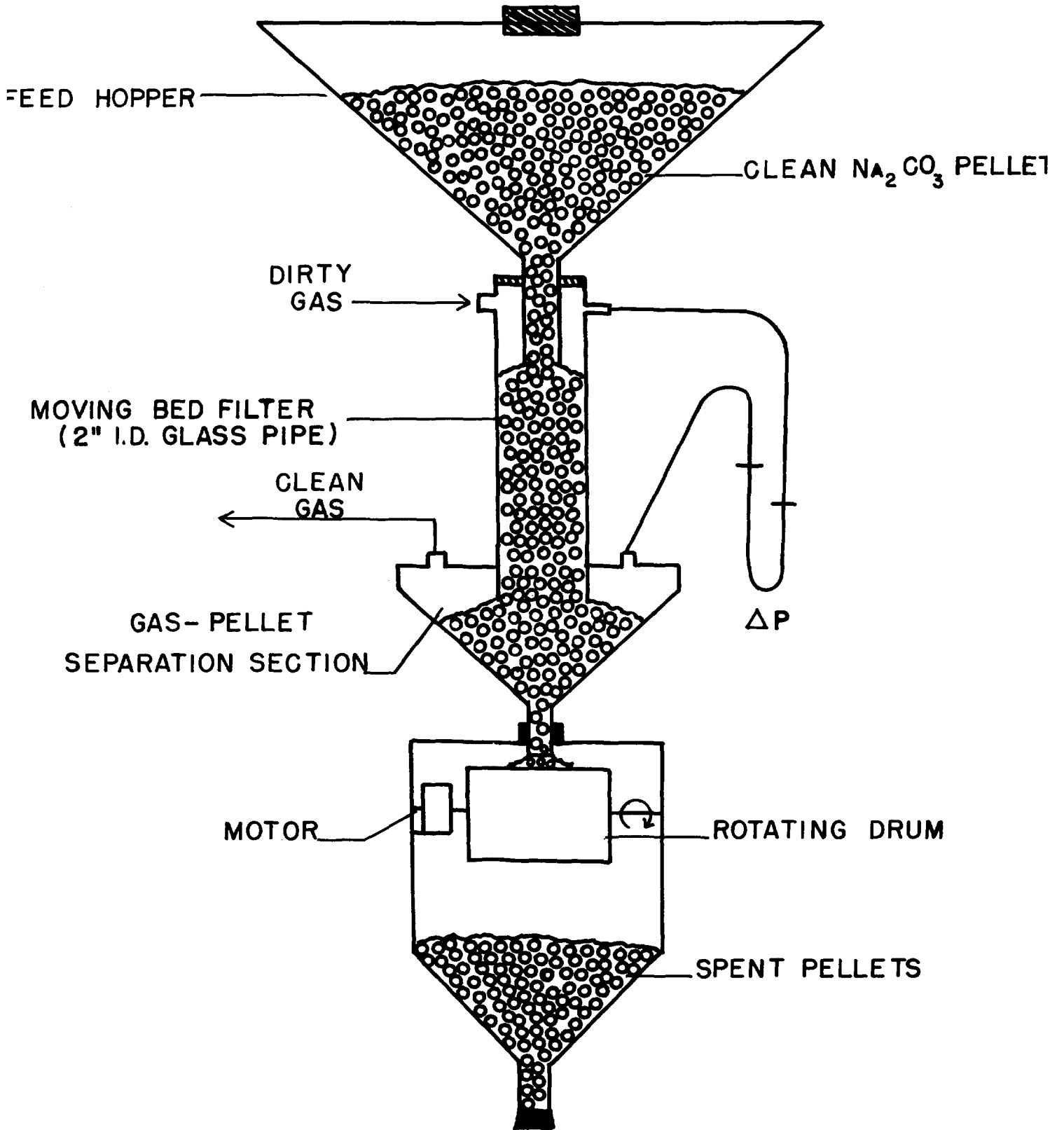


FIGURE 8 Cocurrent moving bed filter.

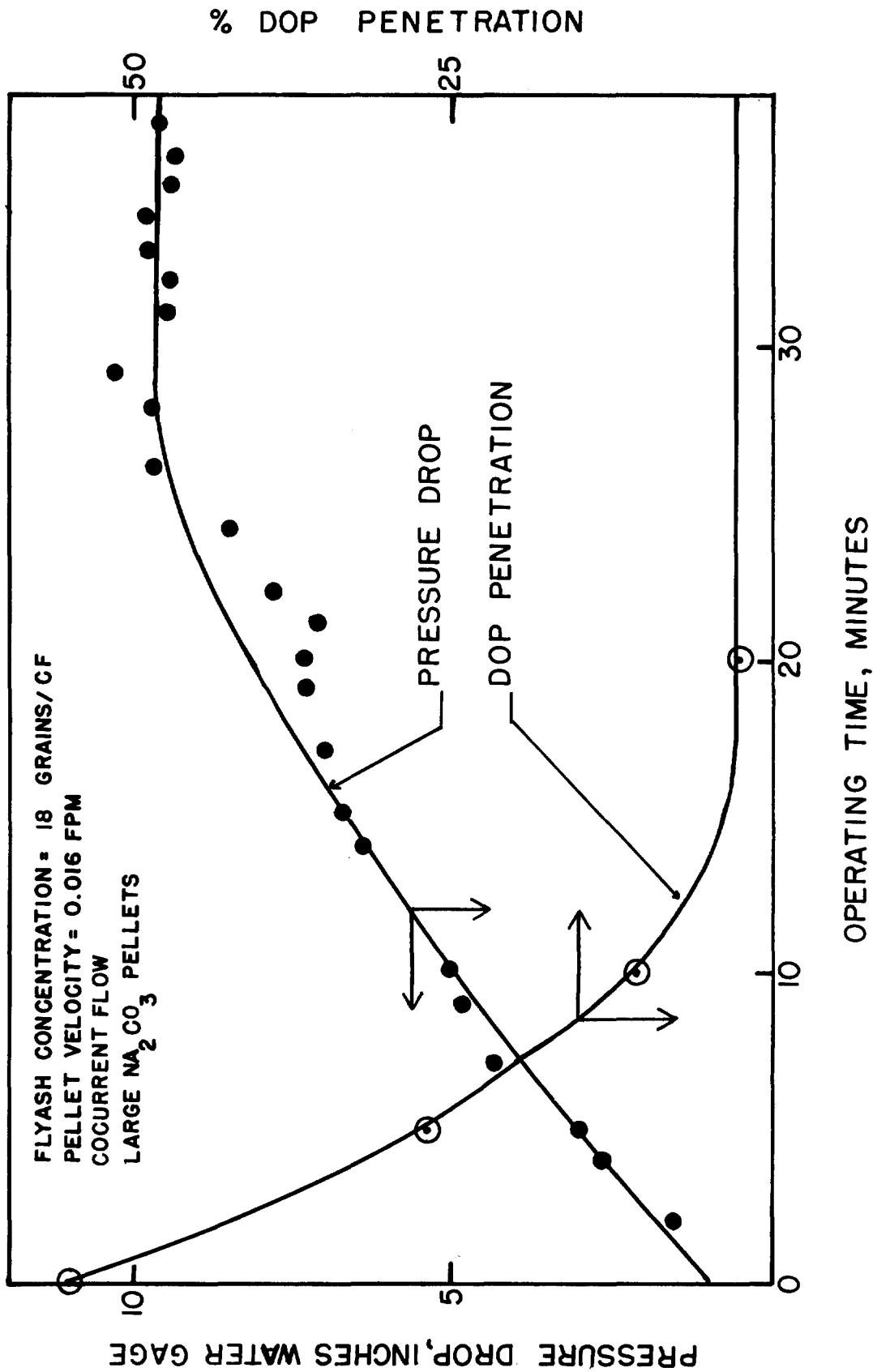


FIGURE 9 PRESSURE DROP AND COLD DOP PENETRATION VS TIME, COCURRENT MOVING BED FILTER

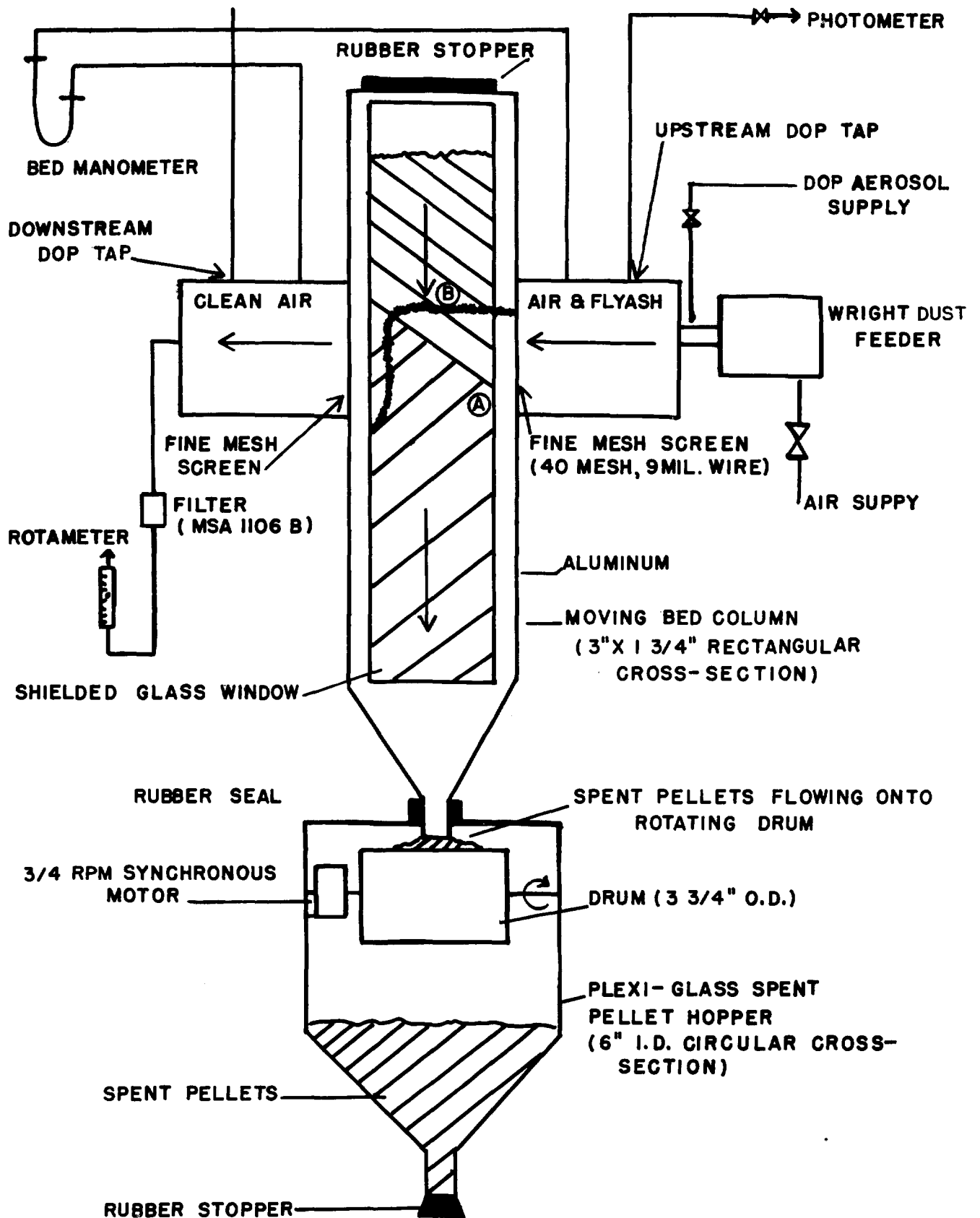


FIGURE 10 CROSSCURRENT MOVING BED FILTER

DISCUSSION

NOTZ: Why did you not test a countercurrent moving bed?

LEITH: The chief problem with a countercurrent bed is that if the gas velocity and pressure drop across it become too high, the bed can fluidize. We did not want to fluidize the bed.

14th ERDA AIR CLEANING CONFERENCE

DESIGN OF OFF-GAS CLEANING SYSTEMS FOR HIGH-LEVEL WASTE VITRIFICATION*

Mark S. Hanson and John D. Kaser**
Battelle, Pacific Northwest Laboratories
Richland, Washington

Abstract

Vitrification of high-level waste to a glassy or ceramic form is being evaluated as a method for final control of high-level nuclear wastes. During vitrification other lower level effluent streams are generated. To obtain complete control of high-level nuclear wastes, all effluent streams from the vitrification system must also be controlled. Off-gas cleanup for the vitrification system poses special problems. The cleanup system must be capable of meeting stringent regulations on both radioactive and nonradioactive pollutants.

High-level wastes are generally nitric acid solutions. Vitrification converts the nitrate salts to oxides, forming nitrogen oxides (NO_x) as a by-product. These NO_x releases can be controlled by nitric acid recovery or by conversion of the NO_x to an acceptable species for release, such as N_2O or N_2 . The off-gas system must also be capable of controlling any fission products which may be volatilized in appreciable quantities and may be controlled in the off-gas system by absorption or adsorption. Whichever method is used, the recovered fission products must somehow be converted to a safe disposal form. Proposed off-gas systems are described, and areas requiring research and development are discussed.

Introduction

Vitrification of high-level waste to a glassy or ceramic form is being evaluated as a method for final control of high-level nuclear wastes. High-level waste is the concentrated remains of chemical solutions used in the reprocessing of nuclear fuels, and contains virtually 100% of the fission products. Although the solutions are aqueous, they do contain undissolved material. Fission products are distributed in both phases.

The conversion of high-level aqueous wastes to solids results in one or more effluent streams with lower levels of activity. The radioactive content of these effluents must be reduced to low levels so that they can be discharged safely. Thus, auxiliary equipment supporting the waste solidification system must be designed to assure sufficient decontamination of effluent streams. Off-gas cleanup must be of sufficient quality to allow the cleaned gas to be released to the atmosphere. Further, the system must be capable of meeting stringent release regulations on both radioactive and nonradioactive constituents.

*Work performed under ERDA Contract E(45-1):1830.

**Presently employed at Atlantic Richfield Hanford Company,
Richland, Washington.

One requirement for the design of the off-gas system is the sufficient cleanup of off-gas to ensure safe operation of the facility. The off-gas system designs depend on many variables: design and operating philosophy, types of solidification equipment, high-level waste composition, allowable release limits, etc. The system can be designed for acid recovery or destruction and many options are available for fission product control.

Process Description

High-level aqueous wastes are generally nitrate salts in nitric acid (HNO_3) solutions. The wastes are the aqueous raffinate from the first solvent extraction step in the Purex process and contain undissolved solids. Fission products are distributed in both the liquid and solid phases. Solidification of these aqueous wastes to insoluble products involves heating the wastes to temperatures above the decomposition temperature of the nitrate salts. This is accomplished by atomizing the waste in a calciner. Various types of calciners are being developed although only two types will be discussed: indirect- and combustion-heated calciners. In an indirect-heated calciner the energy for calcination is provided by resistance or induction electrical heating. A method of indirect heat calcination is spray calcination, in which the high-level waste is atomized into an electrically heated chamber (see Figure 1). In a combustion heated calciner such as a fluidized bed (Figure 2) the energy is provided by the combustion of an organic fuel such as kerosene. Calcining is usually

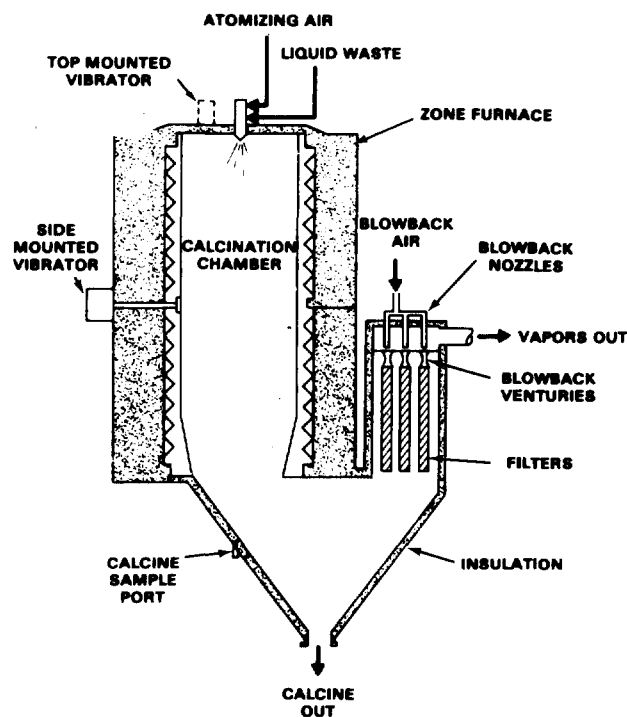


Figure 1 Spray calciner.

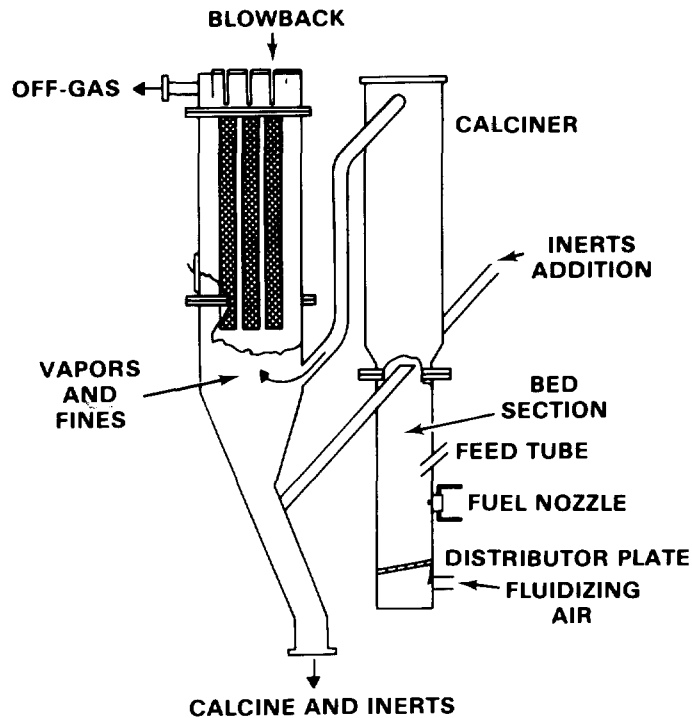


Figure 2 Fluidized bed calciner.

done at a temperature of approximately 500°C. After calcination, the waste is combined with glass-forming materials and falls into a melter where this glass is melted and the waste (now in oxide form) goes into solution with the glass. Melting takes place at approximately 1000°C and the energy for melting is provided by resistance induction, or joule heating (see Figures 3 and 4). Off-gases from the melting process generally pass back into the calciner chamber. These combined melter-calciner off-gases consist of H₂O, nitrogen oxides (NO_x), air, and small amounts of fission products which may be volatilized. As the gas passes through the calcining chamber a large portion of the calcine is entrained. This entrained calcine is then collected on porous sintered metal filters while the process off-gas passes through to the cleanup system. The calcine deposits are periodically blown off the filters by pulses of high-pressure air directed back into the filters by small venturi-type nozzles. The dislodged calcine then falls back into the calciner-melter for processing.

Normal Off-Gas Quantities and Compositions

A 1500-MTU*/yr fuel reprocessing plant will have a typical high-level waste concentration of approximately 378 l/MTU after evaporation. This results in 5.67×10^5 l of high-level waste to be processed per year. For an operating time of 300 days/yr, the vitrification facility must process about 80 l/hr of waste. At a feed rate

*Metric tonnes uranium.

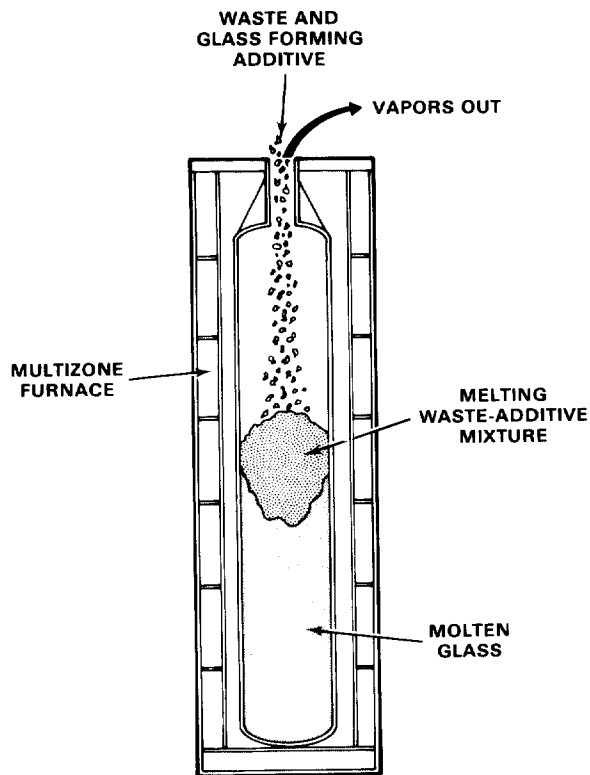


Figure 3 Resistance or induction heated in-canister melter.

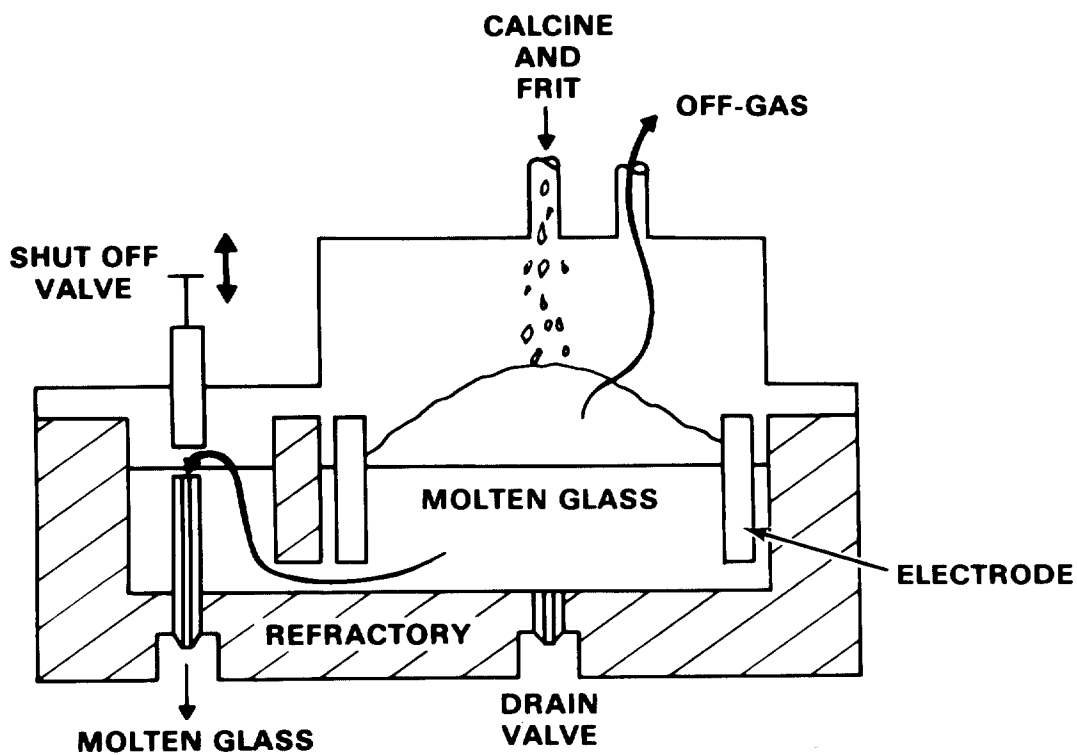


Figure 4 Joule heated ceramic melter.

14th ERDA AIR CLEANING CONFERENCE

of 80 ℓ /hr the off-gas quantity will be approximately 176 actual cubic feet per minute (ACFM) at 350°C and -20 in. H₂O pressure (about 132 ACFM off-gas/ ℓ of feed at these conditions).

Of the 176 ACFM gas produced, about 25 ACFM will be noncondensable with the remainder condensable, mainly steam and NO_x. The volatilized fission products are of extremely small volume when compared to the total volume of gas. As can be seen in Table I, the gas consists mainly of steam, NO_x, and air. The steam and the NO_x are from evaporation and the decomposition of the nitrate salts in the waste while the air is from the pneumatic atomization of the feed as well as from other sources. For example, air may be used for the fluidizing medium in the fluidized bed calciner. Another source of air in the off-gas is inleakage. Since the calciners are operated at less than atmospheric pressure for safety considerations, some air will leak into the system through gaskets and connections.

Table I Typical off-gas composition.*

	Indirect Heating, mole %**	Combustion Heating, mole %
N ₂	49.0	46.2
NO _x [†]	<0.1	0.3
N ₂ O	0.1	0.09
H ₂ O	35.0	35.0
O ₂	15.2	10.4
CO ₂	--	7.4
CO	<0.07	0.6
CH ₄	--	0.01

*Excluding fission products

**Resistance or induction

†Includes N₂O₄

An important constituent of the off-gas is the very small amounts of fission products which may be volatilized or entrained as particulate or droplets in the gas stream. The fission products of particular concern are ruthenium, iodine, and cesium while other potentially troublesome fission products include tellurium and selenium. The following discussions will use fission products levels at discharge of fuel to be conservative. In an actual facility, the waste will be aged and the fission product activities will be lower.

It can safely be assumed that all of the iodine in the high-level waste will pass through the solidification system to the off-gas cleanup system. The high level waste contains about 2% of the iodine in the spent fuel. The waste from a pressurized water reactor (PWR) fuel of 33,000-MWd/MTU burnup at 30-MW power will contain about 5.5 g/MTU of iodine (2.34×10^5 Ci/MTU).⁽¹⁾ At the previously discussed conditions a processing rate of 80 ℓ /hr will therefore give

1.16 g/hr (4.95×10^4 Ci/hr) of iodine being discharged to the off-gas system. Since these levels are at discharge, and it is highly improbable that any fuel this fresh will be processed, a more realistic set of values can be found by discounting the activity of the short half-life isotope ^{131}I (half-life of 8.041 day). Discounting this activity (using a waste age of one year) gives to the off-gas system an activity of 1.59×10^{-4} curies/hr of iodine.

Ruthenium volatility varies widely depending upon the process, the product, and the operating conditions. The formation of borosilicate glass from waste using spray calcination and in-canister melting in the WSEP program⁽²⁾ indicated less than 2% ruthenium volatilities. A typical number of 1% ruthenium volatilization will be used in following discussions. The waste from PWR fuel of 33,000-MWd/MTU burnup at 30-MW power will contain about 2.35×10^3 g/MTU⁽¹⁾ (3.71×10^6 Ci/MTU) of ruthenium. Given the previously discussed conditions and a processing rate of 80 g/hr of waste with 1% losses from the calciner, 4.97 g/hr (7.85×10^3 Ci/hr) of ruthenium will go to the off-gas system.

Cesium losses from volatilization ranged from 0.002 to 0.07% in the WSEP program.⁽²⁾ With 0.07% losses and the same conditions used in the iodine and ruthenium discussions, about 0.4 g/hr (1.04×10^3 Ci/hr) of cesium will go to the off-gas system. Volatility of tellerium and selenium will probably be very low⁽²⁾ and these materials are only mentioned because of their potential to cause problems.

It is assumed that the entrained particulate is a mixture of all the fission products present in the feed excluding the gases (hydrogen, iodine and the noble gases) and the volatilized elements previously discussed. With a conservative vitrification system particulate DF* of 10^3 ,⁽³⁾ approximately 2.43×10^4 Ci/hr of particulate will go to the off-gas system.

In summary, Table II shows the typical amounts of fission products leaving the calciner-melter filters and going to the off-gas system. The degree of decontamination required prior to release is based upon the amount of the isotope present and on the established effluent limit. However, allowable release rates are not well defined in today's licensing environment. The allowable release

Table II Fission products going to off-gas cleanup system.*

<u>Element</u>	<u>Amount, g/hr</u>	<u>Activity, Ci/hr</u>
I	1.16	4.95×10^4
Ru	4.97	7.85×10^3
Cs	0.4	1.04×10^3
Other (Particulate)	--	2.43×10^4

*PWR fuel 33,000 MWd/MTU, 30 MW, 3.3% enriched uranium, at discharge.

*Decontamination factor, as used in this paper, is defined as the ratio of the activity per unit time in the dirty effluent to the activity per unit time in the clean effluent leaving a given unit.

limits were estimated as follows. The 10 CFR-20 limit may be applied to the stack concentration. Since the solidification process is only a part of the whole reprocessing system, its effluents should not represent more than 10% of the allowable limit. The release limit is further reduced for individual isotopes because the limit applies to the total release. Since several isotopes may be present in comparable concentrations the limit for each is somewhat arbitrarily set at 20% of the total. From these factors the allowable stack concentration is 2% of the 10 CFR-20 limit. The DF requirements, based on a stack flow rate of 50,000 cfm, are shown in Table III.

Table III DF requirements for critical isotopes.

<u>Isotope</u>	<u>DF at 6 Months</u>	<u>DF at 2 Years</u>
I - 129	2500	2500
Ru - 106	2.5×10^{11}	0.9×10^{11}
Cs - 137	6×10^{10}	3.5×10^{11}
Particulate	1×10^{12}	1×10^{12}

Off-Gas System Design

The off-gas cleanup equipment supporting the waste solidification system must be designed to assure sufficient decontamination of gaseous effluent streams. The off-gas system must clean the gas sufficiently to meet stringent release regulations on both radioactive and nonradioactive constituents.

Nearly all of the gaseous effluents are condensable. Most that are not can be adsorbed or absorbed (excluding air from atomization, inleakage, etc.). Both condensable and noncondensable streams must be treated to remove radionuclides. The noncondensable streams must be continuously discharged to the atmosphere following treatment. Liquid effluents from the off-gas cleanup system must be treated so they are acceptable for recycle (to a fuel reprocessing plant, for example) or for final release to the environment.

Generally, off-gas cleanup systems can be divided into two categories: with and without acid recovery. Since the aqueous high-level waste is nitric acid based, and the nitrogen oxides from the decomposition of the nitrate salts in the wastes cannot be released to the atmosphere untreated, there is incentive for acid recovery. Also, if the solidification plant is integrated with a fuel reprocessing plant, as will be assumed in this discussion, the recovered acid can be used for fuel dissolution and/or solvent extraction scrub streams. Design of the off-gas cleanup equipment without acid recovery would be reasonable if, for some reason, the acid could not be recycled.

The first stage in the off-gas cleanup is condensation or quenching and, depending upon the type of equipment used, particulate removal. There are two general types of equipment used for the first

stage of cleanup: condensers and scrubbers. The choice would be made depending upon the particular calciner to be used. If the calciner system has potential for high solids loading in the off-gas then an open type scrubber such as a venturi should be used. If the potential for particle loading is low then a shell and tube condenser or a packed bed quench scrubber will be of higher efficiency.

If a shell and tube condenser is used, a single pass with the process fluid on the tubeside allows easy maintenance. Downdraft flow of the vapors in the tubes should be chosen to provide good aerosol de-entrainment, some self-cleaning and good acid absorption. The condenser should be constructed of a highly corrosion resistant material, such as titanium. Shell and tube condensers typically give DFs of 10^3 to 10^4 for ruthenium and 10^3 for particulate. (2,3)

A packed bed type quench scrubber has the advantage of being able to produce high decontamination because of its inherent scrubbing capability. The scrubber can also be divided into two or more sections, accomplishing quenching in one section and scrubbing in another. A packed scrubber has the disadvantages of relatively high pressure drops and plugging potential. Gases entering a packed bed heavily laden with particulate may tend to gum and clog the packing material.

The venturi scrubber can handle relatively high particulate loadings while doing some quenching, and achieves fairly good particulate removal. Acid absorption is not as good as in packed beds. Pressure drop generally varies from high to less than zero depending upon operation (inversely with particulate removal efficiency). Ruthenium DFs of 10 and particulate DFs of 50 to 100 are typical for the venturi scrubber. (4-6)

Of the three pieces of equipment discussed in the previous paragraphs, the venturi scrubber is probably the best choice because of its ability to handle high particulate loadings. In a calciner system using sintered metal filters the possibility of a filter failing does exist. The failure of a filter would allow relatively large volumes of particulate to pass before the equipment could be shut down. If a cyclone separator is used instead of filters, removal efficiency will be normally low. Whenever the possibility of passing large amounts of calcine to the off-gas system does exist, the system should be able to handle it without plugging.

In the next stage of the off-gas cleanup, entrained aerosols are removed. This is accomplished by a knock-out pot or a fiber-type mist eliminator, depending upon what quench technique is used. A venturi would probably require a knock-out pot prior to a mist eliminator to prevent flooding. A mist eliminator type setup will give no volatile ruthenium removal but will give a DF of about 10^3 for particulate. (7)

Assuming that a venturi scrubber followed by a knock-out pot are the first and second stages (Figure 5), the next item in the off-gas train is a condenser which will remove any condensables left after the venturi quenching. This condenser will be similar to the one previously described: a single-pass, downdraft shell and tube condenser with the process fluid on the tubeside.

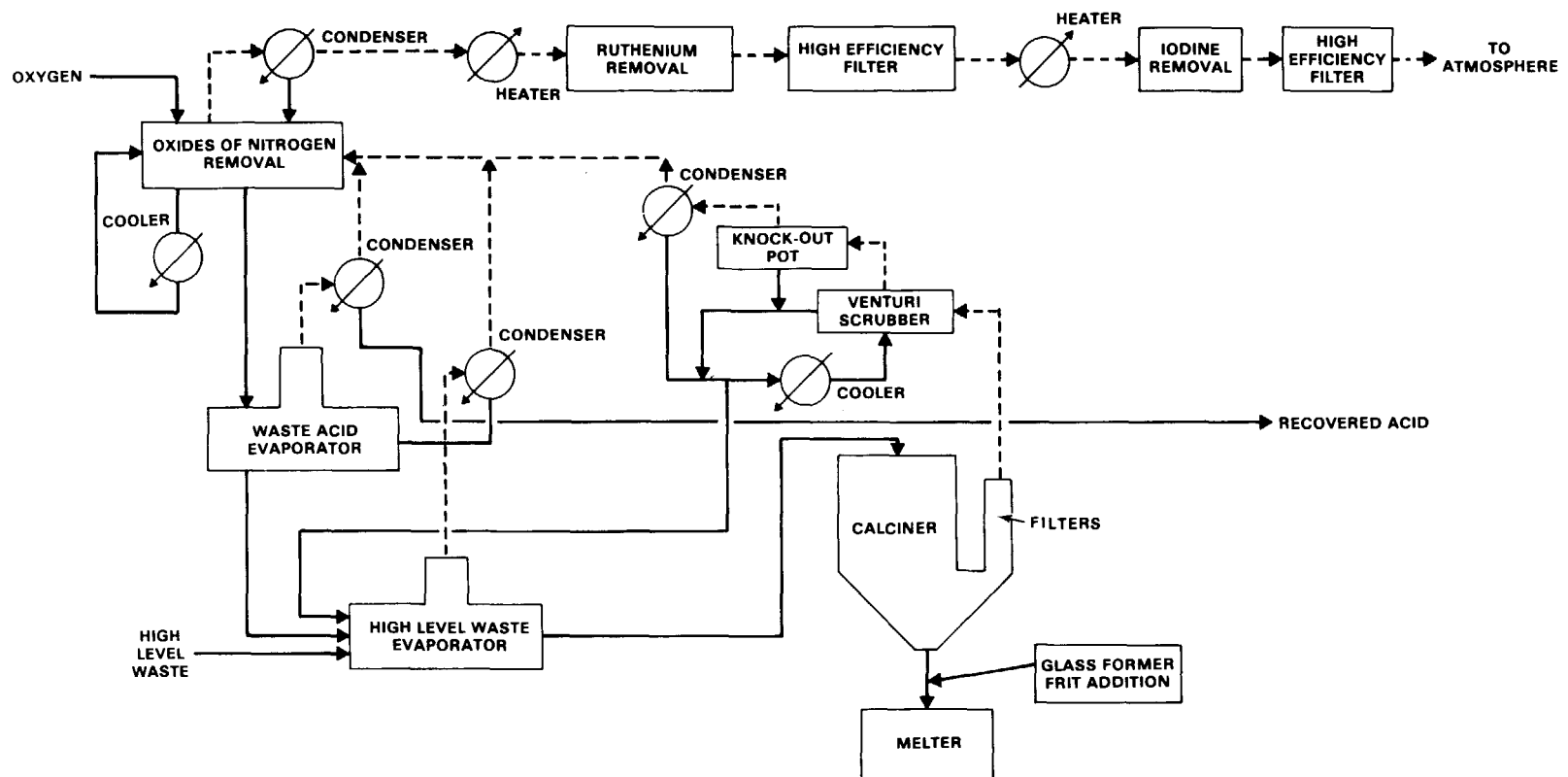


Figure 5 General flow diagram.

Nitrogen Oxide Control

During the next stage in the off-gas train (nitrogen oxide control), the acid will be recovered or destroyed. Control methods may be grouped in three major classes: absorption, conversion, and adsorption.

Absorption. Absorption consists of contacting the gases with liquid, absorbing the NO_x into the liquid. If water or nitric acid is used as the scrubbing liquid, nitric acid may be recovered. Using other liquid scrubbing agents generates a new liquid waste stream.

Absorption of NO_2 into acid solutions takes place as follows:



NO must be oxidized to NO_2 before it can react:



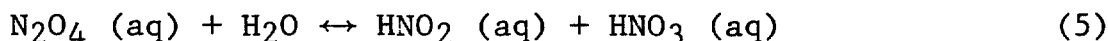
N_2O_4 is an equilibrium product of NO_2 and will react in place of NO_2 in Equation (1):



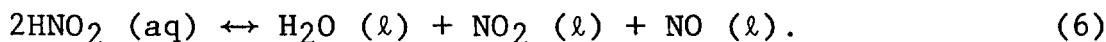
The overall reaction in Equation (1) takes place in several steps. Wendel and Pigford⁽⁸⁾ studied NO_2 absorption and analyzed the results using the penetration theory. The absorption process begins with the dissolution of N_2O_4 gas in water:



This reaction is considered fast; the equilibrium constant is related to the Henry's law coefficient. After entering the liquid phase, the N_2O_4 diffuses away from the gas-liquid interface and reacts with water:



This reaction is considered to be the rate limiting step in the absorption of NO_x in aqueous solutions.⁽⁴⁾ The HNO_2 is unstable in acid solutions and decomposes into H_2O , NO_2 and NO :



The NO is highly insoluble in water and escapes back to the gas phase. Thus, the evolution of NO from the liquid to the gas phase presents a significant limitation on absorption efficiency of NO_2 by acid solutions. Each absorbed mole of NO_2 produces 1/3 mole of NO which must be oxidized before it can be reabsorbed. This oxidation reaction can also be considered as a rate limiting step in the absorption of NO_x into aqueous solutions.

Peters⁽⁹⁾ researched NO_2 absorption efficiency in various absorbers. He found that venturis and spray towers were the poorest absorbers, while packed scrubbers gave intermediate performance, and

bubble cap towers and fritted bubblers gave the best performance. For all of the scrubbers, NO_x removal efficiency decreased with decreasing concentration of NO_2 in the entering gas.

Further, Peters⁽⁹⁾ found that the addition of NaOH has only a minor effect on NO_x removal efficiency. Pennak et al.⁽¹⁰⁾ also found that using NaOH in the scrub solution only gave a minor increase in the efficiency of NO_x removal. Also, the use of NaOH is unattractive because the acid is not recovered and another liquid waste stream is produced.

Efficiencies in removing nitrogen oxides by aqueous scrubbing are typically low. Very few scrubbers⁽⁹⁻¹¹⁾ have shown more than 90% removal of NO_x ; most range from 20 to 70%. Absorption will give a DF of about 10 to 10^2 for ruthenium and 10 for particulate.⁽¹²⁾

A mist elimination step will be required following the absorber to remove any entrained liquid.

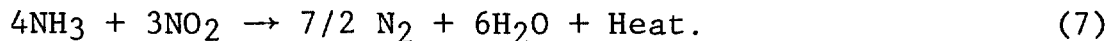
Conversion. Conversion involves the reaction of NO_x to form N_2 and other innocuous gases. A reactant and sometimes a catalyst is required to accomplish the conversion, and acid is destroyed. The three major conversion methods are thermal reduction with hydrocarbon fuel, catalytic reduction with hydrocarbon fuel, and catalytic reduction with ammonia.

Thermal reduction with hydrocarbon fuel involves reducing NO_x to N_2 and H_2O by using a fuel such as propane or natural gas. Temperatures are typically high (1800 to 2000°F).⁽¹³⁾ An NO_x concentration reduction of 90% is possible using 8% combustibles (C_3H_8).⁽¹³⁾ Fuel costs are high because all oxygen in the stream must be consumed before the NO_x is reduced.

Gillespie et al.⁽¹⁴⁾ and Reed and Harvin⁽¹⁵⁾ have studied the use of natural gas in the presence of noble metal catalysts to reduce NO_x . In this case the catalyst operates at temperatures of about 1200 to 1400°F. This enables the catalytic reducer to operate with less fuel than the thermal reducer. However, catalyst life may be short because the operating temperatures are near the catalyst's upper limit capability.

The reduction of NO_x with ammonia over a catalyst is probably the most promising conversion system. The reaction takes place at relatively low temperatures, ammonia reacts only with NO_x , and high degrees of conversion are possible. The process consists of mixing gaseous NH_3 with the process off-gas and passing the mixture through a heated catalyst. Typical catalysts are metal-impregnated alumina and silica,^(14,15) metal exchanged zeolite,⁽¹⁶⁾ and hydrogen and sodium forms of zeolite.⁽¹¹⁾ The reaction forms the products N_2 and H_2O , and sometimes N_2O . A system similar to this is presently being used by Exxon Nuclear Company to eliminate NO_x in the off-gas from the dissolution of uranium oxides. The operation is described by Mays and Schwab.⁽¹⁷⁾ This off-gas is similar to off-gas from the waste solidification process in terms of NO_x emissions. The 25-cfm off-gas stream requires a bed of 10 in. in diameter and 8 in. deep. The catalyst used is 1/16 in. diameter zeolite extrudates. The off-gas is mixed with 50 to 100% excess ammonia and passes down through the bed at a

temperature of 750°F. The conversion reaction(16,17) is:



The reaction rate must be carefully controlled since the bed temperature increases significantly during the conversion (up to 1400°F) due to the exothermic reaction. Conversion efficiencies greater than 99% have been reached.(17) Explosion hazards do exist due to the potential formation of NH_4NO_3 below 600°F. Some type of temperature control is necessary to maintain required bed temperatures and cut the feed if the bed temperature should drop.

Adsorption. Adsorption involves the removal of NO_x from the gas stream by uptake on the surface of solids. Since the process must be cyclic, involving solids regeneration or disposal, two or more sorption beds are required to allow simultaneous adsorption and regeneration or disposal. If the beds are regenerated, the desorbed NO_x would be of relatively high concentration and NO_x control by adsorption would be necessary. The absorption would now be of higher efficiency due to the higher NO_x concentrations. Although high adsorption efficiencies are possible, large beds are required.

Final Off-Gas Cleanup. Up to this point, the gas stream has been treated to remove most of the condensables and the entrained particulate while the NO_x has either been recovered as acid or destroyed. Final cleanup must now be made to remove any fission products that have come through the system, either as volatiles or as particulates. As was stated earlier, the two fission products of primary concern are ruthenium and iodine which can come through the previous parts of the off-gas cleanup system. Since iodine removal methods also tend to remove some ruthenium, but ruthenium removal methods trap little iodine, the ruthenium is trapped first.

Ruthenium Adsorbers. Wet scrubbing is an inefficient method of ruthenium removal, so adsorption is generally used. The adsorbent must be able to: 1) adsorb large quantities of ruthenium while reducing ruthenium concentration in the off-gas effectively, 2) be resistant to attack from the off-gas, and 3) withstand the radioactive environment. There are two ways to handle the adsorption: with and without adsorbent regeneration. If the adsorbent is to be regenerated, it must permit ruthenium desorption quite easily, be resistant to attack from the desorption agent, and have the ability to adsorb effectively after regeneration. If the adsorbent is not to be regenerated, it must be disposable. Since the ultimate disposal method would be to place the adsorbent into the waste glass, the adsorbent should hold most of the adsorbed ruthenium at high temperatures.

Potential ruthenium adsorbers include silica gels, ferric oxide, hydrous zirconium oxide gel, phenolic based ion exchange resins, styrene-divinyl-benzene ion exchange resins, acid resistant molecular sieves, porous glass, impregnated alumina, copper sulfide, zirconium oxide hydrate-dithionite, etc. Of these, silica gel and ferric oxide best meet the requirements for the adsorbent.

- Silica Gel. Barnes and Newby(18) studied the ruthenium adsorption characteristics of silica gel for use in the New Waste Calcining

Facility at the Idaho Chemical Processing Plant. They obtained ruthenium adsorption capacities of greater than 4.8×10^{-3} g ruthenium/cm³ of gel (6-12 mesh particle size bed) and determined that decontamination factors of 10^3 or better are possible, depending upon the depth of the bed. Further, they found that the silica gel can be effectively regenerated (about 80% of the ruthenium can be removed) and that regenerated silica gel adsorbs ruthenium as well as nonregenerated gel. The best operating conditions were found to be at a temperature slightly above the dewpoint of the gas and with a superficial velocity of about 0.4 ft/sec, giving pressure drops of about 1.0 in. of water/in. of bed height. Other investigators have shown similar results. (19,20)

- Ferric Oxide. Elliot et al. (21) found that DFs of 10^3 could be obtained with ferric oxide as the adsorbent. The adsorbent was at a temperature between 150 and 250°C and the superficial velocity about 3 ft/sec. The adsorbent was found to have a capacity greater than 4×10^{-2} g ruthenium/cm³ of bed (18 to 25 mesh particle size bed). Elliot described a system in which the spent adsorber could be put into the glass canister. (21) Barnes and Newby (18) found that ferric oxide cannot be effectively regenerated and the material does not effectively adsorb ruthenium after regeneration. Based on this data, ferric oxide must be used as a nonregenerable adsorber to be disposed in the glass when saturated. The cost of ferric oxide is low, allowing this type of operation.

Depending on whether regeneration is attractive, either silica gel or ferric oxide will effectively remove ruthenium from the off-gas stream.

- Iodine Control. Iodine control is best obtained by using solid adsorbents. Inorganic adsorbents are chosen over wet scrubbing methods and organic adsorbents because they allow a simple design, are relatively noncorrosive, and can be put into permanent storage or recovered as necessary. Adsorbents having potential for use include silver and other metal-exchanged zeolites, silver impregnated, amorphous silicic acid, aluminum and silver oxides, and silver and other metal cation impregnated alumina. Impregnated carbons have potential but may react violently with NO₂. Although only about 15% of the adsorbent is utilized before breakthrough (22) only small amounts are used: 4.2 ft³/yr of iodine containing adsorbent would be accumulated at the previously discussed processing rates. After NO₂ and moisture are removed the product is ideal for long-term storage and decay heat will not be a major problem since the decay energy of ¹²⁹I is low. If silver is used in the adsorbent, high costs may warrant recovery for reuse. Recovery costs will be dependent upon the degree of contamination of the adsorbent by other fission products and the ease of desorption. Should the adsorbent be recovered, some method of disposal must then be found for the desorbed iodine. Decontamination factors of 10^3 or better are obtainable depending upon the adsorbent depth. (22)

Final particulate filtration is used to prevent any particle or entrained droplets from leaving the system. High efficiency particulate filters which provide particulate DFs of 10^3 per stage are used.

Special Problems and R&D Requirements

There are some special areas where problems exist and where further R&D is warranted. The questions of mercury and carbon-14 control are examples of necessary R&D. Since mercury is highly volatile, most mercury in the feed to the calciner-melter system will pass through into the off-gas. Thus, the off-gas system may have to collect and contain the mercury. Carbon-14 has a long half-life (5700 yr) and may have to be controlled.

More R&D is needed in the area of the use and disposal of fission product adsorbers. Can the adsorbers be regenerated successfully? What should be done with the desorbed fission products to prevent revolatilization? Can the adsorbers be successfully placed in the glass with the fission products?

Many of the problem areas will be best researched in an operating situation. None of the problems appear insurmountable and, with the many routes possible in an off-gas train, most problem situations can be overcome.

References

1. M. J. Bell, "ORIGEN - The ORNL Isotope Generation and Depletion Code," USAEC Report ORNL-4628, 1973.
2. W. R. Bond et al., Waste Solidification Program, Volume 8, Spray Solidification Performance During Final Radioactive Tests in Waste Solidification Engineering Prototypes, BNWL-1583, June 1971.
3. J. L. McElroy et al., Waste Solidification Program Summary Report, Volume 11, Evaluation of WSEP High Level Waste Solidification Processes, BNWL-1667, July 1972.
4. 6th AEC Air Cleaning Conference, USAEC Report TID-7539, B. R. Wheeler, "Waste Calcination Off-Gas Studies," July 1959.
5. 6th AEC Air Cleaning Conference, USAEC Report TID-7539, E. F. Edwards, "Waste Calciner Off-Gas System," July 1959.
6. 6th AEC Air Cleaning Conference, USAEC Report TID-7539, H. S. Jordan, G. G. Weltz, "A Venture Scrubber Installation for the Removal of Fission Products from Air," July 1959.
7. Brink Fact Guide, Monsanto Enviro - Chem. Systems, Inc., 1975.
8. M. M. Wendel and R. L. Pigford, "Kinetics of Nitrogen Dioxide Absorption in Water," AIChE Journal, vol. 4, pp. 249-256, 1958.
9. M. S. Peters, "Principles and Processes for Removing Nitrogen Oxides from Gases," Report COO-1015, Engineering Experiment Station, University of Illinois, Urbana, IL, August 1958.

14th ERDA AIR CLEANING CONFERENCE

10. A. F. Pennak, N. R. Leist, and R. C. Kispert, "Reduction of Nitrogen Oxides in Vent Gases by Scrubbing," Proceedings of AEC Pollution Control Conference, Oak Ridge, TN, CONF-721030, October 1972.
11. T. G. Thomas, "Oxides of Nitrogen," Technical Alternatives Document, ERDA-76-43, 1976.
12. C. E. May, K. L. Rohde, B. J. Newby, and B. D. Withers, Ruthenium Behavior in a Nitric Acid Scrubber, USAEC Report IDO-14448, September 1958.
13. G. E. Benedict, G. R. Kiel, and G. J. Raab, "Test Experience with a Commercial NO_x Destructor," ARH-SA-140, Atlantic Richfield Hanford Company, Richland, WA, October 1972.
14. G. R. Gillespie, A. A. Boyum, and M. F. Collins, "Nitric Acid: Catalytic Purification of Tail Gas," Chem. Eng. Progress, vol. 68, pp. 72-77, April 1972.
15. R. M. Reed and R. L. Harvin, "Nitric Acid: Nitric Acid Plant Fume Abaters," Chem. Eng. Progress, vol. 68, pp. 78-79, April 1972.
16. D. T. Pence and T. R. Thomas, "NO_x Abatement at Nuclear Processing Plants," Proceedings of the Second AEC Environmental Protection Conference, WASH-1332(74), April 1974.
17. E. M. Mays and M. R. Schwab, "Elimination of NO_x Fumes," Chemical Engineering, p. 112, February 1975.
18. B. J. Newby and V. H. Barnes, "Volatile Ruthenium Removal from Calciner Off-Gas Using Solid Sorbents," USERDA Report ICP-1078, July 1975.
19. D. H. Rhodes, D. R. Anderson, "Capacity Test Data for the Adsorption of Volative Ruthenium on Silica Gel," USAEC Report IDO-14510, June 1960.
20. D. A. Hanson, B. J. Newby, and K. L. Rohde, "The Adsorption of Ruthenium from Nitric Acid - Air Mixtures," USAEC Report IDO-14458, June 1959.
21. M. N. Elliot, R. Gayler, J. R. Grover, and W. H. Hardwick, "Fixation of Radioactive Waste in Glass. Part III. The Removal of Ruthenium and Dust from Nitric Acid Vapours," from Proceedings of the IAEA Symposium on the Treatment and Storage of High-Level Radioactive Wastes, Vienna, October 1962.
22. D. T. Pence and B. A. Staples, "Solid Adsorbents for Collection and Storage of Iodine-129 from Reprocessing Plants," Presented at the 13th USAEC Air Cleaning Conference, August 1974.

DISCUSSION

BURCHSTED: Is there a possibility of trapping the mercury upon activated carbon that has been properly impregnated?

HANSON: There is a possibility, but we're afraid of having nitrogen oxides passing through our scrubbing system which might cause problems with the charcoal.

FIRST: In connection with nitrogen oxide removal by scrubbing with water, our experiences are very unfavorable. One seldom gets more than about 35 to 45 per cent with water scrubbing at ambient temperatures and ambient pressures. How do you intend to cope with this?

HANSON: We hope to pick up a little bit of efficiency by cooling our scrub stream. Initially, we will be using water. After we are operating, we will be using a weak acid to scrub.

VAN BRUNT: You showed a DF of around 10^{11} . I was wondering about this as it is rather different from the 10^3 DF shown for the adsorber.

HANSON: Yes, there is a difference. The DF of 10^3 is for the adsorber and the 10^{11} is for the entire system.

VAN BRUNT: What kind of DF's do you expect from the absorber?

HANSON: A DF of 10^3 is expected. This can be varied by bed depth, i.e., absorbent depth.

VAN BRUNT: Even with high temperatures?

HANSON: There will be temperature effects, so that the bed temperature will have to be controlled to maintain it within a certain range. By the time we get to the absorbent beds, the gas will be close to ambient temperature.

⁸⁵KR STORAGE BY ZEOLITE ENCAPSULATION*

R. A. Brown, M. Hoza, and D. A. Knecht
Allied Chemical Corporation
Idaho Chemical Programs - Operations Office
Idaho National Engineering Laboratory
Idaho Falls, Idaho 83401

Abstract

This paper describes the technology of ⁸⁵Kr storage by zeolite encapsulation. The process of encapsulation takes place at high temperatures and pressures, and involves the activated diffusion of krypton into zeolite cages. Experimental results for krypton encapsulation in various zeolites are reviewed and discussed. Activated diffusion parameters determined by measuring krypton leakage rates from zeolites at high temperatures and low pressures are used to estimate leakage rates of ⁸⁵Kr during long-term storage. The potential safety benefits are determined for krypton-85 storage by encapsulation in sodalite. Requirements for pilot-scale and process-scale development are discussed briefly.

I. Introduction

Of the noble gases formed by nuclear fission (krypton and xenon), only krypton-85 (⁸⁵Kr) has a half-life sufficiently long to be present at the time of fuel reprocessing. Most of the ⁸⁵Kr in the fuel is released during shearing and dissolution and is removed by the off-gas stream at low concentrations. While the technology exists for dispersal of ⁸⁵Kr to the atmosphere, methods have been proposed for its collection and storage to avoid potential local hazards and long-term global build-up⁽¹⁾.

Annual requirements for storing ⁸⁵Kr (using methods which are applicable to commercial-scale fuel reprocessing) are presented in Table I^(2,3). The production of ⁸⁵Kr from a 1500 tonne/yr reprocessing plant is assumed** to be 9.81 MCi/yr⁽⁴⁾. Pressurized cylinders⁽³⁾ and zeolite encapsulation are compared in Table I. Krypton is assumed to have a relatively pure composition; if impurities such as xenon are present, increased storage positions will be needed in the storage facility. Storage in pressurized cylinders is considered to be available technology. Although storage by zeolite encapsulation will require further development before a production-scale system can be constructed and operated⁽¹⁾, there are potential additional safety benefits in zeolite encapsulation (see Section IV). A program is under way at the Idaho National Engineering Laboratory (INEL) to develop both storage methods to a conceptual design level for a production-scale system.

*Work performed under USERDA Contract E-(10-1)-1375 S-72-1

**Based on a burnup of 25,000 MWd. A burnup of 33,000 MWd would produce 16.8 MCi.

14th ERDA AIR CLEANING CONFERENCE

Table I. Annual ^{85}Kr storage requirements for a
1500 tonne/yr reprocessing plant.*

Storage Method	Pressure		Amount Zeolite, kg	Storage Temperature, °C	Number of 50- λ Cylinders
	Atm	Psi			
Pressurized Cylinders	35	500	--	60**	77
	137	2000	--	127**	24
Zeolite Encapsulation [†]	--	--	2800	120 ^{††}	82

This paper will describe the technology of ^{85}Kr storage by zeolite encapsulation. A technical description of zeolite encapsulation in general will be presented, and laboratory-scale results will be reviewed and will be used to predict long-term storage behavior of krypton-85 in sodalite and zeolite 3A. A brief discussion of the development required for a process-scale encapsulation system will conclude this paper.

II. Technical Description

Zeolite materials are crystalline aluminosilicates which contain a regular array of interconnected cages of uniform size⁽⁵⁾. For a given zeolite type, the cage dimensions are uniquely deter-

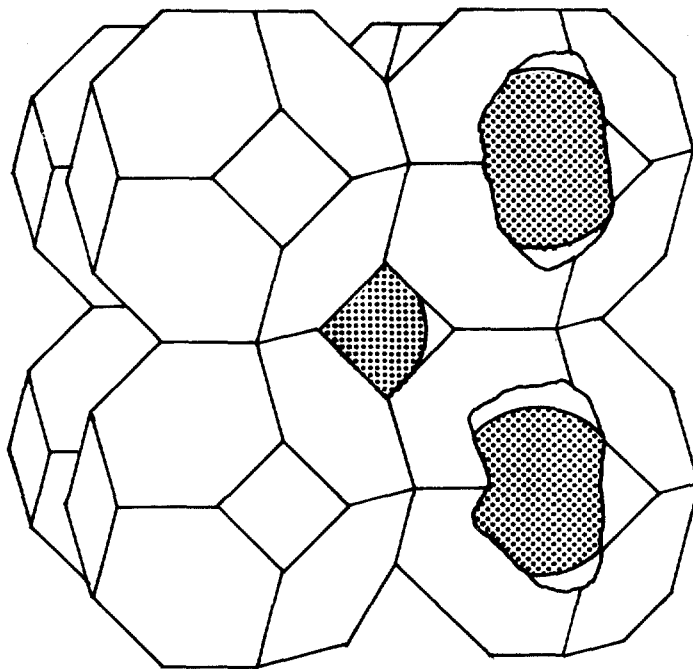


Figure 1. Representation of sodalite cages containing krypton atoms.

*Annual production : 9.81 MCi of 6% ^{85}Kr in krypton; based on a burnup of 25,000 MWd.

**Wall temperature

†Assumed loading : 1.8×10^{-3} mole (40 cm^3 STP) Kr g^{-1} zeolite.

††Mean temperature: center-line temperature is 150°C . See Section IV.

mined by the structure of the crystal⁽⁵⁾. Figure 1 shows the structure of a group of sodalite cages, each containing one atom of krypton. Each sodalite cage consists of a truncated octahedron (~ 6.6 Å free diameter). Each six-ring face is shared with adjoining sodalite cages to make up the overall crystal structure. The krypton atom shown occupying each cage has a room-temperature gas-kinetic diameter of ~ 3.5 Å. Not shown in Figure 1 are the cations (such as sodium) attached to various locations on the aluminosilicate framework. Cations which partially block cage openings (e.g., the six-ring face in Figure 1) can be exchanged with larger or smaller cationic species to alter the dimensions of the opening. Such a modification can have a strong effect on the diffusion of gas molecules.

The process by which krypton diffuses through such a pore structure is known as activated diffusion, since an activation energy is required for krypton atoms to pass through the 2.3 Å apertures⁽⁵⁻⁷⁾. At high temperature and pressure (450°C, 1000 atm)⁽⁶⁾, there is sufficient energy for krypton to diffuse into the crystalline sodalite cages, while at low temperatures (<150°C) the encapsulated krypton does not have enough energy to diffuse out at appreciable rates. Thus, krypton can be introduced into the cages at conditions corresponding to rapid diffusion and then trapped in sodalite at ambient external pressure, even though each krypton atom experiences a high effective "pressure" inside its cage.

While sodalite appears to be a promising trapping medium, krypton encapsulation should be possible with other zeolites. Zeolites with larger cage diameters may be used if the cage openings are kept narrow by suitable ion exchange. Such zeolites include the potassium, cesium, or rubidium-exchanged forms of zeolite A, chabazite, and erionite. Some data on zeolite 3A (potassium-exchanged A) will be presented in Section III.

III. Experimental Results

The experimental study is divided into two general areas: encapsulation and leakage measurements. Experimental encapsulation and leakage studies of krypton in sodalite and zeolite 3A, which have been made at the INEL and elsewhere^(5, 6, 8, 9), will be reviewed and discussed. Theory will be used in interpreting the experimental data and will allow predictions of long-term storage behavior of ^{85}Kr (Section IV).

Encapsulation

A typical process flowsheet for encapsulating krypton in zeolite is shown in Figure 2. Activated zeolite (with interstitial water removed) is loaded into the pressure vessel and heated to the encapsulation temperature. Krypton is introduced at the encapsulation pressure for a preselected time. The temperature is lowered, and the unencapsulated krypton is recycled to the storage cylinder. The krypton-containing zeolite is then removed for further testing. The laboratory-scale system in use at the INEL was obtained commercially and consists of two diaphragm compressors

connected in series to a 250 cm³ vessel (A-286 alloy composition) enclosed in a heating blanket. At temperatures below 500°C, the vessel can be pressurized to 2000 atm (30,000 psi). As the temperature is increased from 500 to 650°C, the maximum operating pressure is decreased from 2000 to 1630 atm (24,000 psi), respectively, at the same safety factor. The high pressure system is housed inside a steel barricade for personnel protection from accidental rupture while pressurized.

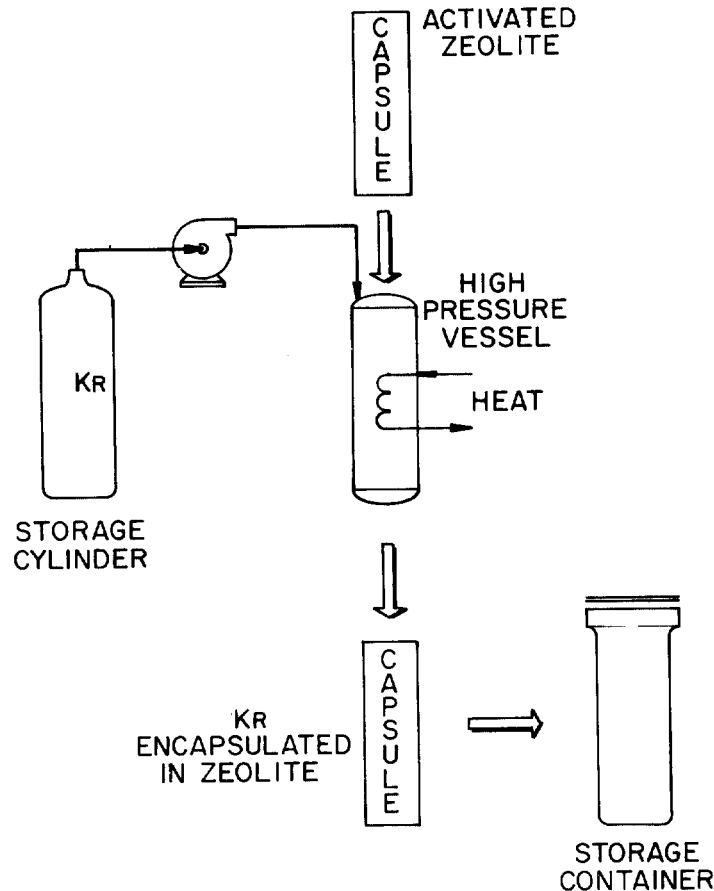


Figure 2. Process for high pressure encapsulation of Kr in zeolite.

We have determined loading densities for argon and krypton in sodalite and zeolite 3A. Representative values are shown in Table II.

Table II. Argon and krypton loaded on zeolite samples.

Gas	Experimental Conditions			Amount Encapsulated, cm ³ STP g ⁻¹ Solid	
	T, °C	P, psi	Time, hr	Sodalite*	Zeolite 3A
Ar	355	10,500	4	32-34	47
Ar	355	28,000	4	38-46	68
Kr	355	28,000	4	10-12	49
Kr	390	28,000	4	18-22	53
Kr	430	26,000	4	25-27	49

The encapsulation of larger amounts of argon than krypton at the same conditions is due to the lower activation energy of diffusion for argon (27 kcal mole⁻¹ in sodalite). (The activation energy for krypton in sodalite is 38 kcal mole⁻¹.) Argon is ~ 0.1 A smaller than krypton, thus lowering the energy barrier for diffusion. As the temperature is raised, more krypton can be encapsulated. Values near 25 cm³ g⁻¹ are considered to be practical for long-term storage of ⁸⁵Kr. If krypton is not readily available, experiments with argon may be used (with a correction factor) to simulate krypton behavior.

Basic sodalite normally contains some intercalated NaOH(10). Thus the unit cell composition of an ideal sodalite hydrate, Na₆(Al₆ Si₆ O₂₄) · 8H₂O becomes Na₆(Al₆ Si₆ O₂₄) x NaOH · (8-2x)H₂O, since each NaOH replaces 2 H₂O molecules(11). The results shown in Table II were obtained using sodalite which had been extracted to remove most of the intercalated NaOH. When samples containing up to ~ 5 weight per cent were encapsulated, ~ 30 -40% reduction in loading densities were observed for a given temperature and pressure (at 4 hr).

A series of krypton encapsulation experiments using sodalite and other zeolites is in progress and will determine the encapsulation behavior in the experimental space : 390-430°C; 20,000-26,000 psi; and 1-4 hr. The results will be used to establish a model for the encapsulation process which can be used to optimize the loadings for given experimental constraints.

Figure 3 presents data obtained by Vaughan for typical isotherms of krypton encapsulated in sodalite(9). A sorption isotherm obtained by Sesny for argon in zeolite 3A at 5000-45,000 psi and 350°C gives a maximum loading of ~ 77 cc/g(8). The values shown in Table II are consistent with the above.

The gas kinetic collision diameter at room temperature for krypton is ~ 3.5 A, and the free diameter of a sodalite cage is ~ 6.6 A (see Figure 1). If one krypton atom occupies each cage of

*Intercalated NaOH has been extracted from these samples.

sodalite, the saturation capacity of krypton for ideal sodalites is 52.6 cm^3 (STP) per anhydrous gram⁽⁶⁾. Ideal sodalite may constitute a nearly perfect sorbent in the sense given by Langmuir. Each cage represents an identical site, and all sites are separated through the 6-ring windows in such a way that the guest species should not be able to interact by direct contact (Figure 1). The experimental isotherms in Figure 3 are of a Langmuir form:

$$K = \frac{\theta}{f(1-\theta)} = \frac{v/v_{\text{sat}}}{f(1-v/v_{\text{sat}})} \quad (1)$$

where K is the equilibrium constant, θ (or v/v_{sat}) is the fraction of saturation capacity sorbed (v , the volume sorbed in cm^3 at STP per anhydrous gram and v_{sat} , the saturation capacity), and f is the fugacity. When f/v is plotted versus f , a straight line results with slope v_{sat} . The data of Figure 3 were used to evaluate v_{sat} as

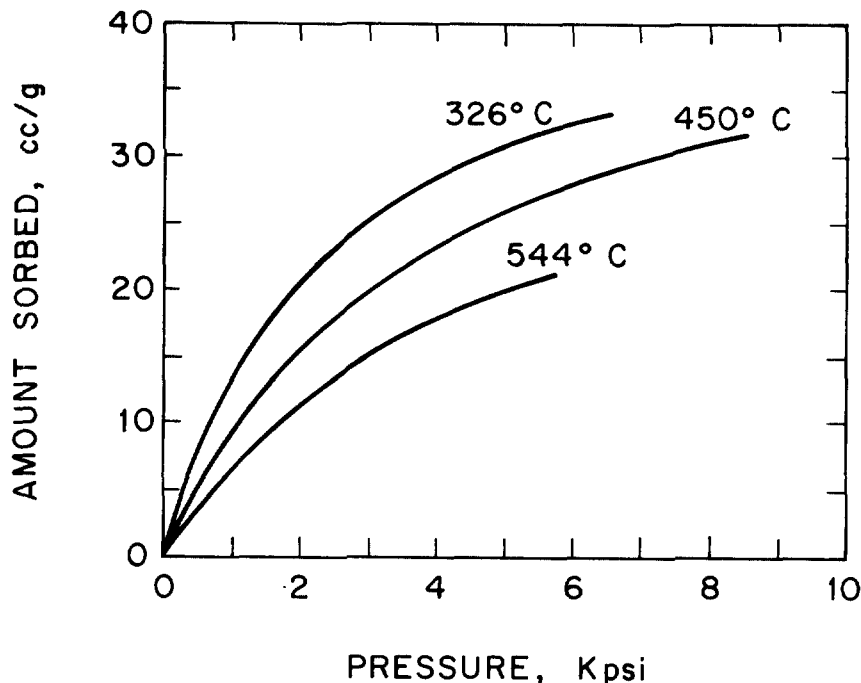


Figure 3. Isotherms of Kr sorbed on extracted sodalite (S2)⁽⁹⁾.

equal to $\sim 45 \text{ cm}^3 \text{ g}^{-1}$, in reasonable agreement with the ideal case⁽⁶⁾. The results shown in Figure 3 were obtained using sodalite (sample S2) which had most of the intercalated NaOH removed by extraction. Sodalite (sample S1) containing NaOH in three times the amount of S2 was also studied⁽⁶⁾. The equilibrium saturation capacities did not change, indicating that krypton could occupy a cage containing sodium hydroxide.

Diffusion Measurements

After krypton has been encapsulated in a zeolite, measurements of its diffusion from the solid at high temperatures can be used to estimate ^{85}Kr leakage under long-term storage conditions. Experimental and theoretical methods of determining the diffusivity of gases in zeolites from leakage measurements will be described in this section, while prediction of krypton-85 leakage will be shown in the following section.

A typical process flowsheet for measuring leakage rates at three different temperatures of krypton encapsulated in a zeolite is shown in Figure 4. The solid sample is placed in each of three sample tubes, and the system is evacuated. After isolating the samples from the vacuum, the sample tubes are heated to temperatures T_1 , T_2 , and T_3 . Measurements can be made of the amount of gas released as a function of time for each tube in turn using the pressure gauge and/or the mass spectrometer. The results of the measurements obtained by Vaughan⁽⁹⁾ for krypton in extracted sodalite (S2) are shown in Figure 5, where Q_t and Q_∞ are the amounts of gas released up to times t and infinity, respectively. Because of the initial temperature rise from room temperature to a higher constant temperature, the curves of the amount desorbed vs time are sigmoid in shape. The theory and method of analysis of the curves has been given elsewhere^(7,12), and only the directly applicable portion of the theory will be described. For fractional leakage (Q_t/Q_∞) less than ~ 0.3 , D (the diffusivity) at the final steady temperature, T , is given by:

$$D = \frac{\pi r_0^2}{36} \frac{d(Q_t/Q_\infty)^2}{dt} \quad (2)$$

where r_0 is an average diffusion path length and is related to the size of the zeolite crystals. Thus, the square root of D can be obtained from the data in Figure 5 using equation (2).

For an activated diffusion process:

$$D = D_0 \exp(-E/(RT)) \quad (3)$$

where E is the activation energy for diffusion and D_0 is a coefficient independent of temperature. If equations (2) and (3) are combined, it is seen that plots of

$$\text{Log}_{10} \left(\frac{d(Q_t/Q_\infty)}{dt^{1/2}} \right) = \frac{1}{2} \log \alpha D \text{ vs } 1/T$$

should be straight lines of slope $-E/(4.606R)$, where $\alpha = (1.3/(\pi r_0^2)) \times 10^5$ and R is the universal gas constant. Such a plot is shown in Figure 6 for the data of Vaughan⁽⁹⁾ (with D in $\text{cm}^2 \text{sec}^{-1}$) obtained using two different sodalite samples, S1 and S2 (S1 contains approximately three times the amount of sodium hydroxide

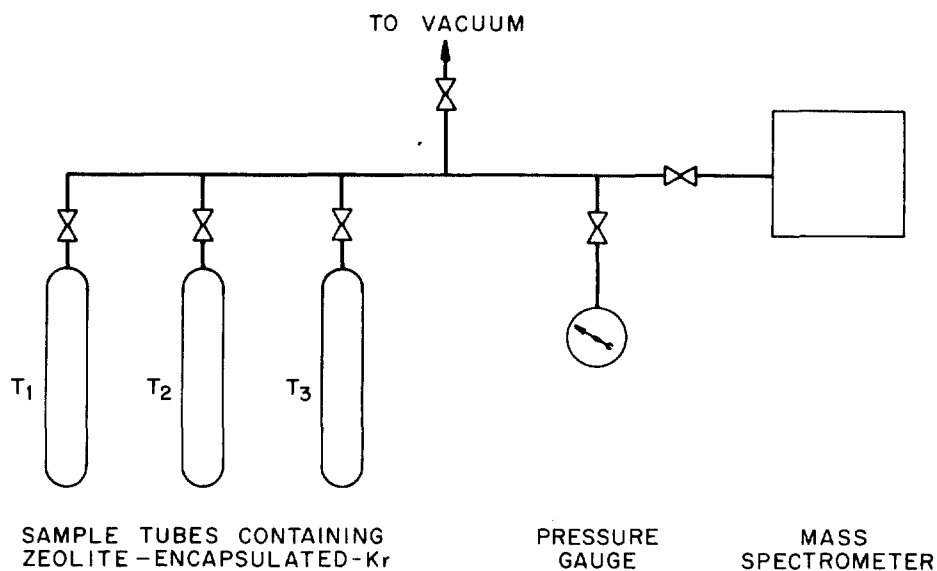


Figure 4. Process for determining rates of leakage of krypton from zeolite.

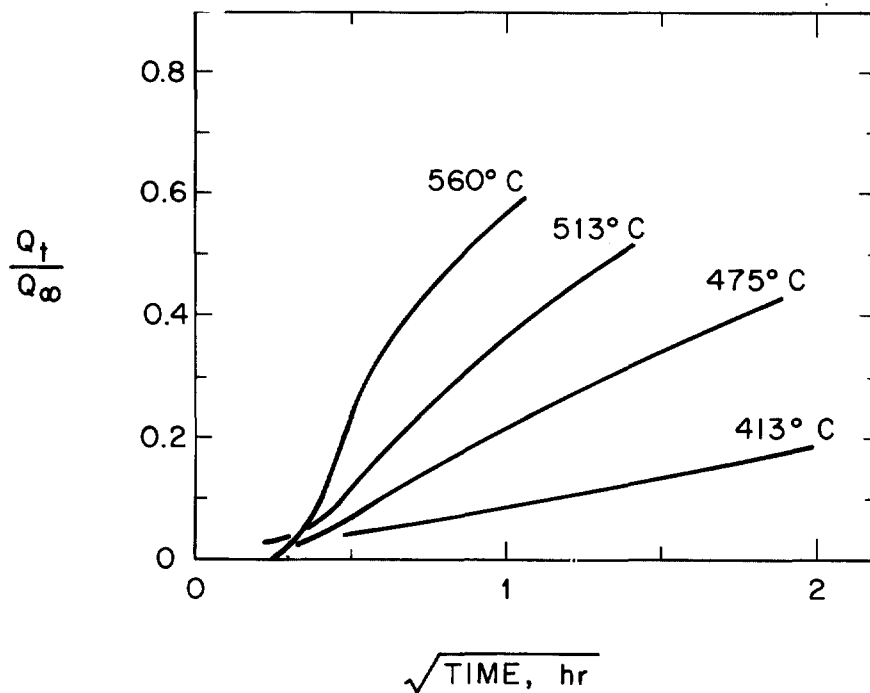


Figure 5. Rate of fractional leakage of krypton from extracted sodalite (S2)⁽⁹⁾.

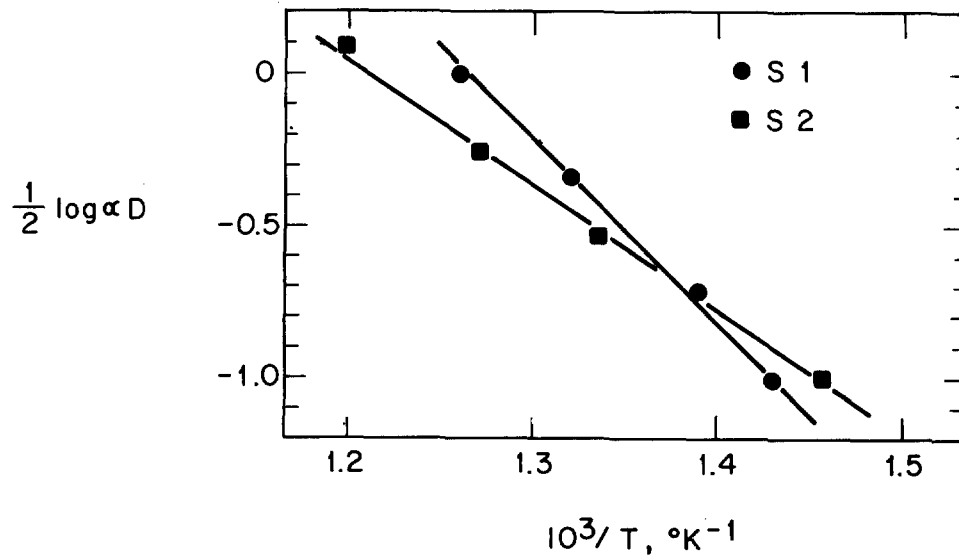


Figure 6. Temperature dependence of diffusion of krypton in extracted sodalite (S2)⁽⁹⁾, D in $\text{cm}^2 \text{sec}^{-1}$.

found in S2). Thus it can be seen that sodalite containing more NaOH has a greater activation energy of diffusion. Using experimental values of $d(Q_t/Q_\infty)/dt^{1/2}$ together with values of r_0 for S1 and S2, Vaughan (6,9) obtains the values of D_0 and E given in Table III. Values of r_0 , D_0 , and E obtained by Walker⁽⁷⁾ for zeolite 3A are also provided.

Table III. Values of E , D_0 , and r_0 for diffusion of krypton in sodalite and zeolite 3A.

Zeolite Sample	r_0, cm	$E, \text{ kcal/mole}^{-1}$	$D_0, \text{ cm}^2 \text{sec}^{-1}$	Reference
Sodalite S1	1.3×10^{-5}	52	1.1	6
Sodalite S2	6.1×10^{-6}	38	1.1×10^{-5}	6
Zeolite 3A	2.0×10^{-4}	16.4	6.0×10^{-7}	7

Using the values of E and D_0 in equation (3), it is possible to calculate D at any temperature for the above.

IV. Long-Term Storage of ^{85}Kr

The laboratory results and theory presented in Section III are used to predict leakage rates of ^{85}Kr from sodalite and zeolite 3A during long-term storage, and the resulting safety factors over pressurized cylinder storage are shown. The same measurements and calculations can be made for other zeolites in which krypton diffusion obeys equations (2) and (3).

The integrated form of equation (2) can be combined with equation (3) to give equation (4), the fractional leakage (up to $Q_t/Q_\infty = 0.3$) of encapsulated krypton at time t and temperature T , once D_0 , E , and r_0 have been determined for a given zeolite sample.

$$Q_t/Q_\infty = 6 \left(\frac{D_0 t}{\pi r_0^2} \right)^{1/2} e^{-E/(2RT)} \quad (4)$$

In long-term storage of ^{85}Kr , the major concern is the leakage of ^{85}Kr (compared to the original amount stored). Radioactive decay effectively reduces the potential leakage of ^{85}Kr by a factor of two every 10.73 years. While the amount of total krypton desorbed increases as a function of the square root of time, the amount of ^{85}Kr which can leak as well as which has leaked is decreasing exponentially. The combined effects are described by equation (5):

$$(Q_t/Q_\infty)_{^{85}\text{Kr}} = 6 \left(\frac{D_0 t}{\pi r_0^2} \right)^{1/2} \exp\left(-\frac{E}{2RT} - \lambda t\right) \quad (5)$$

where λ is the decay constant for ^{85}Kr . The function described by equation (5) reaches a maximum at a value of $t=7.7$ years (corresponding to $1/t=2\lambda$). While the time for the maximum possible ^{85}Kr leakage is fixed, the amount leaked is a function of D_0 , E , r_0 , and T .

Using data obtained by Vaughan⁽⁶⁾ (see Table III) and the value of λ for ^{85}Kr decay in equation (4), it is possible to calculate the release of original ^{85}Kr inventory (fractional net leakage of ^{85}Kr) as a function of time at a storage temperature of 150°C in sodalite samples S1 and S2. Figure 7 shows the results of such a calculation. The fractional leakage of all isotopes of krypton at 150°C and 100 years is $\sim 6 \times 10^{-4}$ and $\sim 2 \times 10^{-2}$ for S1 and S2, respectively. The resulting maximum net leakages ^{85}Kr of 0.3% to 0.01%, if attainable, represent safety factors (based on potential losses from a damaged storage vessel) of 200 to 6000 over pressurized tank storage. Predicted net leakage of (^{85}Kr) from zeolite 3A⁽⁷⁾ (using data from Table III) was 35% for a storage temperature of 50°C .

Since the rate of activated diffusion depends on temperature in an exponential manner, the rate of dissipation of ^{85}Kr radioactive decay heat during storage becomes critical. A heat-transfer model for a 23-cm diameter steel storage cylinder was used to estimate temperature profiles for the cylinder filled with zeolite. At a krypton loading of 1.8×10^{-3} mole ($40 \text{ cm}^3 \text{ STP}$) g^{-1} of zeolite (equivalent to ~ 35 atm, or ~ 500 psi, storage of gas) and an ambient temperature (convective heat transfer) of 50°C , the calculated centerline temperature was 150°C ; the mean temperature was approximately 120°C . The predicted leakage rates at 150°C for sodalite shown in Figure 7 can thus be considered conservative for such conditions. Additional cooling or decreased loading density of ^{85}Kr would be required for encapsulation-storage using zeolite 3A, due to the higher leakage rate.

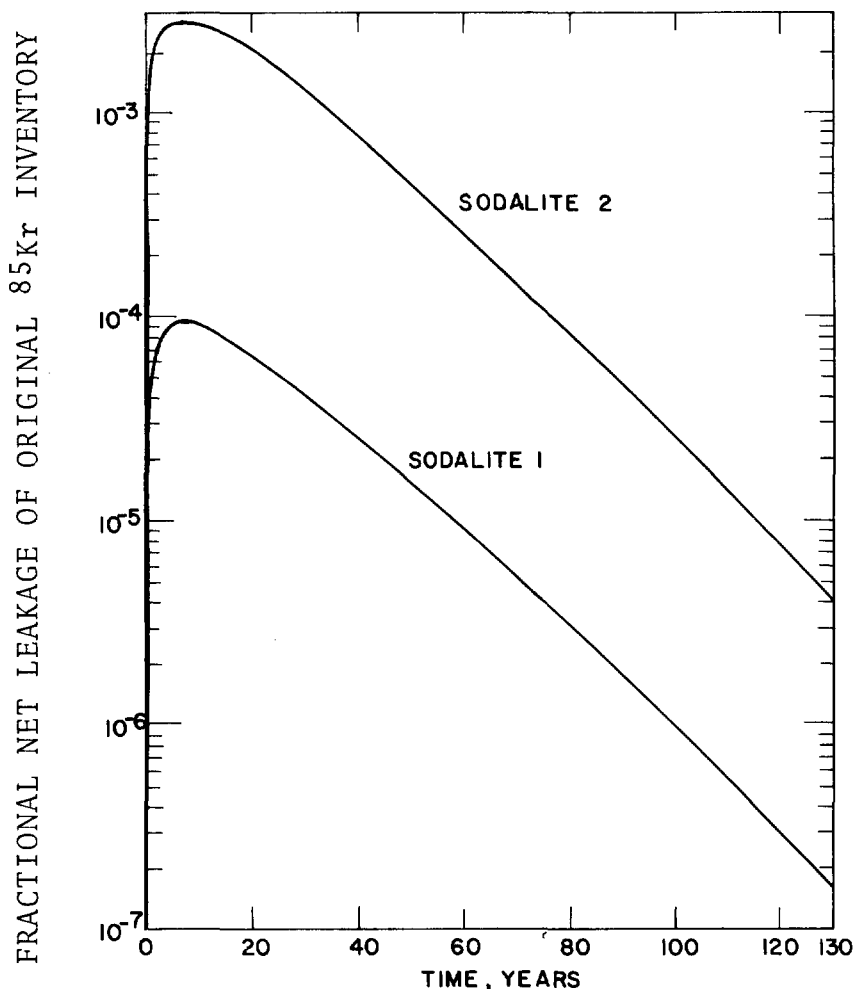


Figure 7. Calculated release of original ^{85}Kr inventory from sodalite at 150°C as a function of time.

V. Program Description

Encapsulation and leakage tests are under way at the INEL using various samples of sodalite and zeolite 3A. New zeolites, including Rb- and Cs-exchanged zeolite A, K-exchanged chabazite and erionite, and a number of different pellet forms of sodalite will be tested as described in Section III. Leakage studies will be used to estimate long-term storage characteristics for the new zeolite forms in the same way as for sodalite and zeolite 3A. Small amounts of the most promising zeolites will be encapsulated with 6% ^{85}Kr in krypton, and long-term storage tests will be initiated under simulated storage conditions. (Krypton with natural background levels of ^{85}Kr is being used for all other testing.) Pilot-scale development will include scale-up of the pressure vessel, possibly to a plant-size prototype, combined with developing remote operation and remote materials handling capability. A conceptual design of the production-scale encapsulation and storage facility will be made.

An estimate of the size and capabilities of a production-scale operation can be made. In a 1500-tonne yr⁻¹ reprocessing plant, ~9.8 MCi yr⁻¹ of ⁸⁵Kr is produced. If 1.8 x 10⁻³ mole (40 std. cm³) g⁻¹ of krypton (with 6% ⁸⁵Kr) is encapsulated in a zeolite such as sodalite, ~2,800 kg yr⁻¹ is required. If 50,000 Ci of ⁸⁵Kr is to be encapsulated in one batch, a 20- ℓ high-pressure vessel would be necessary. The encapsulation process, including solids transfer operations, must be remotely operated due to the high radiation field. In addition to mechanical shielding of the high pressure process equipment, capability for containing the large amount of radioactive krypton is required in the event of failure of the pressurized system. Technology exists for high pressure, remote operation, and remote handling capabilities, and these will be combined into one operational system. Since relatively large amounts of ⁸⁵Kr will be present during the process-scale encapsulation, adequate cooling of radiation-generated heat is required during parts of the process.

Long-term storage criteria will be developed. Stored ⁸⁵Kr in zeolite will generate heat, which in turn must be dissipated so that the storage temperature does not increase to the extent that appreciable diffusion of ⁸⁵Kr out of the zeolite pores can occur (~150°C in Figure 7 for sodalite). Long-term radiation damage to the zeolite structure will be assessed and minimized. The effect of the ⁸⁵Kr decay product, rubidium, will also be determined. (A beneficial effect of rubidium might be to plug up the pores in sodalite.)⁽¹³⁾ In any handling of zeolite-encapsulated-⁸⁵Kr, dust formation must be prevented or contained.

VI. Conclusion

Measurements of loading capacity of krypton in sodalite were made at the INEL and elsewhere^(5,6,8,9). Kinetics of diffusion of krypton out of sodalite have been determined by Vaughan⁽⁶⁾ and can be used to predict leakage of krypton-85 out of sodalite under long-term storage conditions. Based upon these loading and leakage characteristics, the process of encapsulating krypton-85 in sodalite appears to be a feasible storage method. Further developments leading to a conceptual design of a commercial process for krypton-85 encapsulation by zeolites are being pursued at the INEL.

Acknowledgment

The generous assistance of Dr. D. E. W. Vaughan is gratefully acknowledged.

References

1. Alternatives for Managing Wastes from Reactors and Post-Fission Operations in the LWR Fuel Cycle, ERDA-76-43, Chapt 14.1.2.1, Vol. 2, pp. 14.2-14.7 (1976).
2. B. A. Foster, D. T. Pence, and B. A. Staples, "Long term storage techniques for ^{85}Kr ", Proc. Thirteenth AEC Air Clean. Conf., CONF-740807, pp. 293-298 (1975).
3. B. A. Foster and D. T. Pence, "An evaluation of high pressure steel cylinders for fission product noble gas storage", ICP-1044 (1975).
4. Alternatives for Managing Wastes from Reactors and Post-Fission Operations in the LWR Fuel Cycle, ERDA-76-43, Chapt. 2.4.2.4, Vol. 1, pp. 2.63-2.66 (1976).
5. D. W. Breck, Zeolite Molecular Sieves, John Wiley & Sons, New York, 1974.
6. R. M. Barrer and D. E. W. Vaughan, "Trapping of inert gases in sodalite and cancrinite crystals", J. Phys. Chem. Solids, Vol. 32, pp. 731-743 (1971).
7. P. L. Walker, Jr., et al., "Activated diffusion of gases in molecular sieve materials", The Chemistry and Physics of Carbon, Vol. 2, pp. 257-371 (1966).
8. W. J. Sesny and L. H. Shaffer, "Fluid encapsulation product", U. S. Patent 3,316,691 (1967).
9. D. E. W. Vaughan, Encapsulation of Rare Gases, Ph.D. Thesis, Imperial College, London (1967).
10. R. M. Barrer and E. A. D. White, "The hydrothermal chemistry of silicate. Part II. Synthetic crystalline sodium aluminosilicates", J. Chem. Soc., pp. 1561-1571 (1952).
11. R. M. Barrer and J. F. Cole, "Chemistry of soil minerals. Part VI. Salt entrainment by sodalite and cancrinite during their synthesis." J. Chem. Soc. A, pp. 1516-1523 (1970).
12. R. M. Barrer and D. E. W. Vaughan, "Solution and diffusion of helium and neon in tridymite and cristobalite", Trans. Faraday Soc., Vol. 63, pp. 2275-2290 (1967).
13. R. M. Barrer and J. F. Cole, "Interaction of sodium vapor with synthetic sodalite: Sorption and formation of color centers", J. Phys. Chem. Solids, Vol. 29, pp. 1755-1758 (1968).

DISCUSSION

GRADY: I was wondering what the application of this type of process will be to an industrial reprocessing plant? Is the equipment so large and does it require such high pressures and high temperatures that it's not feasible?

D. A. KNECHT: The estimates of the process scale required in an industrial reprocessing plant are presented in the written text of this paper. Roughly, if 50,000 curies of 6% ^{85}Kr in krypton are to be encapsulated in one batch (assuming 50,000 curies per day are generated at a 1,500 ton per year reprocessing plant), a 20-liter high pressure vessel would be required. Multiple encapsulation batches using smaller high pressure vessels, i.e., 5 or 10 liters, can meet processing rate requirements. While high pressure technology does exist for such an operation, further work is under way at the INEL to determine the requirements for commercial-scale operations.

CLOSING REMARKS OF SESSION CHAIRMAN:

We've heard eight excellent papers and it's very difficult to summarize them. The incineration processes that have been described represent intensive development to achieve volume reduction in recognition of the requirements of waste management. Significant reduction is achievable in these primary treatments. However, the net reduction factors of these processes will need to be assessed very carefully.

An important consideration will be the cost of waste management versus the cost of direct disposal without treatment. It will be necessary to derive the net cost-benefit of processes and we need data on the process costs, as well as on ERDA's own cost of storage, in order to make valid cost comparisons. Therefore, cost data from incineration systems is extremely important.

The air cleaning of incinerator effluents is a technical challenge that is having major influence on the design selections and, as you can see, several of these incinerators are designed with special combustion features in an attempt to avoid such things as chlorides or particulate carryover in the offgas and the problems that they raise for air cleaning.

Undoubtedly, air cleaning will dominate the design of incineration development for some time and the successful adoption of these units by commercial industry will probably rest on the ability to clean up the effluents from such units efficiently. We've also heard of the air cleaning needs of several other processes, e.g., high level waste treatment and the need for storage for retention of noble gases. These are indeed significant developments, challenging both the government's laboratories and the industry.

I would like to close by saying that many of you who are members of the air cleaning industry probably recognize what is obvious to

14th ERDA AIR CLEANING CONFERENCE

me and that is that we must devise systems that go all the way back to the design of disposable filters and recognize that they will ultimately be a waste material that has to be treated, packaged, and stored. We must, therefore, use the greatest ingenuity in design with this in mind because, indeed, a significant part of waste management occurs at the head end. I've always said that one of the most important persons in waste management is the procurement officer because he's the one who makes all the selections of what finally winds up in the waste bin and has to be managed as waste.

SESSION III

SYSTEM PROTECTION FROM FIRE, EXPLOSION, AND NATURAL DISASTERS

Monday, August 2, 1976

CHAIRMAN: B. P. Brown

PRELIMINARY RESULTS OF HEPA-FILTER SMOKE PLUGGING TESTS USING THE
LLL FULL-SCALE FIRE-TEST FACILITY

J. R. Gaskill, N. J. Alvares,
D. G. Beason, H. W. Ford, Jr.

TORNADO DEPRESSURIZATION AND AIR CLEANING SYSTEMS

W. S. Gregory, K. H. Duerre,
P. R. Smith, R. W. Andrae

DESIGN AND ANALYSIS OF THE SANDIA LABORATORIES HOT CELL FACILITY
SAFETY VENTILATION SYSTEM

E. A. Bernard, H. B. Burress

EFFECTS OF EXPLOSION-GENERATED SHOCK WAVES IN DUCTS

M. R. Busby, J. E. Kahn, J. P. Belk

14th ERDA AIR CLEANING CONFERENCE

PRELIMINARY RESULTS OF HEPA-FILTER SMOKE PLUGGING TESTS USING THE LLL FULL-SCALE FIRE TEST FACILITY*

J. R. Gaskill, N. J. Alvares, D. G. Beason, and H. W. Ford, Jr.
University of California, Lawrence Livermore Laboratory
Livermore, California 94550

Abstract

As reported in previous Air Cleaning Conferences, hot fire gases can impair the integrity of HEPA filters, and smoke particulates can plug them. This pressurizes the room of fire origin and can lead to the spread of radioactive or other toxic contamination. The heat-damaging effect has been overcome using water sprays in the duct. Previous studies on smoke plugging have been inadequate, however, in determining realistic pyrolysis/combustion rates and in evaluating the effects of fuel arrangements, room geometry, and aging of smoke particulates.

To overcome these deficiencies, Lawrence Livermore Laboratory has constructed a full-size fire-test compartment, equipped it with an exhaust-ventilation system, and provided it with a suitable instrumentation- and data-acquisition system. From a survey of ERDA-contractor facilities, a matrix of fuel loadings (kg/m^2 of combustibles) versus dirty-to-clean ratios (relative yield of particulates) has been prepared. From this, a selected series of fuel arrays is being used to determine the life of HEPA filters during test fires. The effects of high- versus low-exhaust takeoff points, as well as the use or nonuse of sprinklers, are also being investigated.

The fire test facility is described, and the preliminary results obtained to date are reported.

I. Introduction

At the two previous Air Cleaning Conferences, my colleagues and I reported on what we had done to try to ameliorate the effects of unwanted fires on exhaust ventilation systems in facilities where radioactive materials are handled^{(1),(2)}. In 1972, we reported on the successful use of water sprays to overcome the adverse effect of hot fire gases on exhaust ductwork and HEPA filters. In 1974, we reported on an improved method for abating this heat effect, and pointed out some of the difficulties in solving the filter smoke-plugging problem. At that time we indicated that Lawrence Livermore Laboratory was going to build a full-scale fire test facility so that more realistic tests could be conducted. The report today covers a description of the facility and the results of some preliminary fire tests conducted to date.

*Work performed under the auspices of the U. S. Energy Research and Development Administration under contract No. W-7405-Eng-48.

14th ERDA AIR CLEANING CONFERENCE

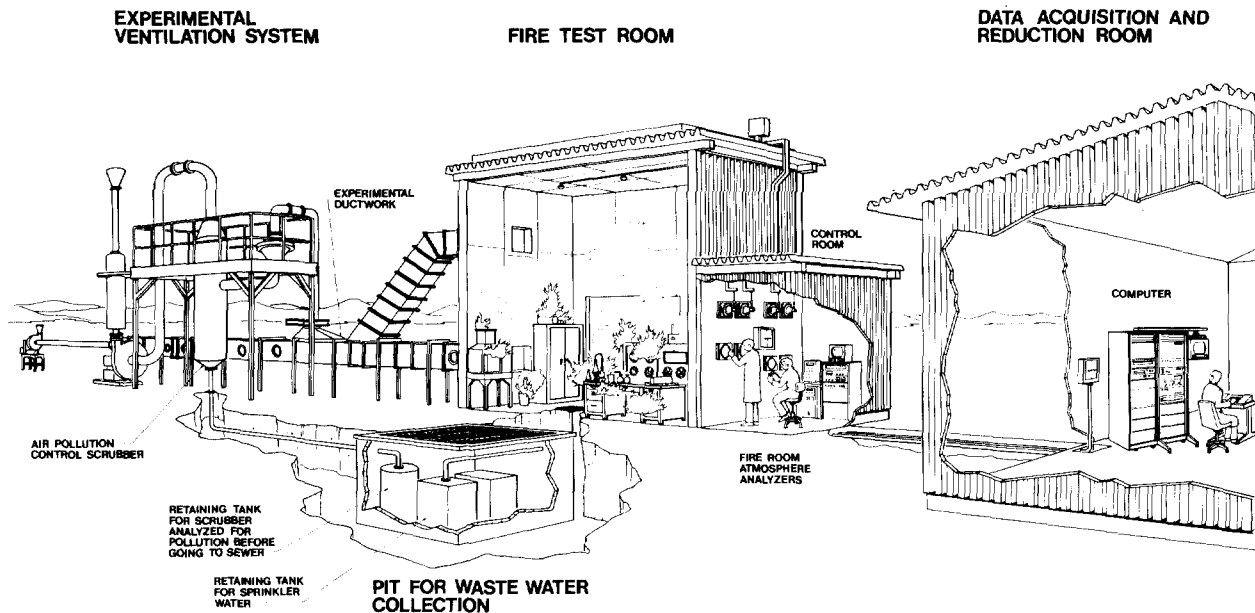


Figure 1 Full-scale fire test facility.

II. Description of Test Facility

As shown in Fig. 1, the full-scale fire facility consists of several elements as follows:

- A fire test room 100 m³ in volume and an associated small control room containing view-ports into the test cell, gas sampling and analytical equipment; a control valve and meter for the sprinkling system; and a cathode-ray display tube capable of showing data obtained from the various centers on a 30-s update arrangement.
- High- and low-takeoff exhaust ductwork leading through a damper to the experimental duct system.
- A bypass air pollution control system (APC).
- A pit for waste water collection and monitoring.
- A computerized data acquisition system.

The fire test cell consists of a rectangular, square-cross-section, columnar steel framework onto which a steel skin with a Q-deck exterior is welded. Some 1600 stainless forks are welded to the inside of the steel skin walls and ceiling for holding the insulation. This insulation consists of 38 mm of Kastolite* SK-7 with a 985°C rating, followed by 100 mm of Kastolite KS-4V with a 1400°C rating. Kastolite is an alumina-silica mixture containing a small amount of lime. The floor of the cell, which is sloped to sprinkler drains, consists of a sand bed overlaid with fire brick, and finally overcast with Kastolite. The finished interior dimensions of the cell are 5.9 m long × 4.0 m wide × 4.2 m high.

*Reference to a company or product name does not imply approval or recommendation of the product by the University of California or the U.S. Energy Research & Development Administration to the exclusion of others that may be suitable.

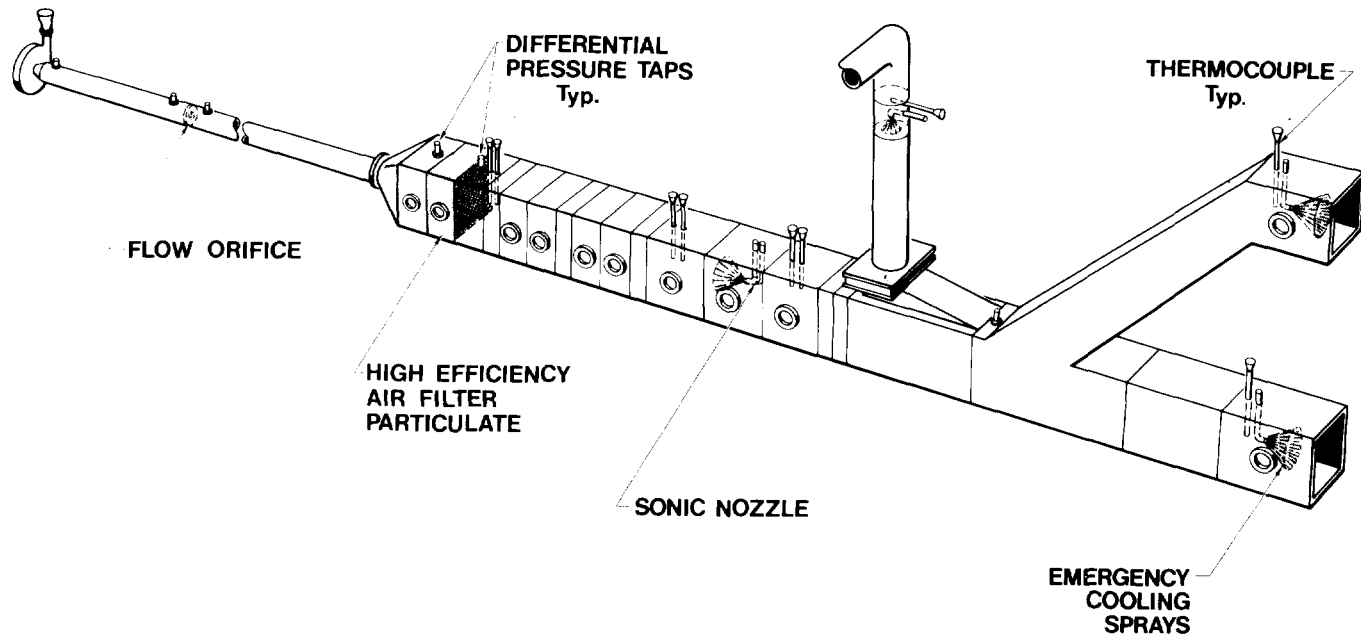


Figure 2 Experimental ductwork for fire test facility.

Figure 2 shows some of the details of the ductwork of which the left-hand section is the experimental modularized portion.

Figure 3 is a photograph of the cell showing one of the two intake air dampers, the exhaust ductwork, the experimental section, and the bypass to the high-pressure-drop venturi scrubber. This latter unit is used when the test is completed and we wish to clear

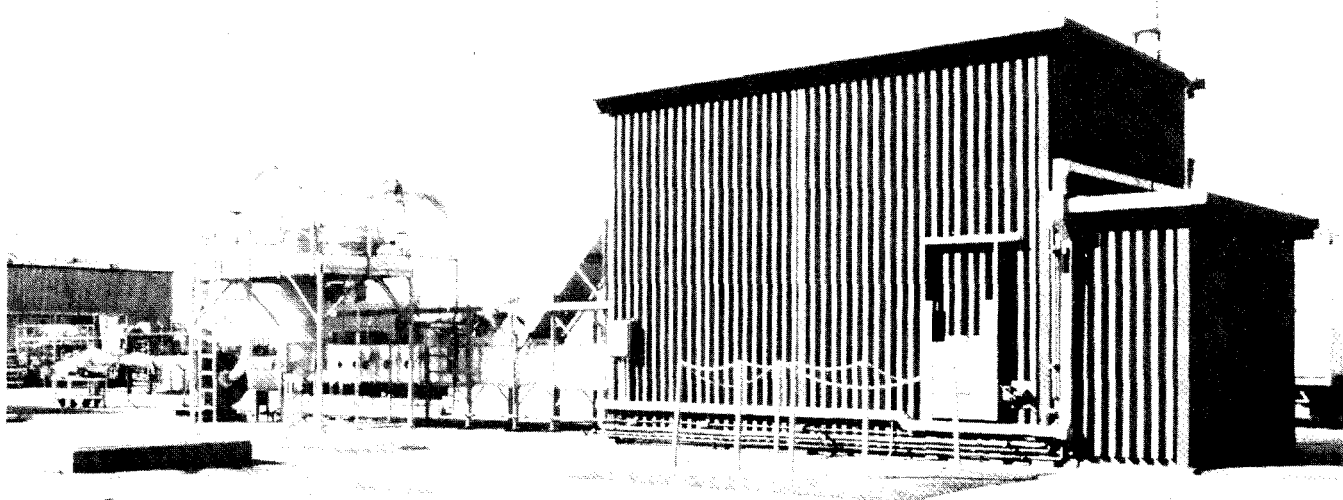


Figure 3 Fire test cell.

14th ERDA AIR CLEANING CONFERENCE

the room of smoke particulates and any toxic gases. In the foreground are shown the guard chains around the waste pit, and the exterior of the control room is to the right. Also shown are two secondary patch panels which lead to pluggable holes in the roof and along the lower sides of the test cell for the introduction of the various sensors. Two other subpanels are located respectively along the experimental ductwork and on the opposite side of the test cell.

Figure 4 is a northeast view of the test cell showing the other intake damper, the doors for taking equipment in and out, and another view of the roof patch panel and instrument wire way.

Figure 5 shows a somewhat detailed view of the air pollution control (APC) system consisting of a high-pressure-drop venturi scrubber, a tank, a high-volume high-pressure blower, and a muffler system. Recently this has been enclosed in a sound-deadening wooden structure.

Figure 6 shows the interior of the test cell looking toward the control room, and shows the viewing ports, light ports, one of the intake dampers, the lower instrumentation ports, and one floor drain.

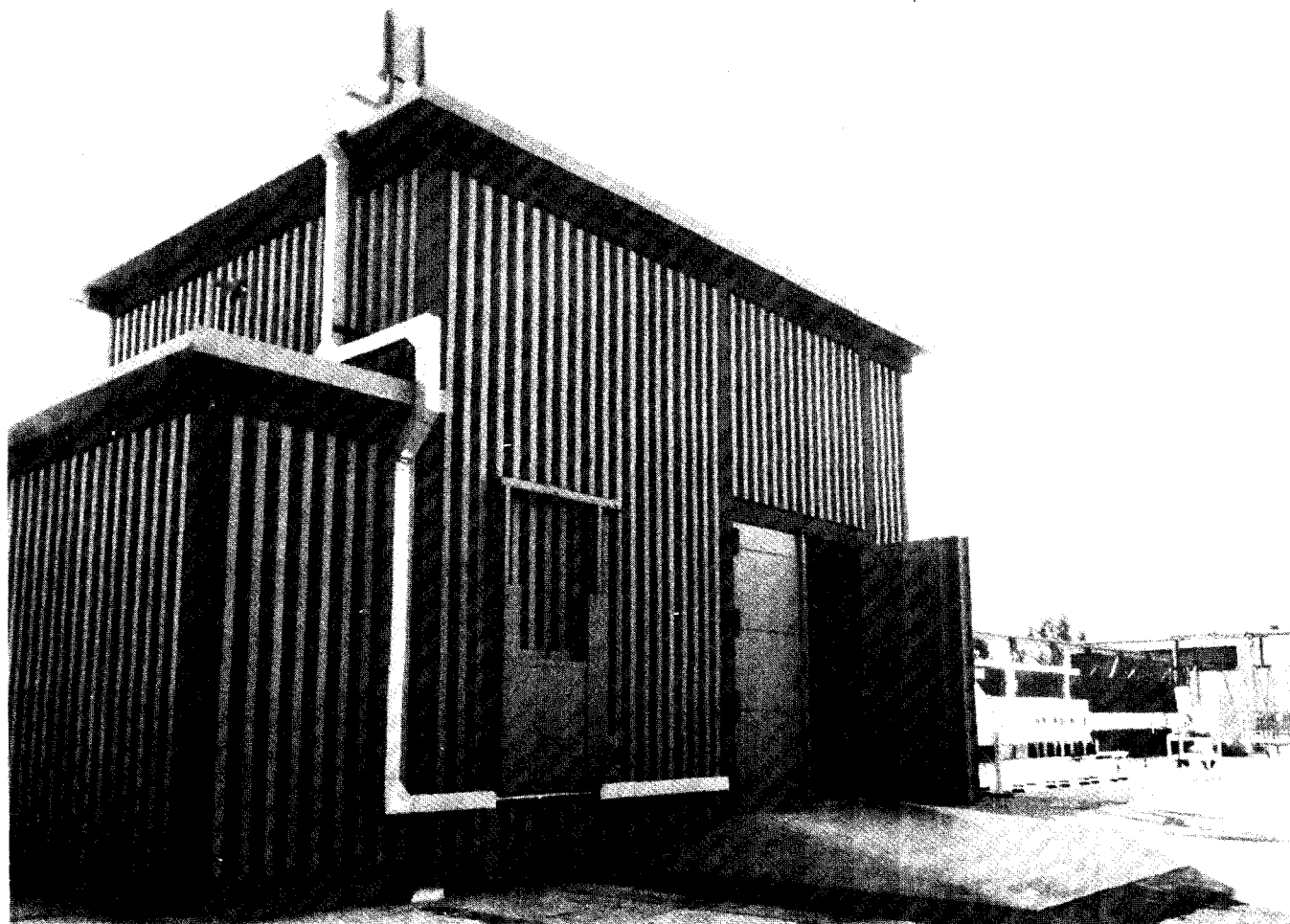


Figure 4 Northeast view of test cell.

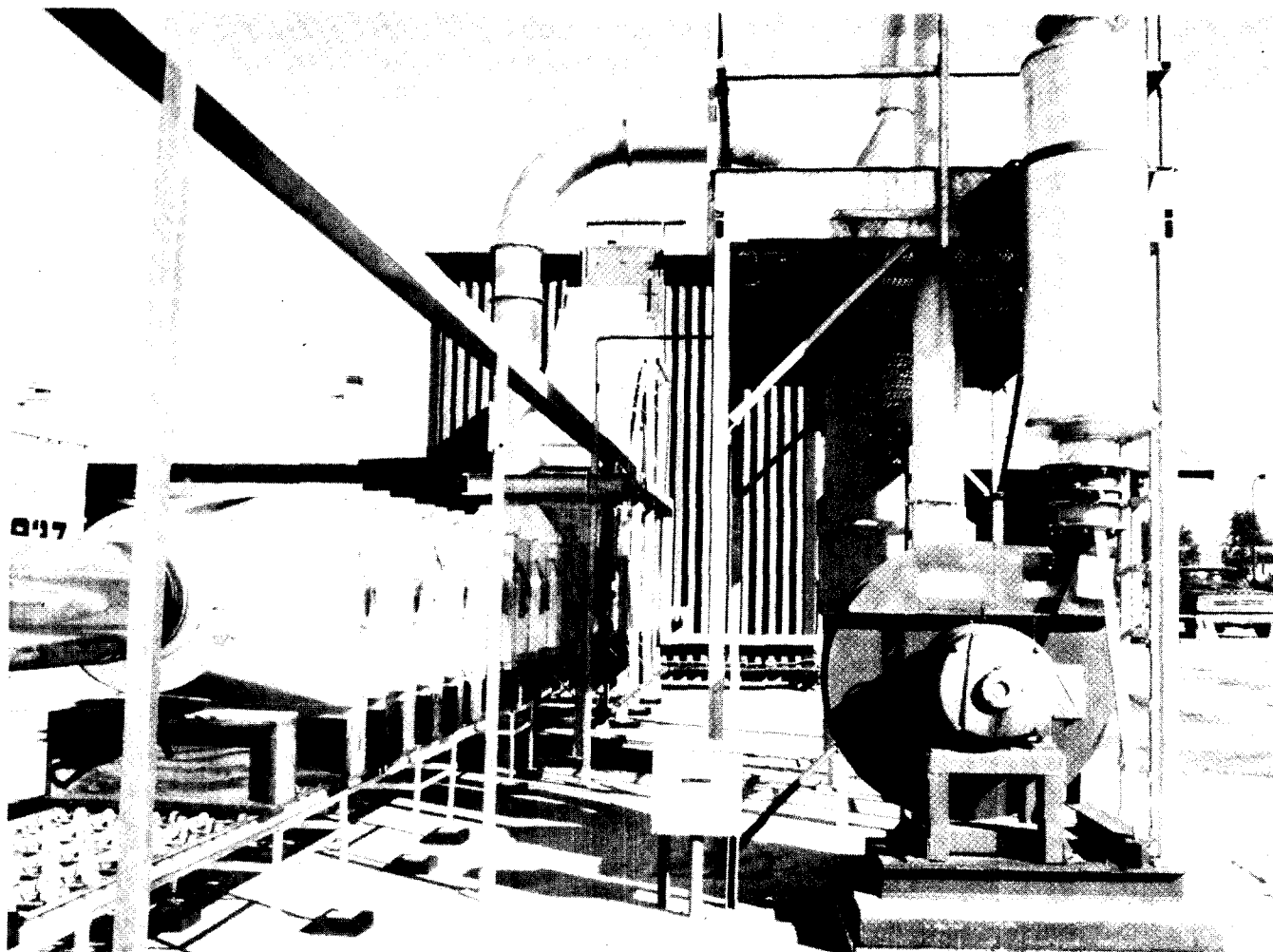


Figure 5 Air pollution control system.

Figure 7 shows the data acquisition/reduction system in the computer room. This consists of the scanner, a magnetic tape storage system, a computer, a CRT display, a display plotter, and a copier.

Figure 8 is an interior view of the control room showing the gas analysis instrument rack. Figure 9 is a view of one of the optical cell systems for determining the light obscuration of the smoke particulates in this test cell. Figure 10 shows a sample intake (currently located in upper exhaust duct) for sampling gases. An external sample port is currently used for taking timed samples for cascade impactor analysis used in determining sizes of smoke-particulates.

Figures 11(a) and (b) illustrate a map of the temperature-measuring sensors, the location of the smoke-density and radiometer sensors, and the pressure-measuring sensors. Figure 12 is a block diagram of the data acquisition system.

Construction of the facility was finished during the summer of 1975. The next several months were spent in installing the ductwork,

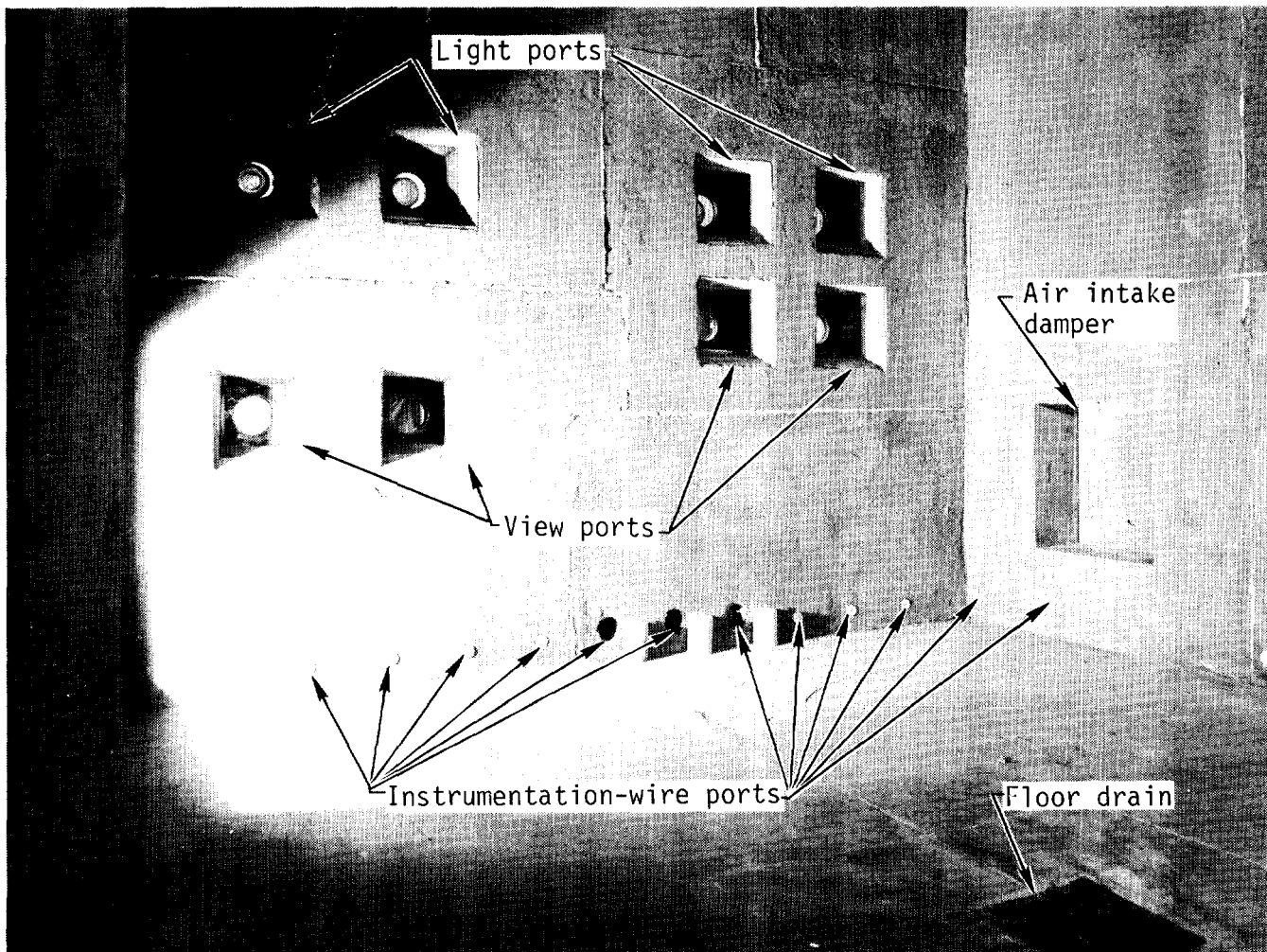


Figure 6 Test cell interior.

APC system, waste drain tanks, and data acquisition system(3). Following this, some time was spent in installing and connecting the sensors, followed by a period of debugging. We have added more instrumentation during the testing program so that additional data are available from the later burns.

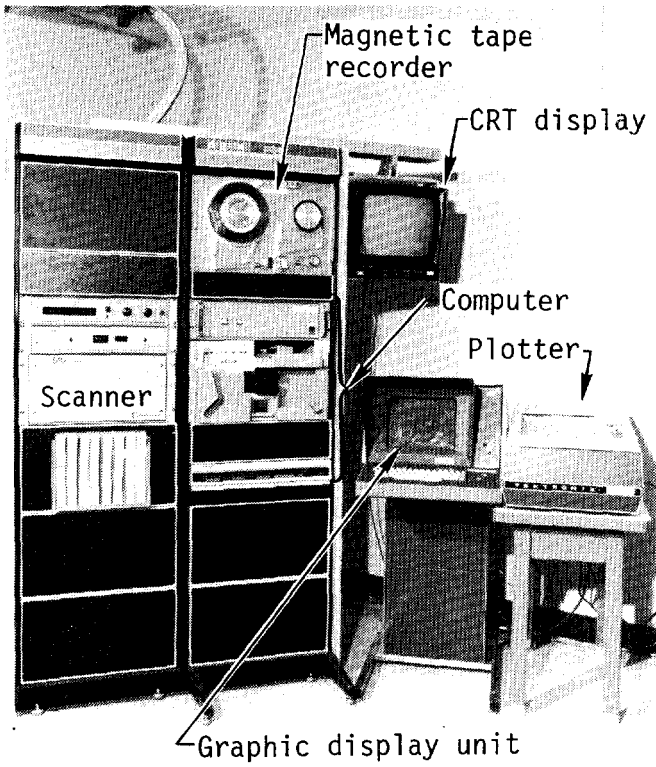


Figure 7 Data acquisition/reduction system.

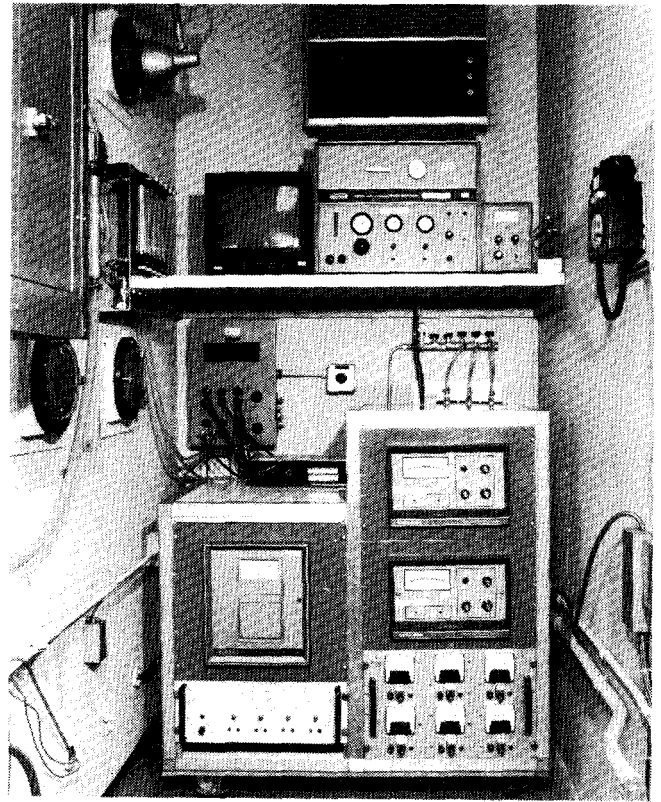


Figure 8 Gas analysis instrument rack.

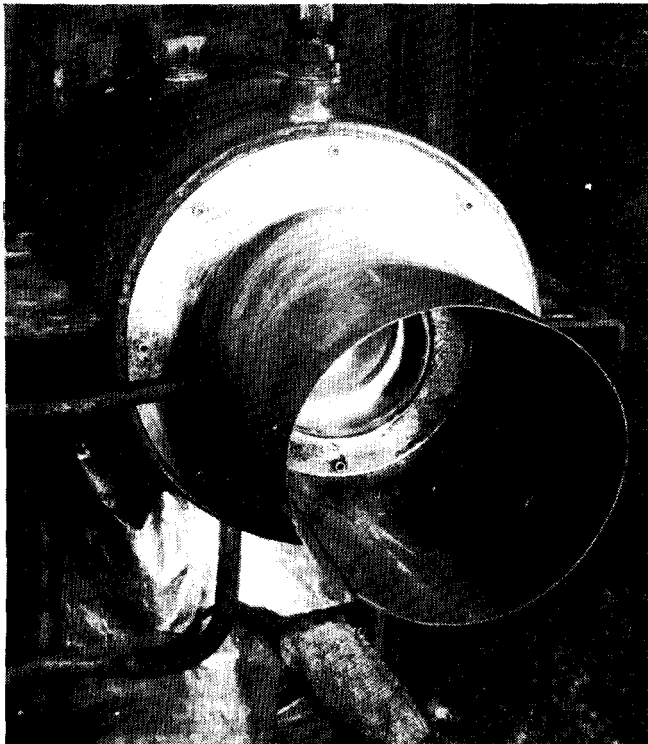


Figure 9 One unit of optical cell for measuring smoke opacity.

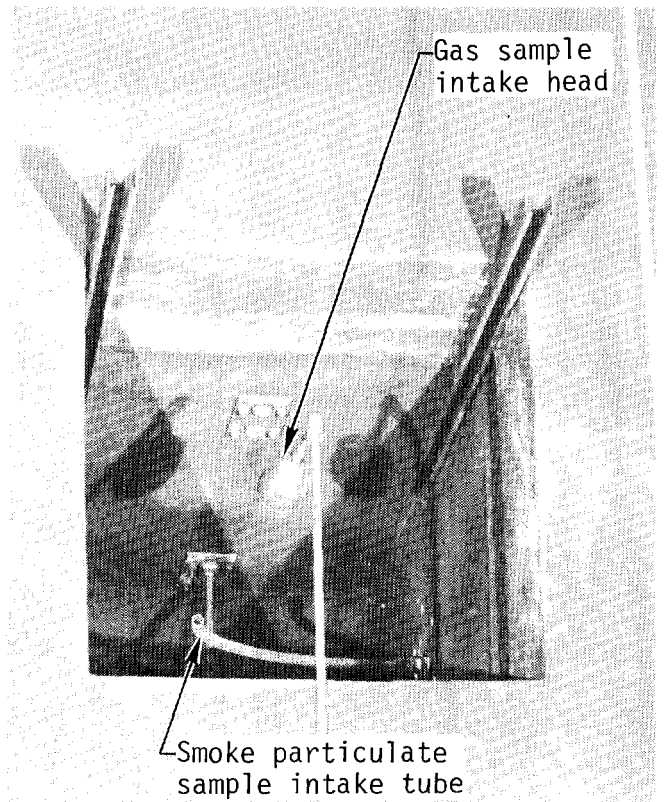
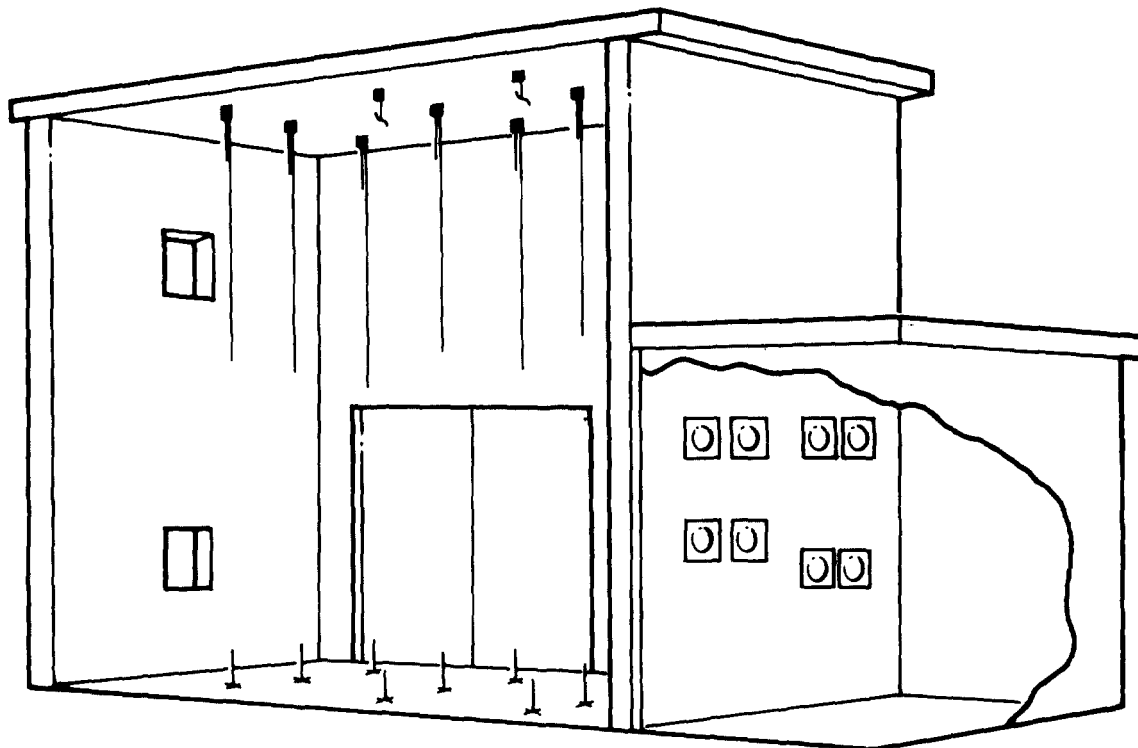
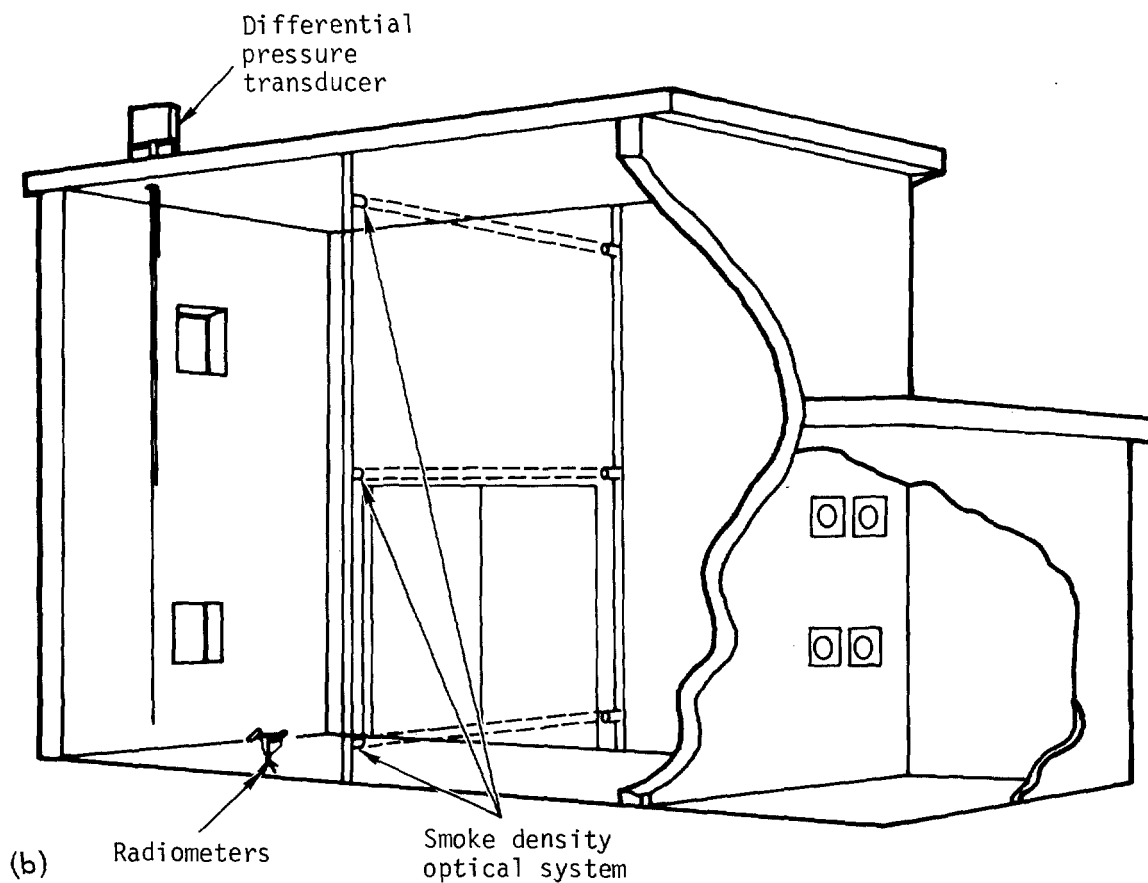


Figure 10 Upper exhaust duct showing gas sample intake tube.



(a) Thermocouple array



(b) Radiometers Smoke density optical system

Figure 11 (a) Map of temperature sensors in test cell; (b) locations of optical-density, pressure, and radiant heat sensors.

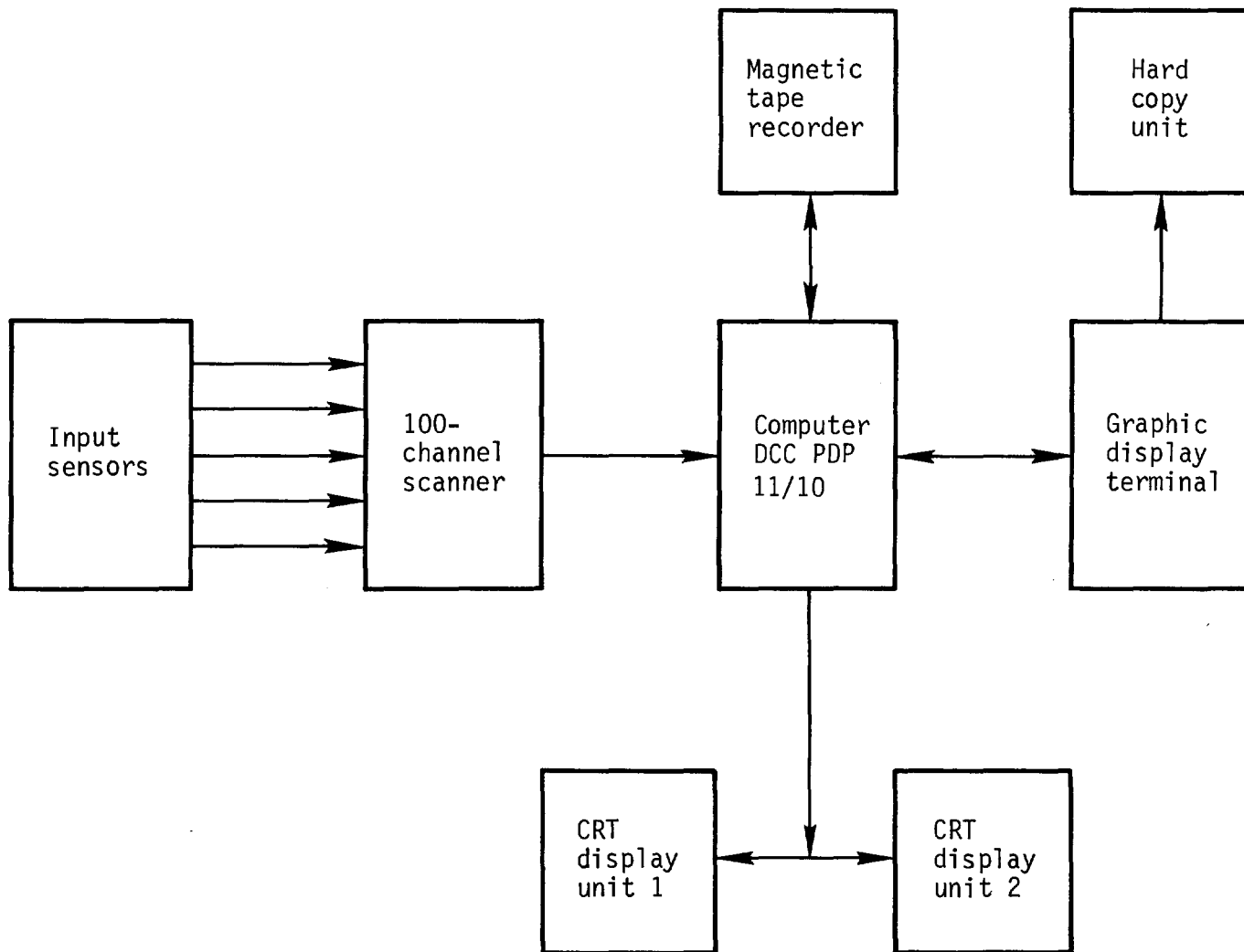


Figure 12 Fire test center data acquisition system.

III. Program Outline

As indicated in our report two years ago⁽²⁾, our program is divided into two phases: the first is an evaluation of the heat- and smoke-plugging insults delivered to the HEPA filter by various likely fire scenarios; and the second is the development and evaluation of countermeasures. The fire scenarios were divided into four sets of parameters as follows:

- Effects of various fuel and smoke loadings (high versus low; dirty versus clean)
- Effects of high versus low exhaust takeoff
- Effects of the use versus nonuse of sprinklers
- Effects of a fire in the room external to any enclosure versus internal to the enclosure.

Information as to actual fuel loadings was kindly supplied by a number of ERDA contractors in the form of lists and weights of materials and photographs. From these data, we prepared tabulations

14th ERDA AIR CLEANING CONFERENCE

expressed as kilograms of combustibles per square meter of floor area in a compartment; we then categorized the various items as "clean" or "dirty" burners. A clean burner is defined as a material or product which when involved in a well-ventilated fire will produce relatively few smoke particulates; a dirty burner is the opposite. Simply expressed, nonfire-retarded cellulosic materials and certain plastic materials are clean burners, whereas fire-retarded materials and a number of plastics are classified as dirty burners.

From these data and categories, a dirty-to-clean (weight) ratio (D/C) for items likely to be found in a laboratory were plotted against the fuel loading (kg/m² of floor area). The results are shown in Fig. 13. Using hand calculation methods, we examined the various concentrations of points and settled on four parameters, which are also shown on the chart. These are D/C ratios of 5 and 0.5 and combustible loadings of 2 and 8 kg/m².

The test parameters were discussed at a meeting of the project committee in the summer of 1975, and it was concluded that priority should be given to: (1) high-combustible loadings (e.g., 20 and 10 kg/m²); (2) an evaluation of sprinkler usage or nonusage; (3) an evaluation of D/C ratios of 3 versus 0.5; and (4) ignition sources external to the enclosures. This then, is the program we have initiated since the facility was first activated.

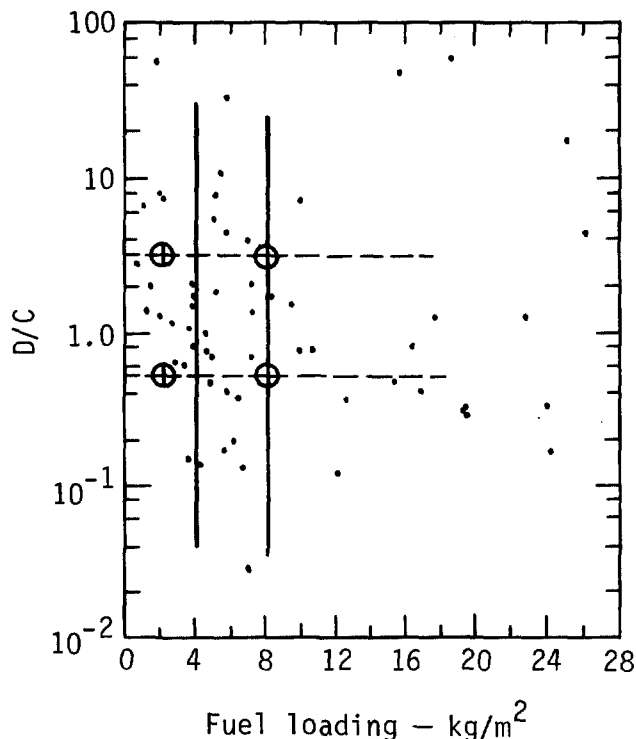


Figure 13 Smoke- versus fuel-loading test parameters.

14th ERDA AIR CLEANING CONFERENCE

IV. Preliminary Burns and Results

To date we have conducted eight burns, all classified as preliminary since during this time, we have been doing further debugging of the system and adding instrumentation. The tests are summarized below, and salient details together with results are included in the Appendix. Test No. 3 was a liquid fuel fire conducted to test the operation of the APC system. The system worked, and no data were obtained.

Test No. 1

The first test, conducted to evaluate the operational and safety characteristics of the test cell and components, involved surplus laboratory furnishings at a moderately heavy but dirty fuel loading. Fire was started by igniting 2 l of isopropanol in pans under the fuel array. The test was categorized by moderate ceiling temperatures, an almost immediate obscuration of light caused by dense smoke generation, and an overpressurization of the cell in about 2 min. Analysis of the smoke particulates taken from the exhaust duct revealed: (1) very heavy accumulation (e.g., 3800 mg/m³), and (2) a particle size distribution which indicated that about half of the weight of the smoke particulates was of 2 μm in size or larger.

Test No. 2

This burn was conducted to determine the effects of a clean, moderately heavy fuel load, and to ascertain whether we could mitigate the overpressurization phenomenon observed in the first test. The ignition source in this case was a plastic waste basket containing milk cartons and paper, the latter soaked with acetone. The results indicate that the fire was clean until the polyester hood ignited, at which time it became very sooty. Efforts to depressurize the room by increasing the exhaust ventilation were unsuccessful because the filter plugged that much sooner. Smoke particulate concentration in the duct was quite heavy - over 3000 mg/m³ mg per cubic meter. The particle size analysis shows that over 75% of the weight exceeded 3 μm in size.

Test No. 4

In this test, we looked at the effects of a free-burning diesel fuel floated on water in a pan. This fuel was allowed to burn for 20 min and then was extinguished using light water (aqueous film-forming foam). Smoke was dense, moderately heavy (about 1000 mg/m³), and rather fine in particulate size (50% by weight less than 1 μm in size). The ventilation uniformly decreased, and the filter plugged at about the time we extinguished the fire.

Test No. 5

In this burn, the loading was moderate but dirty (D/C ratio = 5.1). Included in the furnishings was a table-mounted clear plastic hood. The ignition source was 3 l of acetone poured into pans distributed on the floor and ignited remotely. The fire flared-up

14th ERDA AIR CLEANING CONFERENCE

immediately, but soon started to decay as indicated by the temperature records, probably because the cell pressurized and air could not be drawn into the enclosure. In spite of the dense smoke which obscured vision in 1.5 min, we could occasionally see flames inside the hood. When the hood burned through (about 11 min into the test), the temperatures in the cell started to rise briefly and then to decay again. Shortly thereafter, the ventilation was switched to the APC system which caused the fire to flare up again. The fire was then extinguished, using the overhead deluge system. During the entire test, the gas temperature just upstream of the HEPA filter did not exceed 100°C. Fuel loss in this test was 9% overall and 10% of the dirty items.

Test No. 6

This was a two-stage burn involving an oversized filter* using two 14-kg portions of diesel fuel floated on a pan of water and ignited using a half litre of gasoline which was in turn lit remotely. In the first stage the fire burned well, and the fuel was exhausted in the 19 min. During this time the ventilation decreased from 250 to 180 l/s, and the pressure drop across the HEPA filter changed from 30 to 1800 Pa, indicating an approach to plugging. After refueling, the ventilation was readjusted by opening the exhaust damper to 250 l/s. The second fire burned for a little over 3 min at which time the pressure drop across the HEPA filter increased to such an extent that the filter ruptured. At that time, the flow had decreased to 210 l/s. Smoke concentration in the duct and particulate sizes were about the same as in test No. 4. Significant concentrations of carbon monoxide and unburned hydrocarbons, accompanied by a considerable decrease in oxygen concentrations, were noted in the exhaust duct leading from the cell.

Test No. 7

This was conducted to determine the effect on filter plugging of a well-ventilated, clean-burning fuel. For this purpose, a wood crib (Douglas fir) was constructed so the fuel loading was 8.2 kg/m² and the D/C ratio was zero. An oversized filter was installed in the duct (500 l/s) and the ventilation was adjusted to the filter rating (e.g., equivalent to 18 air changes per hour). A gas burner was installed under the crib and ignited remotely. Gas feed to the burner was 100 l/min throughout the test. The fire burned well for about 16 min at which time it was extinguished. There was little evidence of filter plugging, but much higher temperatures than usual were noted. Half-way through the test a smoke sample taken from the exhaust duct showed a particulate concentration of 1000 mg/m³, 80% of which by weight was of particles larger than 3 µm.

*In all other tests described in this report a filter rated at 250 l/s was used, and the ventilation rate was set initially at 250 l/s. In test No. 6, a filter rated at 500 l/s was used and the flow was adjusted to 250 l/s initially.

Test No. 8

Test 8 was a repeat of Test 7, except that the initial ventilation rate was halved, i.e., to 250 l/s (9 air changes/hr). The fire burned well for 5 min, decayed to a lower steady state for 14 min, and flared up briefly as the APC system was switched over. It was extinguished at 20 min. The cell pressurized at 3-4 min and a dense, acrid, liquid-particulate smoke emanated from the intake ports. During the latter part of the test, liquid tars started to condense downstream of the HEPA filter. Smoke-particulate concentration and size increased during the test. At 16 min the concentration was 12 g/m³; 70% of this weight consisted of particles 2 μm or larger.

V. Discussion and Future Work

Whereas the tests conducted to date have been somewhat preliminary in nature and have not been replicated, we can make some tentative observations and conclusions of a general nature.

First, in all the tests so far where normal ventilation was used and no attempt was made to increase the exhaust ventilation in the event of fire, an almost immediate overpressurization of the compartment has been evident.

Secondly, in the one or two cases where we have increased exhaust ventilation and the fire was dirty, i.e., generating large quantities of smoke particulates, the filter plugged faster and the room finally pressurized as the exhaust ventilation was decreased because of this filter plugging.

Thirdly, one of the "clean" fires became dirty when a significantly large dirty-burning item became involved.

Fourth, the smoke particulate concentration in the exhaust ductwork is, in our opinion, quite high when a heterogeneous mixture of furnishings catches fire and the ventilation is insufficient to cause the fire to burn cleanly if this is at all possible.

Fifth, there are two reasons to hope that the smoke particulates generated in the kinds of fires we have been using can be reduced by scrubbing. The first, is that the particle size distribution in our full-scale fire test compartment seems to be tending toward the larger sizes, which means that they may be able to be targeted by fine water sprays with or without wetting agents or with certain chemicals which can cause them to precipitate. Secondly, our air pollution control system has worked quite satisfactorily. However, this is not a very effective method from the installation-, standby-, and operating-cost per unit volume of gas scrubbed.

During the next several months after we run (and check) a few more test fires, we plan to evaluate a number of smoke-abatement counter-measures. These will include the use of single and sequential water sprays with or without additives, and with or without the use of various prefiltering techniques. By our next meeting, we hope to report on cost-effective methods which we can all use.

14th ERDA AIR CLEANING CONFERENCE

References

1. J. R. Gaskill and J. L. Murrow, "Fire Protection of HEPA Filters by Using Water Sprays," Proceedings of the Twelfth Air Cleaning Conference, Vol. 1 (1972), pp. 103-122.
2. J. R. Gaskill and M. W. Magee, "The HEPA-Filter Smoke Plugging Problem," Proceedings of the Thirteenth Air Cleaning Conference, Vol. 1 (1974), pp. 584-607.
3. J. R. Gaskill, D. G. Beason, and H. W. Ford, Jr., "HEPA-Filter Fire Protection," Hazards Control Progress Report No. 50, UCRL-50007-75-1 (Jan-June 1975), pp. 20-23.

14th ERDA AIR CLEANING CONFERENCE

APPENDIX - TEST RESULTS AND DATA

PRELIMINARY BURN NO. 1 DATE Jan. 23, 1976

PURPOSE To evaluate operational and safety characteristics of Test Cell and components; to determine fire- and filter-plugging effects of dirty, moderately heavy fuel load

FUEL Surplus Laboratory furnishings and equipment

LOADING 9.7 kg/m² D/C RATIO 2.66

INITIAL VENTILATION 250 l/s (9 changes/hr) EXHAUST high

IGNITION 2-l isopropanol in pans under fuel ignited by lighting solvent-soaked train of paper tissue.

RESULTS

SUMMARY Immediate flaming; viewports sooted up/2 min; at 10 min APC (Air Pollution Control) system turned on; cell temps climbed again. At 12-13 min deluge system extinguished fire - fuel loss: 30% total; 38% clean; 27% dirty.

DETAILS

Maximum Temperatures (°C)

In Cell >500/2 min in flame In Cell at ceiling 395

In Cell at exhaust - In Duct at HEPA 115

Cell Pressure Overpressured at ~2 min

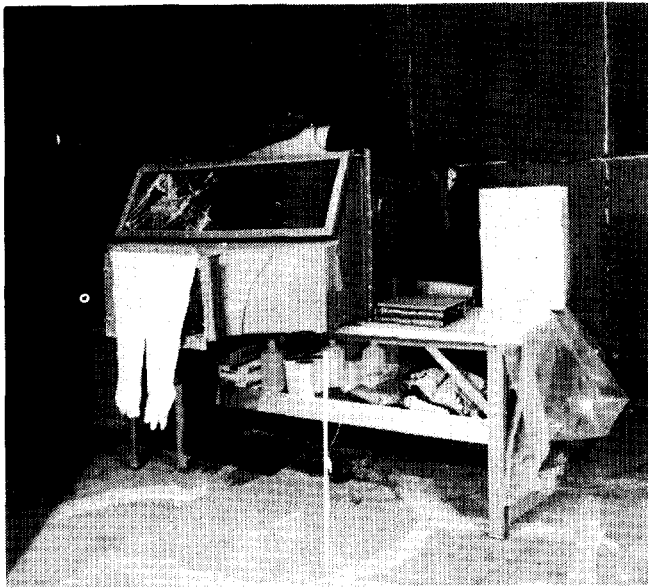
Optical Density Not measured

Exhaust Ventilation Flow Not measured

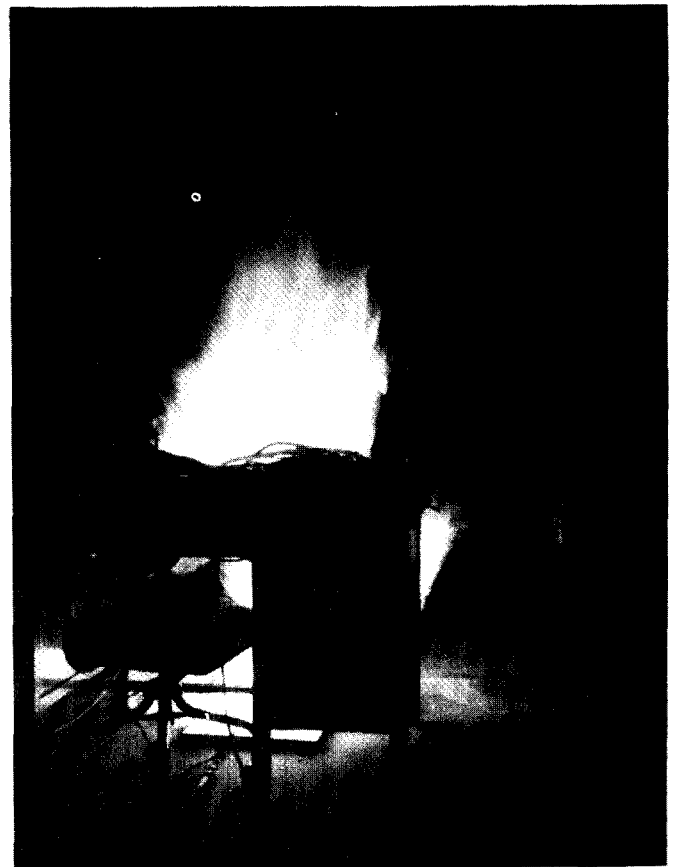
P HEPA (Pa) Not measured

Smoke Particulates-Concentration(mg/m³) 3800 at 4 min.

"Size" (µm) >3/25%; ~2/25%; ~1/28% %



(a).



(b)



(c)



(d)

Figure A-1 Test No. 1. (a) Fuel array; (b) fire at 0.5 min; (c) fire at 1 min; (d) fuel after burn (loss about 23 kg); (e) external view during test.



(e)

Figure A-1 (continued)

14th ERDA AIR CLEANING CONFERENCE

PRELIMINARY BURN NO. 2 DATE Feb. 13, 1976

PURPOSE To minimize overpressurization; to determine effects of clean, moderately heavy fuel load.

FUEL Surplus Laboratory furnishings and equipment

LOADING 10.5 kg/m² D/C RATIO 0.57

INITIAL VENTILATION 250 l/s (9 changes/hr) EXHAUST high

IGNITION Plastic waste basket containing milk cartons & paper soaked with acetone.

RESULTS

SUMMARY Clean fire until polyester hood ignited; then very sooty; attempts to depressurize room by increasing exh. ventil. unsuccessful because filter plugged (1.0 kg of soot); fuel loss: 9.1% of total; 6.6% clean; 12.3% dirty.

DETAILS

Maximum Temperatures (°C)

In Cell ND In Cell at ceiling ND

In Cell at exhaust ND In Duct at HEPA ND

Cell Pressure See narrative

Optical Density

Exhaust Ventilation Flow 250 → 500 → < 150 l/s

P HEPA (Pa) ND

Smoke Particulates-Concentration(mg/m³) 3375 at 16 min.

"Size" (µm) 3/75% %

14th ERDA AIR CLEANING CONFERENCE

PRELIMINARY BURN NO. 4 DATE March 26, 1976

PURPOSE To evaluate effect of free-burning diesel fuel on smoke-
particulate production, filter clogging, and combustion
rate.

FUEL 25-mm layer (13 kg) diesel fuel on water in 914-mm diam. pan

LOADING 0.55 kg/m² D/C RATIO -

INITIAL VENTILATION 250 l/s EXHAUST high

IGNITION 500-m/gasoline floated on surface of fuel; ignited with
torch.

RESULTS

SUMMARY Fuel burned ~20 min; then extinguished; dense smoke;
ventilation decreased & filter plugged ~20 min.
Fuel loss: 8 kg (~62%)

DETAILS

Maximum Temperatures (°C)

In Cell 500 center midheight In Cell at ceiling 320

In Cell at exhaust 160 In Duct at HEPA 60

Cell Pressure

Optical Density Heavy in ~1 min

Exhaust Ventilation Flow 250 → 125 l/s in 20 min

P HEPA (Pa) → 2200 (loading 0.3 kg)

Smoke Particulates-Concentration(mg/m³) ~1000 at min.

"Size" (µm) <1/50%

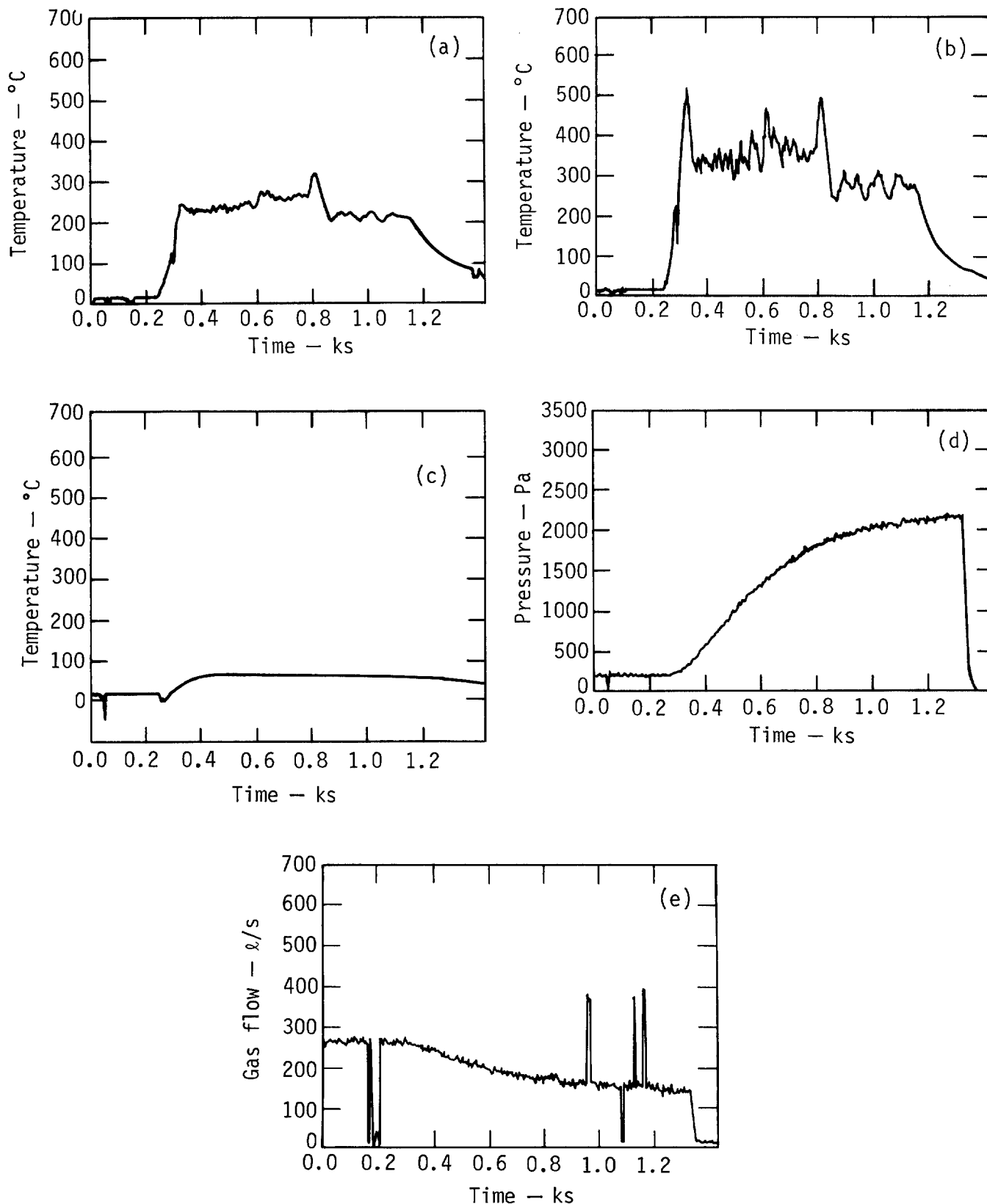


Figure A-2 Test No. 4. (a) Temperature in center of cell 3.7 m above floor; (b) temperature in center of cell 2.2 m above floor; (c) temperature in duct ahead of HEPA filter; (d) pressure drop across HEPA filter; (e) gas flow in exhaust duct.

14th ERDA AIR CLEANING CONFERENCE

PRELIMINARY BURN NO. 5 DATE April 22, 1976

PURPOSE To determine effects of very dirty, moderately heavy fuel loading; to test gas sampling/analytical system; to demonstrate system to local media.

FUEL Surplus Laboratory furnishings and equipment

LOADING 10.5 kg/m² D/C RATIO 5.1

INITIAL VENTILATION 250 l/s EXHAUST high

IGNITION 3-l of acetone in pans on floor ignited remotely using spark coil.

14th ERDA AIR CLEANING CONFERENCE

RESULTS

SUMMARY Room pressurized/vision obscured in 1.5 min; fire decayed at 3 min (lack of oxygen) for 12 min when hood burned through then flared up. Vent switched to APC increase in fire level. Extinguished at 21 min. Fuel loss: total 9%; clean 1.5%; dirty 10%.

DETAILS

Maximum Temperatures (°C)

In Cell 700 in flame In Cell at ceiling 550

In Cell at exhaust 300 In Duct at HEPA 80

Cell Pressure Positive after 1.5 min

Optical Density Dense smoke

Exhaust Ventilation Flow 250 → 220 l/s in 10 min

P HEPA (Pa) Lost data

Smoke Particulates-Concentration(mg/m³) 1000 at min.

"Size" (µm) 3/44% %

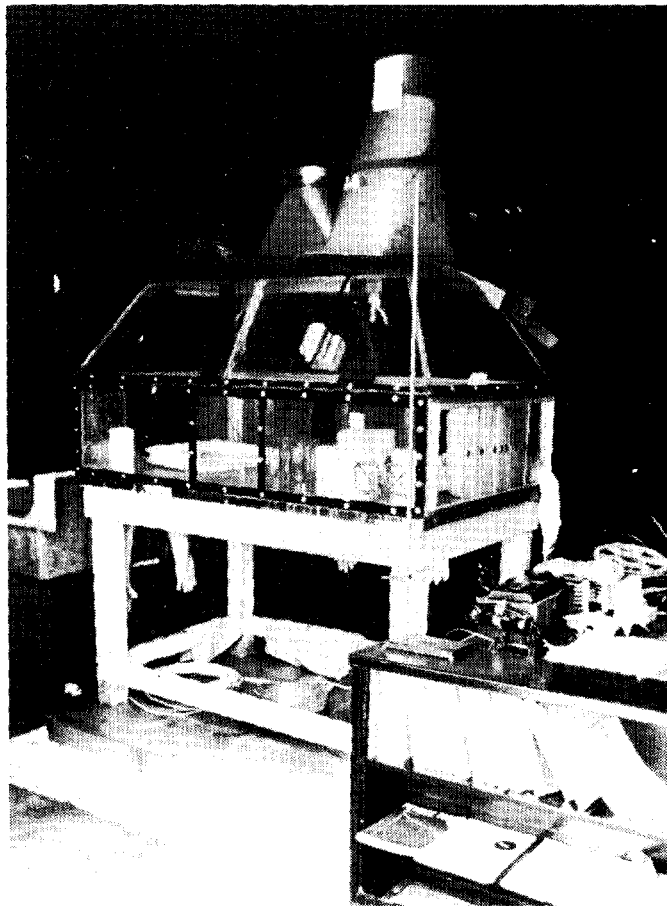
Exhaust-gas Analysis

Unburned hydrocarbons (ppm methane) 3200/5 min MAX

Carbon monoxide (ppm CO) 3600/5 min MAX

Carbon dioxide (% CO₂) ND MAX

Oxygen (% O₂) 11.5 min MIN



(a)



(b)

Figure A-3 Test No. 5. (a) Fuel load before fire; (b) fuel load after fire.

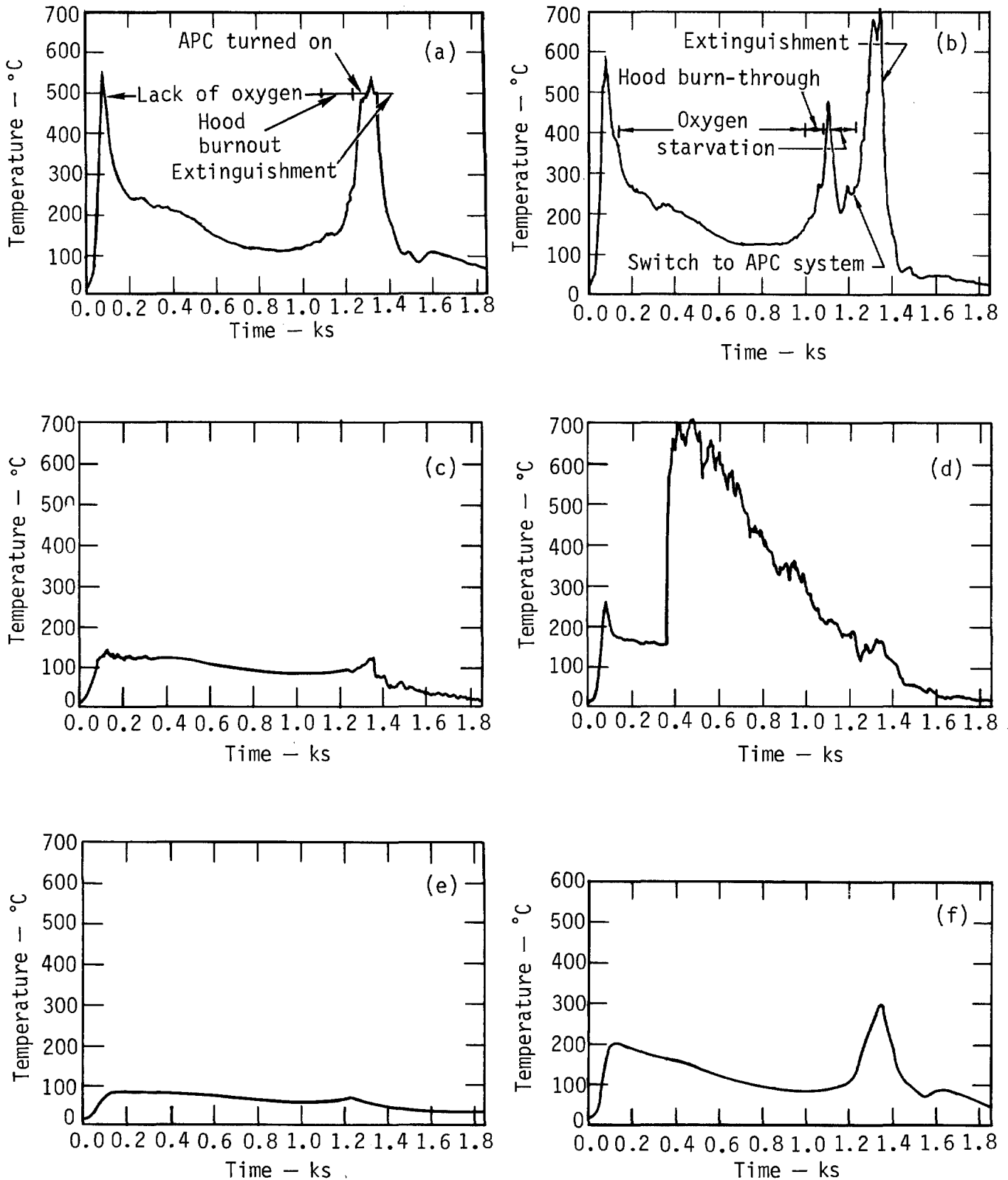


Figure A-4 Test No. 5. (a) Temperature in center of cell 3.7 m above floor; (b) temperature in center of cell 2.2 m above floor; (c) temperature in southwest corner of cell 0.5 m above floor; (d) temperature in hood; (e) temperature in duct ahead of HEPA filter; (f) temperature at cell outlet in duct.

14th ERDA AIR CLEANING CONFERENCE

PRELIMINARY BURN NO. 6 DATE May 7, 1976

PURPOSE Effect on filter plugging of oversize filter using diesel
fuel- two-part burn

FUEL 14-kg diesel, first part - 14-kg diesel, second part

LOADING 0.59 kg/m² D/C RATIO -

INITIAL VENTILATION 250 l/s for each test EXHAUST high

IGNITION 500-ml gasoline floated on diesel; ignited remotely.

Note: Filter rated at 500 l/s was used.

14th ERDA AIR CLEANING CONFERENCE

RESULTS

SUMMARY First fire burned well and burned out in 19 min. Second fire burned 3.3 min when filter reaptured.

Fuel loss: 0.73 kg/min.

DETAILS

Maximum Temperatures (°C)

In Cell 600 (above fire) In Cell at ceiling 300

In Cell at exhaust - In Duct at HEPA 80

Cell Pressure -

Optical Density 1.5 m

Exhaust Ventilation Flow Part 1 Part 2
 250 → 180 l/s 250 → 210 l/s

P HEPA (Pa) first part second part
 30 → 1800 2600 → 2750 (rupture)

Smoke Particulates-Concentration(mg/m³) ~1000 at 5 min.

"Size" (µm) <1/40%; >3/~25% %

Exhaust-gas Analysis

Unburned hydrocarbons (ppm methane) 2800/20 min MAX

Carbon monoxide (ppm CO) 2000/20-min MAX

Carbon dioxide (% CO₂) ND MAX

Oxygen (% O₂) 10/20-min MIN

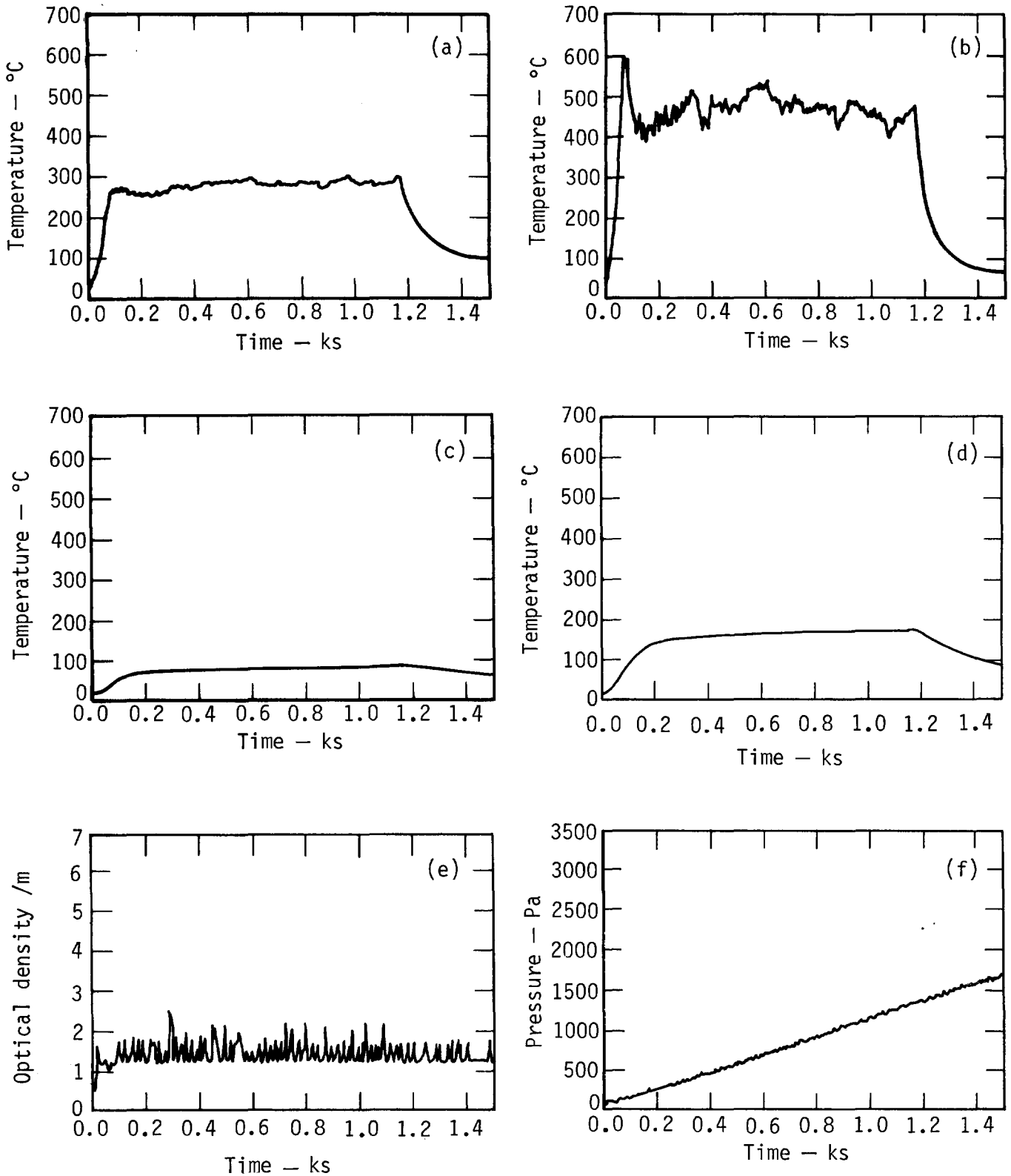


Figure A-5 Test No. 6. (a) Temperature in center of cell 3.7 m above floor; (b) temperature in center of cell 2.2 m above floor; (c) temperature in duct ahead of HEPA filter; (d) temperature in duct 1 m from cell exhaust; (e) optical density in cell 2.2 m above floor; (f) pressure drop across HEPA filter; (g) gas flow in exhaust duct; (h) fuel weight loss.

14th ERDA AIR CLEANING CONFERENCE

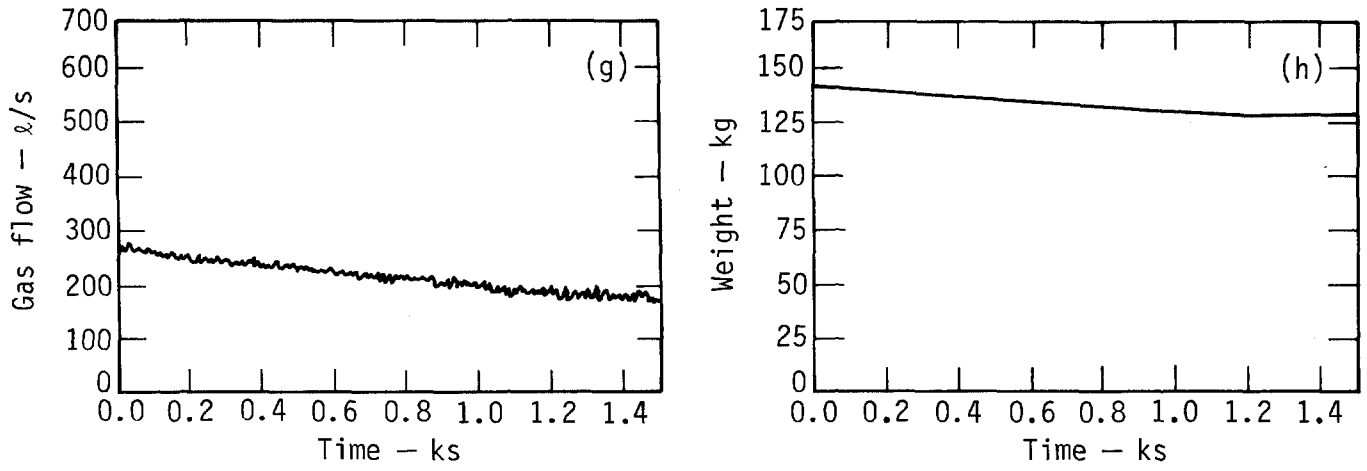


Figure A-5 (continued)

14th ERDA AIR CLEANING CONFERENCE

PRELIMINARY BURN NO. 7 DATE May 28, 1976

PURPOSE Effect on filter plugging of well ventilated clean burning fuel (Douglas-fir, wood crib) plus natural gas

FUEL Douglas fir crib 0.914 × 1.22 × 0.81 m high made up of 51 × 51-mm cross section sticks

LOADING 8.2 kg/m² D/C RATIO 0

INITIAL VENTILATION 500 l/s (18 changes/hr) EXHAUST high

IGNITION Premixed natural gas fire (ignited remotely) under crib at 100 l/min, used throughout test.

14th ERDA AIR CLEANING CONFERENCE

RESULTS

SUMMARY Fire burned well for ~16 min and was then extinguished; little evidence of filter plugging; higher than usual temperatures noted.

DETAILS

Maximum Temperatures (°C)

In Cell ~720-above flame In Cell at ceiling 630

In Cell at exhaust 300 In Duct at HEPA 200

Cell Pressure ~20-30 Pa (negative)

Optical Density ND

Exhaust Ventilation Flow 530 → 470 l/s

P HEPA (Pa) 250 → 420

Smoke Particulates-Concentration(mg/m³) 1000 at 8 min.

"Size" (µm) >3/80%

Exhaust-gas Analysis

Unburned hydrocarbons (ppm methane) ND MAX

Carbon monoxide (ppm CO) 30,000 MAX

Carbon dioxide (% CO₂) ND MAX

Oxygen (% O₂) 6 MIN

14th ERDA AIR CLEANING CONFERENCE

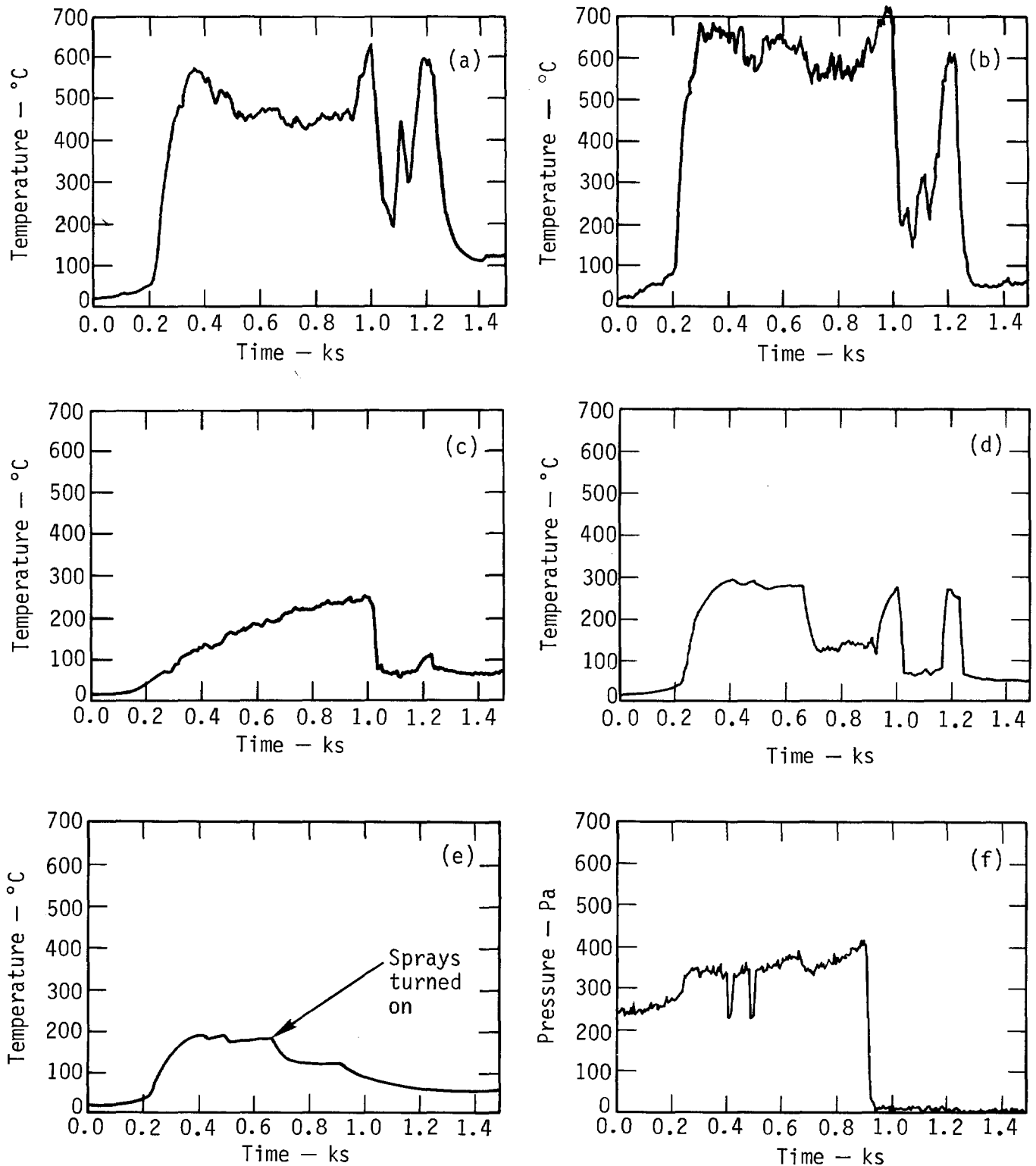


Figure A-6 Test No. 7. (a) Temperature in center of cell 3.7 m above floor; (b) temperature in center of cell 2.2 m above floor; (c) temperature at west end of cell 0.5 m above floor; (d) temperature in duct 1 m from cell exhaust; (e) temperature in duct ahead of HEPA filter; (f) pressure drop across HEPA filter; (g) gas flow in exhaust duct; (h) fuel weight loss; (i) percent oxygen in duct at cell exhaust.

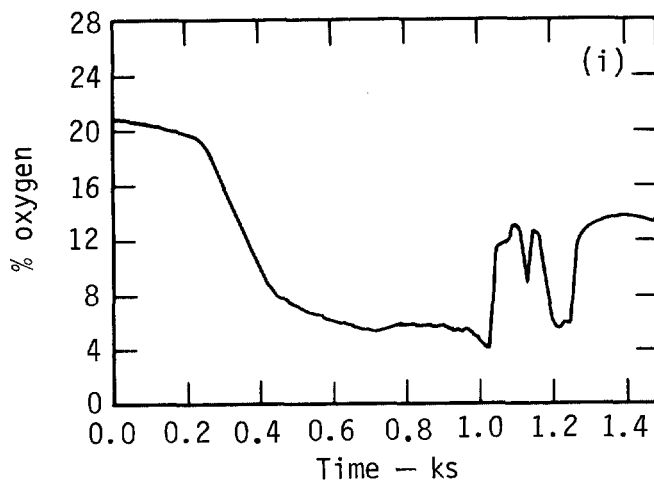
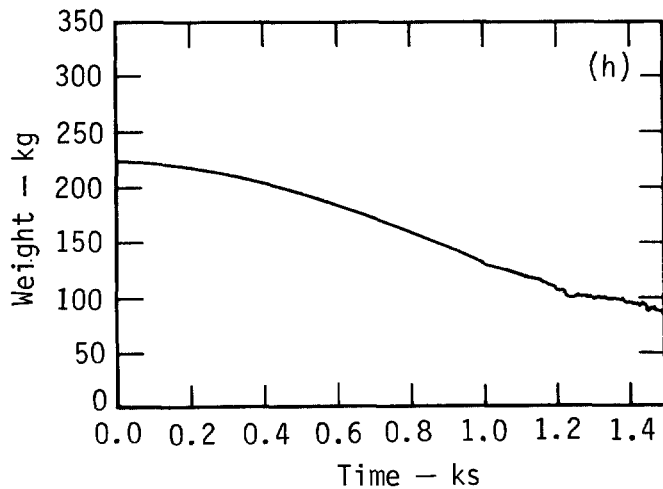
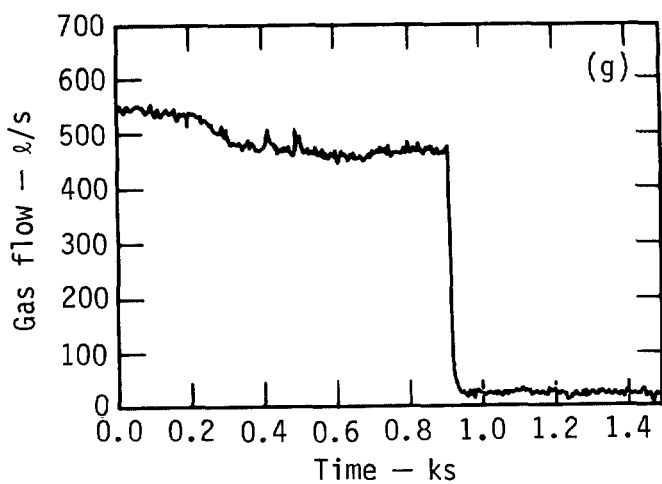


Figure A-6 (continued)

14th ERDA AIR CLEANING CONFERENCE

PRELIMINARY BURN NO. 8 DATE June 22, 1976

PURPOSE To determine effect on filter plugging of moderately well ventilated, clean burning fuel. (Douglas fir wood crib) plus premixed natural gas flame.

FUEL Douglas fir crib, similar to that used in PB-7 plus premixed natural gas flame

LOADING 8.3 kg/m² D/C RATIO 0

INITIAL VENTILATION 250 l/s (9 changes/hr) EXHAUST high

IGNITION Premixed natural gas (ignited remotely) located under crib and kept burning using 100 l/min of gas throughout test.

14th ERDA AIR CLEANING CONFERENCE

RESULTS

SUMMARY Good burning for 5 min; decay to lower steady state for 14 min;
brief flareup during APC switchover; extinguished at 20 min.
Overpressurization at 2-3 min; dense, acrid, liquid-
particulate smoke.

DETAILS

Maximum Temperatures (°C)

In Cell 700 over crib In Cell at ceiling 550

In Cell at exhaust 280 In Duct at HEPA 100

Cell Pressure 20 Pa negative

Optical Density 1/m

Exhaust Ventilation Flow 250 → 100 l/s in 15 min

P HEPA (Pa) 200 → 2000/15 min

Smoke Particulates-Concentration(mg/m³) 12 000 at 16 min.

"Size" (um) >2/70% %

Exhaust-gas Analysis

Unburned hydrocarbons (ppm methane) ND MAX

Carbon monoxide (ppm CO) 60 000/20 min MAX

Carbon dioxide (% CO₂) ND MAX

Oxygen (% O₂) 4.4%/21 MIN

14th ERDA AIR CLEANING CONFERENCE

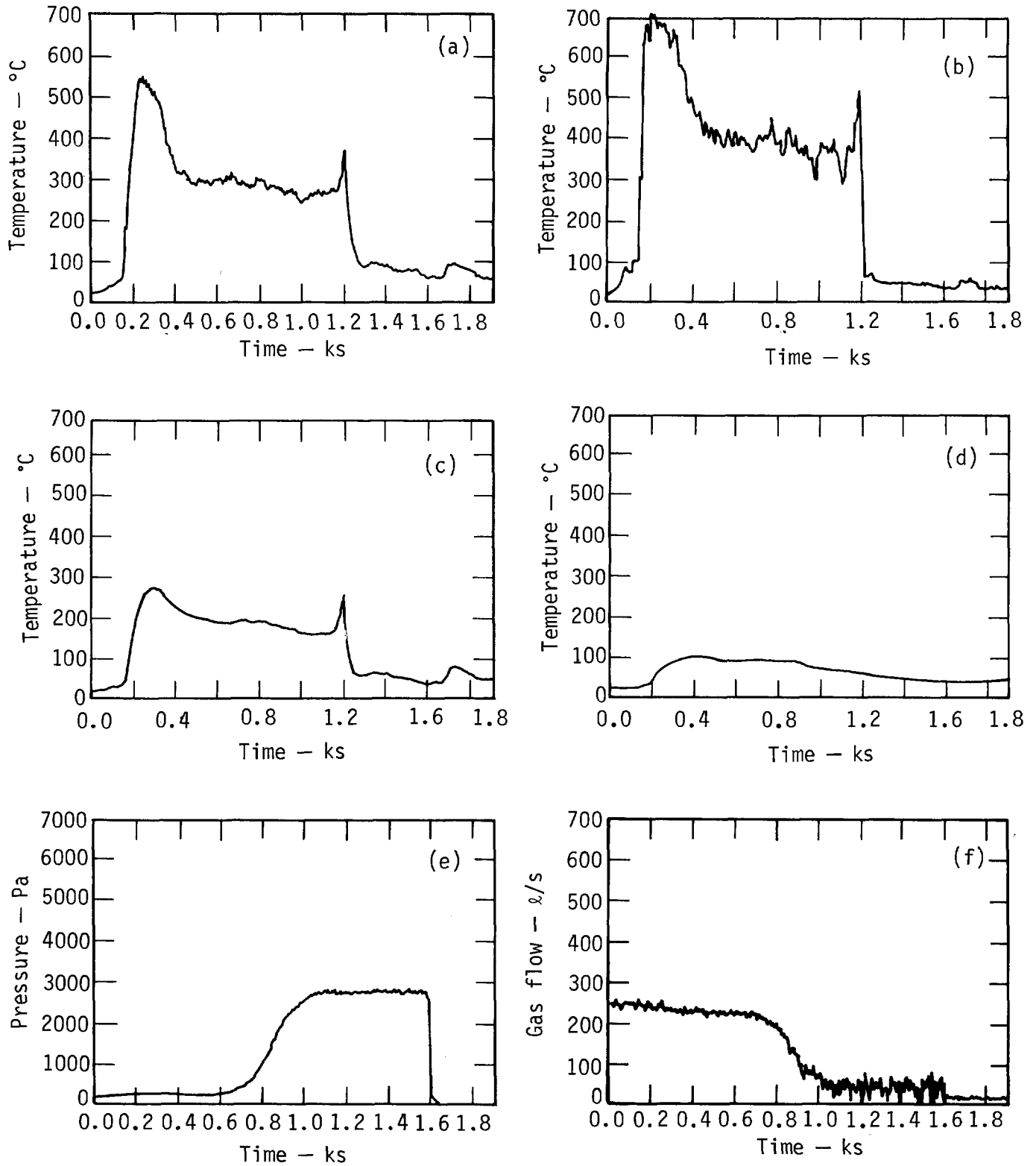


Figure A-7 Test No. 8. (a) Temperature in center of cell 3.7 m above floor; (b) temperature in center of cell 2.2 m above floor; (c) temperature in duct 1 m from cell exhaust; (d) temperature in duct ahead of HEPA filter; (e) pressure drop across HEPA filter; (f) gas flow in exhaust duct; (g) percent oxygen in duct at cell exhaust; (h) percent carbon monoxide in duct at cell exhaust; (i) fuel weight loss.

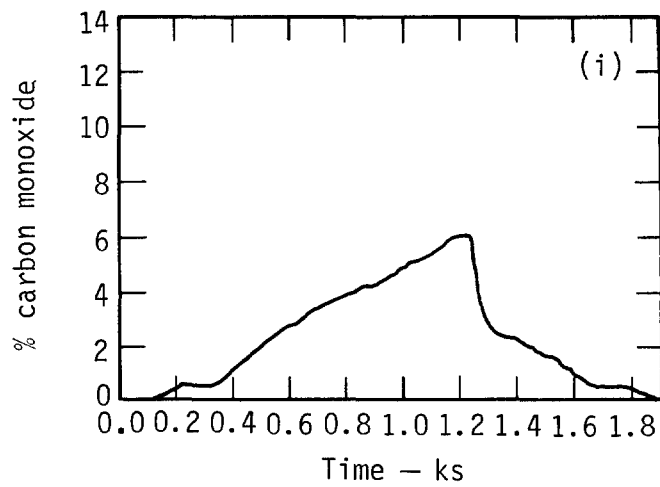
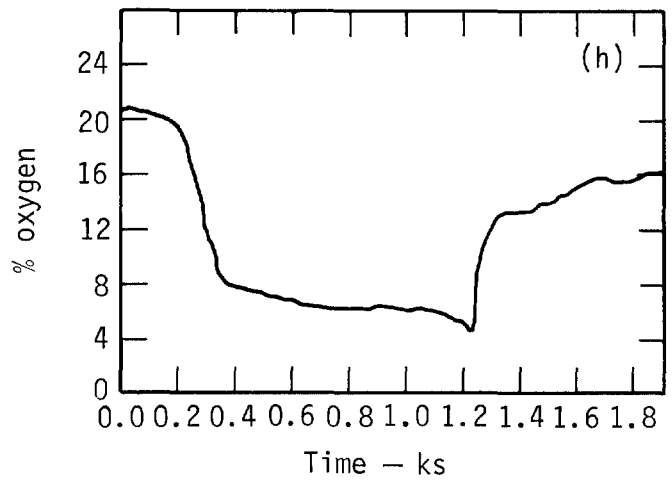
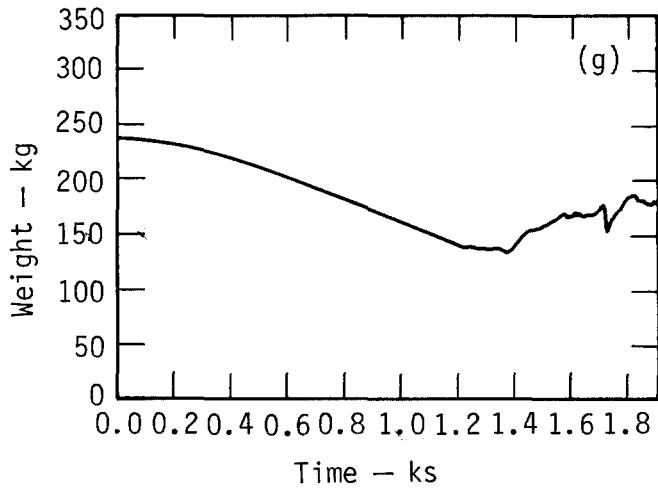


Figure A-7 (continued)

DISCUSSION

BALSMEYER: You talked about filter plugging. Is there any standard definition we can use?

GASKILL: Yes. Three years ago, at an ERDA conference, it was agreed somewhat arbitrarily that after one starts off at a rate of flow, say, 250 liters a second, when one reaches 125 liters per second, the filter is considered to be plugged. Empirically, we have found that this is tantamount to a pressure differential of about 2,100 to 2,300 Pascals across the filter.

BALSMEYER: On filter plugging, did you notice filter breaching or anything else from high pressure flow?

GASKILL: Only in the one case we illustrated. In the other cases, we have stopped short of that. When the filter is plugged, we just say, "That is it", and stop the test. But in the one case where we had the Diesel fuel fire, we were up to around 2,000 Pascals differential at the end of the first fire. The second fire went for three minutes, and we were reading something like 2,800 Pascals when the filter ruptured.

FIRST: I am wondering why you don't go into a more sophisticated filter system by using deep beds of fibers or granules which would have a capacity to protect the absolute filter more capably than is shown.

GASKILL: We may come to that. We have some ideas on scrubbing techniques which we have deferred up to now because our previous work showed that we were dealing with what I will call embryonic particles, mostly of submicron size. Our work now shows they are apparently in the micron size and may be amenable to some of the techniques we have in mind and will be checking. On the other hand, if these are unsuccessful, we will have to use more expensive methods.

W.C. BROWN: I have a question regarding an ERDA interpretation that requires sprinklers in the filter exhaust ahead of the HEPA filters. About two years ago, we designed a system with two stages. Now we are confronted with the possibility that their thinking has changed and that only one stage of sprinklers will be required. The sprinklers will be followed by a demister-prefilter section which tends to protect the HEPA's from carry-over of moisture. Would that be satisfactory?

GASKILL: I don't know that I can completely comment on that. However, as we reported two years ago, using a two-fluid nozzle, we can get 100 per cent evaporation of the water. On a steady basis, with intake gases of 800 degrees Celsius, we can reduce the temperature to 150 degrees Celsius, which I understand is satisfactory, in a distance of about a meter and a half of duct length. We didn't find it necessary to use demisters at that point. On the other hand, I should mention that if, in our scrubbing techniques, we find it necessary to go back to the old inefficient method of spraying where there is a lot of water carry-over, then demisters would probably be indicated. But that remains to be seen.

TORNADO DEPRESSURIZATION
AND
AIR CLEANING SYSTEMS

W. S. Gregory, K. H. Duerre, P. R. Smith*, and R. W. Andrae
Staff Members, Los Alamos Scientific Laboratory
Los Alamos, New Mexico

Abstract

Results from analytical and experimental investigations of tornado depressurization effects on air cleaning systems are presented. Development and use of a computer code that simulates the internal pressures and flows within an arbitrary ventilation system is described. The formulation of fluid motion equations is based upon lumped component response, isothermal or adiabatic compression of air, and conservation of mass. A computer generated movie is shown illustrating the flows and pressures in a simple system.

Also described are experimental investigations to determine air cleaning component response to high flow rates caused by tornado depressurization. HEPA filter is the principal component under investigation. A description of the experimental apparatus is given and preliminary test results presented.

I. Introduction

Air cleaning systems in nuclear fuel cycle facilities must maintain confinement during such natural phenomena as earthquakes and tornados. The operation of a nuclear facility ventilation system is highly dependent on stable atmospheric pressure to maintain proper pressure differentials between containment zones. Atmospheric pressure drops as large as 20.7-kPa (3-psi) are associated with tornados, so that generation of undesirable pressures and flow rates within a ventilation system is possible. Large pressure drops could cause filtration failures, duct collapse or damper failures. Failure of these components in air cleaning systems could result in release of radioactive material to the environment.

Tornado depressurization effects on air cleaning systems are being studied both experimentally and analytically at the Los Alamos Scientific Laboratory and New Mexico State University. A computer code that will predict the magnitude of the pressures and flows within an air cleaning system is the objective of the analytical effort. Experimental testing has centered on evaluating critical air cleaning component response to large pressure pulses. The experimental data obtained will establish empirical relationships for the computer code, and provide structural response information. The status of the experimental and analytical work will be described in the following sections of this paper.

*Professor, New Mexico State University, Las Cruces, New Mexico.

II. Experimental WorkPreliminary Experimental Testing

Small-scale testing of 0.2-by 0.2-m (8-by 8-in.) HEPA filters has been performed at New Mexico State University⁽¹⁾. A blow-down system was used to impose a 20.7-kPa (3-psi) pressure differential across the test filters for three seconds. A pressurized tank (Fig. 1) supplied the air needed to create the required pressure pulse.

The mass flow rate was regulated by sonically choking the flow, and expanding to the desired pressure in a chamber. The chamber served to slow the flow and allow the prefiltering system to operate within design capacity. The flow was exited through a test section of sufficient length to achieve uniform flow before impinging upon the test filter. Flow timing was accomplished by controlling the opening rate of a pneumatically operated ball valve upstream from the sonic orifice.

New 0.2-by 0.2-m (8-by 8-in.) HEPA filters were tested at overpressures of 20.7-kPa (3-psi) with a 6.9-kPa/s (one-psi/s) pressurization rate. Characteristic flow-resistance data were obtained for the filters. The following conclusions were made from these tests.

- A pressurization rate of 6.9-kPa/s (one-psi/s) did not cause physical damage to the filters.
- In some tests, the pressurization rate was larger than 6.9-kPa/s (one-psi/s), which led to failure of the filter. The 0.6-by 0.6-m (24-by 24-in.) filters would be even more susceptible to structural failure because of their larger span.
- At high flow rates the pressure drop across the filter depends upon the duct cross-sectional area, and not on filter depth (Fig. 2).
- Air seems to pass through only a small portion of the filter during the pressure transient. This raises the question of filter effectiveness even if structural failure does not occur (Fig. 3).

Present Experimental Testing

The small filter experiments provided basic information for designing an experimental facility to test 0.6-by 0.6-m (24-by 24-in.) HEPA filters. Results of the small filter tests have led to speculation that high flow rates through HEPA filters can also lead to filter failure. The high velocity air through the folded ends of the fiber mat may open up mat fibers allowing high flow rate air to pass through, and then close after the transient with no evidence of structural failure. (See the change in filter resistance in Fig. 2). Entrapment of particles by the velocity-dependent diffusion mechanism may not occur during turbulent air flow through the fibers. Re-entrainment of smaller particles without a second entrapment could also occur under reversed high flow rate conditions.

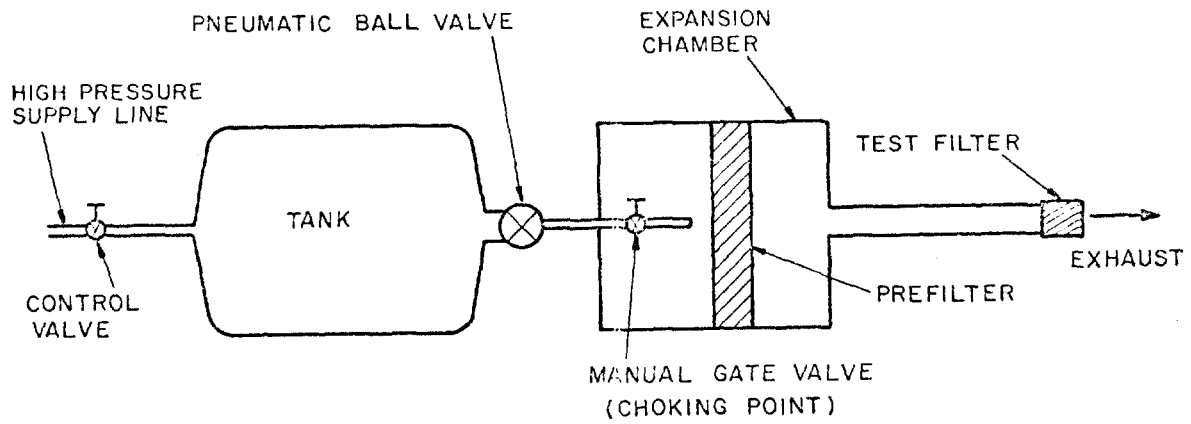


Fig. 1. Small filter experimental apparatus.

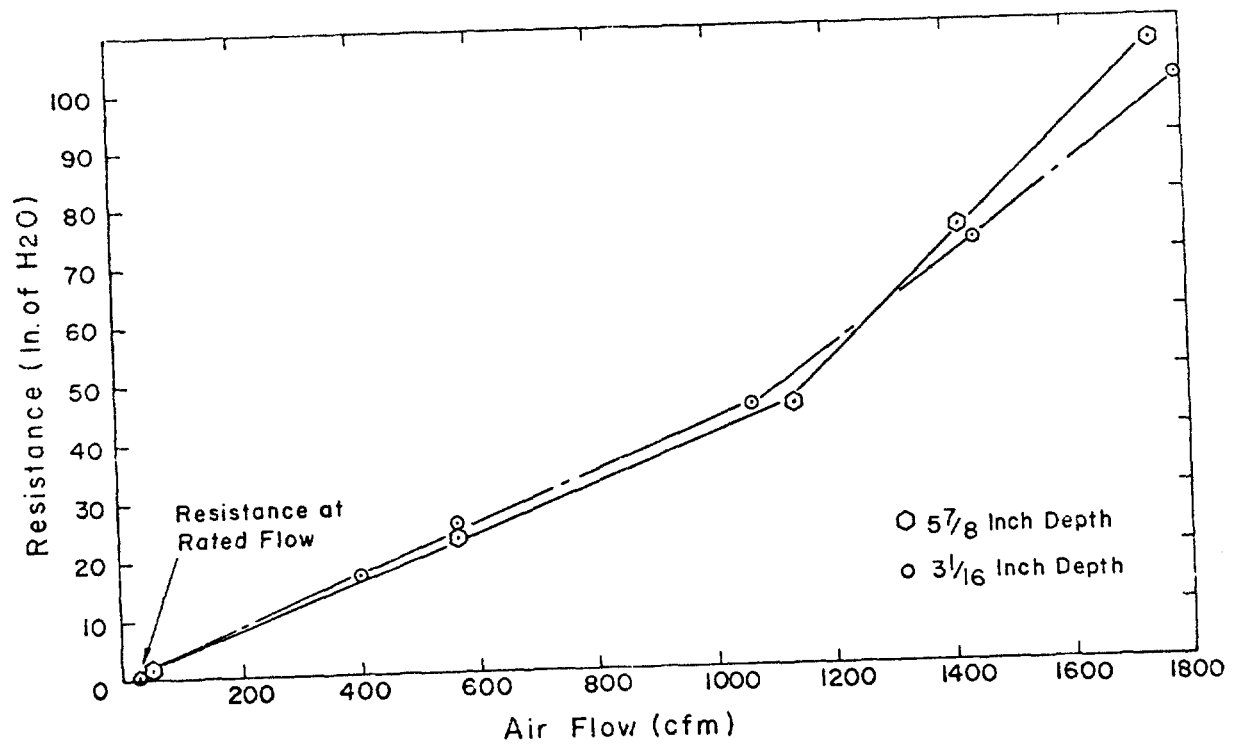


Fig. 2. Flow-resistance curve.

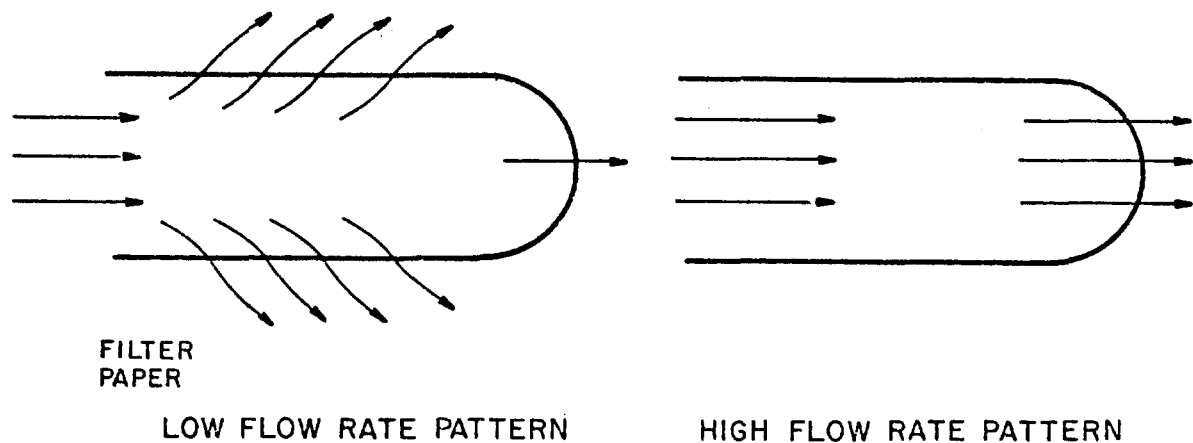


Fig. 3. Flow patterns through HEPA filter.

Objective of the present test program will be to determine the response of 0.6-by 0.6-m (24- by 24-in.) HEPA filters subjected to pressure pulses simulating a NRC Region I tornado (Fig. 4). Two possible failure modes will be investigated; failure from structural damage such that the physical integrity of the filter is destroyed and filter degradation under the NRC Region I tornado pressure conditions.

The experimental program will attempt to answer the following questions:

- Will the structural integrity of the filters be maintained during the pressure pulse?
- How critical is the rise-time of the pressure pulse? When, or at what rate of the pressure rise will the filters invariably fail?
- What is the actual flow-path through the filters during the transient pressure pulse? How does the porosity of the filters change during the pulse?
- If the filters do not fail structurally, is filter effectiveness maintained during the transient pressure pulse? Is filter effectiveness different after the pressure pulse?
- How effective are "loaded" filters during the pressure pulse? Does degree of loading have an effect upon structural failure of the filters?
- How much "release" can be expected during the transient pressure pulse for various degrees of loading?

Proposed Test Methods and Equipment. The equipment to be used to test the 0.6-by 0.6-m (24-by 24 in.) HEPA filters will be a scaled-up version of the preliminary experimental equipment. Two large pressure tanks and compressor equipment were obtained from the Nevada Test Site, and are now located at New Mexico State University at

Las Cruces, New Mexico. The pressure tanks are each 1.5-m (5 ft.) in diameter and 19.8-m (65 ft.) long (Fig. 5). They were made to contain oxygen at pressures to 19.3-MPa (2800-psi.). The compressor is capable of supplying air at 1.7-MPa (250-psi). A pressure of 1.3-MPa (200-psi) in the tanks will provide enough air for one pressure pulse. After each pressure pulse is applied, the tanks will be re-pressurized for the next pulse.

As in the small filter experiment, the mass flow rate will be regulated by sonically choking the flow and expanding into a 3.1-by 3.1-m (10-by 10-ft.) chamber (Fig. 6). The expansion chamber will contain 25 HEPA filters for prefiltering the air. The air will travel through a duct of sufficient length to achieve uniform flow before impinging on the test filter.

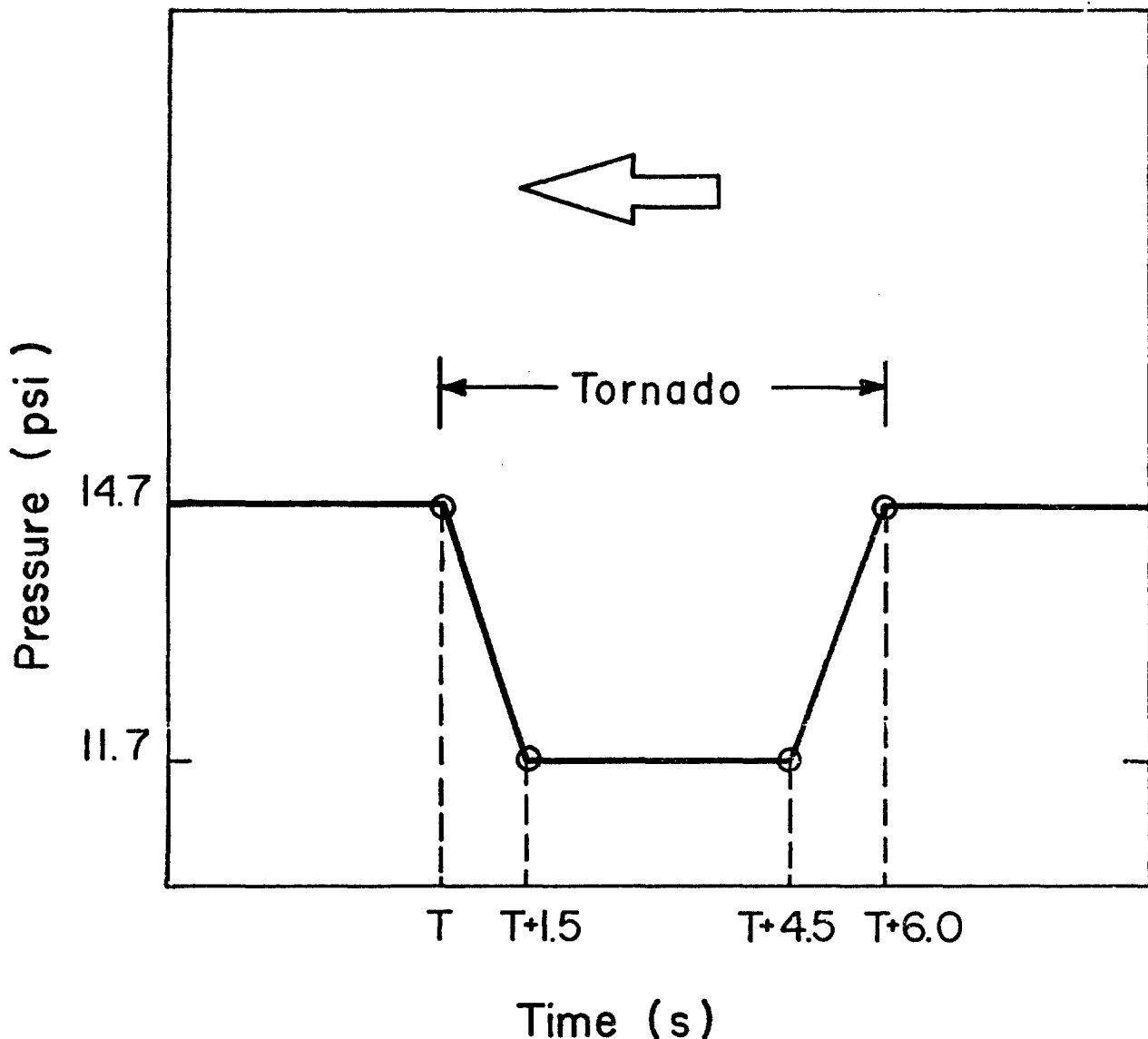


Fig. 4. Assumed pressure transient for Region I Tornado⁽²⁾.



Fig. 5. Pressure tanks.

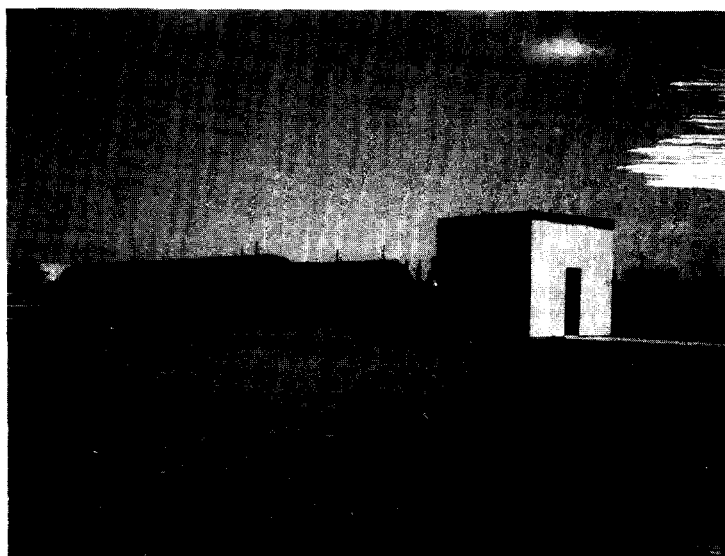


Fig. 6. Expansion chamber under construction.

The pressure pulse rise-time will be regulated by controlling the opening rate of valves between the expansion chamber and the high pressure air supply tanks. A pneumatically operated ball valve will be used with a closely regulated air pressure to actuate the control mechanism. A multiple valve arrangement is also being evaluated to achieve pressure rise times shorter than the NRC Region I tornado of 1.5 seconds.

The key to obtaining answers on questions of effective filtration is an ability to measure filter behavior during a transient pressure pulse. This can be accomplished by injecting particles of uniform size into the supply duct upstream of the filter, and simultaneously measuring particle density upstream and downstream from the filter. Care must be taken to distribute the particles uniformly across the cross-section of the duct. Also, particles of a size and density comparable with reprocessing ventilation systems should be used.

Several methods for determining the particle density upstream and downstream of the filter during the pressure were considered. These included nuclear tracer methods, x-ray defraction methods, and light diffusion or scattering methods. The safety problems inherent with the handling of radioactive materials and x-ray equipment as well as the expense of the instrumentation needed for these methods essentially eliminated them from consideration. The further requirement that the porosity of the filter material be investigated during a transient pressure pulse virtually demanded use of a light scattering method. The fact that particle density must be measured in an airstream having a velocity of 61-m/sec (200-ft/sec) during a time interval of approximately 3 seconds led to the consideration of a Laser Doppler Velocimeter (LDV) as both a particle counter and velocity meter. A slight modification on the optical system of the LDV will allow investigation of a filter porosity using a single laser beam.

The measured particle density will be related to the number of particles passing through a small volume per unit time. The data rate measured by the LDV is proportional to the number of particles passing through its measurement volume per unit time. Hence, the difference in data rate upstream to downstream across the filter gives the filter effectiveness (F_{eff}) during the pulse.

$$F_{eff} = \frac{\text{Data Rate Upstream} - \text{Data Rate Downstream}}{\text{Data Rate Upstream}} \quad (1)$$

A possible configuration of such a system is shown in Fig. 7. We believe that the LDV system could monitor the effectiveness of clean and loaded filters during a pressure pulse. Further, it could give a quantitative measurement of particles released from loaded filters during a pressure transient.

The LDV system would give the mean flow velocity upstream and downstream of the filters, as well as the turbulence level at these points. Furthermore, by traversing the LDV measuring volume (the crossing point of the beams) across the cross-section of the duct downstream of the filters, the flow path of the air through the filters can be determined. Porosity of the filter material during the pressure pulse could be investigated by passing a laser beam through the filter and measuring the change in beam intensity.

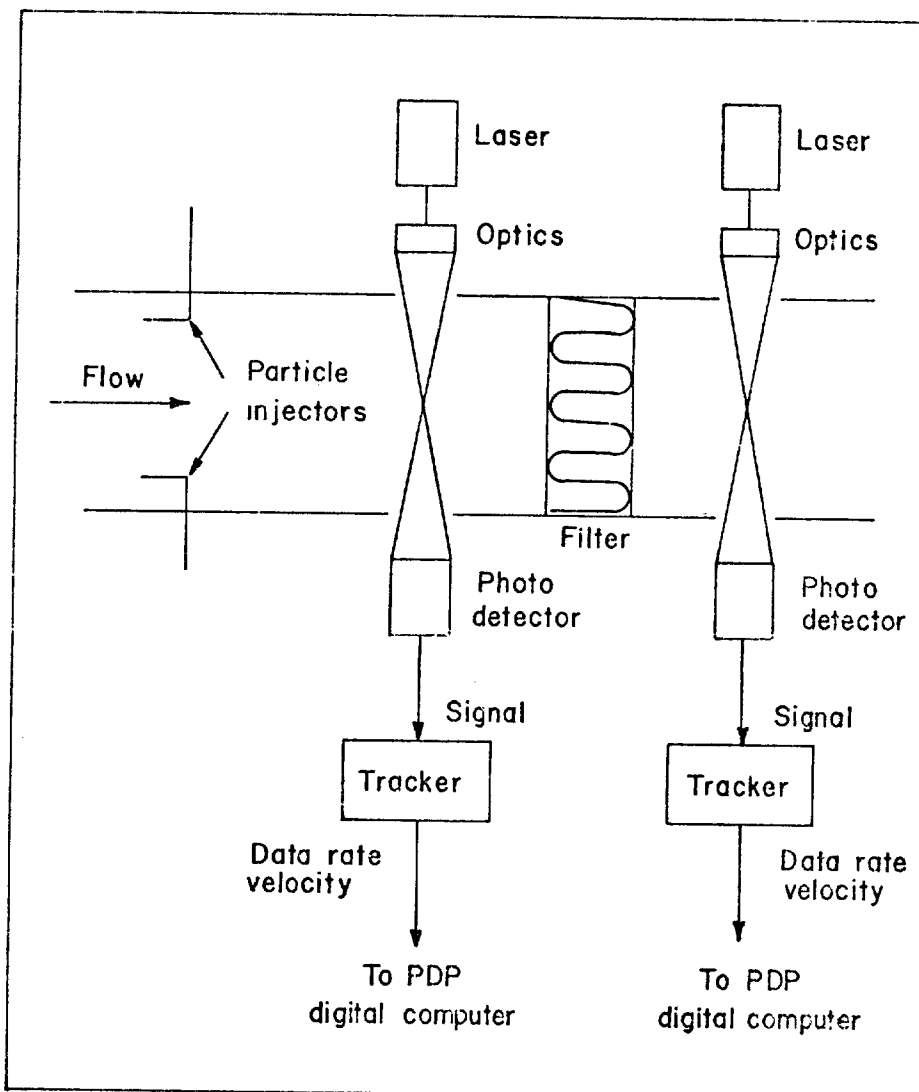


Fig. 7. Laser instrumentation system.

Future Investigations

Further investigations will examine the behavior of other ventilation system components during tornado induced pressure transients. Considerable uncertainty exists concerning the response of a fan or blower to a change in atmospheric pressure. Blowers on either the exhaust or supply side, are probably the components closest to the full impact of tornado depressurization. Blower operation under conditions of out-running flow and flow reversal are not well known.

III. Analytical Work

General

Calculation of pressures and flows, within an air cleaning system for a tornado depressurization requires solution of general fluid dynamic equations, involving the conservation of momentum,

energy, and mass. These equations are not easily solved numerically, but they do provide a basis for development of a simplified set of working equations. Analysis of these equations showing the importance of inertia and shock terms has been described elsewhere⁽³⁾. Simplification and coupling of these equations with empirical fluid-flow relationships, allows development of equations that can be used to calculate the fluid dynamics in a network of connecting ducts and components.

A digital computer code "TVENT" has been developed that utilizes the equations derived in the following section to predict the transient response of arbitrary ventilation systems to tornado induced pressure transients.

Formulation of Equations

The equations are formulated using a "lumped" parameter approximation that neglects spatial distribution of variables. The following equations types will result upon application of the lumped parameter approach:

- o a simultaneous set of coupled nonlinear algebraic equations, and
- o a simultaneous set of ordinary differential equations.

The lumped parameter approach includes a number of system elements or branches joined together at points called nodes. The nodes are the connection points at the upstream and downstream ends of the branches. The pressure variable of the system is lumped into the nodes. Air cleaning system components such as dampers, filters and blowers, that have a resistive nature, are located within the branches of the system. A branch without a component (the duct work) also has a resistive nature. The frictional resistance to flow in the ductwork and system components is lumped within the branches of the network. An empirical pressure-flow relationship suitable for the elements is used for all branches in the system. This relationship can be written as:

$$Q(K) = \alpha(K) + \beta(K)(P(J) - P(I))\gamma(K) \quad (2)$$

where

$$\begin{aligned} K &= \text{branch } K, \\ Q(K) &= \text{flow rate through a branch,} \\ \gamma(K) &= \text{constants for a particular branch,} \\ P(I) &= \text{pressure at node } I, \text{ and} \\ \alpha(K), \beta(K), P(J) &= \text{pressure at an upstream node } J \text{ so that} \\ &P(J) > P(I). \end{aligned}$$

Application of Eq. (2) for the system components will yield a number of forms. These forms are summarized in Table I.

At any particular time, the branch flow and the pressures at the upstream and downstream nodes are unknown. Coupling all branch equations at a particular node through use of a continuity equation, allows the flow variable to be eliminated. Only the system pressures remain to be determined. An iterative process, ideally suited for the digital computer, is used with a linearized form of Eq. (2) to

Table I Pressure-Flow Relationships for Various Branch Components.

Branch Component	$\alpha(K)$	$\beta(K)$	$\gamma(K)$	Flow Equation	Eq. No.
Duct Friction	0	Variable	0.5	$\beta(K) (P(J) - P(I))^{\gamma(K)}$	(3)
Filter (low flows)	0	Variable	1	$\beta(K) (P(J) - P(I))$	(4)
Damper	0	Variable	0.5	$\beta(K) (P(J) - P(I))^{\gamma(K)}$	(5)
Blower (linear approximation)	Variable	Variable	1	$\alpha(K) + \beta(K) (P(J) - P(I))$	(6)

determine a pressure correction (ΔP) at each node. The process is repeated many times until the pressures at the nodes are within an acceptable tolerance.

Calculation of the pressure correction parallels Streeter's procedure for determining the pressures and flows in the steady-state portion of a water-hammer computer code⁽⁴⁾. Streeter located pumps at nodes, whereas this analysis requires all components to be located within the branch connections. In addition, this formulation is a transient analysis with allowance for storage of fluid at particular nodes. This condition requires derivation of a different algorithm for calculation of ΔP at fluid storage nodes.

The pressure correction for a node is calculated assuming that the true pressure at node I is equal to $P(I) + \Delta P$. Using this approximation, Eq. (2) becomes:

$$Q(K) \approx \beta(K) [P(J) - (P(I) + \Delta P)]^{\gamma(K)} \pm \alpha(K). \quad (7)$$

Using a binomial expansion of Eq. (7), neglecting higher order terms and considering $P(I)$ to be the value of pressure at node I for the previous iteration, Eq. (7) becomes:

$$Q(K) \approx \beta(K) [P(J) - P(I)]^{\gamma(K)} \left[1 - \frac{\beta(K) \Delta P}{P(J) - P(I)} \right] \pm \alpha(K), \quad (8)$$

or
$$Q(K) \approx A - C\Delta P. \quad (9)$$

where A and C are known constants from the previous iteration and are equal to:

$$A = \beta(K) [P(J) - P(I)]^{\gamma(K)} \pm \alpha(K) \quad (10)$$

$$C = \beta(K) \gamma(K) [P(I) - P(J)]^{\gamma(K)-1} \quad (11)$$

If $P(I) > P(J)^*$, the values of A and C become:

$$A = -\beta(K) [P(I) - P(J)]^{\gamma(K)} \pm \alpha(K), \text{ and} \quad (12)$$

*J refers to downstream node in this case.

$$C = \beta(K)\gamma(K)[P(I) - P(J)]^{\gamma(K)-1}. \quad (13)$$

Components that have a relatively large volume such as rooms, gloveboxes, and plenums are located at the nodes. These nodes exhibit a capacity for fluid storage and are called capacitance nodes. The compressibility of the system is accounted for by allowing fluid storage at the capacitance nodes. However, in all cases the conservation of mass must hold at the nodes. For an ordinary node, with no storage or blower connection, conservation of mass yields:

$$\Sigma Q(K) = 0, \quad (14)$$

or

$$\Sigma A - \Sigma C \Delta P = 0. \quad (15)$$

Solving for the pressure correction ΔP gives:

$$\Delta P = \frac{\Sigma C}{\Sigma A}. \quad (16)$$

Equation (16) is used to determine successive pressure corrections for an ordinary node without storage. When a node is connected to a duct containing a blower, the constant $\alpha(K)$ must be added or subtracted from ΣA before the correction is calculated. In all other cases $\alpha(K)$ is equal to zero.

If only steady-state values of pressure and flow are of interest, Eq. (16) is sufficient for arriving at the correct pressures. However, during a transient, mass-in does not equal mass-out at nodes containing rooms, gloveboxes or plenums. The equation of state is used at these storage nodes in addition to the continuity equation. The equation of state can be written as:

$$P(I) = \rho RT, \quad (17)$$

where

ρ = density of air at the node,
 R = gas constant for air, and
 T = absolute temperature of the air.

Differentiation of this equation with respect to time yields:

$$\frac{dP(I)}{dt} = CF(Q_{in} - Q_{out}), \quad (18)$$

or

$$\frac{dP(I)}{dt} = CF \Sigma Q(K), \quad (19)$$

where

$$\begin{aligned} CF &= \rho RT/V, \\ Q_{in} &= \text{flow rate into node,} \\ Q_{out} &= \text{flow rate out of node,} \end{aligned} \quad (20)$$

and V is the volume of the node under consideration.

Using finite differencing, Eq. (19) can be written as:

$$\Sigma Q(K) = \frac{1}{CF} \frac{P(I)^n - P(I)^{n-1}}{\Delta t}, \quad (21)$$

where

$$\begin{aligned} P(I)^n &= \text{present iterative value of pressure,} \\ P(I)^{n-1} &= \text{past iterative value of pressure, and} \\ \Delta t &= \text{discrete time step.} \end{aligned}$$

Substituting $P(I)^n + \Delta P$ for $P(I)^n$ in Eq. (21) yields the following equation for determination of the pressure correction at a storage node:

$$\Delta P = \frac{CF \Delta t \Sigma A + P(I)^{n-1} - P(I)^n}{1 + CF \Delta t \Sigma C}. \quad (22)$$

Eqs. (16) and (22) are incorporated within the computer code TVENT so that successive pressures are calculated until the true pressures that balance the system are obtained. After convergence has been achieved, the flows that result from the calculated pressure distribution are computed from the branch component equations.

Modeling Technique

Several facility ventilation systems were reviewed to determine the complexity of these systems and to identify typical components and subsystems (5,6). A small fictitious test-case ventilation system was devised containing many of the components and subsystems common to facility ventilation systems. This test-case ventilation system (Fig. 8 and Fig. 9) was used to test the computer code. The test-case features:

- Natural bypass around rooms,
- Recirculation similar to that used in the Westinghouse Recycle Fuels Plant,
- Combinations of series and parallel arrangements of components,
- Rooms (confinement volumes) with multiple inlets and outlets,
- Duct friction, and
- A network consisting of 30 components and 25 nodal points.

Some components have been omitted from Fig. 8 for clarity, but are included in the schematic of Fig. 9.

A branch is defined as a connecting member between two nodes and includes only one component. Boundary conditions (pressure as a function of time) and capacitance are prescribed at nodal points. The branch and node labeling are somewhat arbitrary, however numbers may not be skipped.

Following the lumped parameter approach, all of the pressure losses for a branch are ascribed to the component contributing the largest pressure loss. Thus, the duct loss may be lumped with the damper loss characterized by Eq. (5) of Table I for Branch 1 of Fig. 9. Similarly the duct pressure loss in Branch 2 of Fig. 9 may be lumped with the filter pressure loss. An inspection of the $\gamma(K)$ Table I shows that Branch 1 is modeled more accurately than Branch 2. A branch should be added to the model if the duct pressure loss is a significant fraction of the component pressure loss.

The blower pressure-flow relationship is approximated by a series of linear segments (Fig. 10). The coefficients (Eq.(6) of Table I)

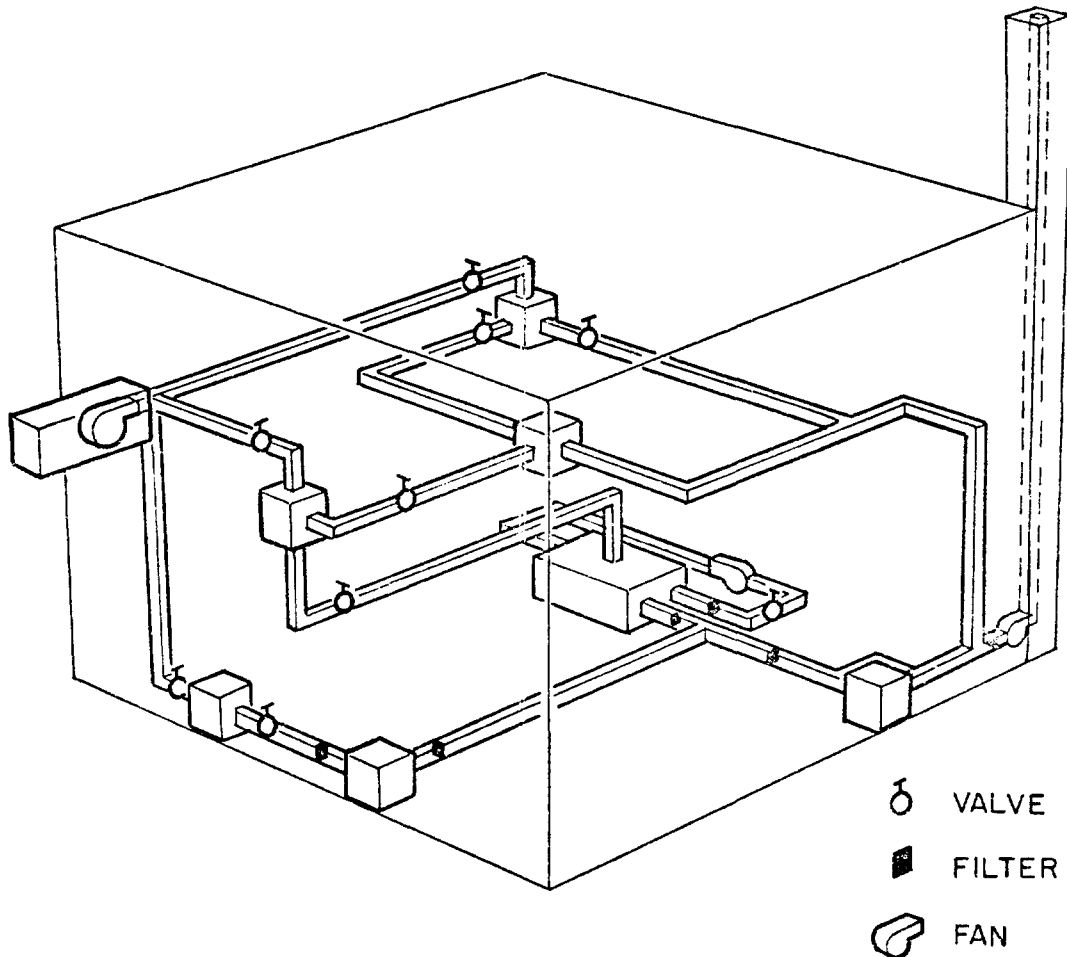


Fig. 8. Fictitious ventilation system within building.

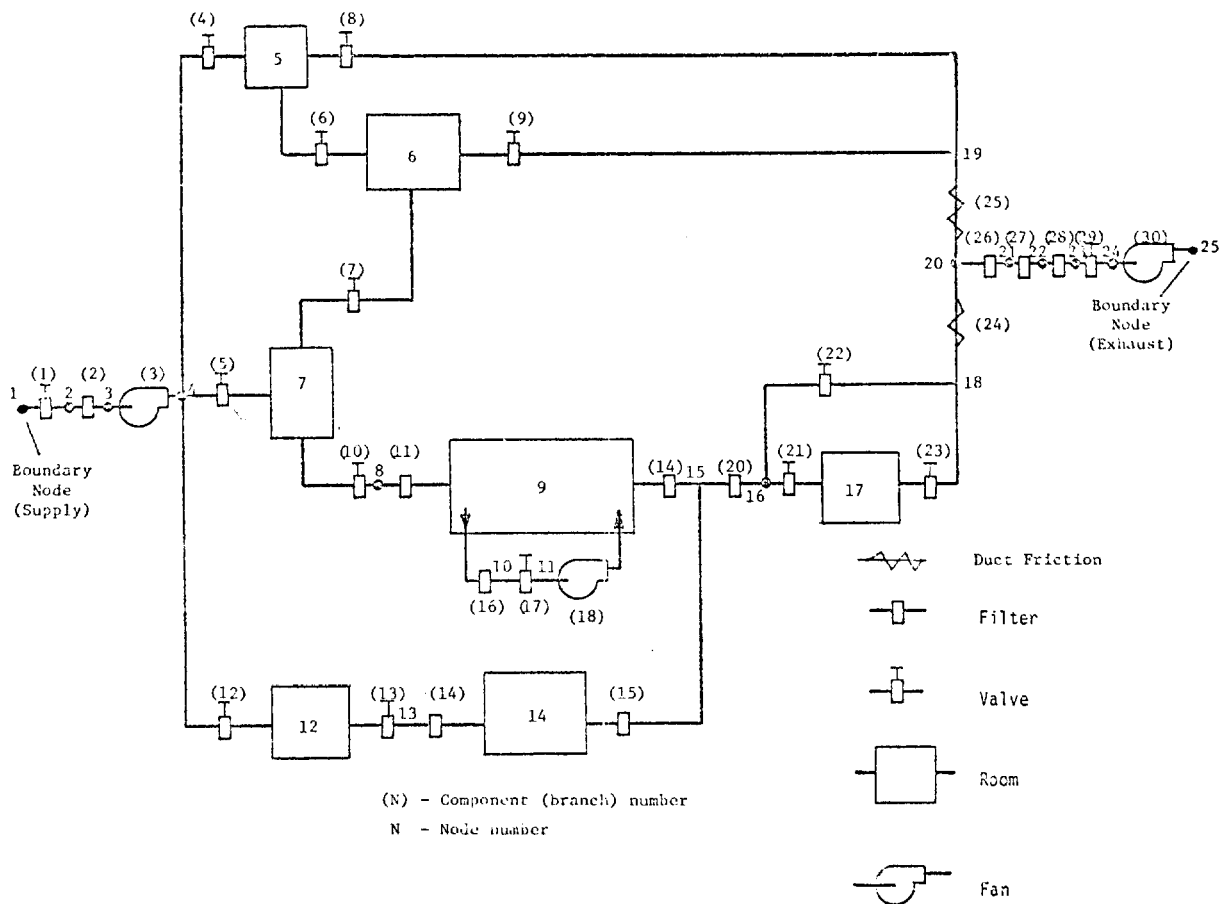


Fig. 9. Lumped parameter model of ventilation system.

are checked at every time-step and changed if necessary to obtain consistent flows and nodal pressures. This technique may also be used for filters with low and high flows as better experimental data become available.

Infiltration or leakage may be specified by the addition of a boundary node attached to a fictitious branch connected to the room with the leak. The resistance can be calculated from the design leak, the design room pressure and the boundary pressure. In this way a variable leakage rate is achieved for the transient.

Duct volumes are checked against the smallest room volume detected by the computer code. An informative message is given if a duct volume exceeds half the smallest room volume, since this would probably indicate a modeling error. Consideration should then be given to adding a capacitance node or possibly eliminating the smallest room(s).

The Computer Program "TVENT"

General. The program is written in the FORTRAN IV language and is designed to be "portable", that is, easily transferred from one computer to another with a minimum of change. Runs have been performed on the CDC 7600 computer and the IBM 360 computer to demonstrate this capability. The portability requirement precludes free format input and film plotting options that are not found on some systems.

The program is structured as a one level overlay (Fig. 11) to permit its use on smaller computers and to allow expansion.

Input. The input consists of two parts: 1) control information specifying how the problem is to be run and 2) a physical description of the system to be analyzed. An attempt has been made to organize and format the input in a way that is "natural" to the designer or engineer preparing the data for analysis. Several common methods exist for designing ventilation systems (7,8). The branch description (Fig. 12) is similar to the working tables given in the above references.

A more common method of representing the pressure-flow relationship is:

$$\Delta H = R \cdot Q^m, \quad (23)$$

where

ΔH = pressure drop across the component (measured or calculated),

R = resistance coefficient,

Q = branch design or measured flow, and

m = flow exponent (equals $1/\gamma(K)$ of Table I).

Equation (23) is used for branch description input and for calculating resistance of leakage nodes. The resistance R, if specified, overrides the resistance normally calculated by the computer using input values of pressure drop and design flow in Eq. (23). Pressures may be specified directly, in which case pressure drops are determined from these pressures and the branch descriptions.

Output. The output produced during problem set-up and transient calculations encompasses:

- Informational and diagnostic messages indicating input or modeling errors.
- Input return in the form of a card-image listing (Fig. 13) and lists associated with arrays generated from the input and used in the system solver.

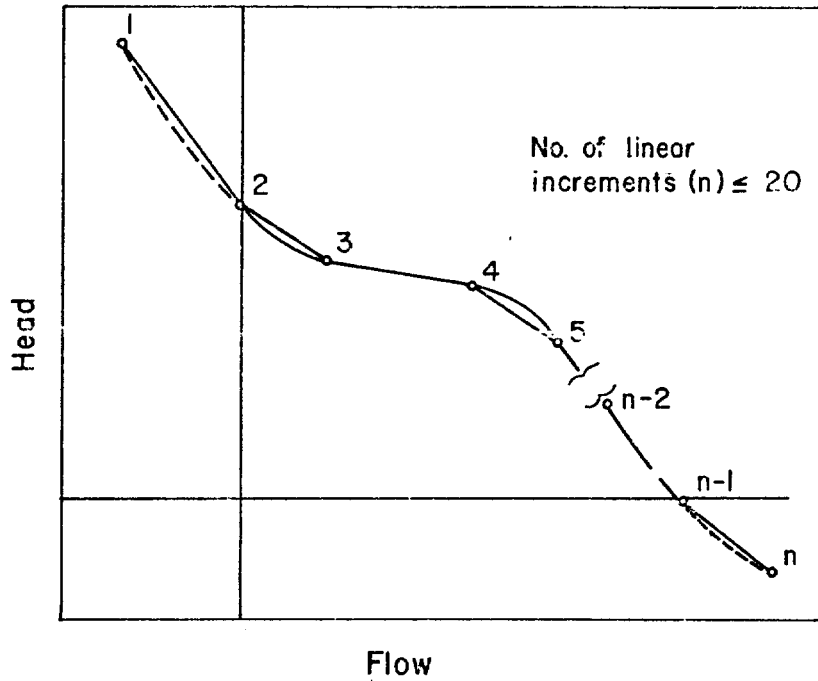


Fig. 10. TVENT blower characteristics.

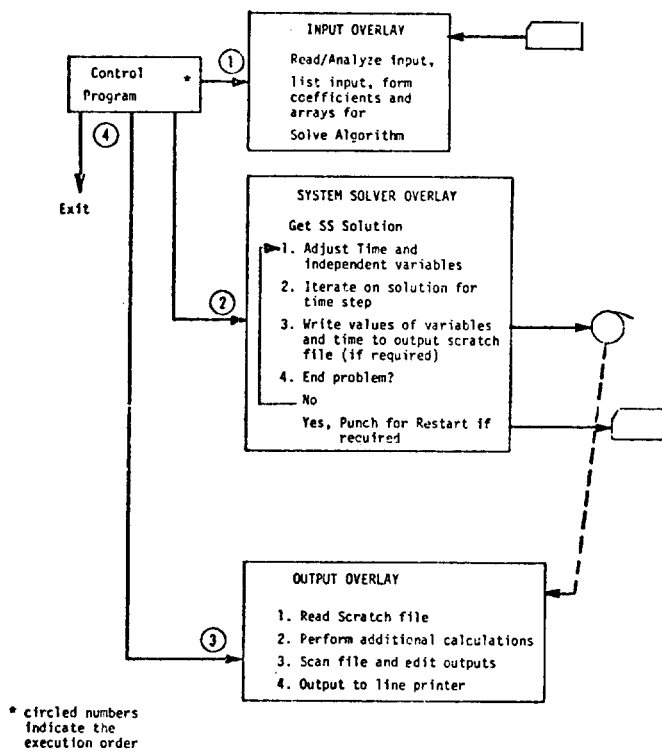


Fig. 11. TVENT program flow and overlay structure.

14th ERDA AIR CLEANING CONFERENCE

NO.	IN NODE	OUT NODE	INITIAL FLOW	HYDRL RADIUS	BRANCH DATA			EXP Q P	RESIST VALUE	BLOWER INTERCEPT,	INITIAL DELTA-P
					TYPE	COMP	BLOWER CURVE				
1	1	2	388.000	0.000	VALV	0	.50	1.203E+03	0.	.104000	
2	2	3	388.000	0.000	FILT	0	1.00	1.003E+03	0.	.387000	
3	3	4	388.000	0.000	BLWR	1	1.00	2.500E+02	1.0000E+03	2.448000	
4	4	5	0.000	0.000	VALV	0	.50	1.000E+02	0.	1.000000	
5	4	7	156.100	0.000	VALV	0	.50	1.201E+03	0.	.016900	
6	5	6	0.000	0.000	VALV	0	.50	1.200E+03	0.	.000050	
7	7	6	0.000	0.000	VALV	0	.50	1.000E+02	0.	1.000000	
8	5	19	0.000	0.000	VALV	0	.50	1.200E+03	0.	.000000	
9	6	19	0.000	0.000	VALV	0	.50	1.200E+03	0.	.000000	
10	7	8	57.400	0.000	VALV	0	.50	1.202E+03	0.	.002280	
11	8	9	57.400	0.000	FILT	0	1.00	3.005E+02	0.	.191000	
12	4	12	100.000	0.000	VALV	0	.50	1.200E+03	0.	.006944	
13	12	13	100.000	0.000	VALV	0	.50	1.200E+03	0.	.006944	
14	13	14	100.000	0.000	FILT	0	1.00	6.993E+02	0.	.143000	
15	14	15	100.000	0.000	FILT	0	1.00	6.993E+02	0.	.143000	
16	9	10	179.800	0.000	FILT	0	1.00	6.996E+02	0.	.257000	
17	10	11	180.100	0.000	VALV	0	.50	1.201E+03	0.	.022500	
18	11	9	200.000	0.000	BLWR	2	1.00	2.500E+02	2.5000E+02	.220000	
19	9	15	57.900	0.000	FILT	0	1.00	3.016E+02	0.	.192000	
20	15	16	190.500	0.000	FILT	0	1.00	3.000E+02	0.	.635000	
21	16	17	79.300	0.000	VALV	0	.50	1.201E+03	0.	.004360	
22	16	18	112.800	0.000	VALV	0	.50	1.200E+03	0.	.000030	
23	17	18	60.200	0.000	VALV	0	.50	1.201E+03	0.	.004460	
24	18	20	193.800	0.000	DUCT	0	.50	1.007E+03	0.	.011500	
25	19	20	0.000	0.000	DUCT	0	.50	1.000E+03	0.	.050000	
26	20	21	395.800	0.000	FILT	0	1.00	7.005E+02	0.	.565000	
27	21	22	395.800	0.000	FILT	0	1.00	3.021E+02	0.	1.310000	
28	22	23	395.800	0.000	FILT	0	1.00	3.021E+02	0.	1.310000	
29	23	24	395.800	0.000	VALV	0	.50	1.204E+03	0.	.100000	
30	24	25	395.800	0.000	BLWR	3	1.00	2.500E+02	1.0000E+03	2.416000	

Fig. 12. Branch description of input data.

14th ERDA AIR CLEANING CONFERENCE

```

          TVENT      JAN 76    LASL
1234567890123456789012345678901234567890123456789012345678901234567890
   A REGION I TORNADO AT THE AIR SUPPLY
   .1875 12.        4
14.3              1      2
  1              1
 25              5
  1              1.5      -83.067    4.5      -83.067
6.              9.8
30 25 3 7 3
  1 1 2 388.8      V      .184
  2 2 3 388.8      F      .387
  3 3 4 388.      B
  4 4 5      V      1.8      1.000E=04    1
  5 4 7 156.1      V      .8169
  6 5 6      V      .00005      6.944E=07
  7 7 6      V      1.8      1.000E=04
  8 5 19      V      .007      6.944E=07
  9 6 19      V      .007      6.944E=07
10 7 8 57.4      V      .00228
11 8 9 57.4      F      .191
12 4 12 100.000      V      6.944E=07
13 12 13 100.000      V      6.944E=07
14 13 14 100.000      F      1.430E=03
15 14 15 100.000      F      1.430E=03
16 9 10 179.8      F      .257
17 10 11 180.1      V      .0225
18 11 9 220.      B
19 9 15 57.9      F      .192
20 15 16 190.5      F      .635
21 16 17 79.3      V      .00436
22 16 18 112.8      V      .00883
23 17 18 80.2      V      .00446
24 18 20 193.000      D      .0115
25 19 20      .05      1.000E=06
26 20 21 395.8      F      .565
27 21 22 395.8      F      1.31
28 22 23 395.8      F      1.31
29 23 24 395.8      V      .188
30 24 25 395.8      B
  5 20. 10. 25.
  6 20. 10. 25.
  7 20. 10. 25.
  9 20. 10. 25.
12 20. 10. 25.
14 20. 10. 25.
17 20. 10. 25.
  1 2
  2 2 4.0 1000.
  0.0 2 1.0 250. 0.0
  3 2 0.0 4.0 1000. 0.0

```

Fig. 13. Card-image listing of input.

- The following lists of steady-state and transient results as shown in Figs. 14 and 15 may be obtained (transient-output times must be requested).
 - pressures and flows for all nodal points and branches, respectively,
 - differential pressures across filters,
 - flows through filters,
 - differential pressures across dampers,
 - differential pressures between rooms, and
 - a summary of peak values.
- A limited number of pressure or flow versus time line-printer plots upon request.

Special Features.

- The input processor accepts an output frequency based on total problem-time less the problem start-restart time with additional special output times (up to 5). The latter are useful when doubt may exist whether a maximum or minimum value of some variable may have been missed.
- A problem may be stopped and subsequently restarted, which is useful for unusually large systems or long transients. It is also useful in simulating duct or filter failures during a transient.
- The input is sufficiently flexible to permit runs for verification of an existing design, and parameter studies for insight into the effects of changing design values.
- The program is easily modified. This is an asset when experimental data may dictate changes in modeling techniques.

IV. Discussion and Results

A computer generated movie has been prepared from four runs made with TVENT for the test case ventilation system.

These runs included:

1. A Region I tornado* occurs at the air supply,
2. A Region I tornado occurs at the exhaust,
3. A Region I tornado occurs simultaneously at both the air supply and exhaust, and
4. A Region I tornado occurs at the air supply, and after a six second delay appears at the exhaust.

14th ERDA AIR CLEANING CONFERENCE

A REGION I TORNADO AT THE AIR SUPPLY

NODAL PRESSURES FOR TIME = 6.00000

	0	1	2	3	4	5	6	7	8	9
0		0.00000	-2.29290	-4.11000	-7.39740	-1.90970	-1.90970	-8.23790	-7.85330	-5.37240
10	-5.62970	-5.65220	-8.03090	-7.24290	-5.71960	-4.83680	-2.24070	-2.13100	-2.14000	-1.94050
20	-2.11820	-2.33090	-2.85080	-3.36280	-3.37940	-0.00000				

BRANCH FLOWS

	0	1	2	3	4	5	6	7	8	9
0		1821.8	1821.8	1821.8	-234.3	1100.9	8.7	-251.6	210.8	210.6
10	-745.5	-745.5	955.2	-1065.3	-1065.3	-617.3	180.8	180.1	180.1	-161.5
20	-778.8	-397.9	-381.8	114.1	-266.9	421.5	154.6	154.7	154.7	155.1
30	155.1									

DIFFERENTIAL PRESSURE (D.P.) ACROSS FILTER

BRANCH	D. P.	BRANCH	D. P.	BRANCH	D. P.	BRANCH	D. P.
2	1.817100	11	2.488900	14	1.523300	15	.882800
16	.257300	19	.535600	20	2.596100	26	.220700
27	.511900	28	.512000				

FLOW THROUGH FILTER

BRANCH	FLOW	BRANCH	FLOW	BRANCH	FLOW	BRANCH	FLOW
2	1821.8	11	-745.5	14	-1065.3	15	-617.3
16	180.8	19	-161.5	20	-778.8	26	154.6
27	154.7	28	154.7				

DIFFERENTIAL PRESSURE (D.P.) ACROSS DAMPER

BRANCH	D. P.	BRANCH	D. P.	BRANCH	D. P.	BRANCH	D. P.
1	2.292900	4	5.487700	5	.840500	6	0.000000
7	6.328200	8	.030800	9	.030800	10	.384600
12	.633500	13	.788000	17	.022500	21	.189700
22	.100700	23	.009000	29	.016600		

Fig. 14. Composite of output listings.

14th ERDA AIR CLEANING CONFERENCE

A REGION I TORNADO AT THE AIR SUPPLY

DIFFERENTIAL PRESSURE BETWEEN ROOMS FOR TIME = 6.00000

NODE	ROOM	1	2	3	4	5	6	7
5	1	0.00000	0.00000	6.32820	3.46270	6.12120	3.80990	.22130
6	2	0.00000	0.00000	6.32820	3.46270	6.12120	3.80990	.22130
7	3	-6.32820	-6.32820	0.00000	-2.86550	-2.20700	-2.51830	-6.10690
9	4	-3.46270	-3.46270	2.86550	0.00000	2.65850	.34720	-3.24140
12	5	-6.12120	-6.12120	.20700	-2.65850	0.00000	-2.31130	-5.89990
14	6	-3.80990	-3.80990	2.51830	-.34720	2.31130	0.00000	-3.58860
17	7	-.22130	-.22130	6.10690	3.24140	5.89990	3.58860	0.00000

S U M M A R Y

```

* * * * *
* HIGHEST PRESSURE OF 0.00000 OCCURS AT NODE 25
* LOWEST PRESSURE OF -6.23790 OCCURS AT NODE 7
* LARGEST POSITIVE FLOW OF 1821.80 OCCURS IN BRANCH 3
* LARGEST NEGATIVE FLOW OF -6023.30 OCCURS IN BRANCH 3
* FILTER WITH LARGEST PRESSURE DIFFERENTIAL OF 2.596100 IS IN BRANCH 20
* FILTER WITH LARGEST FLOW OF 1821.80 IS IN BRANCH 2
* DAMPER WITH LARGEST PRESSURE DIFFERENTIAL OF 6.328200 IS IN BRANCH 7
* ROOM NO. 0 HAS THE HIGHEST POSITIVE PRESSURE OF 0.00000
* ROOM NO. 3 HAS THE LOWEST NEGATIVE PRESSURE OF -6.23790
    
```

Fig. 15. Composite of output listings.

Some preliminary observations can be made based on studies of the test case ventilation system:

- A convergence tolerance of 0.025-Pa (1.0×10^{-4} in. of water) (that is nodal pressures changing by less than this amount on successive iterations) appears to be adequate for accuracy. This has been checked against different algorithms.
- Branches containing small pressure drops (less than five times convergence tolerance) exhibit significant errors. A decrease in the tolerance does not improve the solution.
- Solution accuracy is not a strong function of time-step size.
- The use of linear segments to approximate the blower characteristic curves has not caused convergence problems at those points where the algorithm might tend to search for the correct segment of the blower curve during the transient.
- The CDC 7600 computer time to real time ratio is about one half with a time step of 0.1 second for the test case problem.

V. Summary and Conclusions

The analytical and experimental investigations described in this paper will provide the analyst with some insight into the effects of tornado depressurization on air cleaning systems. The results obtained thus far are preliminary, as the analytical and experimental tools needed to investigate the problem are under development.

Interpretation of preliminary experimental results indicates that there may be a loss of material through the HEPA filters from either filter degradation or structural failure. Further experimental work at the Las Cruces Test facility will be aimed at accurately determining HEPA filter failure mechanisms under tornado conditions.

Analytical investigations with the computer code "TVENT", can provide information on overall air cleaning system response to tornado depressurization. However, this code has not been applied to an actual system. Future plans include its application to an actual system as well as incorporating experimental results for individual components. A second level of analysis using a distributed parameter approach is also planned.

Acknowledgements

The authors would like to express their appreciation for the support provided by the Energy Research and Development Administration, Division of Operational Safety and the Nuclear Regulatory Commission, Division of Safeguards Fuel Cycle and Environmental Research.

References

1. Gregory, W.S., HEPA Filter Effectiveness during Tornado Conditions, LA-5352-MS, Los Alamos Scientific Laboratory, 1973.
2. Markee, E. H. Jr., Beckerley, J. G., Sanders, K. E., Technical Basis for Interim Regional Tornado Criteria, U.S. Atomic Energy Commission Office of Regulation, Wash-1300, 1974.
3. Gregory, W. S., Smith, P. R., Duerre, K. H., "Effect of Tornados on Mechanical Systems", Proceedings Symposium on Tornados, Lubbock, Texas, 1976.
4. Streeter, V. L., "Water-Hammer Analysis of Distribution Systems", American Society of Civil Engineers, HY5, Sept. 1967.
5. Gregory, W. S., Bennett, G. A., Ventilation Systems Analysis During Tornado Conditions - July through December 1974, LA-5894-PR, Los Alamos Scientific Laboratory, March 1975.
6. Bennett, G. A., Gregory, W. S., Smith, P. R., Ventilation Systems Analysis During Tornado Conditions - January - June 1975, LA-6120-PR, Los Alamos Scientific Laboratory, Nov. 1975.
7. ASHRAE Handbook of Fundamentals (Chapter 25), American Society of Heating, Refrigeration and Air Conditioning Engineers, 1972.
8. Carrier Air Conditioning Company, "Air Duct Design", Handbook of Air Conditioning System Design, McGraw Hill Book Company, New York, 1965.

DISCUSSION

OLSON: I would like to know why you are using one and a half seconds for pressure drop rather than three seconds, which I believe is used by NRC.

GREGORY: In the past, the Region 1 tornado criteria have been over a three-second period and, in fact, we did test the small filters over a three second period or with a 1 psi per second ramp. Since then, we are using the interim Region 1 tornado criteria, which, I believe, are in WASH-1300. In the Region 1 tornado, there is a 2 psi per second depressurization which would occur over a one and a half second period, I believe. The computer program will take any kind of condition for any particular transient that you would like to apply.

14th ERDA AIR CLEANING CONFERENCE

DESIGN AND ANALYSIS OF THE SANDIA LABORATORIES HOT CELL FACILITY SAFETY VENTILATION SYSTEM

E. A. Bernard and H. B. Burress
Sandia Laboratories
Albuquerque, New Mexico 87115

Abstract

Sandia Laboratories has designed a Hot Cell Facility (HCF) to support a variety of experimental programs. This facility will provide an on-site capability to conduct glove box experiments with irradiated samples having intermediate levels of radioactivity-2,000 curies of fission products and 200 curies of plutonium.

The HCF uses a combination of existing and new construction to minimize costs and maximize usage of existing facilities. A new safety ventilation system has been designed to service the HCF.

The ventilation system consists of three zones as required by the Plutonium Facilities General Design Criteria, Appendix 6301 (GDC). In conforming with this GDC, the HCF can accommodate several hundred curies of plutonium while actual Sandia requirements are for 1-5 curies.

The maximum credible accident for the HCF is a hypereze (liquid cutting compound) fire. A combination of experimental data and calculational procedures are used to define the fire environment, predict the impact on the ventilation system components and determine the overall system effectiveness in case of such an accident.

I. Introduction

This report describes the Hot Cell Facility (HCF) designed by Sandia Laboratories. The HCF is composed of three steel confinement boxes (SCB's), the hot cell, a support area, the safety ventilation system and a fire protection system. This facility provides Sandia Laboratories with an on-site capability to analyze irradiated samples containing up to 2,000 curies of fission products and 200 curies of plutonium.

The HCF is located in the basement of Building 6580 which is in one of Sandia's major technical areas. Figure 1 shows the floor plan of the HCF. There are three safety ventilation systems serving the HCF. The first system (Zone 1) serves the SCB's and the second (Zone 2A) serves the hot cell. Both of these systems are once-through systems. The third system is a partial recirculation system and serves the support area (Zone 2). The three SCB's are located next to the manipulator wall, the west wall of the hot cell. The separation distance between the SCB's and the other walls of the hot cell allows sufficient space in which to position and unload the sample containers and transfer samples within the hot cell. The walls of the hot cell are 1.07 m (3.5 ft) thick and made of reinforced concrete. An airlock is located at the north end of the hot cell. This airlock permits

access to the hot cell from the support area. The support area (Zone 2) which surrounds the hot cell is used for storage of casks prior to moving them into the hot cell. The area adjacent to the HCF (Zone 3) is not considered a part of the HCF. Make-up air for the safety ventilation system is drawn from the building ventilation system.

The HCF is composed of pre-existing and new construction. The SCB's, the west manipulator wall and part of the south hot cell wall were present before construction of the HCF. The south wall was extended to the ceiling and the new east wall was added to form the walls of the hot cell. The airlock at the north end of the hot cell was added to provide for access into the hot cell. In order to enclose the support area, a new wall was added at the southeast and south boundaries of the HCF. This addition also contains the outside airlock for access into the HCF. A second airlock into the HCF is located adjacent to Room 106.

The mechanical equipment room (MER) which is located above the HCF at ground level has been added to house the HCF ventilation equipment.

Emergency electrical power for critical systems, the fire protection system, evacuation alarms, public address and radiation monitoring systems in Building 6580 have been extended or modified to meet the HCF requirements. A nitrogen fire protection system has been added in Zones 1 and 2A.

The HCF is primarily designed to be a post-irradiation facility for the study of moderately radioactive materials. It is designed to permit safe handling and experimentation with these materials. Several research programs at Sandia--material studies, fuel studies, safety studies and waste solidification studies--require that radioactive materials be analyzed. The HCF meets these requirements.

II. Ventilation System

Functional Requirements

The ventilation system (Figure 2) maintains a safe operating environment within the facility by ensuring that proper differential pressures are maintained so that leakage is from zones of lesser contamination to zones of greater contamination. These zones are as follows:

Zone 1 - Normally Contaminated Area.

Zone 2A - Potentially Contaminated Area.

Zone 2 - Non-contaminated Area.

Exhaust gases from each of these zones are filtered through high efficiency particulate (HEPA) filters to reduce the off-site plutonium exposures to levels less than the Chapter 0524 limits.

14th ERDA AIR CLEANING CONFERENCE

Motor control circuits have been designed to provide sequential start-up of all the ventilation fans so that negative pressures are first established in the innermost zones, thus causing any leakage to be from a zone of lesser contamination to one of greater contamination. Interlocks are employed to shut down the necessary fans to avoid an adverse pressure differential if any fan should fail during operation.

The Zone 1 exhaust fans, the Zone 2A exhaust fans, and the Zone 2 make-up fans have modulating devices to control exhaust air quantities and to aid in maintaining proper static pressure within their respective zones. The Zone 2A make-up fans and Zone 2 recirculating fan will have manually adjusted dampers to provide essentially constant flow through the units. All Zone 1 SCB's have manually adjustable dampers for initial adjustment of air flows. In addition, all Zone 1 supply and exhaust dampers are provided with pneumatic operators which are controlled by energized or de-energized solenoid valves. Some of these dampers are fail-open type and some are fail-closed type.

Pressure differentials between zones are as follows:

Zone 3 - Ambient Condition.

Zone 3 - Zone 2 -0.10 inch w.g.

Zone 2 - Zone 2A -0.25 inch w.g.

Zone 2A - Zone 1 -1.00 inch w.g.

Zone 2 Ventilation System

The Zone 2 area (Figure 3) is maintained at a -0.10 inch w.g. with respect to the Zone 3 area. Zone 2 consists of Rooms 110, 111, and 112, in the east section and Rooms 105, 106, and 107 in the west section.

The Zone 2 make-up damper MUD-2-13 is modulated to maintain -0.10 inch w.g. pressure between Zone 2 (east section) and Zone 3 (Room 114). A differential pressure controller (DPC), with low input located in Room 111 and high input located in Room 114 modulates the make-up damper located on the discharge side of the Zone 2 make-up blower. The west section of Zone 2 is maintained at -0.10 inch w.g. by a DPC with low input in Room 107 and high input located in Room 114 which modulates the return air damper RD-2-12 located in the return air duct downstream of the return air blower.

A majority of the air supplied to the west section of Zone 2 is exhausted through a hood exhaust in Room 106 and the Scanning Electron Microscope System located in Room 105. These exhaust systems discharge into the existing hot exhaust system and are filtered through two HEPA filter banks, one at the glove box and one located at the area stack.

14th ERDA AIR CLEANING CONFERENCE

The make-up air unit supplying Zone 2 receives its air from the existing building distribution system. The volume of make-up air is determined by the amount of air exhausted from the east and west Zone 2 areas, the amount of make-up air supplied to Zone 2A, which includes the Zone 1 supply air, less the amount of infiltration air into Zone 2.

The Zone 2 recirculating blower supplies air to both the east and west sections of Zone 2. In addition to maintaining the correct pressure differential, the Zone 2 system maintains the required number of air changes in the area and supplies the needed heating and cooling. The volume of recirculated air is regulated by a manual intake damper located in the intake duct of the Zone 2 Filter and Cooling Coil Unit.

A cooling coil located in the Zone 2 unit with the controlling thermostat located in Room 107 maintains temperature in the Zone 2 areas. This thermostat also controls the reheat coil located in the building air supply duct to prevent the room temperature from dropping below 68°F during winter and no-load conditions. The water cooling coil is supplied chilled water from the existing building system. A manual by-pass damper in the Zone 2 unit maintains a fixed flow of air through the coil.

Zone 2A Ventilation System

The Zone 2A area (Figure 4) is maintained at -0.25 inch w.g. with respect to the Zone 2 area. Zone 2A is surrounded by the west and east sections of Zone 2.

The Zone 2A exhaust damper ED-2A-8-9 (Figure 4) is modulated to maintain -0.25 inch w.g. pressure differential with respect to Zone 2 (Room 111). This damper is modulated by a DPC, with low input located in Zone 2 (Room 111) and high input located in Zone 2A. The damper is located on the exhaust duct upstream of the Zone 2A exhaust blowers. Effluents are discharged through the exhaust filters at the area stack to the atmosphere.

The make-up air unit supplying Zone 2A draws its air from Zone 2 (east). The volume of make-up air through the Zone 2A make-up unit is controlled by manually adjusting damper MU-D-2A-10 (Figure 4). The volume of make-up air is determined by the supply demands of the Zone 1 SCB's and the air required to meet the cooling requirements of Zone 2A and the Zone 1 SCB's

The exhaust blowers B-8 and B-9 maximum air quantity is set by adjusting the manual damper MD-2A to prevent overloading of the blowers by excess volume of air through the system.

Only cooling, no heating is required in Zone 2A. The make-up air from Zone 2 east (Room 111) is normally maintained within the 69°F to 74°F range.

The heat generated within the Zone 2A comes from lighting of Zone 2A, crane motor and/or other equipment, infiltration, and

by convection and conduction loads from the SCB's. Some air is drawn through the SCB's and removes some SCB heat, but the amount of air through the SCB's is usually very low. Also, if a nitrogen atmosphere is maintained in SCB 1 and SCB 2, very little flow enters the Zone 1 exhaust, resulting in the Zone 2A cooling system handling the total load of Zone 2A and Zone 1. A cooling coil in the Zone 2A make-up air unit, with the controlling thermostat bulb located in the Zone 2A exhaust duct controls the zone temperature. The cooling coil is supplied cooling water from the building chilled water system. Normally Zone 2A is maintained at 68°F but under full load the temperature within the zone can rise to 85°F. This is within the design and operating limits of the Zone 2A area and Zone 1 SCB's.

The exhaust blowers B-8 and B-9 are controlled by a Blower Selector Switch which automatically selects the alternate blower in case of failure of the primary blower, thus assuring continuous exhaust.

Zone 1 Ventilation System

The Zone 1 area (Figure 5) consists of the three SCB's located within the area designated as Zone 2A. These are referred to as SCB 1, SCB 2 and SCB 3. The Zone 1 SCB's are maintained at -1.0 inch w.g. with respect to the Zone 2A area. Zone 2A surrounds Zone 1.

The exhaust of each SCB is connected to the Zone 1 exhaust manifold. The pressure differential between this manifold and Zone 2A is maintained at -2.0 inch w.g. by DPC EM-1. This controller modulates a damper located on the upstream duct of the Zone 1 exhaust blowers which discharge into the existing hot exhaust system. Each SCB is maintained at its designed negative pressure by a DPC that modulates an exhaust damper located on the exhaust duct between the cell and the exhaust manifold.

The exhaust blowers B-6 and B-7 maintain the required static pressure in the exhaust manifold and have sufficient capacity for exhausting the required CFM necessary for purging with air or nitrogen.

Make-up air to the SCB's is drawn from the discharge duct of the Zone 2A Make-up Air Unit. To assure that the supply to the Zone 1 Make-up Air Filter Banks will have sufficient head, a manual damper downstream of the Zone 1 take-off is adjusted to maintain this required head. Each SCB has a pneumatic operated damper on its air supply duct. The volume of air to the SCB is governed by a manual positioning switch in the control line to the damper of the supply duct to the SCB. The maximum open position of each SCB damper will be determined to prevent excessive air flow into the SCB's and to prevent the combined maximum flows of the SCB's from overloading the capacity of Zone 1 blowers B-6 and/or B-7.

In addition, each SCB has a nitrogen supply system, in the event the operations within the SCB demand a nitrogen atmosphere.

The controls for these nitrogen systems will be located on the control console of the SCB. Each SCB has a control console.

The above SCB control console is located on the operator side (west wall) of the manipulator wall. The following items of the Zone 1 ventilation control system of the SCB are located in this console. For each SCB there is:

- (a) A differential pressure indicator to indicate the pressure differential between the SCB and Zone 2A with high and low limit light and alarms.
- (b) A manual positioning switch to regulate volume of make-up air into SCB from "no flow" to "full flow."
- (c) Controls for the nitrogen supply to the SCB.

Cooling of the SCB's is by heat transfer to the Zone 1 air flow and by heat transfer to the air of Zone 2A surrounding the SCB's.

Ventilation Controls

The operating controls for the HCF ventilation system are located in Room 106 adjacent to the existing control panel for the hot and cold exhaust systems. These controls consist of on-off (or automatic) switches, monitor lights and alarm indicators (Alarms are relayed to the area guardhouse.) for the various components of the ventilation system. The electrical motor control center is located in the MER, where disconnect switches are to be used for shutting down the blowers for maintenance purposes. The mechanical control panel for the HCF ventilation system is located in the MER. This panel contains the zone differential pressure controllers and associated auxiliary equipment for the ventilation system operation.

III. Facility Electrical, Radiation and Fire Protection Systems

The electrical service to the HCF is obtained from the Building 6580 service. Critical loads fed by the electrical service (ventilation equipment, including the SCB nitrogen system, selected lighting, and receptacles in containment boxes, monitor and alarm system, remotely-operable airlock doors, etc.) will be served from the existing Building 6580 Emergency Generator System. The emergency generator system starts automatically and picks up the critical loads when the normal power source is interrupted. The system is tested weekly by simulating a normal power source interruption and allowing the generator to automatically start and pick up the critical loads. A new diesel-powered generator was installed in July 1975.

Radiation Protection Systems

Systems. Radiation monitoring is provided by two basic systems, the Remote Area Monitoring System (RAMS) and the Constant Air Monitoring System (CAMS). There is also a stack gas monitor

for the area stack. Selected RAMS and CAMS will be specifically required by the HCF Technical Specifications operating regulations. CAMS will monitor exhaust and environment air in the HCF.

RAMS. The RAMS is designed to monitor radiation levels at locations remote from a central readout station in the Health Physics Office. Each RAMS unit has a local meter readout, a visible alarm, an audible alarm, plus the remote readout in the Health Physics Office. The range for all RAMS units is 1 mr/hr to 100 r/hr. Trip points for each location are established at levels consistent with the values necessary for compliance with Chapter 0524 criteria.

Each RAMS unit employs transistorized circuitry coupled to a detector which responds to gamma radiation. The unit also includes backup power in the form of a battery which has a minimum capacity of 100 hours in no-alarm condition and 8 hours in alarm condition and is capable of full recharge. Batteries presently employed in the RAMS units are Glob Gel/Cel; however, a continuous in-service maintenance program evaluates new battery types, capabilities, etc., and replacements are made when superior batteries are found.

CAMS. The CAMS consist of portable monitors which monitor the air and exhaust for gross beta and gamma activity. CAMS units are located in areas adjacent to the HCF and in adjoining passageways. CAMS units may be placed at other locations at the discretion of the health physicists.

Fire Protection Systems

Systems. The Building 6580 Fire Protection System is utilized for the HCF. Fire Protection is provided within Zone 1 and Zone 2A by limiting the amount of combustibles within the areas, and providing an inert atmosphere when working with pyrophoric materials. Additional protection in the form of nitrogen fire suppression systems is provided inside the SCB's and the hot cell, and water sprays used in conjunction with metal screen scrubbers and demistors in the ventilation exhaust ducts of the SCB's and hot cell.

A wet pipe automatic sprinkler system is provided in Zone 2.

Hot Cell and SCB Fire Protection System. The hot cell has heat detectors to initiate a fire alarm. In addition, these detectors initiate the nitrogen purge system of the hot cell. Control interlocks prevent further introduction of make-up air and maintain negative pressure within the cell through control of the exhaust damper.

SCB 1 and SCB 2 (those involved with examination of capsules containing enriched uranium-dioxide and sodium) have a nitrogen atmosphere for these operations and are also equipped with containers of MET-L-X. SCB 3 (involved with waste solidification studies) has an air atmosphere, but is also equipped for nitrogen

atmosphere operation. All SCB's have heat detectors to initiate a fire alarm and a nitrogen fire suppression system identical to the hot cell system.

Nitrogen Fire Suppression System. The nitrogen fire suppression system is incorporated in the HCF to serve Zone 1 (SCB's) and Zone 2A (hot cell) areas. A 4,400 gallon liquid nitrogen storage tank, located adjacent to the MER, provides nitrogen for daily operation and the fire suppression systems to Zones 1 and 2A. When actuated either manually or by the Zone 1 and Zone 2A fire detection system, nitrogen gas flows into these zones, electrical interlocks prevent further introduction of make-up air and the ventilation controls continue operation of the exhaust fans, maintaining the area negative pressure. Pressure regulators and orifice plates regulate the volume of nitrogen flow into the zones. Within a few minutes after initiation of the nitrogen flow, the oxygen content is low enough to suppress the type of fire that may occur within Zone 1 or 2A.

HEPA Fire Protection System. To protect the HEPA filters from heat damage, a water spray system, including scrubbers, water spray nozzles, and demistors, are incorporated into the Zone 1 and Zone 2A exhaust lines to assure that air temperatures to the HEPA filters is less than 300°F. Temperature sensors are located in the exhaust duct and actuate the water sprays, providing the necessary water flow required to reduce the air temperature to an acceptable level for flow through the HEPA filter. A final water spray, manually operated, is located in the MER filter banks. These filter banks also have a temperature sensor located in the supply air ducts to initiate an alarm within the facility Fire Alarm System.

The residual water, after passing through the spray system, is drained into a storage tank where it is monitored for radioactive content.

IV. Discussion

GDC Conformance

In the early design stage for the HCF it was determined that the GDC would apply in that three ventilation zones would be required. At that time only 1-5 curies were considered to be the upper limit for the plutonium inventory. We considered eliminating Zone 2A but this was not pursued because ERDA/ALO's position was that 5 curies did represent a substantial quantity of plutonium and the GDC requirement for three zones should be met. They also maintained that Zone 2A was necessary to prevent the contamination of Zone 2 (essentially all of the HCF) in the event of a serious incident in the SCB's. In addition, the elimination of Zone 2A would be a major redesign effort. Time was short and sufficient resources were not available to do the redesign work. Also the savings in construction cost were found to represent only a few percent of the total cost. Because of these factors it was decided to retain the three

ventilation zones. However, we did increase the plutonium limit to 200 curies and were permitted to remove one HEPA filter each from the Zone 1 and 2A banks.

In retrospect the early design work was at a disadvantage because the plutonium inventory limit was not well defined. This uncertainty plus the position that 1-5 curies of plutonium is a substantial quantity lead to conservatism in the design and to the three ventilation zones. Consequently, the three zone system required for the New Plutonium Recovery Facility at Rocky Flats and the DP West Plutonium Processing Facility at Los Alamos, both of which can handle significantly more plutonium than is planned for the HCF, is nonetheless still required.

We have three suggestions which might avoid what we consider to be the over design problems which we have encountered with the HCF. (1) Attempt to quantify the meaning of "substantial quantities of in-process plutonium". The disparity that exist between the quantities of plutonium associated with the HCF and major plutonium facilities is such that some modification of the three zone ventilation requirement appears to be justified. We intend to pursue this point with ERDA/ALO. (2) Develop firm upper limit inventories before proceeding with preliminary design of the facility. Thus one can avoid incorporating excessive design margins to deal with the uncertainty in the inventories. (3) Reduce the area devoted to support activities within the confines of any future facilities. The argument about extensive clean-up requirements in case of an incident is certainly valid. The Zone 2 Support Area is probably larger than required because of the constraints of pre-existing construction. If the hot cell boundary was slightly enlarged to accommodate storage of casks and transfer containers, it is conceivable that only two ventilation zones would be needed.

Fire Analysis

In performing the hazards analysis associated with a fire in the SCB's we established an SCB limit of 1 lb of hypereze cutting compound, a high quality kerosene, having a heat of combustion of about 20,000 BTU/lb. With the air available an upper limit burn rate of about 0.5 lb/min could be sustained. Tests at Sandia showed that a maximum flame temperature of 2,000°F existed in the upper position of the flame. Hence our fire environment was defined to be one with a heat release rate of 10,000 BTU/min which lasted two minutes. Air temperature from the flame was assumed to be 2,000°F.

Attempts were made to incorporate a metallic heat sink in the exhaust duct to protect the HEPA filters. The heat sink was found to be very effective in initially cooling the exhaust air. But subsequent to the fire, the heat sink was cooled by the air flow and the temperature rise in the air was enough to present a hazard to the HEPA filters. Two alternatives were considered, an active cooling system for the heat sink (radiator-like system) and bypassing the heat sink once the fire was extinguished. These seemed complex with respect to the conventional water

sprays which we decided to use. However, we are pursuing this concept and intend to incorporate a heat sink alternative if a practical one is developed.

V. Summary

We believe that the HCF is too conservatively designed. Part of this conservatism has been removed by increasing the plutonium limits to 200 curies. Alternatives of two ventilation zone systems and reduced support areas would be considered if the HCF were redesigned. The heat sink concept appears to be a viable option to water sprays for HEPA filters. However this concept does need further development.

References:

Appendix 6301, General Design Criteria, Plutonium Facilities.

ORNL-NSIC-65, Design, Construction and Testing of High Efficiency Air Filtration System for Nuclear Application, January 1970.

UCRL-23800, Fire Protection of HEPA Filters by Using Water Sprays, July 1972.

Argonne National Laboratory, Liquid Nitrogen Fire Extinguishing System Test Report, J. A. Beidelman, May 1972.

SLA-74-0345, Test Results on the Effect of Heating a Confined High Explosive, A. B. Donaldson and D. O. Lee, August 1974.

U. S. ERDA Manual, Chapter 0524, Standards for Radiation Protection, January 1975.

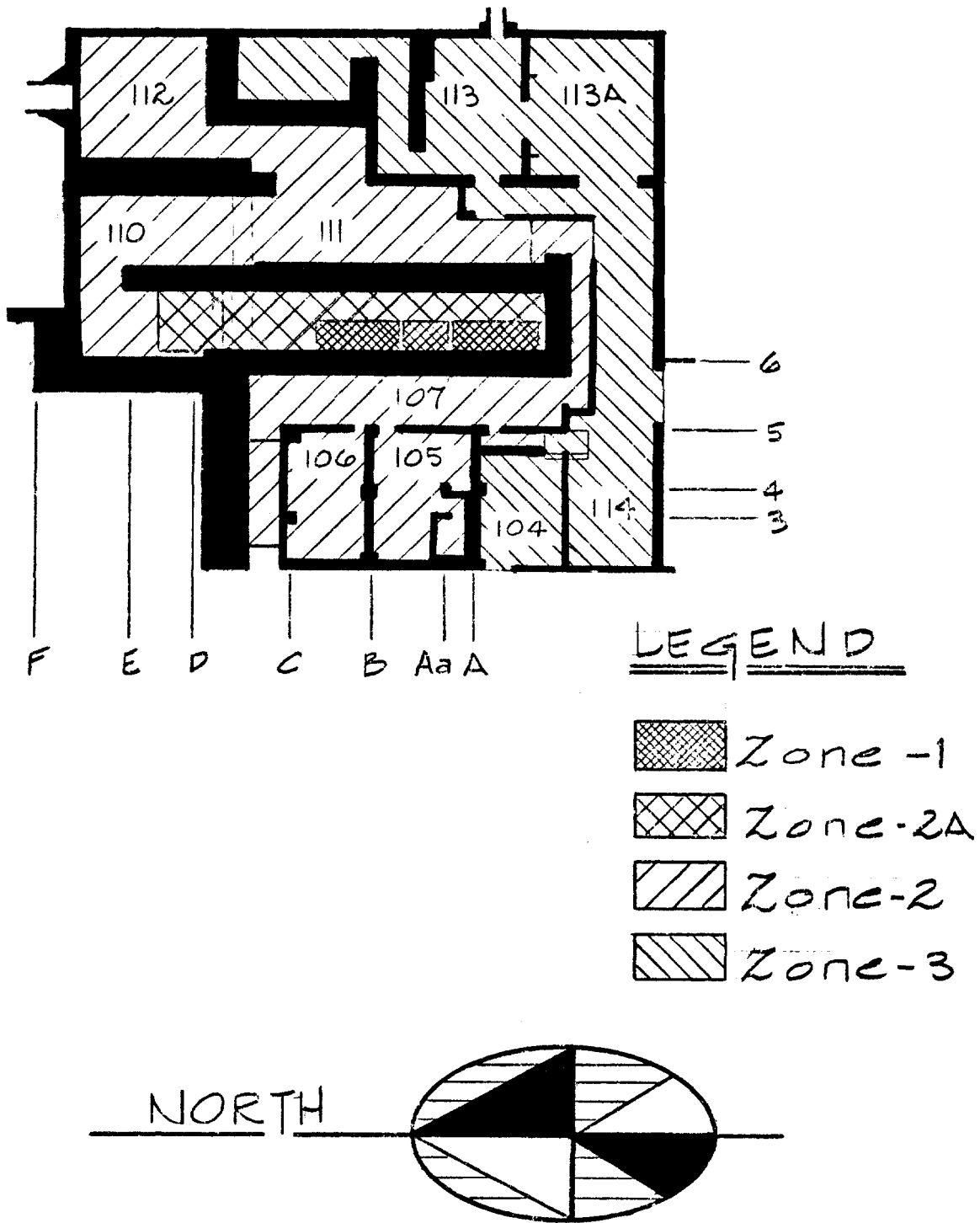


FIGURE 1
HCF FLOOR PLAN

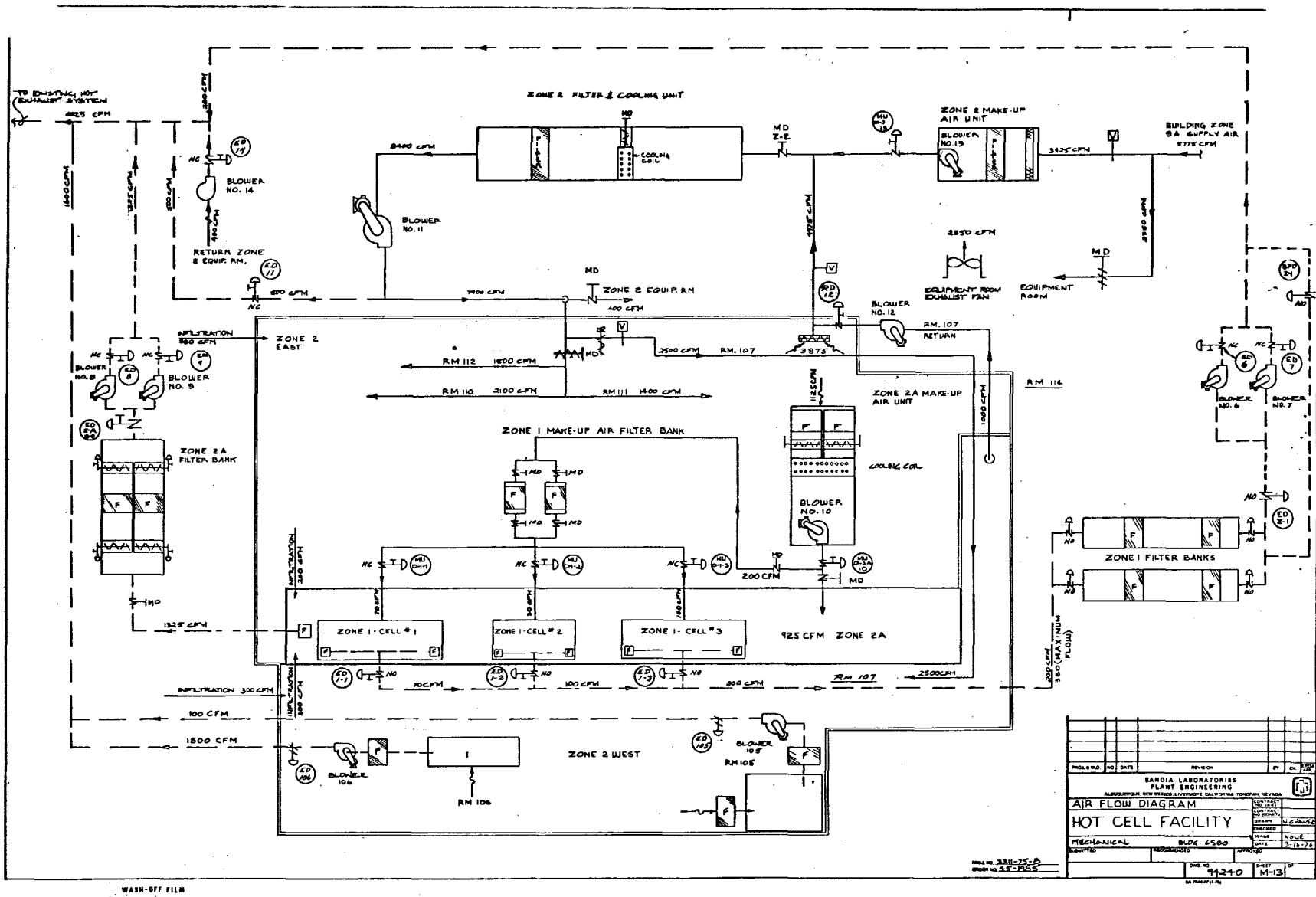


FIGURE 2
VENTILATION SYSTEM

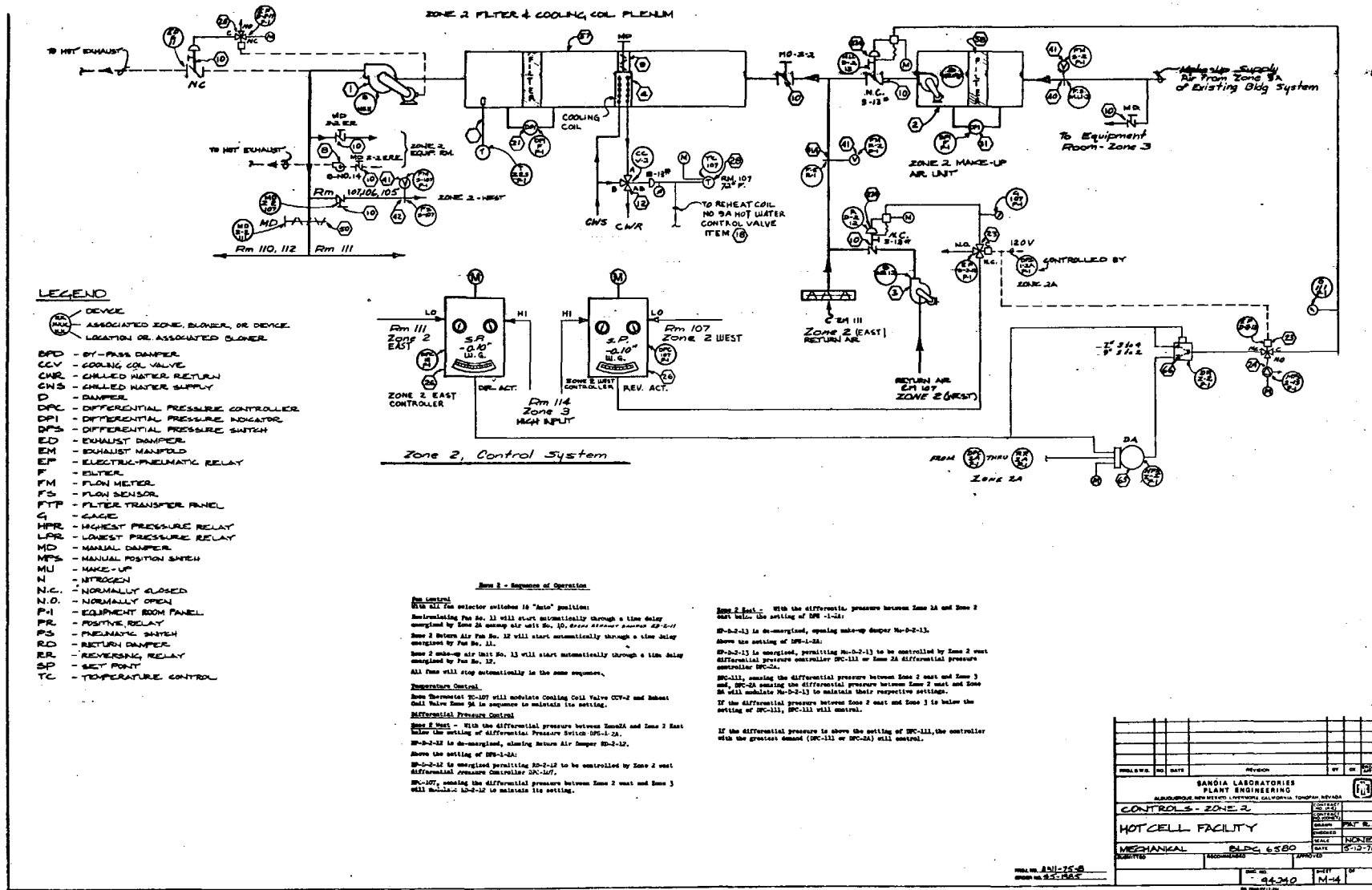


FIGURE 3
ZONE 2

206

WASH-OFF FILM

REVISION	NO	DATE	REVISION	BY	CHK
SANDIA LABORATORIES PLANT ENGINEERING					
ALBUQUERQUE NEW MEXICO LIVERMORE CALIFORNIA TONGVA NEVADA					
CONTROLS - ZONE 2					
HOTCELL FACILITY					
MECHANICAL		BLPG 6580		DATE 5-12-74	
DESIGNED		RECORDED		DRAWN	
		NO. 96340		M-4	

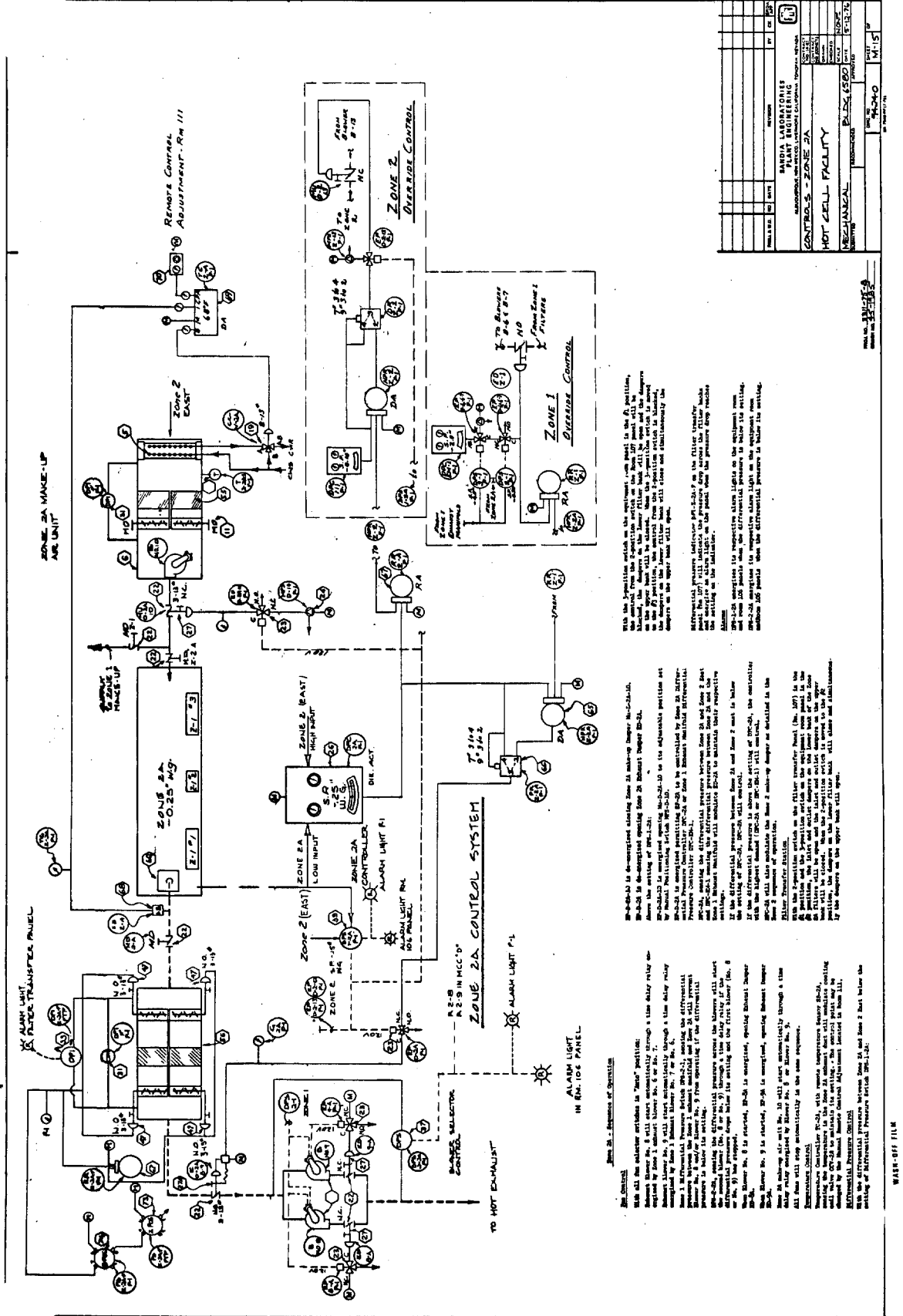


FIGURE 4
ZONE 2A

REVISIONS:

NO.	DATE	DESCRIPTION
1		
2		
3		
4		
5		

PROJECT: MCH-40
 DRAWING NO.: M-15
 TITLE: ZONE 2A CONTROL SYSTEM
 AUTHOR: SANDIA LABORATORIES PLANT ENGINEERING
 CHECKED: []
 APPROVED: []
 PROJECT ENGINEER: []
 CONTRACTOR: []

With the operation switch on the equipment, and panel in the B position, the electrical switch on the Zone 2A main will be closed. When the operation switch is in the A position, the electrical switch will be closed. When the operation switch is in the B position, the electrical switch will be closed. When the operation switch is in the A position, the electrical switch will be closed.

Differential pressure indicator (PS-21) on the filter transfer will indicate when the differential pressure is below its setting. When the differential pressure is below its setting, the indicator will be illuminated. When the differential pressure is below its setting, the indicator will be illuminated.

PS-21-22 indicates the differential pressure on the equipment room and room 108 panels. The differential pressure is below its setting. When the differential pressure is below its setting, the indicator will be illuminated. When the differential pressure is below its setting, the indicator will be illuminated.

PS-23 will also indicate the Zone 2 make-up supply is available to the filter transfer transfer.

With the operation switch on the filter transfer panel (the 107) in the B position, the operation switch on the equipment room panel in the B position will be closed. When the operation switch on the equipment room panel in the B position, the electrical switch will be closed. When the operation switch on the equipment room panel in the B position, the electrical switch will be closed.

Zone 2A - Sequence of Operation

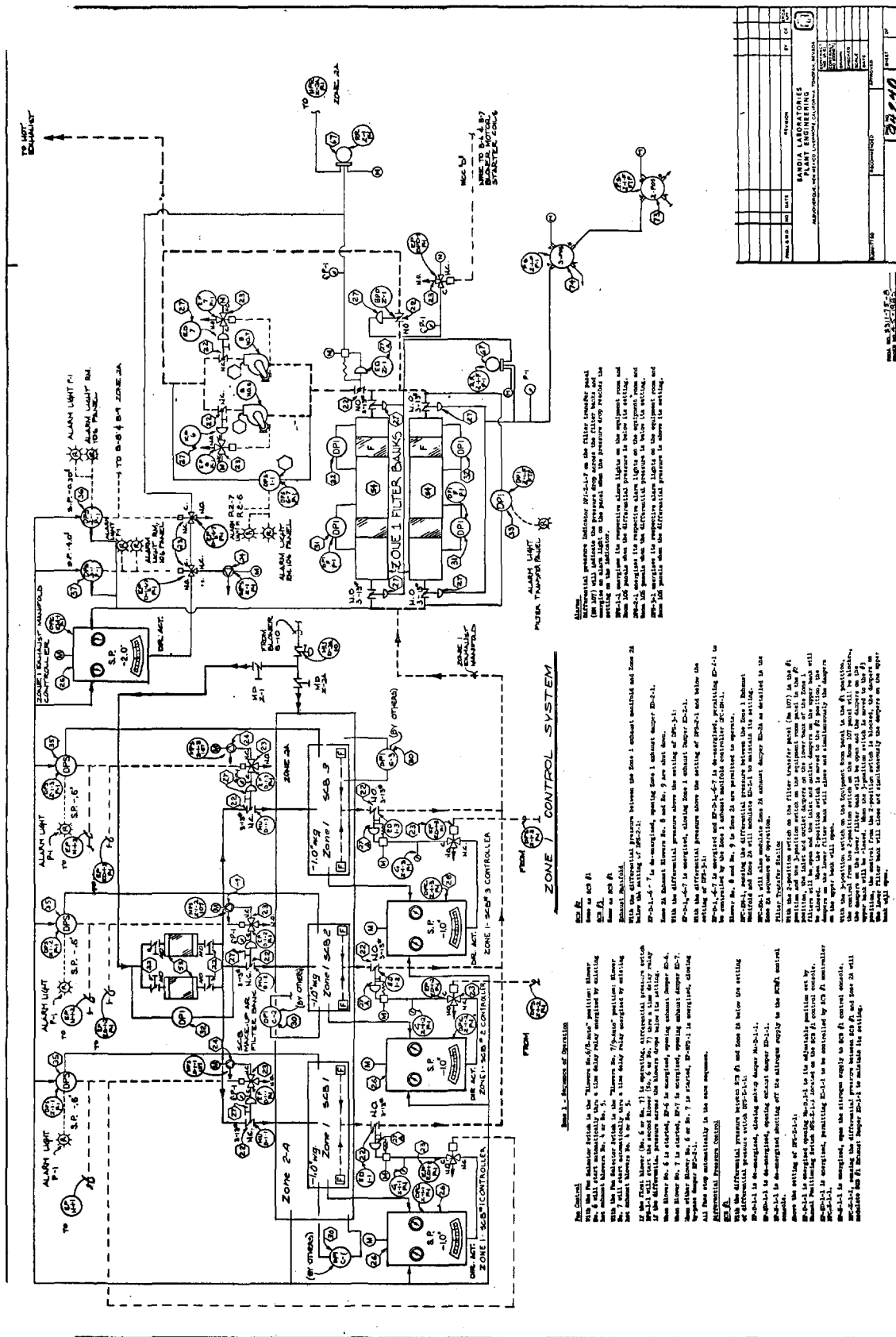
When all the alarm switches in "Alarm" position, the alarm indicator on the Zone 2A panel will be illuminated through a time delay relay.

When the alarm indicator on the Zone 2A panel is illuminated, the alarm indicator on the Zone 2A panel will be illuminated through a time delay relay.

When the alarm indicator on the Zone 2A panel is illuminated, the alarm indicator on the Zone 2A panel will be illuminated through a time delay relay.

When the alarm indicator on the Zone 2A panel is illuminated, the alarm indicator on the Zone 2A panel will be illuminated through a time delay relay.

WAS-8-611-118



5.1.1 - Sequence of Operation

With the differential pressure between Zone 1 and Zone 2 above the setting of DP-1-1, the differential pressure between Zone 2 and Zone 3 above the setting of DP-2-1, and the differential pressure between Zone 3 and Zone 4 above the setting of DP-3-1, the following sequence of operations will occur:

1. Zone 1 scrubber motor (SM-1) will start automatically when the differential pressure between Zone 1 and Zone 2 is above the setting of DP-1-1.

2. Zone 2 scrubber motor (SM-2) will start automatically when the differential pressure between Zone 2 and Zone 3 is above the setting of DP-2-1.

3. Zone 3 scrubber motor (SM-3) will start automatically when the differential pressure between Zone 3 and Zone 4 is above the setting of DP-3-1.

4. When any scrubber motor starts, the differential pressure between the zone it is scrubbing and the zone it is scrubbing into will be reset to the setting of the corresponding differential pressure switch.

5. When any scrubber motor stops, the differential pressure between the zone it is scrubbing and the zone it is scrubbing into will be reset to the setting of the corresponding differential pressure switch.

6. When any scrubber motor stops, the differential pressure between the zone it is scrubbing and the zone it is scrubbing into will be reset to the setting of the corresponding differential pressure switch.

7. When any scrubber motor stops, the differential pressure between the zone it is scrubbing and the zone it is scrubbing into will be reset to the setting of the corresponding differential pressure switch.

5.1.2 - Sequence of Operation

With the differential pressure between Zone 1 and Zone 2 above the setting of DP-1-1, the differential pressure between Zone 2 and Zone 3 above the setting of DP-2-1, and the differential pressure between Zone 3 and Zone 4 above the setting of DP-3-1, the following sequence of operations will occur:

1. Zone 1 scrubber motor (SM-1) will start automatically when the differential pressure between Zone 1 and Zone 2 is above the setting of DP-1-1.

2. Zone 2 scrubber motor (SM-2) will start automatically when the differential pressure between Zone 2 and Zone 3 is above the setting of DP-2-1.

3. Zone 3 scrubber motor (SM-3) will start automatically when the differential pressure between Zone 3 and Zone 4 is above the setting of DP-3-1.

4. When any scrubber motor starts, the differential pressure between the zone it is scrubbing and the zone it is scrubbing into will be reset to the setting of the corresponding differential pressure switch.

5. When any scrubber motor stops, the differential pressure between the zone it is scrubbing and the zone it is scrubbing into will be reset to the setting of the corresponding differential pressure switch.

6. When any scrubber motor stops, the differential pressure between the zone it is scrubbing and the zone it is scrubbing into will be reset to the setting of the corresponding differential pressure switch.

7. When any scrubber motor stops, the differential pressure between the zone it is scrubbing and the zone it is scrubbing into will be reset to the setting of the corresponding differential pressure switch.

5.1.3 - Sequence of Operation

With the differential pressure between Zone 1 and Zone 2 above the setting of DP-1-1, the differential pressure between Zone 2 and Zone 3 above the setting of DP-2-1, and the differential pressure between Zone 3 and Zone 4 above the setting of DP-3-1, the following sequence of operations will occur:

1. Zone 1 scrubber motor (SM-1) will start automatically when the differential pressure between Zone 1 and Zone 2 is above the setting of DP-1-1.

2. Zone 2 scrubber motor (SM-2) will start automatically when the differential pressure between Zone 2 and Zone 3 is above the setting of DP-2-1.

3. Zone 3 scrubber motor (SM-3) will start automatically when the differential pressure between Zone 3 and Zone 4 is above the setting of DP-3-1.

4. When any scrubber motor starts, the differential pressure between the zone it is scrubbing and the zone it is scrubbing into will be reset to the setting of the corresponding differential pressure switch.

5. When any scrubber motor stops, the differential pressure between the zone it is scrubbing and the zone it is scrubbing into will be reset to the setting of the corresponding differential pressure switch.

6. When any scrubber motor stops, the differential pressure between the zone it is scrubbing and the zone it is scrubbing into will be reset to the setting of the corresponding differential pressure switch.

7. When any scrubber motor stops, the differential pressure between the zone it is scrubbing and the zone it is scrubbing into will be reset to the setting of the corresponding differential pressure switch.

FIGURE 5
ZONE 1

WASH-OFF FILM

PROJECT NO.	37240
DATE	
DESIGNED BY	
CHECKED BY	
APPROVED BY	
BARDA LABORATORIES	
AN INSTRUMENTAL ENGINEERING COMPANY	
1100 UNIVERSITY AVENUE, ANN ARBOR, MICHIGAN 48106	
TELEPHONE (313) 763-1000	
FACSIMILE (313) 763-1000	
TELETYPE (313) 763-1000	
CABLE (313) 763-1000	
RADIO (313) 763-1000	
TELEVISION (313) 763-1000	
POSTAL (313) 763-1000	
AIR MAIL (313) 763-1000	
EXPRESS (313) 763-1000	
REGISTERED MAIL (313) 763-1000	
POST OFFICE BOX (313) 763-1000	
CITY (313) 763-1000	
STATE (313) 763-1000	
COUNTRY (313) 763-1000	

DISCUSSION

BURCHSTED: You mentioned you had water sprays on your filters. Do these sprays permit impingement of water on the filter itself, and if so, could the droplets puncture the filter?

BURRESS: The first set of sprays is located in a spray chamber and is about 25 feet from our first bank of filters, both in Zone 1 and Zone 2A. In Zone 2, we do not have a water spray system on the filter. I don't believe we will get any water carry-over on the Zone 2 bank. Also, ERDA has asked us to put a final manual spray on the filter banks in the event that heating continues in spite of the sprays.

BURCHSTED: That might be a last-ditch type of thing. If you have a fire, you put the fire out regardless of what happens to the filter?

BERNARD: Yes. About four failures are needed to produce this situation.

EFFECTS OF EXPLOSION-GENERATED SHOCK WAVES IN DUCTS*

M. R. Busby**

Tennessee State University
Nashville, Tennessee

J. E. Kahn and J. P. Belk

Union Carbide Corporation-Nuclear Division
Oak Ridge National Laboratory
Oak Ridge, Tennessee

Abstract

An explosion in a space causes an increase in temperature and pressure. To quantify the challenge that will be presented to essential components in a ventilation system, it is necessary to analyze the dynamics of a shock wave generated by an explosion, with attention directed to the propagation of such a wave in a duct.

Using the equations of unsteady flow and shock tube theory, a theoretical model has been formulated to provide flow properties behind moving shock waves that have interacted with various changes in duct geometry. Empirical equations have been derived to calculate air pressure, temperature, Mach number, and velocity in a duct following an explosion.

I. Introduction

A comprehensive safety analysis should evaluate the effects of a localized detonation on essential air-cleaning components in an exhaust system. The analysis should predict the capability of critical air-cleaning apparatus to remain functional following a detonation, even if the location of the actual incident is distant from those components and connected to them by a complex path. In order to describe an explosion, it will be necessary to differentiate between normal burning and detonation.

Description of Explosions

Normal burning is a result of heating an optimal volume of a combustible gas mixture to the ignition temperature by an external source, after which the flame propagates through the entire volume.¹ The maximum flame front speed for normal burning of a hydrogen-air mixture is 320 cm/sec, and the maximum post- to precombustion pressure ratio is 8.^{2,3} However, detonation differs from normal burning in that the velocity of flame propagation and pressure ratio are significantly higher (e.g., for a 40% hydrogen-air mixture the detonation wave velocity is 2100 m/sec, and the pressure ratio is approximately 20).^{4,5} Although the phenomenon is not completely understood at present, the steady detonation wave has been modeled as a shock front, followed, after a short time interval, by a combustion zone, and then a region of hot gases in equilibrium. This model has been

*Research sponsored by the U.S. Nuclear Regulatory Commission under contract with Union Carbide Corporation under Union Carbide Corporation's contract with the Energy Research and Development Administration. By acceptance of this article, the publisher or recipient acknowledges the U.S. Government's right to retain a nonexclusive, royalty-free license in and to any copyright covering the article.

**Consultant to Oak Ridge National Laboratory.

used successfully to predict the detonation wave velocities for various gas mixtures.⁶ Detonation velocity depends on the reaction-kinetic properties of the mixture.⁷ Because of the tremendous pressures that such equipment would experience upon wave impact, detonation can be more damaging to air-cleaning components than normal burning.

Initiation and Propagation of Detonation

If an explosive mixture is present in a duct system, there exists the possibility of spontaneous transition from normal burning to detonation at some "induction distance."^{8,9} This phenomenon occurs because, as a flame propagates down a duct, the burning rate increases continuously due to the turbulence of the mixture in front of the flame and the increase in flame surface area. The rapid burning creates a shock wave in the unburned mixture, which ignites the gas downstream from the flame front.

Of particular interest also is the likelihood of detonation waves propagating from a smaller duct to a larger one. From generalizations of earlier experiments,^{10,11} it was erroneously concluded that it is impossible for a detonation wave to propagate to the larger duct.⁹ However, if a detonation wave is transmitted to a large volume or duct from a smaller duct or tube whose cross section is sufficiently large, the detonation wave can propagate into the large duct. For example, Zel'dovich has shown experimentally that the initiation of spherical detonation in an explosive gas mixture is possible by means of a plane detonation wave from a tube, only if the tube diameter is equal to or greater than a certain critical diameter (e.g., for a hydrogen-air mixture, the critical diameter is 19 mm).¹² If the diameter of the tube is less than the critical diameter, a plane detonation wave collapses, and normal burning of the gas takes place. Zel'dovich thus concluded that, at a point where the tube diameter changes, a plane detonation wave can either be attenuated, transformed to slow burning, or transformed to a spherical wave that will propagate within the volume, with all the consequences that follow.

The conclusion concerning attenuation has led to a proposed detonation-control measure by placing orifices with diameters less than the critical diameter for detonation at intervals in a duct less than the "induction distance."⁸ In this paper, less consideration is given to the probability of occurrence of a detonation than to the effects produced by such a phenomenon.

Hydrogen-Air Mixtures

Because a hydrogen-air mixture has so many prevalent possible sources (e.g., radiolytic or thermal disassociation of water, metal fires in the presence of water, sodium-water reaction, etc.) its detonation properties are of major interest. The actual explosive mixture might be air-hydrogen-steam, and a theoretical phase diagram for such a mixture is presented in Figure 1. Theoretically, in an air-hydrogen-steam mixture, 11% steam is sufficient to suppress any detonation.¹³ However, using a "third explosion limit theory", Mathews shows that the water molecule is only as effective as the hydrogen molecule in suppressing the active radicals in a hydrogen-air mixture.¹⁴ Thus the effectiveness of water vapor in suppressing detonations is still open to question, and experimental verification is lacking. In the present analysis, the effect of steam is neglected, and since the water molecule is more effective than the nitrogen molecule in suppressing the active radicals in the hydrogen-air mixtures,¹⁵ an air-hydrogen mixture should have a more destructive potential.

Experimental data for the detonation properties of hydrogen-air mixtures for various percentages of hydrogen are used in the analysis given here. The molecular weight of the mixture, the detonation velocity, the Mach number, and the Mach number based on 100% air are given in Table I.^{12,4} The detonation wave Mach number is defined as the ratio of the wave velocity to the speed of sound in the gas ahead of the wave. The effect of a shock wave passing through a duct containing a nonexplosive gas is independent of the explosive mixture at the initiation of the explosion and

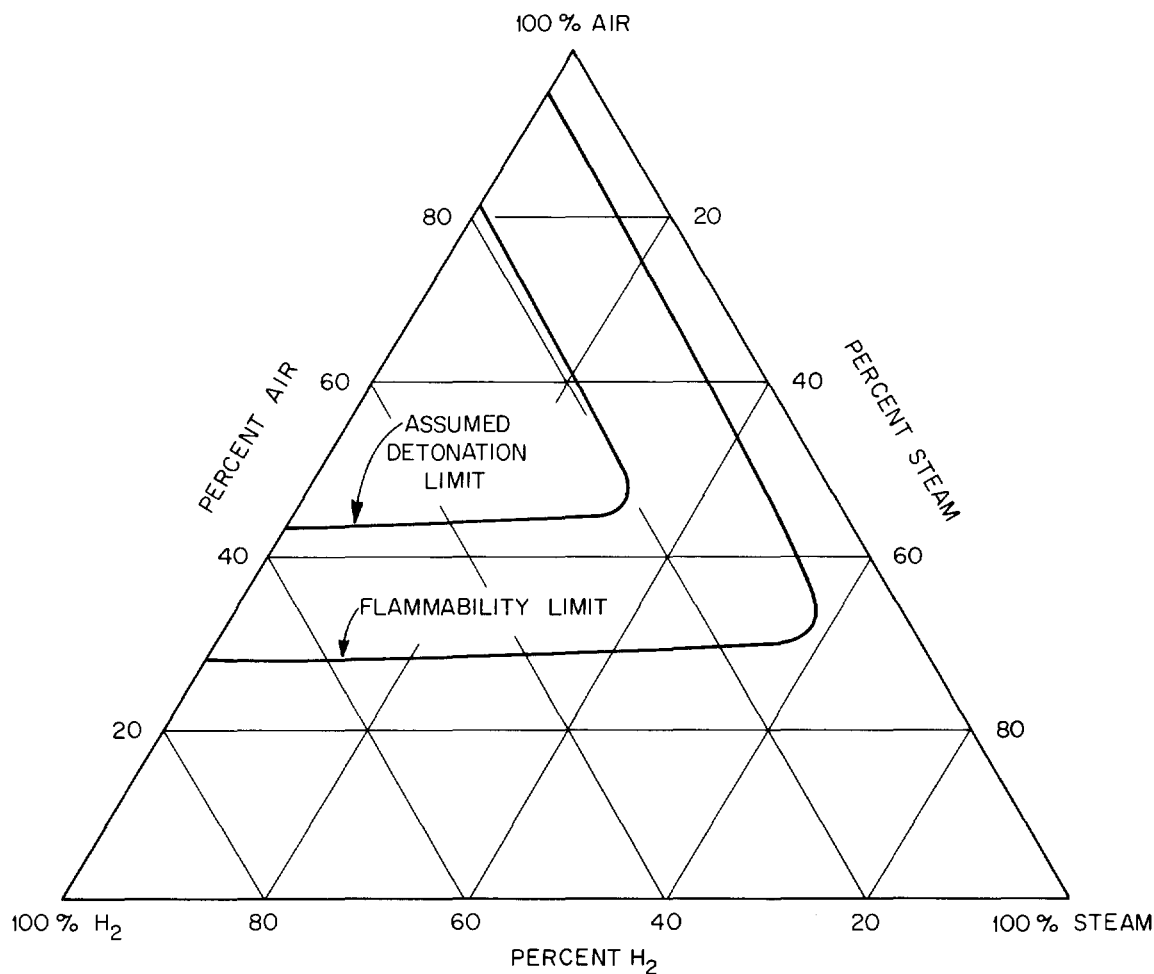


Figure 1: Detonation and flammability limits for air-hydrogen-steam mixtures (ref. 15).

Table I. Detonation data for hydrogen-air mixtures
(1 atm; 300° K)

H ₂ (percent by volume)	Mixture molecular wt.	Detonation velocity m/sec	Wave Mach Number (based on mixture)	Wave Mach Number (based on 100% air)
18.5 ^a	23.98	1300	4.11	3.74
18.8 ^a	23.90	1483	4.70	4.27
19.0 ^b	23.85	1480	4.70	4.26
19.9 ^b	23.60	1650	5.26	4.75
35 ^b	19.53	1950	6.84	5.62
42 ^b	17.64	2100	7.75	6.05
55 ^b	14.14	2200	9.07	6.34
58.9 ^b	13.08	2190	9.39	6.31

^aR. Wendlandt, *Z. Physik Chem.*, 110, 637 (1924).

^bJ. Brenton, *Ann. Office Nat'l. Combustibles Liquids*, 11, 487 (1936).

depends only on the incident shock wave Mach number and the gas-mixture properties and configuration within the duct.

II. The Duct-Detonation Wave Model

For the theoretical model, it is assumed that detonation occurs in a localized section of a duct where a hydrogen-air mixture is present. The blast wave is established and advance with a velocity corresponding to the hydrogen composition as given in Table 1. It is assumed that in the duct there exists an imaginary plane which divides the detonable mixture from 100% air. As the detonation wave crosses this plane into the air, combustion ceases, and the shock wave is then governed by those equations applicable to moving shock systems. Therefore, the Mach number of the wave as it travels in the noncombustible region is based on the speed of sound in 100% air. The variation of Mach number with hydrogen composition is presented in Figure 2. As predicted by this assumption, the values of pressure, temperature, and density behind the wave would be those related to the von Neumann "spike" and are consistent with the assumed model of the detonation wave (i.e., a shock front, followed by a combustion zone, and then a region of hot gases in equilibrium).²

The interactions of the moving shock wave with sudden or gradual duct contractions or enlargements are calculated by utilizing a shock-tube digital-computer program in which the area ratio between duct stages is an independent variable. The program employs the unsteady flow and shock tube equations to determine by an iterative technique the flow conditions as the duct area changes.^{16,2} A variety of flow conditions may be established after the passage of the shock wave. Once the area ratio and gas properties are fixed, the computer program will provide the flow condition that reflects what actually occurs. The program is limited to the unsteady one-dimensional flow of real and ideal gases. The energy- and momentum-dissipative effects of heat transfer and friction at the duct walls have not been considered in the calculation of shock wave properties. Since these effects tend to weaken the wave, neglecting them provides conservative results. Also, for the same reason, the possibility of reflected rarefaction waves overtaking and weakening the shock system has not been included in the model.

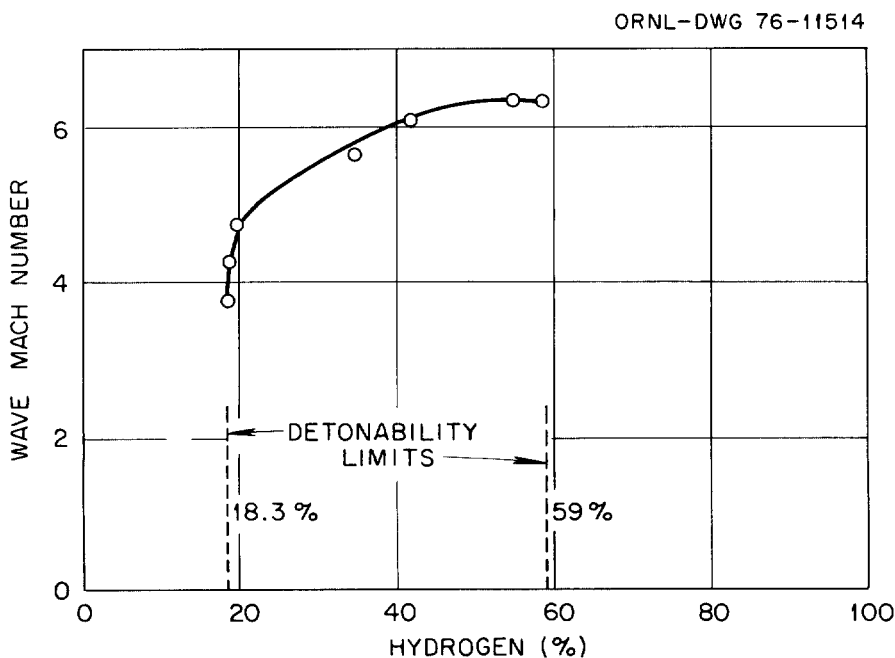


Figure 2: Detonation wave Mach numbers for hydrogen-air mixtures (refs. 4 and 12).

A time-displacement diagram for a typical sudden contraction is presented in Figure 3. As the incoming shock impinges upon the area change, another shock wave is reflected upstream while a stronger shock (i.e., higher Mach number) is transmitted downstream in the smaller duct. A contact surface and an unsteady expansion follow the transmitted wave. For a sudden enlargement, a typical time-dependent diagram is given in Figure 4. As the incident shock wave encounters the sudden

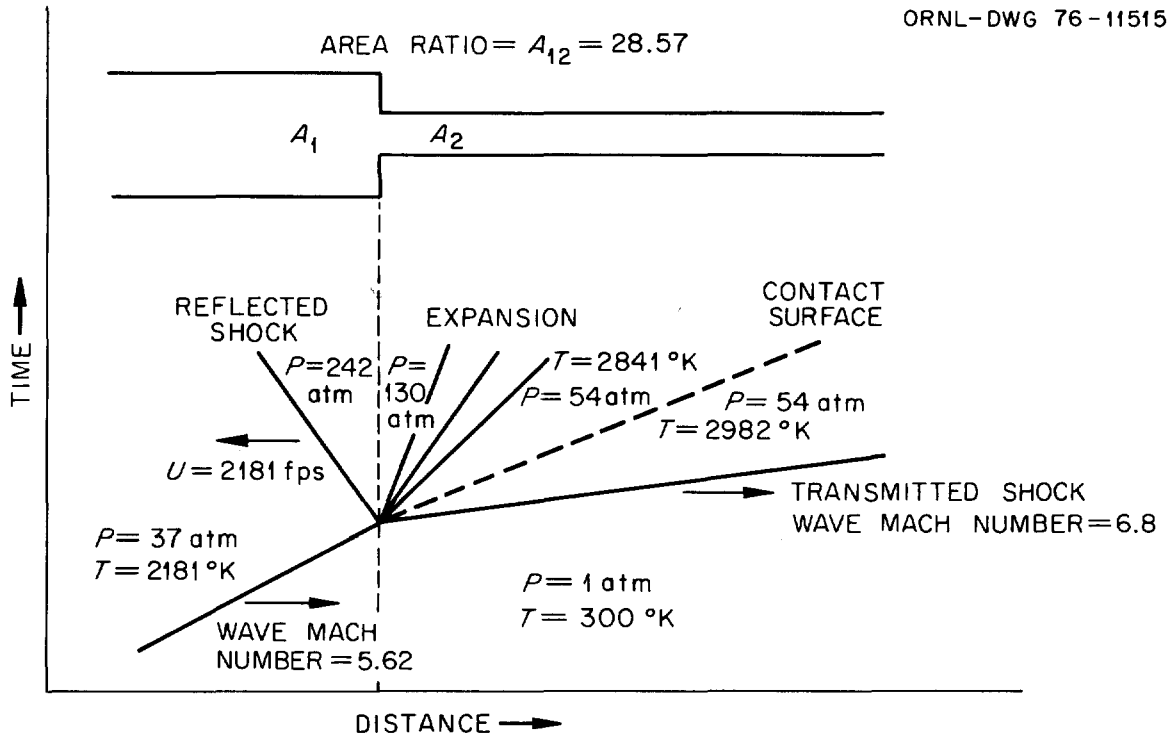


Figure 3: Shock wave interaction with sudden contraction.

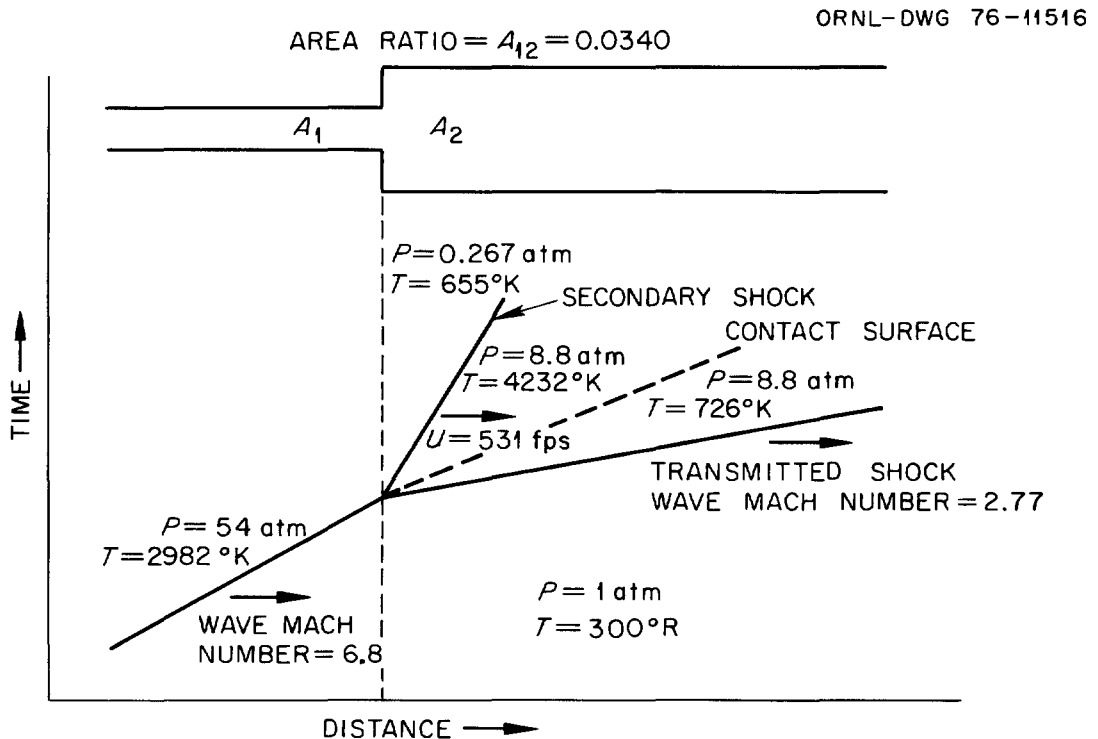


Figure 4: Shock wave interaction with sudden enlargement.

enlargement, a weaker shock wave is transmitted which is followed by a contact surface and a secondary shock that is swept downstream. With assumed ideal air and by utilizing the computer program, surfaces may be constructed in a three-dimensional plot of area ratio vs incident Mach number vs transmitted Mach number, static pressure, static temperature, or velocity. Empirical equations for these surfaces have been derived and are given below for a sudden area contraction or enlargement:

$$M_T = M_S (1 + a_1 \ln A_{12}) \quad (1)$$

$$P_T = a_2 + (M_S)^2 [b_2 + c_2 (\ln A_{12}) + d_2 (\ln A_{12})^2] \quad (2)$$

$$T_T = a_3 + b_3(M_S)^2 + c_3(M_S)^{-2} + (\ln A_{12}) [d_3 + e_3(M_S)^2] + (\ln A_{12})^2 [f_3 + g_3(M_S)^2] \quad (3)$$

$$U_T = a_4 + b_4(M_S) + c_4(M_S)^{-1} + (\ln A_{12}) [d_4 + e_4(M_S)] + (\ln A_{12})^2 [f_4 + g_4(M_S)^{-1}] \quad (4)$$

where

dependent variables are:

- M_T = transmitted shock wave Mach number;
- P_T = transmitted static pressure behind wave, atm;
- T_T = transmitted static temperature behind wave, °K;
- U_T = transmitted velocity behind wave, fps;

and independent variables are:

- M_S = incident shock wave Mach number;
- A_{12} = area ratio, upstream area/downstream area.

The coefficients and range of applicability for the appropriate geometry are given in Table II. It must be emphasized that these equations are empirical, and no inference concerning property functional

Table II. Coefficients and limits for transmitted flow property equations [eqns. (1) to (4)]

Transmitted property	Eqn. no. and subscript	Coefficients						
		a	b	c	d	e	f	g
For sudden contraction limit of applicability: $A_{12} > 1.0$, $M_S > 2.1$								
Mach No., M_T	1	0.070						
Pressure, P_T	2	-0.728	1.19	0.362	-0.066			
Temperature, T_T	3	277	58.7	13.0	-14.7	18.2	2.66	-3.23
Velocity, U_T	4	108	950	-1360	227	91.1	-156	143
For sudden enlargement limit of applicability: $A_{12} > 0.13$, $M_S > 2.5$								
Mach No., M_T	1	0.182						
Pressure, P_T	2	-0.120	1.16	0.443	0.046			
Temperature, T_T	3	288	58.1	-64.1	1.76	22.1	-1.02	2.32
Velocity, U_T	4	19.1	947	-970	72.4	175	37.1	-142

relationships is intended. All the properties behind the shock wave may be determined from the above equations. The equations apply only to ideal air ahead of the shock wave (though the computer program can apply to other ideal and real gases) and are presented in order to facilitate design and safety analyses. The results from the equations agree within about 5% of the computer results.

If a sudden enlargement results in a secondary shock which attempts to propagate upstream (i.e., $A_{12} < 0.13$ and $M_s < 2.5$), the computer program will not calculate the flow-field properties. For such cases, three-dimensional flow-field effects are significant but are beyond the scope of the assumed model. However, if these sudden enlargements are modeled as gradually expanding channels with pre- to post-enlargement ratios equal to that of the actual sudden enlargements, the expansion properties may be estimated for the actual cases. In this model, a stationary shock wave is allowed to stand at some calculated area ratio in the diverging duct, and its presence will adjust the downstream properties to match the flow requirements for the primary shock wave. Specifically, the solution for such a case may be constructed on a pressure-velocity (P-U) diagram in the following way:

1. A stationary normal shock is assumed to stand at a given duct area ratio.
2. An isentropic, steady expansion is assumed up to the shock.¹⁶
3. The normal shock relations are used to calculate flow properties across the shock.¹⁶
4. An isentropic steady expansion is assumed downstream of the shock until the final area is traversed. The pressure and velocity at the final area are plotted on the P-U diagram.
5. By assuming different shock locations, a locus of points may be constructed.
6. The pressure and velocity behind the primary shock wave are given in terms of conditions ahead of the wave by the following relation:¹⁶

$$\frac{U_T}{C_1} = \frac{\frac{P_T}{P_1} - 1}{\gamma \sqrt{1 + \frac{\gamma + 1}{2\gamma} \left(\frac{P_T}{P_1} - 1 \right)}} \quad (5)$$

Also the upstream or transmitted pressure behind the shock wave, P_T , is given in terms of the shock wave Mach number as:²

$$\frac{P_T}{P_1} = \frac{2\gamma M_T^2 - (\gamma - 1)}{(\gamma + 1)} \quad (6)$$

where

- γ = specific heat ratio, C_p/C_v ;
- M_T = transmitted shock wave Mach number;
- U_T = transmitted velocity behind shock wave, fps;
- C_1 = speed of sound in gas downstream, fps;
- P_1 = pressure in gas downstream, atm;
- P_T = transmitted static pressure behind shock wave, atm.

By assuming various values of P_T when P_1 and C_1 are given, a shock polar may be constructed on the P-U diagram.

7. The intersection of the shock polar with the previously constructed curve will give the pressure and velocity behind the primary shock wave.

An example of this procedure applied to a specific duct enlargement is presented in Figure 5. Because the assumption of a gradual enlargement should yield a stronger transmitted shock than that formed in a sudden enlargement, this formulation is conservative (as desired in a safety analysis).

The limits of applicability for a sudden contraction are $A_{12} > 1.0$ and $M_s > 2.1$. Cases for $M_s < 2.1$ are being investigated. Since sudden contractions always produce a stronger transmitted wave, a conservative estimate is made for cases where $M_s < 2.1$ if the incident Mach number is assumed to be 2.1.

The flow properties should also be affected by other geometrical duct arrangements such as bends, tees, valves, or long runs of straight duct. However, in an experimental study of detonation in hydrogen-air mixtures in Savannah River process equipment, Porter found that pipe bends up to 90° had no apparent effect on the formation or propagation of detonation waves.⁵ In addition, a combination of $1/2$ - and 2-in. pipe in a "Y" configuration had no significant effect on the detonation process. Similar results were found by Hishida and Hori for the propagation of pressure waves in water in pipes of various geometries.¹⁷ Thus, experimentally, there appears to be no measurable shock-wave suppression effects in bends or tees. Even though these geometries must have flow losses associated with them, the effects cannot be calculated with the present model; and since these losses appear to be experimentally insignificant, they will be neglected in the present analysis.

As an example, a duct system consisting of contractions and enlargements (Figure 6) will be analyzed for detonation effects. It is assumed that a detonation wave is established near the entrance of the duct and enters a nondetonable mixture (i.e., air) as shown. A sudden contraction at *a* and sudden enlargements at *b* and *c* are encountered. The time-displacement conditions are shown in Figure 6. At point *c* the gradual enlargement assumption is invoked. It is observed that such a duct

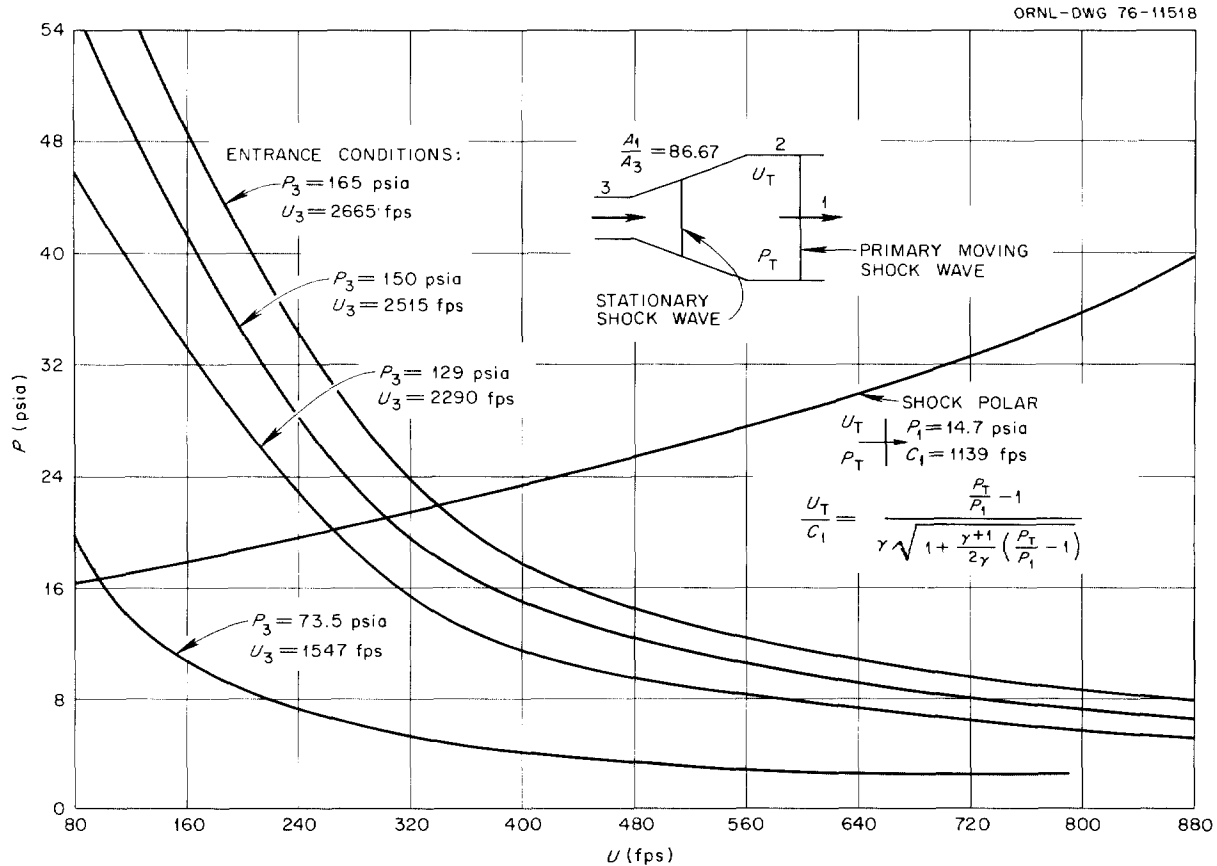


Figure 5: Estimation of conditions behind shock wave propagating through a gradual duct enlargement.

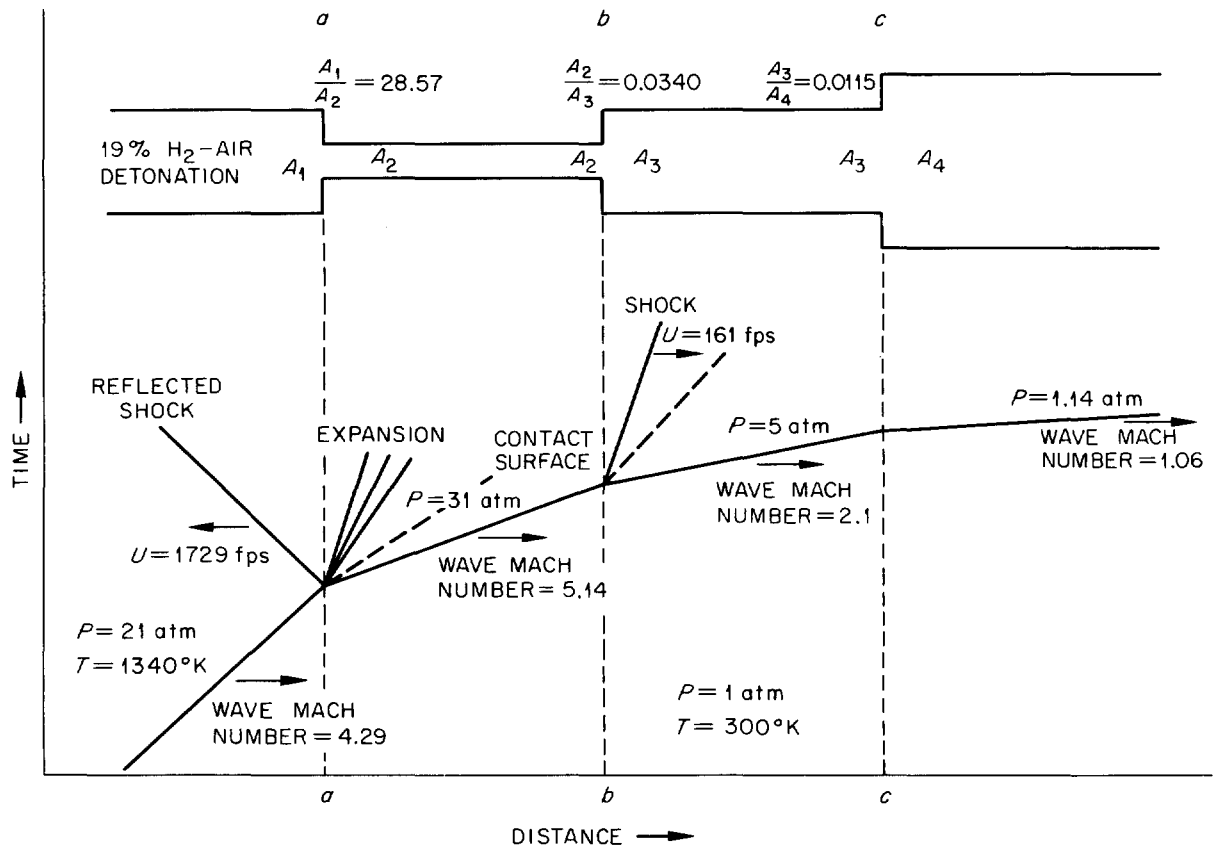


Figure 6: Duct system analysis.

arrangement for the given initial shock condition (i.e., a shock of $M_s = 4.29$ moving into air at 1 atm and 300°K) would produce a pressure drop from 21 to 1.14 atm. Any number of such duct contractions or enlargements may be joined together and analyzed for the final flow properties.

III. Conclusions

A theoretical model has been presented which should aid in a comprehensive safety analysis of explosion-induced shock waves in ducts of various geometries. Empirical equations for a range of sudden duct contractions and enlargements virtually eliminate the necessity of computer computations for the flow-field properties behind the primary shock wave. Also, a method has been presented which can conservatively estimate the flow properties for enlargements outside the range of the computer model applicability. Damage to air-cleaning components in duct systems due to wave impact can be estimated.

References

1. Ia. B. Zel'dovich and N. M. Simonov, *J. Phys. Chem. (USSR)*, 11, 1361 (1949).
2. A. G. Gaydon and I. R. Hurle, *The Shock Tube in High-Temperature Chemical Physics*, Reinhold Publishing Corp., N.Y., 1963, pp. 251-787.
3. W. S. Young and N. W. Kruse, "Properties of Explosive Gas Mixtures," *Trans. Am. Inst. Chem. Engrs.* 35, 337-358 (1939).
4. J. Brenton, *Ann. Office Nat'l Combustibles Liquids*, 11, 487 (1936).
5. J. B. Porter, *Analysis of Hydrogen Explosion Hazards*, DP-1295, E. I. DuPont de Nemours and Co., Savannah River Laboratory, Aiken, S.C. (July 1972).
6. B. Lewis and G. von Elbe, *Combustion, Flames, and Explosions*, Academic Press, N.Y., 1951, p. 606.
7. Ia. B. Zel'dovich, S. M. Kogardo, and N. N. Simonov, "An Experimental Investigation of Spherical Detonation in Gases," *Soviet Phys.—Tech Phys.*, 1, 1689-1713 (1956).
8. B. Lee, J. Lee, and R. Knystautas, "Transmission of Detonation Waves Through Orifices," *AIAA Journal*, 4,(2), 365-367 (1966).
9. W. Jost, *Explosion and Combustion Processes in Gases*, McGraw Hill, N.Y., 1946, pp. 160-209.
10. P. Laffitte, *Comptes rend.* 177, 178 (1923).
11. P. Laffitte, *Comptes rend.* 179, 1934 (1924).
12. R. Wendlandt, *Z. Physik Chem.*, 110, 637 (1924).
13. J. G. Moore and E. V. Gilby, *A Review of Problems Arising from the Combustion of Hydrogen in a Water Reactor Containment*, UKAEA Report AHSB(S) R 101, Authority Health and Safety Branch (1966).
14. R. L. Mathews, *Explosion and Detonation Limits for an Oxygen-Hydrogen-Water Vapor System*, USAEC Report KAPL-M-6564, Knolls Atomic Power Laboratory (June 1966).
15. H. A. McLain, *Potential Metal-Water Reactions in Light Water-Cooled Power Reactors*, ORNL-NSIC-23 (August 1968), p. 90.
16. A. H. Shapiro, *Dynamics and Thermodynamics of Compressible Fluid Flow*, Vols. 1 and 2, Ronald, N.Y., 1953.
17. M. Hishida and M. Hori, *Experiment on Pressure Wave Propagation. I. The Result of Experiments on Branches and Bends*, United States-Japanese Fast Reactor Exchange Program, JAPFNR-137 (November 1974).

DISCUSSION

ETTINGER: Since ventilation systems normally have tapered rather than sudden expansions or contractions, what is the magnitude of the difference between your model for sudden changes in duct size versus the real situation in ventilation systems?

BUSBY: For tapered geometries, the losses would be less than for sudden expansions or contractions. The particular computer model that we have can calculate the flow through tapered geometries.

MURROW: If the shock wave was not such a serious one, but a shock wave generated by an abrupt closing of a valve in a moving air stream, the Mach number might not be 2.1. Would the computer code be able to handle this kind of problem and generate the pressures, the reflected pressures, and the less-than-ambient downstream pressure from the closing valve?

BUSBY: If a moving shock wave has a Mach number less than 2.07, the flow behind the shock wave is subsonic. In some particular cases the flow may be assumed to be incompressible and those corresponding equations will apply. For the closing of a valve, if the incident conditions are known, the reflected conditions can be found from the equations of shock tube theory.

ORTH: Since your calculations, as you've mentioned, are conservative, do you know of any plans to run some experiments to check the real case with calculations?

BUSBY: At Oak Ridge, I do not know of any such program yet.

CLOSING REMARKS OF SESSION CHAIRMAN:

I'd like to thank our four speakers. In summary, just a short one, there always will be requirements for ventilation systems to survive fire, explosion and natural disasters. I think we've had four good papers that will assist us in analyzing and designing facilities. Thank you.

RADIOIODINE REMOVAL AND RETENTION

Monday, August 2, 1976

CO-CHAIRMEN: R. D. Rivers, J. G. Wilhelm

IODINE EVAPORATION FROM IRRADIATED AQUEOUS SOLUTIONS CONTAINING
THIOSULFATE ADDITIVE

A. H. Dexter, A. G. Evans,
L. R. Jones

DEPENDENCE OF GAS PENETRATION OF CHARCOAL BEDS ON RESIDENCE TIME AND
LINEAR VELOCITY

V. R. Deitz, C. H. Blachly,
L. A. Jonas

EFFECT OF SERVICE AGING ON IODINE RETENTION OF ACTIVATED CHARCOAL

A. G. Evans

A METHOD FOR CORRELATING WEATHERING DATA ON ADSORBENTS USED FOR THE
REMOVAL OF CH_3I

H. Parrish, R. C. Muhlenhaupt

IODINE REMOVAL ADSORBENT HISTORIES, AGING AND REGENERATION

J. R. Hunt, L. Rankovic,
R. Lubbers, J. L. Kovach

NEW CHARCOAL IMPREGNANTS FOR TRAPPING METHYL IODIDE

I. Salts of the Iodine Oxyacids with Iodide or Iodine and
Hexamethylenetetraamine

V. R. Deitz, C. H. Blachly

II. Applications to a Variety of Base Charcoals

A. G. Evans

THE BEHAVIOR OF HIGHLY RADIOACTIVE IODINE ON CHARCOAL IN MOIST AIR

R. A. Lorenz, S. R. Manning,
W. J. Martin

REMARKS ON TESTING THE RELIABILITY OF IODINE ADSORPTION IN ION-
EXCHANGING CHARCOAL-FILTERS WITH RESPECT TO SOLVENT LOADINGS

H. J. Strauss, K. Winter

AIRBORNE ELEMENTAL IODINE LOADING CAPACITIES OF METAL ZEOLITES AND A
DRY METHOD FOR RECYCLING SILVER ZEOLITE

B. A. Staples, L. P. Murphy,
T. R. Thomas

AIR FILTRATION PLANTS OF WALL-TYPE FOR SEPARATION OF FISSION IODINE
IN NUCLEAR REACTORS

H. H. Stiehl, M. Neumann, D. Sinhuber

14th ERDA AIR CLEANING CONFERENCE

AN AIRBORNE RADIOIODINE SPECIES SAMPLER AND ITS APPLICATION FOR MEASURING REMOVAL EFFICIENCIES OF LARGE CHARCOAL ADSORBERS FOR VENTILATION EXHAUST AIR

W. A. Emel, D. C. Hetzer,
C. A. Pelletier, E. D. Barefoot,
J. E. Cline

OPERATING EXPERIENCE WITH THE TESTING OF IODINE ADSORBERS ON THE AIR CLEAN UP SYSTEMS OF THE BELGIAN PWR POWER PLANTS

B. Deckers, P. Sigli, L. Trehen

HEAD-END IODINE REMOVAL FROM A REPROCESSING PLANT WITH A SOLID SORBENT

J. G. Wilhelm, J. Furrer, E. Schulte

REPORT OF THE GOVERNMENT-INDUSTRY COMMITTEE ON ADSORBERS AND ADSORPTION MEDIA

C. A. Burchsted

OPENING REMARKS OF SESSION CHAIRMAN: (J. G. Wilhelm)

Thirteen years ago the first charcoals were developed which removed iodine in both organic and elemental form. Today, iodine filters for power reactor stations can be constructed with high decontamination factors, but some problems still remain unsolved. One of the most pressing at this time is the ageing and poisoning of iodine filters (which may take place within a few months, or even weeks) to such an extent that the lowest removal efficiencies acceptable for iodine filters will not be met. Four papers will be given on this subject.

Improved impregnants for activated charcoal are still the goal of R&D work. Of special interest are impregnants which allow operation at higher temperatures and better withstand poisoning. In addition, it is of interest to increase the variety of base charcoals which can be used effectively. Two papers will be presented on this subject.

A new inorganic material was developed for removal of iodine from fuel reprocessing plant effluents. Two papers will discuss the trapping of iodine on silver containing materials; one will discuss a method for recycling expensive silver zeolite adsorbers.

The low discharge levels for radioactive iodides still permissible may limit the number of nuclear plants acceptable in a nuclear park. In some countries - Germany, for example - regulations are so stringent

14th ERDA AIR CLEANING CONFERENCE

that determination of the chemical forms of iodine releases may be a necessary step in calculating the actual hazards from such releases; surely elemental iodine moves most easily through the ingestion path and produces most of the irradiation of the surrounding population. One paper will discuss a sampler which separates effectively airborne radioiodine species.

Two papers will discuss the reliability of tests of sample-bypass canisters in determining the current condition of large-scale filter beds. These papers will consider alternatives of performing these tests, including a convenient test kit for in-situ evaluation of full-scale filter banks with radioiodine compounds.

Another paper will discuss the effects of various additives on the evaporation of iodine from containment spray-cooling solutions. Still another will discuss a facet of the post-LOCA environment which has previously been little studied: the effect of intense radiation on the performance of iodine - trapping charcoals.

One paper will present a new filter system design which allows convenient testing of HEPA filter gaskets and renewal of adsorption media in safe and convenient fashion.

Finally, a report will be given on the March, 1976 topical meeting held by ERDA in Washington, at which preliminary data on some of the items above were given, and matters related to standards, interlaboratory comparisons of adsorber tests, and laboratory certification were discussed.

IODINE EVAPORATION FROM IRRADIATED AQUEOUS
SOLUTIONS CONTAINING THIOSULFATE ADDITIVE*

A. H. Dexter, A. G. Evans, and L. R. Jones
Savannah River Laboratory
E. I. du Pont de Nemours and Co.
Aiken, S. C. 29801

Abstract

Sodium thiosulfate in concentrations of 1 wt% was shown to limit iodine evaporation to 0.5% or less in $\sim 5 \times 10^{-4}$ M aqueous solutions of iodine irradiated to 10^8 rad. Potassium hydroxide in concentrations of 0.05 wt% was almost as effective. Lower concentrations of thiosulfate were ineffective: iodine was almost completely released, and a portion was converted into a form capable of penetrating several inches of activated carbon. Attempts to identify the penetrating form were unsuccessful; it may be either a particulate or an aerosol because it was removable by HEPA filters.

Introduction

This paper reports measurements of the effectiveness of sodium thiosulfate in preventing the volatilization of iodine subjected to a radiation dose of 10^8 rad. Previous studies¹ at the Savannah River Laboratory (SRL) had shown that thiosulfate was very effective in inhibiting this release in a nonradiation environment. Earlier studies at Babcock and Wilcox² and at Oak Ridge National Laboratory³ evaluated the effect of radiation on thiosulfate and demonstrated that a significant fraction of the thiosulfate would survive large doses of radiation. No previous measurements have been reported on the effect of radiation on the water-iodine-thiosulfate system.

In earlier work, in the absence of radiation, small concentrations of thiosulfate were found to be very effective in reducing iodine evolution from aqueous solutions of iodine.¹ For example, in studies that used ^{131}I as a tracer, 32.8% of the iodine in a 5×10^{-5} M aqueous solution volatilized in a 5-hr period; whereas with a 8×10^{-4} M concentration of thiosulfate present as an additive, only 0.00066% of the iodine was volatilized. On the basis of Zittel and Row's work,³ about 60 to 70% of the thiosulfate was expected to be destroyed by the combined effects of temperature and radiation at doses of 10^8 rad. However, with an excess of thiosulfate present (for example, the 16 to 1 molar ratio used in the nonradiation experiments at SRL) - the volatilization of iodine in the presence of radiation was not expected to be significantly different from that in the absence of radiation. Laboratory-scale experiments were designed to evaluate this premise.

* Work done under Contract No. AT(07-2)-1 with the Energy Research and Development Administration.

Experimental

The SRL ^{60}Co Irradiation Facility⁴ which provides $\sim 2.7 \times 10^7$ rad/hr was used to irradiate aqueous solutions of KI to doses of 10^8 rad. The KI in each experiment was "tagged" with ~ 1 mCi of ^{131}I , and scintillation counting equipment was used to measure the volatilization of the ^{131}I as a function of radiation dose imparted to the solution. Typically, 4ℓ of solution in a stainless steel vessel was irradiated for ~ 5 hr while air flowed over the solution surface at 13 ℓ/min. The volatilized ^{131}I was transported by the flowing air and collected on activated carbon that was monitored with a scintillation counter (Fig. 1). An inventory (material balance) was made of the ^{131}I activity of all system components after each test. Pre-irradiation pH was typically about 7, and in several experiments this was increased to >10 by adding KOH. The solutions were not buffered. Solution temperature during irradiation was $\sim 50^\circ\text{C}$.

Results

Experimental results are given in two parts: 1) the effect of additives, and 2) the attempts to identify a penetrating form of iodine that was found during the experiments.

Influence of Additives on Iodine Evaporation

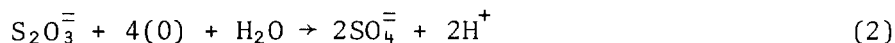
The study included experiments with: a) no additive, b) sodium thiosulfate, c) sodium thiosulfate and potassium hydroxide, and d) potassium hydroxide.

Tests With No Additive. Irradiation of a water solution containing KI ($5.6 \times 10^{-4}\text{M}$) to a dose of 10^8 rad caused the evaporation of 14.6% of the iodine. This result compared with 16 to 34% evaporation of iodine¹ from a solution containing elemental iodine ($\sim 1.5 \times 10^{-4}\text{M}$) in the absence of radiation. These results indicate that radiation converts ionic iodide to volatile iodine, most probably through OH radical attack of the iodide

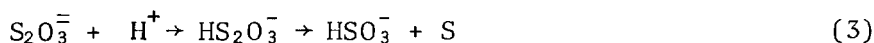


The OH radicals result from the radiolysis of the water. Further, because the iodine evaporation is about equivalent in the two experiments, the conversion of iodide to iodine is thought to be almost quantitative.

Sodium Thiosulfate Additive. When sodium thiosulfate was added at a molarity (5.5×10^{-4}) approximately equal to that of the KI, an almost quantitative release of the iodine occurred (94% in one experiment and 96% in another). The ineffectiveness of the thiosulfate at this concentration is thought to be due to the radiolysis of thiosulfate by the reaction²



augmented by acid decomposition of the thiosulfate by the reaction²



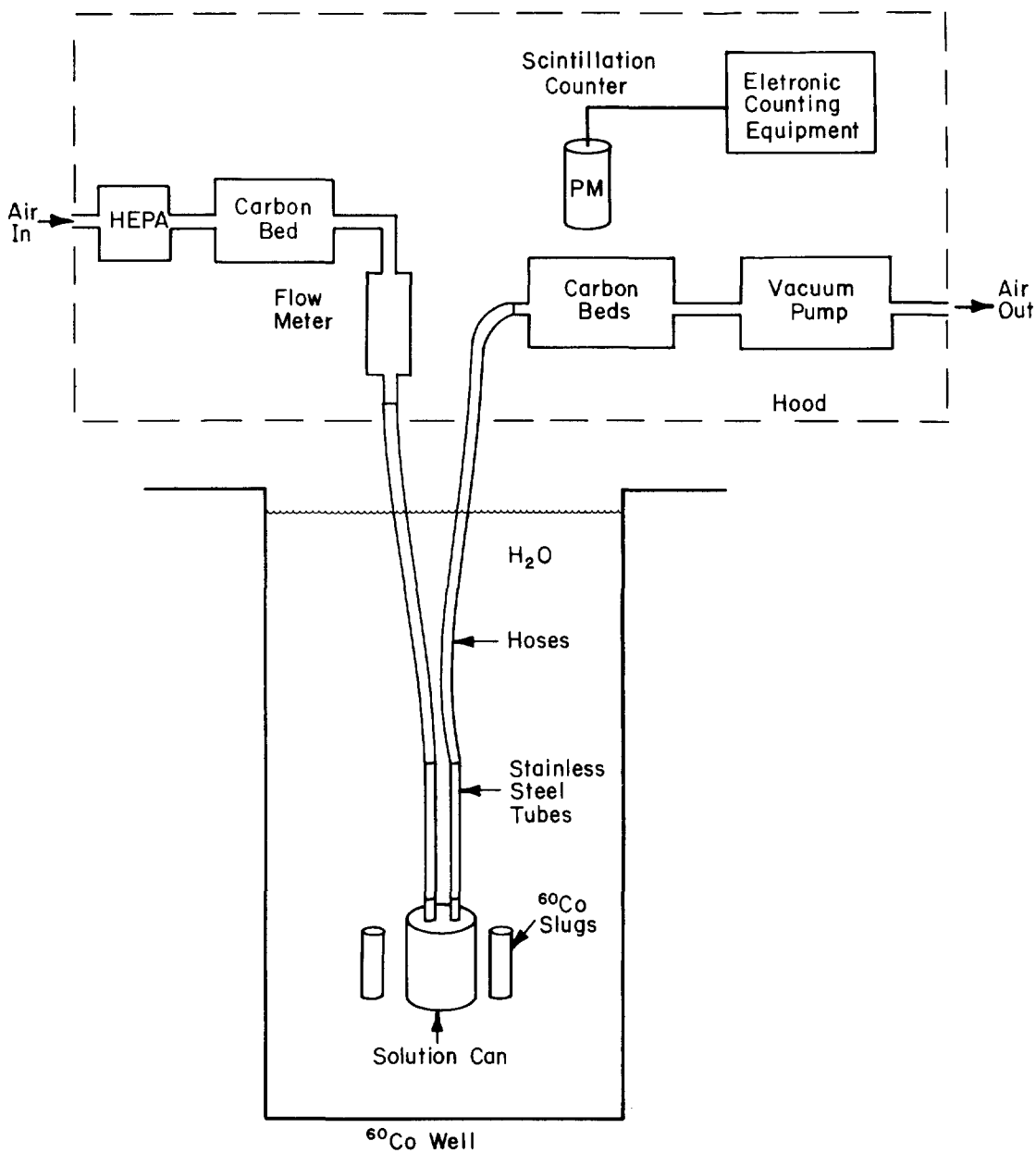


Figure 1. Schematic of iodine evaporation experiment.

However, if all of the thiosulfate were destroyed, the iodine release should be about equivalent to the non-additive release. This was not the case, and the degradation of the thiosulfate or the degradation products is assumed to actually promote the release of iodine from solution.

An unexpected result of this experiment was that about 11 to 15% of the iodine evolved was a penetrating form that passed through the 3 in. of activated carbon designed to collect the iodine. Some of this activity was stopped in a 1-ft-thick backup bed of carbon, but a large portion penetrated it.

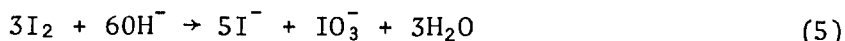
Tests With Sodium Thiosulfate and Potassium Hydroxide. To reduce possible acid decomposition of the thiosulfate, KOH ($10^{-3}M$) was added to increase the pre-irradiation pH of the solution from ~ 7 to >10 . Some improvement was found in that iodine evaporation was reduced to 30%. The penetrating iodine was found again.

With the same KI and KOH concentrations, the thiosulfate concentration was increased to 0.1 wt%. Almost quantitative release of the iodine occurred, but there was no evidence of generation of penetrating form. When the thiosulfate concentration was increased to 1 wt% with the same KI and KOH concentrations, iodine evolution was significantly reduced to 0.044% in one experiment and 0.55% in another. There was no evidence of the penetrating form.

The first of these experiments with KOH added indicates that the KOH served to partially neutralize the reaction product ($2H^+$) of Equation 2 thus reducing acid decomposition by Equation 3. However, when the thiosulfate was increased to 0.1 wt%, the KOH was either ineffective in neutralizing the larger quantity of decomposition products ($2H^+$) or was depleted in neutralizing the lower pH solution resulting from the larger addition of thiosulfate. In the case of the 1 wt% addition of thiosulfate, sufficient thiosulfate was apparently present, even with decomposition, to maintain iodine essentially in the nonvaporizable iodide form by



Tests With Potassium Hydroxide Additive. The alternatives to thiosulfate as an additive for iodine retention are limited. One that has been suggested is KOH. The rationale behind the use of KOH is that it serves two purposes: 1) it promotes formation of the nonvolatile iodide by



and, 2) it increases solution pH to prevent the OH radical attack of the iodide⁵



which occurs in neutral or acidic solutions. In alkaline solution, the OH radicals are dissociated by the reaction



The effectiveness of KOH as an additive was briefly examined. With the same KI concentration as previously used, experiments were performed with KOH concentrations of 10^{-3}M and $8 \times 10^{-3}\text{M}$ (0.05 wt%). The iodine evolutions measured were 2.5 and 1.2%, respectively.

A comparison of these results with the thiosulfate results indicates that 0.05 wt% KOH is almost as effective as 1 wt% thiosulfate. In addition, the change in iodine evolution is slight for an almost 10-fold change in KOH; a 100-fold change in iodine evolution occurs for a 10-fold change in thiosulfate concentration.

The additive experiments (Table I and Fig. 2) indicate that the rate of iodine evolution is a function of radiation dose.

Penetrating Form of Iodine

As previously noted, several thiosulfate additive experiments produced significant quantities of an iodine form capable of passing through several inches of activated carbon. Tests were conducted to identify the penetrating iodine species to determine if it might occur in systems that use activated carbon for removal of radioiodine.

Nine experiments were performed in the ^{60}Co irradiation facility in an attempt to obtain a sample of the penetrating iodine for analysis and identification. The experimental equipment shown in Fig. 3 was designed to freeze out a sample. Nitrogen was also substituted for air as the flow gas to avoid freezing out oxygen. After seven such experiments with KI and thiosulfate concentrations equal to those that had previously given the penetrating iodine, the penetrating iodine was not formed in a nitrogen atmosphere. Oxygen appears to be a pre-requisite for its formation.

Two experiments were then performed with flowing air and a cold trap containing dry ice and trichloroethylene (-70°C) substituted for the liquid nitrogen trap. In both experiments, the penetrating iodine was generated, but the trap was incapable of freezing out a sample. Two experiments were performed to determine if the decomposition products of thiosulfate (SO_4 and S) were involved in the formation of the penetrating iodine. One experiment used KI plus Na_2SO_4 in the radiation field and the other used KI plus sulfur. Neither experiment produced the penetrating form of iodine.

Two additional experiments, with HEPA filters in the air stream, showed that the penetrating iodine was readily removable. This result suggests that the penetrating iodine may exist in the form of either a particulate or an aerosol. Both of these forms can pass through activated carbon beds. In the absence of a suitable analytical technique to apply to the material collected on the HEPA, identification work was halted.

TABLE I

Iodine Evaporated After Exposure to 10^8 Rad

<i>Type Experiment</i>	<i>Concentrations, wt%</i>			<i>Iodine Evaporated, %</i>
	<i>KI</i>	<i>Na₂S₂O₃</i>	<i>KOH</i>	
No Additive	0.010	-	-	14.6
Thiosulfate	0.010	0.014	-	94 ^a
	0.010	0.014	-	96 ^a
Thiosulfate and KOH	0.010	0.014	0.006	30 ^a
	0.010	0.1	0.006	96
	0.010	1.0	0.006	0.044
	0.010	1.0	0.006	0.55
KOH	0.010	-	0.006	2.5
	0.010	-	0.050	1.2

^a. Experiments that gave the penetrating iodine species.

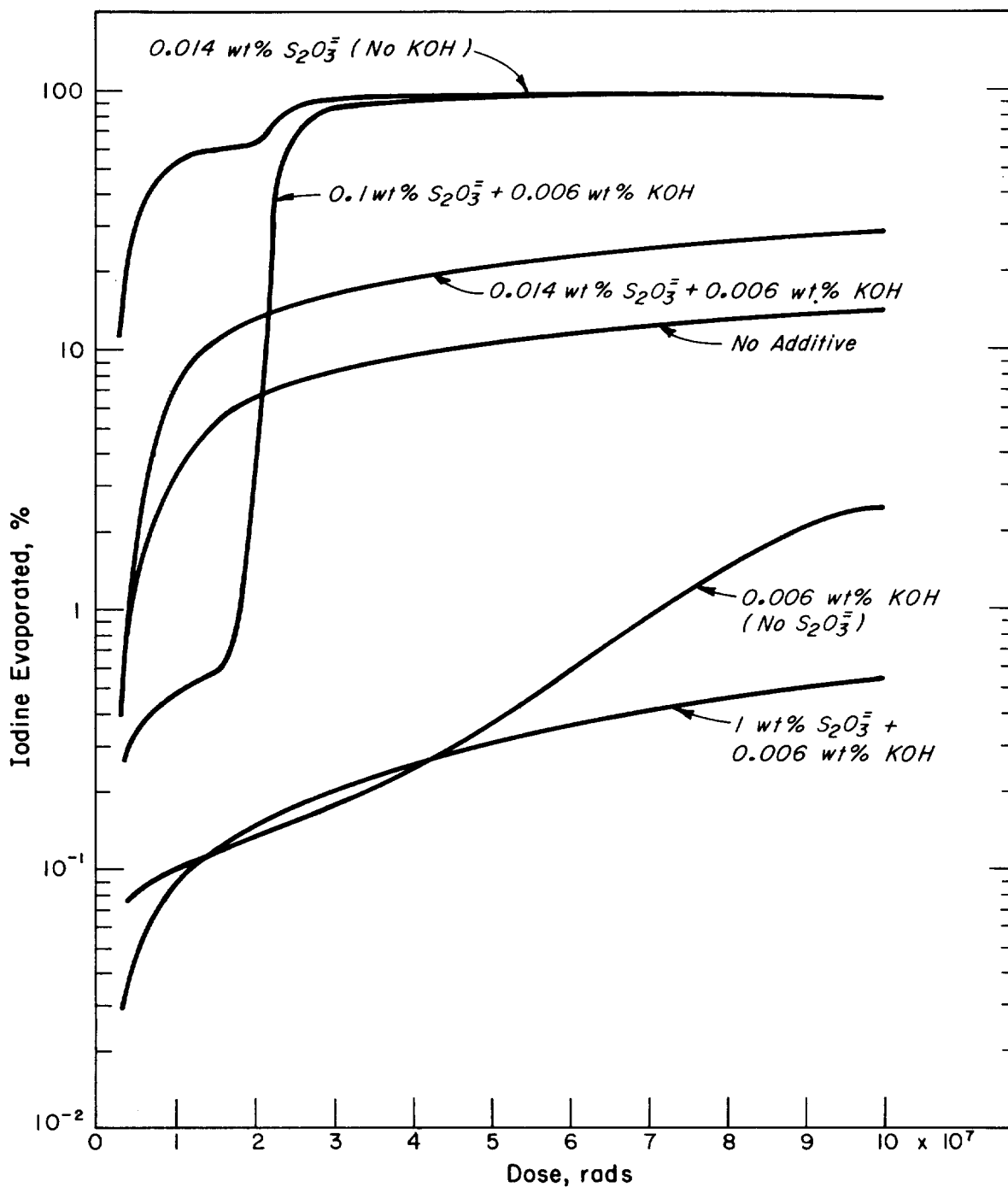


Figure 2. Effect of additive and radiation dose on iodine evaporation ($5.6 \times 10^{-4} \text{M}$ solution of KI).

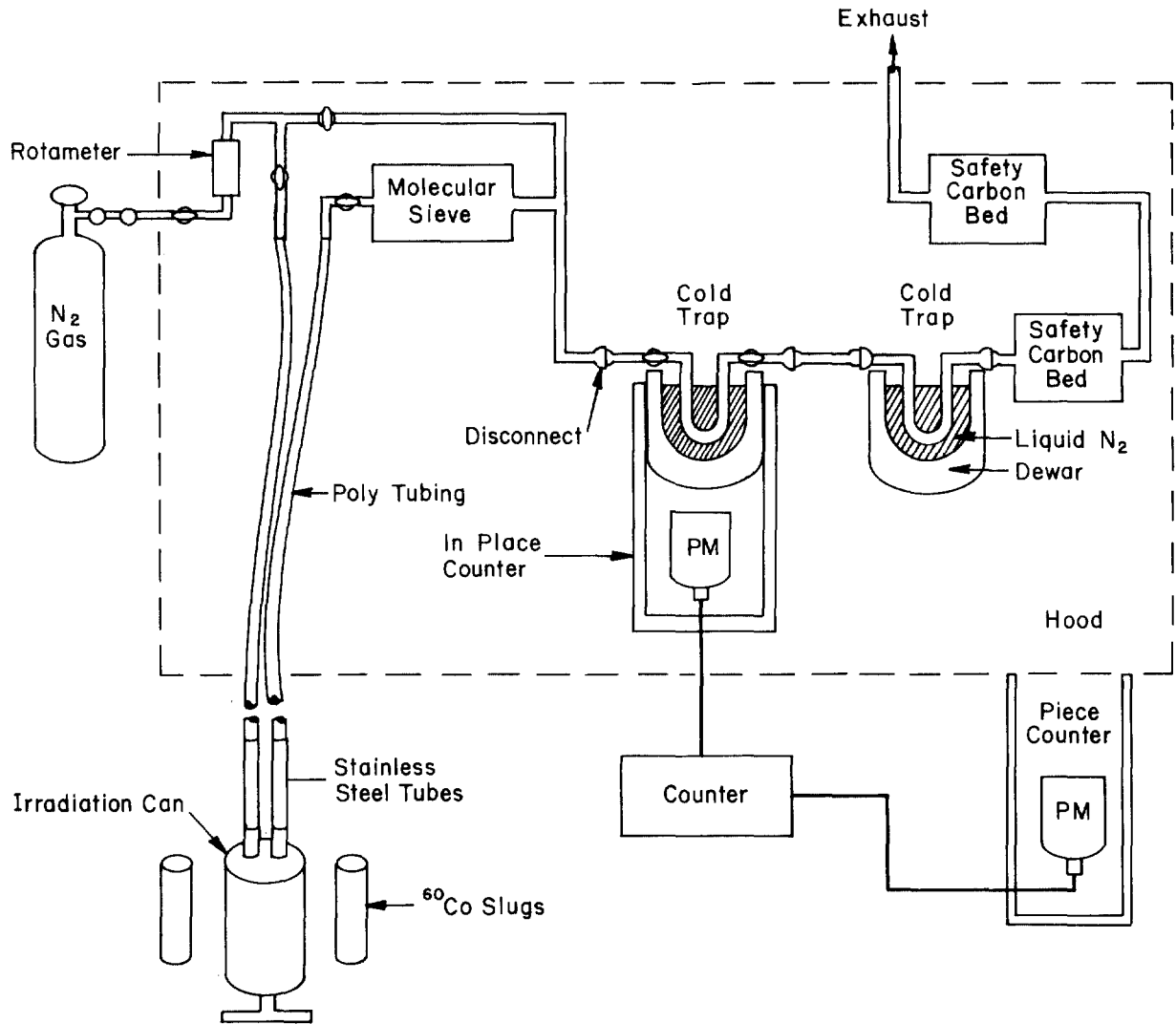


Figure 3. Schematic of iodine penetration experiment.

References

1. A. H. Dexter, A. G. Evans, and L. R. Jones. *Confinement of Airborne Radioactivity*. USAEC Report DP-1390, E. I. du Pont de Nemours and Company, Savannah River Laboratory, Aiken, S. C. (1974).
2. W. N. Bishop and D. A. Nitti. "Stability of Thiosulfate Spray Solutions." *Nucl. Tech.* 10, 436 (1971).
3. H. E. Zittel and T. H. Row. "Radiation and Thermal Stability of Spray Solutions." *Nucl. Tech.* 10, 436 (1971).
4. L. R. Jones. "Effects of Radiation on Reactor Confinement System Materials." *Twelfth AEC Air Cleaning Conference*, Oak Ridge, Tennessee, August 28-31, 1972, USAEC Report CONF-720823 Volume 2 (1972).
5. A. R. Denaro and G. G. Jayson. *Fundamentals of Radiation Chemistry*. Ann Arbor Science Publishers Inc., Ann Arbor, Michigan (1972).

DISCUSSION

RIVERS: Is the current norm for sprays pure sodium thiosulfate?

DEXTER: We don't mean to imply that the results we got are applicable to any other reactor or containment vessel. It is entirely unrelated to that, and we would not want to make any inferences as to how this sulfate would work in that kind of system. Their requirements are different from the sort of problems that we are concerned with. But to answer your question, others use both thiosulfate and caustic in sprays to knock down the iodine in the air over the reactor vessel.

DEPENDENCE OF GAS PENETRATION OF CHARCOAL BEDS ON
RESIDENCE TIME AND LINEAR VELOCITY

V. R. Deitz, C. H. Blachly
Naval Research Laboratory, Washington, D.C. 20375
and
L. A. Jonas
Edgewood Arsenal, Aberdeen Proving Ground, MD 21010

Abstract

The trapping of methylradioiodide ($\text{CH}_3\text{I}^{131}$) was studied in packed columns of different diameters, bed depths, and at various flow velocities, using impregnated granular activated charcoals. The gradient in penetration along the axis of flow was determined after dividing the column into eight equal layers by discs of perforated stainless steel, followed by a back-up section, and counting each layer. In one series of measurements six columns were used in which the depth and the corresponding superficial linear velocity was varied 5.6 fold; the weight and volume of charcoal and the volumetric flow rate were held constant. Although the residence time was constant (0.25 sec) in all six columns, significant decreases in penetration occurred with increase in linear velocity. In other series of measurements, the diameter, depth, and weight of charcoal were held constant and the volumetric flow rate was varied over a wide range of superficial linear velocity. Differences in penetrability, as a result of varying the bed geometry, the residence time, and the flow velocity were examined in accord with recent concepts of adsorption kinetics and catalytic behavior in packed beds.

I. Introduction

During the two decades following World War I the data of adsorption included studies on the flow of gas-air mixtures through granular charcoal (1). A period then followed in which steady-state adsorption data (mostly physical adsorption) dominated the attention of many investigators (2). Within the last two decades, however, there has been renewed interest in dynamic adsorption studies due to the remarkable development of gas chromatography and the applications of adsorbents to engineering processes.

Much of the design of charcoal filters has followed in the footsteps of early jerry-built structures. The many engineering parameters have not been evaluated for their influence on the penetration of an adsorbed gas through the charcoal. This paper is concerned with the dependence of penetration of methyl iodide containing radioiodine 131 on two parameters - residence time and carrier gas velocity - using beds of impregnated charcoals. By counting the radioactivity in each of the equal volume sections into which a bed is divided, the gradient of adsorbed methyl iodide along the axis of flow can be directly determined. The results are examined in accord with recent concepts of adsorption kinetics and catalytic behavior in packed beds.

II. Theoretical

The Wheeler (3) adsorption equation for gas breaking through or penetrating a bed of charcoal, modified by Jonas et al (4) to reflect charcoal bed weights rather than bed depths, was originally derived from a continuity equation of mass balance, and can be expressed as

$$t_b = \frac{W_e}{C_o Q} \left[W - \frac{\rho_\beta Q \ln (C_o / C_x)}{k_v} \right] \quad (1)$$

where t_b is the time (min) at which an exit concentration C_x ($\text{g}\cdot\text{cm}^{-3}$) penetrates the bed when challenged by an inlet concentration C_o ($\text{g}\cdot\text{cm}^{-3}$) at a volumetric flowrate Q ($\text{cm}^3\cdot\text{min}^{-1}$), ρ_β is the bulk density of the charcoal bed ($\text{g}\cdot\text{cm}^{-3}$), W is the bed weight (g), W_e is the adsorption capacity of the charcoal ($\text{g}\cdot\text{g}^{-1}$), and k_v is the pseudo first order adsorption rate constant (min^{-1}). The critical weight of charcoal, W_c , is

$$W_c = \frac{\rho_\beta Q \ln (C_o / C_x)}{k_v} \quad (2)$$

and identified as that weight of charcoal just sufficient to reduce the inlet concentration to the arbitrarily chosen exit concentration. Equations (1) and (2) apply to the kinetics of gas adsorption by activated charcoal.

Since plug flow is usually assumed for gas movement through the charcoal bed, the mean residence time τ in the bed can be shown as

$$\tau = \frac{L}{V_\ell} = \frac{V}{Q} = \frac{W}{\rho_\beta Q} \quad (3)$$

where L is the bed depth (cm), V_ℓ the superficial linear velocity ($\text{cm}\cdot\text{min}^{-1}$), and V the volume of the bed (cm^3). Thus, by substituting into equation (1) one obtains

$$t_b = \frac{W_e \rho_\beta}{C_o} \left[\tau - \frac{\ln (C_o / C_x)}{k_v} \right] \quad (4)$$

Here, the breakthrough time t_b is shown as a function of residence time, τ .

In heterogeneous catalysis, as opposed to heterogeneous adsorption, the attenuation of C_o to C_x can be independent of time and, therefore, the kinetics of this process are studied under steady-state conditions. Under these conditions the first order equation relating the concentration attenuation is

$$\frac{C_x}{C_o} = \exp (-k\tau) \quad (5)$$

where k is the first order catalytic rate constant (min^{-1}).

If, in the case of gas adsorption kinetics, a finite concentration exited the bed immediately, and remained relatively steady and independent of time, equation (1) could apply to these conditions by setting t_b equal to zero. Then, for the equation

$$o = \frac{W_e}{C_o Q} \left[W - \frac{\rho_\beta Q \ln (C_o/C_x)}{k_v} \right] \quad (6)$$

to be satisfied in the non-trivial case where

$$\frac{W_e}{C_o Q} \neq 0 \quad (7)$$

it is required that

$$W - \frac{\rho_\beta Q \ln (C_o/C_x)}{k_v} = 0 \quad (8)$$

and

$$W = \frac{\rho_\beta Q \ln (C_o/C_x)}{k_v} \quad (9)$$

From this one can show that

$$\ln \frac{C_o}{C_x} = \frac{k_v W}{\rho_\beta Q} \quad (10)$$

or

$$\ln \frac{C_x}{C_o} = - \frac{k_v W}{\rho_\beta Q} \quad (11)$$

and in exponential form

$$\frac{C_x}{C_o} = \exp \left(- \frac{k_v W}{\rho_\beta Q} \right) \quad (12)$$

Since we note from equation (3) that

$$\tau = \frac{W}{\rho_\beta Q}$$

we can substitute for $W/\rho_\beta Q$ in equation (12) to obtain

$$\frac{C_x}{C_o} = \exp \left(- k_v \tau \right) \quad (13)$$

Equation (13), applying to the case of a finite yet steady gas concentration exiting a charcoal bed, can be seen as equivalent in form and concept to equation (5), applying to heterogeneous catalysis, with the rate constant k_v denoting sorption and k denoting catalysis.

III. Experimental1. Materials.

The three impregnated charcoals, 4167, 4169, and 4171, were prepared from two base charcoals, and some physical properties pertinent to the present treatment are given in Table I. The impregnation formulation (hexamethylenetetramine, iodine, and sodium hydroxide) is one of many samples reported in another paper presented at this Conference (5).

2. Equipment.

The carrier air flow was first passed through charcoal and then through a high efficiency particulate filter. In all measurements the test charcoal sample was prehumidified for 16 hours with the air flow at 95-97 RH. The methyl iodide-131 was purchased (ICN Life Sciences, Irvine, California) at suitable intervals as a liquid (1 ml) of 5 millicuries activity. The charcoals were counted in aliquots of about 13 cm³ using a Nuclear Chicago Gas Flow Detector, Model 470 and Model 8712 decade scaler.

TABLE I: PHYSICAL PROPERTIES OF ACTIVATED CHARCOALS

Base Charcoal	Lot 4171	Lot 4169	Lot 4167
	G212-coconut	MBV-coal	G212-coconut
Particle dia. (cm)	0.172	0.256	0.172
Bulk dens. (g.cm ⁻³)	0.393	0.391	0.392
Spherical vol. (cm ³)	0.002664	0.008785	0.002664
Particle wt. (g)	0.002033	0.008197	0.001972
Particle dens. (g.cm ⁻³)	0.763	0.933	0.746
Particles per g	492	122	507
Sieve Analysis			
on 6	0	1.5	0
6-8	2.7	61.0	2.7
8-10	14.9	23.1	14.9
10-12	35.6	9.2	35.6
12-16	45.0	4.9	45.0
16-20	1.4	0.2	1.4
Pan	0.4	0.1	0.4

3. Procedure.

The data were obtained for 17 charcoal columns of constant volume (106 cm³), each column initially being divided into eight equal sequential sections. A fixed volume flow of air plus the dose of methyl iodide-131 entered the column for two hours and then the air flow alone was continued for two additional hours. Each of the eight sections (each containing 106/8 cm³ charcoal) was evaluated in terms of its retained radioactive counts per minute (CPM) and likewise in the backup beds, which had a total depth of two inches.

4. Bed Section Penetration Calculation.

Since the bed depth was divided into eight equal sections, each section was challenged by the radioactive methyl iodide penetrating

the previous section (C_x), and the back-up beds retained all the methyl iodide penetrating the eighth section. The total methyl iodide challenge (C_o) to the bed was the sum of the radioactive counts per minute (CPM) found on all eight sections plus that on the back-up beds. The fractional penetration of each section was calculated from the retention (CPM) on each bed section and the total CPM challenge to the bed:

$$\begin{aligned} \text{Fractional Penetration} & & \text{Total CPM Challenge - CPM Retained on} \\ \text{for 1st Section} & & \text{1st Section} \\ (C_x/C_o)_1 & = & \frac{\hspace{10em}}{\text{Total CPM Challenge}} \quad (14) \end{aligned}$$

$$\begin{aligned} \text{Fractional Penetration} & & \text{Total CPM Challenge - Sum of CPM} \\ \text{for nth Section} & & \text{Retained on} \\ (C_x/C_o)_n & = & \frac{\hspace{10em}}{\text{Total CPM Challenge}} \quad (15) \end{aligned}$$

$$= \frac{\text{CPM Penetrating nth Section}}{\text{CPM Challenging nth Section}} \quad (16)$$

The sum of the fractional penetration and the fractional retention, either for a particular bed section, or for the arithmetic means, is unity.

IV. Results

1. Observed Data.

The experimental data are tabulated in terms of the number of radioactive counts per minute (CPM) detected in each of the equal volume sections of the column. The weight, volume, and bulk density of the packed charcoal were maintained invariant, but the bed area, bed depth, volumetric flowrate, gas residence time, and superficial linear flow velocity were varied.

Charcoal #4171 was tested at a constant volumetric flowrate of 25 liters per minute and residence time of 0.254 seconds for the vapor in the bed by varying both the bed depth and area of the charcoal bed. In these tests the superficial linear velocity ranged from 21 to 118 cm.sec⁻¹. In order to extend the lower limit of the linear velocity to 4.2 cm.sec⁻¹ one test was made at a volumetric flowrate of 5 liters per minute. The data are shown in Table II.

TABLE II: RETENTION OF $\text{CH}_3\text{I}^{131}$ BY IMPREGNATED CHARCOAL: CONSTANT
RESIDENCE TIME, VARIABLE SUPERFICIAL LINEAR VELOCITY,
 (LOT #4171)

TEST CONDITION	OBSERVED VALUES						
Vol. flowrate, $\ell.\text{min}^{-1}$	25.0	25.0	25.0	25.0	25.0	25.0	5.0
Bed depth (total), cm	5.33	8.03	11.3	16.1	21.6	30.0	5.33
Bed dia. , cm	5.08	4.10	3.45	2.90	2.50	2.12	5.08
Bed area , cm^2	20.27	13.20	9.35	6.61	4.91	3.53	20.27
Weight , g	41.3	41.3	41.3	41.3	41.3	41.3	41.3
Bulk density, $\text{g}.\text{cm}^{-3}$	0.393	0.393	0.393	0.393	0.393	0.393	0.393
Sup. lin. vel., $\text{cm}.\text{sec}^{-1}$	21.0	31.6	44.6	63.1	84.9	118.0	4.2
Res. time, , sec	0.254	0.254	0.254	0.254	0.254	0.254	1.27
Radioactive CPM on							
Bed section 1	36227	19358	156245	89281	80615	15796	56808
2	25248	13067	104162	58135	40954	9336	49020
3	20487	9520	75753	35709	28970	5707	28409
4	14965	7463	49995	25505	18470	3633	14451
5	10725	5133	34717	16335	11470	2325	7184
6	8301	3965	23580	10960	7323	1431	3392
7	6455	2852	15239	6789	5000	732	1685
8	4685	2206	9799	4328	3004	420	656
Back-up bed	14588	6152	17097	6486	3376	240	680
TOTAL	141681	69716	486587	253528	199182	39620	162285

238

14th ERDA AIR CLEANING CONFERENCE

Charcoal #4169 was tested at constant bed depth and area, but varying volumetric flowrates (5.5 to 50.0 $\ell \text{ min}^{-1}$), so that the superficial linear velocity ranged from 4.52 to 41.1 cm sec^{-1} and the residence time from 1.179 to 0.130 seconds. The data are shown in Table III.

TABLE III: RETENTION OF $\text{CH}_3\text{I}^{131}$ BY IMPREGNATED CHARCOAL: VARIABLE RESIDENCE TIME AND SUPERFICIAL LINEAR VELOCITY (LOT #4169)

TEST CONDITION	OBSERVED VALUES				
Vol. flowrate, $\ell \text{ min}^{-1}$	5.5	11.0	18.0	25.0	50.0
Bed depth (total), cm	5.33	5.33	5.33	5.33	5.33
Bed diameter, cm	5.08	5.08	5.08	5.08	5.08
Bed area, cm^2	20.27	20.27	20.27	20.27	20.27
Weight, g	42.2	42.2	42.2	42.2	42.2
Bulk density, g.cm^{-3}	0.391	0.391	0.391	0.391	0.393
Sup. lin. vel. cm.sec^{-1}	4.52	9.05	14.8	20.6	41.1
Res. time, sec	1.179	0.589	0.360	0.259	0.130
Radioactive CPM on					
Bed section 1	42024	20028	23492	91145	7797
2	16921	11041	15467	65007	6142
3	7862	5754	9947	48287	5564
4	2702	4743	6316	35363	4432
5	2094	2868	4486	28985	3153
6	874	999	3222	20912	2473
7	200	732	2302	14913	2076
8	139	346	1423	11449	1355
Back-up bed	95	365	2595	28256	4464
TOTAL	72911	46876	69250	344317	37933

14th ERDA AIR CLEANING CONFERENCE

Charcoal #4167 was tested at varying flowrates, bed depths, and areas so that the superficial linear velocity ranged from 2.53 to 126.2 cm sec⁻¹ and the residence time from 0.793 to 0.127 seconds. The data are shown in Table IV.

TABLE IV. RETENTION OF CH₃I¹³¹ BY IMPREGNATED CHARCOAL: VARIABLE
RESIDENCE TIME AND SUPERFICIAL LINEAR VELOCITY
(LOT #4167)

TEST CONDITION	OBSERVED VALUES				
Vol. flowrate, l min ⁻¹	2.0	5.5	11.0	18.0	50.0
Bed depth (total), cm	2.01	4.02	6.02	8.03	16.1
Bed dia. , cm	4.10	4.10	4.10	4.10	2.90
Bed area , cm ²	13.20	13.20	13.20	13.20	6.61
Weight , g	10.4	20.8	31.2	41.6	41.6
Bulk density, g.cm ⁻³	0.392	0.392	0.392	0.392	0.394
Sup. lin. vel. cm.sec ⁻¹	2.53	6.94	13.88	22.72	126.2
Res. time, sec	0.793	0.578	0.434	0.353	0.127
Radioactive CPM on					
Bed section 1	92569	249967	32447	45428	58047
2	7119	80613	12294	24245	31553
3		15399	4849	13560	26503
4		2667	1779	8143	20740
5			712	4535	18991
6			247	2345	15059
7				1256	11168
8				831	10324
Back-up bed	488	328	157	848	32536
TOTAL	100176	348974	52485	101191	224921

2. Data Handling.

In order to reduce the relative error when the observed CPM retained on a bed section was of the order of magnitude of the background CPM (coupled with the reproducibility limits of the instrumentation), it was decided to pair data when any one section, or the back-up section, had a CPM less than 100. This occurred in some of the observed data, associated with long residence times, in Charcoal #4167, and in these instances, therefore, the CPM of the preceding section or sections were added to the observed CPM. When this was done the necessary adjustments were made in the values for bed depth, char weight, and residence time of vapor in the bed since in effect the back-up bed increased in size by incorporating the lower sections of the original bed that had a CPM less than 100.

3. Rate Constant.

The trapping and removal of $\text{CH}_3\text{I}^{131}$ vapor by the impregnated charcoals are considered to be primarily catalytic in behavior (5) rather than adsorptive. One necessary condition for the former is that each section, equal in volume to all other active sections in the bed, remove the same fraction of $\text{CH}_3\text{I}^{131}$ under the same test conditions. Thus, when the fractional penetration per section was obtained from the relation

$$\text{Fractional Penetration} = 1 - \text{Fractional Retention} \quad (17)$$

and the total bed penetration calculated from the relation,

$$\% \text{ Bed Penetration (calculated)} = \left(\frac{\text{Fractional Penetration}}{\text{per section}} \right)^n \times 100 \quad (18)$$

where n was the number of sections, the calculated values agree very closely with the observed bed penetration percentages obtained from the relation

$$\% \text{ Bed Penetration (observed)} = \frac{\text{CPM in back-up bed}}{\text{Total CPM Challenge}} \times 100 \quad (19)$$

The close correspondence between these two percentages are shown for all three charcoal lots, and under all test conditions, in Table V. The first order rate constant k in sec^{-1} was calculated from equation (5) using the observed fractional bed penetration values for all charcoal lots and under all test conditions. The results are shown in Table VI.

14th ERDA AIR CLEANING CONFERENCE

TABLE V: OBSERVED AND CALCULATED BED PENETRATION PERCENTAGES
AT VARIOUS RESIDENCE TIMES AND LINEAR VELOCITIES

Char Lot No.	Bed Depth (cm)	Res. Time (sec)	Sup. Lin. Vel. (cm sec ⁻¹)	Ret. Frac. per Sec.	Pene. Frac. per Sec.	% Bed Penetration *	
						Observ.	Calc.
4171	5.33	1.27	4.2	0.492	0.508	0.42	0.44
4171	5.33	0.254	21.0	0.247	0.753	10.30	10.34
4171	8.03	0.254	31.6	0.262	0.738	8.82	8.80
4171	11.3	0.254	44.6	0.342	0.658	3.51	3.51
4171	16.1	0.254	63.1	0.367	0.633	2.56	2.58
4171	21.6	0.254	84.9	0.402	0.598	1.69	1.64
4171	30.0	0.254	118.0	0.465	0.535	0.61	0.67
4169	5.33	1.179	4.52	0.559	0.441	0.13	0.14
4169	5.33	0.589	9.05	0.452	0.548	0.78	0.81
4169	5.33	0.360	14.8	0.336	0.664	3.75	3.78
4169	5.33	0.259	20.8	0.268	0.732	8.21	8.24
4169	5.33	0.130	41.1	0.234	0.766	11.77	11.85
4167	2.01	0.793	2.53	0.930	0.070	0.49	0.49
4167	4.02	0.578	6.94	0.814	0.186	0.094	0.12
4167	6.02	0.434	13.88	0.620	0.380	0.30	0.30
4167	8.03	0.353	22.72	0.450	0.550	0.85	0.84
4167	16.1	0.127	126.2	0.215	0.785	14.47	14.42

*Observed: $\frac{\text{CPM in back-up bed}}{\text{Total CPM challenge}} \times 100$

Calculated: (Penetration fraction per section)ⁿ x 100
where n = no. of sections in bed

14th ERDA AIR CLEANING CONFERENCE

TABLE VI: $\text{CH}_3\text{I}^{131}$ REMOVAL RATE CONSTANTS OF
 IMPREGNATED CHARCOALS UNDER VARIOUS TEST CONDITIONS

Char Lot No.	Bed Depth (cm)	Res. Time (sec)	Sup. Lin. Vel. (cm sec ⁻¹)	% Bed Pene. (Observ.)	Rate Constant (sec ⁻¹)
4171	5.33	1.27	4.2	0.42	4.31
4171	5.33	0.254	21.0	10.30	8.95
4171	8.03	0.254	31.6	8.82	9.56
4171	11.3	0.254	44.6	3.51	13.19
4171	16.1	0.254	63.1	2.56	14.43
4171	21.6	0.254	84.9	1.69	16.06
4171	30.0	0.254	118.0	0.61	20.08
4169	5.33	1.179	4.52	0.13	5.64
4169	5.33	0.589	9.05	0.78	8.24
4169	5.33	0.360	14.8	3.75	9.12
4169	5.33	0.259	20.8	8.21	9.65
4169	5.33	0.130	41.1	11.77	16.46
4167	2.01	0.793	2.53	0.49	6.71
4167	4.02	0.578	6.94	0.094	12.06
4167	6.02	0.434	13.9	0.30	13.39
4167	8.03	0.353	22.7	0.85	13.51
4167	16.1	0.127	126.2	14.47	15.22

V. Discussion

It was shown in Section II (Theoretical) that the equation for the case of a small but finite steady gas concentration at the exit of a charcoal bed is equivalent in form and concept to the equations applying to heterogeneous catalysis. The rate constant k_v denoted adsorption and k denoted catalysis. If the rate of methyl iodide trapping is dominated by a catalytic process, the change in superficial linear velocity, reflected in a reciprocal change in the mean residence time of the gas in the bed, coupled with the observed fractional bed penetration, would be expected to result in an invariant rate constant. However, the actual rate constants for Char 4169 (Table VI) increased nonlinearly with increase of V_ℓ . This phenomenon was observed by Jonas and Rehrmann (6) in a study of the physical adsorption of benzene by activated carbon, and by May and Polson (7), Underhill (8), Ackley (9), and Lorenz and Manning (10) in studies of the trapping of radioactive vapors by impregnated charcoals. A possible explanation of this phenomenon in the case of a simple adsorption process lies in an analogy with heat flow across a stagnant air film. High velocity flow will decrease the thickness of the air film and increase nonlinearly the flow of heat across the film. If diffusional transfer across an air film is controlling in a series of sequential steps, an effect of increased flow velocity, which disturbs and decreases the film thickness, will be to increase the transfer rate until its maximum rate is realized, and then further increase in flow velocity will no longer effect the rate. In the case of an initial physical adsorption followed by chemical reaction, or by a catalytic process, no such maximum appears to exist.

A key point, therefore, in understanding the behavior of impregnated charcoals is the dependence of the fractional penetration on V_ℓ (Fig. 1). The average penetration fraction per section (Table V) was averaged for all values of V_ℓ in each impregnated charcoal with the following results:

char	mean	standard deviation	range
4171	0.632	0.094	0.508 - 0.753
4169	0.630	0.135	0.441 - 0.766
4167	0.394	0.285	0.070 - 0.785

The mean values and range of penetration fraction per section for #4171 and #4169 reflect a behavior toward methyl iodide trapping compatible with a rate constant dominated by a catalytic process. On the other hand, the mean value for #4167 showed an overall weaker dependence on V_ℓ , as evidenced by the lower mean and higher standard deviation. It is suggested that the trapping of methyl iodide by #4167 is compatible with a rate constant dominated by adsorption. This behavior can best be seen in the log - log plot of rate constant versus linear velocity (Figure 2) in which the rate constant at first increases in accord with those for #4169 and #4171 (V_ℓ range from 2.53 to 6.94 cm sec⁻¹), but as V_ℓ continues to increase the rate constant levels off. This relationship is in agreement with the concept of stagnant layer removal described above.

14th ERDA AIR CLEANING CONFERENCE

The effect of linear velocity on reaction rate for catalytic systems was explicitly shown by Wheeler (11), in terms of the mass transfer limited rate, as

$$k \approx 1.86 d_p^{-3/2} V_\ell^{1/2} \tag{20}$$

where d_p is the mean carbon particle diameter in cm, V_ℓ the superficial linear velocity in cm sec^{-1} , k the rate constant in sec^{-1} , and the coefficient 1.86 in consistent units. Since in this study each lot of charcoal was unique both in particle diameter and impregnation details, the $d_p^{-3/2}$ term in equation (20) was considered constant and the equation treated as

$$\log k \approx \log A + 0.500 \log V_\ell \tag{21}$$

where A was set equal to $1.86 d_p^{-3/2}$. Hence, a plot of $\log k$ against $\log V_\ell$ should result in a straight line with a slope of 0.500. Figure 2 shows a plot of $\log k$ vs $\log V_\ell$, and Table VII contains the data for the three impregnated charcoals tested. The slopes of the lines for char #4171 and #4169 are 0.454 and 0.447 respectively, showing excellent agreement with theory. The coefficient of correlation values for these plots are 0.994 and 0.970, indicating high confidence limits for the relationship indicated. The data for char 4171 show at constant residence time that as bed depth and linear velocity increase the rate constant increases; char 4169 at constant bed depth as residence time decreases and linear velocity increases the rate constant increases; char 4167, however, shows an initial increase in rate constant as linear velocity increases and then a leveling off as velocity continues to increase. The behavior of #4167 may be due to non-uniformities in its impregnation.

TABLE VII: RATE CONSTANT DEPENDENCE ON LINEAR VELOCITY

Lot #	Char Particle Diam. d_p , cm	Rate Constant - Velocity Eqn*	
		Calculated **	Experimental
4171	0.172	$k = 26.08 V_\ell^{0.500}$	$k = 2.21 V_\ell^{0.454}$
4169	0.256	$k = 14.36 V_\ell^{0.500}$	$k = 2.85 V_\ell^{0.447}$
4167	0.172	$k = 26.08 V_\ell^{0.500}$	$k = 3.91 V_\ell^{0.581}***$

*Rate constant k , sec^{-1} ; Superficial lin. vel V_ℓ , cm sec^{-1}

**Calc. from eqn (20).

***For the initial increase in rate constant, based on the first 2 k vs V_ℓ values.

Differences between the calculated and experimental values of the coefficient A in Table VII are not considered significant since errors inherent in the determination of the mean spherical charcoal diameters, raised to the negative 3/2 power, could account for the variations. The close agreement between calculated and experimental values for the exponent on V_ℓ , however, which indicates the functional dependence of the rate constant on velocity, are considered very significant.

When the linear velocity, residence time, bed depth, and bed weight

are the same a higher rate constant for one impregnated char over another indicates a greater efficiency for trapping methyl radioiodide. Thus, on the basis of Table VI data, char #4167 appears superior to #4171 since even at a smaller bed depth (2.01 vs 5.33 cm) and a shorter residence time (0.793 vs 1.27 sec) the bed penetration was approximately the same (0.49 vs 0.42%) reflecting for #4167 a rate constant more than 50% greater than for #4171 (6.71 vs 4.31 sec⁻¹). However, at any linear velocity greater than 60 cm sec⁻¹ the ability of #4171 to trap methyl iodide is superior to #4167, as evidenced by Figure 2. An analogous comparison can be made between #4167 and #4169, although the latter exceeds the trapping efficiency of the former at any velocity greater than 35 cm sec⁻¹.

VI. Concluding Remarks

An overview analysis of the trapping of CH₃I¹³¹ by the impregnated charcoals indicates two test parameters which affect its adsorption or catalytic rate constant, namely, residence time and superficial linear velocity. Although the bed residence time is used directly in equation (5) or (13) to obtain the rate constant, the data in Table VI show that for #4171 when the residence time was constant but the superficial linear velocity increased the rate constant increased. When the residence time decreased, as in the case of #4169, but the superficial linear velocity increased, the rate constant also increased. In fact, for all three charcoal lots as the linear velocity increased the rate constant increased, although the functionality depended upon whether the rate constant was dominated by a catalytic or adsorptive type process. The generalized conclusion from these data is that the superficial linear velocity plays a dominant role, whereas the residence time a more subsidiary role, in affecting the rate constant. In addition, a catalytic process appears to be more effective than simple adsorption in trapping methyl radioiodide.

Acknowledgement

The sponsorship of the Division of Nuclear Fuel Cycles and Production, Energy Research and Development Administration, and the complete cooperation of John C. Dempsey, Contract Manager, are gratefully acknowledged.

Selected References

- (1) Deitz V.R., "Bibliography of Solid Adsorbents," 1900-1942.
- (2) Brunauer S., "The Adsorption of Gases and Vapors", Princeton Univ. Press, 1945 (511 pp).
- (3) (a) Wheeler A. and Robell A.J., J. Catal. 13, 299 (1969).
(b) Jonas L.A. and Rehrmann J.A., Carbon 10, 657 (1972).
- (4) Jonas L.A. and Rehrmann J.A., Carbon 11, 59 (1973).
- (5) Deitz V.R. and Blachly C.H., 14th ERDA Air Cleaning Conf. (1976).
- (6) Jonas L.A. and Rehrmann J.A., Carbon 12, 95 (1974).
- (7) May F.G. and Polson H.J., Methyl Iodide Penetration of Char. Beds: Variation with Relative Humidity and Face Vel, AAEC/E322 (Sep74).
- (8) Underhill D.W., Mass Transfer of Krypton-85 in Charcoal Adsorbers, 9th AEC Air Cleaning Conf. (1966).
- (9) Ackley R.D., Removal of Radon-220 for HTGR Fuel Reprocessing and Refabrication Off-Gas Streams by Adsorption, DRNL-TM-4883 (Apr75).
- (10) Lorenz R.A. and Manning S.R., Iodine Sorption on Charcoal, Conf. on Methyl Iodide Retention by Charcoal, (25 March 76).
- (11) Wheeler A., in Catalysis, Vol II, p. 150, Reinhold Publishing Co. New York, N.Y. 1955, edited by Emmett P.H.

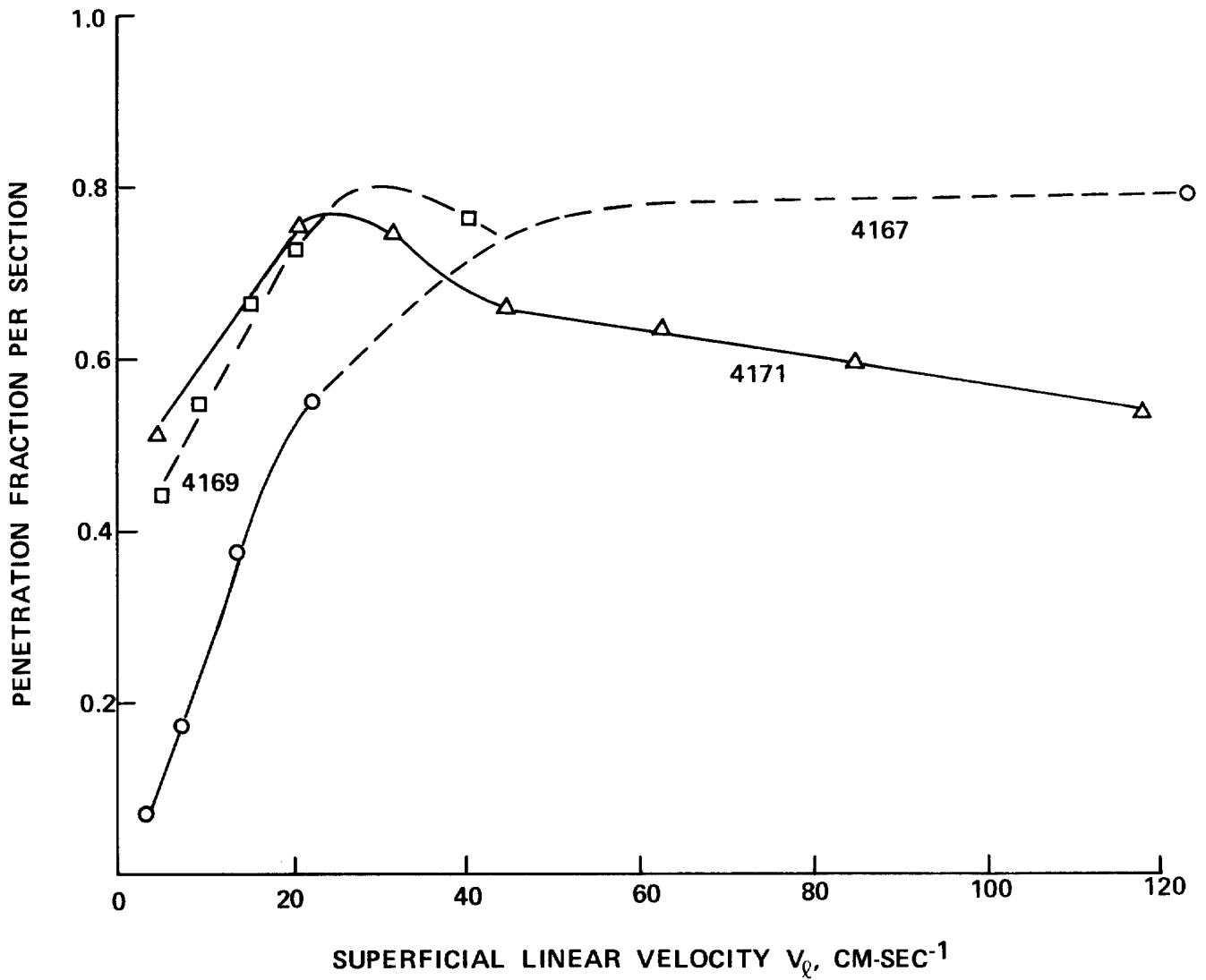


FIGURE 1. PENETRATION FRACTION OF $\text{CH}_3\text{I}^{131}$ THROUGH IMPREGNATED CHARCOALS AS A FUNCTION OF LINEAR VELOCITY

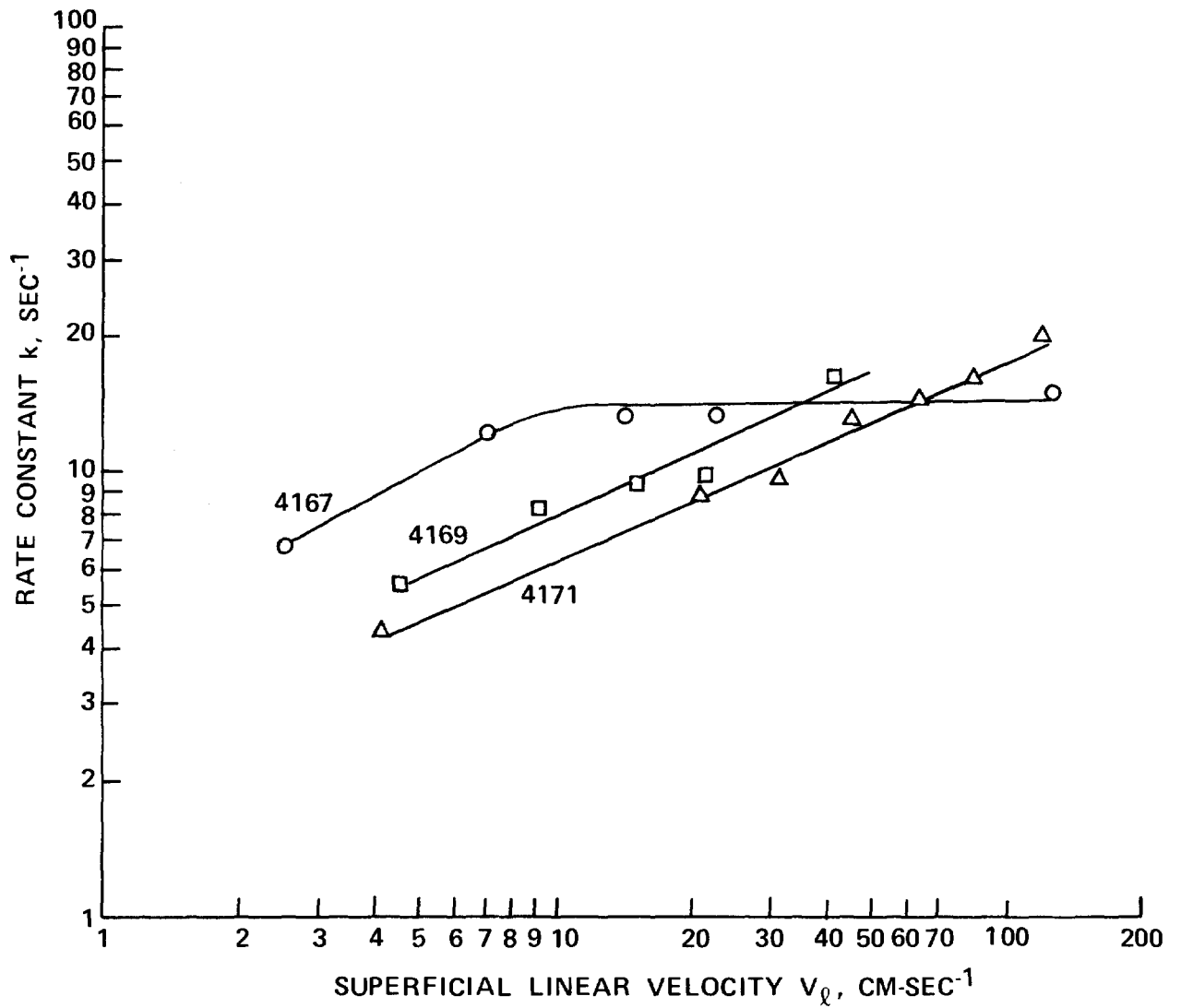


FIGURE 2. RATE CONSTANT FOR $\text{CH}_3\text{I}^{131}$ REMOVAL BY IMPREGNATED CHARCOALS AS A FUNCTION OF LINEAR VELOCITY

DISCUSSION

LIPTON: I have a question on two equations (15 and 16) which you stated as being equivalent. Let's say there is some absorption in each of Section 1 through n-1 but then there is total penetration of Section n. That would make Equation 16 equal to one but Equation 15 less than one.

JONAS: Counts per minute were obtained on each of the eight sections. Then we calculated the penetration per section for each of the eight sections and we found them rather close to the arithmetic mean of the eight values.

LIPTON: It is just an empirical equivalent, not a mathematical equivalent?

JONAS: Yes.

KOVACH: In all of the results, you were using CPM. What assurances did you make that these actually correspond with DPM's?

JONAS: Our CPM represents 12 to 15 per cent of the total disintegrations per minute.

KOVACH: Did you have the same for all of the fractions in that range?

JONAS: Yes, in that range. We deliberately tried to have the various challenges to the total sections the same, as much as possible. They were in the order of magnitude of 10^5 counts per minute. I worried about that because when I had previously seen you in March, you mentioned this.

KOVACH: The other question that I have relates to what we have published in similar work back in 1970 over somewhat different particle size ranges. We also see a definite break in the curve that you published when it switches over from boundary layer diffusion to pore diffusion at very high velocities and at small particle sizes. The validity doesn't exist if you keep increasing a fraction and if you go to smaller particle sizes where you are more liable to be faced with pore diffusion.

JONAS: I believe that as you decrease the particle diameter, you get to the point where you no longer have the queuing-up process and that you change the rate controlling step. And I do feel there would be a change. But over our range, which was a rather wide range, it is still amazing how well the Wheeler equation holds.

KOVACH: A paper in the 11th AEC Air Cleaning Conference Proceedings showed that for beds of fine particle size the relationship between penetration and velocity shown in your work did not seem to exist. Definite breaks were observed when superficial velocity increased, causing a change from laminar to turbulent flow. Have you evaluated other particle size carbons, and do you postulate such breaks using your equations?

14th ERDA AIR CLEANING CONFERENCE

JONAS: The relationship I show is between catalytic rate constant and superficial linear velocity, not between penetration and velocity, per se. However, relative to your question on charcoal particle size, we have only worked on one particle size up to now. It is possible that for very small particle charcoals the effect of increased velocity on the rate constant would be minimized.

EFFECT OF SERVICE AGING ON IODINE RETENTION OF ACTIVATED CHARCOALS*

A. G. Evans
Savannah River Laboratory
E. I. du Pont de Nemours and Company
Aiken, South Carolina 29801

Abstract

The Savannah River reactor confinement systems are continuously operated off-gas cleanup systems whose components include moisture separators, HEPA filters, and halogen adsorber beds of activated charcoal. Charcoal is removed from the system periodically and subjected to a variety of physical, chemical, and iodine penetration tests to ensure that the system will perform within specification in the event of an accidental release of activity from the reactor.

Tests performed on the charcoals include pH measurement of water extracts, particle size distribution, ignition temperature, high-temperature (180°C) iodine penetration, and iodine penetration in an intense radiation field at high humidity. Charcoals used in the systems include carbon Types 416 (unimpregnated), G-615 (impregnated with 2% TEDA and 2% KI), and GX-176 (impregnated with 1% TEDA and 2% KI).

Tests at Savannah River Laboratory show that Type GX-176 carbon (currently in use) performs consistently better than the other two products. Tests performed under simulated accident conditions (the radiation test) showed that Type GX-176 carbon retains iodine better after 18 months service than does Type 416 carbon with no service exposure. The 18-month Type GX-176 carbon also showed lower iodine penetration than did Type G-615 carbon that was service-aged for only nine months. The superior performance of Type GX-176 carbon is attributed to its particle size distribution and impregnants. The high-temperature iodine retention characteristics of all three carbons is shown to be more dependent on pH of the charcoal than on service age. The rate of change of pH of the charcoals also seems to be dependent on the particle size distribution.

Separate experiments at the Naval Research Laboratory show that the methyl iodide retention of aged charcoals decreases rapidly with increasing exposure in the Savannah River Plant systems. Type GX-176 carbon performs slightly better than does Type G-615 carbon.

* The information contained in this article was developed during the course of work under Contract AT(07-2)-1 with the U.S. Energy Research and Development Administration.

Introduction

The airborne-activity confinement system for each of the Savannah River Plant (SRP) production reactors is a continuously online, off-gas cleanup system designed to collect halogens and particulates that could be released following a reactor accident⁽¹⁾. Active components in the system include moisture separators to remove entrained moisture droplets, HEPA filters to remove particulate radioactivity, and beds of activated charcoal to remove halogens. All the air from the process areas of the reactor buildings passes through the confinement system before being exhausted to the atmosphere. A schematic diagram of the air flow through the reactors is shown in Figure 1.

Previous studies of activated charcoals at Savannah River Laboratory (SRL) showed that unimpregnated carbon (the type originally installed in the SRP systems) retains iodine less effectively than do most types of impregnated carbons^(2,3). Those studies showed that the intense radiation field that would result from the accumulation and subsequent decay of radioactive iodine causes organic iodide formation in the carbon bed⁽⁴⁾. The rate of formation and subsequent desorption of the organic iodides is governed by the moisture content and flow rate of the air passing through the beds⁽⁴⁾. The earlier studies also showed that the impregnant triethylenediamine (TEDA), either alone or in combination with iodine salts, improved iodine retention more than did other impregnants tested⁽⁴⁾.

Subsequent studies on TEDA-impregnated carbons showed that limits must be placed on the TEDA impregnation level for high-temperature applications because of the low ($\sim 190^{\circ}\text{C}$) flash point of TEDA⁽⁵⁾. Results of these studies led to the development of Type GX-176* carbon (the type currently installed in the SRP confinement systems)⁽⁶⁾.

Carbon in the SRP confinement system is routinely sampled and subjected to a variety of physical, chemical, and iodine penetration tests to ensure continued operation of the confinement system within performance specifications. Data on these service aging studies are presented in this paper along with observations on factors affecting the performance of several carbons exposed in the SRP confinement system.

* A 10 x 16 (US) mesh coconut carbon impregnated with 1% TEDA, 2% KI, and a proprietary flame retardant. Product of North American Carbon Company, Columbus, Ohio.

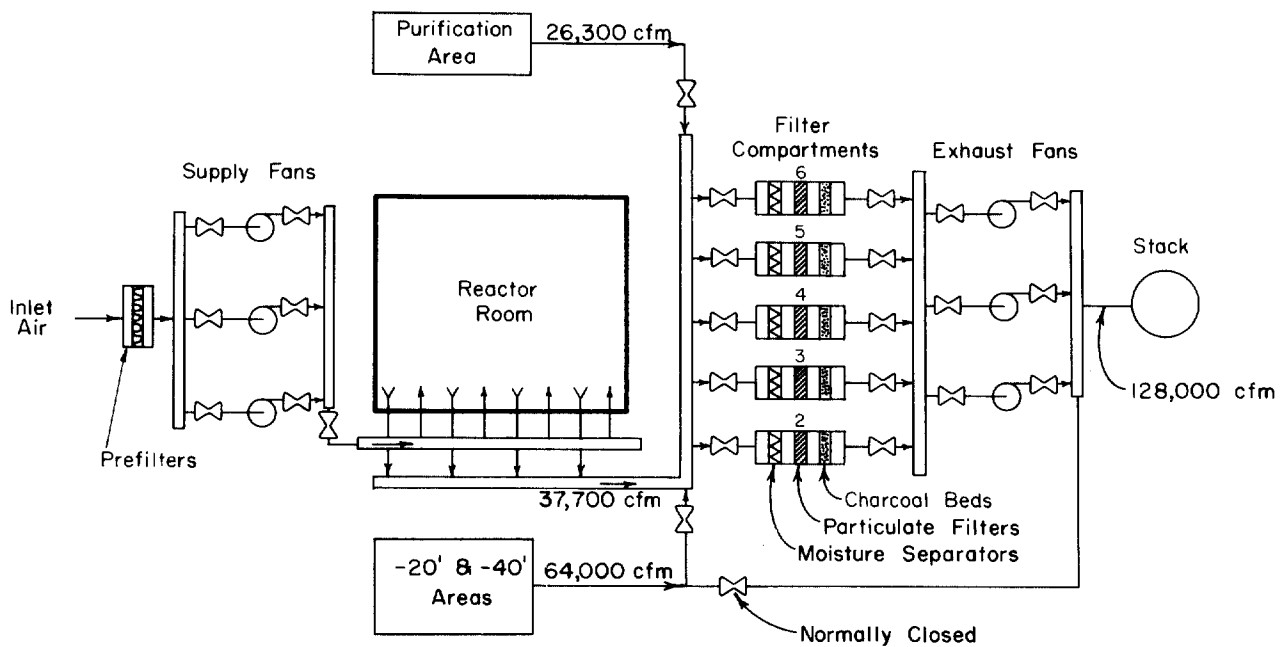


Figure 1 Flow diagram of reactor ventilation system.

Background

Unimpregnated Type 416* carbon was used as a halogen adsorber in all the SRP confinement system charcoal beds until 1975 when replacement with Type GX-176 was completed. Following the discovery of the radiation-induced iodine desorption phenomenon^(2,3), a limited number of beds of Type G-615** carbon were installed in the confinement system for evaluation. Type G-615 carbon was removed from the system after nine months exposure; at that time, detailed evaluation of the ignition characteristics of TEDA carbons^(5,6) along with evaluation of the performance of the confinement system HEPA filters under simulated accident conditions^(7,8) indicated that Type GX-176 carbon can be used effectively in the SRP system with a lesser ignition hazard than can Type G-615 carbon.

Carbon in the SRP system is housed in stainless steel frames (beds) in the confinement compartments (32 beds per compartment, 5 compartments per reactor area)⁽¹⁾. Routine, in-place leak tests are performed on the charcoal beds to ensure gasket and packing integrity⁽⁹⁾. Iodine retention properties of the carbon are determined by performing iodine penetration tests on samples obtained from full-sized carbon beds that have been removed from the system at periodic intervals. Two iodine tests are routinely performed on one-inch-deep beds: (1) a radiation test, a five-hour test in which I₂ is loaded on the carbon and desorbed at 80°C and 95% relative humidity in a radiation field of at least 1.5 x 10⁷ rads/hr, and (2) a high-temperature test, a test in which I₂ is loaded on the carbon in laboratory air and then subjected to four hours of continuous air flow at 180°C⁽²⁾.

Additional tests performed on the carbon samples at SRL include pH measurement of water extracts of the carbon, ignition temperature determinations, and impregnant content measurements. Selected samples of new and used confinement carbons have also been tested for methyl iodide penetration at the Naval Research Laboratory (NRL).

The three types of carbon (Types 416, G-615, and GX-176) exposed in the confinement system were all subjected to the tests described in the two preceding paragraphs.

Test Results

High-Temperature Tests

Earlier studies at SRL showed that the ability of carbon to retain iodine at elevated temperatures declines rapidly with increasing service⁽⁷⁾. The data in Table I show iodine penetration is less in service-aged Type GX-176 carbon than in either carbon Type G-615 or 416. A plot of the data (Figure 2) shows that observed iodine penetrations of Type GX-176 carbon are about 10% of those expected from the other two types of carbon after an 18-month exposure in the confinement system.

* A 10 x 14 (Tyler) mesh coconut carbon. Product of Barneby-Cheney Company, Columbus, Ohio.

** An 8 x 16 (US) mesh coconut carbon impregnated with 2% TEDA, 2% KI, and a proprietary flame retardant. Product of North American Carbon Company, Columbus, Ohio.

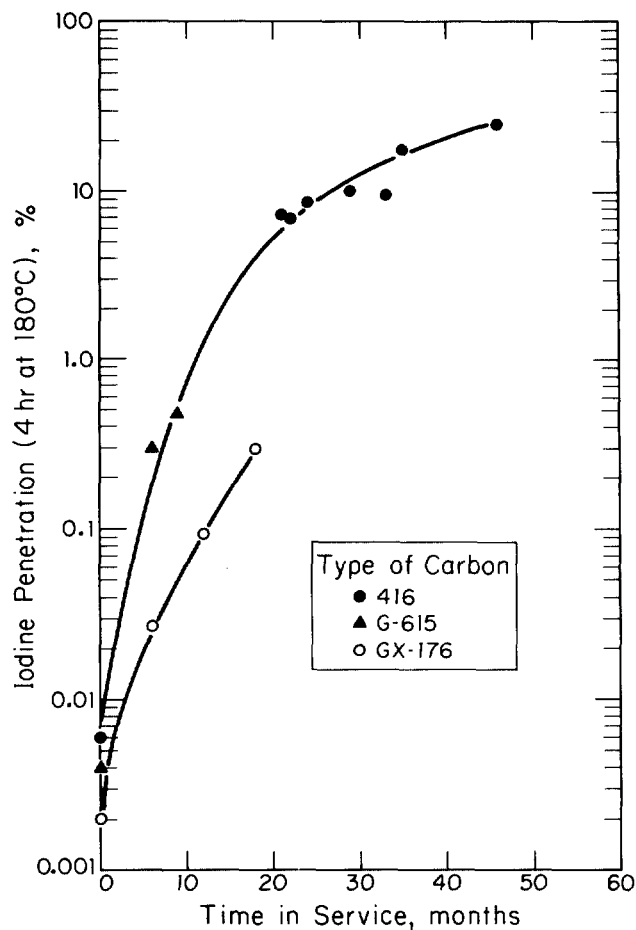


Figure 2 High-temperature tests on confinement carbons.

14th ERDA AIR CLEANING CONFERENCE

Figure 2 also shows that the aging rates of Types G-615 and 416 carbons in the high-temperature test are similar, despite the fact that Type G-615 is an impregnated carbon, and Type 416 carbon contains no additives. Type GX-176 carbon behaves quite differently, even though it contains the same additives as those in Type G-615 (TEDA, KI, and a flame retardant). This anomalous behavior is believed to be caused by differences in the particle size distributions of the carbons and is discussed in greater detail later.

Table I High temperature test data on confinement carbons.

<u>Type of Carbon</u>	<u>Time in Service, months</u>	<u>Compartment Number^a</u>	<u>Iodine Penetration at 180°C, %^b</u>
416	0	-	0.006
	21	C-2	7.22
	22	P-2	6.84
	24	L-2	8.59
	29	P-3	10.2
	33	P-2	9.48
	35	P-3	17.7
	46	K-3	25.2
G-615	0	-	0.004
	6	C-2	0.295
	9	C-2	0.474
GX-176	0	-	0.002
	6	K-2	0.027
	6	P-2	0.093
	12	K-2	0.093
	18	K-2	0.392

^a. Data presented are limited to carbon removed from compartments 2 and 3 only, since previous studies have shown more rapid carbon deterioration in these compartments (5,10). C, K, L, and P designate production reactors.

^b. See text for test conditions.

Radiation Tests

Radiation test data on carbons exposed in the confinement system compartments are presented in Table II and shown graphically in Figure 3. The data show that even after 18 months service, Type GX-176 carbon retains iodine more effectively than does new (unexposed) Type 416 carbon. The data also show that service performance of Type GX-176 carbon is better than that of Type G-615 carbon even though Type G-615 carbon has a slightly lower iodine penetration rate when new.

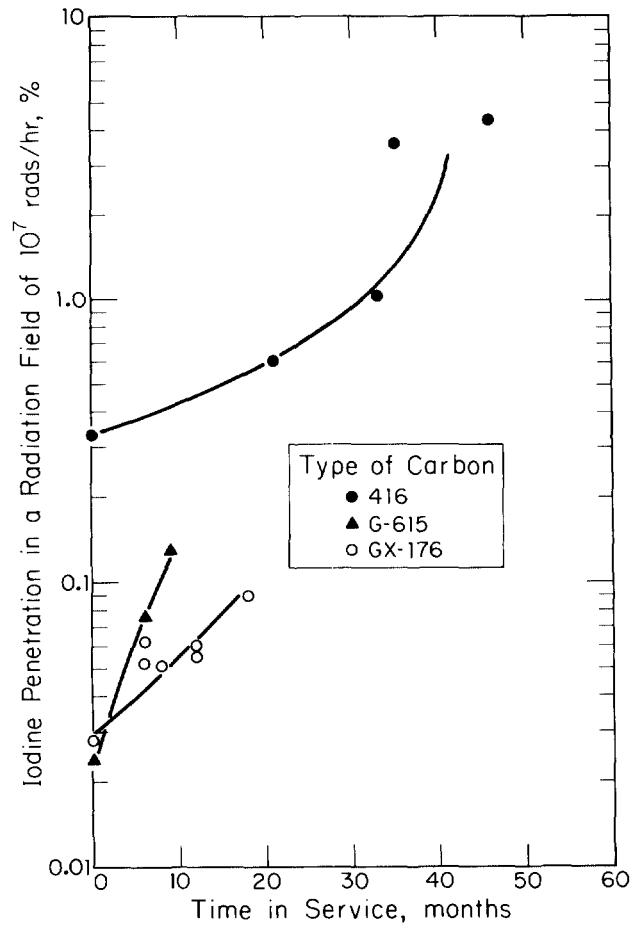


Figure 3 Radiation tests on confinement carbons.

Particle Size Distribution

Particle size distribution is determined on representative samples of all carbons installed in the SRP confinement system. The need for control of the particle size distribution was demonstrated during the early design experiments for the SRP systems⁽¹⁰⁾. Thus, the Type 416 carbon used for many years in the system had a 10 x 14 mesh (Tyler) distribution (approximately equivalent to a 10 x 16 mesh distribution using the U.S. Standard sieves). The Type G-615 carbon installed experimentally in the confinement system was an 8 x 16 mesh (U.S.) material designed for use in deep (2 inches or more) carbon beds in use in power reactor gas treatment systems. The Type GX-176 carbon now used in the SRP system has a 10 x 16 mesh (U.S.) distribution. Typical sieve analyses on the three products are shown in Table III.

Table II Radiation test data on confinement carbons.

<u>Type of Carbon</u>	<u>Time in Service, months</u>	<u>Compartment Number</u>	<u>Iodine Penetration in Radiation Field, %^a</u>
416	0	None	0.329
	21	C-2	0.610
	33	P-2	1.04
	35	P-3	3.63
	46	K-3	4.38
G-615	0	None	0.024
	6	C-2	0.076
	9	C-2	0.129
GX-176	0	None	0.028
	6	K-2	0.052
	6	P-2	0.062
	8	P-2	0.051
	12	K-2	0.060
	12	P-6	0.055
	18	K-2	0.090

^a. See text for test conditions.

14th ERDA AIR CLEANING CONFERENCE

Table III Typical particle size distributions for confinement carbons.

Size Range ^a	Carbon on Sieve for Three Carbon Types, wt %		
	416	G-615	GX-176
on 8	0.0	4.8	0.0
on 10	0.2	24.6	0.5
on 12	14.1	37.1	6.6
on 14	77.2	25.8	35.0
on 16	8.2	6.5	53.8
on 18	0.5	0.9	3.9
Thru 18	0.0	0.3	0.2

a. U.S. Standard ASTM E-11 Sieve Sizes using the method of ASTM D2862 for the determination.

The data in Table III shows that 66.5 wt % of Type G-615 carbon is larger than 12 mesh (greater than ≈ 1.68 mm nominal diameter), but 92.9 wt % of the Type GX-176 carbon is smaller than 12 mesh. The only other known difference between carbon Types G-615 and GX-176 is the TEDA content shown in Table IV.

Table IV Comparison of carbon Types G-615 and GX-176.^a

	G-615	GX-176
Base carbon	Coconut	Coconut
BET surface area ^b , m ² /g	1000	1000
Mesh size (U.S.)	8 × 16	10 × 16
TEDA content, wt %	2.0	1.0
KI content, wt %	2.0	2.0
Flame retardant, wt % ^c	1.0	1.0

a. Vendor-supplied data.

b. Nominal surface area after impregnation.

c. The same proprietary compound is used on both carbons.

14th ERDA AIR CLEANING CONFERENCE

Earlier studies of carbon behavior in a radiation environment indicated that iodine penetration should increase with decreasing TEDA content (3,6). However, test results on service-aged carbons show that Type GX-176 carbon performs consistently better than does Type G-615 carbon, indicating that the particle size distribution is at least as important for iodine retention as is the TEDA content. Particle size data also indicate that smaller carbon granules age more slowly in service than do larger granules.

NRL Methyl Iodide Tests

Samples of new and service-aged carbons of Types G-615 and GX-176 were sent to NRL for methyl iodide penetration testing. Type 416 carbon was not included in this test series because of the known poor methyl iodide retention efficiency of unimpregnated carbon. The NRL test conditions were 25°C temperature, 95% relative humidity, 0.25-second residence time (2-inch-deep carbon bed), 0.1-mg CH₃I/g carbon loading, and 4-hr test time (following 16 hours pre-equilibration at 25°C and 95% relative humidity). This test is intended as a carbon qualification test and is not necessarily indicative of expected carbon performance under accident conditions. Test results are shown in Table V.

Table V Methyl iodide penetration tests of confinement carbons

<u>Type of Carbon</u>	<u>Time in Service, months</u>	<u>Methyl Iodide Penetration, %^a</u>
G-615 ^b	0	0.79
	6	11.4
	9	22.3
GX-176 ^c	0	0.45
	6	5.82
	12	28.5
	18	32.1

-
- a. NRL test data courtesy V. R. Deitz. See text for test conditions.
- b. All samples except the control exposed in the C-2 compartment.
- c. All samples except the control exposed in the K-2 compartment.

Test data show that the methyl iodide retention efficiency of both carbons decreases rapidly with increasing service. The data also show that Type GX-176 carbon deteriorates more slowly than does Type G-615 carbon and confirm the earlier observations on the importance of particle size distribution.

pH Tests

pH tests are performed on the carbon by measuring the pH of water extracts of the carbon. The SRL pH test is made by placing a 5-g sample of carbon in 50 ml of cold, distilled water, heating the slurry to boiling, and then cooling to room temperature in a sealed flask. The pH measurement is made on the liquid decanted from the carbon after the sample has cooled. Data obtained by this method (Table VI) show a rapid decrease in pH with increasing service. As indicated earlier, Types G-615 and 416 carbons show similar behavior when evaluated by the high-temperature test (penetration versus service, Figure 2), but Type GX-176 carbon seemed to deteriorate more slowly. When the high-temperature penetration data are compared with the reciprocal of the pH data (1/pH instead of service age), all three carbons appear to behave similarly (Figure 4). Previous investigations of new carbons showed similar pH effect on iodine retention at elevated temperatures and indicate that one of the principal mechanisms for high-efficiency iodine retention is the conversion of elemental iodine to ionic iodine on the charcoal⁽⁸⁾.

Table VI pH of service-aged carbons.^a

<u>Type of Carbon</u>	<u>Time in Service, months</u>	<u>Compartment Number</u>	<u>pH of Water Extract</u>
416	0	-	9.59
	21	C-2	4.80
	22	P-2	4.75
	33	P-2	4.33
	35	P-3	3.99
	46	K-3	3.01
G-615	0	-	9.86
	6	C-2	7.20
	9	C-2	6.63
GX-176	0	-	9.70
	6	K-2	7.60
	6	P-2	7.70
	12	K-2	6.60
	12	P-6	7.15
	18	K-2	6.46

^a. See text for description of method.

Other Tests

Ignition temperature tests performed on impregnated confinement carbons show an apparent increase in the ignition temperature of Type GX-176 carbon for the first few months of service followed by a decrease. The total iodine content of Type GX-176 carbon also increased during the first few months of service in the confinement system. Data are shown in Table VII.

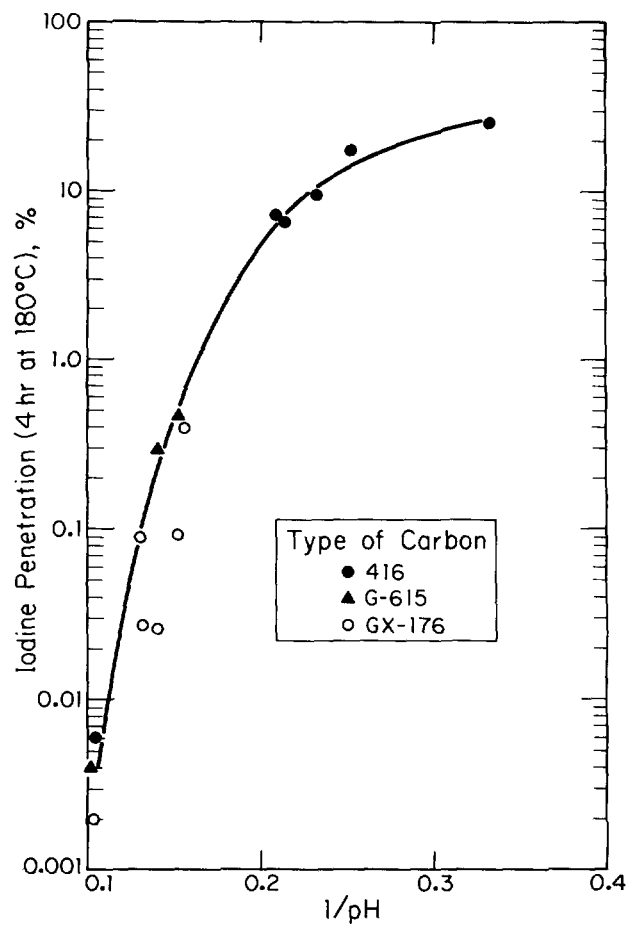


Figure 4 High-temperature iodine penetration as a function of carbon pH.

14th ERDA AIR CLEANING CONFERENCE

Table VII Other data on confinement carbons.

Type of Carbon	Time in Service, months	Compartment Number	Ignition Temp., °C ^a	Total Iodine Content, wt % ^b
416	0	-	340	-
	43	K-3	275	-
G-615	0	-	360	-
	6	C-2	420	-
	9	C-2	415	-
GX-176	0	-	386	1.41
	6	K-2	437	1.72
	6	P-2	420	-
	8	P-2	415	-
	12	K-2	322	1.59
	18	K-2	312	1.59

a. As measured in quartz apparatus at a heating rate of 5°C/minute and linear face velocity of 55 ft/min.

b. Determined by neutron activation analysis.

The TEDA content of Type GX-176 carbon was also determined when the carbon was purchased for installation in the confinement system. Analyses of the full-purchase lot, comprised of 16 sublots, showed variations in TEDA content from 0.86% to 1.08% with an average of 0.99% and a standard error of 0.08%. The analytical procedure consisted of TEDA extraction in carbon tetrachloride with subsequent quantitative analysis by infrared absorption spectrometry⁽¹¹⁾. Attempts to adapt the method to used carbons were unsuccessful because of the accumulation of interfering hydrocarbons on the service-aged charcoals.

14th ERDA AIR CLEANING CONFERENCE

References

1. W. S. Durant, R. C. Milham, D. R. Muhlbaier, and A. H. Peters. Activity Confinement System of the Savannah River Plant Reactors. USAEC Report DP-1071, E. I. du Pont de Nemours & Co., Savannah River Laboratory, Aiken, SC (1966).
2. A. G. Evans and L. R. Jones. Confinement of Airborne Radioactivity - Progress Report: January 1971 - June 1971. USAEC Report DP-1280, E. I. du Pont de Nemours & Co., Savannah River Laboratory, Aiken, SC (1971).
3. A. G. Evans and L. R. Jones. Confinement of Airborne Radioactivity - Progress Report: July 1971 - December 1971. USAEC Report DP-1298, E. I. du Pont de Nemours & Co., Savannah River Laboratory, Aiken, SC (1972).
4. A. G. Evans. "Effect of Intense Gamma Radiation on Radioiodine Retention by Activated Carbon," Proceedings of the Twelfth Air Cleaning Conference, Oak Ridge, TN, August 28-31, 1972. USAEC Report CONF-720823, pp 401-414 (1973).
5. A. G. Evans. Confinement of Airborne Radioactivity - Progress Report: July 1972 - December 1972. USAEC Report DP-1329, E. I. du Pont de Nemours and Company, Savannah River Laboratory, Aiken, SC (1973).
6. A. G. Evans. Confinement of Airborne Radioactivity - Progress Report: January 1973 - June 1973. USAEC Report DP-1340, E. I. du Pont de Nemours & Co., Savannah River Laboratory, Aiken, SC (1973).
7. A. G. Evans and L. R. Jones. Confinement of Airborne Radioactivity - Progress Report: July 1973 - December 1973. USAEC Report DP-1355, E. I. du Pont de Nemours & Co., Savannah River Laboratory, Aiken, SC (1974).
8. A. H. Dexter, A. G. Evans, and L. R. Jones. Confinement of Airborne Radioactivity - Progress Report: January - December 1974. USERDA Report DP-1390, E. I. du Pont de Nemours & Co., Savannah River Laboratory, Aiken, SC (1975).
9. D. R. Muhlbaier. Nondestructive Test of Carbon Beds for Reactor Confinement Applications - Final Progress Report: January - June 1966. USAEC Report DP-1082, E. I. du Pont de Nemours and Co., Savannah River Laboratory, Aiken, SC (1966).
10. G. H. Prigge. Application of Activated Carbon in Reactor Containment. USAEC Report DP-778, E. I. du Pont de Nemours and Co., Savannah River Laboratory, Aiken, SC (1962).
11. A. H. Dexter and A. G. Evans. Confinement of Airborne Radioactivity - Progress Report: January - December 1975. USERDA Report DP-1430, E. I. du Pont de Nemours and Co., Savannah River Laboratory, Aiken, SC (1976).

DISCUSSION

DEMPSEY: I can't understand why particle size should affect the degradation of the charcoal. Do you have a mental picture of what might be happening?

EVANS: I don't have proof positive but one of the problems, of course, is the accumulation of acidic components from the air itself. We know in our particular system, for example, that we have oxides of nitrogen present. We also have some sulfur dioxide present. These will accumulate on the charcoal and on the larger grain size particles, particularly, but they may not penetrate into the deep sites or they may plug the surface pores. A more likely explanation has to do with the surface oxidation phenomena; that is, the trace quantities of ozone present in the atmosphere as well as atmospheric oxygen. Because of the larger surface-to-volume ratio of smaller grain sizes, the larger grain sizes simply do not allow penetration of these species or diffusion down into the internal structure of the charcoal as well as smaller grain sizes. So the smaller grains seem to weather better because they offer more surface area. There's just more surface to oxidize than there is on the larger particles. This may also suggest, if the hypothesis is correct, that there is a finite limit for any charcoal surface based, for example, on the ambient ozone level.

KOVACH: Wouldn't it be easier to determine whether it is particle size dependent or not by trying the GX-176 impregnation on a range of particle sizes? Are you speculating now that particle size is the only difference?

EVANS: Aside from some proprietary things, the only difference between the GX-176 and G-615 charcoal with respect to impregnation is the TEDA level. Two per cent TEDA is present on G-615 new charcoal. In initial tests, with 2 per cent TEDA on the new charcoal, the G-615 showed superior methyl iodide retention properties. It also showed superior properties in our radiation tests. However, it just does not weather as well, all other things being constant except the TEDA level, which very rapidly decreases with service in the case of 615 because TEDA blows off in a flowing air stream. The only other difference is the particle size distribution.

KOVACH: Do you see the identical TEDA level decrease in bulk adsorbents?

EVANS: At the lower TEDA impregnation level, we believe that the rate of depletion of TEDA is slower. We have not been able to prove this, however. Our efforts to analyze the TEDA content of used charcoal have proven, so far, somewhat less than satisfactory.

KOVACH: A word of caution; when you run ignition or high temperature stability experiments, HEMTA decomposition results in extensive HCN generation.

•

A METHOD FOR CORRELATING WEATHERING DATA ON ADSORBENTS
USED FOR THE REMOVAL OF CH₃I

H. C. Parish and R. C. Muhlenhaupt
CVI Corporation
A Division of Pennwalt Corporation
Columbus, Ohio

Abstract

Traditionally, weathering data have been expressed in terms of removal efficiency as a function of time for a select number of bed depths. The test results are inherently a function of a multiplicity of variables, most of whose effects cannot be isolated. In addition to the exposure time and bed depth, these variables include: 1) variations in the efficiency of the adsorbent when new; 2) guard bed design (bed depth, replacement schedule); 3) air quality; and 4) air velocity. This situation has limited the usefulness of existing data to predict the performance of an adsorbent at some specific set of conditions.

This paper discusses the development of a single parameter, namely, the Effective Weathering Rate (EWR), its usefulness in correlating weathering data, and subsequent utilization during design. The effectiveness of the model was checked by analyzing several sets of data. It was found that a single value of EWR could be determined for each set of data such that the model could be used to reproduce, with reasonable accuracy, the adsorber efficiency for various bed depths as a function of time and, in one case, with and without a guard bed.

Values of EWR were determined from the limited available experimental data for air which could be described only qualitatively as ranging from relatively clean to relatively dirty air from a heavily industrialized area. As quantitative data become available, it is expected that the EWR can be correlated with the character and concentration of air contaminants such as hydrocarbons, SO₂, NO_x and O₃.

The EWR, determined from experimental data, can be used to predict adsorber efficiencies for conditions corresponding to a specific application. Thus, the analytical model can be used to extrapolate from the experimental conditions to the actual conditions for a given application. Some of the changes in conditions which can be treated by this method include: 1) bed depth of adsorbent, 2) addition of guard bed or depth of guard bed, 3) effectiveness of the carbon (new), 4) operating time, and 5) air velocity.

Some parametric studies were performed analytically to demonstrate some applications of the weathering model. These included calculating the adsorber efficiency as a function of time and bed depth, for carbons having various efficiencies when new, and for guard beds of variable bed depth and having different replacement schedules for the guard bed material.

1. Introduction

A few experimental studies on weathering have been conducted to date. Understandably, these studies have been largely independent efforts, each involving adsorbents, air quality, bed depths, air velocity and other test conditions generally selected to represent specific systems for which the tests were conducted. The result has been a collection of data that generally could not be compared in a straight-forward manner or applied to a specific application, generally characterized by another set of conditions. The published data on weathering have generally been in the form of CH₃I removal efficiencies, measured after select intervals of exposure time. Most of the experimental efforts involved nominally 2.5 cm and 5.0 cm adsorber beds with exposure times of less than 1 year. Extrapolation of these results to deeper beds and/or longer periods of exposure is difficult. Even in the one test program in which bed depths up to 15 cm were exposed for a period of up to approximately 1.75 years, extrapolation of the data to any specific application having conditions different from those of test conditions is not straight-forward. In particular, a specific application might utilize an adsorbent having different initial performance characteristics than those of the adsorbent used in the test program. In addition, if a guard bed is used, it may have a different bed depth from the one tested and periodic replacement of the guard bed would generally be expected whereas the only known guard bed data did not involve replacement. Furthermore, the guard bed data were taken over a period of only 14 months, whereas it would be expected that an adsorber, when protected by a guard bed, would have a much longer useful life.

An analytical weathering model has been developed to provide a means of calculating the CH₃I removal efficiency for a weathered adsorbent, requiring only known quantities such as bed depth, exposure time, air velocity, initial performance characteristics, etc. and one new parameter, the Effective Weathering Rate

(EWR). The EWR has been evaluated for the known weathering data and is tabulated in Table I. The EWR is expected to be primarily a function of contaminants in the air such as hydrocarbons, NO_x , SO_2 and O_3 . At present, since quantitative data on the concentrations of these species were not available with the weathering data, the EWR can only be correlated loosely as being typical for clean air or dirty air, or some degree between. As more data become available, it is expected that the EWR can be correlated with the concentrations of various air contaminants.

This paper describes an analytical tool that could provide the following benefits:

- 1) a means for describing available weathering data in terms of a single correlating parameter, considered to be primarily a function of the quality of the air.
- 2) a means for simplifying the application of weathering data to specific applications and to maximize the utility of experimental weathering data.
- 3) a means for simplifying future experiments on weathering by minimizing the number of conditions that need be investigated.
- 4) a basis for an analysis of the effectiveness of guard beds and economic evaluation of guard beds.

Two versions of the analytical model were investigated. The more simplified one is referred to as the zero transition model, and the more refined version is described as the finite transition model. Both are discussed in this paper. The two versions of the weathering model provide consistent results when applied to the same set of data, and hence reinforce and support each other. More importantly, since both can be used to evaluate the EWR, the confidence level of the results is enhanced.

The recommended procedure for applying the weathering model includes the use of both the zero transition and the finite transition models to analyze the appropriate data and to determine the combined best estimate of the EWR. This value of EWR would then be used with the finite transition model to calculate the adsorber efficiency for design conditions including bed depth, exposure time, performance of the new adsorbent and guard bed design factors.

The weathering model, the key concepts and the principle equations are given in the Analysis section of this paper. The efficiencies calculated from the weathering model and a comparison of the calculated and experimental efficiencies are presented in the Results section. The calculations were performed for the complete range of both bed depth and exposure time for which there is experimental data.

The EWR used in the analyses were obtained from the experimental data using both the zero and the finite transition models. The consistency of the EWR, determined by the two versions of the weathering model is also illustrated.

II. Analysis

Description of Weathering Model

The conceptual weathering model used in this analysis is an intuitively obvious one. It was assumed that the weathering phenomenon could be represented as a progressively advancing zone of ineffective adsorbent. This assumption was indicated by data from the literature and further justified, post priori, by the results of the subsequent analysis.

Two versions of this model were investigated, and each was found to have certain useful properties. The first model was the simplest in which the transition from weathered to unweathered carbon had zero thickness. The second model considered a finite transition. The general equation as applied to both of these concepts and the associated analytical procedures are described below.

General Performance Equation

A few observations can be made with respect to the removal of CH_3I by the commonly used adsorbents that apply to either of the two weathering models.

In a homogeneous material, CH_3I performance can generally be described by relating the fractional penetration to bed depth by the equation:

$$P = e^{-Bx} \quad (1)$$

where

- P = fractional penetration
- B = characteristic constant of a given adsorbent under a standard set of test conditions [cm^{-1}]
- x = bed depth [cm]

By definition, the fractional penetration at any moment in time for N beds or bed segments in series is given by:

$$P = P_1 \cdot P_2 \cdot \dots \cdot P_N = e^{-\sum_{i=1}^N B_i \Delta x_i} \quad (2)$$

where B_i is considered to be constant over each segment Δx_i . In the limit as $\Delta x \rightarrow 0$, this can be written as:

$$P = e^{-\int B'(x) dx} \quad (3)$$

where $B'(x)$ is a function of x for any moment in time. From Equation 3, the penetration at any moment is given by the exponential of the area under the curve in which $B'(x)$ is plotted as the instantaneous function of x .

Weathering Model with Zero Transition Zone

The initial analyses were performed using the simplest possible model in which it was assumed that the adsorbent in the weathered zone, represented by the cross hatched area in Figure 1-A, was rendered totally ineffective in the removal of CH_3I while the remainder of the adsorbent maintained 100% of its original effectiveness. It is recognized that this is a simplified model since it is unrealistic to expect the demarcation between the weathered and unweathered zone to be a sharp line. Rather, a "gray" area of transition would be expected as illustrated conceptually in Figure 1-B. Nevertheless, the data calculated from this model does provide physically meaningful information.

Based on this weathering model, an equivalent depth of the weathered zone can be calculated from Equation 4, given the new carbon performance (to determine B_0) and a measured penetration, P . See Figure 1-A for physical representation of variables.

$$X_1 - X_2 = \frac{\ln P}{B_0} \quad (4)$$

where

- P = ratio of the outlet to inlet concentrations
- B_0 = the adsorbent characteristic constant
- X_1 = the weathered zone length
- X_2 = the total bed length.

This approach was tried initially. The results were reasonably consistent for adsorbent weathering penetrations up to approximately 45%.

The unweathered zone length, shown in Figure 1-A, can be expressed in terms of the integral of $B'(x)$ by combining Equations 1 and 3. Thus

$$(X_2 - X_1) = \frac{1}{B_0} \int B'(x) dx \quad (5)$$

From Equation 5, the area under the $B'(x)$ vs x curve is equal to the product $B_0 (X_2 - X_1)$ as illustrated in Figure 2-A.

It can be demonstrated that this model provides consistent results independent of the bed length from which the data are taken, provided the leading edge of the transition zone has not "broken through" the bed, that is, if $X_b \leq X_c$ (See Figure 1-B).

For example, consider the variation of $B'(x)$ with x as illustrated in Figure 1-B in which this condition is met. The integral of Equation 5 can be evaluated in two steps, from zero to X_b and from X_b to X_c using the notation shown in the figure. Rearranging the equation then gives

$$B_0(X_2 - X_1) = \int_0^{X_b} B'(x) dx + \int_{X_b}^{X_c} B_0 dx$$

or

$$B_0(X_2 - X_1) = \int_0^{X_b} B'(x) dx + B_0(X_c - X_b). \quad (6)$$

The length of weathered carbon, X_1 in Figure 1-A, is determined from

$$X_1 = X_2 - (X_2 - X_1) \quad (7)$$

where $(X_2 - X_1)$ is calculated from Equation 6.

Thus, for any increment ΔL added to the total length, X_2 , a corresponding ΔL is added to $(X_2 - X_1)$ from Equation 6 and X_1 is unaffected by Equation 7. The same reasoning can also be used to show that the calculated length X_1 will vary with the total length chosen if the transition zone has broken through the section from which the data were taken. Therefore, the calculated value of X_1 will be in error under this condition.

Therefore, one of the principle guidelines to be observed in the application of the simplified model is that the data be taken on a bed of sufficient length and at a time such that the weathering effect has not progressed to the end of the bed. A quantitative criterion was analytically developed requiring that the calculated weathered zone should not exceed 43.8% of the total bed length. If this criterion is met, it can be shown by analysis that the error will be less than 5%. This, of course, does not consider experimental error or "real world" deviations from the analytical model.

Weathering Model with Finite Transition Zone

The simplified model described above was refined to include a transition zone of finite length as illustrated in Figure 1-B. The application of the new model differs somewhat from that of the previous one, in that the simplified model can be used to calculate the weathered zone length directly in the form of a closed solution, whereas the new model utilizes a trial and error process to determine the adsorbent weathering rate.

The analysis was performed in the following manner. The transition zone was divided into 100 equal increments of x , and a function $B(x,t)$ was defined such that an average value of B for each increment at a given time could be determined. The total penetration was then calculated using Equation 2.

The major effort was in determining the correct expression for the function $B(x,t)$ in equation form. The experience with the simplified model suggested defining the effective length of weathered zone (L_w) as the distance into the adsorbent bed at which the characteristic constant B is one half its value for the new adsorbent. That is B equals $B_0/2$ at x equals L_w as illustrated in Figure 2-A. Values for $B(x,t)$ were calculated from data obtained in Table 1 of Reference 1.

The function $B(x,t)$ can be expressed in equation form as:

$$B(x,t) = B''(x, L_w) \quad (8)$$

where

$$L_w = B'''(t) \quad (8A)$$

The function $B''(x, L_w)$ was determined empirically from the data in Table 1 of Reference 1, and is expressed in Equation 11.

The function $B''(x, L_w)$ was not changed after it had been established for that one set of data. It was felt that the usefulness of the correlation procedure would be limited if more than one variable had to be determined for each application. Fortunately, the results of this effort indicated the function $B''(x, L_w)$ to be sufficiently universal.

The function $B'''(t)$, was determined from

$$B'''(t) = L_w = EWR \cdot t. \quad (9)$$

As noted earlier, the EWR is considered to be a constant for a given air velocity and quality of air.

The calculations were then performed in the following manner. Using Figure 2-A as a guide, the position corresponding to B equals $B_0/2$, shown as L_w , was determined from Equation 9. For correlation of experimental data the EWR was determined by trial and error. Also, the zero transition model was initially used to provide a good first estimate of the results. This technique is developed below. If the calculations are for design purposes, the EWR is based on experimental data or obtained from the data reported herein. The location of Q , the trailing edge of the transition region, was determined from:

$$Q = L_w(1 - 0.3565 \cdot L_w^{0.25}) \quad (10)$$

where the units for L_w and Q are cm.

$B(x,t)$ was calculated using Equation 11.

$$B(x,t) = B''(x,L_w) = \frac{B_0}{2} \left(\frac{x-Q}{L_w-Q} \right)^{0.3} \quad (11)$$

The constants for Equations 10 and 11 were determined from the data given in Table 1 of Reference 1. These constants were then used for all subsequent analyses described in this paper. Experimental values for $B(x,t)$ were calculated from the data in Table 1 of Reference 1 and are shown in Figure 2-B as the solid lines. Figure 2-B also shows curves representing $B(x,t)$ calculated from Equations 10 and 11. The calculated data fit the experimental data reasonably well, particularly since the integral of the curve is used in calculating penetration (see Equation 3).

Relationship Between dX_1/dt and EWR

The rate at which the weathered zone progresses through the adsorbent in the zero transition model is described by the derivative dX_1/dt , which has the same units (i.e., cm/yr) as the EWR of the finite transition model. It is interesting and useful to note the relationship between the two quantities.

From the definition of the two models and Figures 1-A, 1-B, and 2-A, it would be expected that a functional relationship should exist between dX_1/dt and the EWR. This was confirmed by calculations, the results of which are presented in Figure 3.

III. Results

The calculated data, illustrated in Figure 4 thru Figure 18, were based on actual experimental conditions and were obtained by essentially the same procedures that would be used in performing design calculations. The experimental data points are plotted along with the calculated data (lines).

Two values of EWR were initially determined for each set of experimental data shown in Figures 4 through 11. One value was calculated using the zero transition model while the other was determined using the finite transition model. The final EWR for each set of data was then established considering the results from both models.

The EWR for the experimental data in Figure 12 was determined entirely from the zero transition model (dX_1/dt) and Figure 3. The resultant EWR was used with the finite transition model to obtain the analytical results illustrated in the figure.

In all cases, the zero transition model was used to calculate dX_1/dt only for data meeting the requirement that X_1 (calculated) did not exceed 43.8% of the test bed depth.

Having determined the EWR from one or both versions of the weathering model, that value was used in the finite transition model to calculate the adsorber efficiency as a function of bed depth and exposure time for the test conditions.

One of the significant results is the degree to which the calculated data fit the experimental data. In some cases, a wide range of bed depths and exposure times were represented by a single set of experimental data. Nevertheless, the data for each set were generally reproduced well by the model using the EWR characteristic for that set of data. In addition, consistency in the results obtained using the zero and finite transition models is apparent from Figures 13 through 18, considering that the EWR (represented by the lines) used with the finite transition model reproduced the experimental data while the EWR from the zero transition model was calculated directly from the data.

Figures 4 thru 12 show the experimental data from the various references plotted as discrete points and the corresponding analytical data plotted in curvilinear form.

The results shown in Figure 4 are based on the data in Table 2.10 of Reference 2. As with all of the data reported to date, no measurements of air contaminants were provided. However, it is expected that the quality of the air would typically be good for the part of the country (Oak Ridge, Tennessee) in which the test was conducted. It is recognized that air from any closed space could be highly contaminated; however, no indication of any unusual contaminants were reported. The air velocity during the exposure period was 10.2 cm/s (20 fpm) compared to the more common velocity of 20.3 cm/s (40 fpm). The velocities are indicated in the graphs using the symbol V .

As may be noted in the figure, the calculated values for both the 2.5 cm and 5.0 cm bed depths agreed well at an EWR of 1.75 cm/yr, for up to 300 days. Consistency of the two models is illustrated in Figure 13. The zero transition zone results at 300 days did not meet the less than 43.8% weathered criterion and hence were not included. However, as noted, the X_1 values calculated directly from the experimental data

from the 2.5 cm and 5.0 cm beds fall very close to the finite transition zone curve (EWR that reproduced the data in Figure 4).

Figure 5 represents the data in Figure 4 (LITR-BSR data) of Reference 3. For this set of data, the best overall (considering both the 2.9 cm and the 5.8 cm beds) fit of calculated efficiencies to the experimental results would be achieved with a slightly lower EWR than the value used. A smaller EWR would tend to raise the calculated efficiencies for both the 2.9 cm and 5.8 cm beds, but the efficiency of the smaller bed would increase more rapidly. However, the 5.33 cm/yr EWR was chosen partially on the basis that this value produced results that correspond favorably to those calculated using the zero transition model (see Figure 14). In addition, since 5 cm beds are much more commonly used for the removal of CH_3I than 2.5 cm beds, it was considered desirable to preferentially fit the 5.8 cm bed depth data.

The experimental data in Figure 6 are also from Figure 4 of Reference 3, but represent the HFIR data. Again, the calculated efficiencies would fit the experimental data a little better using a slightly lower EWR than that shown. However, factoring in the data from the zero transition model, a rate of 4.04 cm/yr was selected for the EWR. Thus, both the zero and finite transition models were used to determine a consistent EWR from the experimental data. The resultant EWR was used with the finite transition model to calculate efficiencies as indicated by the curves in Figure 6.

Figure 7 presents the results of the calculations based on the KI-impregnated carbon data listed in Table 1 of Reference 1. In this case an EWR of 10.8 cm/yr provided the best overall fit (also see Figure 16).

The results shown in Figure 8 are based on data obtained from Figure 3 of Reference 1. An EWR of 7.62 cm/yr provided the best overall fit of calculated efficiencies to experimental data. The calculated efficiencies compare well with the measured efficiencies for bed depths of 2.5, 5.0, 12.5, and 15.0 cm. Although the comparison is not as good for bed depths of 7.5 and 10.0 cm at 387 days, the overall correlation between calculated and experimental data is considered to be very acceptable. Consistency of the two analytical models is illustrated in Figure 17. Only two data points were applicable for the zero transition model, since the others exceeded the X_1/L value of 0.438.

The experimental data in Figure 9 are from Figure No. 5 of Reference 1. In this case an EWR of 10.16 cm/yr provided the best overall fit of analytical and experimental data. The calculated and experimental data compared reasonably well for bed depths of 2.5, 5.0, and 7.5 cm. Even though the comparisons were not as good at 10 and 12.5 cm, the overall correlation between calculated and experimental data is considered to be acceptable. There were no data meeting the X_1/L less than 0.438 requirement; therefore, the zero transition zone model was not used in evaluating the EWR.

Figure 10 shows the results obtained using the experimental data from Figure 2 of Reference 1. These test data were taken using comparable air with the same type of impregnated carbon as that in Figure 7 of this paper, but this time preceded by a guard bed material of the same base carbon but without the impregnant. Therefore, it seemed reasonable to assume that the same function $B(x,t)$ would apply as before, starting at the inlet to the guard bed at time $t = 0$. The penetration through the adsorber can be calculated from Equation 3 at any time "t", where the integral is evaluated from the inlet to the outlet of the adsorber. If the model is valid, the EWR should be the same as that used for Figure 7 of this paper. Accordingly, an EWR of 10.80 cm/yr was assumed with no effort being made to determine a best fit value. Fortunately, as seen in Figure 10, the same value of EWR fit the data with guard bed fairly well.

The results shown in Figure 11 are based on the limited test data shown in Table II of Reference 1. Again, none of the data was suitable for the application of the zero transition model. In addition to the usual test data for the first bed and for two beds in series, the data from Reference 1 included an efficiency for the second bed alone (the first bed in effect being a guard bed). The analysis included a calculation for the same bed. Both the experimental and calculated values for the second bed are shown in Figure 11. The calculated efficiencies are in good agreement with the measured.

The experimental data in Figure 12 are from Figure 4 (TEDA data) of Reference 3. This analysis was performed somewhat differently from the previous ones in that the zero transition model alone was used to calculate the EWR from the experimental data. The EWR thus determined was then used as usual in an analysis by employing the finite transition model to calculate efficiencies for various bed depths and exposure times. It can be seen from Figure 12 that the EWR, as determined solely by the zero transition model, provides a good fit of the data when used in the finite transition model.

It should be mentioned that experimental data shown in Figure 4 and Table III of Reference 1 were not used in this effort. The data from Figure 4 were from a test consisting of a sodium zeolite/silver zeolite,

14th ERDA AIR CLEANING CONFERENCE

guard bed/adsorber bed combination and the current weathering model is not suited to a system in which the guard bed would have significantly different removal characteristics for the weathering agents than that of the adsorbent. However, it is anticipated that this restriction can be removed with some additional development. For now though, the data of Figure 4 is not compatible with the model since, as Wilhelm concluded, the sodium zeolite apparently did not adequately remove the weathering agents that attacked the AgX because the weathering did not seem to be significantly retarded by the addition of the guard bed⁽¹⁾.

Data from Table III of Reference 1 were not included because there was some uncertainty over one of the data points. That is, there appeared to be an inconsistency between the reported CH₃I removal efficiencies at 5 months and 6 months for filter bank No. 1.

Ranges of EWR for Data Evaluated

The values of EWR determined for each set of experimental data are summarized in Table 1. Based on the assumption that the EWR is proportional to the air velocity for a given adsorbent and quality of air, the indicated EWR is adjusted for velocity. The results for EWR, adjusted to a velocity of 20.3 cm/s are listed in the Table. These data are tabulated in ascending order of adjusted EWR.

Table I. Summary of EWR data

Reference Figure No.	Indicated EWR (cm/yr)	Superficial Velocity (cm/s)	EWR Adjusted to 20.32 cm/s (cm/yr.)	Air Quality* Code No.	Adsorbent
4	1.75	10.16	3.51	1	Carbon, KI ₃
6	4.04	20.32	4.04	2	Carbon, KI ₃
12	4.24	20.32	4.24	3	Carbon, TEDA
5	5.33	20.32	5.33	3	Carbon, KI ₃
8	7.62	25.0	6.20	4	Silver Zeolite
9	10.16	25.0	8.26	5	Silver Zeolite
7	10.80	25.0	8.79	4	Carbon, KI
10	10.80**	25.0	8.79	4	Carbon, KI**
11	20.32	30.0	13.74	5	Carbon

*Air Quality Code No. Descriptions --

1. Ambient Air from the Oak Ridge Research Reactor
2. Air from the Oak Ridge High Flux Isotopes Reactor; reasonably steady relative humidity and temperature
3. Air from the Oak Ridge Bulk Shielding Facility -- a swimming pool type. Unsteady relative humidity and temperature
4. Industrial Environment -- "very near to several chemical factories, oil fired power plants, etc."
5. Air from a reactor building

**EWR taken from inlet to guard bed

The data are also coded by numbers "1" thru "5", incorporating the available information with respect to the quality of the air. Although quantitative data on this parameter are not available, the trend appears to be towards increasing EWR with poorer quality air, as would be expected. Relatively little is known about the quality of the air coded as No. 1 from the Oak Ridge Research Reactor Building. However, these data and data coded as No. 2 and 3 were obtained in tests conducted using air from comparatively unindustrialized areas of Tennessee where the air is presumed to be relatively clean. This, of course, is not necessarily true for closed spaces which could be contaminated, for example, by cleaning agents or paints.

The air coded as No. 3 was considered by Davis and Ackley to present a somewhat more severe weathering condition than that coded as No. 2 because of relatively large swings in temperature and relative humidity⁽³⁾. For the two sets of data using air identified as code No. 3, the EWR for KI₃ impregnated carbon was 5.33 cm/yr compared to 4.24 cm/yr for TEDA impregnated carbon.

The air coded as No. 4 is described in Reference 1 as industrial air "very near to several chemical factories, oil fired power plants, etc." As seen in Table 1, the EWR values for data using air coded No. 4 were higher than those for the adsorbents exposed to the Tennessee air. The EWR for KI impregnated carbon was also somewhat higher than that for Silver Zeolite with the same air.

The air coded as No. 5 is from a reactor building. The quality of that air is not indicated; however, Table 1 shows that the EWR is consistently high for both the carbon and the silver zeolite adsorbents.

Example Applications of the Weathering Model

In addition to serving either as the basis for the analysis and correlation of data as described above or as a useful tool in estimating adsorbent life in a specific application, the weathering model can be used in various parametric studies. Two examples are described below to demonstrate some of the possible applications of the model. An EWR of 5.08 cm/yr was used in both examples as a representative value based on the range of EWR indicated in Table 1. It should be emphasized that these results are presented on the basis of actual operating time, not calendar time.

Note: It is recommended that the weathering model be proven by additional comparison to experimental data, especially guard bed data, prior to placing extensive reliance on these or other results from the weathering model.

Calculated Effect of Initial Adsorbent Efficiency on Service Life

An analysis was performed to estimate the effect of the efficiency of the adsorbent (when new) on its predicted life under weathering conditions. These calculations were made for a 5.0 cm bed and a 10.0 cm bed, using the finite transition zone model. As noted earlier, an EWR of 5.08 cm/yr was used in the calculations. The results of this analysis are illustrated in Figure 19. For purposes of discussion, an arbitrary limit of 90% removal efficiency was used as the criterion to define the bed life. Three adsorbents (A, B, and C) having initial efficiencies of 99.99%, 99.9%, and 99.0%, respectively for a bed depth of 5.0 cm were analyzed. Based on the 5 cm bed depths, adsorbent "C" would last 130 days whereas adsorbent "B" would last 223 days (a 72% increase), and adsorbent "A" would last 301 days (a 132% increase). Similar relative increases were determined for a 10 cm bed.

Also, the analytical results indicate a disproportionate increase in bed life with increased bed depth. For example, doubling the bed depth results in an adsorbent life of approximately 5.5 times as long. Wilhelm made a similar observation from his experimental data ⁽¹⁾.

Guard Bed Calculations

The weathering model can be applied readily to calculate the effectiveness of guard beds of various bed depths, within the present limitation that the guard bed and adsorber have approximately the same removal characteristics for the weathering agents. It is believed that this restriction can be removed with a further refinement of the model. The results of a sample guard bed analysis are presented in Figure 20. Although it is beyond the scope of this paper, this type of analysis has been combined with estimated replacement and capital costs to provide economic evaluations for the use of guard beds.

The results in Figure 20 indicate the efficiency of the adsorber as a function of time for two combinations of guard bed thickness and replacement schedule. Both analyses were performed for a 5 cm deep adsorber bed. One analysis was based on a guard bed thickness of 5 cm and a replacement schedule of every six months while the other was based on a guard bed thickness of 10 cm and a replacement schedule of every 12 months. All calculations were based on an EWR of 5.08 cm/yr as discussed earlier and an initial adsorbent efficiency of 99.9%.

IV. Summary

The weathering model was tested by analyzing several sets of experimental weathering data, using the data to determine an EWR and subsequently calculating adsorber efficiency as a function of bed depth and time. The results of all the analyses were considered to be satisfactory, especially in view of the range of bed depths and exposure times covered in many of the experiments. The results of one test, conducted without a guard bed, were even extrapolated to successfully predict the results of another test in which a guard bed was used.

The recommended procedure for applying the weathering model in a design situation is summarized as follows:

If weathering data from the literature is to be used, either refer to Table I of this paper for the appropriate value of EWR or use any other available data to select or calculate an EWR which is associated with the air quality that would be considered to represent a weathering condition at least as severe as the expected operating situation.

If a weathering test is to be performed, the air used in the test should be as representative of the operating air as practicable. Certainly, the more data that are taken, will result in a higher degree of confidence in the results. However, the weathering model has shown sufficient promise that at least interim

design information could be obtained by a relatively modest weathering test program. For example, data taken at 60 days and 120 days on a 5 cm and 10 cm bed (four data points) could be extrapolated to substantially longer operating periods, different bed lengths and various guard bed design configurations, provided the guard bed material meets the conditions described earlier.

Whether the data is taken from the literature or from a weathering test conducted especially for the specific design effort, it is recommended that both the zero transition model and the finite transition model be used to evaluate the EWR, with the selected value being that which provides the best overall fit for the two versions of the weathering model.

Having determined the EWR that characterizes the design conditions, that value should be used with the finite transition model to calculate the adsorber efficiency corresponding to whatever design bed depth and operating time may be required and for the appropriate guard bed parameters, if a guard bed is to be used.

One condition for application of the weathering model should be noted; it is important that the adsorber efficiency test conditions be consistent throughout. That is, the tracer test used to measure the removal efficiency of the adsorber must use the same relative humidity, temperature, air velocity, etc., for testing the new adsorbent and all subsequent tests as the adsorbent is aged.

In addition to its use as a design tool in the sense indicated above, the EWR, used with the weathering model, could be used as a correlating parameter.

If future weathering data are used to calculate an EWR from this weathering model and if quantitative data are taken on the concentration of trace contaminants as well as relative humidity, then it may be possible to correlate the EWR with SO_2 , NO_x , O_3 and hydrocarbon concentrations. If sufficient data become available, it may also be possible to define and correlate a function $B''(x, L_w)$ for each of the contaminants and combine the functions to obtain an overall $B''(x, L_w)$ based on the concentrations of each contaminant. In this event, given a set of air quality measurements, the life of an adsorber could be predicted with relative confidence for various adsorber thicknesses, adsorbents, air velocities, and with or without guard beds, without requiring further weathering tests. Even now, since the range of EWR is not as large as might be expected for the data reported, a value for the EWR or a range of values could be assumed.

The weathering model could also be potentially useful in performing parametric studies including the optimization of adsorber bed depth, adsorber quality (initial performance) and, for guard beds, the optimization of guard bed depth, and replacement schedule for the guard bed material.

Although the results reported herein are encouraging, some refinement of the weathering model may be indicated as additional data become available.

References

1. Wilhelm, J. G., Dillman, H. G., Gerlach, K., "Testing of Iodine Filter Systems Under Normal and Post - Accident Conditions", Proceedings of 12th AEC Air Cleaning Conference 1972, pp. 434-444.
2. Cottrell, Wm. B., "ORNL Nuclear Safety Research and Development Program Bimonthly Report for November-December 1967", ORNL-TM-2095, February 5, 1968, p. 42.
3. Davis, R.G. and Ackley, R. D., "Long-Term Effects on Radioiodine Trapping by Charcoal", Proceedings of 12th ACE Air Cleaning Conference 1972, pp. 469-483.

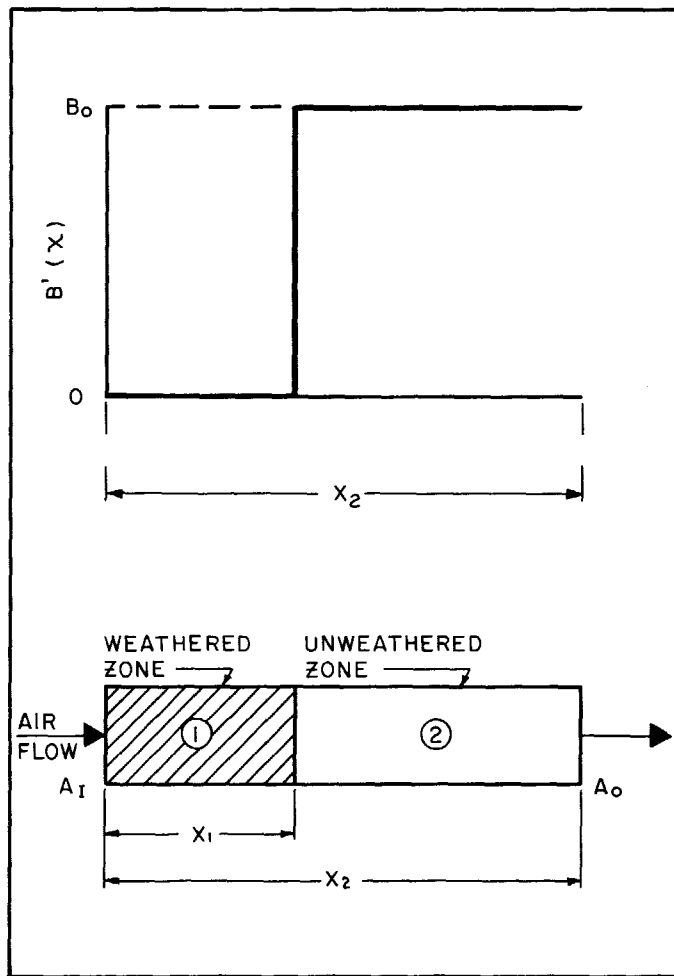


Figure 1-A. Schematic drawing illustrating concepts of simplified weathering model with a transition zone of zero length.

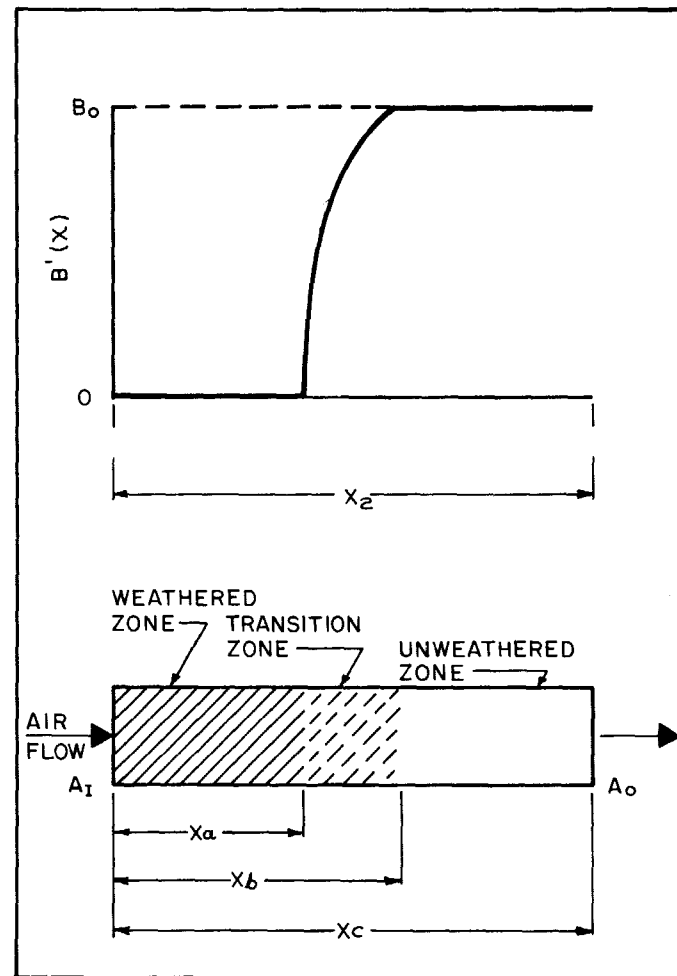


Figure 1-B. Schematic drawing illustrating concepts of weathering model with a transition zone of finite length.

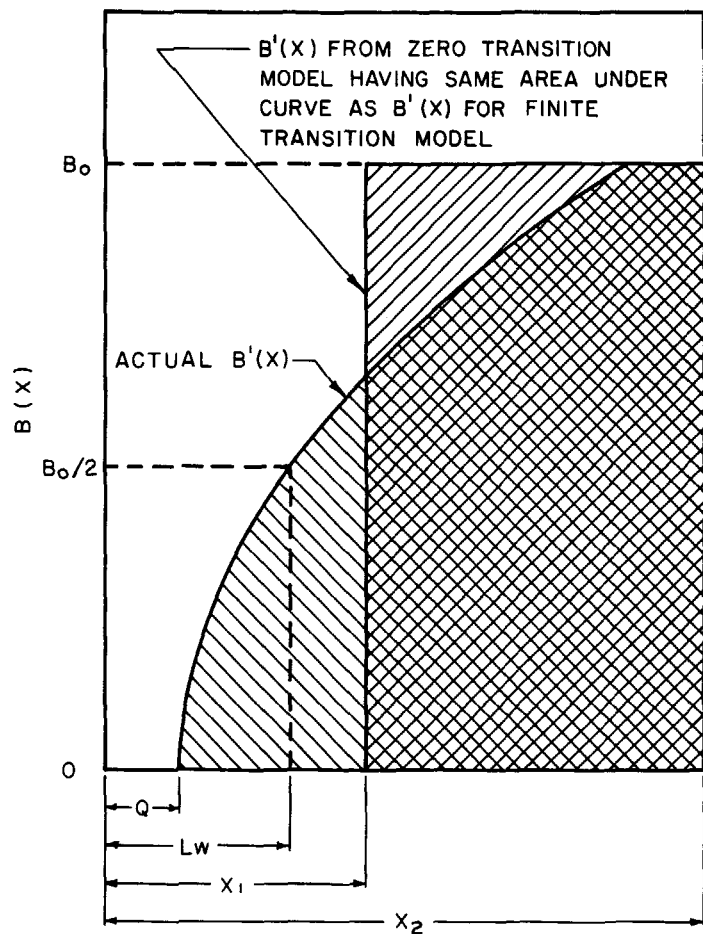


Figure 2-A. Typical curves representing actual $B'(x)$ and step function form of $B(x)$ from simplified model.

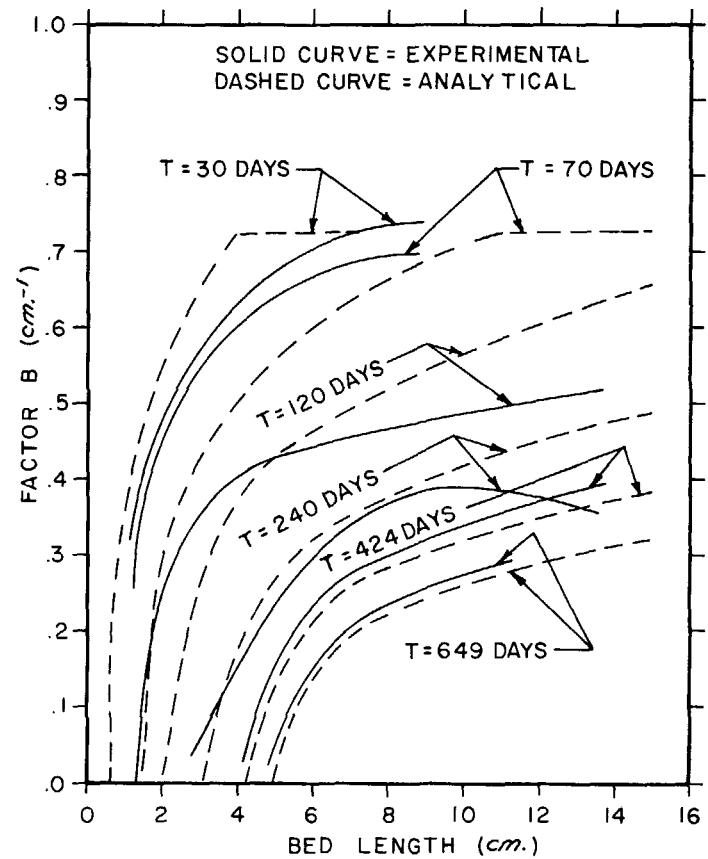


Figure 2-B. Comparison of experimental and curve fit values for performance exponential "B" factor.

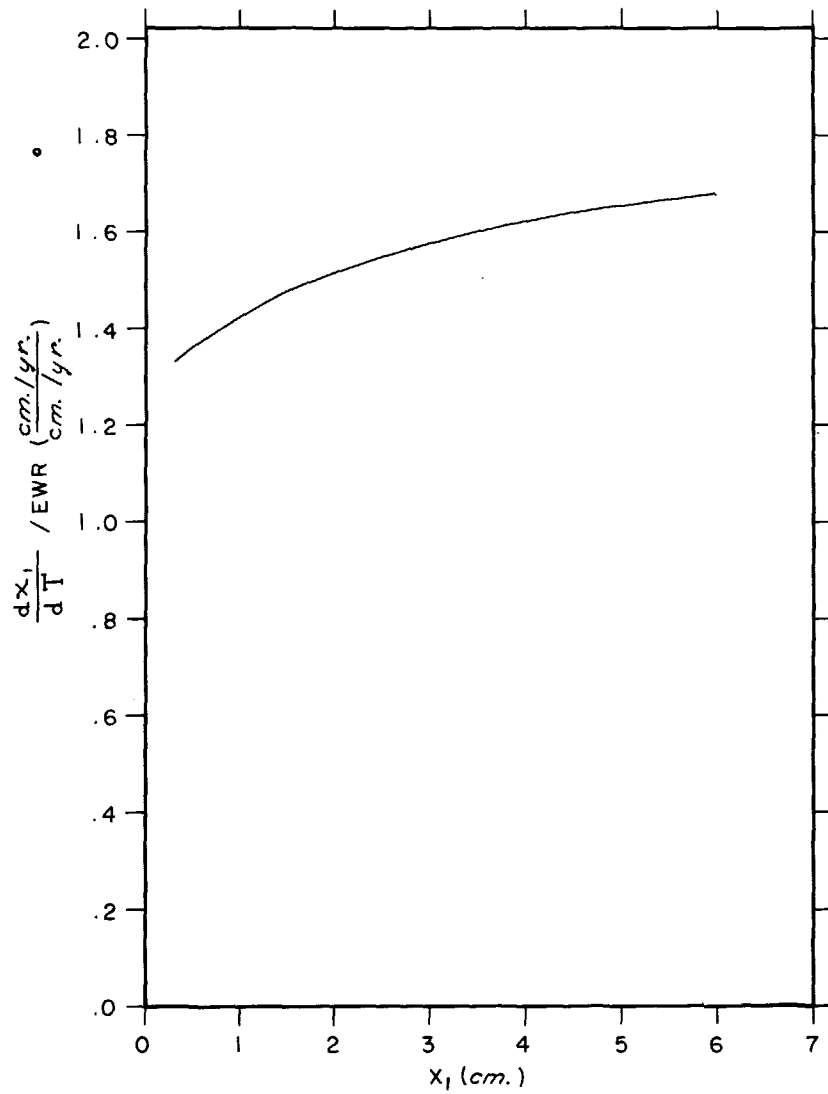


Figure 3. Relationship between rate of weathering calculated using two different weathering models.

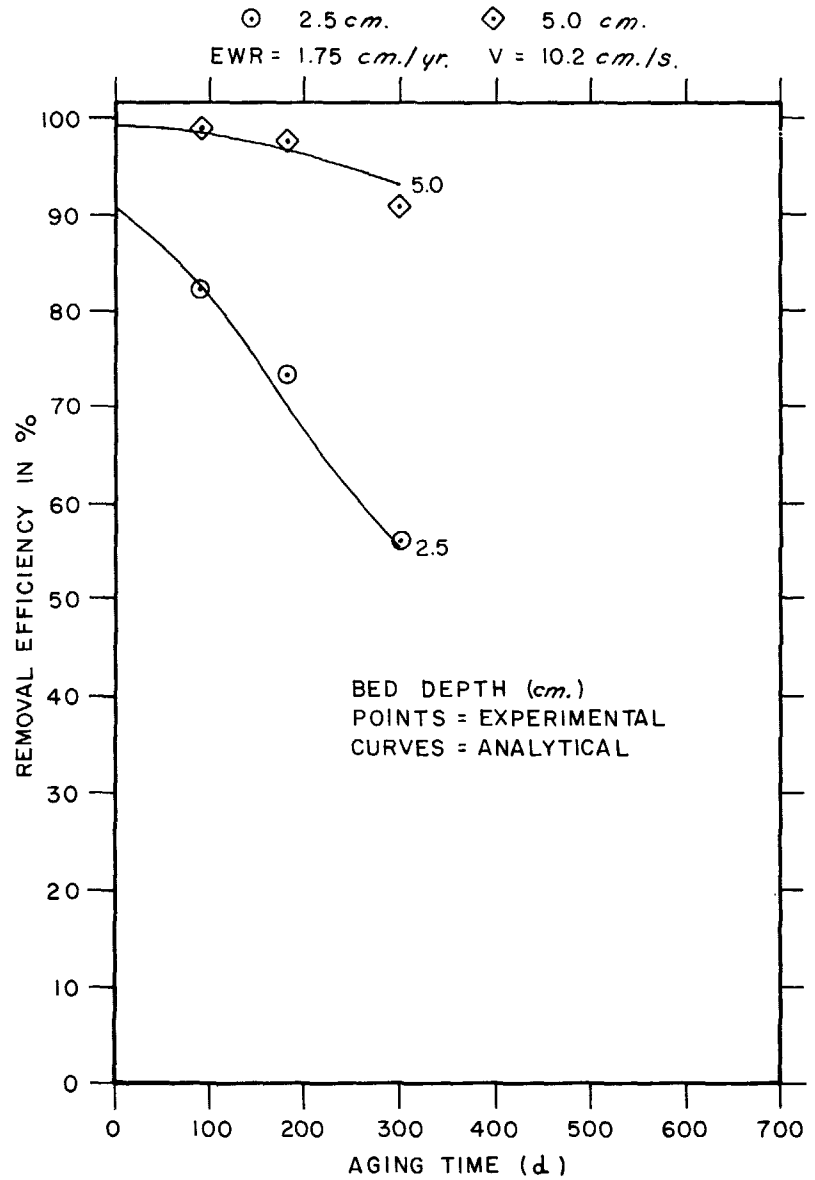


Figure 4. Experimental data from Table 2.10 of Reference 2 and corresponding analytical results.

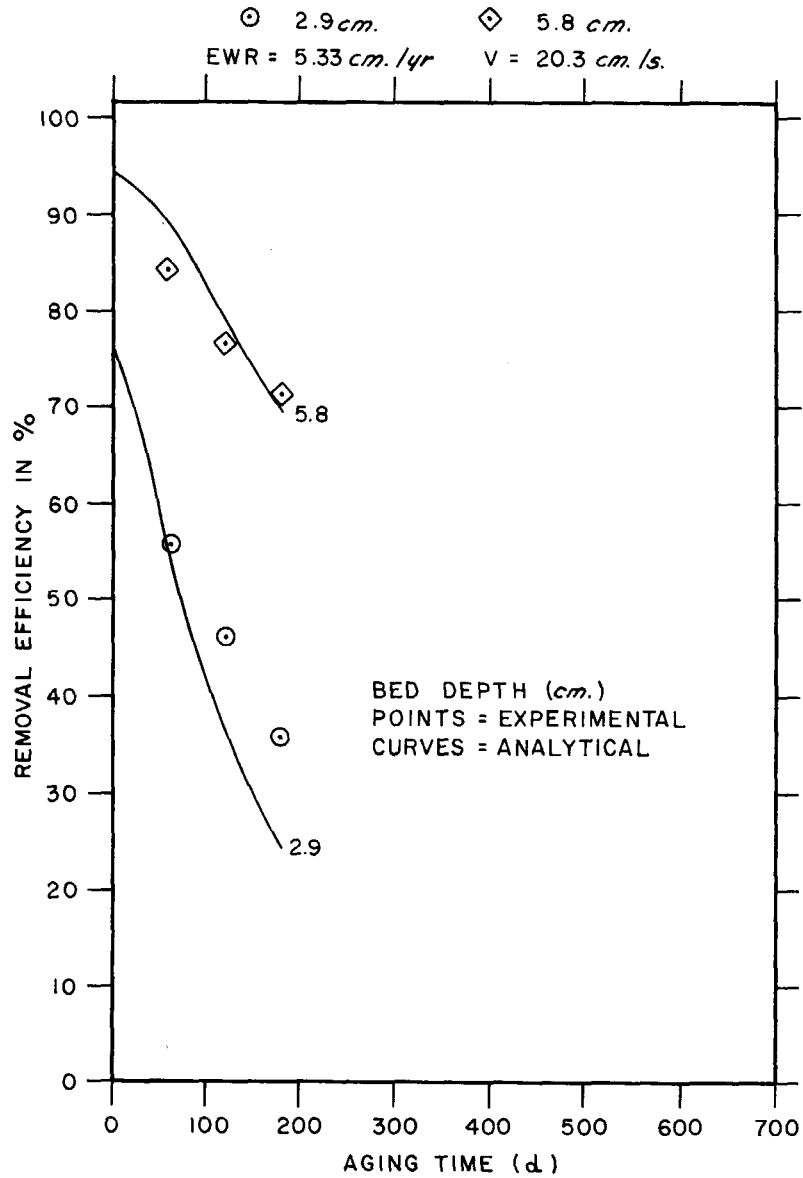


Figure 5. Experimental data from Figure 4 of Reference 3 (G617-BSR) and corresponding analytical results.

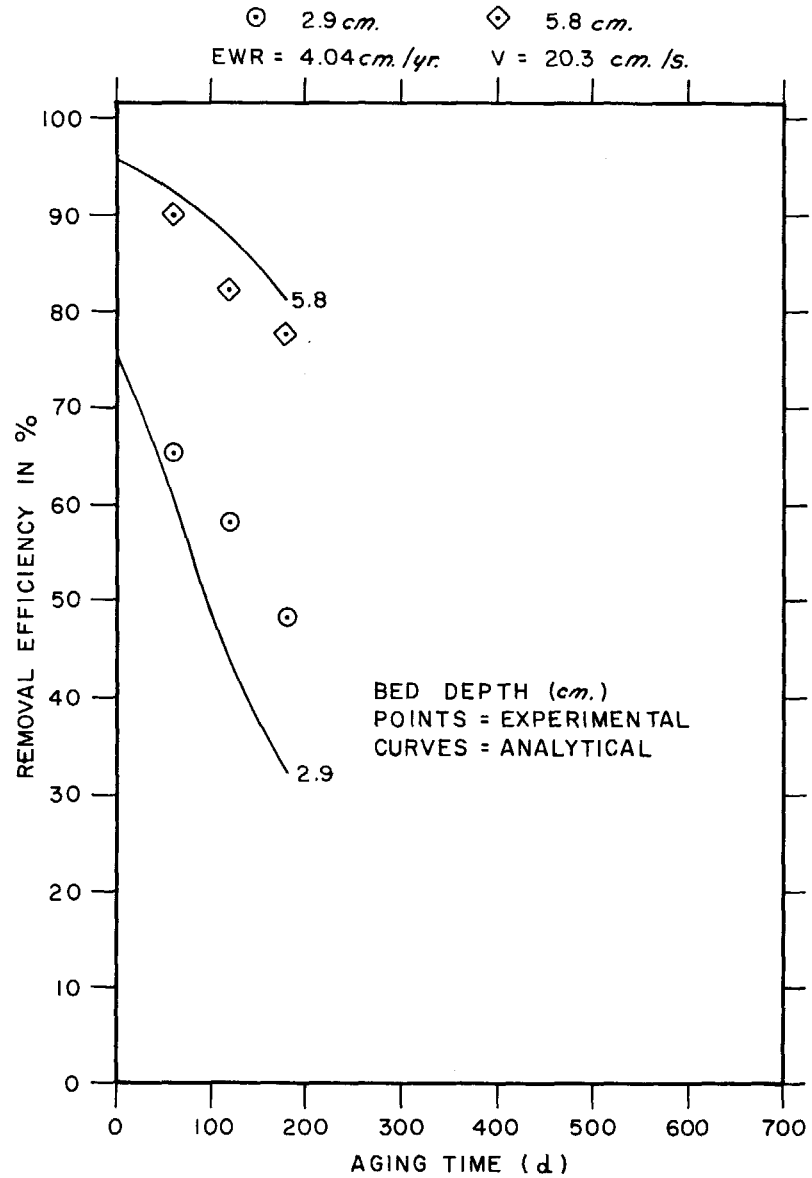


Figure 6. Experimental data from Figure 4 of Reference 3 (G617-HFIR) and corresponding analytical results.

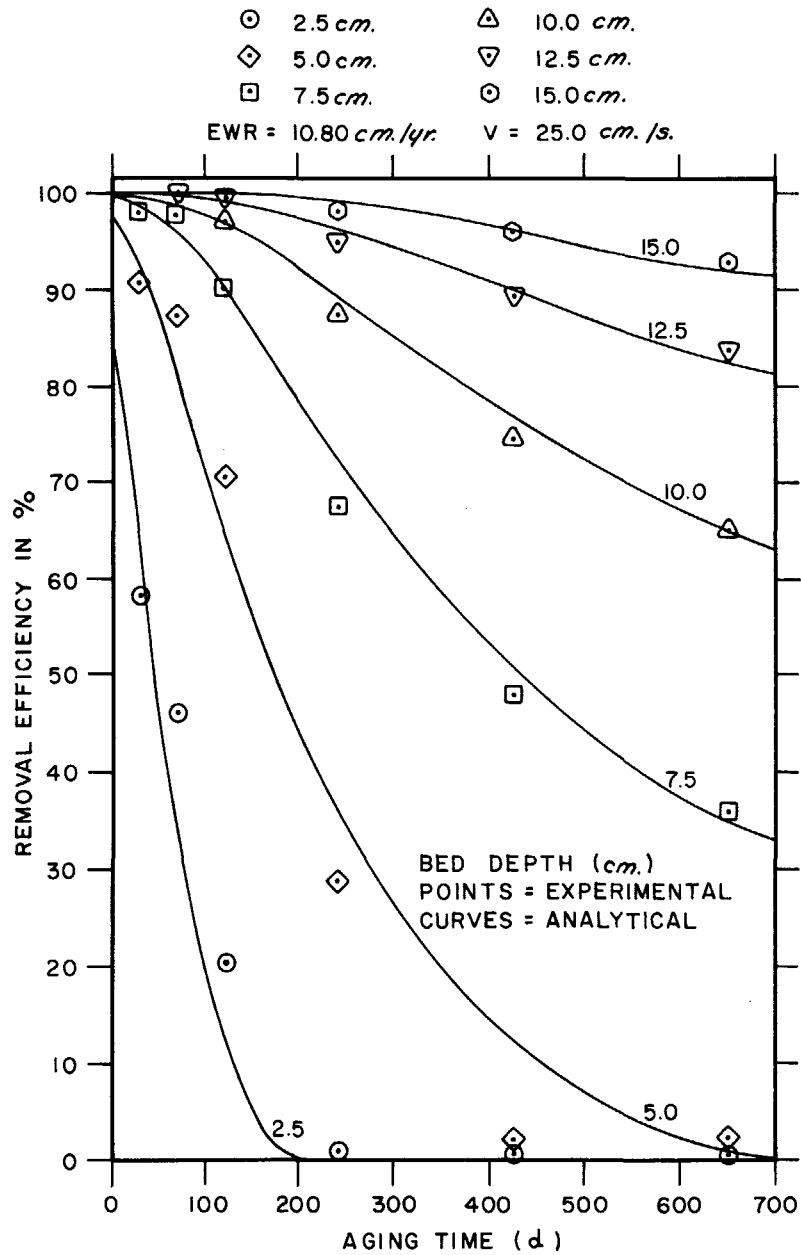


Figure 7. Experimental data from Figure 1 of Reference 1 and corresponding analytical results.

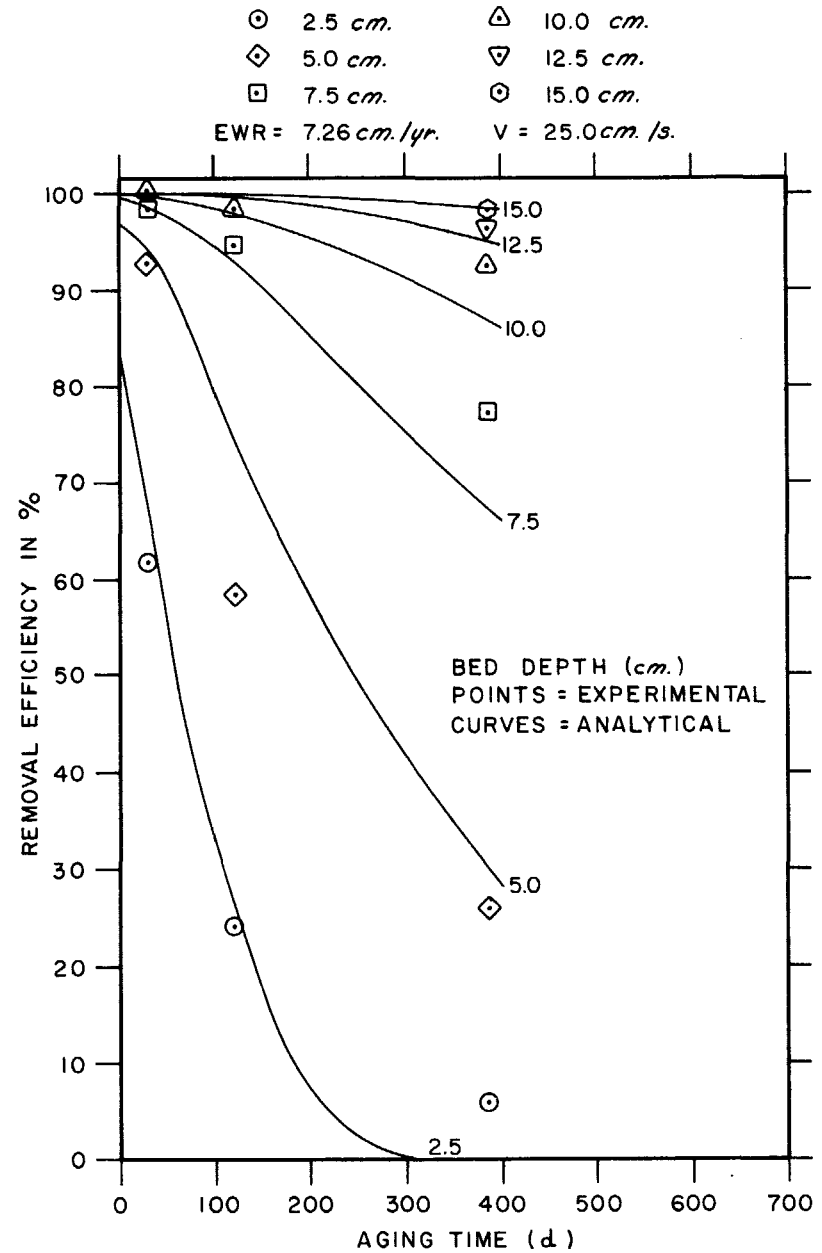


Figure 8. Experimental data from Figure 3 of Reference 1 and corresponding analytical results.

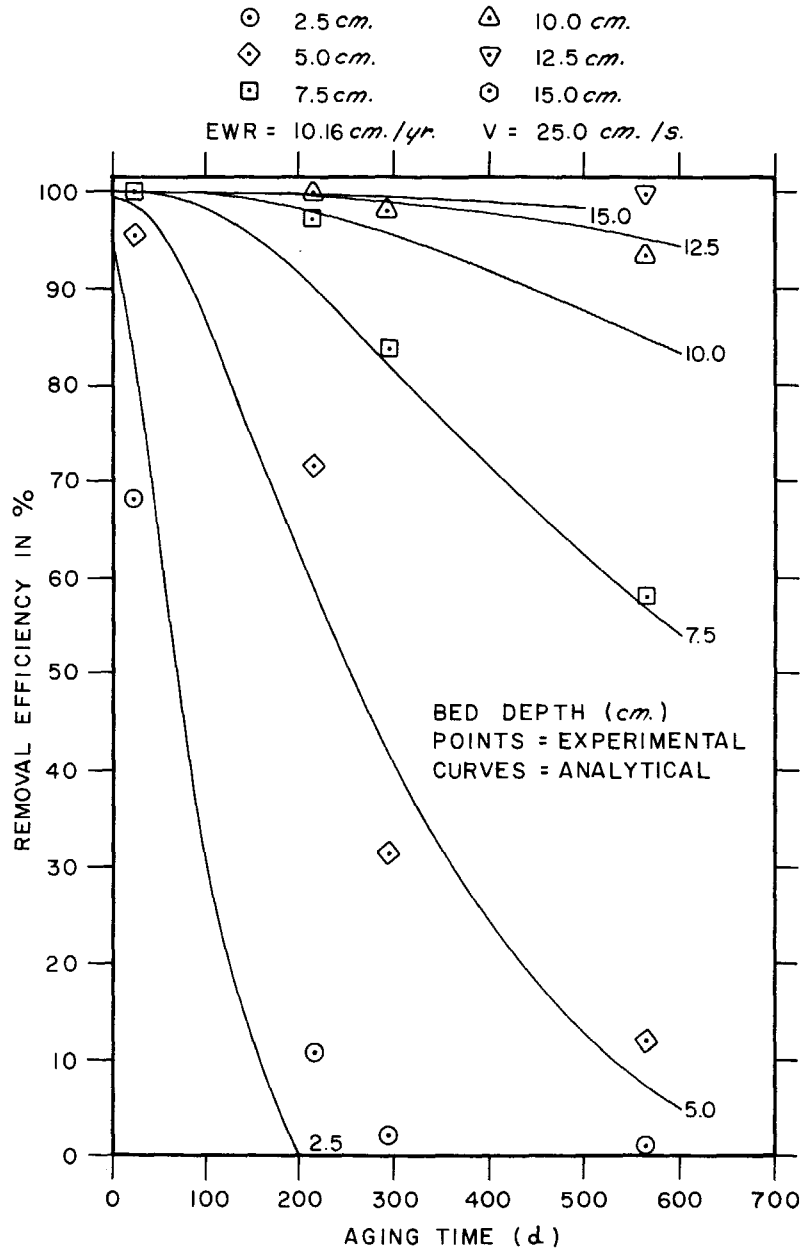


Figure 9. Experimental data from Figure 5 of Reference 1 and corresponding analytical results.

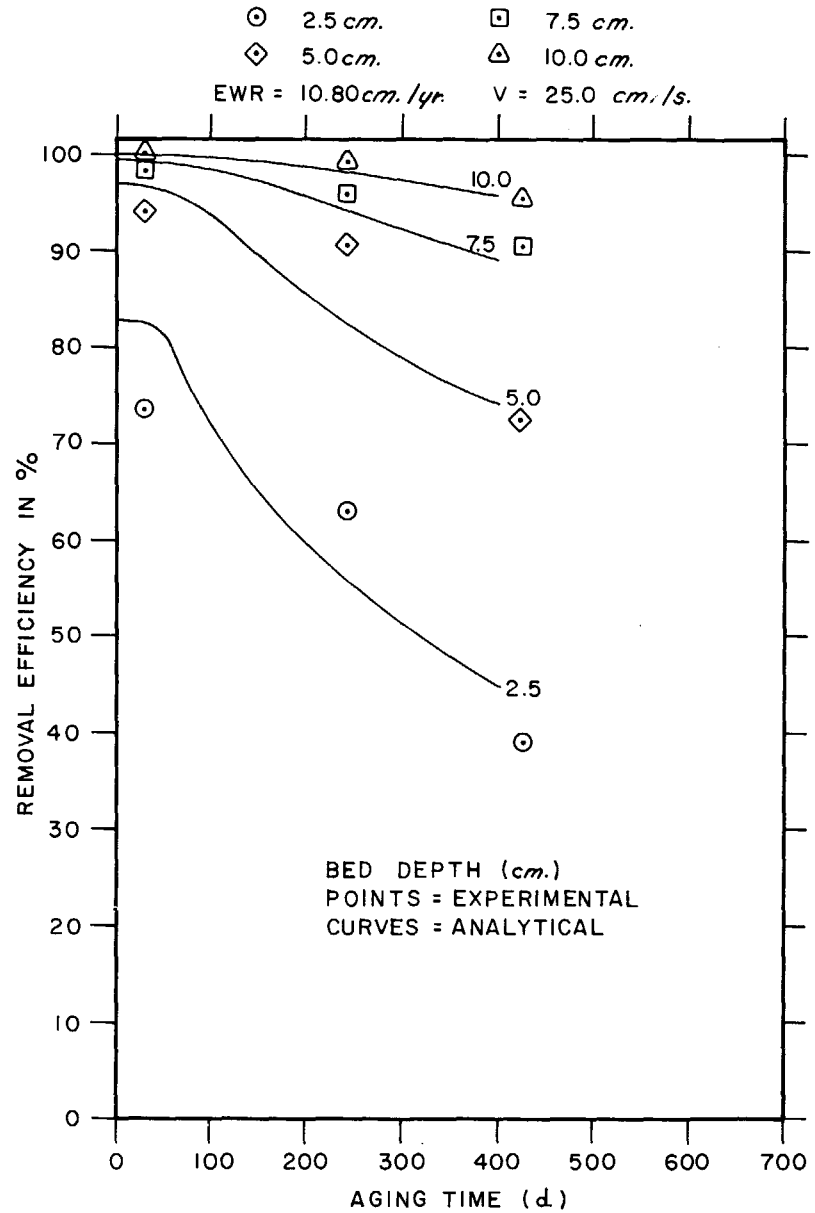


Figure 10. Experimental data from Figure 2 of Reference 1 and corresponding analytical results.

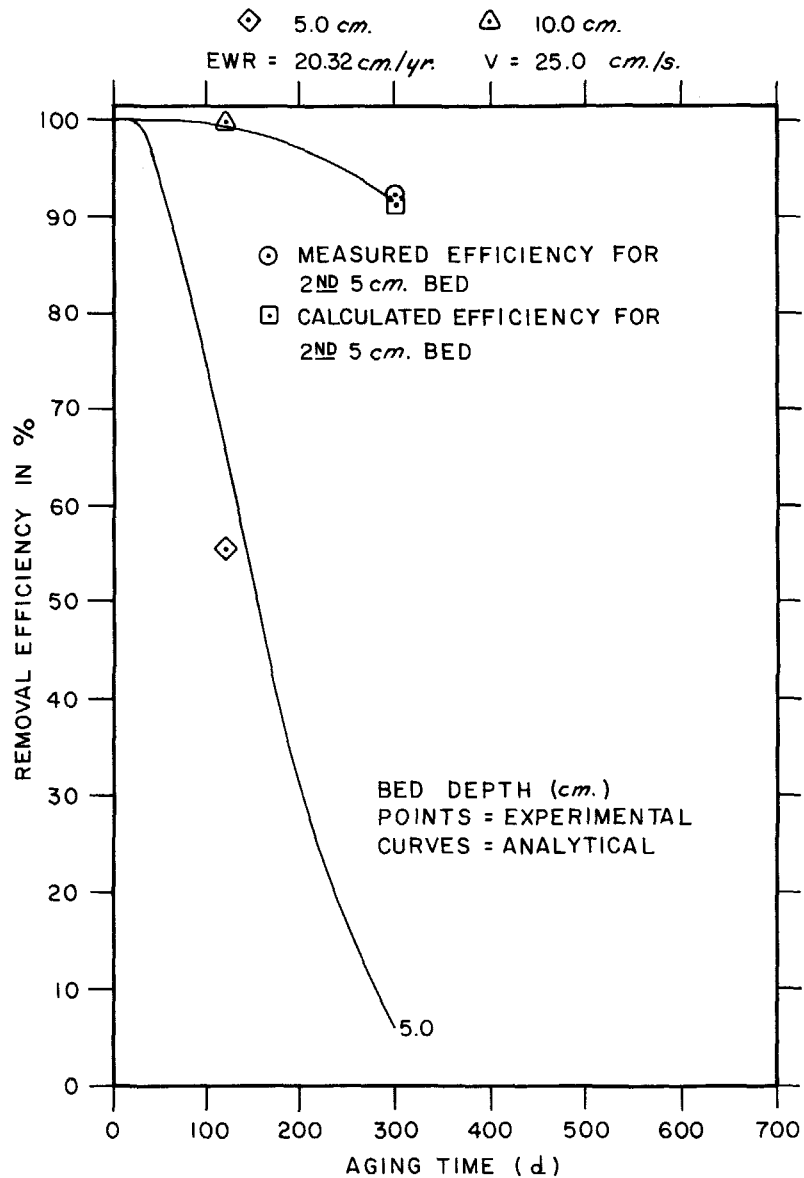


Figure 11. Experimental data from Table II of Reference 1 and corresponding analytical results.

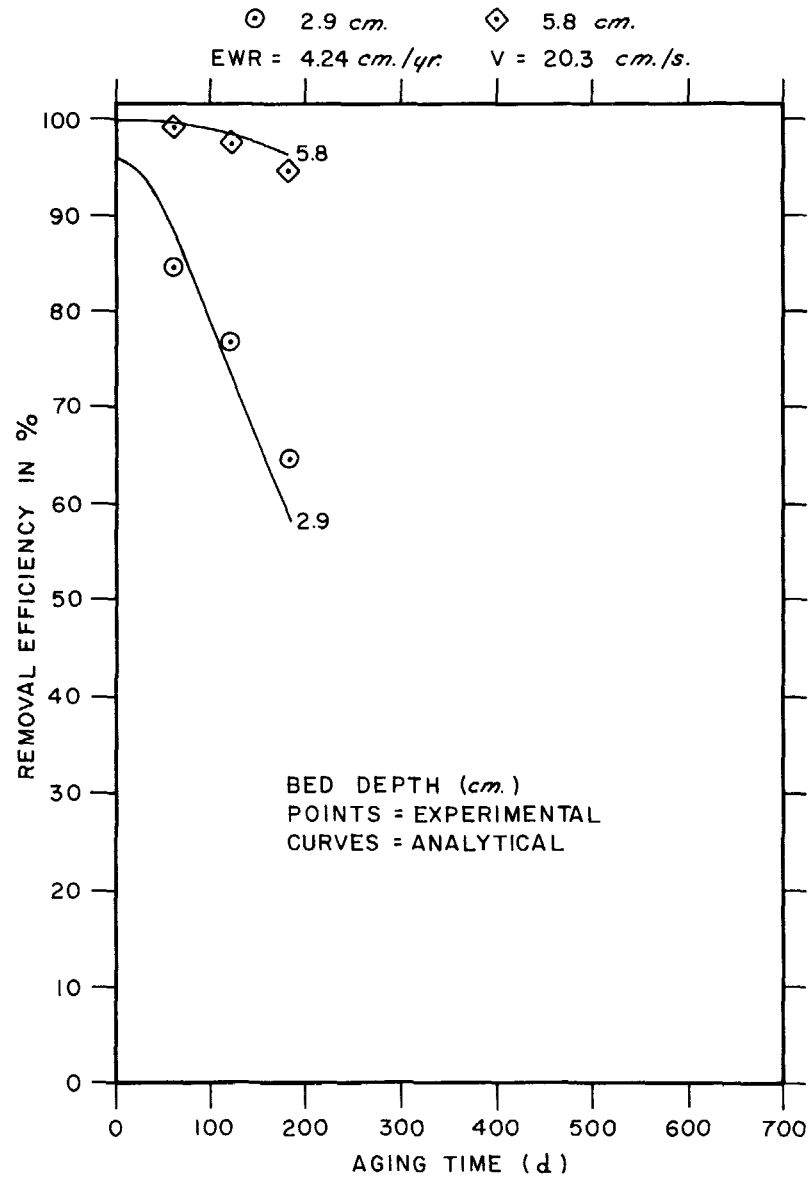


Figure 12. Experimental data from Figure 4 of Reference 3 (G618-E) and corresponding analytical results.

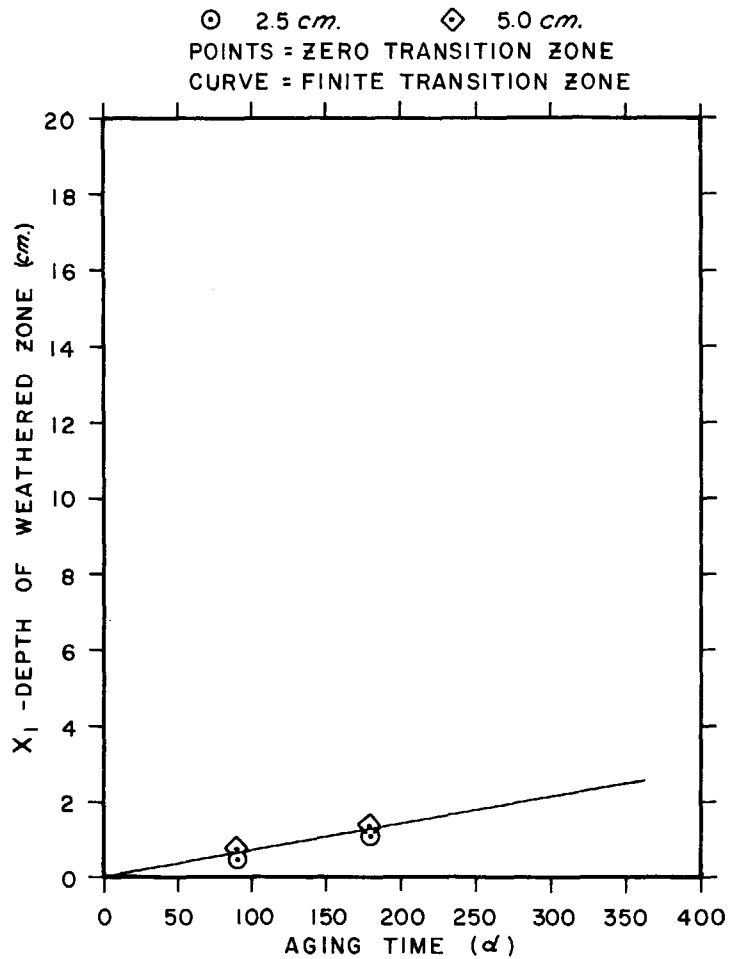


Figure 13. Comparison of results from two analytical models using data in Table 2.10 of Reference 2.

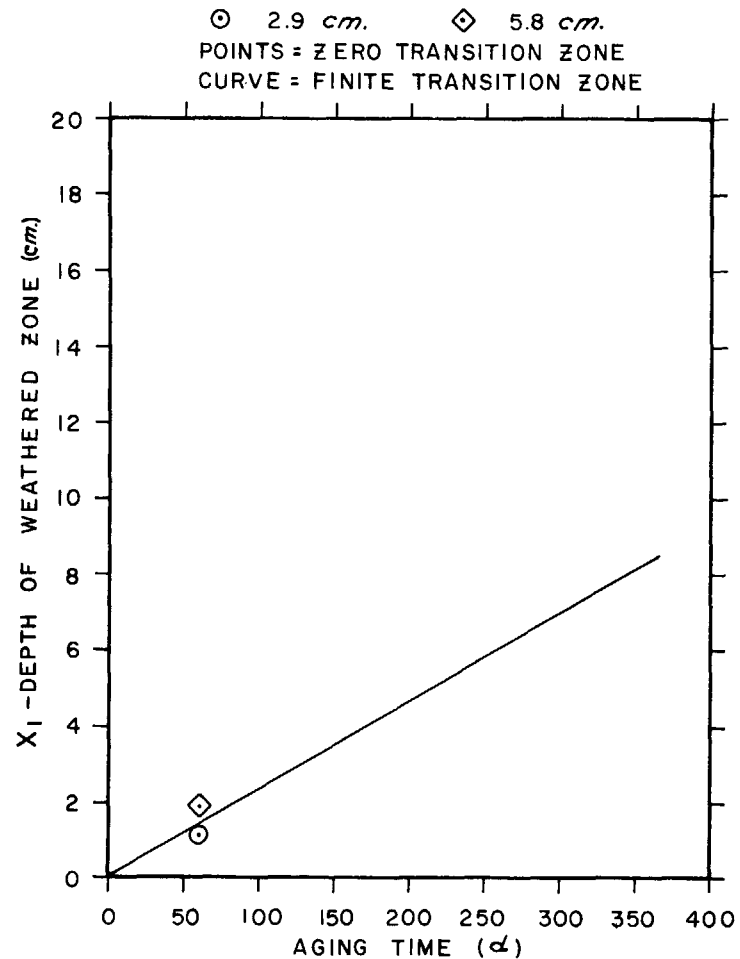


Figure 14. Comparison of results from two analytical models using data in Figure 4 of Reference 3 (G617-BSR).

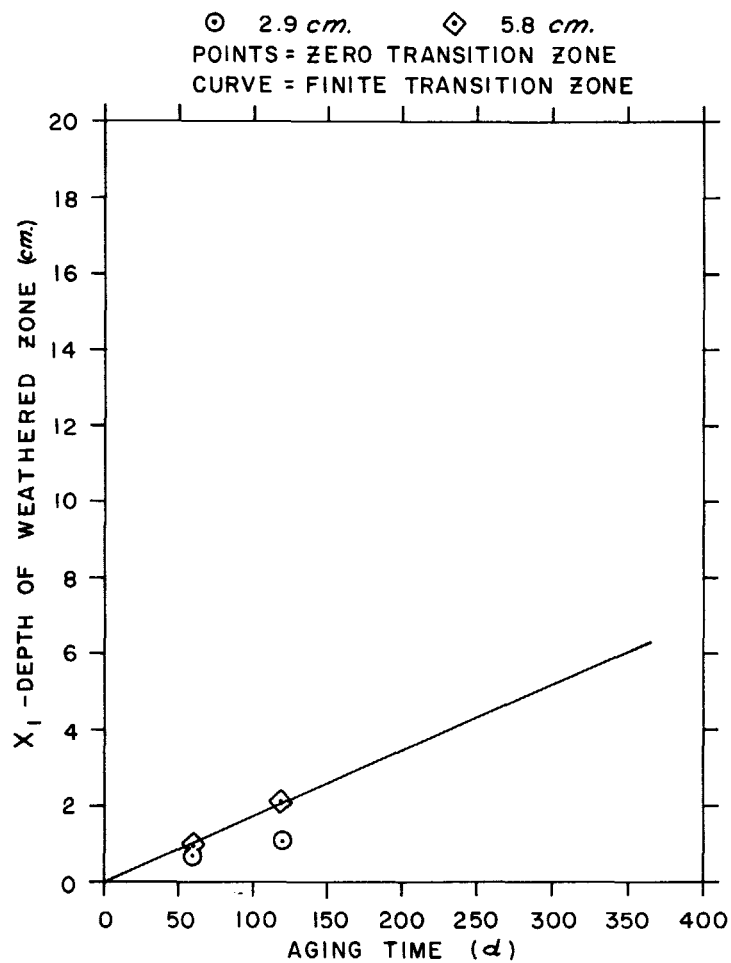


Figure 15. Comparison of results from two analytical models using data in Figure 4 of Reference 3 (G617-HFIR).

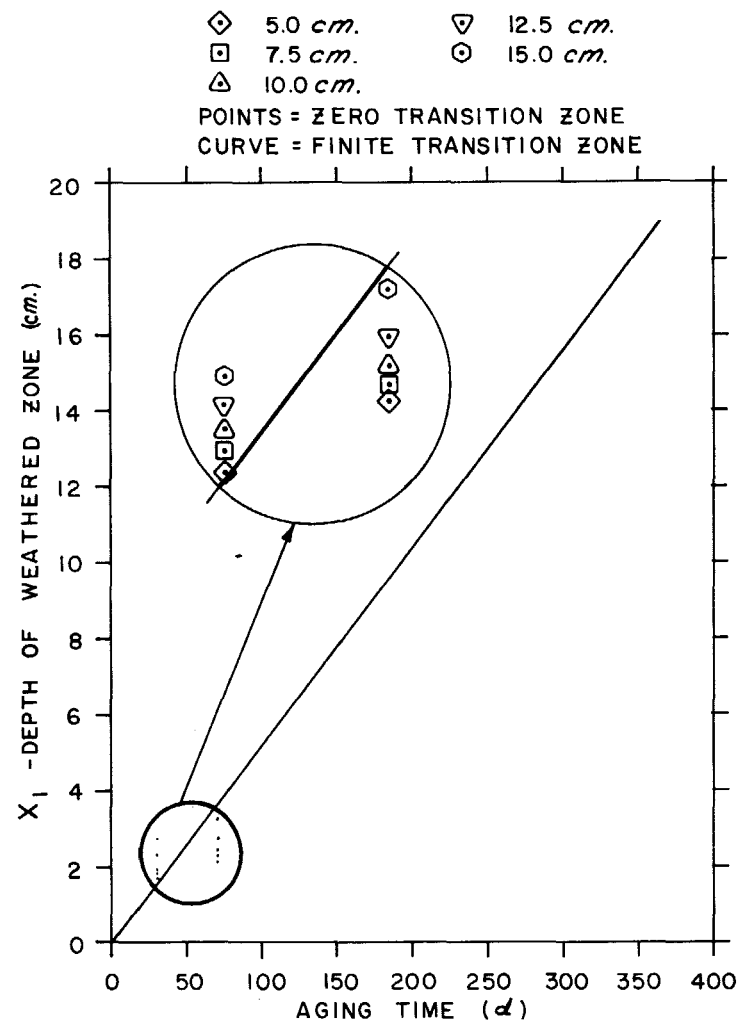


Figure 16. Comparison of results from two analytical models using data in Table I of Reference 1.

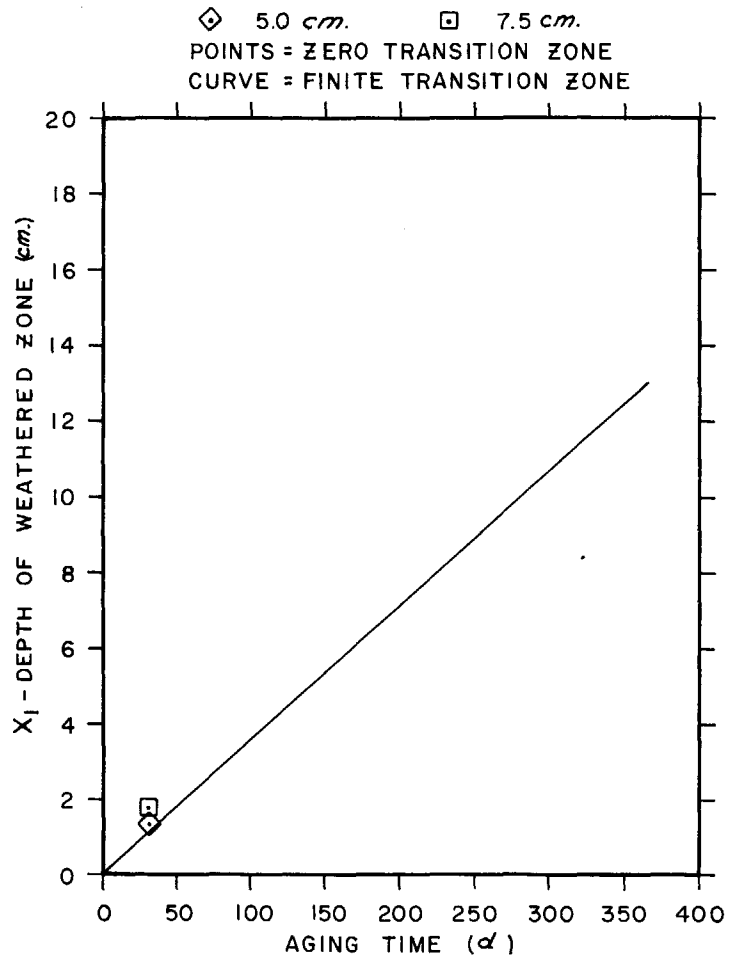


Figure 17. Comparison of results from two analytical models using data in Figure 3 of Reference 1.

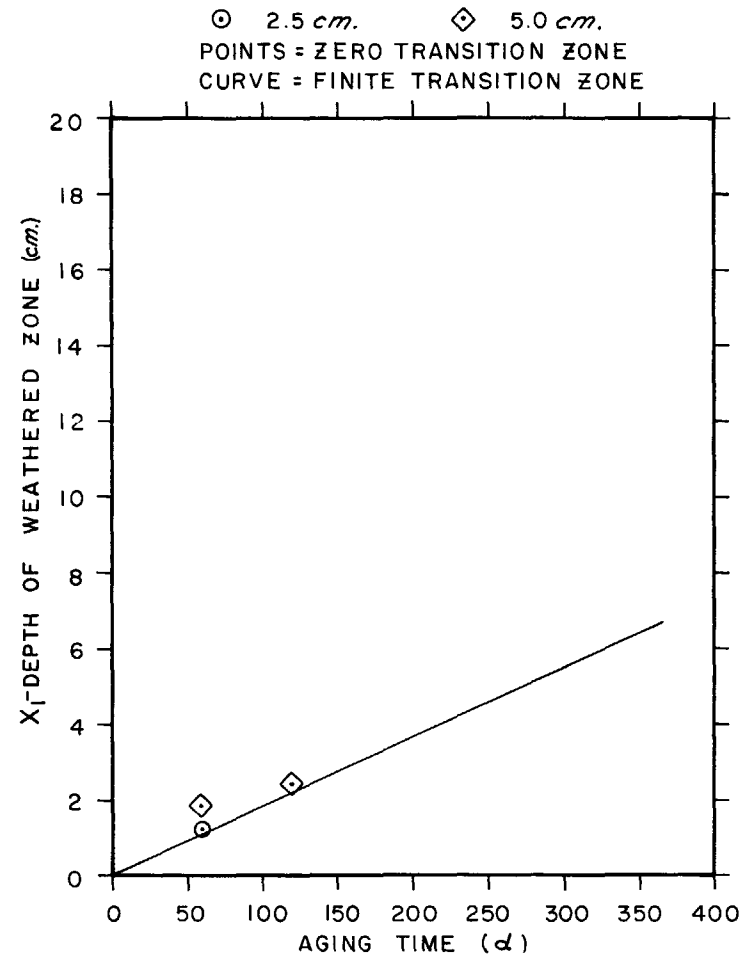


Figure 18. Comparison of results from two analytical models using data in Figure 4 of Reference 3 (G618-BSR).

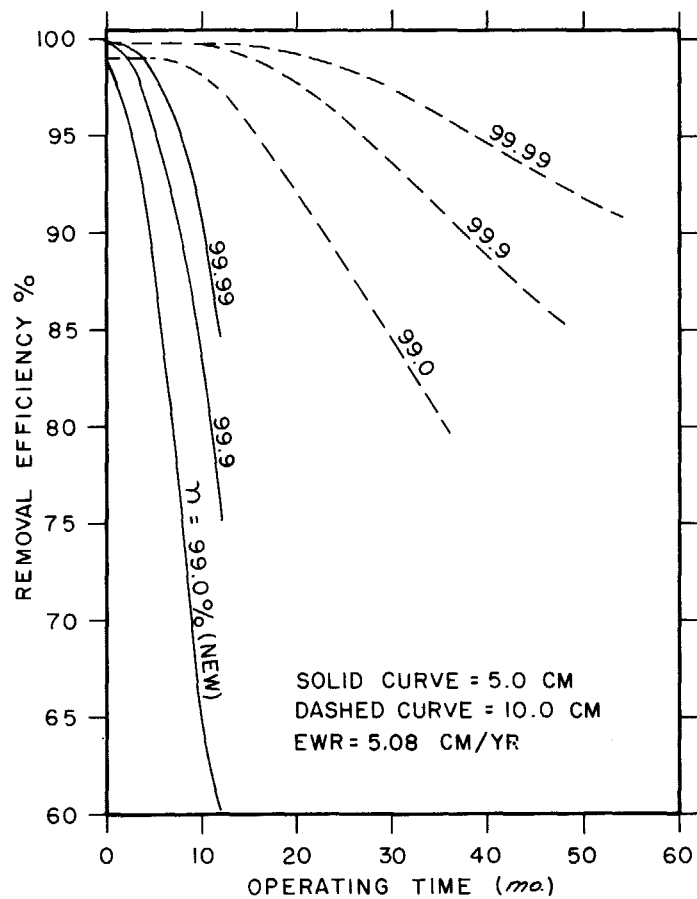


Figure 19. Predicted adsorber efficiency change with time as a function of performance in new condition.

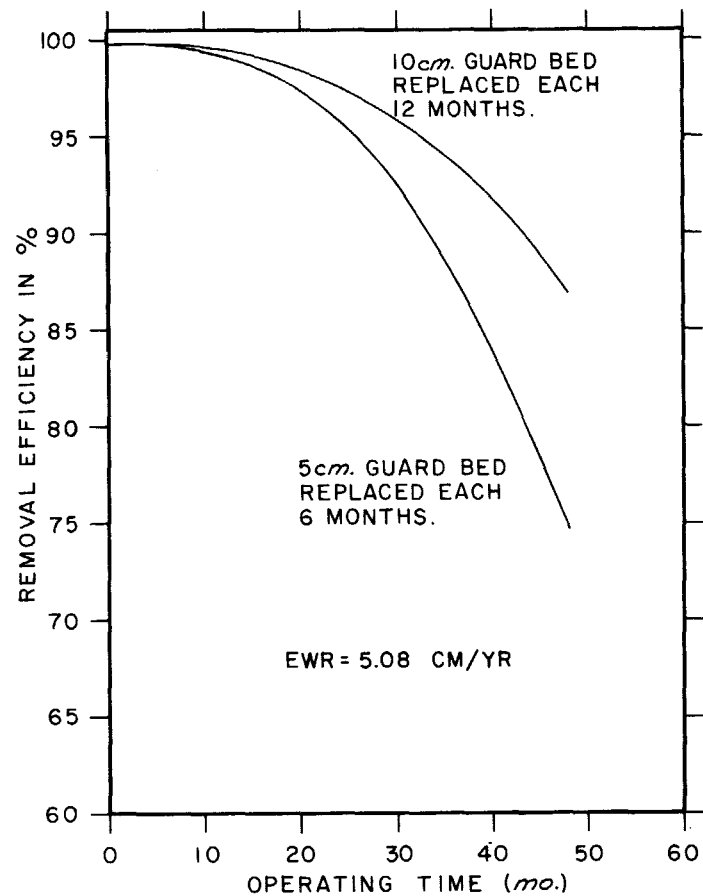


Figure 20. Predicted change in adsorber efficiency with sample guard bed depths and replacement schedules.

DISCUSSION

WILHELM: The reason for very quick loss of removal efficiency is a large amount of solvents and plastics being adsorbed by charcoal. We found that there is no homogeneous function to describe the real effect of the degradation of the charcoal. We found from our early experience in some reactor stations that were erected four years ago that charcoal with a given thickness should last two years. The data didn't fit all the new stations because solvents from recent painting were responsible for rapid degradation. I am a little hesitant to develop functions and correlations for the useful operation time of charcoal.

PARISH: I think we developed these ideas in the paper although I did not have time to elaborate here. It is our contention that the effective weathering rate (EWR) parameter is a function of the air quality. We are anticipating that it is quite possible that, based on analyses from data like this, we could correlate the variation in effective weathering rates with the concentration of hydrocarbons, sulfur dioxide, or other suspected weathering agents. By allowing the EWR parameter to vary, we have been able to fit all of the data that we have examined so far, which included quite a spectrum of data with respect to air quality. Remember that this is an empirical model, requiring experimental data in order to evaluate the EWR parameter. As far as we know, the data in our references were subject to the same limitation, in that they did not reflect performance after painting. Therefore, the analytical model is no more or no less applicable than the published data. As data on adsorbent efficiencies after painting activity become available, we would like to evaluate an EWR for that also. It should also be noted that the weathering model does not inherently require a constant EWR. It could very readily be adapted to a time variant EWR, so that it may be possible to handle transient behavior, also. To retain a proper perspective on this paper, I would emphasize that it is not suggested that this analytical model is a substitute for periodic testing of an adsorbent system. It is intended primarily as a design tool and a means for extending the utility of experimental data.

14th ERDA AIR CLEANING CONFERENCE

IODINE REMOVAL ADSORBENT HISTORIES, AGING AND REGENERATION

J.R.Hunt, L.Rankovic, R.Lubbers, J.L. Kovach
Nuclear Consulting Services Inc.
Columbus, Ohio

Abstract

The experience of efficiency changes with life under various test conditions is described. The adsorbents were periodically removed from both standby and continuously operating systems and tested under various test methods for residual iodine adsorption efficiency.

Adsorbent from several conventional "sampler" cartridges versus the bulk adsorbent was also tested showing deficiency in the use of cartridge type sampling.

Currently required test conditions were found inadequate to follow the aging of the adsorbent because pre-equilibration of the sample acts as a regenerant and the sample is not tested in the "as is" condition.

The most stringent test was found to be the ambient temperature, high humidity test to follow the aging of the adsorbent.

Several methods were evaluated to regenerate used adsorbents; of these high temperature steaming and partial reimpregnation were found to produce adsorbents with near identical properties of freshly prepared adsorbents.

I Introduction

Test conditions currently required by the NRC (1) (2) to follow adsorbent aging have been found inadequate because pre-equilibration of the sample can act as a regenerant and the sample is therefore not tested in the "as is" condition.

The CH₃I removal efficiency evaluation of new activated carbon is a well established technique, however evaluation of impregnated carbon exposed in stand-by or continuous service under a variety of environmental hazards is not as well known. Activated carbon, if exposed to an atmosphere containing organic vapors (paint, plastic outgassing, degreasing solvents, oil vapor, etc.), will adsorb and retain these vapors and such "aging" will decrease its efficiency for isotope exchange type removal of CH₃ ¹³¹I. Most procedures specified for adsorbent evaluation (1) (2) require extensive pre-equilibration under the test conditions to assure the establishment of moisture and temperature equilibrium between the test vapor and the test carbon. If the test conditions are near ambient (25°C) this "precaution" is acceptable even for "aged" carbons which may contain adsorbed organics. However if the postulated use condition is at elevated temperature, the impurities which "poison" the carbon are removed during the "pre-equilibration" period and the carbon regenerated before the introduction of the CH₃ ¹³¹I test charge.

14th ERDA AIR CLEANING CONFERENCE

Therefore the test will show a higher residual efficiency than the system, particularly if the system is normally at ambient and heaters would be activated only in case of humidity control. It is difficult to postulate initiation of heaters and "regeneration" of the adsorbent bed 4-16 hours prior to an accident.

II Procedure & Apparatus

During routine radiiodine testing of adsorbent samples sent to NUCON for analysis by various nuclear power plants, samples are occasionally tested which contain organic "poisons".

In one instance, adsorbed organics were suspected due to an extremely low $\text{CH}_3^{131}\text{I}$ efficiency. Subsequent steam stripping (100°C saturated steam) of the adsorbent revealed a 10-15% loading of organic material with a turpentine-like odor.

In another case, "poisoning" was suspected by a turpentine-like odor of the condensate after pre-equilibration during a steam-air test, not because of a low $\text{CH}_3^{131}\text{I}$ efficiency. Steam stripping of a fresh sample of this adsorbent indicated an organic loading of <1%.

In this experiment, the two adsorbent samples described above (both BC727 KI₃ impregnated coconut shell) and a sample of new BC727 were evaluated under various conditions of temperature, relative humidity and pre-equilibration time for $\text{CH}_3^{131}\text{I}$ removal.

Apparatus

The test apparatus consisted of stainless-steel and glass test bed assemblies fully enclosed in an environmental chamber. Temperature, relative humidity, pressure and flow were monitored continuously. Methyl iodide was supplied at a constant rate from a pressurized stainless steel generator.

Counting was performed in a 4.0 inch NaI well crystal. The counting efficiency of the system for ^{131}I is approximately 63%.

III Results

Table 1 Methyl iodide removal efficiency for new carbon (BC 727)

Temperature	Efficiency
20°C	89.20
40°C	90.80
60°C	94.72
80°C	98.75

Bed Diameter:	2.0 inch
Bed Depth:	2.0 inch
Face Velocity:	40 FPM
Relative Humidity:	95%
Pre-equilibration:	4 hours
Loading:	1 hour
Post Sweep:	2 hours
$\text{CH}_3 \text{I}$ Loading:	0.5 mg/m ³

14th ERDA AIR CLEANING CONFERENCE

Table 2 Decontamination factors for used carbon
(BC 727, 2 years, 10-15% organic contamination)

Temperature	Pre-equilibration time, hours					
	0		4		16	
Bed depth	1"	2"	1"	2"	1"	2"
20°C	---	1.46	1.23	1.42	1.17	1.37
40°C	1.40	2.00	----	----	----	----
60°C	1.89	3.54	----	----	2.3	4.4
80°C	2.19	5.18	----	----	2.2	35.97

Bed Diameter: 2.0 inch
 Bed Depth: as indicated
 Face Velocity: 40 FPM
 Relative Humidity: 70%
 CH₃I Loading: 0.5 mg/m³

Table 3 Methyl iodide removal efficiency for used carbon
(BC 727, 2 years, 10-15% organic contamination)

Temperature	Pre-equilibration time, hours					
	0		4		16	
Bed depth	1"	2"	1"	2"	1"	2"
20°C	----	31.75	18.36	29.76	14.39	26.86
40°C	28.71	49.92	----	----	----	----
60°C	47.02	71.74	----	----	56.53	77.31
80°C	54.41	80.93	----	----	54.62	97.21

Bed Diameter: 2.0 inch
 Bed Depth: as indicated
 Face Velocity: 40 FPM
 Relative Humidity: 70%
 CH₃I Loading: 0.5 mg/m³

Table 4 Decontamination factors for used carbon
(BC 727, < 1% organic contamination)

Temperature	Pre-equilibration time, hours			
	0	1	2	16
25°C	6.37	3.03	2.24	2.17
88°C	357.0	83.3		

14th ERDA AIR CLEANING CONFERENCE

Bed Diameter: 2 inches
 Bed Depth: 2 inches
 Face Velocity: 40 FPM
 Relative Humidity: 95%
 CH₃I Loading: ~0.5mg/m³

Table 5 Methyl iodide removal efficiency for used carbon
(BC 727, <1% organic contamination)

	Pre-equilibration time, hours			
Temperature	0	1	2	16
25°C	84.30%	67.02%	54.44%	53.82%
88°C	99.72%	98.80%		

Bed Diameter: 2 inches
 Bed Depth: 2 inches
 Face Velocity: 40 FPM
 Relative Humidity: 95%
 CH₃I Loading: ~0.5 mg/m³

IV Evaluation of Methyl Iodide Test Results

Table 1 reflects the well-known effect of decreasing CH₃¹³¹I efficiency with decreasing temperature on a new BC727 type carbon.

Although data is incomplete at 40° C (Tables 2, 3), at 60° C the lowering of the decontamination factor due to higher carbon moisture content is masked by the improvement obtained by desorption of the organic. At 80° C the effect is pronounced.

Tables 4 and 5 indicate results similar to those obtained with new BC727 except that due to "aging", the efficiencies are lower. Decreasing efficiency with increasing pre-equilibration time even at 88° C indicates the improvement is not as significant as the decrease in efficiency due to the increased moisture content of the carbon. Although it is not clear from the data available here, it is possible that the change in efficiency @ 88° C between 0 and 1 hour pre-equilibration due to increased carbon water content would have been much greater and in fact significant organic desorption did occur.

From Tables 2 and 3, it is evident that under certain conditions dramatic "improvement" of adsorbent samples may occur due to test methods which do not account for contaminant removal during pre-equilibration.

The degree to which efficiencies are "improved" and the ease with which such "improvements" are identified in the test data depends on a number of factors.

14th ERDA AIR CLEANING CONFERENCE

The results obtained in Tables 2 and 3 make identification of the problem in this particular case more simplified than in others.

More data is needed concerning water adsorption of nuclear grade activated carbons at various relative humidities over time and associated effects on $\text{CH}_3^{131}\text{I}$ efficiencies.

Identification of contaminants and their sources should be performed.

Additional test methods should be devised to assure that reported efficiencies represent the condition of the adsorbent as it will be used.

Although adsorbent regeneration may offer economic promise on a large scale, in the test rig it is often responsible for inaccurate results for systems which can least afford errors in the measurement of their efficiencies.

V Regeneration of Poisoned Carbons

One batch of chemically poisoned iodine impregnated carbon, which was in use at a PWR for four years and had insufficient methyl iodide removal efficiency was treated in various manners to improve or regenerate its efficiency.

The following treatment - CH_3I efficiency values were obtained:

Treatment	pH	$\text{CH}_3^{131}\text{I}$ Efficiency %	
None	5.2	42.60	130° C (RDT)
None	5.2	16.11	25° C (RDT)
16 Hours oven drying at 150° C	6.8	56.70	130° C (RDT)
3 Minutes at 400° C	7.5	78.50	130° C (RDT)
6 Minutes at 400° C	8.2	77.65	130° C (RDT)
Reimpregnate with KOH (1% Wt.)	9.5	86.70	130° C (RDT)
6 Minutes at 400° C and reimpregnate with KOH (1% Wt.) and KI (0.5% Wt.)	10.4	92.50	130° C (RDT)
6 Minutes at 400° C and reimpregnate with KOH (1% Wt.) and TEDA (0.5% Wt.)	10.8	96.82	130° C (RDT)

The residual total iodine both after the 3 and the 6 minutes exposure at 400° C was 1.2%.

Based on the results it appears that some grades of chemically contaminated carbons can be regenerated successfully by flashing-off the impurities and reimpregnating the carbons.

The hardness and ignition temperature of the carbon after regeneration, reimpregnation and rescreening are in the RDT and Regulatory Guide 1.52 specified acceptable region.

Based on evaluation of carbons to date, there appears to be two distinct types of poisoning. One results in acidification of the carbon; the other is solvent contamination, however often both methods of poisoning exist and it is difficult to state generalized treatment for regeneration of all carbons.

14th ERDA AIR CLEANING CONFERENCE

VI Random Observations Regarding Testing of Systems and Adsorbents

Several observations were made which may contribute to the improvement of components and systems.

(1) Adsorber cells, where the rough side of the perforated cell is turned toward the carbon, generate more fines and result in faster loading of downstream HEPA filters.

(2) Adsorber cells which inadvertently got wet if not emptied and washed immediately completely disintegrate due to iodide corrosion.

(3) The mechanical integrity of many cells is inadequate to withstand repeated handling. Cells shipped to NUCON for refilling show missing handles, missing slide plates and broken studbolts.

(4) Many currently installed "sampling" cartridges are totally inadequate. Tests performed on cartridges and on bulk carbon were found to be different by 2-25% in $\text{CH}_3^{131}\text{I}$ removal efficiency--in all cases the cartridges showing higher remaining efficiency. Additionally, the cartridges often contain loose carbon, indicative of faulty filling methods.

(5) Radiation exposure of test personnel during in-containment tests results in 75-500 mR dose primarily from neutron radiation. Such systems should be converted to permit remote leak testing where personnel are in shielded area.

Non-containment systems testing results in average of 5-15 mR dose per test series of 2-4 days' duration.

References

1. "Design, testing and maintenance criteria for atmospheric cleanup system air filtration and adsorption units of light-water-cooled nuclear power plants." Regulatory Guide 1.52 (June 1973)
2. "Gas-phase adsorbents for trapping radioactive iodine compounds." RDT M 16-I (October 1973)

DISCUSSION

RIVERS: In your Table 5, at 25°C the penetration increased steadily as pre-equilibration time was increased; which is rather the reverse of the high temperature situation.

HUNT: In this case, the decrease in efficiency was due directly to the varying pre-equilibration time. In other words, as the pre-equilibration time increased, the adsorption of water on the carbon also increased. Adsorbed water on the carbon decreases methyl iodide efficiency.

EVANS: The regeneration technique that seemed to be most effective was raising the temperature to 400°C. The effect of this was to burn off organic vapor and surface oxides, was it not?

KOVACH: Yes, you are correct.

WILHELM: We agree that if you test aged charcoal in the laboratory, you will find all you have just told us. The question is, really, how meaningful is the test in the laboratory, leaving apart the dependence on the preconditioning time and other conditions. We found that, in most filter systems, the test charcoal in a bypass of the installed filter doesn't have the same air changes as the main unit. Therefore, it doesn't compare well enough to the main unit. One reason may be that the bulk density of the charcoal in a small scale sampler is often lower than the bulk density in big charcoal beds. Thus, laboratory results may not relate directly to full scale performance.

HUNT: I would like to make another comment. The second carbon was run originally in a steam-air test at 130°C and the removal efficiency was really quite good. However, the man that was running the test noticed a distinct odor, and the odor on both of these carbons was something like kerosene. In the condensate after equilibration, this odor was noticed on the sample, which had 1 per cent organic contamination. That is how we discovered there was organic contamination on the carbon; not because we got a poor test result. In fact, probably the reason we got such a good test result was because we steamed off the organic contaminant during pre-equilibration.

14th ERDA AIR CLEANING CONFERENCE

NEW CHARCOAL IMPREGNANTS FOR TRAPPING METHYL IODIDE I. SALTS OF THE IODINE OXYACIDS WITH IODIDE OR IODINE AND HEXAMETHYLENETETRAAMINE

Victor R. Deitz and Charles H. Blachly
Naval Research Laboratory
Washington, D. C. 20375

Abstract

Iodine in its various chemical compounds can have the oxidation states I^- , I^0 , I^{+1} , I^{+5} and I^{+7} . When alkali salts of the iodine oxyacids (KIO , KIO_3 and KIO_4) are mixed with iodides (I^-) and/or elementary iodine in basic solution, the mixtures containing the extremes in valence states are converted into compounds of intermediate charge. A number of charcoals were impregnated with selected mixtures and these proved to be excellent trappers for methylradioiodide. Hexamethylenetetraamine (HMTA), a tertiary amine having a high flash point and low volatility, was also included in the impregnations investigated as a second impregnate. About two hundred samples were impregnated with the iodine mixtures and HMTA using the 2-stage process on a variety of base charcoals and these were evaluated for methyl iodide trapping and ignition behavior. Some of the promising impregnated charcoals were also evaluated in other laboratories. The results are presented and a fundamental interpretation proposed for the trapping mechanism based upon a dissociation-controlled exchange (the exchange controlled by dissociation of one of the species) via a simple effective chain reaction.

I. Introduction

Previous charcoals for trapping methyl iodide have been impregnated with potassium iodide plus iodine (KI_x) and/or with triethylenediamine (TEDA). The impregnation process has been chiefly proprietary information. A detailed study of a trapping process must, however, start with known systems: well-characterized base charcoals, known impregnating solutions, and a well defined test procedure for contacting the charcoals with methyl iodide. Thus, the chemical problems fall within two groups:

- (1) adsorption of the impregnant chemicals from solution including the surface changes that take place upon subsequent drying of the impregnated charcoal, and
- (2) the surface reactions at the gas-solid interface during the trapping process.

The latter have been described in general terms as either an isotope exchange, when a large amount of normal iodine is present as e.g. KI_x , or as the formation of the adsorbed quaternary iodide by dissociative addition when TEDA was present.

The many publications and reports of the Oak Ridge National Laboratory in this country (1a, 1b, 1c) and those of the U.K. Atomic Energy Authority (2) have been very helpful in the present investigations and these are gratefully acknowledged.

II. Adsorption from the Impregnating Solutions

Iodine in its various chemical compounds includes the oxidation states I^- , I^0 , I^{+1} , I^{+5} and I^{+7} . Noteworthy features (3) are the instability of the compounds with respect to disproportionation in alkaline solution, the comparative stability of IO_3^- , and the instability of the +3 oxidation state (i.e. no chemical evidence for its presence has been found). It is apparent, therefore, that the alkali salts of the iodine oxyacids (KIO , KIO_3 and KIO_4) can have a complex solution chemistry when mixed with the iodides (KI) and/or elementary iodine (I_2).

When the salts of the iodine oxyacids are present in basic aqueous solutions, there are several equilibria that convert the initial species to intermediate oxidation state. In general, one of the iodine species is oxidized and the second reduced. Some of the combinations reported in this paper as impregnating solutions on charcoal are: KIO_4+KI , KIO_4+I_2 , KIO_3+I_2 , KIO_3+KI , and $KOH+I_2$. In many cases the calculated heats of formation were favorable for certain postulated reaction products of intermediate oxidation states.

A systematic study of the adsorption from solution of oxyiodine salts by charcoals has not been reported. Although limited solubility is in general accompanied by high adsorption, the oxyiodine salts of interest have a high solubility. Since the adsorption from solution increases with concentration, the impregnating solutions were dispersed by a sprayer into fine droplets which were contacted with a quantity of dry charcoal contained in a slowly rotating cylinder having inclined lifts. Some water in the solution could thus migrate into the microstructure of the charcoal leaving the solute at high concentration to be adsorbed in the outer structure. The conditions were selected so that charcoal always had a dry appearance after impregnation.

Subsequent to the impregnation of the oxyiodine salts, a very effective measure was to impregnate the charcoal with a high flash-point amine such as hexamethylenetetraamine (HMTA)*. As will be shown, such a two-step process was found to yield the minimum penetration of methylradioiodide for most base charcoals. Furthermore, the use of a high flash-point amine after the introduction of the oxyiodine salts was found to raise the ignition temperature of the charcoal. With the concentrations carefully adjusted, the charcoal retained a dry appearance after the 2-stage impregnation.

* Synonyms for hexamethylenetetraamine $(CH_2)_6N_4$ are methenamine, formamine, hexamine and urotropin. The rhombic crystals melt with charring at $270^\circ C$ and the flash point is $233^\circ C$.

The drying of the charcoal after impregnation is an important operation. Times longer than 5 hours and temperatures in the range 95 to 105°C are preferred.

Base charcoals from different sources yield individual trapping efficiencies when the same impregnation formulation is used. The behavior may be due to the extent to which the reactants on the various charcoals yield the necessary intermediate species for trapping methyl iodide.

III. Methyl Iodide Trapping: Procedure and Results

The test procedure outlined in the RDT Standard M-16⁽⁴⁾ was followed. The results given in this paper used the parameters listed below:

Diameter	5.08 cm	2 in
Length	5.08 cm	2 in
Air Flow	25 L/min.	0.88 CFM
Linear Velocity	21 cm/sec.	41.5 ft/min.
Contact time	0.254 sec.	
Relative humidity		
%	95-97	
Prehumidification		
time	16 hours	
Time of dose	2 hours	
Time for purge	2 hours	
Temperature	22°C	

The dose of methyl iodide was 55 microliters or 125 micrograms of the liquid per g. charcoal. The total air flow for 2 hours is equivalent to 3 cubic meters. With sample weights of 40, 50, and 60 grams, the total doses were 5.0, 6.25, and 7.5 mg or 1.67, 2.10 and 2.5 mg/m³. The methyl iodide was purchased from ICN Life Sciences, Irvine, California at 5000 µCi per ml liquid. The liquid was injected with a Gilmont digital micrometer syringe of 0.25 ml capacity directly into the air stream at equal increments over the 2-hour dosing period.

Figure 1 is a diagrammatic sketch of the charcoal test container and the back-up beds. Each component was fabricated from a pair of Pyrex O-ring (Viton) connectors, size 50mm I.D. (Kontes Glass Co., Type M). The Viton did not become radioactive after exposure to methylradioiodide. The connectors were held together with "Pinch Type" clamps. The humidified air stream enters at the top: A is the humidity sensing element, b thermometer, C septum closure, D test sample of charcoal, E backup beds, F location of an O-ring, G exit to flowmeter. The charcoal is supported on discs of perforated stainless steel screen.

The counting was done with a Nuclear-Chicago Model 470 gas-flow detector with the Model 8712 Decade Scaler. The percent penetration of the bed was determined from the relation

$$\% \text{ Penetration} = \frac{\text{CPM in back-up beds}}{\text{Total CPM in sample and back-up beds}}$$

14th ERDA AIR CLEANING CONFERENCE

The reproducibility for several samples may be seen from Table I. The volume of each charcoal, 106 cm³, was divided after mixing into 8 aliquots and each (5.6 mm average depth) was counted. The variance was found to be less than 5%. The efficiency was estimated in the counting of the charcoals with the above facility (Table I) and the value appears to depend on the charcoal, the impregnation and possibly to the extent on prehumidification. The following tests were made keeping the three parameters constant. Preparation 4144 was prehumidified in duplicate (34% weight gain). The top section was counted after methyl iodide dosing and then the section was progressively diluted with equal volumes of non-dosed prehumidified charcoal. A linear dependence (Figure 2) was observed between the count and the dilution factor indicating a constant counting efficiency for the sample.

Table I

Reproducibility in the Counting of Impregnated Charcoals After Exposure to Methyl Iodide - 131

	<u>4017</u> <u>17 June</u>	<u>4184</u> <u>19 June</u>	<u>4185</u> <u>19 June</u>	<u>4186</u> <u>20 June</u>
	13820	5243	2989	79232
	12431	5273	2947	77278
	14079	5273	3023	76003
	13910	5001	2956	81000
	14162	5222	3002	79804
	13278	5357	3026	77178
	13013	5503	3124	75369
	<u>12928</u>	<u>5284</u>	<u>3019</u>	<u>76020</u>
Mean	13452	5269.5	3011	77736
Std. dev.	630.5	140	54.6	2044
Variance	4.7%	2.7%	1.8%	2.6%
Efficiency	12.6%	7.9%	4.6%	2.6%

The results (Table II) are for independent impregnations using a coal-base charcoal (Union Carbide MBV 6/14). The reproducibility of the procedure includes the uncertainties in withdrawing the sample from the supply of base charcoal, the preparation of the solution, the impregnations, and the drying. In addition, the introduction of the impregnants via a 1-step or 2-step process indicates that the latter yields a product of about half the penetration, everything else being kept the same.

14th ERDA AIR CLEANING CONFERENCE

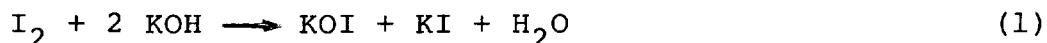
Table II

Penetration of Methylradioiodide Through a Coal-Base Charcoal: 1-step vs 2-step Process of Impregnation

<u>Sample</u>	<u>Impregnant for 100g Charcoal</u>		<u>Methyl Iodide Penetration %</u>
4203	5g HMTA, 1g I ₂ , 1.5g KOH		0.41
4206	5g HMTA, 1g I ₂ , 0.375g KOH		0.58
4208	5g HMTA, 1g I ₂ , 0.375g KOH		0.85
4212	5g HMTA, 1g I ₂ , 0.44g KOH		0.72
4212R	5g HMTA, 1g I ₂ , 0.44g KOH		<u>0.93</u>
			0.70 av.
	<u>Step 1</u>	<u>Step 2</u>	
4215	I ₂ , KI, KOH	HMTA, 5g	0.51
4221	I ₂ , KI, KOH	HMTA, 5g	0.30
4222	I ₂ , KI, KOH	HMTA, 5g	0.43
4225	I ₂ , KI, KOH	HMTA, 5g	0.30
4226	I ₂ , KI, KOH	HMTA, 5g	0.29
4227	I ₂ , KI, KOH	HMTA, 5g	<u>0.29</u>
			0.35 av.

Test conditions: Bed diameter 2-inch; height 2-inch; contact time 0.25 second; prehumidification 16 hrs. at 96 RH %

Two series of impregnations were made with a coal-base charcoal (Union Carbide MBV 6/14) in which the total iodine was maintained at 1 wt. % of the charcoal. The common aspect of these impregnations is the disproportionation to form the hyperiodite group, which is more favorable in alkaline than in neutral media. It is rapid at room temperature



The disproportionation of KOI to form the iodate and the iodide is also rapid at room temperature



There are no substantiated accounts of the isolation of solid hypoiodites. However, in solution the presence of excess base stabilizes

14th ERDA AIR CLEANING CONFERENCE

the OI^- to some extent and it is reasonable that this may be carried over to the adsorbed species on charcoal. The presence of KIO_3 and KI on a charcoal may be viewed as a potential source of KOI in small but finite quantities. The use of KOH plus KI as reactants in the impregnating solutions was likewise found effective. The results (Table III) include variations in the proportion of I_2 and KI , all with KOH present at a solution pH of 10 to 11. The observed penetrations of methyl iodide were quite low, all being in the range 0.1 to 0.4% and an average of 0.25%.

Table III

Impregnation of Coal-Base Charcoal (Total Iodine 1 wt.% of Charcoal)

Sample	Impregnation in 2 Steps		Methyl Iodide Penetration (%)
	1st	2nd	
4236	I_2 , KI , KOH	1% HMTA	0.44
4246	I_2 , KOH	2% HMTA	0.13
4248	I_2 , KOH , Na_2HPO_4	2% HMTA	0.06
4243	I_2 , KI , KOH	1% HMTA	0.17
4242	I_2 , KI , KOH	3% HMTA	0.29
4238	KI , KOH	None	0.29
4229	KI , KOH	None	0.38
4244	I_2 , KOH	None	0.15
4231	I_2 , KI , KOH , Na_2HPO_4	5% HMTA	0.26
4227	I_2 , KI , KOH	5% HMTA	0.29
4225	I_2 , KI , KOH	5% HMTA	0.30

Test Conditions: 2-inch diameter, 2-inch height, contact time 0.25 second; prehumidification 16 hrs. at 96 RH%

The sources of the iodine in one series of impregnations were from the following binary solutions: KIO_3 and KI , KIO_3 and I_2 , KIO_4 and KI , and KIO_4 and I_2 . The total iodine has been varied from 1 to 4 wt.%; about 2 wt.% appears to be optimum. However, it was shown in other preparations that the base charcoal itself is also a strong factor. The quantity of HMTA has been varied from 1 to 5 wt.% and again the base charcoal dictates the particular amount to use for the minimum penetration of methyl iodide. The results in Table 4 were obtained for a 2-step impregnation on the coal-base charcoal (Union Carbide MBV 6/14) and the total iodine in these preparations was 1 wt.%. It will be noted that a second series was repeated without HMTA and for this particular effect charcoal the presence of HMTA appears to contribute a second order effect insofar as methyl iodide penetration is concerned.

14th ERDA AIR CLEANING CONFERENCE

Table IV

Impregnation with Binary Mixtures of Iodate or Periodate with Iodide or Iodine Using the Coal-Base Charcoal

<u>Sample</u>	<u>Impregnations</u>		<u>% Penetration</u>
	Step 1	Step 2	
4250	KIO ₃ and KI	1% HMTA	0.26
4251	KIO ₃ and I ₂	1% HMTA	0.47
4252	KIO ₄ and KI	1% HMTA	0.18
4253	KIO ₄ and I ₂	1% HMTA	0.60
4254	KIO ₃ and KI	None	0.54
4255	KIO ₃ and I ₂	None	0.56
4256	KIO ₄ and KI	None	0.44
4257	KIO ₄ and I ₂	None	0.51

Test Conditions: 2-inch diameter, 2-inch height, contact time 0.25 second; prehumidification 16 hrs at 96 RH %

A total of 45 preparations were made with one particular base charcoal. A frequency plot (Figure 3) indicated that the results might be better presented by a bimodal distribution. For a normal distribution for n=45 and the mean penetration = 0.33, the standard deviation was 0.13. For a bimodal distribution the corresponding values were n=26, mean=0.239, std deviation=.07 and n=19, mean=0.46, standard deviation=.06. The explanation is considered to be in the evaluation procedure for penetration rather than in the uncertainties of the impregnation procedure.

Several parameters were also evaluated for methyl iodide penetration by the American Air Filter Company**. The results (Table V) at ambient temperature are compared from both laboratories and demonstrate the effectiveness of the new impregnation and the good reproducibility.

** The authors are indebted to J. F. Fish, R. D. Rivers and M. Pasha for complete cooperation in these tests.

Table V

Determination of the Penetration of Methyl Iodide
by American Air Filter Co. and NRL

<u>Preparation</u>	<u>AAF Co.</u>		<u>NRL</u>	
	<u>Temp. °C</u>	<u>% Penetration</u>	<u>Temp. °C</u>	<u>% Penetration</u>
4264	132	0.117	22	0.36
4266	131	1.07	22	0.50
4267	129	1.19	22	0.43
4230	32	0.15	22	0.28
4231	30	0.005	22	0.26
4225	28	0.58	22	0.30
4227	27	0.28	22	0.29

IV. Thermal Stability

The thermal stability of impregnated charcoals has been reported (5,6) under a number of conditions pertinent to an unlikely ignition of an adsorbent by the heat of fission-product decay. The new impregnations have, therefore, been examined by determinations of the spontaneous ignition temperature (SIT) upon programmed external heating and by the composition of the effluent gases during heating. Only the SIT behavior is reported in this paper.

The pertinent observation is that a high flash point amine (HMTA) added to the impregnation formulation generally elevates the ignition temperature of the charcoal relative to the case when the amine was omitted. Table VI is a brief summary of the spontaneous ignition temperatures for the original base charcoal and the impregnated products. The desirable behavior of HMTA is evident when the comparison is made with other impregnations.

The evolved gases during the above ignition measurements have been analyzed for elementary iodine, alkyl iodides, carbon monoxide and carbon dioxide. These are decomposition products of the impregnated charcoals in the flow of air and as such are probably not directly responsible for the primary ignition process of the charcoal. The ignition is quite rapid once the critical temperature range is reached as shown by either the rapid rise in effluent gas temperature or by the visual incandescent appearance. Johnson and Woods (7) showed that adsorbed vapors of low flash points determine the SIT of a charcoal in service. For example, n-decane (13 to 30 wt.%) on a coconut charcoal or on a coal-based charcoal showed values of SIT near those of liquid n-decane, i.e. 216°C. There appeared to be no catalytic effect by the charcoals to promote the spontaneous ignition of hydrocarbons; air passing continuously through charcoal beds need not result in any significant temperature rise due to hydrocarbon oxidation. The observations of Johnson and Woods are pertinent to

14th ERDA AIR CLEANING CONFERENCE

charcoals in service. In the nuclear reactor application there is an urgent need to study impregnated charcoals after typical service exposures. In this case there is a potential heat source and good heat transfer to the air stream is essential. While quite satisfactory new materials are available, more information is needed to determine the expectant life of the various impregnated charcoals.

Table VI

Comparison of Spontaneous Ignition Temperatures
of the Base and the Impregnated Charcoals

<u>Prepn.</u>	<u>Charcoal</u>	<u>Impregnation</u>	<u>SIT(°C)</u>
4008	Nuchar 6x16, Coal	None	510
4146	" " "	I ₂ + HMTA	460
G212	Coconut	None	338
4097	"	TEDA	208
4045	"	TEDA	186
4065	"	TEDA	207
4014	JXC 6/14	None	500
4127	"	I ₂ , HMTA	470
4128	"	I ₂ , HMTA	455
4015	MBV 6/14	None	492
4227	"	I ₂ , KI, HMTA	409
4258	"	KIO ₄ , KI, HMTA	445
4244	"	I ₂ , KOH, HMTA	465
4238	"	KI, KOH	334
4229	"	KI, KOH	332
4020	207B 8/12	None	447
4220	"	I ₂ , KI, HMTA	375
GX202	Wood	None	436
4218	"	I ₂ , KI, HMTA	440
4280	"	KI, KIO ₃ , HMTA	395
4239	"	KI, KOH	337

V. Role of the Base Charcoal

The selection of base charcoals for the nuclear industry application of iodine removal must take into account a number of properties:

- (1) After impregnation, the product must, of course, be a satisfactory trapper for organic iodides at high relative humidity.
- (2) The charcoal must be available in the desired particle size range and possess particle integrity against excessive dust formation.
- (3) The charcoal must possess a large surface area in order to adsorb the impregnants and to yield a large final gas-solid interface.

(4) There must be a suitable open porosity within granules to accommodate the adsorbed impregnants and to permit the transport of the gaseous reactants and products.

(5) The charcoal must be compatible with a high pH of the impregnating solution which also serves to protect the impregnant in service.

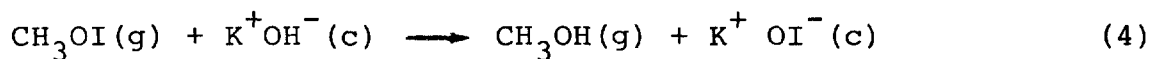
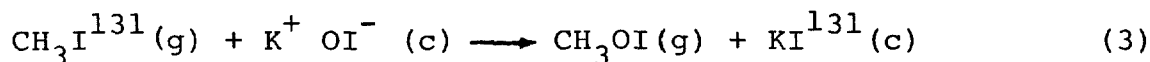
(6) An adequate adsorption capacity must exist after impregnation to handle the pollutants present in the carrier air.

The study in progress at NRL seeks to evaluate these aspects of behavior for many of the available commercial adsorbents (8).

VI. Mechanism for Trapping Methyl Iodide

A reaction mechanism for CH_3I retention is desirable as a guide to an investigator in the conduct of further research and development. Collins, Taylor and Taylor (2) discussed the particular examples of KI_x and the amine impregnants, the latter forming a quaternary iodide.

The many combinations of the salts of iodine oxyacids used as impregnating solutions in the present study have one thing in common. Although starting with various combinations of iodine species, it is possible in basic solutions to form the hyperiodite species. The formation is thermodynamically possible as shown by calculated heats of formation. Postulating a small but finite concentration of OI^- in the boundary surface of a charcoal, the following trapping mechanism may occur:



The calculated total free energy change for the sum of these two reactions is -17.45 Kcal. A CH_3I (131) molecule in approaching a OI^- species on the surface (Figure 4) is oriented with the CH_3 towards the ion and the $\text{I}(131)$ directed away. By means of a Waldon Inversion (9) the transition state I is formed which readily is transformed into products II as indicated in Figure 4. A neighboring mobile OH^- surface group then rapidly forms the transition state II which results in the formation of products III, CH_3OH and the original reactive OI^- species. A chain reaction is thus established with the following overall features:

1. The chain reaction involves the regeneration of the active species OI^- and furnishes a stable sink for radioiodine, namely KI^{131} .

2. The free energy change is quite favorable.

14th ERDA AIR CLEANING CONFERENCE

3. The charcoal support could serve as a sink for the CH_3OH molecules produced.

4. The mechanism accounts for high trapping efficiency when the pH is high and for a low efficiency observed when the pH is reduced.

5. Economical quantities of impregnants are employed.

6. The observed I(131) concentrations in the charcoal bed in the direction of air flow follows catalytic kinetics (10).

One test for the reaction mechanism is the detection of methyl alcohol as a reaction product. Obviously, excess methyl alcohol will serve as a "poison" in the proposed mechanism.

The complete reaction mechanism is doubtlessly very complex. In some cases the adsorption process appears to dominate the trapping kinetics. However, in most cases, efficient trapping appears to occur via the catalytic process.

VII. Concluding Remarks

The base charcoal is not an inert carrier for the impregnant. For example, the pH of the water extract of the impregnated charcoal is normally lower by 3 to 4 pH units than that of the impregnating solution, a behavior compatible with surface interaction.

The advantages of the oxyiodine salts as impregnation agents may be summarized as follows:

1. When paired with suitable base charcoals, excellent trapping agents are obtained for methyl iodide that are efficient in air flows at 95-97 RH, contact times of 0.25 second, and in 2-inch bed depths of charcoal.

2. The cost of the impregnants is nominal and the shelf life under dry conditions appears to be indefinite.

3. A number of domestic charcoals, mainly those prepared from coal, are available as satisfactory base charcoals.

4. A high ignition temperature can be realized, in the range 350 to 450°C, using impregnated coal-based charcoals.

A number of unsolved problems and complications arise in the practical applications, but an optimistic view may be justified based on the current laboratory work in progress.

Acknowledgements

The sponsorship of the Division of Nuclear Fuel Cycles and Production, ERDA, and the complete cooperation of John C. Dempsey, Contract Manager, are gratefully acknowledged. Many thanks are due

14th ERDA AIR CLEANING CONFERENCE

to A. G. Evans, Savannah River Laboratory, for his close cooperation in several aspects of the investigation.

References

- 1a. Adams, R. E., Ackley, R. D., and Browning, W. E., Jr., ORNL-4040 UC-80-Reactor Technology, January 1967.
- 1b. Adams, R. E., Ackley, R. D. and Combs, Zell., Nuclear Safety Program Annual Report, ORNL-4374, 93-105, Dec. 31, 1968.
- 1c. Ackley, R. D. and Adams, R. E., ORNL-TM-2728, December 1969.
2. Collins, D. A., Taylor, L. R. and Taylor, R., Proc. 9th AEC Air Cleaning Conference 1, 159-198 (1966); TRG Report 789(W) 1964, U.K.A.E.A., Windscale.
3. Downs, A. J. and Adams, C. J., "The Chemistry of Chlorine, Bromine, Iodine and ASTATINE", Pergamon Texts in Inorganic Chemistry, Vol. 7, Pergamon Press (1975).
4. RDT Standard M16-1T, October, 1973. Division of Reactor Research and Development Technical Information Center, Oak Ridge, Tennessee.
5. Evans, A. G. and L. R. Jones, DP-1355, Savannah River Laboratory, Aiken, S. C. 29801.
6. Evans, A. G., Proc. 13th AEC Air Cleaning Conference, 743-755 (1974).
7. Johnson, J. E. and Woods, F. J., J. Fire & Flammability 2, 141-156 (1971).
8. Deitz, V. R. and Burchsted, C. A., "Survey of Domestic Charcoals for Iodine Retention", NRL Memo Report 2960, January 1975.
9. Fieser, L. F. and Fieser, M., "Advanced Organic Chemistry", pp. 320-321 (1961 Edition), Reinhold Publ. Corp., New York.
10. Deitz, V. R., Blachly, C. H. and Jonas, L. A., Proc. 14th ERDA Air Cleaning Conference (1976).

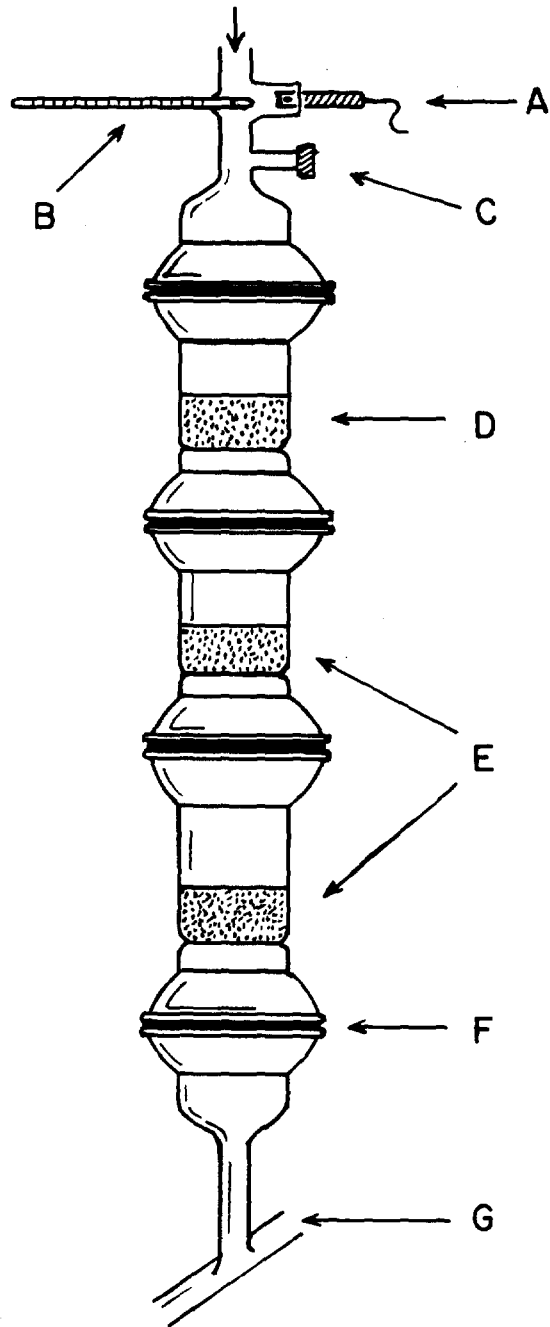


Figure 1: Diagrammatic Sketch of the Charcoal Test Chamber

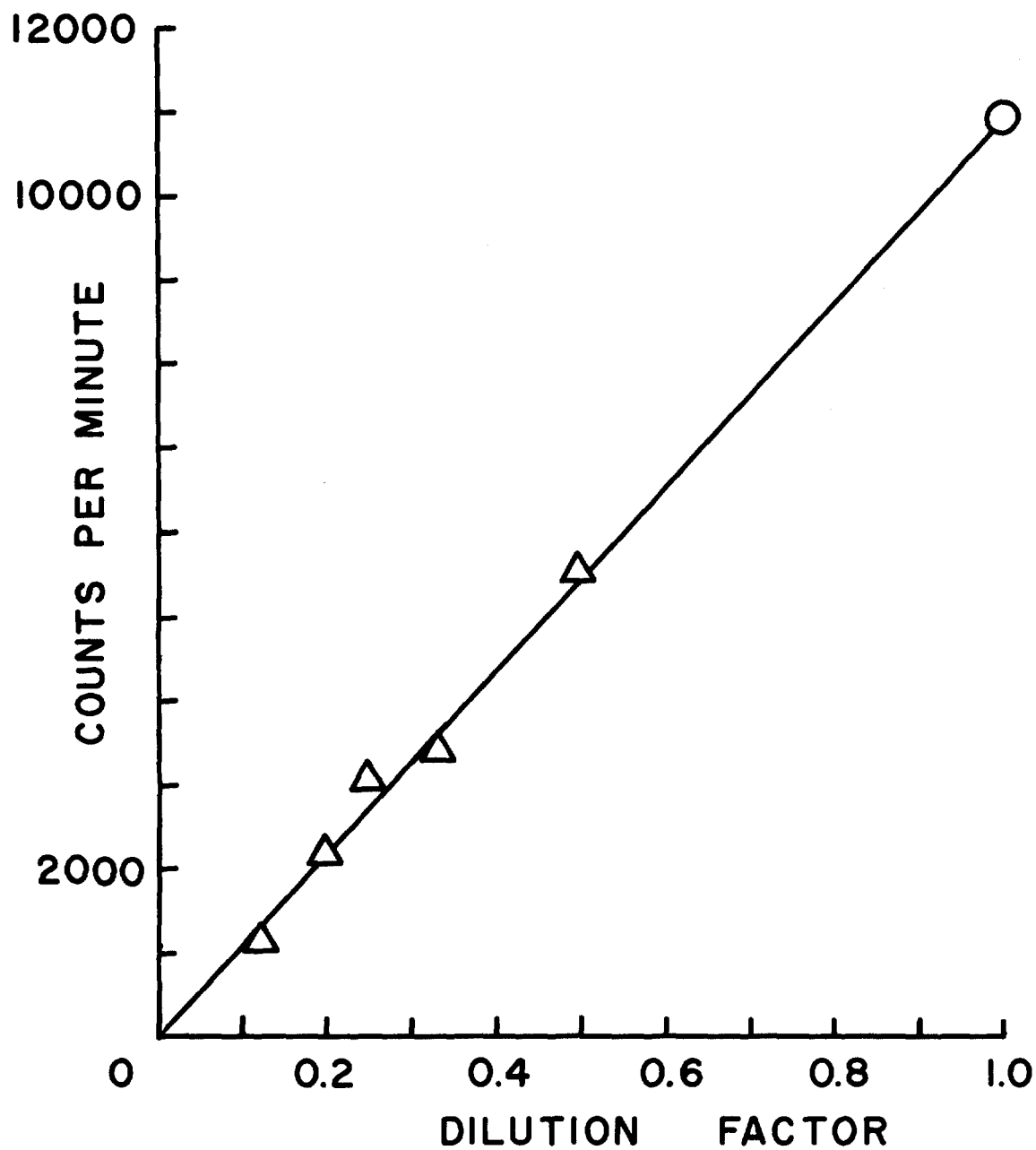
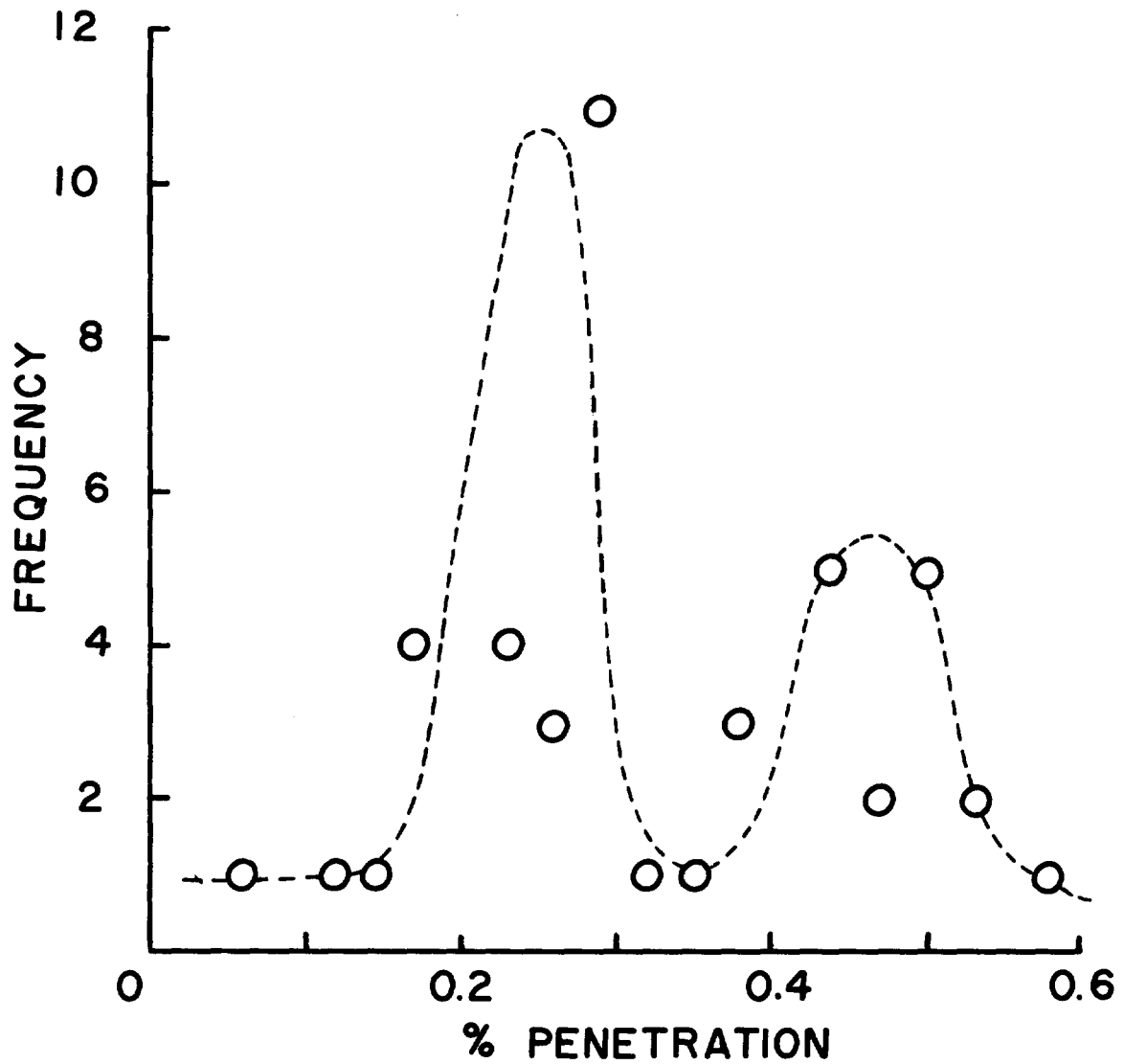


Figure 2: The Counting of Adsorbed $\text{CH}_3\text{I}(131)$ on Impregnated Charcoal (4144) Diluted with Humidified Original Sample



<u>DISTRIBUTION</u>	<u>n</u>	<u>MEAN</u>	<u>STD. DEV.</u>
Normal	45	0.33	0.13
Bimodal {	26	0.239	0.07
	19	0.46	0.06

Figure 3: Frequency Plot of the Penetration Values using MBV Impregnated Charcoals

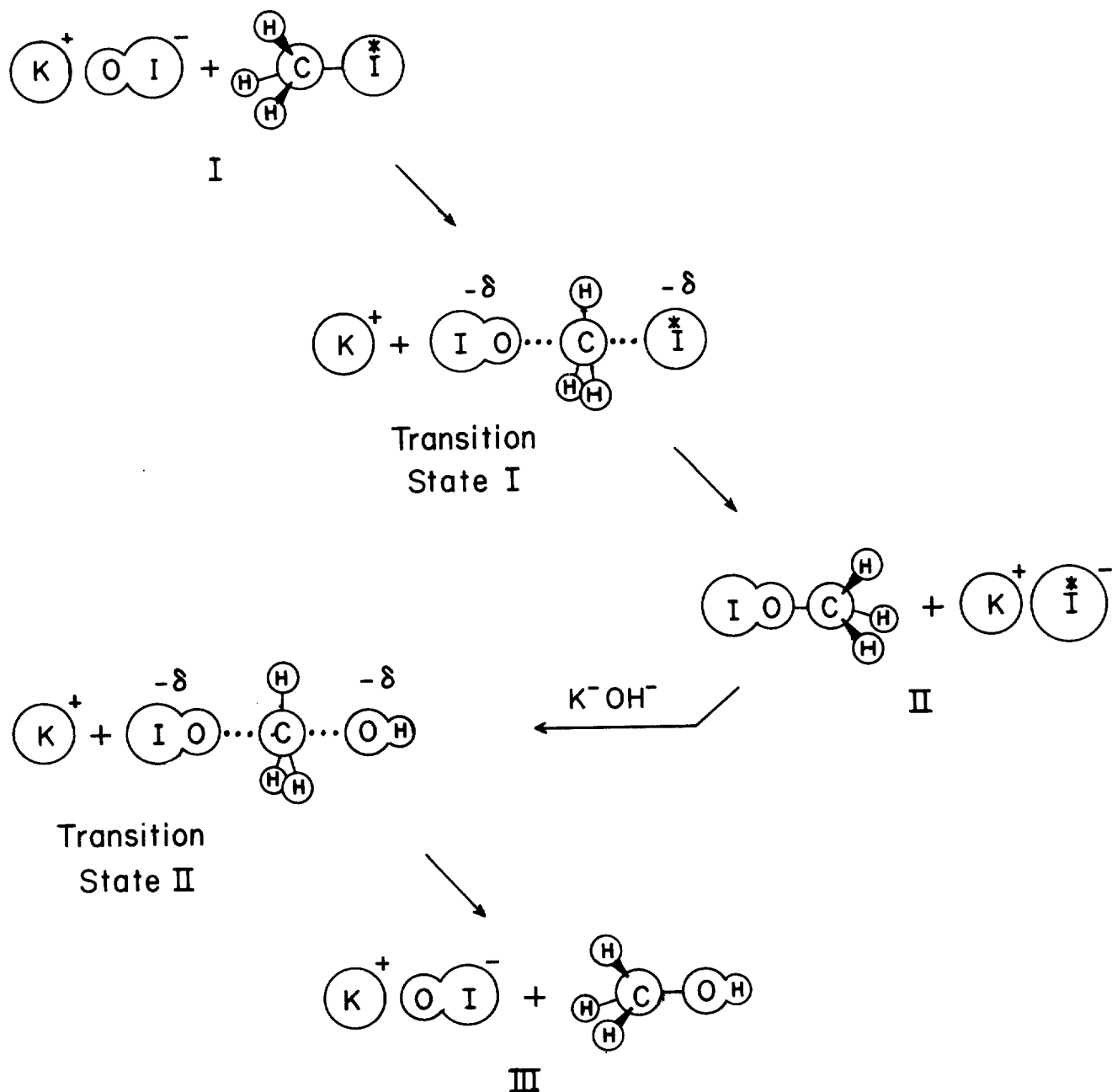


Figure 4: A Catalytic Mechanism for the Trapping of Methyl Iodide on Oxyiodine-Impregnated Charcoals

NEW CHARCOAL IMPREGNANTS FOR TRAPPING METHYL IODIDE
PART II. APPLICATIONS TO A VARIETY OF BASE CHARCOALS*

A. G. Evans
Savannah River Laboratory
E. I. du Pont de Nemours and Company
Aiken, South Carolina 29801

Abstract

The most common impregnated charcoals in use at nuclear power reactors in the United States are coconut carbons containing iodine salts or a combination of iodine salts and TEDA (triethylenediamine). Although carbons impregnated with TEDA have proven to be quite effective for trapping methyl iodide, enough undesirable characteristics of TEDA have been observed (e.g., high cost, high vapor pressure, and low flash point) to stimulate a search for other effective impregnants.

Cooperative efforts between the Naval Research Laboratory (NRL) and Savannah River Laboratory (SRL) have led to the development of several promising new impregnation formulations containing HMTA (hexamethylenetetramine) and iodine salts. SRL has applied the new formulations to base carbons derived from coconut shells, coal, petroleum, and wood. The newly developed impregnated carbons, according to tests at NRL, perform as well as, or better than, commercial charcoals containing TEDA. The most successful combinations consist of coal carbon impregnated with 2% HMTA, 2% iodine (as KI and KIO₃), KOH, and NaH₂PO₄•H₂O.

Performance data are reported for the complete series of tests performed on the charcoals. Tests include methyl iodide retention tests, high-temperature I₂ penetration tests, ignition temperature tests, measurement of the carbon pH (water extracts), and confirmation of impregnation levels by neutron activation analysis. Specific impregnation techniques are also discussed.

*The information contained in this article was developed during the course of work under Contract No. AT(07-2)-1 with the U. S. Energy Research and Development Administration.

Introduction

In the United States, the most commonly used impregnated charcoals for trapping radioiodine and methyl iodide are prepared by treating coconut shell-base carbons with iodine salts or with combinations of iodine salts and TEDA (triethylene-diamine). Several studies have shown that TEDA-KI formulations are more effective than those containing KI or KI_x⁽¹⁻³⁾. However, the use of TEDA in some gas treatment systems is limited by some of its physical and chemical characteristics, and by its high cost.

On carbon, TEDA has a flash point of ~190°C^(4,5). In some accident situations, the combination of radioiodine decay heat and TEDA combustion heat may exceed the heat removal capacity of the system and cause carbon ignition at temperatures as low as 190°C^(5,6,7).

TEDA has a finite vapor pressure over much of the operating temperature range of gas treatment systems. Consequently, some TEDA is lost from the system when air flows through the carbon beds. The manufacture of TEDA carbons therefore requires careful drying to minimize TEDA losses and impregnation costs. At a TEDA cost of eight dollars per pound, impregnation costs are about ten cents per pound for each weight percent TEDA in the final product.

Efforts began at SRL and NRL in 1974 to find an effective impregnant to replace TEDA. Desired characteristics of the new impregnant included: (1) methyl iodide removal efficiency equal to or better than that of TEDA, (2) low enough vapor pressure at 100°C to prevent significant loss of impregnant in service or during manufacture, (3) thermal stability to withstand temperatures up to at least 300°C without ignition and 200°C without decomposition, and (4) a lower cost than TEDA.

NRL studies showed that HMTA (hexamethylenetetramine) had the characteristics stated above when used in combination with iodine or iodine salts⁽⁸⁾. SRL and NRL have collaborated in efforts to adapt the HMTA formulations to a variety of base carbons.

Base carbons from coconut, petroleum, coal, and wood have been impregnated at SRL with several combinations of HMTA, iodine, and iodine salts. Tests that were run on all the carbons include methyl iodide penetration measurements, elemental iodine penetration measurements at 180°C, ignition temperature measurements, pH determinations (on water extracts), and specific analyses for sodium, potassium, and iodine by neutron activation analysis. Samples of six of the experimental carbons were also installed in the SRP Carbon Test Facility (CTF) for service aging studies.

Discussion

The basic techniques for HMTA impregnations were developed at NRL. SRL modifications to the formulations included adjusting iodine and potassium contents to achieve more favorable [(I/K)/pH] ratios^(9,10) and the addition of flame retardants to the formulations to obtain more favorable ignition characteristics.

The initial SRL samples were impregnated by a one-step technique, i.e., all the impregnants were dissolved in a single solution. A two-step impregnation technique (two solutions applied serially), developed later, simplified preparation of the impregnation solution. Both techniques are discussed below.

One-Step Impregnation

The first step in the preparation of impregnating solution is grinding HMTA and I₂ crystals together (with a mortar and pestle, or a laboratory ball mill for larger samples). NRL tests showed that intimate mixing of HMTA and I₂ is necessary. Water, KOH, and other ingredients are added to the iodine-HMTA mixture in a flask, and the slurry is stirred until a solids-free solution is obtained. Complete dissolution of the ingredients frequently requires several hours of stirring. Application to the carbon by drip or spray addition techniques was most effective for uniform carbon impregnations when solution volume was carefully adjusted to saturate (but not flood) the carbon sample. Experience showed that the solution should be prepared with slightly less than two-thirds of the volume of water necessary to saturate the carbon.

The first SRL series of HMTA samples were prepared with the one-step technique and consisted of systematic variations of the iodine and HMTA contents to determine optimum impregnation level for each component. Samples were prepared with and without flame retardants to determine the most effective additive to improve the ignition characteristics of the final product. Type G-210* carbon was chosen as the base material for this series of samples so comparisons could be made with Type G-615* carbon containing TEDA. Impregnation levels and test results are shown in Tables I (constant HMTA) and II (constant iodine). The constant HMTA samples were prepared and tested first to select the optimum combination of iodine and iodine salts. The data show that methyl iodide retention is best, i.e., penetration is lowest, when contents of iodine as I₂ and I⁻ are each 1 wt % (Sample 2). Although addition of KI to the sample increased the ignition temperature (compare Sample 2 with Sample 3), the ignition temperature was still lower than the desired 350°C. Addition of 1% monobasic sodium phosphate (NaH₂PO₄•H₂O) to the formulations brought the ignition temperatures into the desired range, but the methyl iodide penetration values increased also (compare paired Samples 3 and 6 and 2 and 7). Addition of the dibasic sodium salt (Na₂H₂PO₄•2H₂O) also increased the ignition temperature, but caused an even greater increase in methyl iodide penetration (Samples 2, 7, and 8). Thermal desorption data (I₂ desorption at 180°C) are all quite low because of the low [(I/K)/pH] values.

* An 8 x 16 mesh coconut carbon having surface area of ~1100 m²/g (before impregnation). Product of North American Carbon Company, Columbus, Ohio.

14th ERDA AIR CLEANING CONFERENCE

After the optimum combination of I₂, I⁻, and KOH was determined, a group of samples was prepared in which iodine contents were constant and HMTA content was varied from 1 to 6%. The data (Table II) show that the lowest methyl iodide penetration was obtained at the 2% impregnation level (Sample 10). Note that the methyl iodide penetration for Sample 10 compares favorably with that of the commercial TEDA carbon (G-615). Sample 10 exhibits a slightly higher I₂ penetration at 180°C than do other SRL formulations, but its I₂ penetration remains lower than that of the commercial product.

Table I One-step impregnations of coconut carbon^a with constant HMTA (5%)

Sample No.	Impregnation Level, wt %				Ratio (I/K)/pH ^c	Ignition Temp., °C	Iodine Penetration, %	
	I ₂	I ^{-b}	KOH	Other			I ₂ ^d	CH ₃ I ^e
1	1.0	-	0.7	-	0.024	275	0.00061	9.32
2	1.0	1.0	0.7	-	0.041	325	0.00031	1.33
3	2.0	-	1.4	-	0.037	265	0.00041	2.53
4	3.0	-	2.1	-	0.043	265	0.00045	2.61
5	1.0	2.0	0.7	-	0.050	315	0.00060	2.39
6	2.0	-	1.4	1.0 ^f	0.036	355	0.00060	3.05
7	1.0	1.0	0.7	1.0 ^f	0.038	390	0.00052	1.86
8	1.0	1.0	0.7	1.0 ^g	0.045	355	0.00057	3.18

a. Type G-210 base carbon, see text for description.

b. KI used. Addition calculated on the basis of weight percent iodine added.

c. Determined from analyses of carbons after impregnation (see Reference 9).

d. SRL thermal desorption test at 180°C.

e. NRL methyl iodide test data. Test run at 25°C, 95% relative humidity, 0.1 mg CH₃I/g C loading, and 0.25-second residence time in 2-in.-deep carbon bed.

f. NaH₂PO₄•H₂O (monobasic sodium phosphate) flame retardant added.

g. Na₂HPO₄•2H₂O (dibasic sodium phosphate) flame retardant added.

14th ERDA AIR CLEANING CONFERENCE

Table II One-step impregnations of coconut carbon^a with constant iodine (1% I₂, 1% I⁻)

Sample No.	Impregnation Levels, wt %			Ratio (I/K)/pH ^b	Ignition Temp., °C	Iodine Penetration, %	
	HMTA	KOH	Other			I ₂ ^b	CH ₃ I ^b
9	1.0	0.7	1.0 ^c	0.034	350	0.00067	0.99
10	2.0	0.7	1.0 ^c	0.038	370	0.00141	0.65
11	3.0	0.7	1.0 ^c	0.029	415	0.00105	1.19
12	4.0	0.7	1.0 ^c	0.036	422	0.00092	1.37
7	5.0	0.7	1.0 ^c	0.038	390	0.00052	1.86
13	6.0	0.7	1.0 ^c	0.037	435	0.00076	1.76
G-615 ^d	TEDA	-	1.0 ^e	0.039	360	0.0060	0.79

a. Type G-210 base carbon, see text for description.

b. See Table I for details.

c. NaH₂PO₄·H₂O.

d. A commercial carbon containing 2% TEDA and 2% KI.

e. Proprietary flame retardant.

Two-Step Impregnation

Additional NRL studies on impregnation techniques revealed that addition of the iodine salts and HMTA in separate impregnation steps saved substantial time in the solution preparation step and resulted in improved methyl iodide retention by the impregnated product⁽⁸⁾. In this technique, the inorganic ingredients (I₂, KI, KOH, NaH₂PO₄·H₂O, etc.) are dissolved in one solution that is added to the carbon in a volume of water equal to approximately half that required to saturate the carbon. A second solution containing the HMTA (with enough KOH added to adjust solution pH) is added to the carbon (without drying the partially wetted charcoal) in an equal volume of water. The total volume of water required to prepare the two solutions is only slightly less (~95%) than the volume of distilled water required to saturate the carbon.

The initial SRL samples impregnated by the two-step technique were prepared with 5% HMTA and the I₂-KI-KOH formulation found best in the first one-step sample series (test results on samples of varied HMTA content were not yet available). Additional samples were prepared using 2% HMTA with KI, KIO₃, and KOH instead of the I₂-KI-KOH combination used in earlier formulations. The chemistry of specific formulations will be discussed in greater detail later. A third set of samples was prepared with KI, KIO₃, KOH, and NaH₂PO₄·H₂O to show the effect of HMTA on iodine retention. Base carbons used for these three sets of samples included charcoals derived from coconut shells, coal, petroleum, and wood. Test data are shown in Tables III (coconut and wood carbons) and IV (coal and petroleum carbons).

The data in Tables III and IV show that two types of carbon (Type G-212, a high surface area coconut carbon, and Type GX-202, a wood base carbon) do not retain

14th ERDA AIR CLEANING CONFERENCE

Table III Two-step HMTA impregnations on coconut and wood carbons.

Type of Carbon	Impregnation Levels, wt %				(I/K)/pH ^b	Ignition Temp., °C	Iodine Penetration, %	
	HMTA	Iodine Salts	KOH	Other ^a			I ₂ ^b	CH ₃ I ^b
G-210	5.0	2.0 (I ₂ , I ⁻)	0.7	PO ₄ ³⁻	0.030	398	0.00289	1.74
	2.0	2.0 (I ⁻ , IO ₃ ⁻) ^c	0.8	PO ₄ ³⁻	0.028	320	0.00104	0.46
	2.0	2.0 (I ⁻ , IO ₃ ⁻)	0.8	BO ₃ ³⁻ ^d	0.034	275	0.00084	4.45
	0.0	2.0 (I ⁻ , IO ₃ ⁻)	0.4	PO ₄ ³⁻	0.040	377	0.00079	4.10
G-212 ^e	5.0	2.0 (I ₂ , I ⁻)	0.7	PO ₄ ³⁻	0.027	335	0.00231	2.47
	2.0	2.0 (I ⁻ , IO ₃ ⁻)	0.4	PO ₄ ³⁻	0.026	335	0.00120	0.91
GX-202 ^e	5.0	2.0 (I ₂ , I ⁻)	0.7	PO ₄ ³⁻	0.048	436	0.00450	0.90
	2.0	2.0 (I ⁻ , IO ₃ ⁻)	0.4	PO ₄ ³⁻	0.042	412	0.00115	1.49
	0.0	2.0 (I ⁻ , IO ₃ ⁻)	0.4	PO ₄ ³⁻	0.044	403	0.00153	1.42

a. Flame retardant, 1.0% NaH₂PO₄·H₂O unless otherwise indicated.

b. See Table I for details.

c. 2.2% KI, 0.6% KIO₃.

d. 0.8% H₃BO₃.

e. Products of North American Carbon Company, Columbus, Ohio.

Table IV Two-step HMTA impregnations on coal and petroleum carbons.

Type of Carbon	Impregnation Levels, wt %				Ratio (I/K)/pH ^b	Ignition Temp., °C	Iodine Penetration, %	
	HMTA	Iodine Salts	KOH	Other ^a			I ₂ ^b	CH ₂ I ^b
G-352 ^e	5.0	2.0 (I ₂ , I ⁻)	0.7	PO ₃ ³⁻	0.045	450	0.00141	0.50
	2.0	2.0 (I ⁻ , IO ₃ ⁻) ^d	0.7	PO ₃ ³⁻	0.065	435	0.00121	0.36
	2.0	2.0 (I ⁻ , IO ₃ ⁻)	0.8	BO ₃ ^{3-e}	0.062	395	0.00160	1.17
	0.0	2.0 (I ⁻ , IO ₃ ⁻)	0.8	PO ₃ ³⁻	0.060	420	0.00325	0.21
BPL ^f	5.0	2.0 (I ₂ , I ⁻)	0.7	PO ₃ ³⁻	0.087	433	0.00337	0.53
	2.0	2.0 (I ⁻ , IO ₃ ⁻)	0.6	PO ₃ ³⁻	0.065	420	0.00184	0.69
	0.0	2.0 (I ⁻ , IO ₃ ⁻)	0.8	PO ₃ ³⁻	0.057	392	0.00079	1.30
W-965 ^f	5.0	2.0 (I ₂ , I ⁻)	0.7	PO ₃ ³⁻	0.095	425	0.00721	0.73
	2.0	2.0 (I ⁻ , IO ₃ ⁻)	0.8	PO ₃ ³⁻	0.055	415	0.00057	0.44
	0.0	2.0 (I ⁻ , IO ₃ ⁻)	0.8	PO ₃ ³⁻	0.057	417	0.00173	1.09

a. 1.0% NaH₂PO₄•H₂O unless otherwise indicated.

b. See Table I for details.

c. Ground and sieved to 10x16 mesh. Product of North American Carbon Company, Columbus, Ohio.

d. 2.2% KI, 0.6% KIO₃.

e. 0.8% H₃BO₃.

f. 10x16 mesh fraction. Product of Calgon Corporation, Pittsburgh, PA.

g. Witcarb-965 (formerly grade 337). Product of Witco Chemical Corporation, New York, NY.

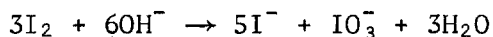
methyl iodide as effectively as do the other types of carbons impregnated with these HMTA formulations. The fact that penetration values of one percent or less were obtained, however, suggests that specific formulations could be developed for these carbons that would perform as well as some of the commercial TEDA products.

The data also show that the addition of HMTA to the formulation usually improves methyl iodide retention performance over that obtained with iodine compounds alone. The anomalous behavior of Type G-352 carbon with and without HMTA is still under investigation.

Flame retardant experiments included in the data in Tables III and IV are also worth noting. Two samples prepared with H_3BO_3 as a flame retardant (on carbon Types G-210 and G-352) both showed significantly poorer methyl iodide retention than did their companion samples containing monosodium phosphate $NaH_2PO_4 \cdot H_2O$. Examination of ignition temperature data on these same samples shows that boric acid is also less effective as a flame retardant than is the phosphate.

Chemistry of Impregnation Formulations

Choice of Reagents. Preliminary NRL data indicated that an I_2 -HMTA reaction, prior to impregnation, is needed to produce a carbon with effective methyl iodide retention. The development of the two-step impregnation technique suggested that the "activation" of the HMTA molecule can take place on the carbon either during or after the impregnation step. During the transition from one- to two-step impregnations, samples were first prepared with I_2 and KI as in earlier studies. The SRL formulations were specifically designed to contain an excess of potassium to achieve a favorable I/K ratio ($<0.6:1$ atom ratio)⁽⁹⁾ and a high pH. As a result, the I_2 incorporated in the solutions was always converted to ionic iodine before the impregnation step. The idealized reaction is⁽¹¹⁾:



Other oxyiodides may be formed during the reaction of iodine with caustic as discussed in detail in Part I of this paper⁽⁸⁾ and in Reference 12.

To optimize the impregnant formulations for possible commercial use, the cost of reagents and the safety of reagent handling must be considered. Since I_2 is converted to ionic iodides before impregnation, the less costly and less hazardous iodine salt forms were used, rather than I_2 . Once dissolved, the same mixtures of iodides and oxyiodides should form in solution as would be formed from dissolution of I_2 in caustic.

Thus, all the later SRL formulations are based on 2% total iodine and derived from KI and KIO_3 in the weight proportion to achieve the ratio $5I^-:IO_3^-$. KOH is added to bring the I/K weight ratio to approximately 2:1 (an atom ratio of $<0.6:1$) both to maintain the iodine in ionic form and to neutralize the NaH_2PO_4 added.

Preparation of Solutions. Experience has shown that the order of combination of reagents is as important as the amounts of reagents used. The specific order of combination of reagents for the one-step impregnation was discussed earlier. When solutions were prepared for the first two-step impregnations, I_2 and KI were used rather than the KI- KIO_3 combination. Thus, KOH addition was required early in the

preparation phase in order to dissolve the I_2 . The phosphate was added last, and the solution remained clear and colorless after KOH addition through the time the solution was added to the carbon. Test data show that the two methods produce carbons with essentially the same methyl iodide retention (compare Sample 7 in Tables I and II with the first sample of Type G-210 carbon in Table III).

When the KI-KIO₃ combination was tested, the first samples were prepared in the same manner. That is, the KI, KIO₃, and KOH were dissolved first, and the phosphate salt was added last. Again a clear, colorless solution was formed and remained up to the time of addition to the carbon. In later experiments with custom-designed solutions for different base carbons (base carbon pH's vary as a function of the natural potassium content), the KI, KIO₃, and phosphate salt were combined first, and the solution was titrated with a known concentration KOH solution.

Addition of the NaH₂PO₄ to the KI-KIO₃ salt solution resulted in the formation of the I₃⁻ ion because of the lower solution pH (the pH typically dropped from about 8.6 to 7.2 with the addition of NaH₂PO₄). Solutions are typically deep red in color after phosphate addition. The intensity of the color varies with the volume of solution used for a particular carbon. Back-titration of dummy solutions showed that a pH in excess of 13 is required to decolorize the solution once the I₃⁻ ion is formed. KOH addition required to adjust solution pH to 13 or more corresponds to addition of 0.8-1.0 weight percent KOH to the final product and lowers the ignition temperature substantially (especially on coconut carbons). KOH additions to the red solutions corresponding to 0.4-0.7% addition to the final product result in a solution ranging from red (0.4% addition, solution pH = 10.0) to straw yellow (0.7% addition, solution pH = 12.2).

Samples prepared from colored impregnating solutions show significantly higher methyl iodide penetration as well as exhibiting a lower pH. Typical data on two base carbons are shown in Table V.

Experiments currently in progress involve dissolution of caustic and phosphate together in a concentrated buffer solution (molar ratio KOH:NaH₂PO₄·H₂O ≈ 2:1). Addition of buffer solution to the KI-KIO₃ solution brings the pH of impregnation Solution 1 to about 12.4. The solution remains colorless during the buffer addition indicating that the I₃⁻ ion is not formed. Preliminary data show that this solution preparation technique results in a more satisfactory product (carbon pH's are in the 9.2-10.3 range, ignition temperatures are all above 340°C, and the carbons all have high-temperature iodine penetration values less than 0.002%). Methyl iodide penetration data were not available when this paper was being prepared.

Table V Effect of impregnation solution on methyl iodide penetration.

Basic Formulation: Solution 1 2.18% KI, 0.56% KIO₃,
1.0% NaH₂PO₄•H₂O + KOH
Solution 2 2.0% HMTA + KOH^a

Type of Carbon	Total KOH, wt %	Solution pH	Carbon pH	Ignition Temp., °C	CH ₃ I Penetration, %	Solution Color
G-210	0.41	10.0	9.70	375	3.57	Bright red
	0.48	11.1	10.30	337	2.59	Bright yellow
	0.81	Unknown ^b	10.48	320	0.46	Colorless
Witcarb 965	0.67	11.2	9.62	445	2.08	Bright yellow
	0.65	11.3	9.77	432	1.10	Pale yellow
	0.81	Unknown ^b	10.10	415	0.44	Colorless

a. KOH added to HMTA solution to bring solution pH to same value as Solution 1.

b. KOH added before NaH₂PO₄•H₂O. Solution pH not measured.

Service Aging Studies

Samples of six of the HMTA-impregnated charcoals have been installed in the CTF at SRP for service aging studies. Base carbons include Types G-210, Witcarb 965, G-352, MBV*, and GX-202. Other samples will be included in the evaluation program as test positions become available in the CTF. Particular emphasis is being placed on both the iodine retention properties and the mechanical stability of the carbons.

Observations made during the impregnation of several of the base carbons show that most of the non-coconut charcoals "dust" badly in the rotary drum impregnator used at SRL. This dusting characteristic raises the question as to how well the carbons will withstand the stress of air flowing through the carbon beds in service.

HEPA filters placed ahead of the backup beds used in the SRL high-temperature test accumulate more carbon dust during the testing of coal carbons than during testing of other types of carbons even though all test beds are blown out with an air jet prior to testing. No settling of the test beds has been observed during these tests, but the test period (4.17 hr) is not of sufficient duration to cause much loss of carbon. The longer exposure periods anticipated in the CTF (6-18

* Product of Union Carbide Corporation, New York, N.Y.

months of continuous air flow at a face velocity of 55 ft/min) should be sufficient to ascertain whether attrition is a problem in tightly packed beds.

Conclusions

Several solutions containing HMTA and iodine salts have been used on a variety of base carbons to produce impregnated charcoals for trapping methyl iodide. Test data show that some of these charcoals retain methyl iodide as well as or better than commercial charcoals containing TEDA. Coal carbons retain methyl iodide better with HMTA formulations, but acceptable trapping efficiencies have been achieved with coconut and petroleum carbons as well. The performance of the product also is sensitive to both the chemicals used in the formulation and the techniques used during the preparation of impregnation solutions.

Acknowledgment

The author wishes to express his appreciation to V. R. Deitz of NRL for furnishing methyl iodide penetration test data for this paper and to C. H. Blachly of NRL for performing the methyl iodide tests.

14th ERDA AIR CLEANING CONFERENCE

References

1. D. A. Collins, L. R. Taylor, and R. Taylor. "The Development of Impregnated Charcoals for Trapping Methyl Iodide at High Humidity." Proceedings of the Ninth AEC Air Cleaning Conference. USAEC Report CONF-660904, Vol. 1, p 154-198 (1967).
2. A. G. Evans and L. R. Jones. Confinement of Airborne Radioactivity - Progress Report: January 1971-June 1971. USAEC Report DP-1280, E. I. du Pont de Nemours and Company, Savannah River Laboratory, Aiken, SC (1971).
3. A. G. Evans and L. R. Jones. Confinement of Airborne Radioactivity - Progress Report: July 1971-December 1971. USAEC Report DP-1298, E. I. du Pont de Nemours and Company, Savannah River Laboratory, Aiken, SC (1971).
4. R. E. Adams, R. D. Ackley, and R. P. Shields. "Application of Impregnated Charcoals for Removing Radioiodine from Flowing Air at High Relative Humidity." Treatment of Airborne Radioactive Wastes, Proceedings of a Symposium, New York, NY, August 26-30, 1968, IAEA, Vienna p 398 (1968).
5. A. G. Evans. Confinement of Airborne Radioactivity - Progress Report July 1972-December 1972. USAEC Report DP-1329, E. I. du Pont de Nemours and Company, Savannah River Laboratory, Aiken, SC (1973).
6. A. G. Evans. Confinement of Airborne Radioactivity - Progress Report: January 1973-June 1973. USAEC Report DP-1340, E. I. du Pont de Nemours and Company, Savannah River Laboratory, Aiken, SC (1973).
7. J. L. Kovach and J. E. Green. "Evaluation of the Ignition Temperature of Activated Charcoals in Dry Air." Nucl. Safety 8, 41 (1966).
8. V. R. Deitz and C. H. Blachly. "New Charcoal Impregnants for Trapping Methyl Iodide, Part I, Salts of the Iodine Oxyacids with Iodide or Iodine in Basic Solution." Paper presented at the Fourteenth ERDA Air Cleaning Conference, Sun Valley, Idaho, August 2-4, 1976. Naval Research Laboratory, Washington, DC (1976).
9. A. G. Evans. "Effect of Alkali Metal Content of Carbon on Retention of Iodine at High Temperatures." Proceedings of the Thirteenth AEC Air Cleaning Conference, San Francisco, CA, August 12-15, 1974, USAEC Report CONF-740807 (1975).
10. A. H. Dexter, A. G. Evans, and L. R. Jones. Confinement of Airborne Radioactivity - Progress Report: January 1974-December 1974. USERDA Report DP-1390, E. I. du Pont de Nemours and Co., Savannah River Laboratory, Aiken, SC (1975).
11. Therald Moellar. Inorganic Chemistry. John Wiley & Sons, Inc., New York (1952).
12. A. J. Downs and C. J. Adams. The Chemistry of Chlorine, Bromine, Iodine and Astatine. Pergamon Texts in Inorganic Chemistry, Vol. 7, Pergamon Press, New York (1973).

DISCUSSION

R. J. WILLIAMS: One question I have is how well any of these charcoals will perform if one gets an iodine release after a fire. Do you have any information on the effect of the accumulation of combustion products on iodine retention?

EVANS: Not to my knowledge. Perhaps Dr. Deitz has some data on the effects of pollutants on HMTA-impregnated charcoals.

DIETZ: The results that we have today are on new impregnated charcoals. We have, at present, a whole series of weathering experiments where pollutants are being added to the charcoal and we will, maybe at the next charcoal meeting in Washington, be able to report on some of the results.

EVANS: In addition to Dr. Deitz's studies, we have some of the HMTA-impregnated charcoals installed in a weathering facility at Savannah River.

KOVACH: Rather than a question, I would like to make a comment regarding HMTA. At about 380°C, it decomposes and the major decomposition product is HCN, so if you are running ignition temperature studies or any secondary hazard studies, even on a laboratory scale, the quantity of cyanide generated is rather high. I caution you to try not to do away with your lab technicians if you are running decomposition studies.

EVANS: For obvious other reasons, tests that we run are performed in a fumehood. If the carbon itself ever gets exposed to 300°C or more, you might just as well forget its effectiveness. The iodine is gone, anyway, from a practical point of view.

DIETZ: Tomorrow afternoon, we will show that iodine is rather volatile. It will start coming off around 180 to 190°C, depending on the impregnation.

WILHELM: I have a feeling that in most of the containment systems constructed to date, the charcoal filters won't work. Both the primary containment and the secondary containment will work and they will work properly. If the primary containment doesn't fail, the secondary containment will work properly. But what happens when the primary containment fails? I think the secondary containment will fail, too, because it will "see" conditions it can't handle. In this situation, we can't claim safety, we don't normally have the safety, and this situation is strictly not allowed.

14th ERDA AIR CLEANING CONFERENCE

THE BEHAVIOR OF HIGHLY RADIOACTIVE IODINE ON CHARCOAL IN MOIST AIR*

R. A. Lorenz, S. R. Manning, and W. J. Martin
Oak Ridge National Laboratory
Oak Ridge, Tennessee 37830

Abstract

The behavior of highly radioactive iodine adsorbed on charcoal exposed to moist air (average partial pressure of water vapor, 110 torr) was investigated in a series of six experiments. The amount of radioactive ^{130}I on a well-insulated 28-cm³ bed ranged from 50 to 570 Ci. The relative humidity was 47% at the bed inlet temperature of 70°C.

Radioactive iodine was released from the test beds at a continuous fractional release rate of 7 to 10 x 10⁻⁶/hr for all types of charcoal tested. The chemical form of the released iodine was such that it was very highly penetrating with respect to the nine different types of commercial impregnated charcoals tested in backup collection beds. Two types of silver nitrate-coated adsorption materials behaved similarly to the charcoals. Silver-exchanged type 13X molecular sieve adsorbers were 20 to 50 times more efficient for adsorbing the highly penetrating iodine, but not as efficient as normally found for collecting methyl iodide. The chemical form of the highly penetrating iodine was not determined.

A species behaving like methyl iodide was released from the main test beds only during the period that the radioactive iodine was being loaded onto the test beds. An exception was a sample of charcoal that had been in service for four years in an air cleaning system associated with a reactor building at Oak Ridge National Laboratory. This charcoal, which contained 108 mg of adsorbed atmospheric contaminants per gram of charcoal, released a methyl iodide-like material continuously at a fractional rate of 80 x 10⁻⁶/hr in addition to the highly penetrating iodine form. A different type of charcoal, which had been exposed for nine months at the Savannah River Laboratory and was found to contain a much lower concentration of adsorbed organic impurities, released only the highly penetrating form of iodine.

When the velocity of the moist air was decreased from 28.5 fpm (25°C) to as low as 0.71 fpm (25°C), the temperature of the charcoal bed rose slowly and reached the ignition point in three of the experiments. At 0.71 fpm (25°C), the ignited charcoal beds reached maximum temperatures of 430 to 470°C because of the limited oxygen supply. The charcoal exposed for four years at Oak Ridge ignited at 283°C compared with 368°C for unused charcoal from the same batch.

Two of the experiments used charcoal containing 1 or 2% TEDA (triethylene-diamine) and a proprietary flame retardant. The oxidation and ignition behavior of these charcoals did not appear to be affected adversely by the presence of the TEDA.

* Research sponsored by the Energy Research and Development Administration under contract with the Union Carbide Corporation.

14th ERDA AIR CLEANING CONFERENCE

I. Introduction

We have completed a series of experiments which had the primary objective of determining whether the ignition of charcoal can occur from the decay heat of highly radioactive iodine before the iodine desorbs. The second objective of our program was to provide supportive data for the calculation of charcoal bed temperatures, and the third objective was to study the movement of iodine within charcoal beds and the desorption of iodine from these beds during exposure to intense radiation fields and elevated temperatures. Seven experiments conducted with dry air have been reported previously;⁽¹⁾ six experiments conducted with moist air are reported here.

We used four types of charcoal in our moist air experiments, Runs 8-13 (see Table I). All of them are coconut-based charcoals except for WITCO Grade 42, which is petroleum-based. Each batch had performed satisfactorily in other iodine or methyl iodide adsorption tests. Because some large differences in iodine desorption and oxidation rates or ignition temperature have been observed from batch to batch of a given manufacturer's type number, we caution that the experimental results presented here apply only to the particular lots of material tested.

Our experimental apparatus is shown schematically in Fig. 1. The charcoal is contained to a depth of 2-1/8 in. (5.4 cm) in a quartz Dewar flask with an inside diameter of 1.03 in. (2.62 cm). A heater on the outside of the flask is adjusted to follow the temperature of the center of the bed in order to further reduce the chance for heat loss through the side, in simulation of an essentially semi-infinite reactor adsorber system. Except for a small heat loss via conduction and heat radiation, the only cooling mechanism is the forced flow of air upward through the bed. Thermocouples measure the temperature distribution in the charcoal. The inlet temperature was controlled at 70°C in simulation of an accident ambient temperature, while the charcoal reached a higher temperature, depending on the amount of radioactive iodine present and the air flow rate.

II. Experimental Procedure

The radioactive ^{130}I was obtained by irradiating a mixture of 86% ^{129}I --14% ^{127}I in the chemical form PdI_2 packed as powder in quartz ampoules and seal-welded in an aluminum capsule. We irradiated this material for 30 hr (except Run 13) in the High Flux Isotope Reactor (HFIR) at a thermal flux of 2.5×10^{15} neutrons/cm². sec, which resulted in specific activities of 5.7 Ci ^{130}I /mg I and 1.4×10^{-3} Ci ^{131}I /mg I at the time of removal from the reactor.

After irradiation, the capsule was transported to the hot cell and sealed into the recirculating loop system. The tips of the capsule and ampoules were then sheared off, allowing the ampoules to fall into a quartz-lined furnace where the PdI_2 was thermally decomposed at 600 to 700°C to palladium metal and I_2 . Air circulating at the normal flow rate carried the radioactive iodine through two layers of Cambridge 1G HEPA filter medium into the test charcoal bed.

A collimated radiation detector was moved in 1/8-in. increments to follow the distribution of iodine in the bed as the experiments progressed. The collimator, located 6 in. from the bed, contained a slit that was 1/16 in. wide and 8 in. long (8-1/2 in. long beginning with Run 10).

Iodine that penetrated or was desorbed from the test bed was collected in sequentially operated traps. HEPA filters (Cambridge 1G) were used to collect particulate matter, and charcoal and silver-exchanged zeolite were used to collect

Table I Characteristics of charcoal investigated

Charcoal type	ORNL lot No.	Experiment No. ^a	Dry mass in each experiment (g)	Dry density (g/cm ³)	Apparent density ^b (g/cm ³)	Mean surface particle size ^c , D _p (cm)	K ^d (%)	I ^d (%)	pH ^e
MSA 85851 ^f	51969	1, 2, 3, 4, 8, 13	11.2	0.420	0.45	0.161	2.85	4.41	9.1-8.6
BC-727 ^g	1683	5	13.1	0.461	0.562	0.169	1.87	3.79	8.2-8.2
WITCO Grade 42 ^h	62469	6, 9	10.9	0.384	0.389	0.171	0.90	3.07	8.3-7.8
		10 (first in.)	6.77	0.513	0.564	0.168	0.83	2.72	3.6-3.3
		10 (second in.)	6.14	0.449	0.513	0.174	0.96	3.32	7.1-6.8
GX-176 ⁱ	SR-7	7, 11	14.7	0.524	0.563	0.151	1.26	1.30	9.1-8.8
G-615 ^j	SR-6	12	14.9	0.539	0.626	-	1.0	1.3	7.3-7.1

^aExperiments 1-7 reported in ref. 1.

^bApparent density of the moist charcoal according to the method of ASTM D-2854-70.

^cParticles collected on 8-mesh or passing 16-mesh (U.S.) screens eliminated. $D_p = W/\Sigma (W_i/D_{pi})$.

^dWeight percent based on apparent density of moist (as-received) charcoal. Moisture content varied because of different storage conditions.

^eFirst value obtained from 5 g charcoal in 20-ml water for 30 min at room temperature. Second value after heating to boiling and cooling to room temperature in covered container.

^fProduct of Mine Safety Appliances Company, Pittsburgh, Pa.

^gProduct of Barnebey-Cheney, Columbus, Ohio. Charcoal obtained from A. G. Evans, Savannah River Laboratory.

^hProduct of WITCO Chemical Corporation, New York, N.Y.

ⁱProduct of North American Carbon, Inc., Columbus, Ohio. This charcoal also contains 1% TEDA (triethylenediamine) and a proprietary flame retardant. Charcoal and chemical analyses obtained from A. G. Evans, Savannah River Laboratory.

^jProduct of North American Carbon, Inc., Columbus, Ohio. This charcoal also contains 2% TEDA and a proprietary flame retardant. The charcoal was obtained from A. G. Evans after 9 months service at Savannah River Laboratory.

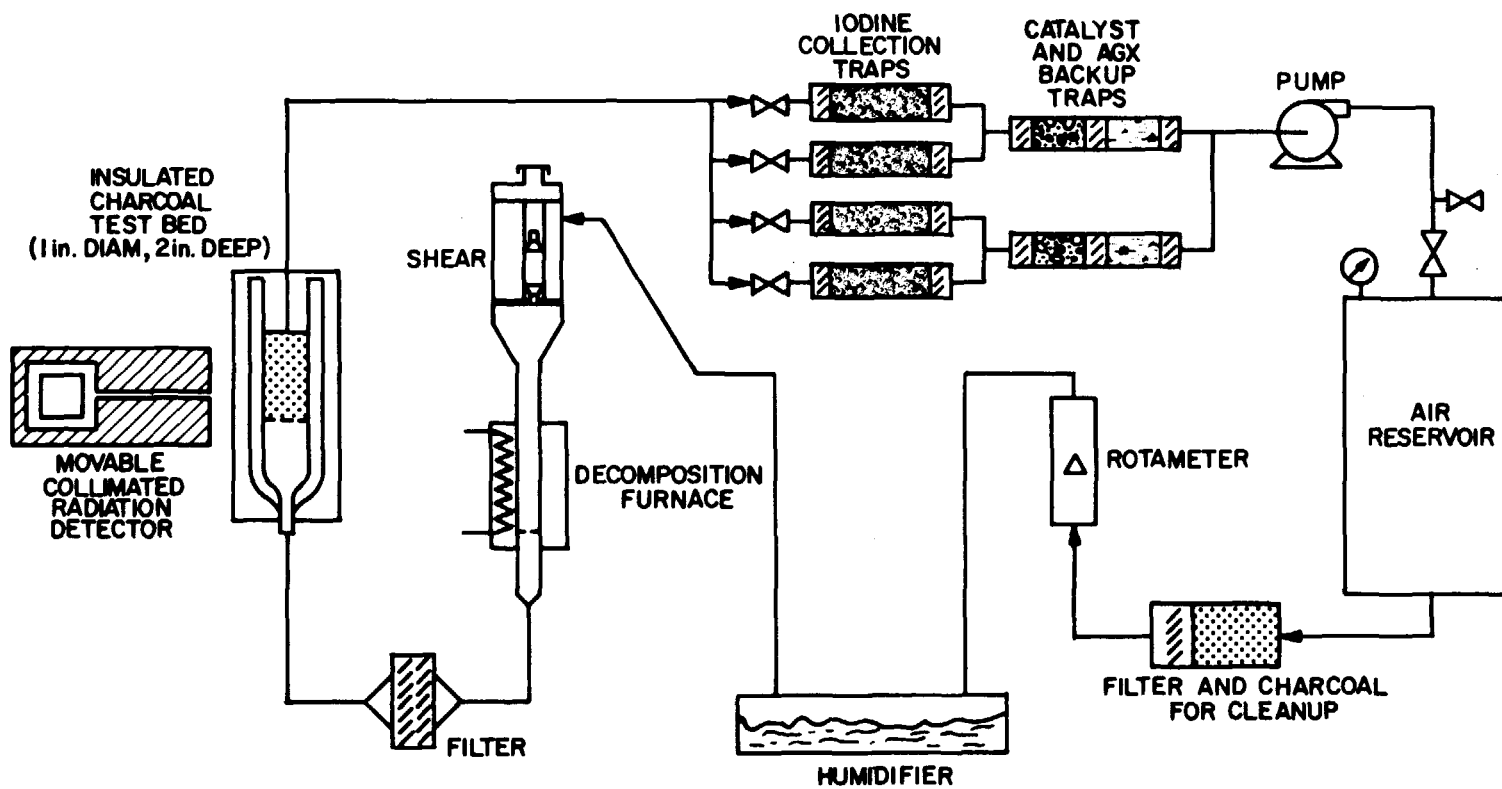


Fig. 1 Flow diagram for experiments with moist air.

both elemental iodine and the more penetrating organic forms of iodine. We examined the distribution of iodine among the cartridges to determine the relative amounts of elemental and organic iodine present.

The experimental procedure can be described as follows. The installed collection traps and heated loop were purged with dried and filtered air, using a once-through mode and a flow rate of 4.9 liters/min for 2.5 hr to dry the loop and remove volatile contaminants. A 28-cm³ volume of the test charcoal in the as-received moisture condition was then poured into the insulated bed through the outlet tube. (The presence of many thermocouples and the restricted fall resulted in a packing density somewhat less than that measured by the method of ASTM-D-2854-70. Assuming a void fraction of 0.43 for normal packing, we estimate a void fraction of 0.45 for the test bed.) Subsequently, the loop heaters were turned on, the irradiated capsule installed, air circulation started, and the capsule sheared when the desired bed temperature was reached. The humidifier was heated to 54 or 55°C to maintain proper humidity.

The air inlet temperature to the bed was controlled at 70°C, and the charcoal bed was heated by the decay heat to some higher temperature, depending on the level of radioactivity and air flow rate, as shown in Tables II-VII. The period of operation at normal air flow rate at the beginning of each experiment enabled observation of the iodine movement and desorption at nearly constant-temperature conditions. The air flow rate was subsequently reduced allowing the temperature to rise, in simulation of an accident situation (except in Run 13). The operating conditions are also summarized in Tables II-VII.

III. Oxidation of Charcoal

The temperature behavior during several of the runs is shown in Figs. 2-5. The accelerating temperature rise during a period of each of these experiments was the result of an increasing rate of heat release from the oxidation of charcoal as the temperature rose. The rate of rise depended on the amount of radioactive iodine decay heat, the oxidation characteristics of the charcoal, and the air flow rate. We calculated the heat balance for the test bed, described in more detail previously,⁽¹⁾ and obtained the rate of heat release also shown in Figs. 2-5. At the very low air flow rates employed in these experiments, the rate of heat release decreased following ignition, possibly due to consumption of the chemically active sites and poisoning of the charcoal surface.

Figure 6 shows the calculated rate of heat release from oxidation as a function of temperature. The heat release data prior to ignition can be correlated for each experiment using the Arrhenius-type equation

$$H = H_0 e^{-A/RT}, \quad (1)$$

where

- H_0 = a constant (cal/min·g charcoal),
- A = an activation energy (cal/mole),
- R = 1.987 cal/mole·°K,
- H = the rate of heat release by oxidation (cal/min·g charcoal).

The values of H_0 and A are given in Table VIII. The experimental heat release data are fairly accurate within the range of 0.5 to 20 cal/min·g charcoal; however, the accuracy of extrapolations beyond this range is uncertain.

The rate of heat release for MSA 85851 during Run 8 was only approximately one-third that observed during Run 4, which was conducted in dry air with charcoal

Table II Summary of conditions and radioiodine release, Run 8 - type MSA 85851 charcoal

Time interval (min)	-340 to -240 ^a	-240 to -120	-120 to 0	0 to 150	150 to 465
Main bed activity (Ci ¹³⁰ I) ^b	465	415	370	320	240
Bed midpoint temp. range (°C)	72-93	80-93	79-80	79-147	147-429
Flow velocity (fpm at 25°C) ^d	28.5	28.5	28.5	3.8	e
Water vapor partial pressure (torr)	85	95	95	100	105

Iodine form	Fraction of radioactive iodine released (10 ⁻⁶)				
Elemental	<0.3	<0.4	0.05	0.13	0.74
Particulate	0.004	0.001	0.001	0.001	1.20
Moderately penetrating	0.5	<0.4	<0.05	<0.1	<0.4
Highly penetrating	~3.0	~8.6	~11.5	f	f
Total ^g	~3.7	~8.6	~11.5	>2.4	>3.4

^aLoading of 100 mg of radioactive iodine took place during this period.

^bActivity at end of time period. The half-life of ¹³⁰I is 12.3 hr.

^cThe ignition temperature (assumed to be 310°C) was reached at 396 min at approximately 0.8-in. bed depth.

^dMoist air at 0.98 atm.

^eVelocity was reduced to 1.43 fpm at 150 min (147°C), reduced to 0.71 fpm at 300 min (195°C), increased to 1.9 fpm at 457 min (369°C), and increased to 3.8 fpm at 460 min (412°C).

^fThese collection traps did not contain silver-exchanged zeolite. Total fraction found in the trap charcoal, loop cleanup charcoal, and humidifier was 47 x 10⁻⁶. Total of all penetrating iodine released was 68 x 10⁻⁶.

^gGrand total fractional release of radioactive iodine was 71 x 10⁻⁶.

Table III Summary of conditions and radioiodine release, Run 9 - WITCO Grade 42 charcoal

Time interval (min)	-465 to -360 ^a	-360 to -240	-240 to -120	-120 to 0	0 to 180	180 to 360
Main bed activity (Ci ¹³⁰ I) ^b	535	480	430	380	320	270
Bed midpoint temp. range (°C)	70-92	81-92	80-81	79-80	79-166	166-181 ^c
Flow velocity (fpm at 25°C) ^d	28.5	28.5	28.5	28.5	3.8	0.71
Water vapor partial pressure (torr)	95	100	95	95	95	95

Iodine form	Fraction of radioactive iodine released (10 ⁻⁶)					
Elemental ^e	~0.4	<0.3	<0.3	<0.3	<0.5	<0.5
Particulate	0.03	0.05	0.06	0.001	0.4	0.002
Moderately penetrating	0.4	0.2	0.2	≤0.2	<0.2	<0.2
Highly penetrating ^f	>1.2	>7.0	>2.6	>12	15	3.1
Total	>1.6	>7.1	>3.2	>12	15.5	3.2

^aLoading of 123 mg of radioactive iodine took place during this period.

^bActivity at end of time period. Half-life of ¹³⁰I is 12.3 hr.

^cIgnition was not reached because of the low radioactivity and the high ignition temperature of WITCO Grade 42 charcoal.

^dMoist air at 0.98 atm.

^eTotal fractional release of elemental iodine was probably in the range 0.4×10^{-6} to 1.4×10^{-6} .

^fThe fraction which penetrated the four collection beds used during normal air flow operation and was collected in the backup bed and humidifier was 21×10^{-6} . Total fractional release of penetrating iodine was 63×10^{-6} .

^gGrand total fractional release was 65×10^{-6} .

Table IV Summary of conditions and radioiodine release, Run 10 - WITCO Grade 42 charcoal from HFIR air cleaning system

Time interval (min)	-470 to -360 ^a	-360 to -300	-300 to -120	-120 to 0	0 to 180	180 to 296
Main bed activity (Ci ¹³⁰ I) ^b	485	460	390	345	290	260
Bed midpoint temp. range (°C)	70-88	83-88	78-83	77-78	77-139	139-376 ^c
Flow velocity (fpm at 25°C) ^d	25.7	28.5	28.5	28.5	3.8	0.71
Water vapor partial pressure (torr)	100	100	110	110	110	110

Iodine form	Fraction of radioactive iodine release (10 ⁻⁶)					
Elemental	-	~1.4	-	-	-	1600
Particulate	<0.2	<0.03	2.5	<0.7	<0.03	<1
Moderately penetrating	130	~76	266	156	24	≤630
Highly penetrating	8	~8	25	15	20	18
Total ^e	139	86	294	171	44	2200

^aLoading of 100 mg of radioactive iodine took place during this period.

^bActivity at end of time period. Half-life of ¹³⁰I is 12.3 hr.

^cIgnition temperature of 283 reached at 275 min at approx. 0.3-in. bed depth. Ignition temperature is based on thermocouple rate-of-rise first reaching 20°C/min. Maximum recorded temperature was 473°C.

^dMoist air at 0.98 atm.

^eGrand total fractional released was 2950 x 10⁻⁶ or 0.295%.

Table V Summary of conditions and radioiodine release, Run 11 - type GX-176 charcoal

Time interval (min)	-470 to -360 ^a	-360 to -300	-300 to -120	-120 to 0	0 to 180	180 to 360
Main bed activity (Ci ¹³⁰ I) ^b	570	540	455	410	345	291
Bed midpoint temp. range (°C)	70-93	89-94	80-87	79-80	79-120	120-396 ^c
Flow velocity (fpm at 25°C) ^d	26-28	16-26	28.5	28.5	5.8	1.9
Water vapor partial pressure (torr)	105	105	110	110	110	110

Iodine form	Fraction of radioactive iodine released (10 ⁻⁶)					
Elemental	<0.3	<0.2	<0.2	<0.2	<0.2	6.4 ^e
Particulate	0.05	0.26	3.0	1.5	0.19	0.50
Moderately penetrating	0.34	<0.2	<0.2	<0.2	<0.2	<0.2
Highly penetrating	6.3	5.2	28.1	20.7	27.7	19.7
Total ^f	6.7	5.5	31.1	22.2	27.9	26.6

^aLoading of 133 mg of radioactive iodine took place during this period.

^bActivity at end of time period. Half-life of ¹³⁰I is 12.3 hr.

^cIgnition temperature of 307°C was reached at 319.5 min after first flow reduction. Maximum recorded temperature was 504°C.

^dMoist air at 0.98 atm.

^eThis amount of iodine was leached from tubing network between the main test bed and the adsorber traps. Most of the release probably occurred at the high bed temperature and was probably mostly elemental iodine.

^fNot included were 7.2 x 10⁻⁶ found in loop cleanup bed and 0.4 x 10⁻⁶ in humidifier. Grand total release was 124.6 x 10⁻⁶, or 0.0125%.

Table VI Summary of conditions and radioiodine release, Run 12 - type G-615 charcoal used 9 months at SRL

Time interval (min)	-491 to -361 ^a	-361 to -300	-300 to -120	-120 to 0	0 to 180	180 to 450
Main bed activity (Ci ¹³⁰ I) ^b	480	455	380	340	290	225
Bed midpoint temp. range (°C)	71-85	85-95	80-85	74-80	74-113	113-219
Flow velocity (fpm at 25°C) ^c	21.5	9-22	22	23	5.8	2.9
Water vapor partial pressure (torr)	110	110	115	115	110	115

Iodine form	Fraction of radioactive iodine released (10 ⁻⁶)					
Elemental	<0.6	<0.6	<0.3	<0.6	<0.5	6.0 ^d
Particulate	0.09	0.06	0.5	0.3	0.02	0.008
Moderately penetrating	0.6	<0.6	<0.3	<0.6	<0.5	<2.9
Highly penetrating	8.5	10.9	44.7	28.8	35.0	73.7
Total ^e	9.2	11.0	45.2	29.1	35.0	79.7

^aLoading of approximately 110 mg of radioactive iodine took place during this period.

^bActivity at end of time period. Half-life of ¹³⁰I is 12.3 hr.

^cMoist air at 0.98 atm.

^dThis amount of iodine was leached from the tubing network between the main test bed and the adsorber traps. Most of the release probably occurred at the high bed temperature and was probably mostly elemental iodine.

^eNot included were 10.9×10^{-6} found in the loop cleanup bed and 0.3×10^{-6} in the humidifier water. Grand total release was 221×10^{-6} , or 0.022%.

Table VII Summary of conditions and radioiodine release, Run 13 - type MSA 85851 charcoal

Time interval (min)	-145 to 0 ^a	0 to 60	60 to 195	195 to 315	315 to 2895	2895 to 3015
Main bed activity (Ci ¹³⁰ I) ^b	50	47	42	37	3.3	2.9
Bed midpoint temp. range (°C)	70-71	67-71	69-71	70	68-70	70
Flow velocity (fpm at 25°C) ^c	28.5	21.1	28.5	28.5	28.5	28.5
Water vapor partial pressure (torr)	120-150	120-150	120-150	140	140-145	140-145

Iodine form	Fraction of radioactive iodine released (10 ⁻⁶)					
Elemental ^d	<0.2	<0.05	<0.06	<0.1	<20	<0.6
Particulate	0.001	0.003	0.008	0.0006	0.004	0.007
Moderately penetrating	0.2	<0.05	<0.06	<0.1	<20	<0.6
Highly penetrating	8.3	6.6	13.9	15.3	111	1.6
Total ^e	8.5	6.6	13.9	15.3	111	1.6

^aLoading of approximately 77 mg of radioactive iodine took place during this period.

^bActivity at end of time period. Half-life of ¹³⁰I is 12.3 hr.

^cMoist air at 0.98 atm.

^dThe fraction 0.8×10^{-6} was leached from the tubing network between the main test bed and the adsorber traps.

^eNot included were 2.6×10^{-6} found in the loop cleanup bed and 0.3×10^{-6} in the humidifier water. Grand total release was 160×10^{-6} , or 0.016%.

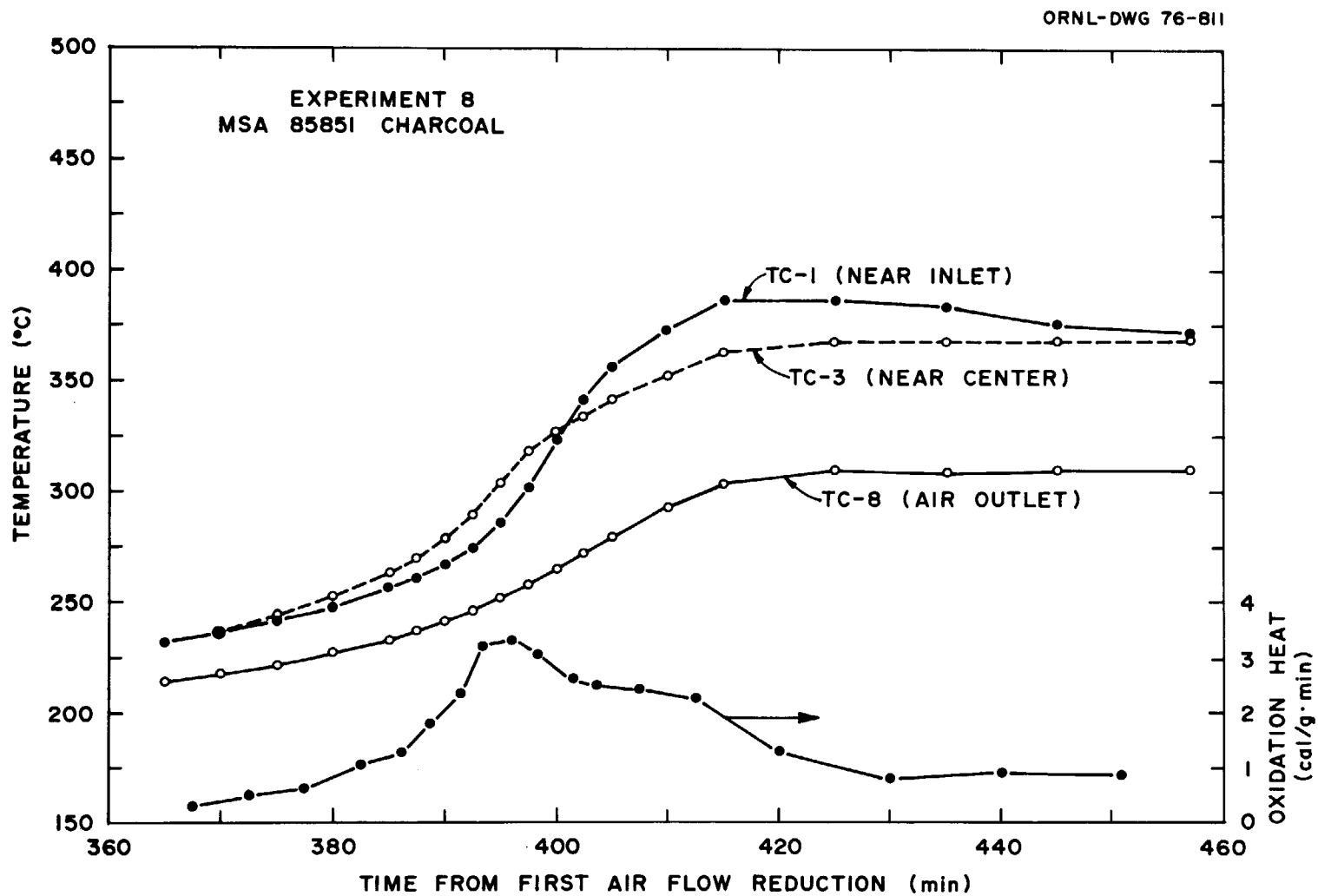


Fig. 2 Temperature behavior during Run 8 with MSA 85851 charcoal.

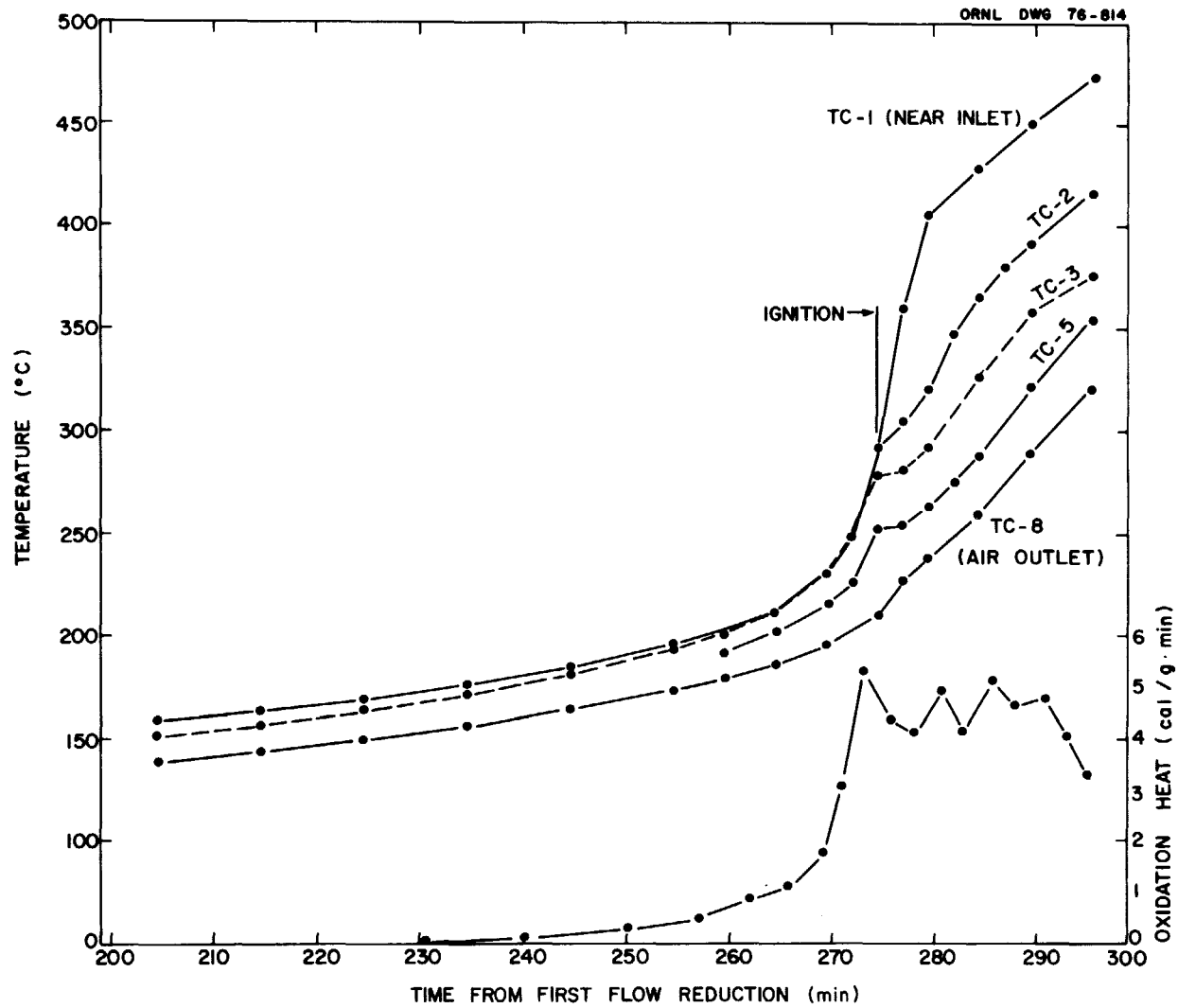


Fig. 3 Temperature behavior during Run 10 with WITCO Grade 42 used four years in the HFIR.

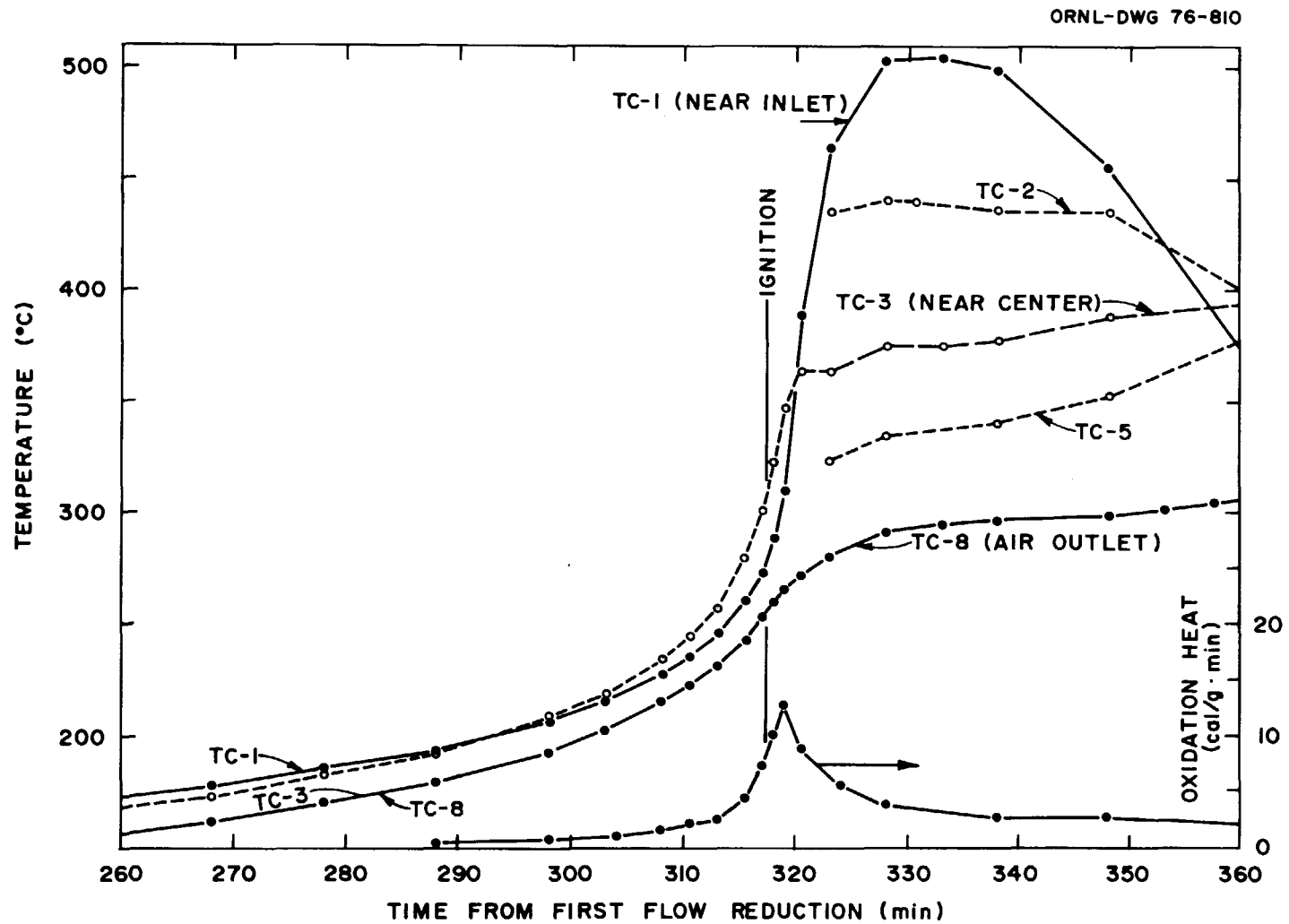


Fig. 4 Temperature behavior during Run 11 with GX-176 charcoal.

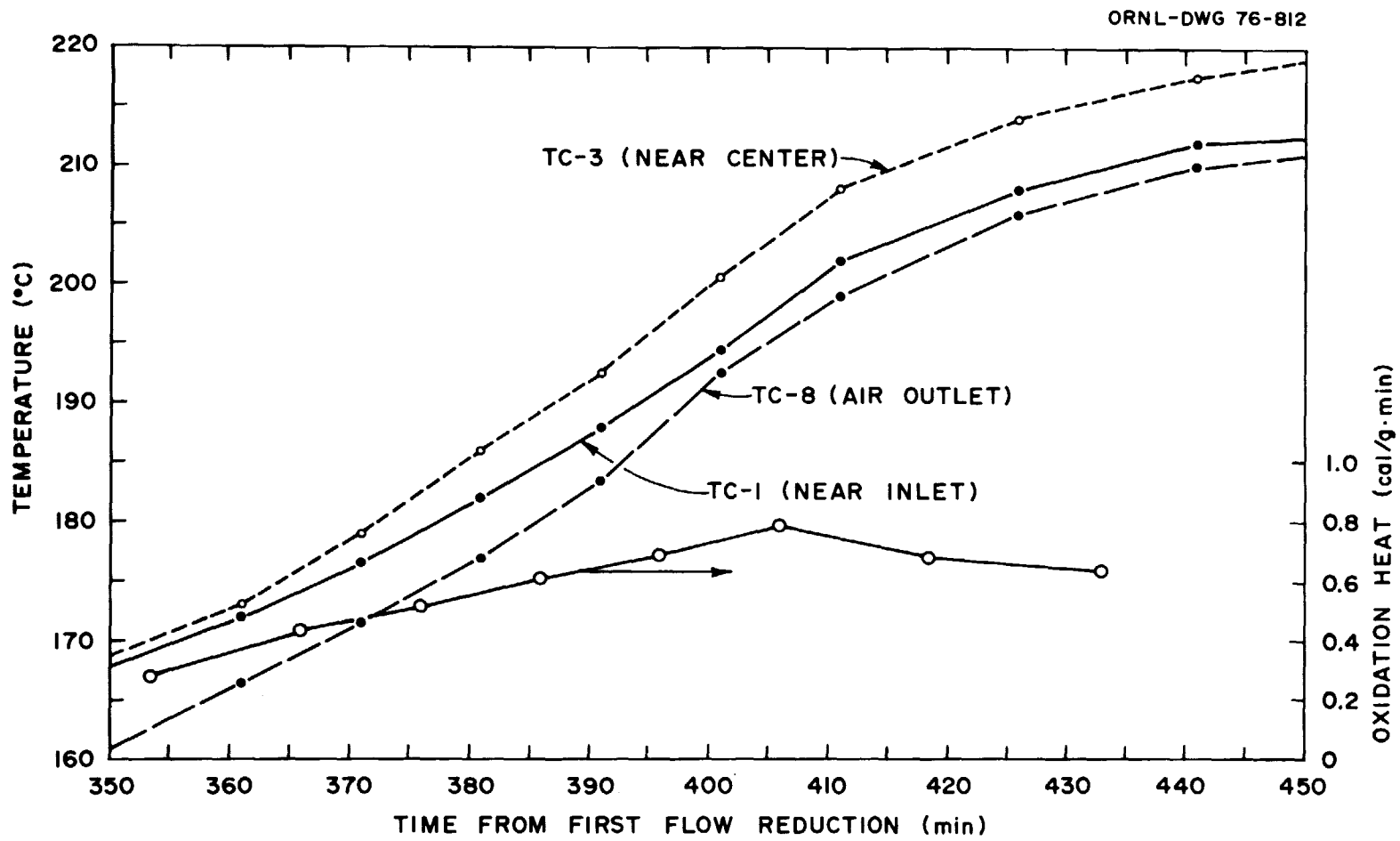


Fig. 5 Temperature behavior during Run 12 with G-615 charcoal used nine months at SRL.

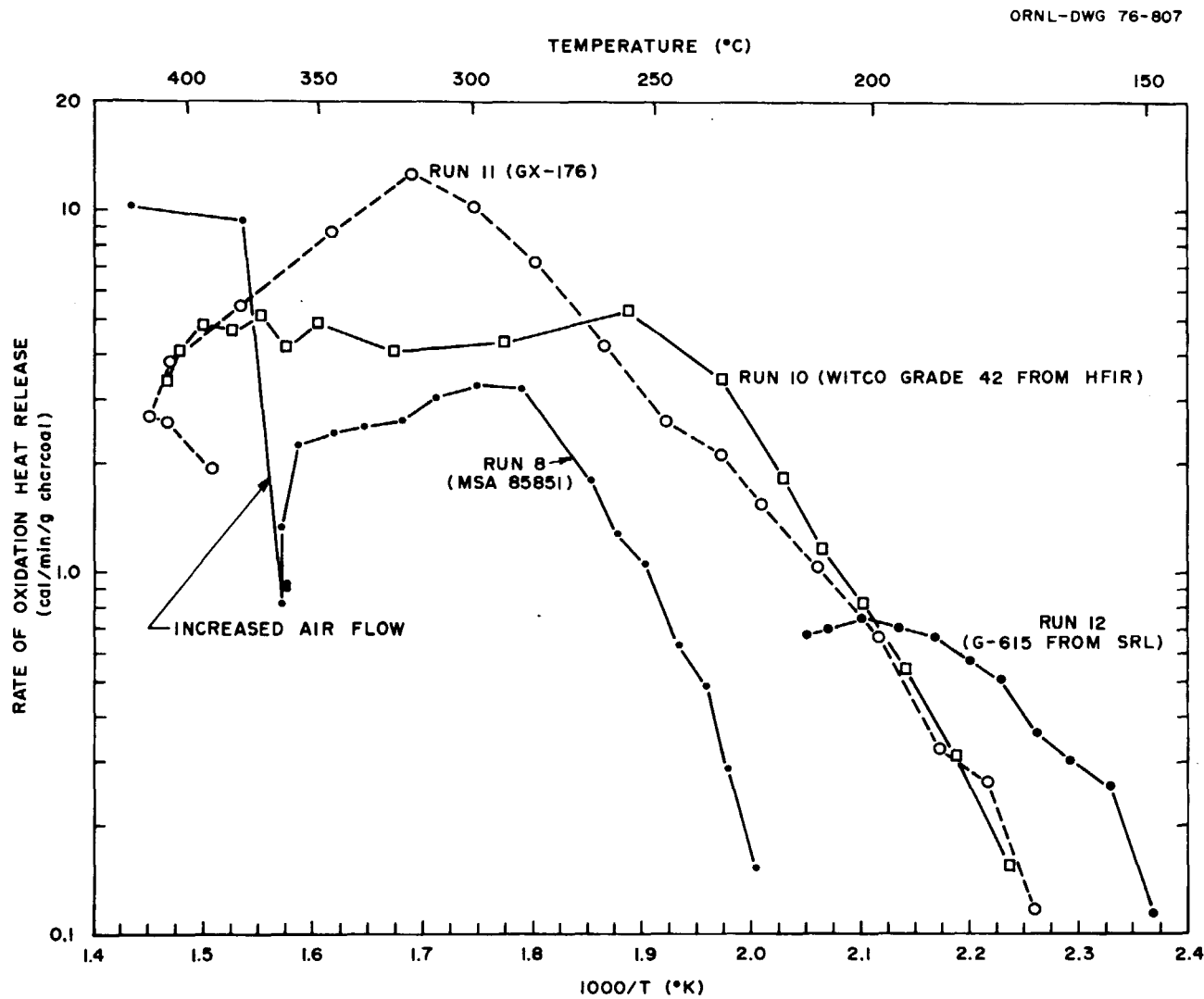


Fig. 6 Rate of oxidation heat release during experiments with moist air.

Table VIII Charcoal oxidation characteristics

Type of charcoal	Run No.	Air velocity (fpm at 25 °C)	Oxidation rate parameters		Ignition temp. (°C)
			$\frac{H_2O}{A}$ (cal/min·g charcoal)	A (cal/mole)	
MSA 85851 Lot No. 51969	8	0.7	2.05×10^8	20,000	a
WITCO Grade 42 HFIR, 4 yr service	10	0.7	1.25×10^9	20,000	283
GX-176 SR-7	11	1.6	3.37×10^6	14,500	307
G-615 (9 mo. service) SR-6	12	2.5	5.41×10^6	14,500	a

^aNot determined.

from the same batch and nearly three times as much radioactive iodine. We believe that much of this difference resulted from the very slow rate of heatup during Run 8, which allowed consumption of chemically active sites in the charcoal. When the air flow rate was increased for the final 7 min of the experiment, the oxidation heat release rate and the bed temperatures increased rapidly as seen in Fig. 6.

In Run 9, which used WITCO Grade 42 charcoal, a maximum temperature of 184°C was reached and measurable heat was not evolved from oxidation at that temperature. In Run 10, charcoal from the same purchase lot that had been used for four years in the High Flux Isotope Reactor (HFIR) air cleaning system at Oak Ridge released heat by oxidation at much lower temperatures and ignited at 283°C. Previous tests with unused charcoal from the same purchase lot indicated an ignition temperature of approximately 368°C.⁽¹⁾ It is quite clear that the adsorbed atmospheric contaminants promoted ignition of the base charcoal. The first 1-in. depth of our test bed contained charcoal from the first 1-1/8 in. bed in the HFIR system and the second 1-in. depth was taken from the second 1-1/8 in. HFIR bed. Infrared analysis of CCl₄ extracts revealed hydrocarbon concentrations of 145 and 71 mg/g in the respective HFIR charcoals. Based on the reported air flow during the four years of service, the concentration of adsorbed hydrocarbons was approximately 50×10^{-9} g per gram of air. This is compatible with the 290×10^{-9} g/g (excluding methane) concentration found in the HFIR building in 1967.⁽²⁾ The apparent density of the HFIR charcoal indicates a total weight gain almost twice that given by the CCl₄-infrared method.

The heat from oxidation measured for GX-176 during Run 11 was slightly lower than that measured previously during Run 7.⁽¹⁾ As shown in Fig. 5, the oxidation heat release rate decreased and the bed temperatures stabilized after ignition.

Run 12 was made with type G-615 charcoal that had been in service for nine months at the Savannah River Laboratory (SRL) and contained 16 mg of hydrocarbons per gram according to infrared analysis of a CCl₄ extract. As shown in Figs. 5 and 6, the organic contaminants and/or TEDA impregnant apparently oxidized at relatively low temperatures, but the heat released was insufficient to ignite the base charcoal. We believe that a higher rate of temperature rise provided either by a lower air flow or a higher radiation decay heat could have resulted in ignition of the base charcoal. Both G-615 and GX-176 are reported to contain a proprietary flame retardant that could influence the oxidation heat release rates.

A sophisticated computation of temperatures of a charcoal bed containing organic material would properly assume separate oxidation heat release rate equations for the base charcoal and for the organic material, and provide a maximum total heat release for the organic material, depending on the amount present.

IV. Release and Desorption of Iodine

As mentioned previously, we used sequentially operated traps composed of high-efficiency filters, charcoal cartridges, and silver-exchanged zeolite to distinguish the iodine forms released during the course of the experiments. The results are summarized in Tables II-VII. Identification of the form of the collected iodine was uncertain in some cases. For example, most of the released elemental iodine plated out in tubing common to all of the individual collection traps. Many of our collection beds operated at an unusually low air velocity, a condition for which very little I₂/CH₃I adsorption efficiency data have been reported. For constant residence time, adsorption efficiency decreases when velocity is lowered. Our rather scattered data suggest that, for velocities in the range of 1 to 10 cm/sec, the adsorption (trapping) efficiency for methyl iodide on good-quality impregnated

charcoal will not exceed values extrapolated from the data of May and Polson⁽³⁾ for nearly dry air. Another departure from conventional iodine adsorption testing techniques was the absence of clean air purging following a collection period. This permitted loosely adsorbed forms of radioactive iodine to be spread throughout the collection bed.

Highly Penetrating Iodine

Our first experiment with moist air, Run 8, revealed that most of the radioactive iodine released from the main test bed was in a chemical form unusually penetrating with respect to impregnated charcoal. For subsequent runs we eliminated the silver-plated honeycombs (used for trapping elemental iodine) and increased the number of cartridges containing silver-exchanged zeolite (AgX).

The highly penetrating nature of the released radioactive iodine is illustrated in Fig. 7. The collection trap from which these data were obtained was operated for 2 hr, beginning 4 hr after loading was completed. The trap temperature was 130°C, the air velocity was 17.3 cm/sec at 130°C, and the total residence time (charcoal + AgX) was 0.43 sec. (The collection traps were heated in order to produce low relative humidity and therefore promote high adsorption efficiency.) With the exception of Run 10, the distribution of radioactive iodine among the charcoal cartridges indicated loosely held or poorly sorbed species. We believe that the large amount of radioactive iodine on the first cartridge in Run 10 was methyl iodide. Under the operating conditions of this collection bed, each charcoal cartridge should collect more than 95% of the entering methyl iodide. In addition to G-618, eight other types of commercial impregnated charcoal were tested in other collection traps without significant difference in adsorption efficiency.

The silver-exchanged zeolite was much more efficient for collecting the highly penetrating radioactive iodine. The decrease in slope between the AgX cartridges (Fig. 7) suggests that at least two forms of highly penetrating iodine were present. Our AgX material was prepared from type 13X molecular sieves in the 1/16-in.-diam pellet form (mean particle diam, 0.20 cm; void fraction, 0.55) exchanged to > 95% silver content. Two other batches of the same size AgX prepared by others were tried in other collection beds; no efficiency difference was observed. AgX beads in the 10-20 mesh range and granular AgX in the 12-16 mesh range (particle diam, 0.16 cm; void fraction, 0.43) were also tried, and both were found to have higher efficiencies. The mean particle size and void fraction differences could easily account for the higher adsorption efficiency because of improved gas-phase mass transfer.

Beginning with Run 10, we added high-temperature backup beds in the circuits used during operation at normal air flow rates. Beginning with Run 12, all flow lines were routed through these beds which contained a total of 45 cm³ of Hopcalite, an oxidizing catalyst, MSA lot No. 21215.* This was followed by a total of 42 cm³ of silver-exchanged zeolite pellets, all in a 2.84-cm-diam tube. Table IX shows the results of most of the high-temperature backup traps. Although the AgX appears to have performed efficiently, a large amount of radioactive iodine reached the loop cleanup filter which contained 550 cm³ of BC-72L, an unimpregnated charcoal.

* Mine Safety Appliances Co.

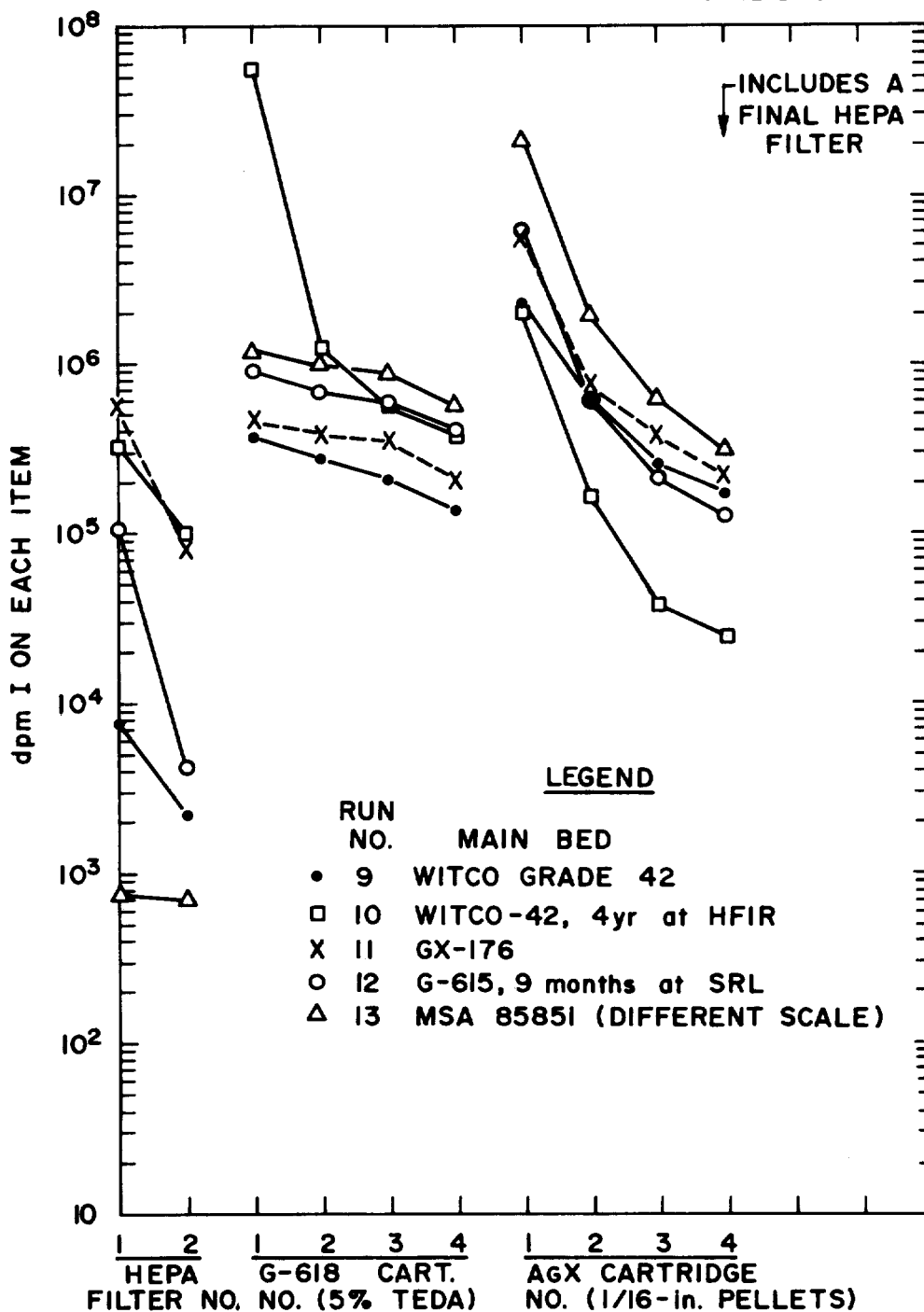


Fig. 7 Distribution of radioactive iodine among components of a collection trap.

Table IX Performance of high temperature backup beds

Component	Approximate temperature (°C)	Run 10	Run 11	Run 12	Run 13	
		(10 ⁵ dpm ¹³¹ I)	(10 ⁵ dpm ¹³¹ I)	(10 ⁵ dpm ¹³¹ I)	(10 ⁸ dpm ¹³⁰ I)	(10 ⁸ dpm ¹³⁰ I)
HEPA filter	150	0.0005	0.0010	<0.002	0.004	0.0001
1st Hopcalite	280	0.41	0.52	0.34	0.010	0.24
2nd Hopcalite	320	0.52	0.65	0.63	0.009	0.26
3rd Hopcalite	360	0.78	1.64	1.5	0.036	0.30
1st AgX	380	17.7	72.2	1.9	13.2	20.0
2nd AgX	400	0.0034	18.2	0.007	3.3	0.14
3rd AgX	420	0.0069	1.1	0.005	0.0002	0.006
HEPA filter	200	<0.0005	0.0003	Not used	Not used	Not used
Loop cleanup bed ^a	70	16.5	31.8	37.7	5.98	
Time in use (min)		300.0	410.0	491.0	460.0	2700.0

^a Apparent penetration of above high temperature backup beds.

Such large penetrations are difficult to understand. The distribution of radioactive iodine in the loop cleanup filter was examined to determine whether back-diffusion from the humidifier and main test bed during the 8-day cooldown period could be the source of the iodine. We discovered that some back-diffusion had occurred, but only perhaps 10% of the total on the cleanup bed. Ackley and Davis tested this same catalyst and found it to be beneficial when CH_3I was used but detrimental when I_2 was being tested.⁽⁴⁾ A single test with AgX only in a high-temperature backup trap in our system was inconclusive because of possible penetration through a Hopcalite-AgX combination used later in the same run. Our calculations indicate that much of the improved performance of AgX with methyl iodide with increased temperature can be accounted for by improved gas-phase mass transfer.

Two other adsorbing materials were tested for their ability to trap the highly penetrating iodine. AC-6120* is a noncombustible adsorbent which traps I_2 and CH_3I very efficiently.⁽⁵⁾ It is a porous form of amorphous silicic acid impregnated with AgNO_3 . We tested this bead-shaped material in our standard collection beds at 130°C during Run 13. Its performance was shown to be comparable to the charcoals and inferior to AgX for trapping our highly penetrating iodine. Similar results were obtained for GX-135, a granular silver nitrate-coated aluminum silicate-based material which is not currently being manufactured.

The rates of release of highly penetrating iodine and the moderately penetrating form, which behaved like methyl iodide, are summarized in Table X. The release rates for the highly penetrating form were generally within the range 7 to 10×10^{-6} / hr. Release rates during the first time periods shown for each run were lower. This was the period for loading of the radioactive iodine and, on the average, only half of the iodine was on the main test bed available for desorption. Based on the true amount on the bed, these first period rates should be approximately doubled. In Run 13, with reduced radioactivity, the release rates were essentially normal for the first two time periods listed, but then decreased slowly as time progressed and the radioactive iodine decayed to much lower intensities.

Samples of gas taken from the air reservoir tank were analyzed by gas chromatography. Methane was always detected and occasionally other hydrocarbons as well. Following Run 9 the reservoir contained 10 ppm methane (CH_4). The sample of gas following Run 10 contained 160 ppm methane, approximately 15 ppm ethane (C_2H_6), and approximately 45 ppm propane (C_3H_8). Gas from Run 11 contained 95 ppm methane and a trace of ethane, and gas from Run 12 contained 16 ppm methane.

Characteristics of the Highly Penetrating Iodine

Beginning with Run 10, we added a sampling circuit (not shown in Fig. 1) in an attempt to collect and identify the highly penetrating iodine form(s). The circuit consisted of two HEPA filters, a condenser at 0°C , a freeze trap at -78°C , and a trap at -78°C containing cartridges of type 13X sodium zeolite, silica gel, Tenax, and Porapac-Q (the latter two are commercial chromatograph packings) alone or in combinations, depending on the experiment. The HEPA filters, condenser, and freeze traps collected only very small amounts of the radioactive iodine. All of the sorbents retained the radioactive iodine efficiently at -78°C , but the Porapac-Q appeared to release the iodine more easily when the sorbents were subsequently warmed for transfer of the radioactive iodine to an evacuated stainless steel holding tank.

* Bayer/Leverkusen.

Table X Rate of release of penetrating forms of radioactive iodine

Run No.	Amount of radioactive iodine (Ci ^{130}I)	Time from first flow reduction (min)	Average temp. ($^{\circ}\text{C}$)	Partial pressure of water (torr)	Release rate x 10^6 (fraction/hr)	
					Moderately penetrating iodine	Highly penetrating iodine
8	0-465	-340 to -240	82	85	0.3	~2
	465-370	-240 to 0	82	95	<0.1	~5
	370-240	0 to 465	~150	105	<0.1	~6
9	535-380	-360 to 0	81	95	0.2	~7
	380-320	0 to 180	125	95	<0.1	5
	320-270	180 to 360	174	95	<0.1	1.0
10	0-485	-470 to -360	79	100	51	4.4
	485-345	-360 to 0	79	110	83	8.0
	345-290	0 to 180	~110	110	16	13
	290-260	180 to 296	~260	110	<325	9.3
11	0-570	-470 to -360	82	105	0.2	3.4
	570-410	-360 to 0	82	110	<0.1	9.0
	410-345	0 to 180	~100	110	<0.1	9.2
	345-290	180 to 360	~260	110	<0.1	6.6
12	0-480	-491 to -361	78	110	0.3	3.9
	480-340	-361 to 0	80	115	<0.3	14
	340-290	0 to 180	~94	110	<0.2	12
	290-225	180 to 450	~170	115	<0.6	16
13	0-50	-145 to 0*	70	135	0.08	3.4
	50-37	0 to 315	70	135	<0.04	6.8
	37-3.3	315 to 2895	69	142	<0.5	2.6
	3.3-2.9	2895 to 3015	70	142	<0.3	0.8

*For Run 13, time "0" corresponds to end of loading of radioactive iodine.

14th ERDA AIR CLEANING CONFERENCE

After several days to allow reduction of the radiation intensity by decay, the contents of the tank were admitted to a mass spectrometer for mass identification. Relatively large amounts of air and CO₂ adsorbed along with the radioactive iodine during the experiment were present in the holding tank and provided a high background which interfered with the iodine-containing mass peaks in the mass spectrometer. A positive peak at mass 130, presumably H¹²⁹I, was observed in the gas from Run 10; however, we believe that this is a result of reaction with some system component. In later experiments we decreased the air + CO₂ background by concentrating the radioactive iodine in a small trap containing cooled Tenax, but the mass results were inconclusive.

The original radioactive iodine loaded onto the main test bed contained ¹²⁹I and ¹²⁷I in the ratio of 6:1. The mass spectrometer revealed several paired mass peaks with approximately this same ratio. The larger of the paired peaks occurred at masses 131, 141, 168, 181, 186, 191, and 198. Mass peaks at 262, 278, 281, 331, and 354 were also seen frequently but appeared to be associated with the background emanating from within the needle valve, probe, and mass spectrometer internals.

None of these masses corresponds to a common iodine compound; in reality, we do not know whether any of them actually contained iodine. Since all of the charcoals in the main test bed contained impregnated iodine (¹²⁷I) in greater quantity than the loaded radioactive iodine, we expected that the highly penetrating iodine leaving our test bed might have ¹²⁹I/¹²⁷I ratios of much less than 6:1.

Several incidental noniodine-containing masses were observed. From Runs 11 (new GX-176) and 12 (new MSA 85851) we observed masses 101, 103, and 105, corresponding to the fragment CFC1₂⁺. From Run 12 (G-615 used nine months at SRL) we observed Freon 113 (1,1,2-trichloro-1,2,2-trifluoroethane), Freon 112 (1,1,2,2-tetrachlorodifluoroethane), and a large amount of trichloroethylene.

From the amount of radioactive iodine collected in the condenser in this circuit we could estimate the solubility of the form of iodine present. For Run 10 (which contained predominantly a methyl iodide-like form), as well as later runs (which exhibited only the highly penetrating form of iodine), we calculated partition coefficients $\leq 10 \text{ g I/cm}^3 \text{ water/g I/cm}^3 \text{ air}$ at 0°C. The radioactive iodine in the condensate was readily extracted by carbon tetrachloride. This behavior and the low partition coefficient suggest some organic iodide form(s). Formation and release from the main test bed was essentially independent of air velocity and temperature. Only traces of highly penetrating iodine were observed during the dry air experiments. We observed that most of the radioactive iodine became tightly bound after a long holdup time on most of the mentioned adsorbents (including charcoal). J. G. Wilhelm⁽⁶⁾ has shown that aryl iodides exhibit much of the behavior described above, but we have not been able to detect any of this class of compounds.

Release of Methyl Iodide

A small amount of methyl iodide-like material either penetrated through or was released from the main test bed during the loading phase of each experiment. The identification was based only on its trapping behavior on impregnated charcoal. Methyl iodide-like material was not observed later in the runs except for Run 10 in which this type of material was continuously released. With the dry air experiments,⁽¹⁾ most of the form of iodine described as "penetrating" is believed to have been methyl iodide although no positive identification was made. Small amounts of the highly penetrating form were present in at least some of the dry air experiments; however, it was rarely detected because of smaller collection beds, only occasional use of AgX sorbent, and concealment by ^{131m}Xe radioactivity (a daughter of ¹³¹I) that accumulated in the recirculating loop.

14th ERDA AIR CLEANING CONFERENCE

Desorption of Elemental Iodine

Since very little elemental iodine was released from the end of the main test bed, we used data collected with the collimated gamma scanner to calculate iodine adsorption/desorption coefficients. Gamma scan data are shown in Fig. 8 and in Table XI. A computer program was written to calculate the partial pressure of iodine in equilibrium with the charcoal according to the observed rate of movement within the bed. The rate of mass transfer for elemental iodine is very rapid, so that there is an essentially continuous equilibrium between the charcoal and the vapor phase. Therefore, the extent of movement of iodine should be directly proportional to the air velocity within the bed. The gamma scanner monitored 17 increments, or slabs, along the length of the bed. We assumed that iodine which desorbed from the first (inlet) slab was re-adsorbed on the second slab, etc. We assumed a linear adsorption isotherm; this means that the partial pressure of iodine is directly proportional to the mass concentration on the charcoal, $P = x/k$, where P is the partial pressure of iodine (atm), x is the total concentration of iodine on the charcoal, and k is the adsorption coefficient.

The calculation is most accurate for the first 1/2-in. of bed depth; hence we correlated experimental k values for this region with the temperature obtained from a thermocouple located in that region of the bed. Results are shown in Fig. 9. For each type of charcoal we can express the value of k satisfactorily with the equation $k = k_0 e^{-A/RT}$, where A is the activation energy (cal/mole), R is the gas constant, T is the absolute temperature ($^{\circ}K$), and k_0 is a constant for each type of charcoal (g I/g charcoal·atm I_2).

The coefficients calculated for these moist air experiments are essentially the same as those determined previously for the dry air experiments.⁽¹⁾ The one exception is Run 10, which used heavily contaminated charcoal that desorbed iodine at a rate approximately six times greater than other charcoals.

When test bed temperatures remained constant, the calculated coefficients generally rose somewhat with longer times indicating stronger adsorption. Therefore, the coefficients shown in Fig. 9 should be used only for short-term situations such as those in our experiments. The relatively large mass of radioactive iodine used in our experiments may have contributed to this behavior.

We had expected that significant differences in adsorption coefficient might be observed for different charcoals since previous observations have demonstrated a strong effect of relative potassium and iodine concentrations on iodine desorption.^(1,7,8) Our assumption that the observed movement of iodine within the test bed was simple elemental iodine adsorption/desorption could be in error; the high radiation field could enhance the movement by some yet unrecognized mechanism. The ion chamber gamma scanner readings contained distortions introduced by collimator inefficiency and the inclusion of scattered radiation. No corrections were made for these distortions which made the low-activity readings appear higher than their true levels. F. G. May performed a calibration that demonstrated the type of distortion inherent in the system.⁽⁹⁾

V. Conclusions

Heat from the oxidation of charcoal and organic contaminants is an important contributor to attainment of ignition. Computer programs such as CHART⁽¹⁾ and TOO HOT⁽¹⁰⁾ have demonstrated satisfactory calculation of charcoal bed temperatures, including ignition, when heat release resulting from oxidation of the charcoal was included.

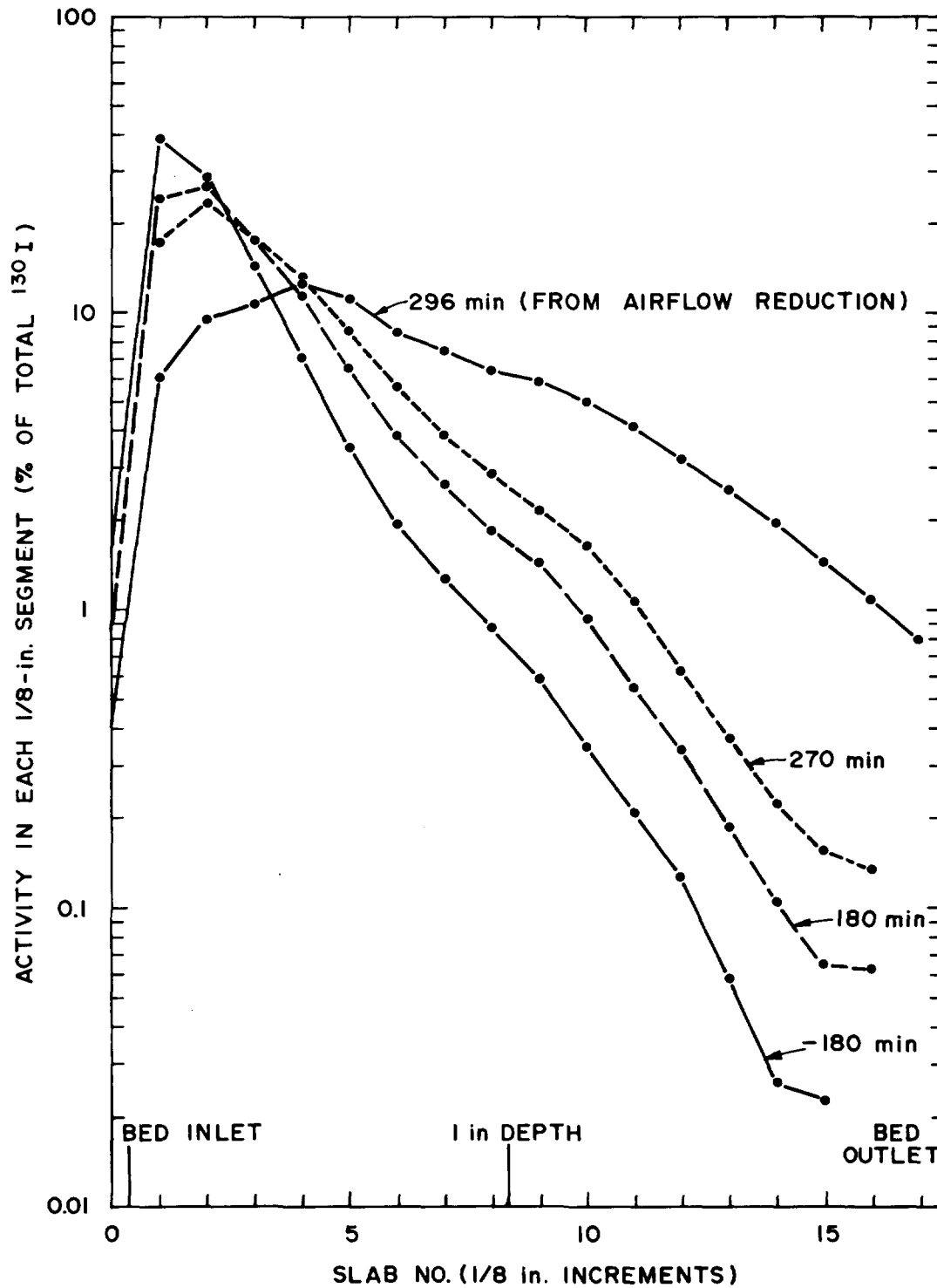


Fig. 8 Distribution and movement of radioactive iodine in the main test bed of Run 10.

Table XI Distribution of radioactive iodine in main test bed

Slab No. *	Percent of total radioactivity in each slab																	
	Run 8				Run 9			Run 11			Run 12				Run 13			
	Time from flow reduction (min)				Time from flow reduction (min)			Time from flow reduction (min)			Time from flow reduction (min)				Time from end of loading (min)			
	-235	0	300	465	-360	0	360	-360	0	180	360	-360	0	180	450	0	1440	2880
1	17.7	12.4	7.5	3.2	16.1	13.9	6.3	6.3	4.7	2.9	0.5	4.9	3.2	2.6	1.4	2.5	2.1	2.0
2	59.7	61.4	57.4	26.2	55.2	53.3	46.8	64.2	61.4	59.7	7.8	59.0	55.3	54.3	37.2	61.3	58.2	56.4
3	13.3	15.9	23.3	22.8	16.2	18.3	26.9	20.2	23.5	26.4	11.2	22.6	25.9	27.0	34.8	25.2	27.9	29.0
4	3.92	4.48	5.93	17.7	5.04	6.33	10.2	4.62	5.37	5.78	11.6	7.36	8.60	8.90	15.2	5.56	6.16	6.46
5	1.62	1.89	2.27	12.7	2.45	3.11	4.21	1.71	1.97	2.07	12.2	2.47	3.01	3.12	5.53	2.12	2.31	2.38
6	0.86	0.95	1.03	7.74	1.01	1.24	1.56	0.91	1.00	1.02	11.8	1.24	1.46	1.49	2.44	1.00	1.06	1.11
7	0.52	0.55	0.55	4.09	0.60	0.75	0.84	0.59	0.61	0.62	10.8	0.75	0.86	0.88	1.23	0.65	0.70	0.72
8	0.39	0.42	0.40	2.34	0.38	0.47	0.55	0.42	0.43	0.44	9.47	0.49	0.54	0.55	0.72	0.44	0.45	0.51
9	0.27	0.28	0.27	1.18	0.23	0.29	0.34	0.30	0.31	0.31	7.59	0.33	0.36	0.36	0.43	0.31	0.31	0.38
10	0.18	0.19	0.16	0.55	0.14	0.18	0.21	0.21	0.22	0.23	6.10	0.24	0.25	0.26	0.31	0.23	0.23	0.29
11	0.13	0.13	0.11	0.28	0.10	0.11	0.14	0.15	0.16	0.16	5.50	0.17	0.19	0.18	0.22	0.16	0.16	0.22
12	0.09	0.09	0.07	0.13	0.07	0.08	0.10	0.10	0.11	0.11	2.75	0.11	0.12	0.12	0.15	0.12	0.11	0.16
13	0.08	0.07	0.04	0.08	0.07	0.07	0.08	0.07	0.07	0.07	1.44	0.07	0.08	0.08	0.10	0.06	0.07	0.10
14								0.04	0.04	0.05	0.61	0.05	0.05	0.05	0.07	0.04	0.04	0.09
15											0.26							
16											0.18							
17											0.16							
Background																		
Bed midpoint temp. (°C)	85	82	196	429	87	81	178	85	78	120	394	83	78	113	219	73	73	73

* Each slab is determined by collimator movement of 0.125 in. (0.318 cm).

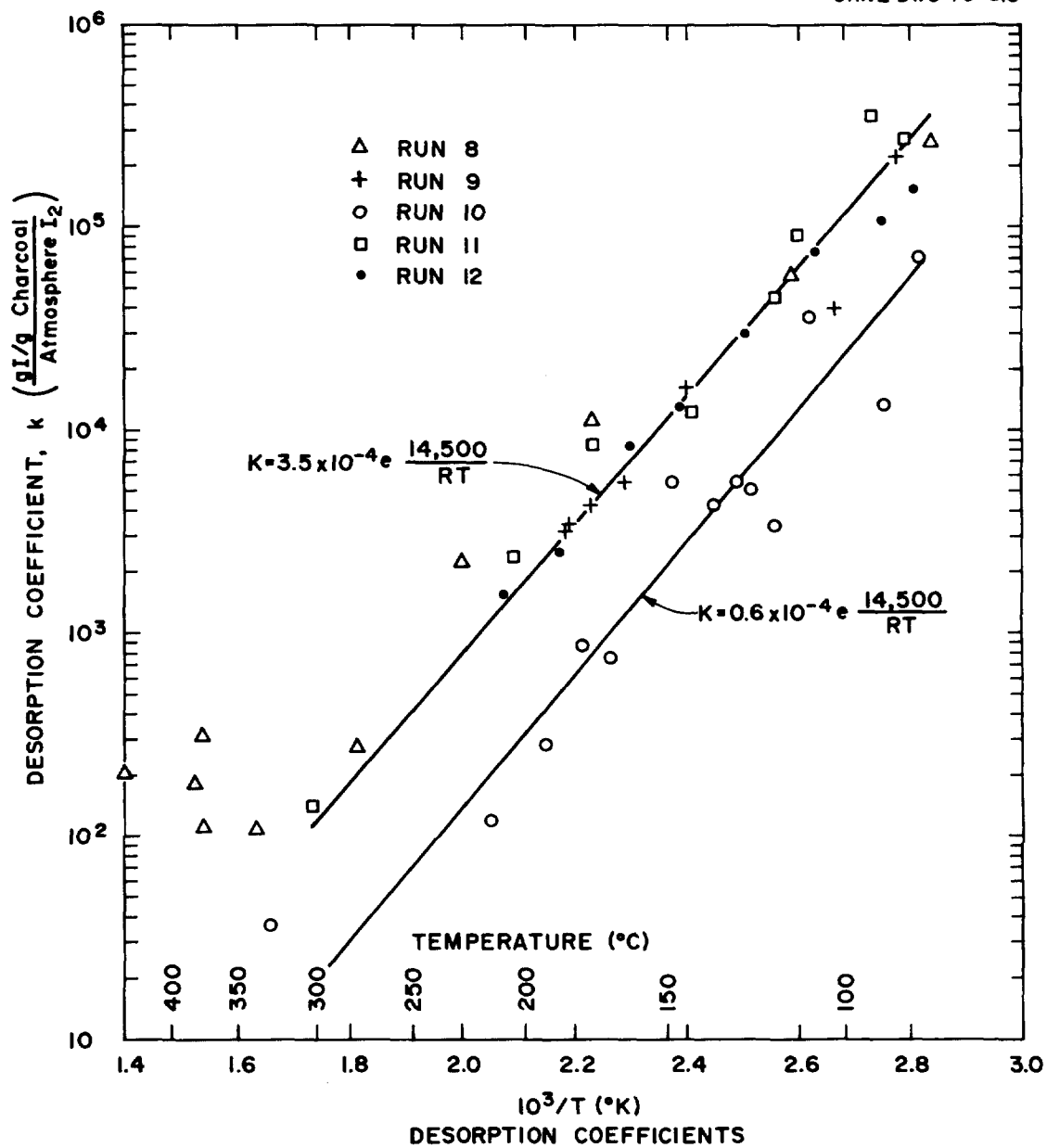


Fig. 9 Desorption coefficients calculated for radioactive iodine in the main test bed of experiments conducted in moist air.

14th ERDA AIR CLEANING CONFERENCE

Movement of radioactive iodine within the charcoal bed and desorption from the end of the bed were trivial before ignition at the low air flow rates used in our experiments (0.7 to 3.8 fpm at 25°C reference). Higher flow rates would enhance radioactive iodine movement and desorption to some extent, but unusually large heat sources would be required to reach crucial temperatures.

The decreasing heat release rate, stabilized bed temperatures, and very slow radioiodine desorption rates following ignition when low air velocities prevail provide both time and opportunity for combating the combustion. Increased air velocity or induced turbulence would tend to increase the rate of heat release following ignition.

The formation and release of highly penetrating iodine, although occurring at a very low rate, appear to be promoted by moisture and radiation. The radiation effect apparently saturated above 1.0 Ci $^{130}\text{I}/\text{cm}^3$ charcoal. Identification and trapping of this material were not completely solved; nevertheless, the use of some silver-exchanged zeolite is recommended in the collection system whenever the highly penetrating form is suspected to be present.

VI. References

1. R. A. Lorenz, W. J. Martin, and H. Nagao, "The behavior of highly radioactive iodine on charcoal," in Proceedings of the Thirteenth AEC Air Cleaning Conference, CONF-740807 (March 1975), pp. 707-35.
2. R. E. Adams et al., Nuclear Safety Program Annual Progress Report for Period Ending December 31, 1967, USAEC Report ORNL-4228 (April 1968), p. 118.
3. F. G. May and H. J. Polson, Methyl Iodide Penetration of Charcoal Beds: Variation with Relative Humidity and Face Velocity, AAEC/E-322 (September 1974).
4. R. D. Ackley and R. J. Davis, Effect of Extended Exposure to Simulated LMFBR Fuel Reprocessing Off-Gas on Radioiodine Trapping Performance of Sorbents (Final Report), USAEC Report ORNL-TM-4529 (August 1974).
5. J. G. Wilhelm and H. Schuettelkopf, "Inorganic adsorber materials for trapping of fission product iodine," in Proceedings of the Eleventh AEC Air Cleaning Conference, CONF-700816 (December 1970), pp. 568-99.
6. J. G. Wilhelm, Kernforschungszentrum Karlsruhe, personal communication.
7. R. O. Lingjaerde and L. Podo, A Study on the Trapping of Iodine at High Temperatures on Activated Charcoal, Dragon Project Report DP-Report-213 (September 1963).
8. A. G. Evans, "Effect of alkali metal content of carbon on retention of iodine at high temperatures," in Proceedings of the Thirteenth AEC Air Cleaning Conference, CONF-740807 (March 1975), pp. 743-57.
9. F. G. May, Comparison of Charcoals in Removing Iodine from Air-Streams at High Temperature, AERE-R4145 (1962).
10. E. A. Bernard and R. W. Zavadoski, "The calculation of charcoal heating in air filtration systems," in Proceedings of the Thirteenth AEC Air Cleaning Conference, CONF-740807 (March 1975), pp. 845-61.

DISCUSSION

WILHELM: Do you think the penetrated compound could be an aryl iodide in which the iodine won't react or isotopically exchange because of the structure?

LORENZ: I know that you have mentioned this possibility before and have published some experimental results with that type of compound. In our attempts to identify this material, we used the mass spectrometer, but were not successful in finding masses of common iodine compounds, including the type of aryl iodides you described.

REMARKS ON TESTING THE RELIABILITY OF IODINE
ADSORPTION IN ION-EXCHANGING CHARCOAL-FILTERS
WITH RESPECT TO SOLVENT LOADINGS

H.J. Strauss , Dr. rer.nat., Dortmund*
K. Winter , Dipl.-Phys. , Dortmund*

* Ceagfilter und Entstaubungstechnik GmbH, Dortmund

Abstracts:

The reliability of high-efficient removal of fission iodine and its compounds depends on the condition of iodide-impregnated charcoal, especially on foreign loads, e.g. solvents. Samples of the charcoal taken from monitor-filters will have an equivalent load if flow-velocity is equal to that in the iodine-filter. But, the influence of geometric form and of bulk density is not to be neglected, insofar as conditions for identic flow-velocity cannot be assumed. It seems, that a good sample only can be taken directly out of the charcoal by pipette. Foreign loads below about 3% have practically no influence on the reliability of high-efficient-iodine-removal. When operating a charcoal-filter at temperatures in the range of 70°C to 90°C the equilibrium of adsorption of solvents is below this level with respect to the concentrations occurring in practice. Further advantages are: The relative humidity is lowered and the humidity of the carbon is lowered. Therefore the iodine-removal can be kept to a high efficiency.

Introduction:

One cause of failures in iodine removal with iodide impregnated ion-exchanging charcoal filters, here briefly called iodine-filters, is caused by foreign load on the charcoal, e.g. with solvents from painting or cleaning. This effect often is called poisoning or ageing of the charcoal. To ensure the reliability of iodine removal with the necessary high efficiency, the condition of the charcoal has to be checked at not too long intervals. Therefore samples of the charcoal are to be analyzed and their efficiency against methyl-iodide is tested. The problem is to get a good average sample. One solution for this task is to install parallel to the iodine-filter several monitor-filters with a small diameter and a depth of the bed equal to the depth of the bed of the iodine filter, filled with charcoal up to the same bulk density as the charcoal in the iodine-filter has (fig.1). If these requirements are fulfilled the flow velocities should be equal and correct informations on the

conditions of the charcoal is to be expected.

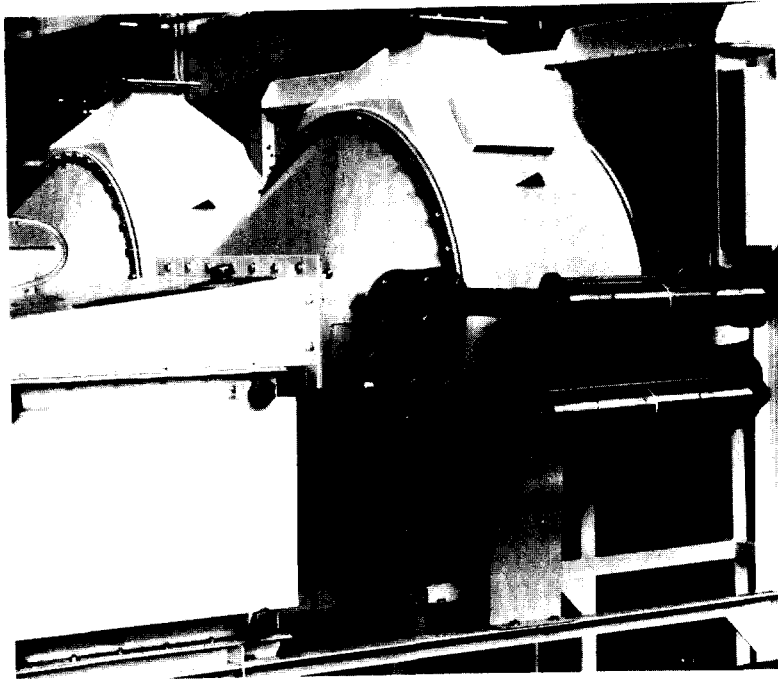


Fig. 1:
Iodine adsorption filter
with deep-bed filter
type KCR and 2 monitoring
filters
(Courtesy Ceagfilter und
Entstaubungstechnik
Dortmund, BRD)

Influence of geometry, bulk density and pipe diameter on flow velocity

In practice the iodine filter is not a cylindrical vessel. Above there is a dome to fill the filter with charcoal and below there is a hopper to remove the charcoal.

Let us assume that the iodine-filter has a circular cross-section with a diameter D and an area A (fig. 2), then the pressure drop Δp at the airflow \dot{V} may be written as

$$\Delta p = c \cdot \frac{\rho}{2} \cdot \left(\frac{\dot{V}}{A} \right)^2 \quad A = \frac{\pi \cdot D^2}{4} \quad A' = \frac{\pi \cdot D}{4} (D + 2 \delta D) \quad (1)$$

where C stands for a resistance-coefficient and ρ for the air-density. The dome and the hopper (fig. 3) give an enlargement of the cross-section of flow. Let us assume that this new cross-section becomes elliptic with

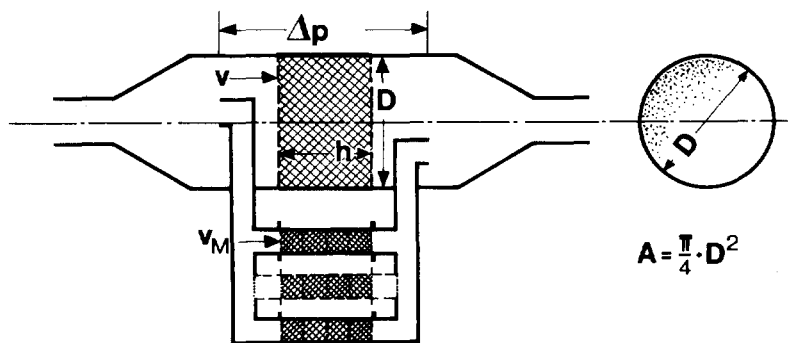


Fig. 2:
Iodine-filter with
monitoring-filter; the
deep-bed-vessel with
circular cross-section
(schematic drawing)

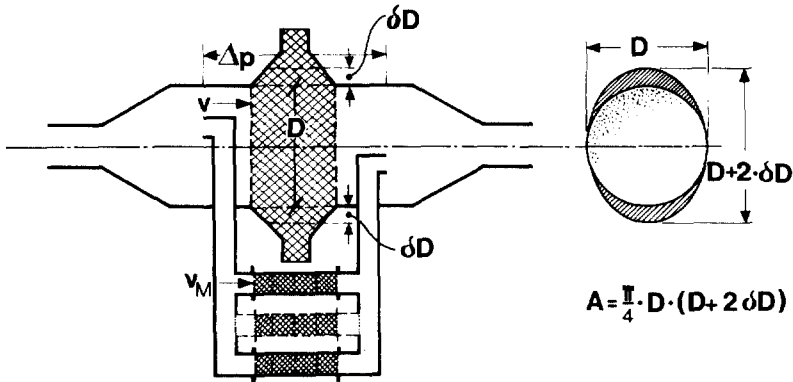


Fig. 3:
Iodine-filter with
monitoring-filter; the
deep-bed-vessel with dome
and hopper and elliptical
cross-section
(schematic drawing)

the small axis D and the large axis $(D+2\delta D)$, the new pressure-drop $\Delta p'$ becomes

$$\Delta p' = \Delta p \left(\frac{1}{1+2\delta D/D} \right)^2 \sim \Delta p \left(1-4 \frac{\delta D}{D} \right) \quad (2)$$

(with $\delta D/D \ll 1$)

This pressure drop gives the acting force to drive a flow through the monitor-filters. The question is, what flow-rate will be caused by this pressure drop. To get an estimated figure, let us assume that flow and pressure drop are in accordance with the formula given by FEHLING (1), which is secured by experiment in the limits of Reynold's Number $15 < Re < 300$. For a flow-velocity of $.5 \text{ m s}^{-1}$ and a charcoal-grain size of $.003 \text{ m}$ the Reynold's Number is about 30, so that the premise is fulfilled. The FEHLING formula gives a relationship between the acting pressure drop Δp , the coefficient of resistance of a single grain c_w , the mean diameter of the grain \bar{a}_g and their shape-factor m , the depth of the bed L , the relative pore-volume of the bed V_p air-density ρ and air-velocity w :

$$\Delta p = \frac{c_w \cdot m}{\bar{a}_g \cdot L} \cdot \frac{1}{V_p^4} \cdot \frac{\rho}{2} w^2 \quad (\text{according to FEHLING /1/}) \quad (3)$$

Or, for the air-velocity through the monitor filters (marked with the index M)

$$w_M = \sqrt{\frac{2\bar{a}_g L}{\rho c_w m} V_{p,M}^4 \Delta p'} \quad (4)$$

with $\Delta p'$ from (2) and Δp from (3) the ratio w_M/w is obtained

$$\frac{w_M}{w} = \sqrt{\frac{2\bar{a}_g L}{\rho c_w m} V_{p,M}^4} \cdot \sqrt{\frac{\rho c_w m}{2\bar{a}_g L} \frac{1}{V_p^4}} \cdot \sqrt{1-4 \frac{\delta D}{D}} \quad (5)$$

or

$$= \sqrt{\frac{V_{p,M}^4}{V_p^4}} \cdot \sqrt{1-4 \frac{\delta D}{D}} \sim \frac{V_{p,M}}{V_p} \left(1-2 \frac{\delta D}{D} \right) \quad (6)$$

(with $\delta D/D \ll 1$)

FEHLING (1) studied further the influence of the wall, and he found that the pore-volume is to be corrected. His result is given by

$$V_{p,M} = V_{p,\infty} \left(1 + 8 \frac{\bar{a}_g}{D_M}\right) \quad (7a)$$

where V_p stands for the pore-volume of a charcoal-bed in a large vessel at the maximum packing density. The relationship between the pore-volume at maximum packing density and a pore-volume at lower packing density may be written as

$$V_p = V_{p,\infty} \left(1 + \frac{\delta V_p}{V_p}\right) \quad (7b)$$

The formula (9a) is of importance for the monitoring-filter, due to their small diameter; (9b) gives the pore-volume with variations in the packing density. Therefore (9b) relates mainly to the iodine filter itself, because the packing density of the charcoal in the monitoring-filter can be kept near the attainable maximum, while the packing density of the iodine filter varies from charging to charging. Inserting (7a) and (7b) into (6) the ratio w_M/w becomes:

$$\frac{w_M}{w} = \frac{V_{p,\infty}^2 \left(1 + 8 \frac{\bar{a}_g}{D_M}\right)^2}{V_{p,\infty}^2 \left(1 + \frac{\delta V_p}{V_p}\right)^2} \left(1 - 2 \frac{\delta D}{D}\right) \quad (8)$$

or

$$\sim \left(1 - 2 \frac{\delta V_p}{V_p}\right) \left(1 - 2 \frac{\delta D}{D}\right) \left(1 + 16 \frac{\bar{a}_g}{D_M}\right) \quad (9)$$

(with $\delta V_p/V_p \ll 1$ and $\bar{a}_g/D_M \ll 1$)

In practice these correction numbers are in the following range:

$$0 < \frac{\delta V_p}{V_p} < .2 \quad \text{(bulk-density varies about 7\%)}$$

$$0 < \frac{\delta D}{D} < .16 \quad \text{(half height of dome and of hopper)}$$

$$\frac{16 \bar{a}_g}{D_M} \sim .3$$

(charcoal-grain-size
about 1 mm, diameter of
monitor-filter 50 mm)

With these correction numbers the ratio of flow-velocities goes to

$$.5 < \frac{w_M}{w} < 1.3$$

and the correction numbers are in the nature of systematic errors.

To examine this conclusion, experiments were carried out. The iodine-filter was a deep-bed filter of the KCR-type (fig. 1). The hollow space for the charcoal was 324 litres. This filter was charged with charcoal of cylindric grain with a diameter of 1.5 mm and a ratio between length and diameter of about 2 with a narrow distribution; it was charcoal of CEAG-type CB 1.5. The iodine-filter (with its monitoring filters) was installed in a loop and the air-flow through it was found by measuring the rotation speed of the blower (which had previously been calibrated), and by use of the blower characteristics.

Due to this, there is a hysteresis at low flow velocities, i.e. less than $.35 \text{ m}_s^{-1}$; this hysteresis may be caused by the effect of "rotating stall", but it does not influence the results which were taken by measuring the pressure drop at flow velocities above this critical limit.

The monitor-filters were tested in a separate test-device. The flow was measured by flow meters. The pressure drop itself was taken by static taps before and behind the filter under test and was measured with a water-gauge. Iodine-filter and monitor-filter were charged with practically identic charcoal up to the same depth of the bed. The packing-density at the monitor filter, which is easy to handle, was brought to the highest attainable level. The packing density of the charcoal in the iodine-filter was kept to a low level for the first run. After this, the packing density was increased by hammering. Due to this, up to about 7% of the volume of charcoal had to be filled up. Apart from this packing density the bed of charcoal in the iodine-filter and in the monitor-filter are to be assumed as identical.

The pressure drop flow velocity characteristic of the monitor-filter so charged is shown in fig. 4. The uncertainty is in the range of $\pm 10\%$. The pressure drop / flow-velocity-characteristic of the iodine-filter depends on the packing density and varies within the characteristics of "low-bulk-density" and high-bulk-density". The characteristics show that the pressure drop for a flow velocity of $.5 \text{ m}_s^{-1}$ may vary between 400 Pa m^{-1} and 540 Pa m^{-1} . This pressure drop drives the flow through the monitor-filter only with a velocity of $.27 \text{ m}_s^{-1}$ to $.34 \text{ m}_s^{-1}$. The ratio w_M/w was found to be in the range of .55 to .68. This is in the lower range of the figures to be expected.

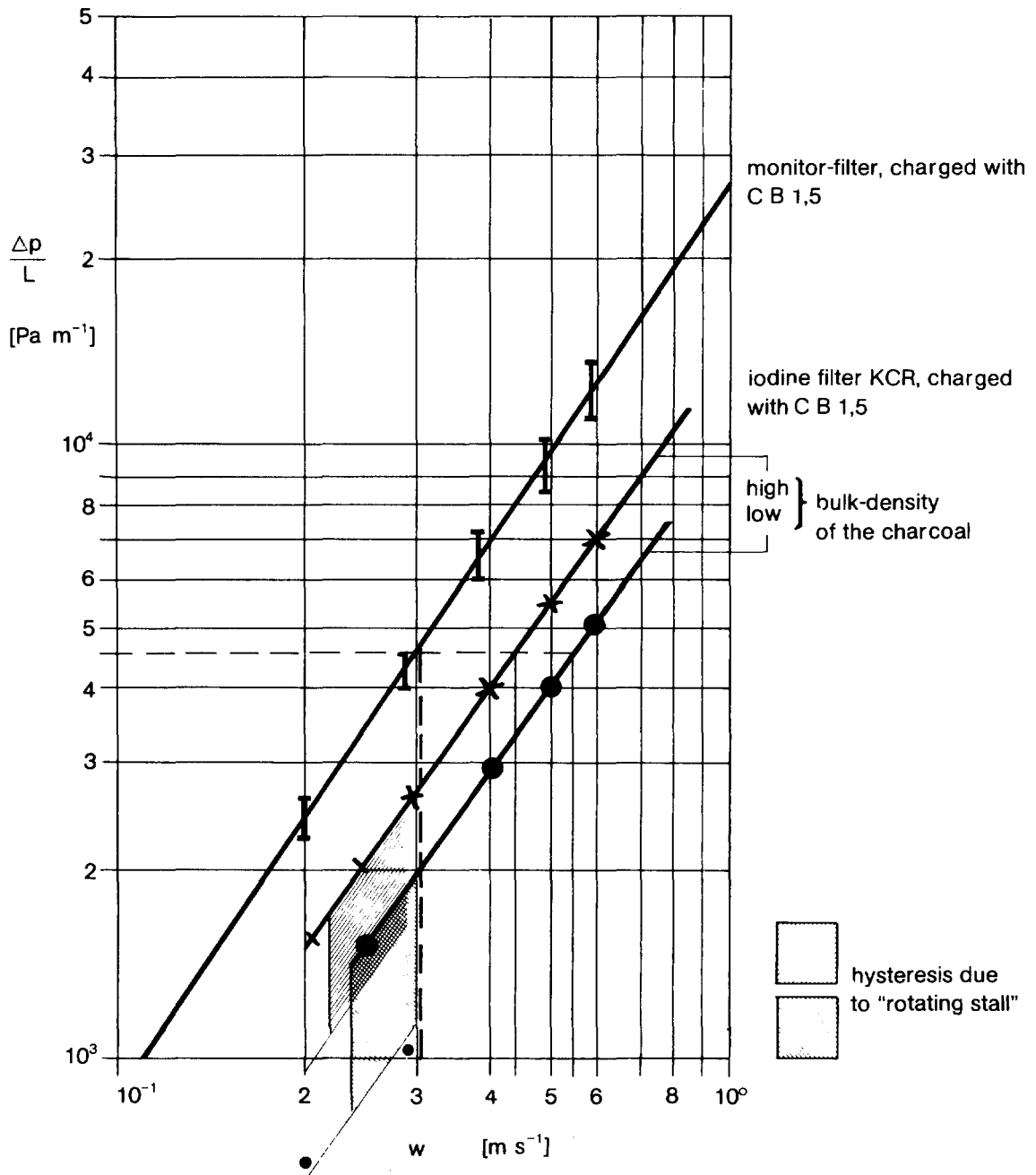


Fig. 4: Pressure drop / flow velocity characteristics of monitor filter and iodine filter type KCR

The use of charcoal with a wider distribution of the ratio length to diameter, or the use of broken charcoal will give a ratio of w_M/w still below the result obtained with this special type of cylindrical charcoal.

In addition to the studies of the relationship between pressure drop and flow velocity with respect to the packing density, efficiency tests against radio-active methyl-iodide are carried out. First results lead to the conclusion that the packing density (within the limits mentioned) has no remarkable influence on the methyl-iodide efficiency. A final report

of these studies is intended to be published later.

According to this it seems improbable that a ratio near 1 can be obtained and that good average samples can be got by taking charcoal from monitor filters.

Another solution for getting charcoal samples is independent on the flow and the influences mentioned on it. The samples are taken by pipette (fig. 5) direct from the bed. Therefore the pipette is inserted into the

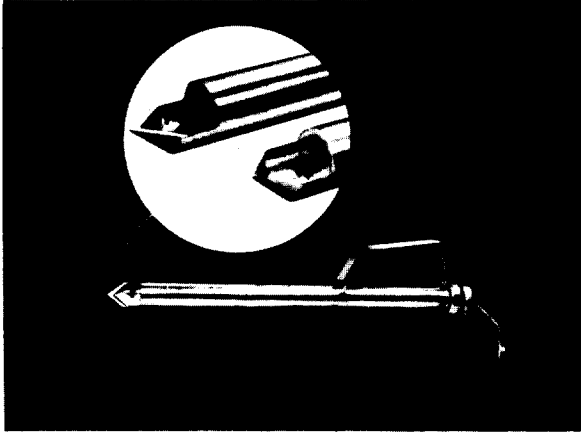


Fig. 5:
Pipette to get samples from the deep-bed
(Courtesy Technische Universität Stuttgart
Abteilung Mechanische Verfahrenstechnik,
Stuttgart, BRD)

filter vessel and into the charcoal bed by means of guide bushes provided.

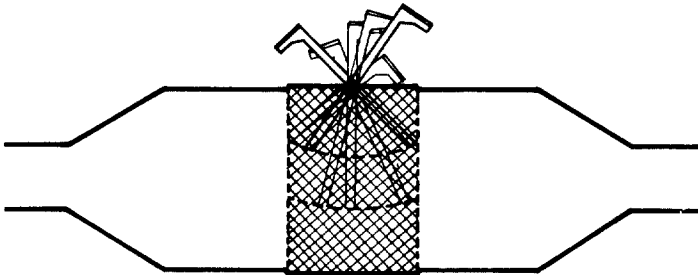


Fig. 6:
Pipette used to take samples from two different planes

If, for example, three samples are to be taken in two planes (fig. 6), the filter vessel should have a handhole, closed with a plate bearing the guide bushes, in this case six, fixed in the desired directions (or there may be one turnable and with adjustable groves for the different angles, under which the pipette is to be inserted).

In connection with the uncertainty of getting good average samples already mentioned by monitor filters, the question arises whether there is any possibility of preventing such foreign loadings and there are two possible solutions:

- i : to remove the foreign impurities before they reach the iodine filter,
- ii : to prevent the adsorption of these foreign impurities.

The first solution leads to prefilters (fig. 7).

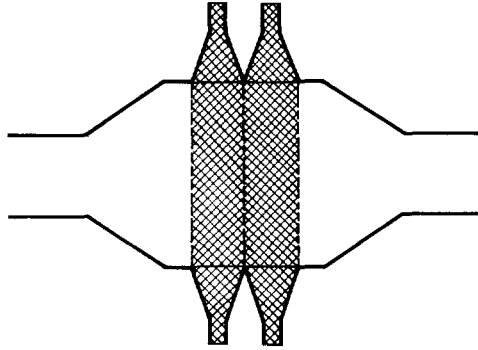


Fig. 7:
Deep-bed-filter with double
layer: The first acts as
prefilter, the second as
iodine filter

But using adsorption-type prefilters, one has to remember that the amount of adsorbed matter depends on the vapour-pressure of this matter in the ambient air. If, some time after painting or cleaning, the vapour pressure drops to (or near to) 0, adsorbed matter will leave the charcoal, will be desorbed. Therefore the charcoal in the prefilter may get a peak charge of solvent but will not be a safe storage over a long time. In consequence the charcoal of the prefilter has to be changed in short intervals, but nobody knows the time at which a surge of organic matter e.g. from painting reaches the prefilter and what time is needed to lower the high loading in front of the prefilter and to distribute the load over prefilter and iodine filter. This problem may be solved by protection filters which act as prefilters during that time the air contains organic matter. This may be tested by infrared or ultra-violet spectroscopy, by flame photometry or by combustion analysis. These protection filters (fig. 8) are by-passed by a duct, which can be closed if foreign matter is detected.

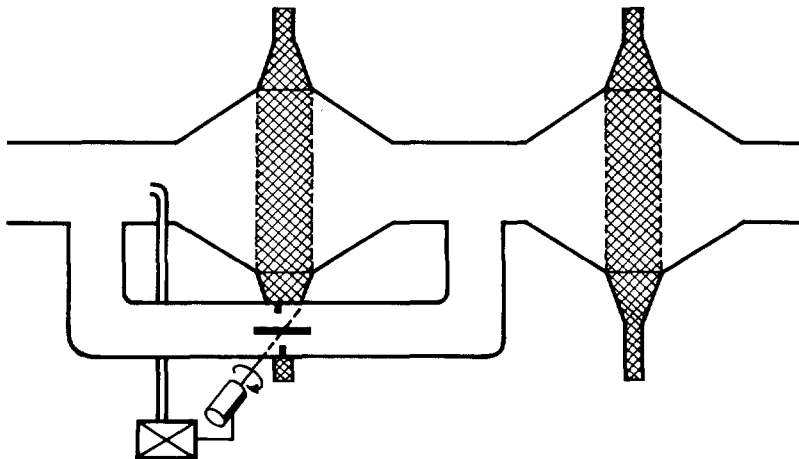


Fig. 8: Iodine-filter with by-passed protection-filter

DISCUSSION

DEITZ: Is the change in packing densities to be ascribed to particle breakdown or are we describing something due to the ordering of particles? Is there any way to sort this out?

STRAUSS: I think that the rise in packing density or the lowering of the pore-volume of the charcoal depends on the grains, which are, after filling, in randomly distributed directions. After hammering, they turn a little bit and they give a higher packing density.

DEITZ: But not particle breakdown?

STRAUSS: No, there is no particle breakdown. This has been checked in other connections. We are sure there is no particle breakdown.

WILHELM: There is another effect when you fill a big charcoal unit, as shown by Dr. Strauss. The pellets will have a horizontal orientation and the flow will be horizontal, too, i.e., parallel to grain layers. If you fill the bypass control filter vertically, the gas stream in the bypass filter flows perpendicular to the charcoal grain layers. In the case of pelletized charcoal and of charcoal in the form of little plates, this is a very important effect. When the charcoal is in horizontal layers and the air is coming down vertically, the canister has a much higher resistance than when flow is parallel to the particle layers. If you have little plates, you have the same effect.

PARISH: I would like to comment and also ask a question. First, I concur with the findings of Mr. Strauss. We have also evaluated the test canisters and have found that when proper consideration is not given to packing the adsorbent, the resultant test canister flow may be very nonrepresentative. However, when properly packed, we have repeatedly obtained very representative velocity through the canisters, varying from 8 per cent to minus 5 per cent relative to the main bed. I would like to ask if you would define for us what you mean when you say "hammer the large bed for packing purposes?"

STRAUSS: I agree fully with your remark. It is a problem to get good distribution, but one can do this by filling to the upper level and then bringing up the packing density with hammering. We fill up in this way with airflow to a point where the pressure drop becomes a constant value at rated flow.

RIVERS: The use of the canister is very convenient and gives you an easily obtainable sample, with which you can say whether the bed needs changing, for example, without doing anything to the main bed. Would it not be possible to make a shallower test canister which would then, of course, have less resistance and greater penetration than the main bed? At least it would be on the conservative side as a test device.

STRAUSS: If I understand you right, you want to keep canister

14th ERDA AIR CLEANING CONFERENCE

filters to check the main beds?

RIVERS: My canisters in parallel with the filter bed would have less depth and therefore less resistance and could be made to pass the same velocity as the main bed, but would last for less time than the main bed.

STRAUSS: But in normal cases, the difference in flow geometry and lower packing density in the main filter results in a lower relative velocity through the monitoring filter. Lowering the flow-resistance cannot solve this problem because our legislation forces us to use an identical bed.

AIRBORNE ELEMENTAL IODINE LOADING CAPACITIES OF METAL
ZEOLITES AND A DRY METHOD FOR RECYCLING SILVER ZEOLITE*

B. A. Staples, L. P. Murphy, and T. R. Thomas
Allied Chemical Corporation
Idaho National Engineering Laboratory
Idaho Falls, Idaho

ABSTRACT

Several metal-exchanged zeolites have been tested to determine their elemental-iodine-loading capacities at breakthrough in air streams. The experiments were directed toward the application of the adsorbents for the removal of iodine-129 from the process off-gas of nuclear fuel reprocessing plants. The effects of the bed temperature, face velocity, bed depth, water vapor, and NO₂ on the loading capacities were examined. Only silver-exchanged zeolite was found to have a high chemisorption capacity for elemental iodine both in dynamic and static loading tests. The chemisorption capacities of lead-, cadmium-, and silver-exchanged zeolites for iodine are discussed in terms of thermodynamics.

Experiments were conducted to develop a method for recycling silver-exchanged zeolite. Iodine-desorption tests were performed by purging iodine-loaded silver-exchanged zeolite with pure hydrogen at bed temperatures of 400 to 700°C. The predicted rates of hydrogen iodide removal from silver iodide based on thermodynamic calculations are compared to the rates of removal observed from silver iodide dispersed in a zeolite matrix. The characteristics of test beds which were regenerated and reloaded several times are described. The use of lead-exchanged zeolite as an adsorbent for the hydrogen iodide purged from the silver-exchanged zeolite was studied. The potential application of silver-exchanged zeolite as a primary adsorbent for radioiodine removal from process off-gas and lead-exchanged zeolite as a secondary adsorbent for storage is evaluated.

INTRODUCTION

Fission-product iodine-129 is produced in nuclear power reactors and subsequently released as organic iodides and elemental iodine (I₂) into the process off-gas of reprocessing plants during fuel dissolution. Based on an iodine-129 content⁽¹⁾ of 40 mCi/MTU burned at 40,000 megawatt days and 90% volatilization of the iodine, it is estimated that as much as 330 kg/yr (54Ci) would be released from the stack gas of a 5 tonne/day reprocessing plant without the use of iodine-recovery systems. The proposed⁽²⁾ EPA release limit could require at least 99.5% abatement of iodine-129 from the gaseous effluents (calculations are given in Appendix A). Even though the total release of iodine-129 would pose little concern on a world-wide scale, collection and storage will probably become necessary to avoid localized buildup in the environs of

*Work performed under USERDA Contract E-(10-1) 1375 S-72-1.

reprocessing plants.

Numerous low-loading tests (less than 10 mg iodine per gram substrate) have been run and decontamination factors (DF's) of 10^2 to 10^5 have been reported^(3,4,5,6,7) for the removal of iodine from airstreams. However, very little data have been reported for long-term tests in which iodine-loading capacities at breakthrough were studied. For application of iodine-recovery systems to reprocessing plants, both high DF's and loading capacities will be necessary to minimize capital costs and the amount of waste generated. Pence, Duce and Maeck⁽³⁾ found that silver-exchanged zeolite (AgX) would adsorb 84 mg of methyl iodide (CH_3I) per gram of AgX in dry air at 25°C with a $\text{DF} > 10^4$. Ackley and Combs⁽⁷⁾ reported a loading of 209 mg $\text{CH}_3\text{I}/\text{g}$ AgX in air containing 3% water vapor at 200°C with a $\text{DF} > 100$. At a DF of $> 10^4$ their loading was about 87 mg $\text{CH}_3\text{I}/\text{g}$ AgX. Wilhelm and Schüttelkopf⁽⁶⁾ obtained loadings of about 40 mg I_2 or CH_3I per gram Ag-KTB for DF's > 100 at bed temperatures of 150°C in the presence of 3% H_2O and 2.5% NO_2 . The silver content of Ag-KTB is about 78 mg Ag/g Ag-KTB as compared to 360 mg Ag/g AgX. Collard and coworkers⁽⁸⁾ reported a maximum loading of 52 mg I_2/g AgX at bed temperatures between 30 and 100°C . The DF and composition of the test gas were not given. To our knowledge, no systematic study of the effect of experimental variables on the iodine-loading capacity of silver-loaded adsorbents has been conducted. In our program, the effects of face velocity, bed depth, bed temperatures, water vapor and NO_2 on the elemental-iodine-loading capacity of AgX were studied.

It has been suggested⁽⁹⁾ that lead-exchanged zeolite (PbX) might be used for elemental-iodine removal in place of AgX. Although data exist^(3,7,10) which indicate that metal-exchanged zeolites (except AgX) generally have poor efficiencies and/or low capacities for CH_3I removal, their efficiency for I_2 remains an open question. Pence and coworkers⁽⁴⁾ indicated that high DF's with PbX were obtainable in dry-air streams and low loadings (about 1 mg I_2/g PbX) but that the efficiency was extremely poor at high relative humidity. Gal and coworkers⁽¹⁰⁾ have indicated that partial chemisorption with CH_3I was observed on PbX and cadmium-exchanged zeolite (CdX) in static adsorption-desorption tests. In our program screening and loading tests were conducted on CdX, PbX, zinc- and copper-exchanged zeolites (ZnX, CuX) to determine if they would be potential adsorbents for elemental-iodine removal.

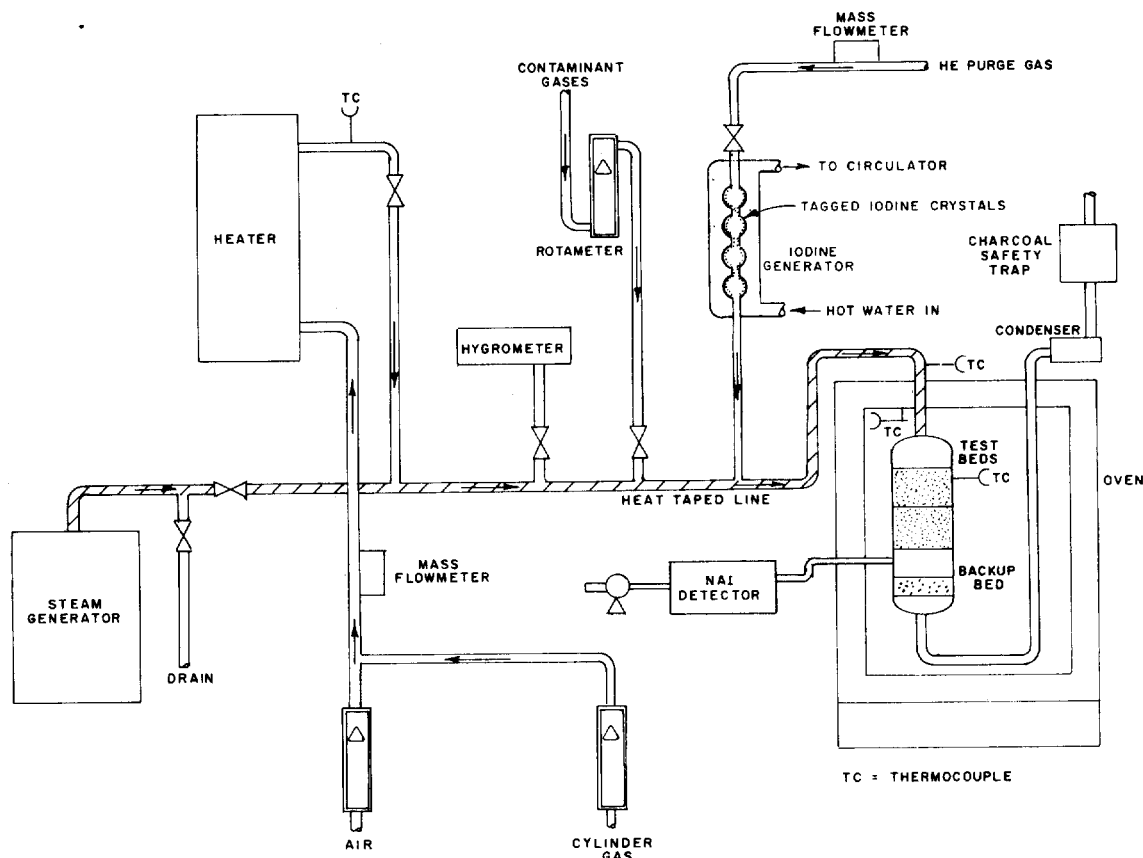
Because silver is a valuable resource, a method to regenerate spent AgX would improve the economic feasibility of adsorbent technology. Scoping studies on a dry method to regenerate and recycle spent AgX were conducted. In conjunction with this, PbX was used as a secondary adsorbent for the final collection and storage of iodine. The results of the comprehensive study on the adsorption characteristics of AgX, the screening tests on metal-exchanged zeolites, and the regeneration tests are discussed below. Application of adsorbent technology to reprocessing plants is also treated.

EXPERIMENTAL PROCEDURE

The metal-exchanged zeolites used in these studies were prepared by ion-exchange with 1.6 mm spheres of Linde Molecular Sieve Type 13X. Batch-exchange procedures were used in which the zeolite was contacted several times with a hot solution of the desired metal nitrate or acetate. The exchanged zeolites were washed with distilled water until excess cations were removed and dried by purging with dry air at 100°C. The extent of exchange was measured by dissolving samples in nitric acid and analyzing the amount of sodium which remained in the exchanged zeolites by flame-emission spectroscopy. Analysis indicated 99.9, 98, 92, 85, and 75% exchange for Ag⁺, Pb⁺⁺, Cd⁺⁺, Cu⁺⁺, and Zn⁺⁺ respectively.

Screening and iodine-loading tests were conducted using the apparatus illustrated in Figure 1. Heated-air streams containing desired amounts of water vapor, contaminant gases and airborne-elemental iodine tagged with iodine-131 were passed through the test beds. Iodine breakthrough was detected by passing an effluent slipstream through a small-adsorbent bed monitored by a gross-gamma counter. Silver-exchanged zeolite was used for backup beds. A Pyrex cylinder 5 cm in diameter was used for a test-bed holder. Up to 15-cm-bed depths could be tested and each 2.5-cm segment could be analyzed for its iodine content. A gamma spectrometer was used to determine the amount of iodine-131 in the test beds and based on the known ratios of iodine-127/iodine-131, the iodine loadings were obtained. Up to 60 g sources of tagged iodine were prepared by adding 10 mCi of iodine-131 to elemental iodine dissolved in diethyl ether. The solution was evaporated to dryness and the crystalline iodine was transferred in the vapor phase by a heated airstream into a condenser where it was recrystallized. Airborne iodine was introduced into the carrier gas by passing hot water through the outer jacket of the condenser and purging the crystalline iodine with helium. The experimental conditions used for testing are summarized in Table I.

Iodine-desorption tests were conducted using an apparatus which is illustrated in Figure 2. Silver-exchanged zeolite containing iodine (AgIX) was purged with pure hydrogen (H₂), and the desorbed hydrogen iodide (HI) was recovered downstream on PbX. During the desorption tests the effluent from the AgIX bed was sampled with a 10-cm-quartz-absorption cell and the absorbance by HI in the cell was measured with a UV-VIS spectrophotometer. The partial pressure of HI (P_{HI}) was obtained from the equation: $P_{HI} = A/ab$ where A = the measured absorbance, a = the molar absorptivity (7.22 atm⁻¹cm⁻¹ at 21°C)¹¹ at 215 nm, and b = the path length (10 cm).



ACC-A-1859

Figure 1. Test Apparatus for Iodine-Adsorption Studies

Table I
EXPERIMENTAL CONDITIONS

Experimental Variable	Screening Tests	Loading Tests
Dry-bed weight (g)	99	99, 198, 297
Bed diameter (cm)	5	5
Bed depth (cm)	5	5, 10, 15
Carrier gas	air	air
Superficial-face velocity at 25°C (m/min)	15	15, 30, 60
I ₂ concentration (mg/m ³)	~90	~500
Loadings (mg I ₂ /g bed)	~1.4	3.5 to 170
H ₂ O concentration (%)	0 to 10	0 and 5
NO ₂ concentration (%)	0	0 and 2
Pretest purge (hr)	1	1
Test period (hr)	1	1 to 60
Post-test purge (hr)	0.25	20

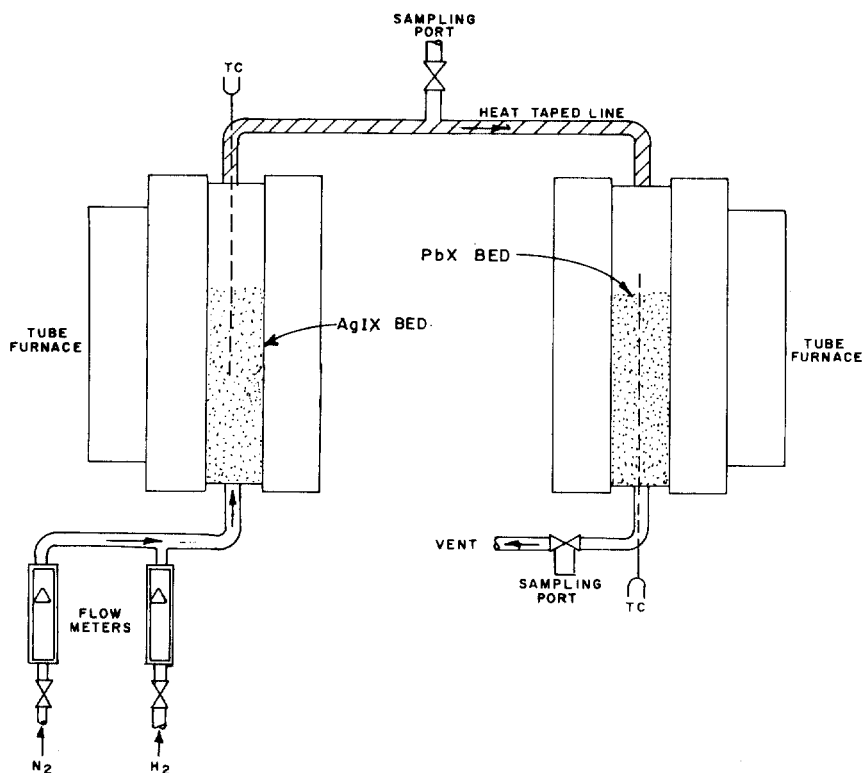


Figure 2. Test Apparatus for Iodine-Desorption Studies

EXPERIMENTAL RESULTS

Screening Tests

Several metal-exchanged zeolites were tested for the effect of cation, bed temperature, and water-vapor content on I_2 removal efficiency from air streams. The results are given in Table II.

Table II

SCREENING TESTS FOR 5-cm-DEEP BEDS

<u>Adsorption Test Conditions (a)</u>		<u>I_2 Adsorption Efficiency (%)</u>				
<u>Water Vapor (%)</u>	<u>Bed Temp ($^{\circ}C$)</u>	<u>CdX</u>	<u>NaX</u>	<u>PbX</u>	<u>ZnX</u>	<u>CuX</u>
1.5	100	99.986	99.86	93.45	--	31.67
1.5	200	99.836	99.93	88.15	--	0.45
8.5	100	99.992	80.69	56.88	4.17	4.96
8.5	200	99.985	64.39	77.61	4.15	0.50

(a) Test conditions: 60-min-pretest purge, 60-min-test period, 15-min-post-test purge, 15 m/min face velocity, 90 mg I_2/m^3 airborne concentration, 1.4 mg I_2/g substrate loading at 99% efficiency.

The high efficiency of NaX in the presence of 1.5% water vapor indicates that considerable physical adsorption is taking place in the unexchanged substrate with the low loading used. The extremely low efficiencies observed for ZnX and CuX relative to NaX was unexpected and is not understood. Using the same test conditions as above, the test space for PbX and CdX was expanded to study the response surface for I₂ removal efficiency as a function of water-vapor content and bed temperature. The results are given in Figure 3. The response surface for CdX is almost flat in the region between 100 and 250°C with an average-adsorption efficiency of 99.82%. The efficiency appears to drop off sharply around 250°C. No trend is apparent with the PbX and except for one data point, iodine-adsorption efficiencies above 99% were not observed.

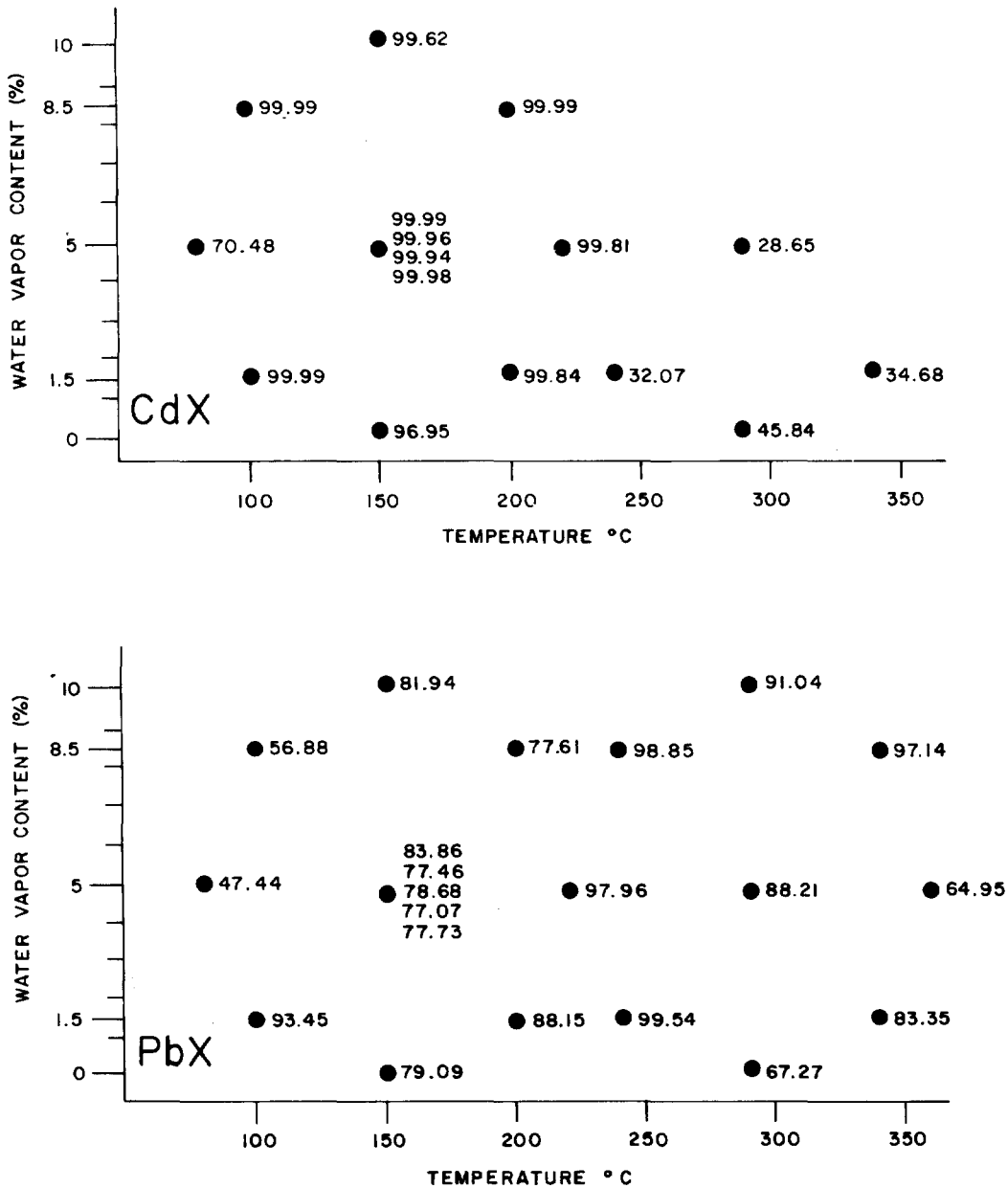


Figure 3. Screening Tests for PbX and CdX

Saturation Tests

Tests were conducted to determine the maximum-loading capacity of NaX, PbX, CdX and AgX under nearly static conditions. The adsorbents were saturated by exposure to airborne I₂ using a face velocity of 1 cm/sec and a bed temperature of 150° until constant weight was obtained. They were then purged with air (up to 120 hr at 150°C) until the rate of I₂ desorption was negligible. The remaining iodine was considered chemisorbed. The results are given in Table III.

Table III

MAXIMUM IODINE ADSORPTION CAPACITIES OF
METAL ZEOLITES AT 150°C. (mg I₂/g bed)^a

<u>Adsorbent</u>	<u>Saturated</u>	<u>Physisorbed^b</u>	<u>Chemisorbed</u>
NaX	364	334	30
AgX	349	135	214
PbX	179	153	26
CdX	374	329	45

(a) Based on dry weights of 0.61 g/cm³ for NaX, 0.71 g/cm³ for CdX and 0.85 g/cm³ for PbX and AgX.

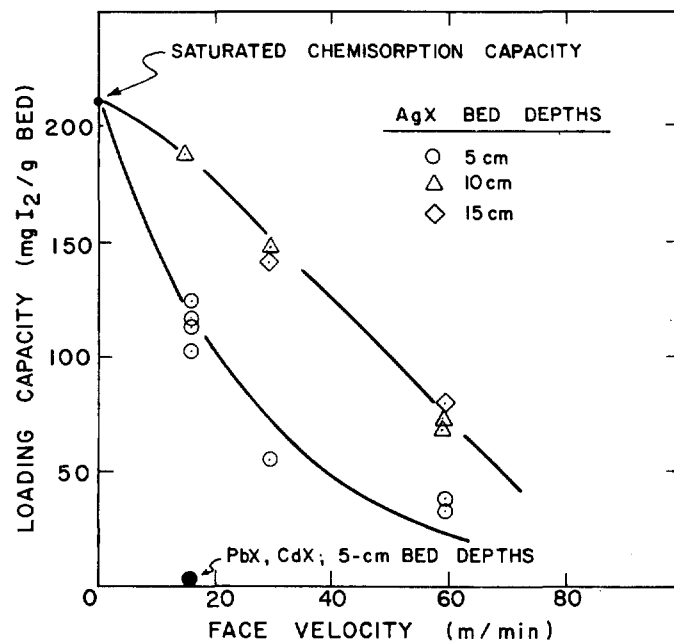
(b) Iodine removed from bed during air purge.

It was anticipated that all of the adsorbents would have saturation capacities similar to NaX. The lower capacity of PbX indicates that partial blocking of the adsorption sites is occurring. The chemisorption capacities of PbX, CdX and NaX are only about 9% of the saturated NaX capacity; no effect due to the cation is apparent. The data indicate that considerable chemisorption occurs in AgX.

Loading-Capacity and Effect Tests

The iodine-loading capacity of AgX at breakthrough (DF ~ 200) was studied as a function of bed depth and face velocity. The data given in Figure 4 indicate:

- (1) The loading capacities of the 10-cm beds are considerably larger than the 5-cm beds at all face velocities tested. No significant increase in loading capacity occurs between 10- and 15-cm-bed depths.
- (2) A large decrease in loading capacity occurs with increasing face velocity at each bed depth.
- (3) For bed depths 10 cm or greater, face velocities below 15 m/min would not greatly increase the loading capacity.
- (4) The loading capacities of 5-cm-deep beds of CdX and PbX is less than 3.5 mg I₂/g bed (based on two sets of duplicate tests).



TEST CONDITIONS: AIRBORNE-IODINE CONCENTRATION, 500 mg/m³; PRETEST PURGE, 1 hr; TEST PERIOD, UP TO 60 hr; POST-TEST PURGE, 20 hr; DF, ABOUT 200; DENSITY OF DRY AgX, 0.85 g/cm³

Figure 4. I₂ Loading Capacity of AgX in Dry Air at 150°C

Using a three-level-factorial design, the effects of bed temperature, water-vapor and NO₂ on the iodine-loading capacity of AgX were studied. The results are given below.

Table IV

EFFECT TESTS ON THE I₂-LOADING CAPACITY OF AgX

Bed Temp (°C)	Water Vapor (%)	NO ₂ (%)	Loading ^{a, b} (mg I ₂ /g AgX)
100	0	0	139
200	0	0	94
100	5	0	67
200	5	0	35
100	0	2	32
200	0	2	37
100	5	2	42
200	5	2	55

(a) Loadings are based on a dry density of 0.85 g/cm³

(b) Test conditions: bed depth, 10 cm; face velocity, 60 m/min; airborne-iodine concentration, 500 mg/m³; pretest purge, 1 hr; test period, 5 to 16 hr; post-test purge, 20 hr; DF, about 200.

The data indicate:

- (1) The main effect variables (temperature, water vapor and NO₂) cannot be analyzed independently because their interactions are so large.
- (2) The interaction between water vapor and NO₂ decreases the loading from 67 to 42 mg at 100°C but increases the loading from 35 to 55 mg at 200°C.
- (3) The interaction between bed temperature and NO₂ decreases the loading from 139 to 32 mg at 100°C and 94 to 37 mg at 200°C.
- (4) Very little if any interaction between bed temperature and water vapor exists. The drop in loading capacity is about the same at both 100 and 200°C.

Iodine-Desorption and Recycle Tests

Iodine-desorption tests were run on AgX beds which had been loaded with iodine in dry-air streams at 15 m/min. The partial pressures of HI, which ranged between 0.0005 to 0.005 atmospheres, were obtained for several bed temperatures and superficial-face velocities throughout the test space. The rates of HI desorption were calculated by:

$$\frac{(P_{HI})(\text{cm}^3 \text{ H}_2/\text{min})(128 \text{ mg HI}/24.1 \text{ cm}^3)}{(\text{cross-sectional area of the test bed})} = \text{mg HI}/\text{min-cm}^2$$

The response surface (see Figure 5) of the desorption rate vs the two experimental variables was obtained by fitting the experimental data to the second order model:

$$Y = 3.09 + 8.81X_1 + 2.93X_2 + 1.98X_1^2 + 0.26X_2^2 + 2.89X_1X_2$$

where the units for Y are mg HI/min-cm², X₁ = (temp-500)/100, and X₂ = (face velocity - 350)/250. All observed-desorption rates agree within 10.7 ± 5.8% (95% confidence level) of the predicted rates on the response surface. However a tailing effect at 400 and 500° occurs in which the P_{HI} continually decreases to zero after about 80 to 90% of the iodine is desorbed. The tailing effect causes the average desorption rate for 99%+ removal of iodine to be about 2.5 times less than that predicted by the response surface.

Recycle tests (see Figure 6) on three 5-cm-deep beds, in which iodine was repeatedly loaded and stripped, were run to test the effect of regeneration temperature on loading capacity. When regenerating at 600°C, the loading capacity decreased about three-fold after three cycles. Using regeneration temperatures of 400 or 500°C caused the loading capacity to decline about two-fold after five cycles. There is no apparent difference between using a regeneration temperature of 400 or 500°C, but a large one exists between 500 and 600°C. The total exposure of the beds to 400, 500 and 600°C were 500, 90 and 10 hr respectively.

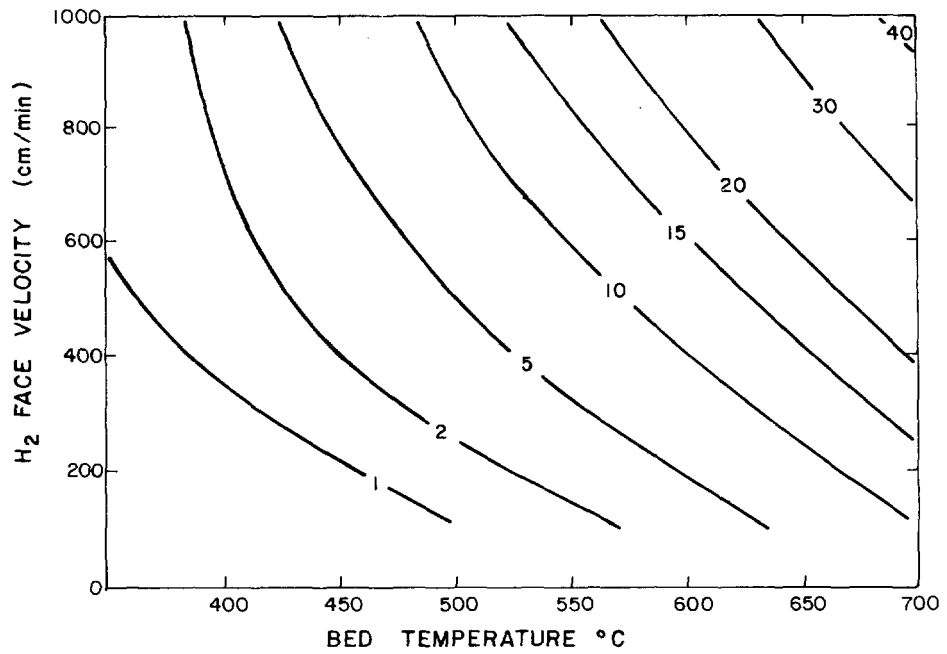
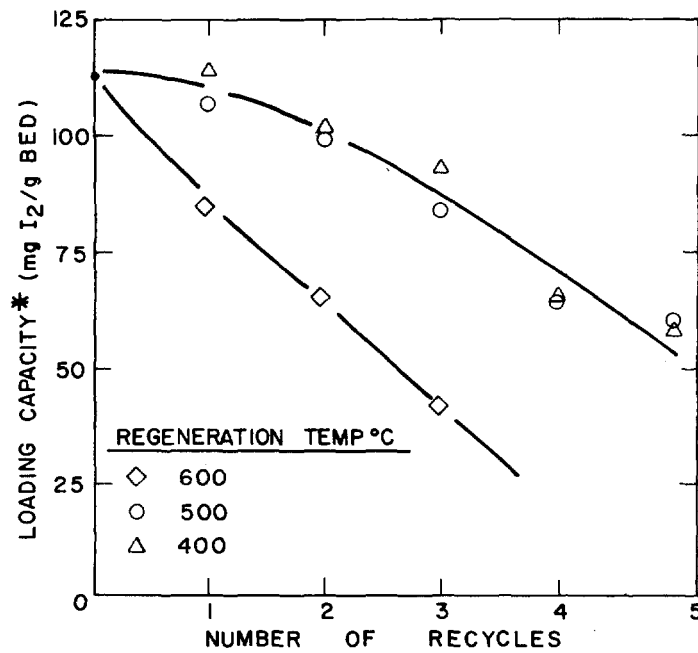


Figure 5. Desorption Rate of HI from AgIX(mg HI/min-cm²)



* LOADING-TEST CONDITIONS: BED DEPTH, 5cm; FACE VELOCITY, 15 m/min; BED TEMPERATURE, 150°C; AIRBORNE-IODINE CONCENTRATION, 500mg/m³; PRETEST PURGE, 1 hr; TEST PERIOD, UP TO 16 hr; DF, ABOUT 200.

Figure 6. I₂ Loading Capacity of Recycled AgX in Dry Air

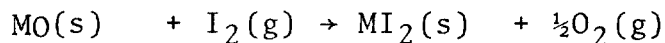
The desorbed iodine was adsorbed on PbX beds at 150°C downstream of the AgX beds being stripped. Using a superficial-face velocity of 500 cm/min, an average loading capacity at breakthrough of 317 mg I₂/g PbX based on four tests was obtained. One of the loaded-PbX beds was post-purged with H₂ at 150°C for 16 hr and no detectible loss of iodine occurred. Another loaded-PbX bed was immersed in distilled water at room temperature for several days and the solubility of the adsorbed iodine was found to be about 26 mg I₂/100 mls H₂O.

DISCUSSION OF RESULTS

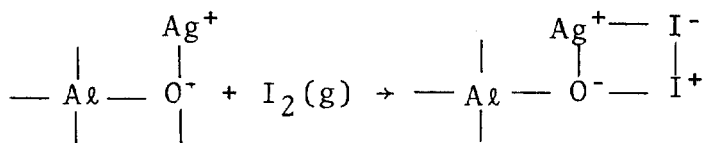
Chemisorption vs Physisorption

The tests on maximum-loading capacities (Table III) indicate that both physisorption and chemisorption occur in the substrate (NaX). The similar chemisorption capacities of CdX, PbX and NaX imply that the chemisorptive bonds which are formed are not metal iodide bonds per se, although bonding may be occurring near the metal sites. The chemisorption capacity of NaX at 150°C is about 30 mg I₂/g NaX. Therefore screening tests on metal-exchanged zeolites which are conducted at lower loadings can be misleading. Typically loadings of about 1 to 10 mg I₂/g substrate are used. Our screening tests (Table II and Figure 3) indicated that CdX might be an efficient adsorbent below 250°C. However, when the loadings were increased from 1.4 to 3.5 mg I₂/g CdX (Figure 4), the efficiency decreased. We decided that most of the data gathered for CdX and PbX represented the response of the substrate and had little to do with the exchanged cation.

The chemisorption capacity of AgX at 150°C is about 214 mg I₂/g AgX (Table III). This is 60% of the stoichiometric capacity based on the number of silver sites per gram. It can be inferred from the data in Table III and Figure 4 that there is a fundamental difference in the type of chemisorption which takes place in AgX as compared to PbX and CdX. If one assumes to the first approximation that the metal ions exist as oxides in the zeolite, the reaction taking place could be viewed as:



where M = Pb or Cd. The standard free energies of the reactions are -16.1, 2.5 and 0.3 kcal/mole for Ag, Cd and Pb respectively. Similarly the conversion of Cu, Co, Fe, Ni, and Zn oxides to iodides involve positive-free energy changes of 20 kcal or more. All the above metal oxides are more stable than their corresponding iodides with the exception of silver, which may explain partially why only AgX has a large-chemisorption capacity. Since the oxygen anion is bonded into an aluminum tetrahedron, a plausible mechanism for the reaction taking place in AgX might be:



It would be expected that only partial bond breakage and formation would be involved to give a cyclic structure. But this reaction should also be thermodynamically favored because the iodide is more stable than the oxide and the O-I bond is stronger than the I-I bond.

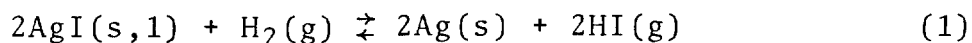
Effect Tests

Application of adsorbent technology to reprocessing plants will generally involve bed depths greater than 10 cm. The results in Figure 4 point out the need to conduct tests with at least 10-cm-bed depths. Otherwise the predicted-loading capacities will be quite conservative. The data in Figure 4 also indicate a large loss in loading capacity with increased face velocity. However, it may be necessary to use high face velocities to avoid unfavorable ratios of bed diameter to bed length.

From the results given in Figure 4 and Table IV, one can infer that the conditions of optimum-loading capacity lie in the direction of lower temperatures, slower-face velocities and the absence of contaminant gases. This is of course to be expected, but practical application usually requires operating conditions which deviate far from ideality. Since the negative effects of increasing face velocity, bed temperature, NO₂ and water vapor are all large, the response surface of loading capacity as a function of all these variables will be studied. It is expected that face velocity will not interact with the other three variables.

Iodine-Desorption Thermodynamics

As previously explained, the formation of silver iodide (AgI) appears to be thermodynamically favorable in the reaction between I₂ and AgX. The rate at which HI is desorbed from iodine-loaded AgX (AgIX) also indicates that AgI is formed within the substrate. The reaction, which we believe occurs, is:



Assuming that the solid and liquid phases have unit activity in the substrate and the gases have unit fugacity, the free energy (ΔG) of reaction is given by:

$$\Delta G = \mu_{\text{HI}} - \mu_{\text{AgI}} \quad (2)$$

Where μ equals the molar free energy of the compounds. The equilibrium partial pressure of HI (P_{HI}) is equated to ΔG by:

$$\log K_{\text{eg}} = \log(P_{\text{HI}}^2/P_{\text{H}_2}) = -\Delta G/2.3RT \quad (3)$$

where K_{eg} is the equilibrium constant. The experimental pressure of H₂ was maintained at one atmosphere. Therefore, equation (3) can be simplified to:

$$\log P_{\text{HI}} = -\Delta G^0/4.6RT \quad (4)$$

where $T = ^\circ K$, $R = 2 \text{ cal/mole}$, and ΔG is the standard free energy of reaction. Using values of μ^0 for $HI(g)$ from the JANAF tables (12) and values of μ^0 for $AgI(s,1)$ from the National Bureau of Standards, (13) the following data were calculated from equations (2) and (4):

$T^\circ C$	400	450	500	550	600	650	700
$\Delta G^0(kcal)$	23.26	22.29	21.32	20.40	19.71	19.13	18.55
$P_{HI}(10^3 atm)$	0.18	0.45	1.01	2.00	3.52	5.59	8.47

The calculated P_{HI} along with the observed P_{HI} (using a superficial-face velocity of 500 cm/min of H_2 through the test bed) are plotted in Figure 7. The observed P_{HI} is three times larger than the calculated P_{HI} at 400°C. This corresponds to a standard free energy of formation of -12.76 kcal/mole for chemisorbed AgI as compared to -14.39 kcal/mole for the pure compound. Although the iodide bond is undoubtedly weaker due to a matrix effect, the discrepancy between partial pressures and free energies are small. At 600°C the discrepancy between partial pressures is less than 50%. It was also observed that at constant temperature, the P_{HI} was constant over a large range of H_2 flow rates which indicates that equilibration of equation (1) is instantaneous under these conditions.

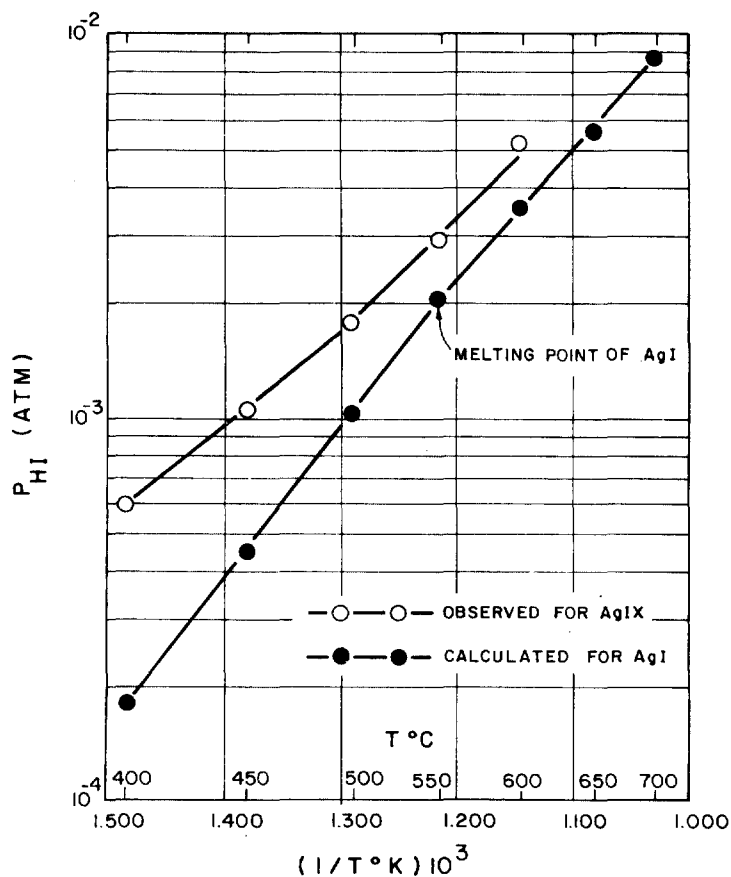


Figure 7. Partial Pressures of HI over AgI and AgIX

Recycle Tests

The loss in iodine-loading capacity of the recycled AgX (see Figure 6) is believed due to the progressive pore collapse of the zeolite structure. Studies by Thomas and coworkers⁽¹⁴⁾ with Type 4A zeolite have shown that starting at 550°C a transformation of the zeolite phase into a non-zeolite solid occurs. The rate of the transformation increases with temperature and the resulting solid has virtually no adsorption capacity for water vapor. In our studies, silver whiskers were observed on the surface of the zeolite when the regeneration was performed at 600°C. It is possible that some of the AgI, which melts at 552°C, migrated to the surface and deposited silver after the iodine was desorbed. Considerable structural damage would be expected if this were occurring. At 500 and 400°C the silver deposit was not observed which may explain the large difference in the recycle data given in Figure 6 at 600°C vs the lower temperatures. We also observed that the rate of iodine removal from AgIX decreased to about half of its original rate by the fifth regeneration at both 400 and 500°C. This is again probably related to increased diffusion resistance from pore collapse. We plan to examine other silver-loaded substrates which have higher thermal stability.

Chemisorption in PbX

As previously mentioned the chemisorption of I₂ in PbX doesn't appear to be thermodynamically favored. However the reaction: $\text{PbO} + 2\text{HI} \rightarrow \text{PbI}_2 + \text{H}_2\text{O}$ has a negative free energy of -47 kcal/mole at 150°C. Since the oxygen anion is bonded into an aluminum tetrahedron, the reaction would involve the chemisorption of both iodine and hydrogen to form PbI₂ and two hydroxyl groups (i.e., 2 Al-OH). In the absence of O₂ the chemisorbed PbI₂(PbI₂X) is stable at 150°C. Once cooled to room temperature, the PbI₂X is kinetically stable in the presence of air. A loading of 317 mg I₂/g PbX represents 88% of the stoichiometric capacity of the PbX based on the number of lead sites per gram.

APPLICATION OF ADSORBENT TECHNOLOGY

A typical application in a 5 tonne/day reprocessing plant might be to remove 600 kg/yr (iodine-129 plus iodine-127) of iodine from a 140 m³/min off-gas stream. Assume that a loading of 50 mg I₂/g AgX could be obtained at a DF of 10³ using a superficial-face velocity of 60 m/min in the presence of NO₂ and water vapor. Figure 8 illustrates a conceptual design of an iodine removal system which uses two-2 m³ beds of AgX. The resulting bed dimensions would be a diameter(d) of 1.71 m and length (ℓ) of 0.86 m for a d/ℓ ratio of 2 and bed weights of 1.78 metric ton each. If the iodine-loading rate averaged 2 kg/day, then one of the beds would last about 40 days before breakthrough. Using a regeneration temperature of 500°C and a hydrogen-face velocity of 200 cm/min (flow = 4.66 m³/min), the predicted desorption rate (from Figure 5) would be 1.5 mg HI/min-cm². When adjusted for tailing the average desorption rate would be about 0.6 mg HI/min-cm², which would require about 4.2 days to regenerate the bed. Each bed would be recycled about four times per year or 20 to 30 times in a five year period. During

this period the loading capacity would be declining and the frequency of recycle increasing. The important feature is that the loaded beds could easily be stripped of iodine and reused several times. This would permit small AgX inventories and more favorable d/l ratios since a maximum loading would not be necessary. In the end, the silver could be reclaimed by conventional-wet-chemistry techniques provided the bed was not too contaminated by other radiosotopes. The stripped iodine would be loaded onto PbX beds for permanent fixation and storage. For 600 kg of I_2 about 2.5 metric ton or 1.7 m^3 of waste per year would be generated. The vessel would be designed so that it could both house the bed during loading and later be used for a storage container. Stoichiometrically, about 4.7 kg H_2 or 9 cylinders of H_2 would be needed per year.

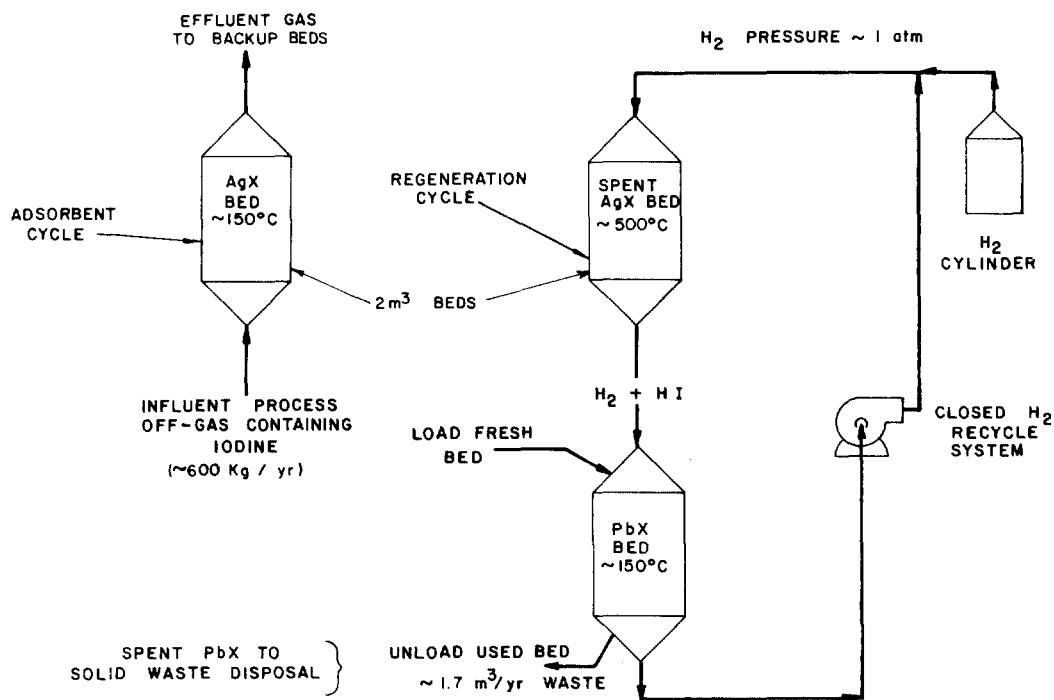


Figure 8. Adsorbent System for Iodine Removal

ACC - A - 2180

If integrated-cleanup systems for the removal of HTO, NO_x , iodine-129/131, Kr-85, etc. are required in the future, then it may be possible to simplify the regeneration process. In dry-nitrogen streams void of any contaminants, Collard and coworkers^{8,15} have reported loadings up to 760 mg I_2/g substrate at 50% breakthrough using NaX at $25^\circ C$. Based on their mathematical analysis of the breakthrough data, it appears that iodine loadings in the range of 200 to 300 mg I_2/g NaX could be obtained with 10-cm-deep beds, face velocities of 15 to 50 m/min, and DF's of 1000. Since the reaction $I_2(l) + H_2(g) \rightarrow 2HI(g)$ has a negative free energy of -1.5 kcal/mole at $127^\circ C$, lower bed temperatures and faster regeneration rates would be possible than with AgX. The problem of pore collapse and loss of loading capacity should not be significant. The PbX would still

14th ERDA AIR CLEANING CONFERENCE

be used as the adsorbent for fixation and storage as the chemisorbed PbI_2 .

APPENDIX A

Iodine-129 Abatement Potentially Required for LWR Reprocessing Plants

The following is assumed:

- (A) The amount⁽¹⁾ of iodine-129 present in spent fuel is about 0.04 Ci per 40,000 MWD.
- (B) The proposed EPA guideline⁽²⁾ for iodine-129 release is a maximum of 0.005 Ci per gigawatt year electrical (GW-YR)_{e1}.
- (C) The conversion efficiency of thermal MWD to electrical is about 30%, therefore from assumption (A) there are 0.04 Ci iodine-129 per 12,000 (MWD)_{e1}.
- (D) Up to 90% of the iodine-129 is discharged as gaseous waste⁽¹⁾.

Based on these assumptions, the amount of unabated iodine-129 released would be:

$$(0.04 \text{ Ci}/12,000(\text{MWD})_{e1})(10^3 \text{ MW/GW}) = 0.0033 \text{ Ci}/(\text{GWD})_{e1}$$

$$(0.0033 \text{ Ci}/(\text{GWD})_{e1})(365 \text{ day/yr})(0.9) = 1.095 \text{ Ci}/(\text{GW-YR})_{e1}$$

The required efficiency of an iodine-129 abatement system would be:

$$(1 - (0.005 \text{ Ci}/1.095 \text{ Ci})) 100 = 99.5\%$$

REFERENCES

1. J. L. Russell and P. B. Hahn, "Public Health Aspects of Iodine-129 from the Nuclear Power Industry", Radiol. Health and Data Report, 12, p. 189, April 1971.
2. Chemical Engineering, p. 36, June 9, 1975.
3. D. T. Pence, F. A. Duce, and W. J. Maeck, "A Study of the Adsorption Properties of Metal Zeolites for Airborne Iodine Species", Proceedings of the 11th AEC Air Cleaning Conference, CONF 700816, p. 581, September 1970.
4. D. T. Pence, F. A. Duce, and W. J. Maeck, "Developments in the Removal of Airborne Iodine Species with Metal Substituted Zeolites", Proceedings of the 12th AEC Air Cleaning Conference, CONF 720823, p. 417, August 1972.
5. J. G. Wilhelm and H. Schüttelkopf, "Inorganic Adsorber Materials for Trapping of Fission Product Iodine", Proceedings of the 11th AEC Air Cleaning Conference, CONF 700816, p. 568, September 1970.
6. J. G. Wilhelm and H. Schüttelkopf, "An Inorganic Adsorber Material for Off-Gas Cleaning in Fuel Reprocessing Plants", Proceedings of the 12th AEC Air Cleaning Conference, CONF 720823, p. 540, August 1972.
7. R. D. Ackley and Z. Comps, Applicability of Inorganic Sorbents for Trapping Radioiodine from LMFBR Fuel Reprocessing Off-Gas, ORNL-TM-4227, May 1973.

14th ERDA AIR CLEANING CONFERENCE

8. G. Collard et al., "Gas Purification Technology in Reprocessing", private communication from L. H. Baetsle, S.C.K./C.E.N., Mol-S.A. Belgonuclearie, Brussels Belgium, May 1976.
9. W. J. Maeck and D. T. Pence, "Application of Metal Zeolites to Radioiodine Air Cleaning Problems", Proceedings of the 11th AEC Air Cleaning Conference, CONF 700816, p. 607, September 1970.
10. I. J. Gal et al., "Adsorption of Methyl Iodide on Impregnated Alumina", Proceedings of the 13th AEC Air Cleaning Conference, CONF 740807, p. 815, August 1974.
11. J. Ramand, "Absorption Ultraviolette Dans La Region De Schumann Etude De: C&H, BrH et IH Gazeux", Annales de Physique (Paris) Series 12. v. 4, p. 528, September 1949.
12. JANAF Thermochemical Tables, 2nd Edition, NSRDS-NBS 37, June 1971.
13. W. J. Hamer et al., "Theoretical Electromotive Forces for Cells Containing a Single Solid or Molten Fluoride, Bromide, or Iodide", J. Electrochem. Soc., 112, p. 750, 1967.
14. J. L. Thomas, M. Mange and C. Eyraud, in "Molecular Sieve Zeolites-I", R. F. Gould, Ed, A.C.S., 1971, Chapter 34, p. 443.
15. G. Collard et al., "Dynamical Adsorption of Iodine on Molecular Sieves", S.C.K./C.E.N. Report BLG 429, 1974.

DISCUSSION

SKOLRUD: In your tests, have you evaluated loading of methyl iodides, or have you looked at the effects of organic contaminants?

STAPLES: The only contaminants we have looked at so far are NO₂ and water. We plan consideration of CH₃I and have discussed how to set up the experiments. We have to look at it because there are organic iodides in the off-gas stream. There have been past studies of the loading capacities of silver X for methyl iodide. One number that comes to mind is about 200 milligrams of iodine per gram of silver X. Rather than repeat some of this work, we have gone to elemental iodine because that is probably the major iodine form released in fuel processing plants.

PARKER: Considering the intensity of capital costs of fuel reprocessing facilities, I wonder if you have done a complete economic study of this system.

STAPLES: We haven't done a complete cost analysis on this.

PARKER: Licensing is very difficult for reprocessing facilities. This hydrogen generation system could add more problems to licensing.

14th ERDA AIR CLEANING CONFERENCE

STAPLES: We believe that designing a fail-safe system to handle hydrogen is within our current technical capability.

DEITZ: We have estimated the thermal stability of potassium iodide relative to silver iodide by a thermal analysis procedure. When heated above 450°C the former appears to be more silver than silver iodide. The total iodine emission was determined and that from silver iodide exceeded that from potassium iodide. Is this your experience?

STAPLES: We have not made this comparison.

WILHELM: What is the price of silver zeolite, of lead zeolite, and of the regeneration process, and is the decontamination factor of silver Z the same as for the X type?

STAPLES: Under the same loading test conditions, the DF's of silver Z and silver X appear to be the same. For Silver X, the latest cost figure I have heard was around \$67 a pound if bought in ton lots. Lead X may cost about \$12 a pound if bought in ton lots.

SKOLRUD: When regenerating loaded beds, is the HI sorbed on PbX stable? That is, is it chemisorbed or physically adsorbed?

STAPLES: We believe the HI is chemisorbed by the PbX. We have performed purging and solubility tests which give us strong evidence to support chemisorption.

PARKER: What problems can arise in licensing fuel reprocessing plants with a H₂ regeneration system? For example, how much hydrogen does a plant producing 600 Kg of I₂ per year require?

THOMAS: Nine ordinary pressurized cylinders of hydrogen per year.

ORTH: Have there been tests in the H₂ regenerant diluted with some inert gas to reduce the hazard from an ignition standpoint? I worry about the safety analysis of a system with hot hydrogen gas containing the active iodine that we have gone to the pains of concentrating.

STAPLES: We have regenerated iodine-loaded silver zeolite only with pure hydrogen. Dilution of hydrogen with an inert gas would slow down the regeneration rate. For scale-up, we have discussed installing monitors to detect either leakage of air or outleakage of hydrogen. If either leak occurs, the process would be shut down and repaired.

Air Filtration Plants of Wall-Type for Separation
of Fission Iodine in Nuclear Reactors

Authors: H.-H. Stiehl, M. Neumann and D. Sinhuber
DELBAG-LUFTFILTER GmbH
P.O. Box 31 04 69 · D-1000 Berlin 31

Abstract

The increasing density of nuclear power stations and increased safety requirements will lead in future to higher flow rates and longer residence times in the adsorption filter layer of the iodine sorption filter plants of nuclear power stations. The safety requirements in the Federal Republic of Germany have been complied with so far in the conventional way by means of duct-type filter constructions. For the higher flow rates and longer residence times necessary in future, we propose a filter construction of wall-type, which complies with the safety regulations of the Federal Republic of Germany. The economic and technical advantages are discussed.

The output of nuclear power plants has been standardized in the past years to values of 800 and 1200 MW and is expected to be maintained for the next 10 years. Contrary to this it is to be expected that the safety requirements will become more stringent during the next years on account of the increasing density of nuclear power stations and the increasing safety conscience of the public by taking advantage of the experience and new research results.

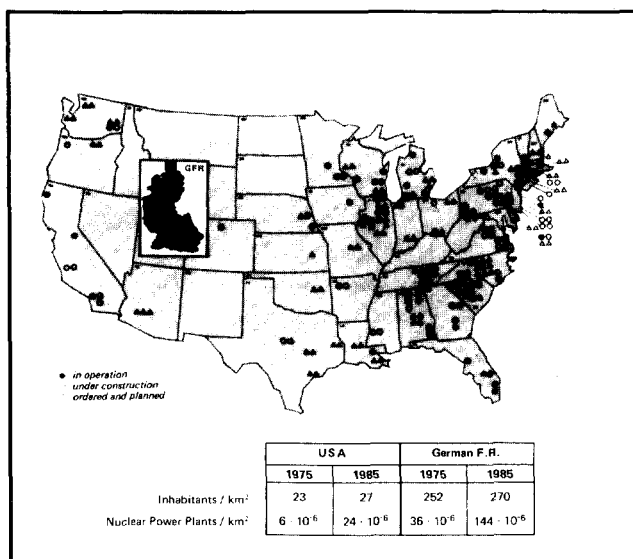


FIGURE 1:
Nuclear Power Plants USA and the Federal Republic of Germany up to 1985

Figure 1 shows a comparison between the density of nuclear power stations in the USA, and in the Federal Republic of Germany in 1985. Whereas in the Federal Republic of Germany an essentially higher density of nuclear power stations is planned than in the United States of America

on account of the greater population density related to the area of the country, there will be comparable nuclear power station densities in the densely populated area at the East Coast of the United States. The political consequences of this development resulted for example in the Federal Republic of Germany in passing the more strict regulation for protection against radiation (1). As examples are cited the increase of the all-year dosis ingestion factor for iodine to $4,4 \times 10^5 \text{rem.m}^3/\text{Cisec}$, the consideration of the soil roughness when calculating the long-term dispersion factor and the necessity to consider of late the dosis values of all loading tracks at the thyroid gland dosis of 90 mrem. By maintaining strictly the principle "as low as practicable" a further reduction of iodine release has to be expected in the proceeding of approval for nuclear power plants. Therefore, it is necessary to discuss new ways for the concept of design of iodine sorption filters. Based on the safety layout criteria in the Federal Republic of Germany the present concept of construction of duct-type is presented and from this the proposed wall-type is being developed. Finally the technical and economical advantages of this type are being discussed.

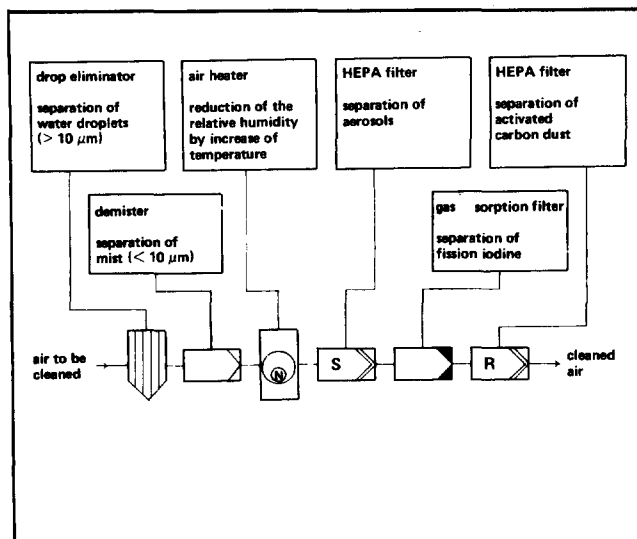


FIGURE 2:
HEPA filter and gas sorption filter plant for separation of aerosols and fission iodine

criteria	regulations
efficiency to DIN 24184 1st filter stage 2nd filter stage	$E \geq 99,97\%$ $E \geq 98\%$ } for paraffine oil mist $0,3 < \phi < 0,5 \mu\text{m}$
leak-proof to DIN 24184	no oil mist thread visible by scattered light
tight filter seat	leak flow rate through filter seat < 0,01 % of the nominal flow rate
Prevention of activity release when changing filters	replacing of filter elements by means of protective bags

TABLE 1:
Safety concept for HEPA filter plant

Figure 2 explains the well known principal construction of iodine filters by means of the drop eliminator, the demister, which may at the same time serve as prefilter, the air heater for reducing the relative humidity, the HEPA filters for elimination of aerosols, the gas sorption filter for separation of fission iodine, and the HEPA filter for separation of activities attached to fines of activated carbon. According to the most important safety layout criteria given in Table 1 for the HEPA filter installations, the efficiency of the HEPA filter elements of the first filter stage must reach at least 99,97 % for a paraffin oil mist of 0,3 to 0,5 micrometer particle diameter. In the second filter stage an efficiency of 98 % is sufficient. In order to ensure that the efficiencies obtained in the type test are reached by the individual filter elements, these must be tested before installation for leak tightness by means of the oil mist test. During this test there shall be no visible oil mist threads in the scattered light of an intensive spot lamp. In order to guarantee the same efficiency of the individual filter elements also for the complete unit, the tightness of the filter seat that is between the gasket of the HEPA filter element and the sealing surface of the frame or housing must be suitable for being tested. For avoiding release of activity, replacing of the HEPA filter elements into a protective bag has to be made possible

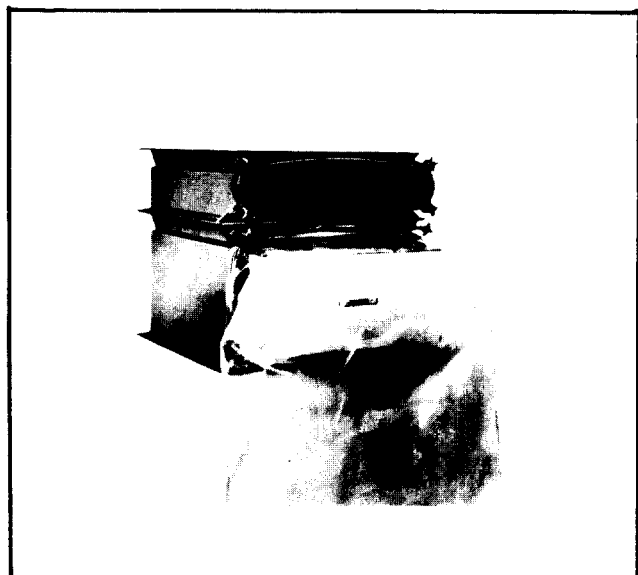


FIGURE 3:

Filter housing consisting of prefilter for fine dust separation and HEPA filter with protective bag

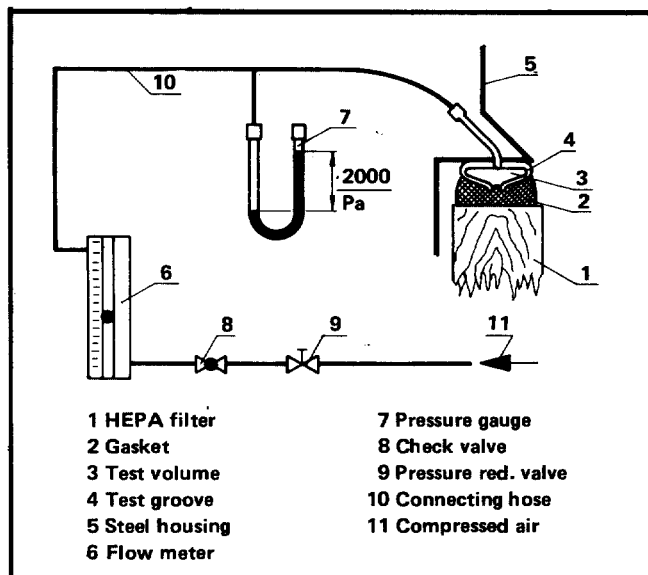


FIGURE 4:

Leakage test of filter seat for HEPA filter

as shown in Figure 3. — The principle of the filter seat test is explained in Figure 4. Air of a pressure of 2000 Pascal is pressed into a groove which is fitted gastight to the filter housing and is covered by the gasket of HEPA filter element. The leak flow rate given by the flowmeter shall not exceed 0,01 % of the nominal flow rate passing the HEPA filter element. Similar to the HEPA filter installations there are safety criteria for the iodine filters the most important of which are summarized in the Table 2. The efficiency for radioactive gaseous fission iodine in the form of methyl iodine must be higher than 99 % for the off-gas filtration units, and higher than 95 % for the recirculated air filtration units.

criteria	regulations
efficiency for radioactive iodine	E ≥ 99 % for CH ₃ 131 J for off gas E ≥ 95 % for CH ₃ 131 J for rec. air
type	self-sealing fixed bed for accident filter
bed depth	minimum 200 mm for accident filter, addition with respect to the relative air humidity, loading with solvents and aging for reaching the required efficiency for 6 to 12 months.
checking of the sorption material during operation	By-passing of a partial flow rate through dismantable control filter
prevention of activity release when replacing the sorption material	replacing of the carbon by means of protective bags

TABLE 2:

Safety concept for fission iodine sorption filter plants

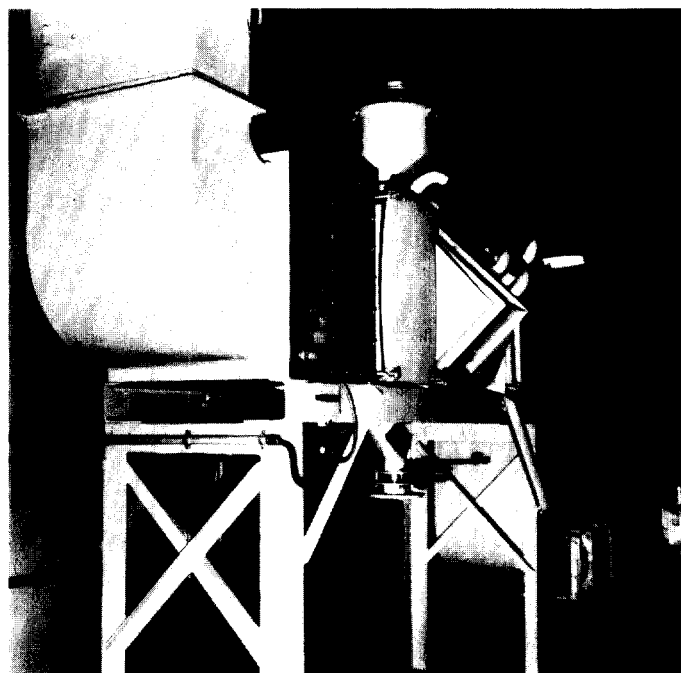


FIGURE 5:

Atmosphere cleanup system with fixed-bed iodine sorption filter, duct type

Accident filters must be of a self-sealing construction comprising a heaped fixed bed filter whose layer thickness must be at least 200 mm. When determining the layer thickness it should be ensured that the required efficiency is maintained for a period of 6 months to 1 year taking into consideration the relative humidity of the carrying air, the preloading especially by organic solvents and the aging of the sorption material. An example for the construction of such fixed bed sorption filters is shown in Figure 5. This filter may be charged and discharged with sorption material by airtight valves on top and at the bottom of the filter layer. For checking the sorption material during operation a partial airstream is separated and directed through removable control filters whose connections as shown in Figure 5 are parallel to the filter layer. Figure 6 shows such control filter. After dismantling the control filter the connections are closed by means of airtight valves.

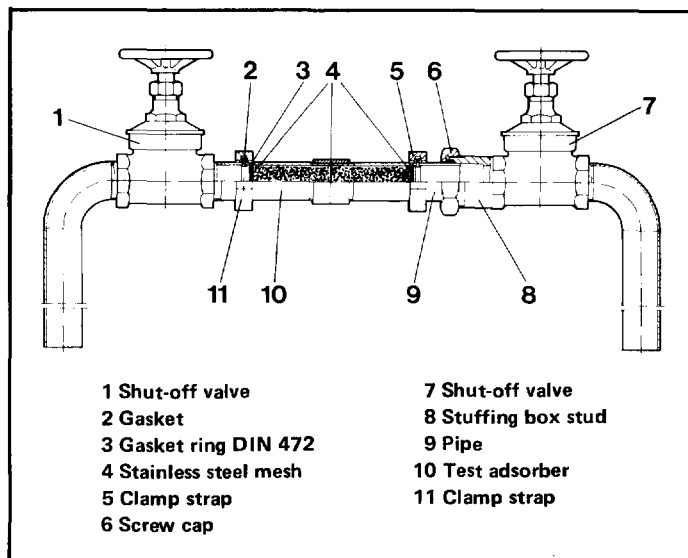


FIGURE 6:
Control filter in parallel with sorption filter

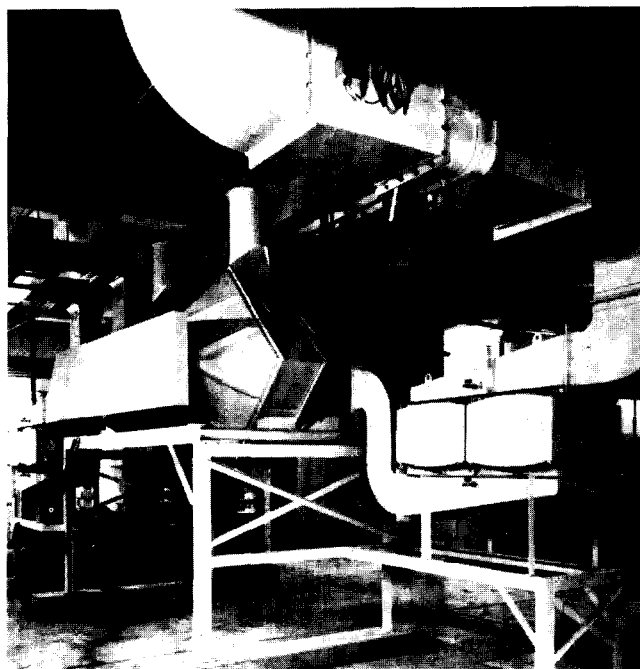


FIGURE 7:
Post accident off-gas filter plant, nominal flow 4000 m³/h, in a nuclear power plant

The used sorption material of an iodine sorption filter bed is discharged into standardized waste containers. During this operation protective bags have to be applied for avoiding release of activity. According to the German regulations the iodine sorption filter units for filtration of waste air from controlled areas must be installed within the control range of the reactor. The technical realization of an accident off-gas filter plant for 4000 m³/h such as installed in the Biblis nuclear power station is shown in Figure 7.

Equipments visible are the drop eliminator, the air heater, the first HEPA filter stage, the fixed bed sorption filter and the second HEPA filter stage. The fixed bed filters are installed at a height which allows discharge into standardized waste containers. Compared with this accident filter unit for 4000 m³/h planned in 1972, the accident filters being planned today are provided for a flow rate of approx. 20 000 m³/h. When maintaining the shown concept of filtration plant of duct-type for flow rates increased to 20 000 m³/h, the following disadvantages will occur (2):

- high space requirement
- high material cost, especially for the stainless steel construction
- high production cost by working steel sheet for housing, connections and ducts

- high cost for 4-fold corrosion-resistant finish suitable for decontamination when using ordinary sheet metal
- difficult and time wasting decontamination
- increased pressure drop of the filtration plant caused by pressure loss in ducts, deviations, cross section changes, and consequently increased operating cost
- high transport and assembly cost.

The disadvantages given may be avoided if the HEPA filter stage and the fixed bed sorption filter are realized in wall-type while the safety criteria valid at present in Germany are maintained. HEPA filter walls with test groove for checking filter seat tightness which are equipped with oval rubber seals for replacing the HEPA filter elements by plastic bags may be assembled from frames by bolting or welding as shown in Figure 8. As the HEPA filter elements are completely surrounded by the plastic bag when removing them from the receiving frames, walls of this type may be serviced from the clean air side (3). The left half of the Figure shows the test groove and the leak rate measuring instrument.



FIGURE 8:
Mounting frame for HEPA filter with filter seat test groove

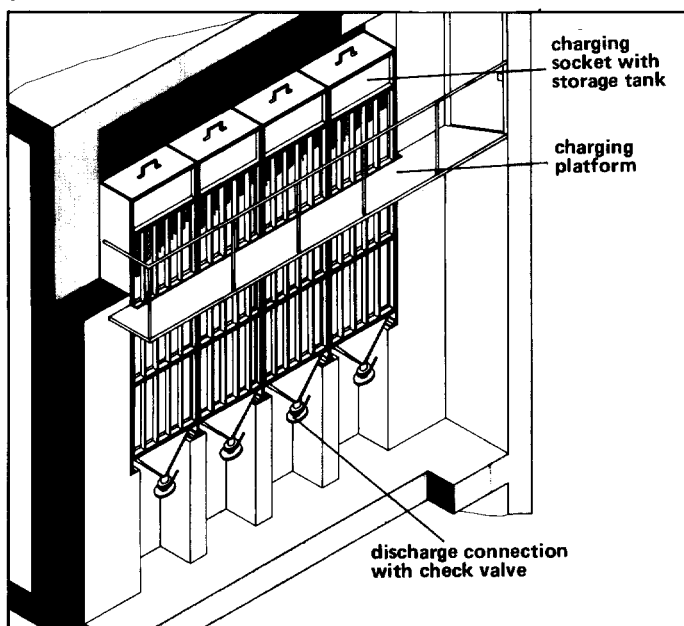


FIGURE 9:
Wall-type gas sorption filter for iodine separation

The view of the fixed bed sorption filter of wall-type seen from the clean airside is given by Figure 9. This shows 4 parallel filter sections, which may be filled after removing the cover from a maintenance platform on top of them. There is a spare quantity of sorption material arranged in the dead zone of the flow which settles automatically during operation in case of possible sagging of the sorption material, and which in this way prevents leakages between the inlet and outlet side of the filters. The used sorption material is discharged by means of a discharge connection into the waste container. The discharge connection is equipped with a sealing gasket in connection with plastic bags for replacing the sorbent. The control filter specified is arranged in such way that a tube is cast airtight in the concrete wall between the inlet and outlet side. This tube can be closed with an airtight valve on the outlet side of which the control filter may be vertically screwed. For reducing the danger of radiation for the maintenance staff the outlet connections may be discharged by means of tubes into the floor beneath. In addition it is possible to provide an automatic charging of the single filter sections from outside. When erecting the filter housing both of steel or of concrete paint finishing has to be provided in the clean room chambers which is suitable for decontamination. For protecting the sorption material from

preloading by organic compounds which are used in the nuclear power stations for example for repairs, painting and for decontamination, and which are of negative influence to the efficiency for methyl-iodine, among others there are at present considerations for using an adsorption prefilter (4, 5). This adsorption prefilter may also be realized as wall-type such as shown in Figure 9. It is arranged between the first HEPA filter stage and the gas sorption filter wall. This adsorption prefilter will increase the life time of the main sorption filter which has high safety significance and will ensure greater availability. The extra cost for the prefilter may be partially compensated by longer service life of the high-quality sorption material of the main filter and by the lower cost for safety control.

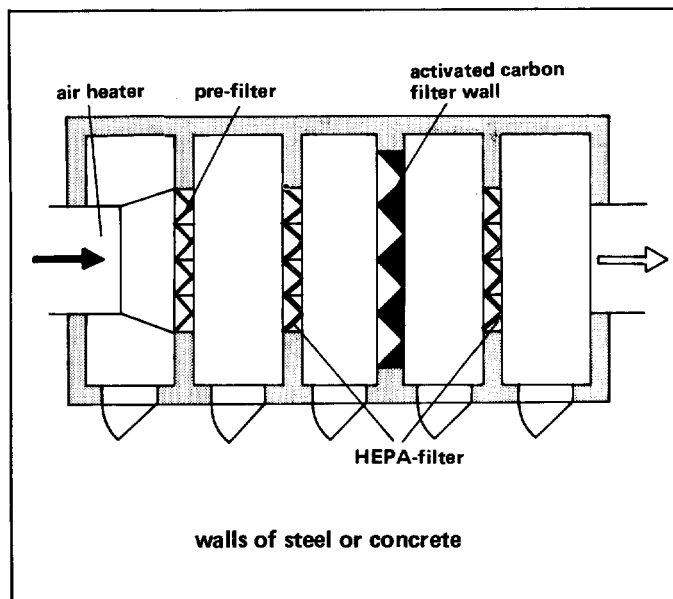


FIGURE 10:
Air filter plant of wall-type for 20 000 m³/h, usual design

The new HEPA filter and gas sorption filter walls may be arranged in the classic parallel construction the way such as shown in Figure 10. The drop eliminator, demister and the air heater are arranged in the intake duct. In order to extend the service life of the first HEPA filter wall, a particulate prefilter wall is provided for. The flow velocity on the following HEPA filter wall is approx. 1,5 m/s at the nominal flow rate of the HEPA filter element. For avoiding high pressure drops and whirling up of the sorption material, the face velocity on the iodine filter unit has to be limited to 0,5 m/s. This change of cross section causes a non-uniform flow distribution over the face area of the sorption filter. This disadvantage is avoided by giving the same cross section to the HEPA filter wall and the activated carbon filter wall, which of course results in higher cost of the installation. Another possibility is arranging the HEPA filter wall and the sorption filter wall at angle to each other. This configuration is shown in Figure 11. It helps to reduce and uniform the air velocity before passing the gas sorption filter wall and to reduce the space requirement.

Comparison of cost was made for a four stage standard filter unit for 20 000 m³/h of the conventional duct-type construction mentioned before, of the arrangement of parallel filter walls and of the arrangement of filter walls at angle to each other. This was based on an HEPA filter element being charged with an air flow rate of 1700 m³/h and a residence time in the gas sorption filter of 0,6 seconds. The cost of the drop eliminator, the demister and the air heater were not included in the calculations as similar conditions were assumed in all three cases. For comparison all steel parts of ordinary steel were calculated with a 4-fold finish suitable for decontamination. Only the components of the gas sorption

filter wall were provided for of stainless steel. For all three cases it was assumed that a floor height of 6 meters is available. The prices for the walls of the plenum chambers of both wall types were calculated for construction of steel as well as of concrete. From the Figure 12 it can be seen that with the concept of filter walls arranged at angle to each other, 58 % of the space is required as compared with the concept of the duct-type air filter. A comparison of the respective prime cost of the filter walls arranged at angle to each other in a steel chamber and of the duct-type filter shows savings of 34 %. Another reduction in price is possible, if the filter walls can be mounted in a concrete room. In such case a saving of 44 % is possible. For the new plant design the values given for the reduction of space and prime cost are minimum savings.

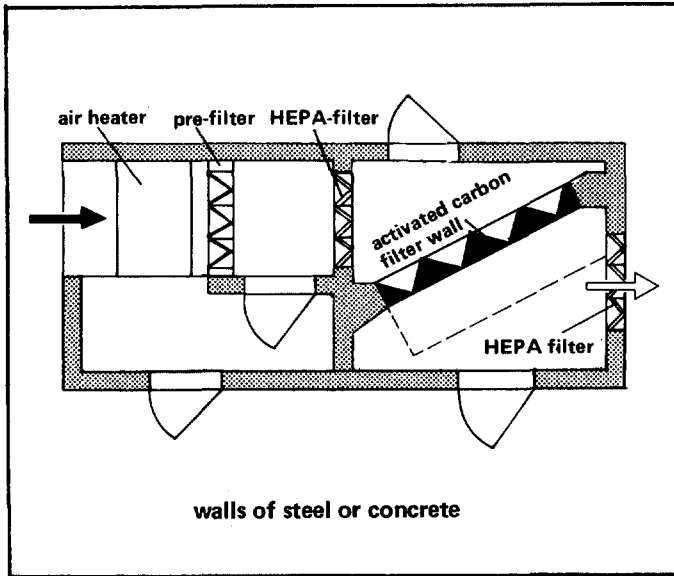


FIGURE 11:

Air filter plant of wall type for 20 000 m³/h, compact unit

Type	steel housing	wall type	compact type
V [m ³ /h] (cf/m)	20000 (11700)	20000 (11700)	20000 (11700)
Space required	100	70	58
Prime cost [%] steel walls	100*	73	66
Prime cost [%] concrete walls	—	62	56

**Remarks: Prime cost for steel housing without wall equal 100 %*

FIGURE 12:

Comparative cost analysis and space requirements for different types of filter units

Conclusion

Replacing of the conventional duct-type iodine filter units by wall-type filter designs while maintaining the safety requirements in Germany is technically feasible. A new HEPA filter wall with device for testing the tightness of filter seats and system of replacing of filter elements by plastic bag as well as a iodine sorption filter wall with heaped fixed bed are introduced. For filter plants of high flow rate and long residence time in the layer of the adsorbent the new solution will give an essential reduction of the space requirement and the production cost.

Literature

- (1) Verordnung über den Schutz vor Schäden durch ionisierende Strahlen (Strahlenschutzverordnung), Bundesrepublik Deutschland 1976
- (2) D. Sinhuber, M. Neumann, H.-H. Stiehl „Gassorptions-Filterwand zur Spaltjodabscheidung aus der Abluft von Kernkraftwerken“, Doc. Nuclex 75, Coll. D 2
- (3) C.A. Burchsted, A.B. Fuller “Design, Construction, and Testing of High-Efficiency Air Filtration Systems for Nuclear Application”, ORNL-NSIC-65, January 1970
- (4) J.G. Wilhelm „Verhalten von Jod-Sorptionsmaterialien“, Euratom-Seminar, Dec. 1973, Doc. V/559/74
- (5) J.G. Wilhelm et al., Jahresbericht 1973 der Gesellschaft für Kernforschung, KFK 1973

DISCUSSION

RIVERS: It's not unusual for nuclear reactor plant equipment to go to the low bidder. The lowest figure on your chart was for concrete structures. Our experience with concrete-cased units has been terrible, and I wonder how you cope with edge leakage and through-the-wall leakage?

STIEHL: As far as we've discussed this problem with the companies who make the concrete for the reactor buildings, they didn't see any problems. The sealing between the sorption filter stages and the concrete wall will be performed by the activated charcoal bed itself. To ensure the tightness of the HEPA-filter stages, experience with the installation of HEPA-filter walls for clean rooms are available. From the experience of running reactors, the diffusion of radioactive components through concrete walls can be avoided by careful concrete buildup and a special concrete coating on the walls. Nevertheless, steel construction will give fewer problems if uncontrolled leakage occurs during filter installation and repairs become necessary.

AN AIRBORNE RADIOIODINE SPECIES SAMPLER AND IT'S
APPLICATION FOR MEASURING REMOVAL EFFICIENCIES OF LARGE
CHARCOAL ADSORBERS FOR VENTILATION EXHAUST AIR

W. A. Emel*, D. Hetzer, C.A. Pelletier, E.D. Barefoot
and J.E. Cline

A. AN AIRBORNE RADIOIODINE SPECIES SAMPLER
FOR NUCLEAR POWER PLANTS**

Abstract

A program, sponsored by the Electric Power Research Institute, is underway to determine the chemical species of radioiodine coming from LWR power plants and their persistence in the nearby environment. In support of this program, an airborne radioiodine sampler, developed and used by the AEC was modified and tested. This sampler consists of five components. The components are: 1) a particulate filter, 2) CdI_2 on a matrix of chromosorb-P to retain I_2 , 3) 4-Iodophenol on a matrix of activated alumina to retain HOI, 4) silver exchanged molecular sieve-13X to retain organic iodides, and 5) impregnated charcoal to serve as a control. The AEC sampler has not been proof-tested for periods over 48 hours or for flow rates above 0.10 l/s. For maximum sensitivity, a sampler is required to be used for periods of one to two weeks and at a flow rate giving a bed residence time of 0.1 sec. The AEC sampler was scaled up in size to attain an air sampling rate of 0.9 l/s. Each media for this sampler (except the particulate filter) was tested in the laboratory for retention of the iodine species; I_2 , Organic, and HOI. The tests were conducted at typical conditions observed at the main iodine release points at nuclear power plants. Confirmatory tests were run at operating nuclear power plants. The test results showed that under normal plant conditions the sampler could be operated at flow rates up to 0.80 l/s and differentiate the iodine species I_2 , HOI, and CH_3I . The retention efficiencies of each media for its specie of radioiodine were found to be:

I_2 on CdI_2 - $87 \pm 5\%$, HOI on IPH $94 \pm 4\%$, and CH_3I on Ag 13-X or KI charcoal $99 \pm 1\%$.

* Present affiliation Allied Chemical Corporation, Chemical Research and Engineering Branch, Idaho Falls, Idaho

** Work performed under contract with the Atomic Industrial Forum.

I. Introduction

Extensive work was done in preparing activated charcoal air filters for nuclear power stations, to prevent a large accidental radioiodine release as had occurred at Windscale in 1957. Regular activated charcoal was found to retain essentially all of the elemental iodine, yet was rather inefficient to organic iodide, especially at high humidities. An extensive series of experiments by Collins, Taylor and Taylor at Windscale in 1967¹, showed that impregnated charcoals would solve the organic iodide problem. Maeck, Pence, and Keller developed a silver loaded zeolite with similar performance for retaining methyl iodide, but with some advantages over impregnated charcoal². Cartan suggested the existence of a third chemical form of radioiodine³. At this time, the need for complete iodine species differentiating became apparent.

The Iodine Species Sampler was developed for air sampling for the proposed Loss-of-Fluid Test. The objective was to have a sampler which could differentiate non-iodine particulates, elemental iodine and organic iodine in steam-air mixtures.

The sampler which was tested is basically one which was developed and used by the AEC⁴. The sampler consists of five components. The components are: 1) A particulate filter, 2) CdI₂ on a matrix of chromosorb-P support to retain I₂, 3) Iodophenol on activated alumina to retain HOI, 4) Silver exchanged molecular sieve - 13X to retain CH₃I, and 5) charcoal to serve as a control. This sampler as it exists had not been tested for sampling periods over 48 hours or for flow rates above 0.11 l/s. For the required sensitivity, the sampler is required to be used for periods of one to two weeks. It is desirable to operate the sampler at residence times >0.1 sec.

To increase the sensitivity, we scaled the AEC sampler to a 6.3-cm diameter size and retained the 2.5-cm depth. This larger sampler operates at flow rates up to 0.9 l/s.

Each medium for this larger sampler was tested in the laboratory for retention of the iodine species; elemental, organic and HOI and for its limitations. Tests were conducted at typical conditions observed at the main iodine release points at nuclear power plants. These locations vary in temperature and humidity. The range of temperature is about 60°F for the lowest and 140°F for the highest. The range of humidity found at the major ventilation points is from 7% R.H. to 90% R.H. Confirmatory tests of the species sampler were run at operating nuclear power plants.

II. Previous Testing of the AEC Radioiodine Species Sampler

The first report on the performance of the radioiodine species sampler was given in the 11th USAEC Air Cleaning Conference⁶. In these tests, the sampler was run at 100 per cent relative humidity and at temperatures from ambient to 90°C. Due to the difficulty of generating pure HOI, the HOI test beds were preceded by a bed of CdI₂-chromosorb-P to remove the elemental iodine present. The results showed retention efficiencies of 99+% for elemental iodine on the CdI₂, IPH and CuX, retention efficiencies of 3-4% for HOI on CdI₂ and >95% for HOI on IPH and CuX, and retention efficiencies for organic iodide of <1% on all three media.

The copper zeolite beds exhibited breakthrough at high humidity when the beds were saturated with steam. Due to the difficulty of preparing Cu-Zeolite, it was abandoned as an HOI adsorbent in favor of 4-Iodophenol on alumina.

Additional testing of the AEC sampler was reported by Keller, et al at the 12th AEC Air Cleaning Conference⁵. Several tests were run to determine the samplers ability to differentiate iodine species at <100% R.H. In these tests, he found that the ability to differentiate species was good. Retention efficiencies for organic iodine were >99%, for HOI >80%, and for elemental iodine >90%. Again it was noted that there was little if any retention (<3%) of methyl iodide on the CDI and IPH adsorbents.

Kabat has tested two of the components (IPH & AGX) of the sampler for HOI retention⁷. The tests were at "room humidity" (55±5% relative humidity), iodine loadings of ~10⁻³ µg/m³, a residence time of 0.14 sec for a 30mm bed, and at ambient temperatures. His results indicate that the 5 weight % 4-Iodophenol-Alumina (30-60 mesh) supplied by Keller exhibited 20-40% breakthrough. The AGX tests showed a ~2% breakthrough of HOI at 50% relative humidity and room temperature and a 30% breakthrough of HOI at 100% R.H. The results do not seem to be consistent with other reported data⁸.

The sampler has been used to measure the iodine species in the delay line of a BWR⁵. It has also been used to measure iodine species for the USAEC Regulatory Operations program of independent measurements of radioactivity in BWR ventilation effluents⁹ and by Reid in his work on removal of iodine by hydrazine sprays in containment¹⁰. The nuclear power divisions of both Westinghouse and General Electric have used the iodine species sampler. Performance data for the sampler, however is somewhat limited. The sampler was tested for use in experiments related to post accident radioiodine air concentrations. Post accident concentrations of radioiodine are significantly higher than the ventilation air concentrations found at nuclear power plants for which the sampler has been primarily used. The temperature and relative humidity conditions are also significantly different. Limited additional data has been presented^{5,7} at conditions closer to plant air conditions. However, it is not complete and some information is contradictory. Further testing of this sampler under normal plant air conditions was required.

III. Test System for the Iodine Species Sampler

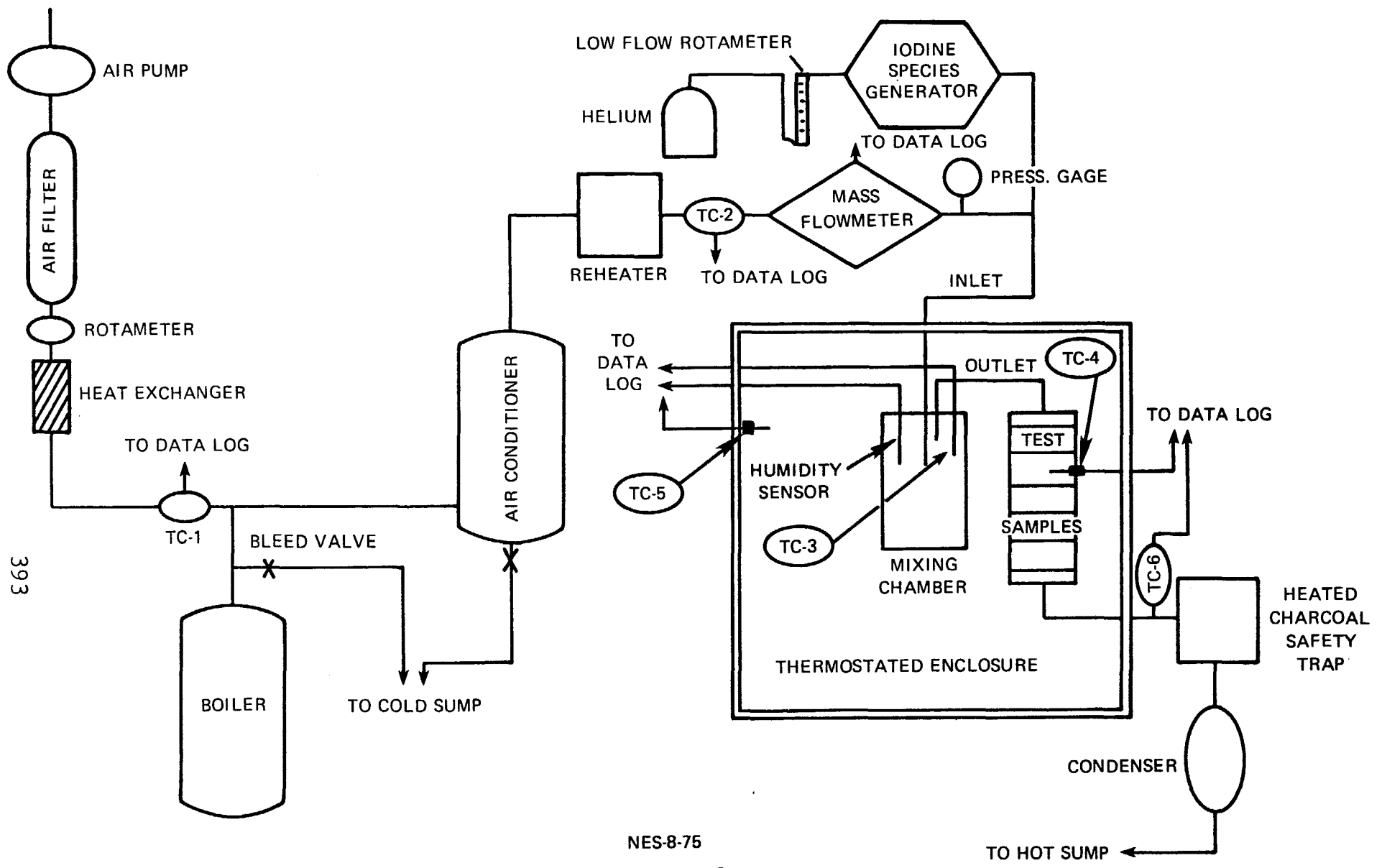
A. Equipment

The test system built for this study is similar to the systems used by Wilhelm¹¹, and by Pence⁸. The system is diagrammed in Figure 1. The inlet air is supplied by a carbon vane air pump. Pressurized supply air is filtered through a HEPA filter, two-2.5-cm beds of impregnated charcoal and another HEPA filter. The inlet air filters were installed based on recommendations in the RDT Standard M-16-1T¹². The air then passes through an aluminum line which can be heated. After this point, water vapor, as required, is supplied by passing the air stream through a pyrex flask containing distilled water. The flask rests in a heating mantle. The air then passes through a pyrex "air conditioner" to adjust the temperature and relative humidity. The temperature of the "air conditioner" is controlled by a refrigerated circulator capable of output temperatures of -20° - +150°C, controlled to ±.05°C. Immediately downstream of the "air conditioner" is a second heater for reheating the air stream. Air then passes through a mass flowmeter where the flow is monitored. Downstream of the mass flowmeter is a pressure gauge. After the pressure gauge, an inlet is provided for the introduction of the different chemical forms of iodine. The iodine species are swept into the test system with a controlled helium purge of the iodine generator solution. Typical flows are 100-400cc He per minute. After the introduction of the iodine specie, the air passes directly into a thermostated enclosure to a stainless steel mixing chamber where the relative humidity and temperature of the air are monitored. The thermostated enclosure is an oven with mechanical air convection and a proportional heat controller. The oven has been modified for cooling by installing coils with circulating coolant. The air then passes through the test beds of media in the sampler. There is provision for monitoring the temperature in a maximum of two beds during a test. The air exits the oven, is reheated, passes through a heated charcoal safety trap, a water-cooled condenser, a vacuum pump and is exhausted to the hood.

The heating stations are individually controlled by variable powerstats. All parts of the air system downstream of the boiler are Type 316 stainless steel or pyrex. A minimum of 1.3cm of insulation is provided for the "air conditioner" and all tubing outside the oven. Data from the tests are logged on a 12-channel digital recorder. During a test, all data are logged at 5 minute intervals or on demand by the operator. The following data points are monitored: Temperatures: room air, inlet air, circulator supply to "air conditioner", downstream of reheater, circulator supply to oven, mixer, test bed #1, test bed #2, oven, backup bed reheater. Outputs from the mass flowmeter and the relative humidity sensor are also monitored.

Two rotameters were used in the system. 0-1.1ℓ/s capacity rotameter was used on the inlet air line and a second of 0-150 sccm air capacity was used to monitor and control the helium purge gas.

SPECIES SAMPLER TEST SYSTEM



NES-8-75
FIGURE 1

393

A. Continued

The main flow monitoring device was a linear mass flowmeter with a range of 0-2.4ℓ/s air. The mass flowmeter was compared against a 0-4.7ℓ/s rotameter and 0-0.5ℓ/s mass flowmeter. In all cases, the output flows agreed within the error of the measurements. The specified accuracy of the mass flowmeter is $\pm 1\%$ of full scale for the output reading and $\pm 2\%$ of full scale for the meter reading with gas temperatures of 0° - 40°C.

Relative humidity measurements were taken with hygrosensors. The output signal of the sensor is converted and monitored. The output of the indicator was recorded by the data logger. Due to the importance of the relative humidity measurements, a check of the calibration of the two wide range sensors was made at the NES lab. The method used for checks was that first reported by Wexler and Hasegawa¹³. The sensors were reported to be accurate to $\pm 1.5\%$ RH. However, extensive recalibrations were required as the first checks indicated errors of $\pm 10\%$ RH at the higher humidities. The recalibrations were made using carefully thermostated salt solutions. The low range sensor has an operation range of 40°F and $\sim 5-45\%$ relative humidity. This sensor was calibrated for three relative humidities at seven temperatures. The high sensor has an operating range of 40° to 140°F and $\sim 30\%$ to 95% relative humidity. The high range sensor was calibrated for five relative humidities at seven temperatures. The accuracy is based on the error stated by Wexler of $\pm 1\%$ R.H. control of the saturated salt solutions and our measurement errors as determined by the deviation of the fitted curves from the measurement points. This latter error ranged from 0.07 to 4.1% relative humidity. Table 1 gives the estimates of error of the relative humidity measurements taken during the tests:

TABLE 1

<u>Temperature</u>	<u>Measured % R.H.</u>	<u>Estimated Error</u>
60°F	20%	$\pm 1\%$ RH
60°F	90%	$\pm 2\%$ RH
110°F	10%	$\pm 1\%$ RH
110°F	83%	$\pm 4\%$ RH

IV. General Description of Sampler

The in plant species sampler consists of five cups in series in an aluminum holder. The cups are machined from aluminum tubing and are 6.3 cm ID and 3.5 cm deep and have a 3-mm thick wall. An O-ring groove is machined at the inlet of each cup. The normal order of the cups as the sample gas sequentially passes through them is as follows: PF-particulate filter, CDI-cadmium iodide media for I₂ retention, IPH-4-iodophenol on alumina for HOI retention, AGX- or BC-151 charcoal-silver loaded zeolite or KI impregnated charcoal for organic iodine retention, and CH-BC-151 charcoal for a breakthrough monitor. The PF cup contains two F-700 filters, sealed by teflon washers and stainless steel snaprings. The filters are recessed 7mm

IV Continued

in the cup to allow for a plenum. The cups of media (IPH, CDI, and AGX) are loaded using paper filter on the front and a screen on the back to hold the material in place, retained by stainless steel snap rings. Each medium is loaded by weight and then packed lightly to give a 2.5-cm depth. To assemble the sampler, the cups, with o-rings are stacked in required sequence and placed in a 7.5 cm OD aluminum sleeve. The ends are attached by three long bolts passing outside the sleeve. The inlet and outlet on the sampler are stainless steel 0.95-cm tubing fittings.

V. Laboratory Tests

1.0 General Comments

1.1 Inlet Iodine Concentrations

Nominal total iodine concentrations in reactor building ventilation air have been estimated¹ at approximately $4 \times 10^{-4} \mu\text{gI}/\text{m}^3$. This value represents the fission produced iodine isotopes 127, 129, and 131. In addition, assumptions are made regarding decay and hold up time for fission product iodine in the fuel such that the weight ratio of Total Fission Product Iodine/ $^{131}\text{I} \approx 10$ at the sampling point. Selection of the test iodine concentrations was made using the ratio of $\frac{\text{Total I}}{^{131}\text{I}} \approx 10$, and the typical range of ^{131}I concentrations found at nuclear power plants. The typical range is 10^{-7} to $10^{-12} \mu\text{Ci } ^{131}\text{I}/\text{cc}$ which translates into approximately 10^{-5} to $10^{-10} \mu\text{g total I}/\text{m}^3$. Sufficient tracer was used to allow an accurate ($\pm 10\%$ or better) measurement of a few per cent penetration of iodine specie through a test bed. In general, the test inlet concentration was $\sim 10^{-5}$ to $10^{-7} \mu\text{g total I}/\text{m}^3$. The effect of ambient iodine (10^{-2} - $10^{-3} \mu\text{g total iodine}/\text{m}^3$) in plant exhaust is not considered. Any exchange of ambient iodine with the chemical species of iodine in the plant air would increase the individual species concentration. This would result in the same or higher specie retention by the specific media. The only ambient iodine in the tests is that which passed the two inches of charcoal adsorbent at the inlet to the test apparatus.

1.2 Iodine Tracer

^{131}I The tracer used for all the tests was high specific activity ^{131}I from Union Carbide in Tuxedo, New York. The iodine tracer contains typically 20-25 atom percent ^{131}I (Cat. #1-131-P-2). The inlet concentration was calculated using the total iodine collected on the sampler beds (correcting the specific activity for decay from the tracer calibration date to sample count time) and dividing this total iodine value by the total flow during the generation period.

1.3 Relative Humidity

The relative humidity was monitored at 5 minute intervals throughout each test. The stated % R.H. is a numerical average of the observed values during a test. Typical ranges of humidity were from 1% R.H. to 3% R.H.

1.4 Temperature

The temperature was also monitored at 5 minute intervals during a test. The typical range of temperature was 1°F .

1.5 Species Generation

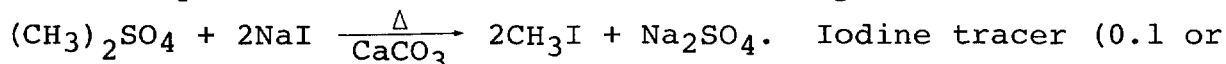
As had been observed by other workers^{5, 6, 7}, pure species of HOI could not be generated at the low iodine concentrations used in these tests. The purity of HOI generated was $\sim 30 - 70\%$ with the majority of the remaining species being organic iodide. A similar difficulty was experienced with the generation of elemental iodine. I_2 was generated with purities of $\sim 30\% - 80\%$ and organic iodides the bulk of the balance. A potential source of the problem was the small amount of epoxy resin used to seal the lid of the mixing chamber.

1.5 continued

There were no problems with the generation of methyl iodide. The CH_3I yields were high (20-80%) and the purity of the specie was greater than 99%. All species generation times were ~ 1 hour followed by two hour purge at the test condition.

1.5.1 Methyl Iodide Generation

The procedure was based on the commonly used reaction:



0.5ml) in 0.05N NaOH was fed into \sim seven milliliters of water containing three milliliters of dimethyl sulfate and ~ 100 mg calcium carbonate. The solution was purged by helium passing through a bubbler tip at a flow of 200-400cc helium per minute. A hot air stream, from a heat gun, was intermittently directed at the flask base to keep the solution hot, but not boiling.

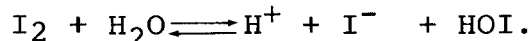
1.5.2 Elemental Iodine Generation

The chemical reaction used to generate I_2 was one which is commonly accepted. The reaction is as follows:

$\text{IO}_3^- + 5\text{I}^- + 6\text{H}^+ \rightleftharpoons 3\text{I}_2 + 3\text{H}_2\text{O}$. Iodine tracer (0.1 or 0.5ml) was added to 1ml of 0.05N NaOH in a dropping funnel mounted on top of a reaction flask containing a 10ml solution of 50mg NaIO_3 in 2N H_2SO_4 . The I_2 produced in the reaction was swept from the solution by a 200cc/min flow of helium into the test system.

1.5.3 Hypoiodous Acid Generation

The procedure for HOI was based upon passing I_2 through a solution with a pH of 12. The reaction is:



The I_2 generation method described in V.B.1.5.2 was used. The I_2 in the helium gas stream was passed through a glass frit diffuser in a gas washing tower containing ~ 200 ml of 0.01N NaOH. The gas stream then passed into the test system.

1.6 Residence Times

The residence time calculations are based on the internal diameter of the test cartridge, the depth of the media, and the volumetric flow per unit time through the cartridge. The times are expressed in seconds as calculated from the expression

$$\frac{\text{Volume of Media}}{\text{Volumetric flow per second}} = \text{seconds R.T.}$$

1.7 ^{131}I Analysis System

All samples from the lab tests as well as the in-plant tests were counted on one of two gamma pulse height analysis systems. Both systems have computer controlled pulse height analyzers coupled with germanium gamma-ray detectors. The systems are calibrated using NBS standards. Each detector has a lucite structure for precise positioning of samples. Complete details of the systems, their calibrations, and procedures for use have been reported¹⁴.

1.8 Efficiency Determinations

If a pure specie of radioiodine is generated, the efficiency of a media for that specie can easily be determined. The method is to measure the activity which penetrated the test media. This is accomplished by placing a total radioiodine adsorber behind test media. This was done in the methyl iodide tests on the AGX/CH media using impregnated charcoal as the total iodine adsorber. When a mixture of species are generated, as in the I₂ - CDI and HOI - IPH tests, this method cannot be used. An alternate method is the dual bed technique. This technique requires that of the species presented to the test bed, only one is retained with any significant efficiency. When this condition is met, two beds of the same media may be placed in series. The activity found on the second bed is a measure of the efficiency of the media for that specie.

In all tests, the assumption is made that the second bed has the same specie efficiency as the first bed. An extrapolation of the efficiency through successive theoretical beds was made for each test to calculate the total penetration of the first test bed. The following equation was used for all the tests to calculate the media efficiency:

$$\left(1 - \frac{\mu\text{Ci Bed B}}{\mu\text{Ci Bed A}} \right) \times 100 = \% \text{ Efficiency.}$$

2.0 Organic Iodide Adsorber Tests

The tests for the retention of CH₃I on AGX in humid atmospheres and on CH (KI loaded charcoal) for dry atmospheres are presented in Table 2. A full species sampler consisting of a particulate filter, elemental iodine adsorbent, non-elemental inorganic iodine adsorbent, an organic iodide adsorbent, and a charcoal backup bed was used in these tests. The tests consisted of an approximate one hour generation of the methyl iodide followed by a two hour purge, all at the individual test conditions.

The tests show that less than 0.03% of CH₃I is retained on any of the media ahead of the organic iodide adsorber in the species sampler. The two tests with detectable radioiodine on the CDI beds had more elemental iodine generated than normal. The activity on these beds most likely is I₂ and not CH₃I. The lowest efficiencies were observed in tests with high humidities and AGX. The samples from the three tests where a few percent penetration occurred were rechecked. No explanation other than normal penetration could be found. The two high temperature - high humidity tests have results reversed from what one would expect. At the shorter residence time, the AGX has less penetration. The test with (~3% penetration) did experience a condition where the humidity sensor was pegged for ~25 minutes. It is highly possible that condensation may have occurred in the bed. Excluding the one test, the efficiency of AGX for methyl iodide under these test conditions is 99-100%.

3.0 Elemental Iodine Tests

Test results for the retention of elemental radioiodine on CDI media are presented in Table 3. The sequence of the test beds was as follows: CDI bed "A", CDI bed "B", IPH, and CH.

Table 2
AGX/CH Media
Methyl Iodide Tests

<u>TEMP.</u> <u>°F</u>	<u>% R.H.</u>	<u>RES. T.</u> <u>(sec)</u>	<u>INLET</u> <u>µgI/m³</u>	<u>PER CENT RETENTION OF I-131 ON TEST MEDIA</u>					
				<u>PF</u>	<u>CDI</u>	<u>IPH</u>	<u>AGX</u> <u>or CH</u>	<u>CH</u>	<u>% Effi.</u>
86	50	0.16	3.4 (-5)	<.01	<.01	<.01	>99.99	<.01	>99.99
60	22	0.16	6.4 (-6)	<.01	<.01	<.01	>99.99	<.01	>99.99
60	26	0.08	3.0 (-6)	<.01	<.01	<.01	99.95	.05	99.95
60	90	0.16	2.2 (-5)	<.01	<.01	<.01	99.94*	.06	99.94
60	90	0.08	9.1 (-6)	<.01	<.01	<.01	98.79*	1.22	98.77
110	10	0.16	2.9 (-5)	<.01	.02	<.01	99.98	<.01	>99.99
110	16	0.08	9.8 (-6)	<.01	.02	<.01	99.98	<.01	>99.98
110	83	0.16	2.4 (-5)	<.01	<.01	<.01	97.08*	2.92	96.99
110	81	0.08	1.9 (-6)	<.02	<.02	<.02	99.22*	.78	99.21

* - AGX media

Table 3
CDI Test Data

<u>Temp. °F</u>	<u>% R.H.</u>	<u>Res. Time (sec.)</u>	<u>Inlet μgI/m³</u>	<u>% Efficiency</u>
61	37	0.082	1.3(-6)	88.4
60	25	0.167	1.1(-5)	91.1
61	90	0.082	1.7(-6)	78.2
60	90	0.168	1.1(-8)	90.1
60	90	0.168	1.7(-5)	84.0
111	10	0.083	1.0(-6)	85.5
111	9	0.167	4.0(-6)	92.6
110	82	0.082	9.9(-7)	85.8
110	82	0.169	1.9(-6)	90.4

The CDI data has been corrected for HOI retention ($3.9 \pm 1.4\%$ of HOI in air stream). In all cases except one the correction resulted in an increase of $<1\%$ in the efficiency. The one case resulted in a correction of $+3\%$.

The average efficiency is $87.3 \pm 4.5\%$ within the range of conditions used for testing. There appears to be a correlation between residence time and the efficiency for radioiodine. At a flow rate of 0.9 l/s (0.08 sec. R.T.) the retention efficiencies are $\sim 84 \pm 4\%$. At 0.5 l/s the efficiencies are $90 \pm 3\%$. While these two groups of data are not mutually exclusive, there is a trend. It is logically consistent that for reaction times on the same order as the residence time the shorter the contact period for adsorption/reaction, the lower the retention.

4.0 Hypoiodous Acid Tests

The tests for the retention of HOI on the IPH media are presented in Table 4. The sequence of the test beds was as follows: CDI bed "A", CDI bed "B", IPH bed "A", IPH bed "B", CH. The two CDI beds were used to remove the elemental iodine present in the inlet stream.

4.0 continued

Table 4
IPH Test Data

<u>Temp. °F</u>	<u>% R.H.</u>	<u>Res. Time (sec)</u>	<u>Inlet₃ µgI/m³</u>	<u>% Efficiency</u>
60	21	0.092	5.8(-6)	98.9
60	20	0.155	1.3(-5)	94.1
60	90	0.080	8.2(-6)	80.5*
61	90	0.140	2.4(-5)	96.9
60	90	0.164	1.5(-5)	91.1*
110	11	0.117	1.8(-5)	93.4
109	10	0.155	1.0(-5)	95.6
111	50	0.111	9.4(-6)	98.3
110	83	0.081	9.2(-6)	30.1
109	82	0.052	4.1(-7)	78.3*
110	82	0.149	8.4(-6)	81.1*
112	78	0.147	5.3(-5)	99.2

*Tests run with bad batch of IPH

At the longer residence times of >0.1 sec, the efficiency of IPH for HOI is 94±4% using all data points. The test which gave 30.1% efficiency experienced condensation in the test beds. The relative humidity sensor was operating at its response limit and we exceeded not only 83% R.H. but 100% R.H. and condensation occurred. The bad batch of IPH was not detected until tests with high temperature and low humidity were run. Since previous tests had been run under the same conditions with radically better results (~95% versus 37% efficiency), obviously something had failed. Several things were checked. When a new batch of IPH was prepared and tested the efficiencies did return to ~95%. Upon further checking, it was learned that during the preparation of the suspect batch, a dark brown third phase formed when the 4-iodophenol was dissolved in the ligroin. A modification in the procedure remedied this problem.

4.1 Activity Profiles of Selected IPH Tests

In the last four IPH tests, the IPH test beds were removed in sections to determine their activity profiles. Each fraction of the first IPH bed contained within ~10% the same amount of material and were well mixed before counting.

14th ERDA AIR CLEANING CONFERENCE

4.1 Continued

Test 39 - Conditions: 109°F, 10% R.H., 0.155 sec. R.T.,
Efficiency 95.5%, 1 inch deep bed

Section:	<u>Front 1/4</u>	<u>Second 1/4</u>	<u>Third 1/4</u>	<u>Last 1/4</u>
Per Cent Acti- vity of Total Bed:	91.8±2.4	3.5±.6	2.7±.5	2.0±.5

Test 40 - Conditions: 60°F, 20% R.H., 0.155 sec R.T., Efficiency
94.0%, 1 inch deep bed

Section:	<u>Front 1/2</u>	<u>Middle 1/4</u>	<u>Last 1/4</u>
Per Cent Acti- vity of Total Bed:	94.8±2.3	2.0±.3	3.2±.3

Test 41 - Conditions: 60°F, 21% R.H., 0.092 sec R.T., Efficiency
98.9%, 1 inch deep bed

Section:	<u>Front 1/3</u>	<u>Middle 1/3</u>	<u>Last 1/3</u>
Per Cent Acti- vity of Total Bed:	92.3±1.3	6.5±.4	1.2±.2

Test 42 - Conditions: 110°F, 83% R.H. (Saturation occurred),
0.097 sec R.T., Efficiency 30.0%, Three IPH beds, each
1 inch deep.

Bed:	<u>A</u>		<u>B</u>		<u>C</u>	
Section:	<u>First 1/2</u>	<u>Last 1/2</u>	<u>First 1/2</u>	<u>Last 1/2</u>	<u>First 1/2</u>	<u>Last 1/2</u>
% Activity of A+B+C	32.0±1.2	18.9±.9	27.3±1.0	16.5±.8	2.2±.3	3.2±.3

The tests 39, 40, 41 show that more than 90% of the ¹³¹I acti-
vity is on the front one-half inch of the IPH bed. Test 39 had ~92%
of the beds activity on the first 0.75 cm section.

Test 42 is presented to show the activity profile of a special
sampler with three IPH beds in series which had been exposed to con-
densation. It is interesting that even under poor conditions, the
retention of the HOI appears complete in three 2.5 cm thick beds.

4.2 Effect of 4-Iodophenol loading on IPH media

Before the tests were begun, it was suggested that five weight
percent 4-iodophenol on alumina may work as well as ten weight per-
cent. If this were true, the cost of the media would be reduced by
1/3. A series of tests were run to determine if any difference
existed. In the tests, two identical samplers, with identical ma-
terials were run. One sampler contained beds of 5 w/o IPH media and
the other had 10 w/o IPH media.

In two of the tests (60°F - 90% R.H., and 110°F, 50% R.H.),
the two samplers were run at the same time, each using one half of
the total flow. In these two tests, the residence time is calcula-
ted from the total flow and the proportion of the activity retained
by each sampler. The results are presented in Table 5.

Table 5
Impregnant Effect on IPH Media

<u>T °F</u>	<u>% R.H.</u>	<u>R.T. sec</u>	<u>Inlet μgI/m³</u>	<u>% Eff.</u>	<u>Note</u>
63	88	0.21	2.0(-5)	89.8	5 w/o MCB
61	90	0.140	2.4(-5)	96.9	10 w/o MCB
60	90	0.157	1.5(-5)	48.5	5 w/o MCB
60	90	0.164	1.5(-5)	91.1	10 w/o MCB
110	11	0.164	1.8(-5)	90.9	5 w/o MCB
110	11	0.117	2.3(-5)	93.4	10 w/o MCB
110	50	0.105	9.4(-6)	98.2	5 w/o MCB
110	50	0.111	9.4(-6)	98.3	10 w/o MCB
109	78	0.125	4.9(-5)	93.0	5 w/o MCB
110	78	0.147	5.3(-5)	99.2	10 w/o MCB

In every case the 5 w/o IPH had a lower efficiency. There is a significant difference in the efficiency 5 w/o IPH at the combination of lower temperature and high humidity, as indicated by the 48.5% efficiency at 60°F and 90% R.H. This value looks anomalous. Since both the 5 w/o and 10 w/o samples were run simultaneously under the same conditions, it is felt that the value of 48.5% maybe real. While it is possible to use 5 w/o near the high temperature range tested, the 10 w/o is recommended. Based on these results all further tests were made with 10 w/o IPH.

4.3 Effect of Mesh Size on IPH Media

A brief evaluation of the effect of the grain size of the IPH media was made at an operating nuclear power plant. Two samplers were connected to a stainless steel manifold to sample the same vent air. The inlet air concentration was $\sim 10^{-10}$ μCi¹³¹I/cc or $\sim 10^{-8}$ μgI total/m³. The samplers were run for 382 hours, sampling an air stream of 121°F and $\sim 10\%$ R.H. About 162 m³ of air was sampled during the test. The results of the test are presented in Table 6.

Table 6

IPH Mesh Size Comparison

<u>Cup</u>	<u>5 w/o IPH 20-40 mesh (Tyler)</u>	<u>5 w/o IPH 8-14 Mesh (Tyler)</u>	<u>Previous Measurement</u>
	<u>Percent of Total Sampler</u>	<u>Percent of Total Sampler</u>	<u>5 w/o - 20-40 Mesh Percent of Total</u>
PF	29.5	19.1	27
IPH-A	63.8	34.5	66 (47% I ₂ + 19% HOI)
IPH-B	<2%	3.7	--
CH-A	6.7%	42.7	7
CH-B	<2%	<3%	<3%
Residence Time	~0.11	~0.19	0.12 est.

The 20-40 mesh IPH results agree well with a previous 170 hr species sampler that was taken in the same location. The data show a significant fraction of the I₂ and HOI breakthrough the large mesh IPH. They are collected on the first charcoal bed along with the organic iodide fraction. The results clearly show that 8-14 mesh IPH is inferior to 20-40 mesh IPH.

4.4 Change in IPH Efficiencies by Varying the Substrate

The procedures for preparing IPH media call for "activated alumina" as the base material for the 4-iodophenol. No type of alumina was specified. For the early tests in this study, activated alumina (Cat. #AG612-1) supplied by Matheson Coleman and Bell was used. After the AGX/CH tests, it was learned that MCB no longer supplied the AX612 alumina. An alternate source was found at Fisher Scientific. Their activated alumina, Cat. #A541, in 8-14 mesh, was ground and sieved to 20-40 mesh and used in the first IPH tests. The results of the tests are in Table 7.

Table 7

HOI Efficiencies of IPH Media Based on Fisher A541 Alumina

<u>T °F</u>	<u>% R.H.</u>	<u>R.T. (sec)</u>	<u>Inlet₃ µgI/m³</u>	<u>% Efficiency</u>
61°	47	0.158	1.6(-5)	93.7
63°	85	0.168	5.6(-6)	<10
111°	9	0.147	4.9(-6)	92.3
110°	82	0.145	2.6(-6)	38%

The high humidity data were surprising. All published information had indicated IPH had better performance at high humidities. The published data gave >80% efficiency at lower humidity. An immediate investigation was begun into the source of the problem. The only change that had been made in the IPH was the source of the alumina. It was learned that two distinctly different types of activated alum-

4.4 continued

ina were involved. The original MCB AX612 was cleaned and sieved from Alcoa type F-1 alumina, a crystalline, highly active material. The Fisher A541 was Alcoa type F-5 activated alumina. Type F-5 is made from type F-1 and has ~ 12 w/o CaCl_2 added to it. A supply of Alcoa type F-1 28-48 mesh activated alumina was secured for use in completing this study. The alumina was sieved as is and the 30-40 mesh fraction used in preparing the IPH media.

4.5 Retention of I_2 on IPH

As could be predicted, elemental iodine is retained on IPH media. Two tests were conducted to verify this. The tests were made by reversing the order of media in one sampler (PF/IPH/CDI/AGX/CH) and comparing the results with a sampler using media in the normal sequence (PF/CDI/IPH/AGX/CH). The sum of the activity on the CDI and IPH beds in the normal sampler should equal the activity on the IPH beds in the second sampler. The data are presented in Table 8. The tests were run under the same conditions $\sim 110^\circ\text{F}$, $\sim 10\%$ R.H. for the same period of time ~ 22 hours. The results clearly show that IPH is a good adsorber for I_2 .

Table 8
 I_2 on IPH

<u>Normal Sampler</u>		<u>Reversed Beds in Sampler</u>	
<u>Component</u>	<u>% Total ^{131}I</u>	<u>Component</u>	<u>% Total ^{131}I</u>
PF + CDI	67.8	PF + IPH	90.2
IPH	23.2	CDI	<1.5
AGX	8.9	AGX	8.7
CH	<1%	CH	<1%

4.6 IPH Reproducibility

A test was designed to determine the performance reproducibility of two different batches of IPH media, Batch #5 and Batch #8. Both batches were prepared using the same materials and the same procedure. The two batches of IPH were loaded into the aluminum cups and the cups loaded into the samplers in the following sequence: CDI/CDI/IPH-A/IPH-B/CH. They were run through the standard one-hour HOI generation and two hour purge. After the purge, the test beds were removed and counted. The IPH-A beds from the two samplers were then placed in new samplers for purging. The new samplers were loaded in this sequence: IPH-A/CDI-P/IPH-P/CH-P. The results are listed in Table 9 and Table 10.

Table 9
IPH Batch Comparison

Conditions: 110°F , 10% R.H., inlet concentration $4.6(-5)\mu\text{gI}/\text{m}^3$,
HOI Purity 72%.

	<u>IPH Batch #5</u>	<u>IPH Batch #8</u>
Residence Time:	0.12 sec	0.23 sec
HOI Retention:	$98.2 \pm 2\%$	$99.2 \pm 3\%$

4.6 continuedTable 10Purge Tests of IPH Batch Comparison

Conditions: Lab air, 6 slm flow rate, 18.5 hr duration, 75^o-80^oF.
20-60% R.H.

<u>Component</u>	<u>IPH Batch #5 Percent of Total</u>	<u>IPH Batch #8 Percent of Total</u>
IPH-A	97.0±2.2	96.1±1.4
CDI-P	<0.2	<0.2
IPH-P	1.6±.2	1.9±.4
CH-P	1.4±.2	2.0±.5
Total Loss	~3%	~4%
<u>Bed Sections</u>		
First 1/3	99.0±3.0	97.5±1.8
Middle 1/3	0.8±.4	1.0±.3
Last 1/3	0.2±.1	1.5±1.4

The two batches compared quite well. The losses of ¹³¹I during the purge, though small, again may be due to the heavy organic iodide from the mixer resin. Losses of ~6% of the activity on the IPH bed were observed for purges of 4 days. It is possible that the losses are due to oxidation of the iodine bound to the 4-iodophenol near the surface of the alumina particle. If this is the case, the rate of loss would diminish as a function of time and would not exceed ~6%.

VI. In Plant Tests

A series of tests were run to compare with laboratory data. Each media (CDI, IPH, AGX), were run for two week periods at operating plants. Two studies were made of the species sampler's stability over 4 to 48 hours. A study of the form of iodine lost during 4 day lab air purges of samplers returned from the field. These studies are detailed below.

1.0 Special Dual Bed In-Plant Break-Through Tests

Special samples were run in 2-3 week tests at two of the plants. One method for verification of sampler media is the dual bed technique. This technique involves placing two cartridges of the same media in sequence in a sampler. It assumes that a chemical form of iodine is retained with the same efficiency by both beds. Therefore, the amount of radioiodine retained on the second bed is considered breakthrough. This method can easily be used with media that have retention efficiencies greater than 75%. We have used it for testing of the CdI₂ and the Iodophenol.

1.1 CDI

Three dual bed tests have been run to date. These are listed below. The results indicate a 10% to 20% loss of radioiodine when CdI₂ is run from 9 to 18 days.

CDI

<u>Test</u>	<u>1</u>	<u>2</u>	<u>3</u>
Run Time	210 hrs.	310 hrs.	432 hrs.
μCi ¹³¹ I/cc	10 ⁻¹⁰	10 ⁻¹²	10 ⁻¹²
Temperature	105°F	120°F	120°F
Rel. Humidity	<10%	<20%	<20%
Residence Time	0.13 sec.	0.1 sec.	0.12 sec.
Breakthrough	9.0%	16.6%	18.6%

1.2 IPH

Again, three dual bed tests were run. The results show essentially no breakthrough for two week exposures.

IPH

<u>Test</u>	<u>1</u>	<u>2</u>	<u>3</u>
Run Time	359 hrs.	358 hrs.	432 hrs.
μCi ¹³¹ I/cc	5 x 10 ⁻⁹	3 x 10 ⁻⁹	2 x 10 ⁻¹⁰
Temperature	105°F	120°F	120°F
Rel. Humidity	<10%	<20%	<20%
Residence Time	0.1 sec.	0.1 sec.	0.1 sec.
Breakthrough	0.3%	0.7%	<1%

14th ERDA AIR CLEANING CONFERENCE

2.0 Study of Sampler Stability Over 48-hour Periods

To study the ability of the sampler to differentiate species over 48-hour periods, two comparison studies were performed. In these measurements, parallel samples were collected simultaneously. One of these was collected continuously for 48 hours and the other was changed every 4 to 24 hours. Comparisons could then be made between the results from the shorter and the longer sampling periods. The results of these measurements are shown below. The uncertainties listed are the two sigma counting error.

2.1 Test #1 - 120°F, <20% Relative Humidity

(% ^{133}I Retained)

Duration of Sampling (Hours)

<u>Media</u>	<u>4.4</u>	<u>15.8</u>	<u>24.1</u>	<u>44.3</u>	<u>Average of 1st 3</u>
PF+CdI ₂	68±7	78±8	83±8	74±7	76±6
IPH	27±3	19±4	12±3	22±4	19±3
AgX	4±1	4±1	5±1	4±1	4.3±1.0

2.2 Test #2 - 100°F, <40% Relative Humidity

(% ^{131}I Retained)

Duration of Sampling (Hours)

<u>Media</u>	<u>13</u>	<u>11.3</u>	<u>13</u>	<u>13.3</u>	<u>51.2</u>	<u>Avg. of 1st 4</u>
PF+CdI ₂	66±6	63±6	63±6	69±7	60±6	65±6
IPH	27±3	29±3	28±3	23±3	31±3	27±3
AgX	8±1	8±1	9±1	8±1	9±1	8.3±1.0

The data indicate that under the conditions of these tests there is no evidence of any change in the performance of the species sampler during the span from 4 to 48 hours.

3.0 Loss of Iodine From Species Components During Purging

Tests were made to evaluate the losses from each component of the species sampler from a continuous flow of air through the media after the activity had been deposited. These measurements were made in such a way so as to determine also the species form of the activity being removed from each media. Samples collected in the plants were purged with air containing no radioiodine in two experiments. The first of these used normal air containing normal concentrations of stable iodine. The second used air filtered through charcoal used to remove the iodine from the air. In the experiments, the initial species sampler was disassembled and each component was used as the front section of a new species sampler. Following the purge, each component was analyzed for activity. The results are described as follows.

14th ERDA AIR CLEANING CONFERENCE

3.1 Test 1

Unfiltered Air

Length of Purge: 94 hours
 Temperature: 73±2°F
 Relative Humidity: 60±15%

	<u>Original Cartridge</u>			
	<u>PF</u>	<u>CdI₂</u>	<u>IPH</u>	<u>AgX</u>
% Loss from each Component	63.8%	5.4%	6.2%	3.2%
<u>Form</u>				
Particulate	5.9%	3.4%	<.1%	<0.3%
I ₂	85.9%	73.8%	2.3%	<0.3%
HOI	6.1%	22.8%	54.6%	<0.3%
Organic	2.1%	<.1%	43.1%	>99%

PF

The results indicate a significant loss of iodine from the particulate filter. The chemical form was primarily elemental. The small (6%) amount of ¹³¹I collected on the 2nd PF is possibly due to adsorption of I₂ as it passed through.

CdI₂

Approximately 5% of the ¹³¹I retained on the CdI₂ was lost over the 4 day period. Once again a small fraction (~4%) of the ¹³¹I was retained on the PF. Again this is possibly due to elemental iodine adsorption. The loss from the CdI₂ was mostly elemental (75%) and the balance HOI.

IPH

The loss from the IPH cartridge was ~6% of the total and was mostly HOI (55%) and Organic (43%). A small amount (~2%) of elemental was observed.

AgX

Organic iodine was the only form lost that could be detected. The amount lost was ~3%.

Filtered Air

Length of Purge: 94 hours
 Temperature: 75±3°F
 Relative Humidity: 70±20%

14th ERDA AIR CLEANING CONFERENCE

3.1 Continued

	<u>Original Cartridge</u>			
	<u>PF</u>	<u>CdI₂</u>	<u>IPH</u>	<u>AgX</u>
%Loss from each Component	7%	<1%	~2%	~3%
<u>Form</u>				
Particulate	38%	--	<0.4%	<1%
I ₂	57%	--	<0.4%	<0.4%
HOI	<1%	--	<0.4%	<0.4%
Organic	5%	--	>99%	>99%

In contrast with the previous test, little radioiodine was removed from any of the species components. The particulate filter lost ~3% of the second count. The loss was ~1/3 "particulate" (probably elemental) and ~2/3 elemental. No detectable (<1%) ¹³¹I was lost from the CdI₂ cartridge. In the previous test, ~5% of the ¹³¹I was lost as I₂ and HOI. On the IPH Cartridge, ~2% of the ¹³¹I was lost as organic iodide. The Agx cartridge lost ~3% of its ¹³¹I as organic iodide. Previous losses were also ~3%.

3.2 Test 2

Unfiltered Air

Length of Purge: 76 hours
 Temperature: 75±3°F
 Relative Humidity: 60±15%

	<u>Original Cartridge</u>			
	<u>PF</u>	<u>CdI₂</u>	<u>IPH</u>	<u>Char</u>
% Loss from each Component	11.8%	2.5%	1.1%	<1%
<u>Form</u>				
Particulate	17%	<1	<1	-
I ₂	78%	100%	<1	-
HOI	5%	<1	45%	-
Organic	<1%	<1	50%	-

In this test, very little was lost from any of the components. That which was purged off, behaved very much as in Test 1, with the principal losses occurring to the particulate filter, the iodine purging off as elemental iodine. However, the loss from the filter with the unfiltered air purge was less than 1/5 that in test 1.

3.3 Speculation on Nature of the Losses in Purging.

Loss of radioiodine from the sampler components may be caused by one or more of three mechanisms. One is oxidation of the adsorbed iodine to I_2 or even to HOI when water vapor is present. Another is exchange, where an atom of stable iodine replaces a radioactive iodine atom. The last is revolatilization of the adsorbed iodine in its original chemical form.

The TEDA charcoal used for the filtered air test would remove the ambient iodine, ozone and other strong oxidants and most of the organic vapors in the lab air.

Oxidation of the particulate iodine to I_2 or exchanges with ambient iodine may be the major loss mechanism for the PF cartridge. When the air was filtered the amount of radioiodine lost from the PF in test 1, dropped by a factor of ~ 9 . Oxidation or exchange may also be the primary cause of the radioiodine loss from the CDI cartridge. Test 2 seems to indicate a different type of particulate iodine. The small amount of iodine listed as I_2 lost from the IPH may be HOI retained on the elemental iodine adsorber. The loss of HOI from the IPH can possibly be explained as revolatilization or simple exchange. The organic iodine loss from the IPH may likely be due to the formation of these iodides in the IPH media. This can be supported by the observation that $\sim 3\%$ of the total radioiodine on the IPH was lost as organic iodine in both tests. We can offer no reasonable explanation for the loss of radioiodine from the AGX cartridge. It is possible that some unreacted organic iodide has slowly been purged from the cartridge.

4.0 Comparison of In-Plant and Lab Tests

In-plant efficiencies are determined from the dual bed tests.

CDI Media

	<u>Inlet $\mu\text{gl}/\text{m}^3$</u>	<u>Temp. °F</u>	<u>%R.H.</u>	<u>R.T. (sec)</u>	<u>R.T. (hr.)</u>	<u>%Eff.</u>
In Plant	10^{-8} - 10^{-10} est.	105-120	<20	0.1-0.13	200-400	82%-91%
Lab	~ 2 (-6)	111	10	0.08-0.17	3	86%-93%

IPH Media

	<u>Inlet $\mu\text{gl}/\text{m}^3$</u>	<u>Temp. °F</u>	<u>%R.H.</u>	<u>R.T. (sec)</u>	<u>R.T. (hr.)</u>	<u>%Eff.</u>
In Plant	10^{-7} - 10^{-8}	105-120	<20	0.1	360-430	>99
Lab	~ 2 (-5)	110	10	0.1-0.16	3	93-96%

AGX Media

	<u>Inlet $\mu\text{gl}/\text{m}^3$</u>	<u>Temp. °F</u>	<u>%R.H.</u>	<u>R.T. (sec)</u>	<u>R.T. (hr.)</u>	<u>%Eff.</u>
In Plant	$\sim 10^{-7}$	~ 100	<20	0.16	210	99.4%
Lab	~ 2 (-5)	110	10-16	0.08-0.16	3	99.9%

4.0 Continued

In all cases the in-plant tests agreed well with the lab tests. Before the IPH tests were run, it was suspected that the 4-iodophenol impregnant might be slowly volatilized from the media under hot dry conditions. This is shown not to be a problem. If significant amount of 4-iodophenol were lost, the species fractions at this same condition would appear different between samples taken for 12 hours, 48 hours, and 400 hours. We have found this not to be the case.

VII. Comparison of Results With Other Investigators

The data from this study compare favorably, with one exception, with the work by Keller, et.al. described in Section II of this work, the one exception is the CDI. His reported efficiency for I₂ by CDI is >90%. The CDI efficiency, under the conditions we tested, is ~85%. At the concentration levels of the tests, we never obtained a CDI efficiency of greater than 93%. Attempts were made to determine the reason for the lower efficiency. No cause was found. Even with the ~84% efficiency of CDI for I₂, this sampler will give the required data for Phase II of the program.

The IPH results of this study while comparing well with Keller's data, do not compare well with the more recent information released by Kabat¹⁵. It was reported that the "Chemical reaction of HOI with the presently used impregnanta (including 4-Iodophenol) is slow". "Slow" is a relative term. Based upon our limited profile work, and at the flow rates tested, the IPH media retained >90% of the HOI on the first one-third of the one inch bed. Whatever reaction occurred, did so in ~30 milliseconds. This is fast relative to the residence time in the bed. Certainly fast enough a reaction to be able to determine the HOI component in an air stream of radio-iodine. Also, it was stated by Kabat that "4-Iodophenol impregnated alumina has a low efficiency for HOI adsorption when several hours sampling time is applied at low humidity conditions (<50% R.H.)". We find high HOI efficiencies (~94%) for IPH at ~10% R.H. for periods of 2, 6, 11, 48, and up to 432 hours. Furthermore Kabat has stated that "Adsorption of HOI on both 4-Iodophenol impregnated and non-impregnated alumina is negligible at 70% RH when sampling time exceeds 2 hours". Since non-impregnated alumina has not been tested for this study, no comment on its HOI efficiency can be made. However, the test data reported above at 90°F and 70% R.H. show an efficiency of ~95%. We have no explanations for the differences in results. No experimental data or detailed test procedures were reported by Kabat.

VIII. Summary and Conclusions

A. Use of the Iodine Species Sampler

The lab test ranges of temperature (60° - 110°F) and humidity (10% - 90% R.H.) cover the anticipated sampling points fairly well. Two exceptions exist. First, some temperatures have run as high as 140°F inside of a turbine building. It is felt that this will not be a problem. Results reported above show adequate sampler performance for periods up to 18 days at 120°F. Secondly, relative humidity of ~100% occurs at sampling points such as a gland-seal exhaust line. If possible, a sampler should be placed in a sampling line after the relatively small flow of the high humidity duct is mixed with a large air flow of lower relative humidity. If this is not possible the sampler and inlet lines should be heated to reduce the relative humidity to 80%-90%. This technique of heating the sampler has been used successfully at plants. The recommended use parameters for the present sampler are given in

A. Continued

Table 11. The media efficiencies for the species are given in Table 12.

Table 11

Recommended Use Parameters
For the Radioiodine Species Sampler

Temperature:	60° - 140°F
Relative Humidity:	10% - 90%
Residence Time:	0.1 - 0.17 sec
Air Sample Flow Rate:	0.47-0.80 l/s

Table 12

Media Efficiencies

<u>Species</u>	<u>CDI</u>	<u>IPH</u>	<u>AGX/CH</u>
I ₂	84±4%*	>98%	99±1%
HOI	~4%	94±4%	99±1%
CH ₃ I	<.02%	<.02%	99±1%

* If the sampler is run at a residence time >0.17 sec the efficiency for I₂ collection on CDI would be 90±3%.

The results presented in Tables 11 and 12 show the sampler can be used in typical nuclear power plants to monitor the total gaseous releases of radioiodine. The use parameters do not rule out the sampler performing well outside these limits. They merely define the limit of adequate performance as defined by the testing.

B. Conclusions

Based upon the test results, the following conclusions are offered.

1.0 Radioiodine Species Sampler for Effluent Measurements

1) The radioiodine species sampler tested in this program will differentiate the known chemical forms of radioiodine in gaseous effluents for sampling periods of at least two weeks and for relative humidities up to 90% and temperatures of at least 120°F. A residence time of 0.1 second gives satisfactory differentiation.

2) There is no indication of imminent failure of the sampler to differentiate species at more severe conditions than those used in our testing. Based on our tests and those of others, relative humidity appears to be the most critical parameter.

14th ERDA AIR CLEANING CONFERENCE

3) Until such time as tests can be made which show the limits at which the sampler will fail to differentiate, it would be prudent to heat the incoming air and the sampler when used to sample streams with relative humidities greater than 90%. Heating will reduce the relative humidity. Examples of gas streams with very high related humidities are off-gas, gland seal exhaust and steam generator blow down vents.

B. RADIOIODINE REMOVAL EFFICIENCIES OF
CHARCOAL ADSORBERS FOR VENTILATION EXHAUST AIR*I. Introduction

On May 28, 1975, a sampling program was initiated at the Ginna nuclear power station to measure the radioiodine removal efficiencies of two charcoal adsorbers over an extended time period. Two installations were evaluated. One consists of 665 liters of charcoal in 32 trays each having dimensions of 72.4 cm. by 56.5 cm. and 5.1 cm. in depth. The installation which has no HEPA filters carries 1.33×10^5 liters/min. (4700 cfm), and the residence time of air in the charcoal is 0.3 seconds.

The other installation carries about 7.08×10^5 liters/min. (25,000 cfm) and has 3750 liters of charcoal in 168 trays each having dimensions of 67.3 cm. by 62.2 cm. and 5.1 cm. in depth. The installation contains HEPA filters in series before the charcoal adsorbers. The residence time of air in the charcoal is also 0.3 seconds.

The charcoal adsorbers in the small filter are changed periodically due to high pressure drop. They were replaced on June 6, 1975, which is at the beginning of the sampling program. The HEPA filters in the large installation are changed periodically due to high pressure drop, but the charcoal has not been changed since the filter was installed in June 1973.

Methods

Figure 2 shows the layout of two installations and the 6 sampling points used. Single tipped probes were used for sampling. To assure representativeness of sampling, a helium tracer was introduced at a known rate upstream of the sampling point and if the airflow rate in the duct computed from the measured helium concentration and the known release rate was the same as that measured by conventional techniques, using the standard pitot tube, the sampler was assumed to be taking a representative sample.

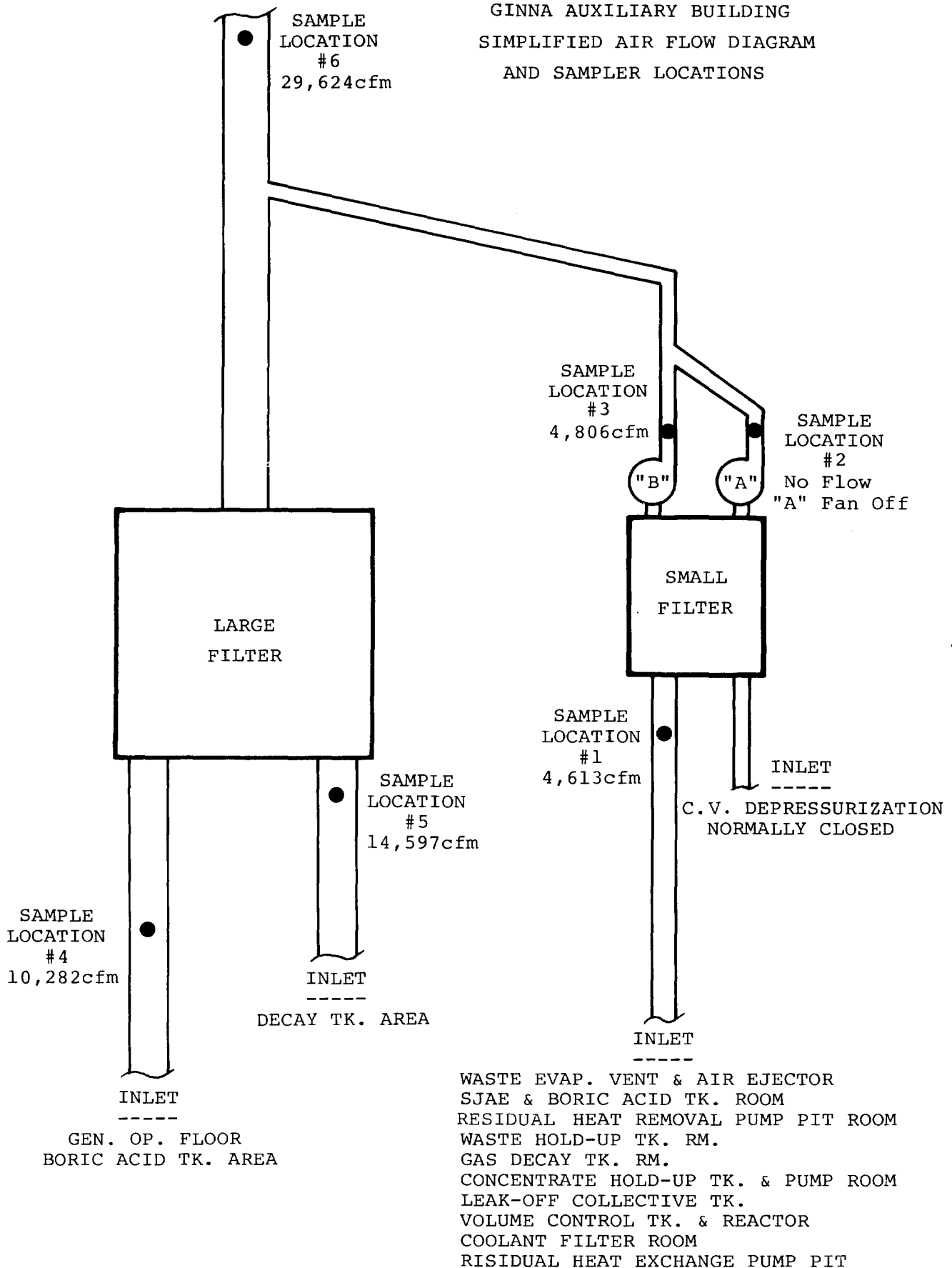
From May 28 to October 2, 1975, the sampling train consisted of a particulate filter (Flanders 700) followed by two charcoal adsorbers in series. A constriction was put in the line behind the charcoal and particulate filters and a small flow was bypassed through a 400 gram silica gel tower to measure tritium in the airstream. Nominal flow rates through the particulate and charcoal filters and the silica gel were 42.5 liters/min. (1.5 cfm) and .056 liters/min. (0.002 cfm) respectively. The second charcoal adsorber in the sampler was used for the purpose of measuring breakthrough of the first adsorber. Seldom was more than 1% of the iodine-131 found on the second adsorber. A layer of tell-tale silica gel was employed

*This work is supported by the Electric Power Research Institute under contract RP274-1.

14th ERDA AIR CLEANING CONFERENCE

FIGURE 2

GINNA AUXILIARY BUILDING
SIMPLIFIED AIR FLOW DIAGRAM
AND SAMPLER LOCATIONS



at the exit end of the silica gel tower to measure column saturation. This was never observed with any of the samplers.

On October 2, 1975, the particulate filter and total iodine sampler was replaced with the species sampler described in section A above. With the exception of two sampling periods from 11/25 to 12/29, species measurements were made until March 24, 1976. The reason for discontinuing species sampling in favor of total iodine sampling was the fact that we experienced difficulties with the IPH adsorber media. When the cause was found and rectified species sampling was resumed.

Iodine-131 was measured using a 4096 channel Ge(Li) spectrometer. Tritium was measured with a liquid scintillation detector. The average sampling duration ranged from 13 days to 25 days and averaged 17 days. Each measured concentration was corrected for decay from the end of the sampling period to the time of counting. Concentrations were also corrected for the decay during the finite sampling interval.

Decontamination factors for the small and large charcoal filter installations were calculated as follows.

$$\begin{aligned} \text{D.F. (small filter)} &= C_1/C_2 \text{ (or } C_3), \\ \text{D.F. (large filter)} &= (Q_4C_4 + Q_5C_5)/(Q_6C_6 - Q_2C_2 \text{ or } 3), \end{aligned}$$

where C's are the concentrations and
Q's are the flow rates in ducts.

The subscripts refer to the sampling locations shown in figure 1.

Results

Table 13 shows results of the measurements of total iodine-131 and tritium.

Table 14 shows the results of the iodine-131 species measurements. In addition to the long duration measurements started on October 2, the results of a set of shorter duration species measurements made from September 3-5, 1975 are included for completeness.

Tables 15 & 16 summarize the calculations of the decontamination factors for the large and small filters respectively. They are listed in order of elapsed time since the charcoal was installed and the corresponding number of air changes experienced by the filters.

Discussion

As shown in Table 14 the results listed are concentrations (release rates) as measured on each adsorber. No corrections have been made for the efficiency of each adsorber for the various species. The reason for this is the uncertainty arising from unknown behavior of iodine-131 on particulate matter. In our other work for EPRI we have observed on one occasion that iodine-131 could be purged off the

14th ERDA AIR CLEANING CONFERENCE

TABLE 13 GINNA AUXILIARY BUILDING
¹³¹I & TRITIUM RELEASES (μCi/sec)

	<u>¹³¹I</u>	<u>³H</u>
<u>7/17/75 - 8/6/75</u>		
#1 Inlet Sm. Filter	7.1±0.4(-4)	1.1±0.2(-1)
#2 "A" Fan Off & Dampers closed - no flow	--	--
#3 "B" Fan Outlet Sm. Filter	3.0±0.8(-6)	1.2±0.2(-1)
#4 Gen. Op. Floor	1.7±0.1(-4)	1.4±0.3(-1)
#5 Decay Tk. Area	3.7±0.2(-4)	1.2±0.2(-1)
#6 Outlet Lg. & Small Filters	5.4±0.3(-5)	4.0±0.8(-1)
<u>8/6/75 - 8/19/75</u>		
#1 Inlet Sm. Filter	7.9±0.4(-5)	1.1±0.2(-1)
#2 "A" Fan Off - No Flow	--	--
#3 "B" Fan Outlet Sm. Filter	1.5±0.3(-6)	1.2±0.2(-1)
#4 Gen. Op. Floor	2.6±0.3(-5)	1.3±0.3(-1)
#5 Decay Tk. Area	8.0±0.4(-5)	1.3±0.3(-1)
#6 Outlet Lg. & Small Filters	1.3±0.1(-5)	3.8±0.8(-1)
<u>8/19/75 - 9/3/75</u>		
#1 Inlet Sm. Filter	2.5±0.3(-4)	1.4±0.3(-1)
#2 "A" Fan Off - No Flow	--	--
#3 "B" Fan Outlet Sm. Filter	1.6±0.3(-6)	1.7±0.3(-1)
#4 Gen. Op. Floor	1.4±0.2(-5)	1.3±0.3(-1)
#5 Decay Tk. Area	6.3±0.7(-5)	1.8±0.4(-1)
#6 Outlet Lg. & Sm. Filters	9.7±1.0(-6)	4.6±0.9(-1)
<u>9/5/75 - 9/18/75</u>		
#1 Inlet Sm. Filter	2.4±0.1(-4)	1.1±0.2(-1)
#2 "A" Fan Off - No Flow	--	--
#3 "B" Fan Outlet Sm. Filter	3.1±0.5(-6)	1.2±0.2(-1)
#4 Gen. Op. Floor	8.2±1.3(-6)	9.6±1.9(-2)
#5 Decay Tk. Area	5.9±0.6(-5)	1.1±0.2(-1)
#6 Outlet Lg. & Sm. Filters	1.1±0.2(-5)	3.4±0.7(-1)
<u>9/18/75 - 10/2/75</u>		
#1 Inlet Sm. Filter	7.0±0.4(-5)	1.0±0.2(-1)
#2 "A" Fan Off & Dampers closed - no flow	--	--
#3 "B" Fan Outlet Sm. Filter	1.4±0.4(-6)	1.6±0.3(-1)
#4 Gen. Op. Floor	3.3±1.0(-6)	1.3±0.2(-1)
#5 Decay Tk. Area	3.9±0.2(-5)	1.5±0.3(-1)
#6 Outlet Lg. & Small Filters	5.5±1.7(-6)	4.5±0.9(-1)
<u>10/2/75 - 10/16/75</u>		
#1 Inlet Sm. Filter	5.1±0.3(-4)	1.2±0.2(-1)
#2 "A" Fan Off & Dampers closed - no flow	--	--
#3 "B" Fan Outlet Sm. Filter	1.3±0.9(-6)	1.2±0.2(-1)
#4 Gen. Op. Floor	8.9±0.8(-6)	8.4±1.7(-2)
#5 Decay Tk. Area	2.2±0.1(-4)	1.1±0.2(-1)
#6 Outlet Lg. & Small Filters	3.5±0.2(-5)	3.6±0.7(-1)

14th ERDA AIR CLEANING CONFERENCE

TABLE 13 (continued)

	^{131}I	^3H
<u>10/16/75 - 11/5/75</u>		
#1 Inlet Sm. Filter	6.6±0.4(-5)	1.9±0.4(-1)
#2 "A" Fan Off - No Flow	--	--
#3 "B" Fan Outlet Sm. Filter	1.6±0.5(-6)	9.7±1.9(-2)
#4 Gen. Op. Floor	5.0±1.2(-6)	6.2±1.2(-2)
#5 Decay Tk. Area	6.7±0.5(-5)	1.0±0.2(-1)
#6 Outlet Lg. & Small Filters	7.4±1.3(-6)	3.2±0.6(-1)
<u>11/5/75 - 11/25/75</u>		
#1 Inlet Sm. Filter	3.3±0.2(-4)	1.2±0.2(-1)
#2 "A" Fan Off - No Flow	--	--
#3 "B" Fan Outlet Sm. Filter	1.0±0.2(-6)	1.1±0.2(-1)
#4 Gen. Op. Floor	2.4±0.5(-6)	6.0±1.2(-2)
#5 Decay Tk. Area	4.4±0.7(-5)	1.2±0.2(-1)
#6 Outlet Lg. & Sm. Filters	9.8±1.6(-6)	3.3±0.7(-1)
<u>11/25/75 - 12/11/75</u>		
#1 Inlet Sm. Filter	1.1±0.1(-4)	1.3±0.3(-1)
#2 "A" Fan Off - No Flow	--	--
#3 "B" Fan Outlet Sm. Filter	4.7±1.4(-7)	1.4±0.3(-1)
#4 Gen. Op. Floor	1.5±0.4(-6)	9.5±1.9(-2)
#5 Decay Tk. Area	4.1±0.3(-5)	2.0±0.4(-1)
#6 Outlet Lg. & Sm. Filters	<8(-6)	5.5±1.1(-1)
<u>12/11/75 - 12/29/75</u>		
#1 Inlet Sm. Filter	1.2±0.1(-4)	2.4±0.5(-1)
#2 "A" Fan Off & Dampers closed - no flow	Changed Fans 12/22 results of #2 & #3	- Averaged
#3 "B" Fan Outlet Sm. Filter	1.5±0.1(-6)	1.9±0.4(-1)
#4 Gen. Op. Floor	1.2±0.3(-5)	8.9±1.8(-2)
#5 Decay Tk. Area	4.5±0.2(-5)	3.4±0.7(-1)
#6 Outlet Lg. & Small Filters	7.3±1.2(-6)	5.9±1.2(-1)
<u>12/29/75 - 1/13/76</u>		
#1 Inlet Sm. Filter	7.2±0.3(-3)	2.3±0.5(-1)
#2 "A" Fan	3.4±0.2(-4)	1.2±0.3(-1)
#3 "B" Fan Off & Dampers closed - no flow	--	--
#4 Gen. Op. Floor	9.9±0.5(-4)	1.3±0.3(-1)
#5 Decay Tk. Area	1.0±0.1(-2)	5.2±1.0(-1)
#6 Outlet Lg. & Small Filters	2.0±0.1(-3)	7.7±1.5(-1)
<u>1/13 - 1/27/76</u>		
#1 Inlet Sm. Filter	3.1±0.2(-3)	2.7±0.5(-1)
#2 "A" Fan - Changed Fans 1/22/76 - Averaged Results		
#3 "B" Fan Outlet Sm. Filter	1.6±0.1(-5)	2.4±0.5(-1)
#4 Gen. Op. Floor	1.4±0.1(-3)	1.2±0.3(-1)
#5 Decay Tk. Area	6.2±0.3(-4)	1.3±0.3(-1)
#6 Outlet Lg. & Small Filters	4.1±0.2(-4)	1.4±0.3(-1)

14th ERDA AIR CLEANING CONFERENCE

TABLE 13 (continued)

	^{131}I	^3H
<u>1/27 - 2/13/76</u>		
#1 Inlet Sm. Filter	2.5±0.1(-3)	2.2±0.4(-1)
#2 "A" Fan Off & Dampers Closed - no flow	--	--
#3 "B" Fan Out Sm. Filter	3.1±0.3(-5)	1.6±0.3(-1)
#4 Gen. Op. Floor	3.1±0.2(-4)	8.1±1.6(-2)
#5 Decay Tk. Area	5.4±0.3(-3)	4.7±0.9(-1)
#6 Outlet Lg. & Small Filters	1.5±0.1(-3)	1.3±0.2(1)*
<u>2/13 - 3/3/76</u>		
#1 Inlet Sm. Filter	1.7±0.1(-4)	1.8±0.4(-1)
#2 "A" Fan Off & Dampers Closed - no flow	--	--
#3 "B" Fan Outlet Sm. Filter	8.6±1.1(-6)	1.5±0.3(-1)
#4 Gen. Op. Floor	8.0±0.6(-5)	8.6±1.7(-2)
#5 Decay Tk. Area	3.0±0.2(-4)	2.3±0.5(-1)
#6 Outlet Lg. & Small Filters	6.4±0.6(-5)	4.5±0.9(-1)
<u>3/3 - 3/24/76</u>		
#1 Inlet Sm. Filter	5.5±0.3(-5)	3.6±0.7(-1)
#2 "A" Fan Off & Dampers Closed - no flow	--	--
#3 "B" Fan Outlet Sm. Filter	4.7±2.6(-7)	9.1±1.8(-2)
#4 Gen. Op. Floor	4.3±0.3(-5)	6.1±1.2(-2)
#5 Decay Tk. Area	4.9±0.3(-5)	1.5±0.3(-1)
#6 Outlet Lg. & Small Filters	1.9±0.2(-5)	3.4±0.7(-1)

*Believe this to be a sampling error.

TABLE 14 RESULTS OF ¹³¹I CHEMICAL FORM

MEASUREMENTS* AT GINNA

		9/3 - 9/5/75	10/2 - 10/16**	10/16 - 11/5**	11/5 - 11/25**
#1 Inlet Small Filter	PF	2.3%	.3%	.6%	--
	CdI ₂	24.9%	4.0%	10.9%	1.7%
	IPH ²	57.4%	9.2%	--	.1%
	CHARCOAL	15.4%	84.3%	88.5%	98.2%
	TOTAL (μCi/sec)	<u>4.1±0.3(-4)</u>	<u>5.1±0.3(-4)</u>	<u>6.6±0.4(-5)</u>	<u>3.3±0.2(-4)</u>
#2 "A" Fan - Fan Off and Dampers Closed - No Flow					
#3 "B" Fan	PF	27.3%	33.7%	--	--
	CdI ₂	--	28.4%	32.4%	--
	IPH ²	59.5%	--	--	--
	CHARCOAL	13.2%	37.9%	67.6%	100%
	TOTAL (μCi/sec)	<u>5.3±2.8(-6)</u>	<u>1.3±0.9(-6)</u>	<u>1.6±0.5(-6)</u>	<u>1.0±0.2(-6)</u>
#4 Gen. Op. Floor	PF	84.3%	--	--	--
	CdI ₂	10.6%	13.3%	13.0%	--
	IPH ²	5.1%	--	17.8%	--
	CHARCOAL	--	86.7%	69.2%	100%
	TOTAL (μCi/sec)	<u>8.6±7.6(-5)</u>	<u>8.9±0.8(-6)</u>	<u>5.0±1.2(-6)</u>	<u>2.4±0.5(-6)</u>
#5 Decay Tank Area	PF	--	2.8%	1.8%	--
	CdI ₂	17.1%	17.9%	25.4%	18.6%
	IPH ²	59.2%	.8%	16.2%	--
	CHARCOAL	23.7%	78.5%	56.6%	81.4%
	TOTAL (μCi/sec)	<u>8.0±2.8(-5)</u>	<u>2.2±0.1(-4)</u>	<u>6.7±0.5(-5)</u>	<u>4.4±0.7(-5)</u>
#6 Outlet Large & Small Filter	PF	--	--	--	--
	CdI ₂	--	--	--	--
	IPH ²	--	--	--	--
	CHARCOAL	100%	100%	100%	100%
	TOTAL (μCi/sec)	<u>6.9±4.3(-6)</u>	<u>3.5±0.2(-5)</u>	<u>7.4±1.3(-6)</u>	<u>9.8±1.6(-6)</u>

*Values are ¹³¹I measured on each adsorber in sampler. No corrections for the efficiencies of each bed for various chemical forms have been made.

**Efficiency of IPH media for HOI collection is suspect.

TABLE 14 (continued)

		12/29 - 1/13	1/13 - 1/27	1/27 - 2/13	2/13 - 3/3
#1 Inlet Small Filter	PF	.2%	.1%	.3%	1.6%
	CdI ₂	6.5%	4.85%	9.7%	23.9%
	IPH ²	22.1%	7.63%	25.3%	38.4%
	CHARCOAL	71.2%	86.5%	64.7%	36.1%
	TOTAL (μCi/sec)	7.2±0.3(-3)	3.1±0.2(-3)	2.5±0.1(-3)	1.7±.09(-4)
#2 "A" Fan	PF	2.8%	Changed Fans	Fan Off and	Fan Off and
	CdI ₂	22.3%	1/22/76	Dampers	Dampers
	IPH ²	48.7%	Averaged	Closed	Closed
	CHARCOAL	26.2%	Results		
	TOTAL (μCi/sec)	3.4±0.2(-4)			
#3 "B" Fan -	PF	Fan Off and	Had only char.	7.8%	8.6%
	CdI ₂	Dampers	on "B" Fan so	7.9%	25.3%
	IPH ²	Closed	% of Species	6.3%	20.9%
	CHARCOAL		could mislead	88.0%	45.2%
	TOTAL (μCi/sec)		1.6±0.1(-5)	3.1±0.3(-5)	8.6±1.1(-6)
#4 Gen. Op. Floor	PF	.1%	.2%	.4%	--
	CdI ₂	2.5%	2.7%	3.6%	6.3%
	IPH ²	7.9%	5.9%	14.4%	14.8%
	CHARCOAL	89.5%	91.2%	81.6%	78.9%
	TOTAL (μCi/sec)	9.9±0.5(-4)	1.4±.07(-3)	3.1±0.2(-4)	8.0±0.6(-5)
#5 Decay Tank Area	PF	.2%	.8%	1.2%	4.7%
	CdI ₂	13.4%	22.0%	12.3%	36.3%
	IPH ²	57.5%	38.8%	40.7%	35.7%
	CHARCOAL	28.9%	38.4%	45.8%	23.2%
	TOTAL (μCi/sec)	1.0±0.1(-2)	6.2±0.3(-4)	5.4±0.3(-3)	3.0±0.2(-4)
#6 Outlet Large & Small Filter	PF	.8%	--	--	3.5%
	CdI ₂	.8%	.1%	.2%	3.0%
	IPH ²	.8%	--	.4%	2.1%
	CHARCOAL	97.6%	99.9%	99.4%	91.4%
	TOTAL (μCi/sec)	2.0±0.1(-3)	4.1±0.2(-4)	1.5±.08(-3)	6.4±0.6(-5)

TABLE 14 (continued)

		<u>3/3 - 3/24/76</u>
#1 Inlet Small Filter	PF	1.0%
	CdI ₂	10.0%
	IPH ²	27.2%
	CHARCOAL	61.8%
	TOTAL (μCi/sec)	<u>5.5±0.3(-5)</u>
#2 "A" Fan	PF	Fan Off and
	CdI ₂	Dampers
	IPH ²	Closed
	CHARCOAL	
	TOTAL (μCi/sec)	
#3 "B" Fan	PF	51.8%
	CdI ₂	48.2%
	IPH ²	--
	CHARCOAL	--
	TOTAL (μCi/sec)	<u>4.7±2.6(-7)</u>
#4 Gen. Op. Floor	PF	--
	CdI ₂	5.5%
	IPH ²	47.6%
	CHARCOAL	46.9%
	TOTAL (μCi/sec)	<u>4.3±0.3(-5)</u>
#5 Decay Tank Area	PF	--
	CdI ₂	22.7%
	IPH ²	42.2%
	CHARCOAL	35.1%
	TOTAL (μCi/sec)	<u>4.9±0.3(-5)</u>
#6 Outlet Large & Small Filter	PF	--
	CdI ₂	--
	IPH ²	--
	CHARCOAL	100%
	TOTAL (μCi/sec)	<u>1.9±0.2(-5)</u>

14th ERDA AIR CLEANING CONFERENCE

TABLE 15 DECONTAMINATION FACTORS FOR
IODINE - 131 ACROSS THE
LARGE FILTER (~25,000 cfm)

Exposure Time (d)	10 ⁸ Air Changes	Part.	D.F.			
			CdI ₂	IPH	Char.	Total
730	2.1	NS	NS	NS	NS	2.0
743	2.1	NS	NS	NS	NS	11.0
758	2.2	NS	NS	NS	NS	12.0
778	2.2	NS	NS	NS	NS	11.0
791	2.3	NS	NS	NS	NS	9.5
816	2.3	NS	NS	NS	NS	9.5
818	2.3	>37	>4.6	>13	2.8	100.0
831	2.4	NS	NS	NS	NS	8.8
845	2.4	NS	NS	NS	NS	10.0
859	2.5	>6.2	>20	>0.9	5.2	6.8
879	2.5	>1.2	>9.0	>6.0	6.5	12.0
899	2.6	(1)	>4.1	(1)	4.3	5.3
915	2.6	NS	NS	NS	NS	6.0
933	2.7	NS	NS	NS	NS	9.9
948	2.7	3.2	(2)	(2)	2.0	6.7
962	2.7	>6.8	>85	>160	3.8	5.1
979	2.8	>65	1300	730	1.8	4.1
998	2.8	9.3	>55	> 60	2.4	7.0
1019	2.9	(1)	>14	>21	1.9	5.0
Average		>18	>190	>140	3.4	13.0

* Both the inlet and outlet concentrations were undetectable

** The quantity of iodine-131 measured at the outlet of the small filter was greater than that measured for the total quantity

14th ERDA AIR CLEANING CONFERENCE

TABLE 16 DECONTAMINATION FACTORS FOR
IODINE - 131 ACROSS THE
SMALL FILTER (4,700 cfm)

Exposure Time (d)	10 ⁸ Air Changes	D.F.				Total
		Part.	CdI ₂	IPH	Char.	
(1)	(1)	NS	NS	NS	NS	50
26	0.075	NS	NS	NS	NS	180
41	0.12	NS	NS	NS	NS	250
61	0.18	NS	NS	NS	NS	248
74	0.21	NS	NS	NS	NS	54
99	0.29	NS	NS	NS	NS	167
101	0.29	6.7	>200	75	90	77
114	0.33	NS	NS	NS	NS	70
128	0.37	NS	NS	NS	NS	54
142	0.41	3.4	54	>240	870	405
162	0.47	>2.7	14	>1.0	53	43
182	0.52	>1	> 28	>1.7	320	333
198	0.57	NS	NS	NS	NS	238
216	0.62	NS	NS	NS	NS	87
231	0.67	1.5	6.2	9.4	57	22
245	0.71	NS	NS	NS	NS	200
262	0.75	3.1	96	320	59	82
281	0.81	3.7	19	36	16	21
302	0.87	2.3	24	> 75	>170	122
Average		>3.1	> 55	> 95	>200	142

* Charcoal adsorbers changed after 9 days of a 22 day sampling period

particulate filter with clean room air and be caught on the CdI₂ adsorber. On two other occasions we have observed no purging of iodine-131 from the particulate filter when treated the same way. As will be seen below, iodine-131 on particulates was probably important in determining the effectiveness of the small installation. In this work efficiency corrections would make a relatively minor impact on the reported release rates, and they have no effect on the observations made of the effectiveness of the charcoal adsorbers being tested.

As pointed out in Table 14, the efficiency of the IPH media was suspect for the first three long duration sampling periods. Lab tests showed that the efficiency for the HOI species was from 30% to 50% during that period. This had no effect on the iodine-131 on particulates or on the CdI₂, but most likely increased the apparent organic fraction. The total iodine-131 reported in Table 13 for these periods was unaffected.

The measurements of tritium provided a continuing check on the quality of the sampling. The charcoal adsorbers should have little or no effect on the tritium concentrations and one would expect the D.F. calculated for tritium to be 1. The average tritium D.F. for the small filter was 1.26 with a standard deviation of the mean equal to 0.18. This D.F. is not significantly different than 1.0 ($X=.05$). The average D.F. and standard deviation of the mean for tritium for the large filter was 0.90 and 0.038 respectively. This D.F. is significantly different than 1 ($X = .0125$) and there may be a bias in the sampling which would give slightly lower D.F. for iodine-131 than were real. On the whole however, we believe that the tritium measurements tend to verify the effectiveness of the sampling for iodine-131.

The reason for the many "greater than" symbols in Tables 15 and 16 is the fact that the I-131 activities on the particulate filter, the CdI₂ adsorber, and IPH adsorber were often less than our detection limit. In some cases radioiodine was not detectable at the inputs. The low concentrations undoubtedly add to the observed variability in the calculated D.F.s.

None-the-less, it is clear from Table 15 that the D.F. for total iodine-131 and the organic fraction decreased with time. The low concentrations preclude such observation for the particulate, CdI₂ and IPH fractions. It is apparent however, that for the large filter, the D.F.s for these forms were much higher than the D.F.s for organic iodine. This is what one might expect. Table 16 shows the opposite for the small filter. The average D.F. for the organic fraction was much higher than that for the other more reactive iodine species. We believe that the low D.F. for iodine-131 on particulates is due to the penetration of the filter by particulates. As pointed out, the small filter has no HEPA filters. The lower D.F.s for the elemental and HOI forms may be due to the purging of the iodine-131 off the particulate filter in the sampler after collection.

To put the decrease in the D.F.s for organic and the total iodine with time into perspective we have compared our results to

14th ERDA AIR CLEANING CONFERENCE

those reported by Collins, et al¹. Their "accelerated aging" tests for organic iodine showed the following relationship between filter performance and the number of air changes experienced by the filter: (The air they used was regular laboratory air).

$$\text{Log}(D.F./R.T.) = \log (D.F./R.T.)_0 e^{-r} (A.C.)$$

where D.F. = Decontamination factor
 R.T. = Residence time
 A.C. = Number of 10⁸ air changes
 r = Constant

Their value for r was about 0.69 for tests with KI and TEDA Charcoal.

The data for total and organic iodine-131 in tables 15 & 16 were fit to exponential curves of the type shown above and the results were as follows:

	<u>log(D.F./R.T.)₀</u>	<u>r</u>	<u>Coeff. of Determination</u>
Large Filter*			
Total	5.9	0.57	0.61
organic	5.9	0.67	0.89
Small Filter *			
Total	5.8	-1.8	0.13
organic	11.6	-2.4	0.29

For the large filter installation the rate of decrease in performance for organic iodine with exposure is remarkably similar to that found by Collins, et al¹. The very good agreement is considered fortuitous, but it does support the form of their expression for the decrease in performance of impregnated charcoal for collecting organic iodine with continued exposure. The rate of decrease in performance for total iodine-131 was less than that for organic iodine-131. This indicates that the ability of the filter to collect the other, more reactive forms, has not decreased as fast.

The fit to the exponential curve was not nearly as good for the small filter as evidenced by the low coefficient of determination. This is due to the much higher variability in the data. Some of the variability is due to experimental error and the relatively high D.F.'s encountered.

The performance of the small filter for organic iodine appears to have decreased faster than that of the larger filter. This could also have happened in the early stages for the large filter or it could be due to accelerated poisoning by materials not caught on HEPA filters. We have no way of knowing at this point. As for the large

*The short duration sample for 9/3-9/5/75 was not used in the curve fitting nor were the results from the first sampling period 5/28-6/19 used. The 9/3-9/5 sample had an unusually high fraction of particulate and elemental iodine. The 5/28-6/19 sample gave unusually low D.F. values and there may have been an experimental error.

14th ERDA AIR CLEANING CONFERENCE

filter, the decrease in performance for total-131 was less than for organic.

We plan to continue these measurements into July 1976.

14th ERDA AIR CLEANING CONFERENCE

VIII. REFERENCES

1. D.A. Collins, L.R. Taylor, and R. Taylor, "The Development of Impregnated Charcoals for Trapping Methyl Iodide at High Humidity" UKAEA-TRG Report 1300(W) 1967
2. W.J. Maeck, D.T. Pence, and J.H. Keller, "A Highly Efficient Inorganic Adsorber for Airborne Iodine Species (Silver Zeolite Development Studies)" IN-1224, October, 1968.
3. F.O. Cartan, H.R. Beard, F.A. Duce, and J.H. Keller, "Evidence for the Existence of Hypoidous Acid as a Volatile Iodine Species Produced in Water-Air Mixtures", Proceeding of the 10th AEC Air Cleaning Conference, CONF-680821 December 1968.
4. J.H. Keller, F.A. Duce, and F.O. Cartan, Retention of Iodine on Selected Particulate Filters and A Porous Silver Membrane Being Considered for the LOFT Maypack, IN-1078, May 1967, p.10
5. J.H. Keller, T.R. Thomas, D.T. Pence, and W.J. Maeck, "An Evaluation of Materials and Techniques used for Monitoring Airborne Radioiodine Species", in Proceedings of the 12th USAEC Air Cleaning Conference August, 1972.
6. J.H. Keller, F.A. Duce, and W.J. Maeck, "A Selective Adsorbent Sampling System for Differentiating Airborne Iodine Species" in Proceedings of the 11th USAEC Air Cleaning Conference, August 1970
7. M.J. Kabat, "Testing and Evaluation of Adsorbers for Gaseous Penetrative Forms of Radioiodine", in Proceedings of the 13th AEC Air Cleaning Conference, San Francisco, August, 1974.
8. D.T. Pence, F.A. Duce, and W.J. Maeck, "A Study of the Adsorption Properties of Metal Zeolites for Airborne Iodine Species" in Proceedings of the 11th USAEC Air Cleaning Conference, August 1970
9. C.A. Pelletier, compiler, "Results of Independent Measurements of Radioactivity in Process Streams and Effluents at Boiling Water Reactors" USAEC, May 1973 (unpublished)
10. D.L. Reid, B.M. Johnson, A.K. Postma Final Report: Research on Removal of Iodine by Containment Sprays Containing Trace Levels of Hydrazine. Contract 212B52000 for Consortium of Private Power Utility Companies. June 1974.
11. J. Wilhelm, Testing of Iodine Filters for Nuclear Installations, SM-110/60 Symposium on Operating and Developmental Experience in the Treatment of Airborne Radioactive Wastes, United Nations, New York, August 1968.
12. C.A. Burchsted, RDT M-16-1T, Gas-Phase Adsorbents for Trapping Radioactive Iodine and Iodine Compounds. ORNL October, 1973.
13. A. Wexler, and S. Hasegawa, Relative Humidity-Temperature Relationships of Some Saturated Salt Solutions in the Temperature Range 0° to 50°C. J. of Research of the N.B.S., pp 1926 53, No. 1, July 1954.

14th ERDA AIR CLEANING CONFERENCE

VIII. REFERENCES, cont'd.

14. Nuclear Environmental Services, Task 1, Plans and Procedures, Rev. 1 A Report to Electric Power Research Institute under Contract RP 274-1, April 1, 1975.
15. M.J. Kabat, Iodine Forms and Removal Efficiencies, Invited paper to panel on "Radioiodine Behavior Related to Power Reactors" sponsored by the Environmental Sciences Division, ANS. Trans, Amer. Nucl. Soc., Annual meeting p.86., New Orleans, La., June 1975.

DISCUSSION

WILHELM: How much elemental iodine was adsorbed on the aerosol filters and how can you distinguish between elemental iodine and particulate iodine on your aerosol filters?

EMEL: It is very difficult to distinguish between the elemental and the truly particulate radioiodine on the sampler. Some of the radioiodine retained on the aerosol filter is converted to elemental iodine and removed from the filter by air purging. This was shown in the purge tests in Section VI of the paper. The amount of elemental iodine on the filter will vary depending on the sampler location in the plant. The lab tests did indicate a few per cent of the elemental iodine was retained on the aerosol filter used in the tests.

KABAT: This is a comment on paragraph VII of this paper. The large discrepancy in HOI adsorption efficiencies reported in ref. 15 and in this paper, is due to a different quality of alumina used in these two experiments. Alumina supplied by Fisher - Scientific was used in the experiment described in ref. 15. This alumina was highly efficient for water vapour adsorption. Therefore, the measured efficiency for HOI absorption was very low at humidity levels exceeding 70%. Six sets of the sampler described in this paper were purchased from SAI and recently tested in our laboratory. The measured HOI adsorption efficiency was significantly higher than the value reported in ref. 15 but the performance of two sections of the sampler (I₂ and HOI absorbents) still did not fulfill our requirements. Further, I suggest that the residence time of HOI for its chemical reaction with 4-iodophenol, be in the order of one hour rather than approximately 30 milliseconds as given in this paper. I believe that the physical adsorption of HOI on alumina, preceding its chemical reaction with 4-iodophenol, is the basic factor controlling the process of HOI collection on this material .

EMEL: The substrate for the 4-iodophenol coating and the Fisher alumina (which turns out to be Alcoa F5) contains about 12 weight per cent calcium fluoride and it doesn't work worth a darn, as we indicated in the paper. We stumbled across it at first. The original paper said "activated alumina", therefore, we immediately went out and bought activated alumina. Activated alumina can be any of three or four different types. The type that works is Alcoa F1, a crystal form of alumina.

OPERATING EXPERIENCE WITH THE TESTING OF IODINE ADSORBERS
ON THE AIR CLEAN UP SYSTEMS OF THE BELGIAN PWR POWER PLANTS.

B. Deckers, Association Vinçotte, Belgium
P. Sigli and L. Trehen, Département de Protection,
Commissariat à l'Energie Atomique, France.

Abstract.

The in situ test method of iodine adsorbers used in France and Belgium has been developed by the French Atomic Energy Authority (CEA). Iodine 131 (in the form of elemental iodine or as methyl iodide) is injected in the ventilation duct up-stream to the adsorber ; the filter decontamination factor (DF) is derived from up-stream and down-stream samplings.

The main results obtained on Belgian plants are given considering two view points : acceptance of the installation and periodical testing. The results obtained are discussed in terms of :

- comparison of DF obtained by in situ and by laboratory measurements on activated carbon samples ;
- effect of air flow rate and relative humidity of the air flow through the adsorber ;
- determination of ventilation air flow from measurement of injected versus retained iodine as a possible cross check ;
- ageing of tested adsorbers.

This technique that has been widely tested for several years is particularly interesting as it allows determination of the whole adsorber conditions at the time of the tests and also because it yields a lot of valuable supplementary information.

1. Introduction.

For some years now, the gaseous effluents of nuclear power plants have been equipped with filtration systems for radioactive particulates that can originate after an accident as well as during normal plant operation. To complete these filtration systems an iodine 131 trapping on activated carbon impregnated with potassium iodide or triethylenediamine is used to improve the efficiency for the most penetrating iodine forms - in particular methyl iodide.

However, one essential problem is the ageing of the activated carbon : in fact it is established that permanently in service adsorbents as well as normally by-passed adsorbents age, resulting in a reduction of their efficiency with time.

As it is not possible to precisely predict what the ageing will be, it seems absolutely necessary to test these adsorption units initially and periodically to assure that their efficiency is satisfactory and in any case, higher than the safety requirements.

Many test conceptions can be envisaged. In parallel with a permanently used adsorption unit, one or more samples of the same batch as the main adsorbent can be installed. These samples are then periodically tested in a laboratory to determine the state of the adsorbent. These tests must however be accompanied by a system leak test to verify that no unacceptable leaks appear through or around the installed cells.

This is the solution used in the United States where the representative samples are periodically tested in a laboratory with methyl iodide and in some cases with molecular iodine, whilst the leak test is carried out with freon (1)(2). This solution presents nevertheless the disadvantage that the actual efficiency at a given moment of the whole installed filtration system is not determined.

Another answer consists of testing periodically in situ the whole installed system with methyl iodide and/or with molecular iodine. This method has the advantage of giving an idea of the actual state of the whole system - adsorbent and possible leaks - at the moment when the test is performed. This last solution seems to be presently preferred in Europe (3),(4),(5) and has been utilized up to now in the Belgian nuclear power plants. In addition to these periodical tests, it is possible to install in parallel with the adsorption unit one or more representative adsorbent samples subjected to regular laboratory tests : in this way, some supplementary information on the state of the adsorbent can be obtained (3),(4),(5).

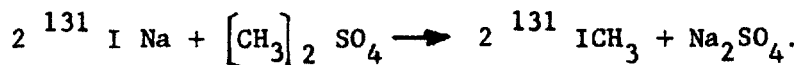
In the present paper, we intend to give a résumé of the utilized technique, and also the conclusions obtained from 70 in situ tests carried out during the years 1974 to 1976 in the Belgian nuclear power plants.

2. In situ test technique.

The details of the iodine and methyl iodide injection and sampling devices have already been described elsewhere (5). We shall therefore only briefly recall their main features.

2.1. Molecular iodine or methyl iodide injection.

Molecular iodine is obtained by isotopic exchange between $^{131}\text{I Na}$ and $^{127}\text{I}_2$; in this case, a negligible amount of methyl iodide is formed. Methyl iodide is obtained by the reaction of methyl sulfate on the sodium iodide :



Either of these generation reactions take place directly in situ with the same device.

The whole generation and injection device (cfr. figure 1) is actuated by an air trump in glass especially designed for this use, which maintains the injection line in depression with regard to the atmosphere of a protective glove box, itself in depression with regard to the outside.

This system which we have used for several years is perfectly safe and we have never had any contamination incident. We note a low internal contamination on the glove box due to successive dismantlings and rebuildings when a series of tests have been performed; the adsorption on the carbon cartridge between the glove box and the outside prevents in this case a contamination of the ambient air.

2.2. Sampling device.

The samples, up-stream and down-stream of the adsorber, are taken with the device represented in figure 2. This device generally includes two carbon beds of 50 mm depth, but may accomodate as many supplementary beds as necessary. Each carbon bed is packed in the laboratory with a vibrating machine and the charcoal is maintained in place with springs.

The instantaneous sample flow is measured by the depression in a calibrated venturi tube. The air velocity through the sample is adjustable and lies in normal operation between 25 and 30 cm.s^{-1} .

Figure 3 gives a scheme of the typical arrangement for testing an installed adsorber bank.

To obtain representative samples in a homogeneous gaseous stream, the up-stream sample is taken near the adsorption unit, at a distance at least equal to 10 duct diameters from the injection point, whilst the down-stream sample is also taken at an equivalent distance of the adsorption unit. This arrangement seems essential since we want to determine the actual efficiency of the whole system with no influence of possible local defects. When the main adsorption unit can be by-passed, it is also desirable to include the by-pass valve between the up-stream and the down-stream sampling point. Indeed, we have frequently noted that the efficiency of an air cleaning system in this case is limited by the leak through the valve by-passing the trap, and not by the performance of the adsorbent itself.

3. In situ test procedure.

At least six hours before each test, the adsorption unit is put in operation to assure that the charcoal has reached the hygrometric equilibrium with the air passing through the bed.

The relative humidity of the air is measured before the test in the ventilation duct just up-stream and down-stream to the trap to determine the relative humidity appearing at the adsorbent level. On some units, especially on those preceded by heaters, we have noted that the air temperature (and hence the relative humidity) can vary widely from one point to another in the ventilation duct.

In parallel, we perform a flow measurement by means of a Pitot tube or a heated wire anemometer to estimate the residence time during the test.

The injection phase of the test lasts thirty minutes. The amount of iodine 131 to be injected is a function of the ventilation flow, of the highest efficiency sought to be measured and of the counting sensitivity. So, an activity of $3 \cdot 10^{-5}$ Ci is sufficient to determine an efficiency of 1,000 with a ventilation flow of $20,000 \text{ m}^3 \cdot \text{h}^{-1}$ since the minimum detectable activity on our equipment reaches $5 \cdot 10^{-12}$ Ci (sampling corresponding to $3 \text{ m}^3 \cdot \text{h}^{-1}$). With this method, the testing of air cleaning systems with very high ventilation flows does not provide any problems.

After the injection phase, sampling is still performed during one hour to take into account a possible desorption.

The countings are performed in the laboratory, by means of γ spectrometry, to prevent any interference with other artificial or natural radioisotopes (^{214}Pb for example, originating from the decrease of the radium emitted by the concrete of the buildings).

Taking into account the time to perform the test itself, to install the test equipment and to dismantle it, it is possible for two persons to carry out three tests a day.

4. Brief description of the tested systems.

All the tests, used as a basis for this study, have been performed on the air cleaning systems of the Doel 1 and 2 and Tihange 1 Belgian nuclear power plants.

The Doel power plant is a twin unit Westinghouse type PWR plant of $2 \times 390 \text{ MWe}$; the Tihange power plant is a Westinghouse type PWR plant of 870 MWe . These two plants have a double containment: in accident conditions, a depression is maintained in the space between primary and secondary containment

14th ERDA AIR CLEANING CONFERENCE

where the air is filtered both in closed loops and before extraction. There are no adsorption systems located inside the primary containment which have to operate in LOCA conditions. These power plants were put in operation in 1974 and 1975.

Among the tested adsorber banks, we have principally :

- the filtration systems of the atmosphere inside the space between the two containments,
- the filtration systems of the air extracted from this space in order to maintain it in depression,
- the filtration systems on the extraction of the auxiliary building, especially the spent fuel pool hall,
- the filtration systems of the control room and emergency plan room air.

On the whole, we have performed tests on 22 distinct filtration units. These units include prefilters, HEPA filters and iodine adsorbers.

The iodine adsorber cells installed in these units have been manufactured by SOFILTRA POËLMAN with activated charcoal impregnated with 1 % potassium iodide. Initially, the adsorbent beds were 25 mm deep with an air velocity of 0.3 m.s^{-1} . Very rapidly, measured efficiencies appeared low, sometimes insufficient, and the ageing process very fast. They have been progressively replaced first by 50 mm deep cells filled with coconut charcoal impregnated with potassium iodide, and with a nominal air velocity of 0.4 m.s^{-1} , afterwards by 50 mm deep cells filled with carboniferous charcoal with the same impregnation but with a nominal air velocity of 0.3 m.s^{-1} .

All the tested air cleaning systems are not in service during the normal operation of the plant. In the space between the two containments, the fans are normally not in service but are automatically put in operation after an accident. The other filtration systems are normally by-passed : only on high activity alarm signals, the by-pass valves close and the filtration systems are put in service. Consequently, the expected and observed ageing is essentially a static ageing, the operation time being practically limited to the periodical tests of the system.

5. Discussion of the results of the tests.

5.1. Comparison of the efficiencies obtained by in situ measurements and by laboratory measurements.

The apparent residence time of the air in the adsorbent directly influences the final efficiency : in practice now, none of the filtration systems installed in a power plant operate at the nominal flow for which the cells have been designed. To allow a comparison of results obtained on different units, we shall express them in the form of the index of performance, following the notation of Collins et al. (6) :

14th ERDA AIR CLEANING CONFERENCE

$$K = \frac{\log DF}{t}$$

where DF is the decontamination factor and t the residence time of the gas in the charcoal bed.

Although strictly, with constant residence time, the index of performance K is a function of the velocity of the air passing through the bed, we have neglected this variation in a first approach, the air velocities generally being between 20 and 35 cm.s⁻¹.

A sample of each activated carbon batch with which the adsorption units are filled, is subjected to laboratory tests, in order to determine the removal efficiency for molecular iodine and for methyl iodide. The efficiency for methyl iodide is determined at different relative humidities between 40 and 95 %. We have thus at our disposal the curve representing the index of performance K as a function of the relative humidity (cfr. figure 4).

On the same figure, we have drawn the values of the K index for methyl iodide, measured in situ by means of the above mentioned method.

With regard to the in situ measured K values below the values foreseeable by the laboratory tests (on figure 4, indicated by a circle with a cross), the inspection of the corresponding units have showed that the by-pass valves were not fully air-tight : hence, the efficiency of the whole system, by-pass valve included, is considerably lower than the removal efficiency of the activated carbon. It appears thus that this test method allows one, to a certain extent, to distinguish between a by-pass leak and a penetration through the bed.

Concerning the other K values (on figure 4 indicated by a circle), contrary to what should logically be expected, they are all higher than the values foreseeable by the laboratory tests. Several assumptions can be advanced to explain this phenomenon.

a) An error in the in situ measurement of the relative humidity of the air or of the air flow : it seems however unlikely that errors, systematically in the same direction appear in the measurement of these parameters.

b) The adsorbents have not reached the hygrometric equilibrium with the air passing through the beds. To prevent this lack of equilibrium, we have taken the precaution to put the adsorption units in operation at least 6 hours before the tests are carried out.

c) A certain amount of the injected iodine is adsorbed on the equipment other than the carbon adsorber, between the up-stream and the down-stream sampling points. We do not measure any activity retained by the absolute filter of the up-stream sampler. Thus, the injected iodine does not appear in the form of aerosols : it is therefore unlikely that the HEPA filters installed in the filtration systems remove a great deal of the methyl iodide. In addition, the adsorption on the ventilation ducts could only explain partially the observed differences of efficiency (cfr. § 5.2).

We have not performed such a comparison of the measured efficiencies for molecular iodine because we have not for the moment many experimental results. In addition, the removal efficiency of the activated carbon for molecular iodine is very high. Therefore, the in situ tests with molecular iodine demonstrate predominantly possible small by-pass leaks rather than a penetration through the activated carbon bed.

5.2. Cross check of the ventilation air flow by the iodine balance.

Knowing the total injected iodine activity, the sampled activity up-stream the adsorber and the sample flow, it should be possible to determine the air flow passing through the adsorber unit : thus, the efficiency of the system and the ventilation air flow could be verified by one unique test.

In practice, we have established that relative important differences appear between the air flow measured with the Pitot tube and the air flow calculated by the iodine balance.

If the injection point is not too distant from the up-stream sampling point, we have obtained cross checks of the measured air flow with the air flow calculated by the iodine balance, with a spread whose mean square root is 25 %.

When the injection point is more distant from the up-stream sampling point, we have observed that even during the methyl iodide tests, an important amount of injected iodine settles on the ducts. So, on a duct about 70 m long and 0.6 m² section, including 4 elbows at 90° and with an air flow of 6,000 m³.h⁻¹ (gas velocity of 2.8 m.s⁻¹), we have observed that on average about 40 % of injected methyl iodide has deposited. During the tests performed with molecular iodine, about 70 % of the injected activity has deposited on this duct.

Consequently, in the present position, the cross check of the measured air flow with the air flow calculated by the iodine balance, is not perfectly realized : it can only give us an indication that the test has been well performed.

5.3. Adsorber ageing for methyl iodide.

From experimental measurements carried out on impregnated carbon, L.R. Taylor and R. Taylor (7) have proposed a relationship allowing calculation of the static as well as the dynamic ageing of impregnated carbon for methyl iodide :

$$\log_{10} K_t = \log_{10} K_o - 0.3 \cdot 10^{-8} N - 1.3 \cdot 10^{-3} t$$

where :

K_o = index of performance mentioned above at the start of ageing,

K_t = index of performance after t weeks ageing,

$$N = \frac{\text{total volume of gas passed through the bed}}{\text{geometric volume occupied by charcoal granules}}$$

t = age in weeks.

We have tried to compare the in situ observed ageing with the ageing foreseen by this relationship. To compare the in situ measurements, we have normalized the results at the same relative humidity. To do this, we have used the curves, representing the efficiency in terms of relative humidity that have been determined by laboratory tests (cfr. figure 4).

Taking into account that the tested filter banks are normally out of service, the observed ageing will essentially be a static ageing : we have verified that, under these conditions, by applying the relationship of L.R. Taylor and R. Taylor, the dynamic ageing must be negligible with regard to the static ageing for all the tested units.

The values used result from efficiency tests performed in situ on 9 adsorber banks ; the time between the successive tests has varied from 1 to 1.5 years for the different units. The results are presented in table 1.

We have observed that the ageing appearing on the adsorber units of the Doel power plant as well as those of the Tihange power plant is faster than the ageing foreseen by this relationship. However, a relatively important dispersion appears between the observed values of this ratio.

Taking into account

- a) the limited amount of measurement results that we have obtained in situ on aged adsorber units,
- b) the fact that these results have been obtained on recent plants where it cannot be excluded that some poisoning could occur,
- c) the uncertainties introduced by the normalisation at a same relative humidity, we think it is however premature to draw definite conclusions about the velocity of the ageing process on adsorption units installed in power plants.

6. Conclusions.

In situ tests of iodine adsorption systems are quite feasible with labeled methyl iodide and can be performed without great inconvenience.

The main conclusions of these tests have shown that :

- the efficiencies obtained in situ seem to be appreciably higher than can be deduced by laboratory tests carried out on representative samples ;
- the ageing appears to be faster than expected. In the future, to increase the lifetime of the adsorbers, it would be desirable to increase the residence time and/or decrease as much as possible the relative humidity of the air passing through the adsorber.

14th ERDA AIR CLEANING CONFERENCE

This technique which permits a gross test takes into account simultaneously, in the measurement of decontamination factors, all the parameters which influence finally the efficiency of the air clean up systems.

References.

- (1) USAEC Regulatory Guide 1.52 "Design, testing and maintenance criteria for atmosphere clean up system air filtration and adsorption units of light-water-cooled nuclear power plants" June 1973.
- (2) ANSI N 510 - 1975 "Testing of nuclear air cleaning systems".
- (3) J.J. Hillary "Iodine sorption plant test procedures in the United Kingdom". Proceedings of the seminar on iodine filter testing, Karlsruhe 1973, pp. 237-248.
- (4) J.G. Wilhelm, H.G. Dillmann and K. Gerlach "Prüfung von Jodfilteranlagen" Proceedings of the seminar on iodine filter testing, Karlsruhe 1973, pp. 211-235.
- (5) P. Sigli and L. Trehen "Contrôle des pièges à iode des centrales nucléaires". Proceedings of the seminar on iodine filter testing, Karlsruhe 1973, pp. 259-269.
- (6) D.A. Collins, L.R. Taylor and R. Taylor "The development of impregnated charcoals for trapping methyl iodide at high humidity" TRG report 1300 (W) 1967.
- (7) L.R. Taylor and R. Taylor "The ageing of impregnated charcoals". Proceedings of the seminar on iodine filter testing, Karlsruhe 1973, pp. 121-148.

TABLE 1. AGEING OF IODINE ADSORBERS

Adsorber unit	Time between the two tests	Measurements during the tests			Normalisation		Time foreseen by the Taylor relationship to obtain the same ageing	Ratio of the observed ageing by the ageing foreseen by the Taylor relationship
		flow	relative humidity	K	relative humidity	K		
N°	weeks	m ³ .h ⁻¹	%	-	%	-	weeks	-
1	72	7.500	56	14,7	79	6,1	427	5,9
		6.500	79	1,73	79	1,7		
2	72	7.500	58	17,6	83	6,8	212	2,9
		6.300	83	3,57	83	3,6		
3	80	7.500	57	27,3	74	15	486	6,1
		6.400	74	3,51	74	3,5		
4	69	4.000	48	9,0	55	6,9	613	8,9
		4.000	55	1,1	55	1,1		
5	77	36.500	53	11,8	33	25	565	7,3
		36.500	33	4,6	33	4,6		
6	58	4.080	62	11,4	33	30	585	10
		4.080	33	5,2	33	5,2		
7	58	3.560	58	11,3	37	23	378	6,5
		3.560	37	7,4	37	7,4		
8	58	1.000	65	10,4	90	4,5	114	2,0
		120	90	3,2	90	3,2		
9	58	830	65	11,5	86	5,7	446	7,7
		120	86	1,5	86	1,5		

171

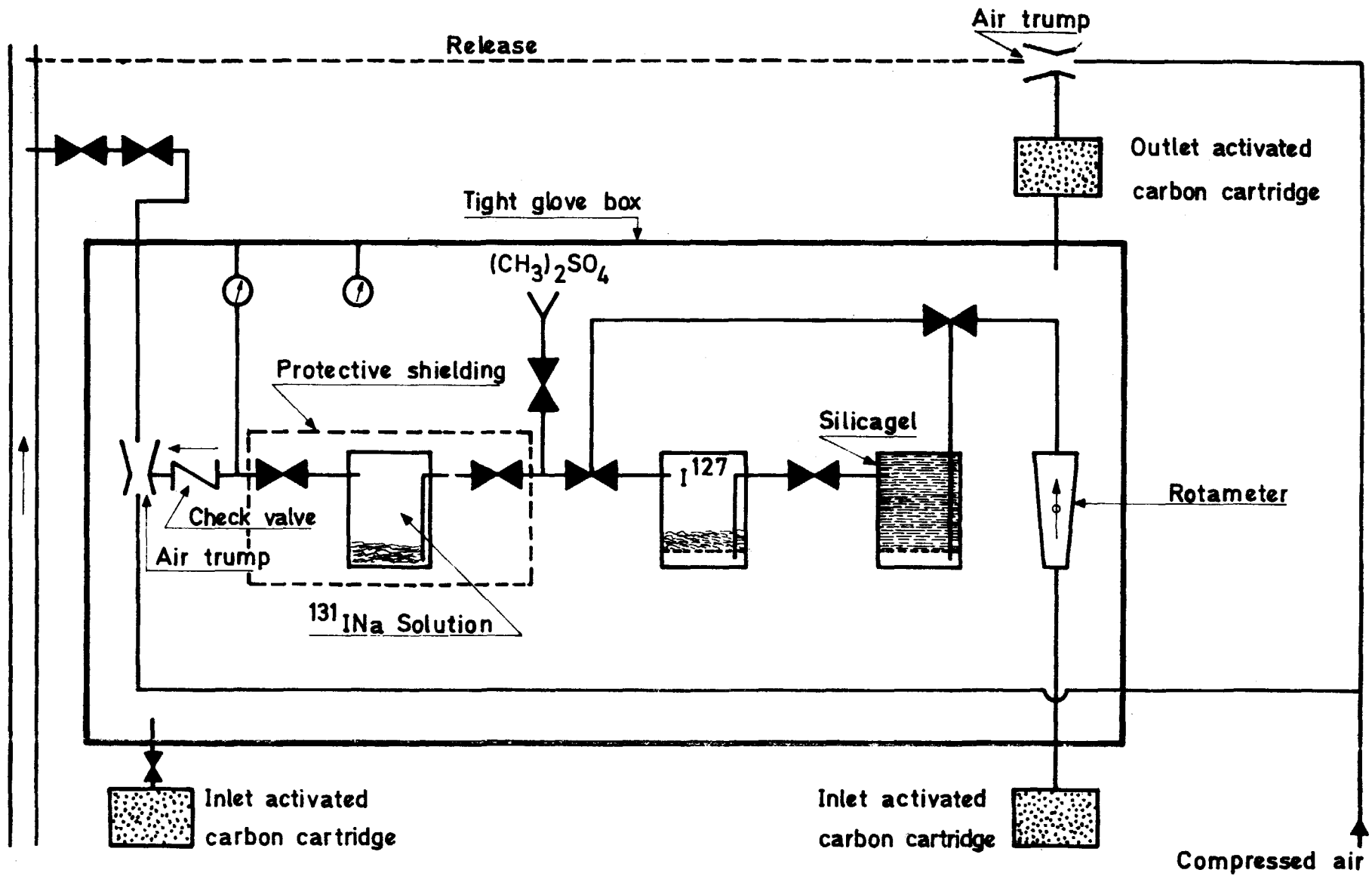


FIGURE 1: Injection device

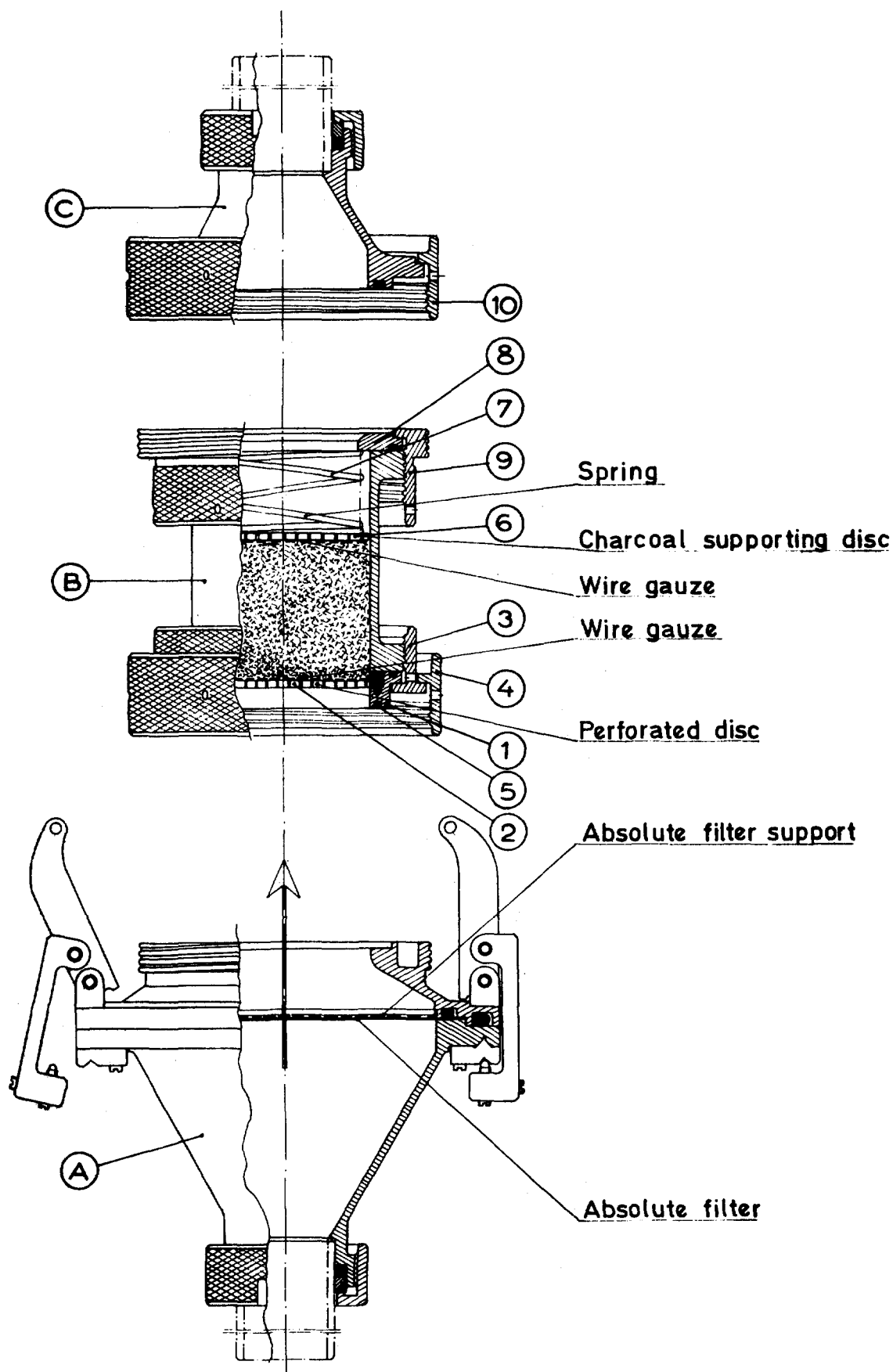


FIGURE 2 : Sampling device

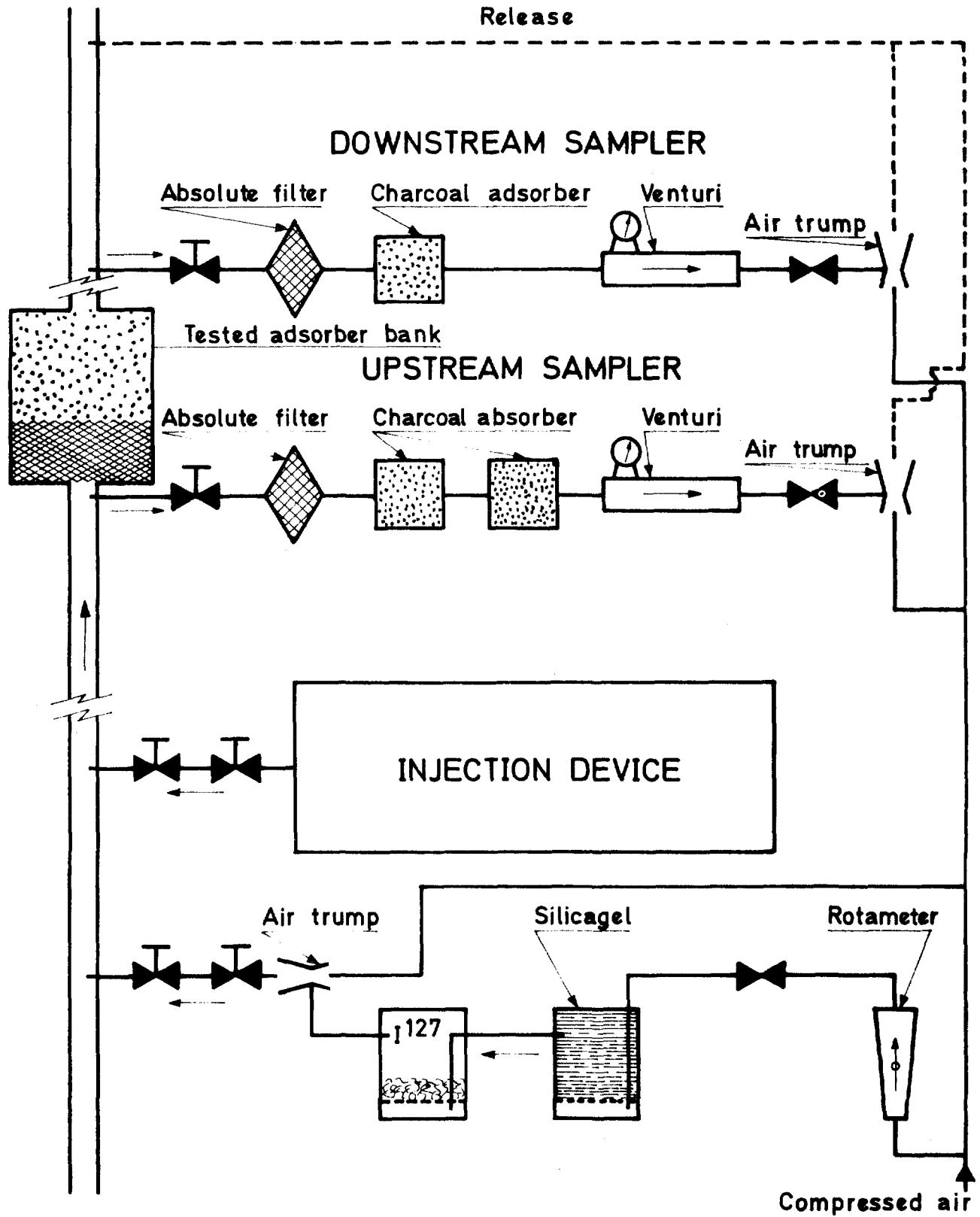
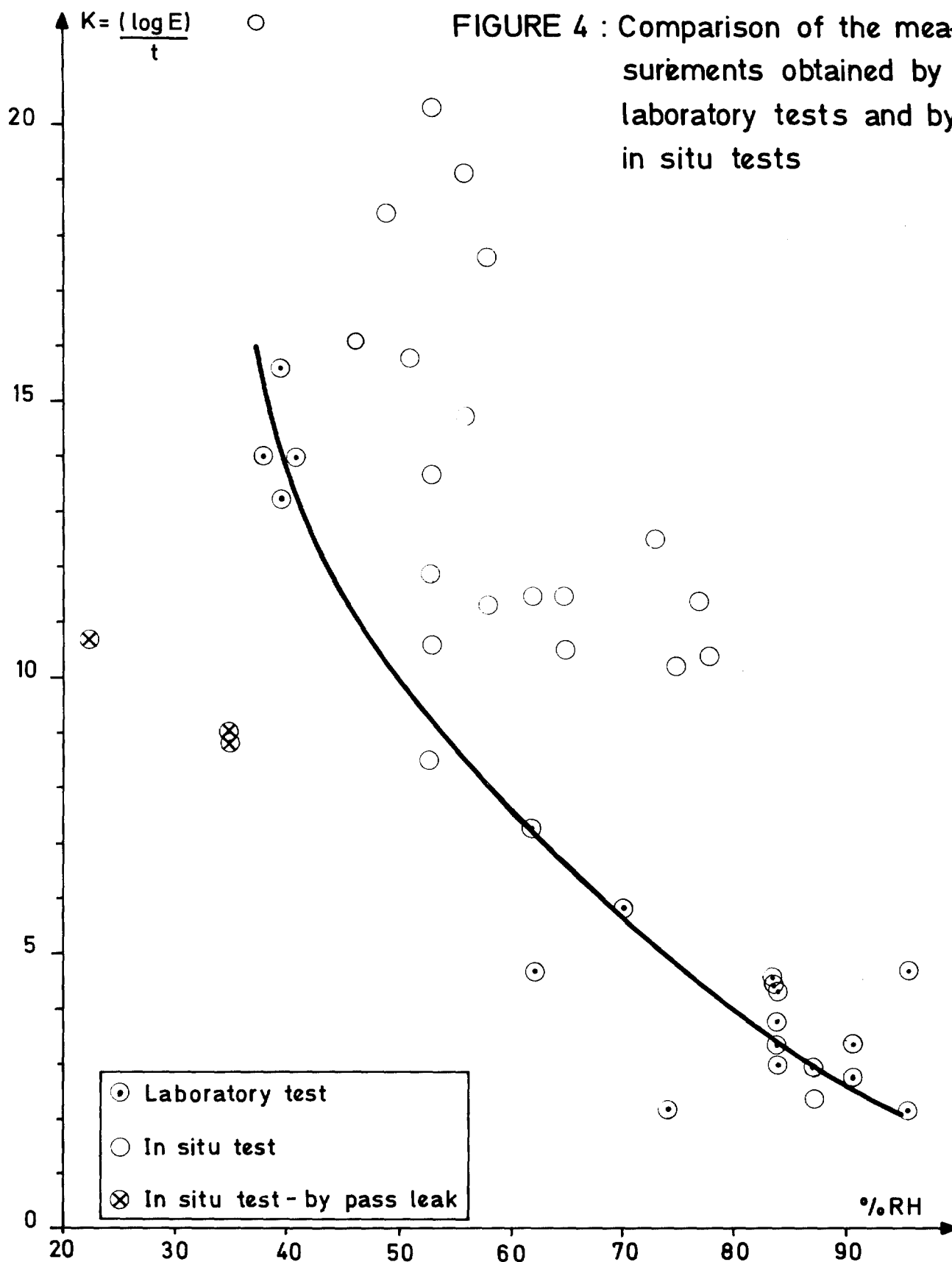


FIGURE 3 : Typical arrangement for testing an installed adsorber bank.

FIGURE 4 : Comparison of the measurements obtained by laboratory tests and by in situ tests



DISCUSSION

WILHELM: Did you ever try to test large charcoal units under controlled conditions and compare this with the results of the laboratory tests also under controlled conditions? I mean could you perform a kind of an in-situ test under well controlled conditions?

DECKERS: We cannot control conditions during the in-situ test, but in-situ tests have been performed over a wide range of relative humidities and at about the same residence time as during laboratory tests.

WILHELM: There is definitely a difference between your results under presumed equal conditions. We applied your method for full scale and bench scale adsorbers and we got the same results for both adsorbers. There was no scale-up factor. I think that different humidity conditions and different percentages of adsorbed water existed between the in-situ filters and the laboratory test beds.

DECKERS: In the space between primary and secondary containment, the relative humidity was very constant due to the confinement. Therefore, it was nearly equivalent to a controlled atmosphere. Due to the fact that the adsorbents were in this atmosphere, it seemed that 6 hours of operation was sufficient to obtain hygrometric equilibrium. However, it is possible that it was not the case.

HEAD-END IODINE REMOVAL FROM A REPROCESSING PLANT
WITH A SOLID SORBENT

J.G. Wilhelm, J. Furrer
Laboratorium für Aerosolphysik und Filtertechnik
Gesellschaft für Kernforschung mbH, Karlsruhe (GfK)

E. Schultes
Gesellschaft zur Wiederaufarbeitung von Kernbrennstoffen mbH (WAK)

Abstract

In the first large-scale reprocessing plant planned in the Federal Republic of Germany a total amount of 580 kg of iodine per annum will be released in the fuel dissolution process for a maximum heavy metal throughput of 1800 tons per year and 40,000 MWd/t of burnup. The main portion of the iodine is formed by the ^{129}I ($T_{1/2} = 1.6 \times 10^7$ a) isotope of which 82 Ci at the maximum are released every year. With the scheduled fuel element storage time of > 220 d the simultaneous release of ^{131}I is < 12.5 Ci the mass of which does not play any part.

If the off-gases were released from the dissolver in the absence of iodine removal, long-term contamination by ^{129}I of the environment would have to be expected, which would increase with continued operation. Besides, Kr separation from the off-gas, which is to be carried out in a large-scale reprocessing plant, calls for preliminary removal of the iodine.

According to the computer model presently imposed in the Federal Republic of Germany for treatment of the environmental impact by radioiodine, a total decontamination factor of 340 must be attained. This implies a long-term diffusion factor of 1×10^{-7} s/m³ for releases via the stack of the reprocessing plant and a limit value of 50 mrem/a at the maximum for the thyroid dose to the critical group of the population via the ingestion path.

The target of current R & D work is an iodine filter attaining for safety reasons a decontamination factor higher by the factor of 10, viz. 3400. This filter is so designed that it is capable of adsorbing the total amount of iodine from the fuel. In the loaded iodine filters the iodine occurs in a solid, nearly insoluble form suitable for transportation so that no further processing steps are required.

The amount of radioiodine carried over into the process solutions of a reprocessing plant should be as low as possible. If this condition is fulfilled, filtering for iodine of the vessel off-gases and of the off-gases originating in the solidification process of radioactive waste might not be necessary. Laboratory tests as well as measurements performed in the Karlsruhe Reprocessing Plant have shown that a fraction > 99.5 % of the iodine inventory can be transferred from the fuel solution into the dissolver off-gas.

In this report the flowsheet for dissolver off-gas cleaning in a reprocessing plant employing solid iodine sorption material and the arrangement of filter components are discussed. The principle of an iodine sorption filter is described which allows exhaustive loading of the iodine sorption material. The removal reactions of different organic iodine compounds and the loading capacity and removal efficiency of the iodine sorption material in the original dissolver off-gases of reprocessing plants are indicated. Studies on the influence of filter poisons are reported.

14th ERDA AIR CLEANING CONFERENCE

Operating experience gathered with a first iodine sorption filter in operation is discussed; this filter has been used to remove practically all iodine produced in the dissolver off-gas of the Karlsruhe Reprocessing Pilot Plant (WAK).

Direct measurement of ^{129}I in samples of filter material using a low energy photon spectrometer is briefly reported.

I. Introduction

In the first large-scale reprocessing plant planned in the Federal Republic of Germany a total amount of 580 kg of iodine per annum will be released in the fuel dissolution process for a maximum heavy metal throughput of 1800 tons per year and 40,000 Mwd/t of burnup. The main portion of the iodine is formed by the ^{129}I ($T_{1/2} = 1.6 \times 10^7$ a) isotope of which 82 Ci at the maximum are released every year. With the scheduled fuel element storage time of ≥ 220 d the simultaneous release of ^{131}I is ≤ 12.5 Ci the mass of which does not play any part.

If the off-gases were released from the dissolver in the absence of iodine removal, long-term contamination by ^{129}I of the environment would have to be expected, which would increase with continued operation.

II. Decontamination Factors Required for Iodine Removal

Since at present adequate data are not available on the dilution of radioactive iodine from the exhaust air with the inactive natural iodine occurring in the atmosphere and in the environment of the reprocessing plant, the relatively high dose ingestion factor for infants of 2×10^6 rem \times m³/Ci \times s is used to calculate the thyroid dose of the critical group of population. When this value is used the calculated thyroid burden by ^{129}I largely exceeds that caused by ^{131}I (calculated on the basis of a dose ingestion factor of 4.4×10^5 rem \times m³/Ci \times s and a cooling time of ≥ 220 d for the spent fuel) and determines to a considerable extent the requirements to the total decontamination factor for radioiodine of a plant. This value is 340 taking into account the data indicated above, a long-term diffusion factor of 1×10^{-7} s/m³ for the iodine release via the stack, the occurrence of all the radioiodine in its elemental form, and a tolerable thyroid burden of 50 mrem/a of the critical group of population via the ingestion path.

If provisions are made for Kr removal from the dissolver off-gas, iodine must be removed with a high removal efficiency ($> 99\%$), independent of the previous considerations, so that the subsequent process steps for Kr removal are not interfered with.

Present R & D work concentrates on the construction of an iodine filter for a reprocessing plant of the size stated in the introduction. For safety reasons the decontamination factor of the filter will be at least 10 times higher than required by Radiation Protection Regulations for the total decontamination factor of the plant.

Therefore, the filters are to provide a decontamination factor > 3400 and be so designed that the total iodine produced in the fuel can be removed. Taking into account the expected volume of off-gas and the wish to achieve the maximum possible loading capacity of the iodine sorption filter and to minimize the number of filter replacements, we obtain a filter design by which a much higher decontamination can be expected than required for reasons of radiation protection.

III. Removal of Aerosols - Concept of Procedure

The aerosol activity mainly originates in the shears and in the dissolver. Suitable layout of the dissolver vapor room and conduction of the sweep gas are to assure that the dust generated during fuel element cutting is separated by sedimentation in the vapor room and likewise dissolved by nitric acid.

Boiling and stirring of the fuel solution in the dissolver generates droplet aerosols whose particle diameters should be mainly above 10 μm .

On account of condensation processes and dilution in the condenser and in the NO_2 absorption and I_2 desorption columns the fuel fraction in the droplet aerosols occurring in the off-gas of individual process steps can be expected to decrease with distance to the dissolver.

The aerosol removal facilities downstream of the desorption column were selected under the following aspects:

1. Droplet aerosols must be removed as much as possible quantitatively in such a way that the liquid can be returned into the process. The fraction of aerosols removed by the HEPA - filters and consequently not eligible for recycling should be as low as possible.

2. To maintain high removal efficiencies over extended operating periods only solid aerosols should be removed by the HEPA - filters; droplet aerosols should be separated previously by appropriate devices. Droplet aerosols passing the droplet and moisture separator should have a low diameter so that they can be easily transformed into solid aerosols by heating and evaporation.

3. If possible, the iodine filter should not be exposed to radioactive aerosols so that the filter can be most conveniently handled after loading without requiring additional shielding.

Fig. 1 shows a flowsheet of the aerosol and iodine filter arrangement which is investigated under the simulated off-gas conditions of a large-scale reprocessing plant.

Fig. 2 shows the components of head end off-gas treatment in a large reprocessing plant.

IV. Position of the Filter Train in the Flowsheet

If measurements at the test benches show that the aerosol concentration in the dissolver off-gas can be kept low, that aerosol removal safely performs also at higher NO_x -concentrations, and that the removal of droplets leads to a sufficient reduction in aerosol off-gas activity, the use of the iodine sorption filter and of the other components of the filter section, even upstream of the NO_2 absorption column for acid recovery, should be discussed (Fig. 2). By iodine removal directly from the dissolver off-gas stream before the off-gas is washed, off-gas treatment could be substantially simplified, since

1. the iodine from the recovered acid must no longer be volatilized which means that the expensive desorption step is avoided;

2. the concentration of the recovered acid might be increased by evaporation without release of residual iodine;

3. alternative methods have not to be developed to increase the concentration of the recovered acid, which would exclude an evaporation step.

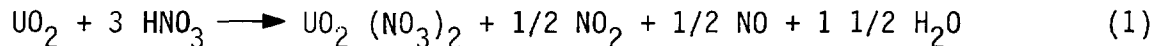
The efficiency of droplet removal is decisive for the expenditure required in the subsequent stages of off-gas treatment, and therefore it must be the topic of detailed future investigations.

It was shown in laboratory tests and removal tests performed with the off-gas of reprocessing plants that the planned iodine sorption filter can be installed both upstream and downstream of the NO₂ absorption column in case that the AC 6120 iodine sorption material is used.

V. Fission Product Iodine Volatilization from the Fuel Solution

To avoid that iodine released from the fuel gets distributed in the process solutions of the reprocessing plant, the total iodine should be volatilized as completely as possible from the fuel solution already in the dissolver. This avoids and minimizes, respectively, the iodine release of the individual process steps including vitrification of high level wastes intended for ultimate storage.

For fission product iodine volatilization from the fuel solution a value of > 99 % can be assumed. Iodine, in the form of iodate, cannot be volatilized. By dissolution of UO₂ in nitric acid according to the formula



sufficient amounts of NO are produced to reduce iodate to elemental iodine. If necessary, NO or nitrite can be added⁽¹⁾.

The volatilization of elemental iodine is decisively determined by the distillation rate of the acid from the dissolver during the process of dissolution. Based on experimental work and experience gathered with the Karlsruhe Reprocessing Plant (residual iodine in the feed solution < 0.5 %⁽⁷⁾) fission product iodine can be expected to be volatilized almost completely from the fuel solution. Part of the residual iodine contained in the fuel solution will be present in the vessel off-gas system. Since radiochemical reactions of tributyl phosphate, its decay products, and dodecane give rise to quite a number of organic compounds susceptible to reacting with iodine, it can be expected that in the vessel off-gas the percentage is high of organic compounds contained in total iodine release. Besides, filter pollutants occur which are an additional handicap to removal.

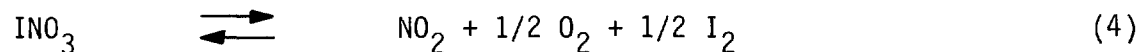
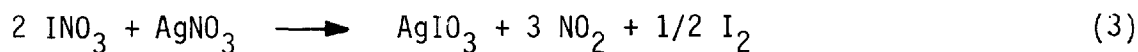
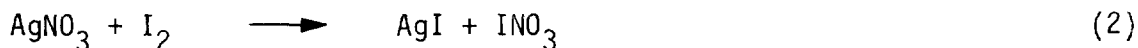
VI. Fission Product Iodine Removal by Solid AC 6120 Iodine Sorption Material

As an alternative to wet washing of dissolver off-gases the total fission product iodine can be directly removed by a solid sorption material. Since the off-gases contain NO_x, only inorganic iodine sorption materials such as molecular sieves and impregnated inorganic carrier materials can be used. Activated carbon is ruled out because of the risk of poisoning and ignition. Fission product iodine removal by solid sorption materials offers major advantages in cases where

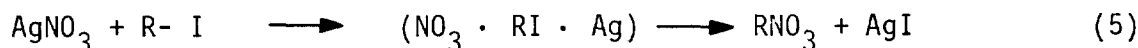
1. high removal efficiencies can be achieved with the sorption material;
2. the fission product iodine is removed in a form immediately suitable for storage so that further treatment steps can be avoided;

3. the filters are designed in a simple and reliable way and can be replaced by remote handling.

The AC 6120 iodine sorption material, in a new highly impregnated version, namely AC 6120/H₁, largely satisfies the conditions enumerated above. This material is now being produced and marketed on an industrial scale. The removal of fission product iodine is due to the conversion of the AgNO₃ impregnation into the hardly dissolvable silver iodide and silver iodate, respectively^(2,3):



Methyl iodide and other alkyl halides enter into reactions with the silver nitrate impregnation to become silver iodide as well, following the equation⁽⁴⁾



VII. Removal Efficiency of the AC 6120 Iodine Sorption Material

VII. 1 Laboratory Scale Tests

Comprehensive experimental data on the removal efficiency of AC 6120 have already been published⁽⁵⁾. Since it is intended to remove by AC 6120 the total iodine from the large reprocessing plant, the fraction of AgNO₃ impregnation was increased to get a higher loading capacity. The new high impregnation version AC 6120/H₁ contains 12 wt.% of Ag. Compared with the less impregnated AC 6120 this yields a slightly higher removal efficiency in the laboratory test (Tables I and II)

VII. 2 Tests Performed with the Dissolver Off-gas of SAP Marcoule

In the process of KNK fuel element dissolution, samples were taken with a sampler of the off-gas upstream and downstream of an AC 6120/H₁ test bed installed in the dissolver off-gas line. For this purpose shortly cooled EL-4 fuel was added which contained high ¹³¹I fractions. To achieve high iodine loading of the test bed, K¹²⁷I was added to the fuel solution in the dissolver. Every sampler was provided with 4 successive AC 6120 beds of 2.5 cm depth, the residence time of the off-gas in the samplers was about 0.6 s. The filter box with the test beds and the aerosol filters was coupled alternatively downstream of the dissolver and of the NO₂ absorption column of the dissolver off-gas line. In the removal tests the whole dissolver off-gas was passed over the aerosol filters and over the iodine sorption material.

In the first removal test the test beds were loaded downstream of the NO₂ absorption column over a period of 2 hours during dissolution. About 3 m³ of off-gas (1.5 m³/h) were passed over the filter system.

Integral measurement of the removal efficiency during sampling for the ¹³¹I activity of the fission product iodine at 150°C and 35 cm bed depth yielded 99.998 % for a residence time of 1.6 s.

In the second removal test the test bed was placed upstream of the NO₂ absorption column. The filter was loaded from the beginning of HNO₃ boiling until

the process of dissolution was terminated. The sorption material already used in test No. 1 was further loaded by iodine in this removal test. 10.5 m^3 ($1.5 \text{ m}^3/\text{h}$) of dissolver off-gas were passed over the filter section during a 7 hours period.

Integral measurement of the removal efficiency at 150°C and with the bed depth and residence time indicated above yielded 99.9992 %. This value was also measured via the ^{131}I activity removed by the upstream and downstream samplers.

The difference in penetration, 2×10^{-3} as compared to 8×10^{-4} %, is within the experimental accuracy and does not allow to draw conclusions as to the differences in removal efficiencies of the AC 6120/ H_1 test bed as a function of preconditioning of the dissolver off-gas.

The results of these and other removal tests have been presented in Table III. Fig. 3 shows the removal profiles of the upstream samplers for the tests Nos. 2, 7, 5, and 6.

Fig. 4 shows a test rig installed at WAK, which allows to continue the investigations of iodine sorption materials. A set-up similar to this test rig was used for the investigations at SAP Marcoule.

VII. 3 Operating Behavior of an Iodine Sorption Filter Used to Clean the WAK Dissolver Off-gases

Complying with requirements by the authorities an iodine sorption filter made up of AC 6120 was installed at WAK in September 1975 which provides for cleaning of the dissolver off-gas during operation. Fig. 5 shows a flowsheet of the WAK off-gas cleaning system and of the sampling points for control of the iodine sorption filter. The filter bed consisted of 26 kg of low impregnation AC 6120 (7 % Ag) since at that time sufficient amounts of the high impregnation AC 6120/ H_1 material were not available. For an average volumetric flow of $148 \text{ m}^3/\text{h}$ of the dissolver off-gas the residence time was $1.0 \pm 0.4 \text{ s}$ at an operating temperature of 130°C . The NO_x concentration in the off-gas was $< 2 \text{ vol. } \%$; this value has been averaged over the whole period of dissolution. Short-term concentration peaks up to 20 vol.% of nitric oxides must be assumed. During the use of the iodine sorption filter LWR fuel was processed which had an average burnup of 25.000 MWd/t of uranium. More than 99.5 % of the fission product iodine contained in the fuel were transferred into the dissolver off-gas. At the end of dissolution only fractions $< 0.5 \%$ of the theoretical ^{129}I content of the fuel (calculated with the ORIGEN code (6)) were found in the feed solution(7).

The washing solution in the washer preceding the iodine sorption filter was from neutral up to 3 M of nitric acid and attained a removal efficiency of about 1 % for ^{129}I . The washing solution was returned by batches into the dissolver.

The decontamination factor of the iodine sorption filter was determined from the ratio of ^{129}I concentrations in the upstream and downstream gas and ranged from $1.0 + 0.4 \times 10^4$ to $2.0 + 0.5 \times 10^4$ over the whole 120 days of service life of the iodine filter. At the end of filter operation a fission product iodine mixture was removed with 172 mCi ^{129}I corresponding to a total iodine amount of about 1.3 kg I_2 . This is equivalent to about 60 % of the capacity of the iodine sorption filter.

Fig. 6 shows the removal profiles of upstream and downstream samplers used to monitor the iodine sorption filter installed in WAK. The ^{129}I activity was plotted over the number of successive individual beds. The samplers were provided with 8 successive 2.5 cm deep filter beds made of AC 6120 and exposed to a 220 l/h partial flow at $110 \pm 10^\circ\text{C}$. The residence time of the dissolver off-gas in a

sampler was about 1.6 s. Two different iodine compounds can be clearly distinguished in the removal profile of the upstream sampler represented in Fig. 6. They are retained with considerably differing removal efficiencies. In the filtered gas only the component is found which is more difficult to remove. At the time of sampling (Fig. 6) the iodine sorption filter had taken up about 70 mCi of ^{129}I corresponding to 24 % of the theoretical capacity. During the period of exposure of the sampler shown in the figure 420 kg of fuel with a theoretical ^{129}I content (according to the ORIGEN code) of 12 mCi had been dissolved.

Complying with a requirement of the licensing authority the iodine sorption filter was monitored without interruption over the whole period of operation and the samplers were replaced after dissolution of 3 to 5 fuel batches each containing 140 kg of fuel. After about 60 % of the silver in the iodine sorption filter had reacted with the fission product iodine, the filter was withdrawn according to the requirements. The surface dose rate of the filter was 80 mrem/h at the end of its service life.

So, the iodine sorption filter was dismantled after 120 days of use. AC 6120 had an excellent flow capacity and showed but slight yellow and grey shading.

All the ^{129}I determinations for the WAK iodine sorption filter were made by direct measurement with a Low Energy Photon Spectrometer (LEPS) after the accuracy and usefulness of the method had been proved by comparison with the results obtained with activation analysis. The agreement of measured values with the ^{129}I yields calculated using the ORIGEN code with a tolerance limit of 10 % can be considered as the experimental validation of the measurement technique.

VIII. Silver Consumption and Loading Capacity of Iodine Sorption Filters

Made of AC 6120/H₁

The consumption of silver is a decisive cost factor of the removal method described. It is attempted to achieve as much as possible a quantitative reaction of silver. According to the reaction equations (2) to (5) on page 5, 143 g of ^{129}I can be removed by 1 kg of AC 6120/H₁ when AgNO_3 reacts by 100 % with iodine.

Laboratory studies have shown that 75 - 94 % of silver in the impregnation react with iodine (see Tables IV to VII). Fig. 7 shows a removal profile obtained in the laboratory test for loading an AC 6120/H₁ filter bed with radioactively marked I_2 up to 58 % of its capacity, whose bed depth is the same as that planned for a large reprocessing plant. The plot shows the amount of iodine removed by each bed section and the penetration dependent on the bed depth and on the loading. The filter beds loaded with I_2 in the laboratory tests usually achieved a decontamination factor of the order of 10^4 up to some 60 % utilization of the loading capacity (measured for the total period of loading).

The iodine sorption filter used for cleaning during operation₄ of the dissolver off-gases from WAK yielded a decontamination factor of 10^4 after 60 % of the total silver had reacted with fission product iodine. This indicates that also in practical filter operation the reacted amount can be high.

With silver molecular sieves, type Linde 13 X Ag, a lower utilization of silver was measured in the laboratory under identical conditions. The reacted amount (Tables VIII and IX) ranged from 35 % (5 % NO_2 , 150°C) to 56,4 % (0 % NO_2 , 150°C). A comparison of the silver utilisation as a function of bed depth for the iodine sorption materials AC 6120/H₁ and MS 13 X Ag is also given in Fig. 15.

IX. Reaction of AC 6120 Iodine Sorption Material with Organic Iodine Compounds

Since in the off-gases of a reprocessing plant, in particular in the vessel off-gas, the presence of organic iodine compounds must be anticipated, the reaction behavior with respect to AC 6120 was investigated for a number of organic iodine compounds. Detailed investigations were made of the reactions of straight chain alkyl iodides $C_n H_{2n+1}I$ ($n = 1-12$), secondary and tertiary alkyl iodides (model substance: secondary and tertiary butyl iodide), alicyclic iodine compounds (model substance: iodine cyclohexane), side-chain substituted aromatic cyclic compounds (model substance: benzyl iodide) and ring substituted aromatic iodide compounds (model substance: iodobenzene) with AC 6120 under cover gas atmosphere. The reaction products were trapped in cooling traps and separated by gas chromatography. They were identified by determination of the retention time and, if necessary, by IR-spectrometric analysis in addition⁽⁸⁾.

Figs. 8 and 9 show some of the gas chromatograms of the model substances and their reaction products following the reaction in a 2.5 cm deep AC 6120 bed and with a residence time of 0.1 s. The reaction temperature was 150°C in the tests shown in Fig. 9. The iodine compounds and reaction products are given in Tab. X.

According to these tests on the removal of organic iodine compounds difficulties should not be encountered in iodine sorption with the inorganic AC 6120 sorption material in the off-gases of a reprocessing plant.

The primary alkyl iodides react with AC 6120 to become AgI and alkyl nitrates and into alkanes with a lower yield. The secondary alkyl iodides form AgI, alkenes and HNO_3 when they react with AC 6120. The tertiary alkyl iodides convert into AgI, alkenes and HNO_3 .

As for the primary alkyl iodides the reaction rate of the secondary and tertiary alkyl iodides decreases with the chain length. Tertiary alkyl iodides react much faster with AC 6120 than primary and secondary alkyl iodides.

Iodocyclohexane reacts with the $AgNO_3$ impregnation like a straight chain secondary alkyl iodide while forming AgI and cyclohexene. Like the primary alkyl iodides benzyl iodide reacts with $AgNO_3$ to become AgI and benzyl nitrate. Also at temperatures up to 180°C iodobenzene does not react with the $AgNO_3$ impregnation of AC 6120.

With respect to the German fuel reprocessing plant, it is not planned to use aromatic compounds in the extraction procedure. So it is not expected that aryl halides will occur in the exhaust air in quantities which would substantially impair the filter efficiency.

In case that the previous dissolution and extraction steps will be modified, aromatic substances, which are susceptible to iodination, should not be used.

X. Influence of Filter Pollutants on the AC 6120 Iodine Sorption MaterialX. 1 Behavior of AC 6120 with Respect to Dodecane and Tri-n-butyl Phosphate

When recycled acid is used the dissolver off-gases might contain small amounts of dodecane employed as the solvent and of tributyl phosphate and its decay products used as an extractant in the PUREX process.

In the vessel off-gas higher fractions of these organic pollutants must be expected; dodecane and radiolytic products of tributyl phosphate were detected. The reactions in air between AC 6120 and dodecane and tributyl phosphate, respectively, were investigated at the operating temperature provided for the iodine sorption filter.

The concentration was 1.9×10^{-2} g dodecane/l air and 6.1×10^{-3} g tributyl phosphate/l air while the residence time of the gas mixture in the iodine sorption bed was 0.4 s and the linear air velocity was 25 cm/s. The reaction products were detected by gas chromatographic analysis.

Dodecane was completely inert with respect to AC 6120. Tributyl phosphate was converted into a silver phosphate of not clarified structure. Butyl nitrate at low concentrations (< 5 % related to the total tributyl phosphate inventory) was determined by gas chromatography as a gaseous reaction product.

While AC 6120 in the NO_x carrying off-gas from the dissolver normally yielded but slight discoloration and no major reduction in removal efficiency as a result of the reaction with pollutants, AC 6120 used in the vessel off-gas underwent a very intensive grey-blue discoloration which was accompanied by a substantial reduction in removal efficiency and is attributable to a conversion of AgNO_3 of the impregnation resulting in Ag_2O . Part of the organic impurities in the vessel exhaust air acted as a reductant with respect to AgNO_3 of the impregnation.

X. 2 Regeneration of the AC 6120 Iodine Sorption Material after Poisoning in the Vessel Off-gas

It was observed that the discoloration resulting from vessel off-gas was eliminated by an NO_2 -air mixture flow and that at the same time the removal efficiency could be largely restored.

Fig. 10 shows the results of three laboratory tests (plots 1, 2 and 3) with AC 6120 previously exposed over 20 days to the vessel off-gas from a reprocessing plant.

Plot 1 shows the penetration of the poisoned AC 6120 test beds by $\text{CH}_3^{131}\text{I}$ in air (temperature 150°C , dew point 30°C , linear air velocity 25 cm/s). The penetration is very high with respect to fresh AC 6120 (plot 4). Plot 2 shows the penetration of AC 6120 after a regeneration period of 24 hours in a mixture of air and 2.5 % NO_2 . During exposure to methyl iodide the carrier gas was also NO_2 containing air. The other conditions are the same as indicated above.

Plot 3 shows the penetration of AC 6120 after a regeneration period of 21 h in air with 2.5 % NO_2 ; however, the apparatus and the adsorber material were flushed by NO_2 -free air over several hours. During exposure to methyl iodide only air (no NO_2 added) was used as the carrier gas in order to avoid the influence of NO_2 on the methyl iodide used as the test medium (other conditions as above).

Fig. 11 shows the results of two removal tests performed in the laboratory with AC 6120 previously exposed to dissolver off-gas over 20 days.

The conditions of the laboratory tests (the results of which have been represented by plots 1 and 2 in Fig. 11) correspond to that indicated for plots 1 and 2 of Fig. 10. Since the dissolver off-gas contains NO_2 and organic impurities of the gas stream are negligible only, poisoning as in the vessel off-gases is not expected. Accordingly, no regeneration effect can be observed in the removal

test performed in the laboratory when NO₂-bearing carrier gas is used.

The following conclusions can be drawn from the plots:

- AC 6120 is poisoned in the vessel off-gases in addition to iodine loading. By the action of NO₂ the effect of poisoning is largely cancelled (comparison of plots 1 and 3, Fig. 10).
- By a low NO₂ content in the off-gases to be filtered AC 6120 poisoning can be largely avoided. Lower penetration and longer service lives of the iodine filter can be expected as a result.
- Since NO₂ appears in the dissolver off-gases of a reprocessing plant, the off-gases from the vessel and from the dissolver could be mixed upstream of the iodine filter. However, this should be done only in case that the amounts of iodine in the vessel off-gases are so high that they must be removed and that by admixture of the vessel off-gases upstream of the filter the removal efficiency is not markedly reduced for the relatively high iodine amounts from the dissolver off-gases. If the iodine released from the fuel is to be removed as completely as possible with the help of the iodine sorption material (off-gas cleaning without iodine washer) separate iodine filtering is recommended for the dissolver and the vessel off-gases. Also the admixture of the NO₂-bearing dissolver off-gases, already cleaned in an iodine sorption filter, to the vessel off-gas upstream of the iodine sorption filter installed for the vessel off-gas is recommended.

X. 3 Influence of NO₂ and NO on the Removal Efficiency of Fresh AC 6120

The operating temperature provided for the iodine sorption filter is 150°C. This excludes condensation of nitric acid and a higher adsorption of nitric oxides on the iodine sorption material.

According to the reaction equation indicated above (4) it can be expected that the removal efficiency decreases with increasing NO₂ concentration. In high loading tests with I₂ and air as the carrier gas no systematic influence of NO₂ concentration on the removal efficiency was observed in the range under investigation up to 5 % of NO₂ (cf. Tables IV to VII).

In a test series investigating the influence of NO₂ concentration on CH₃¹³¹I removal an increase in penetration from 0.0004 to 0.003 % of a 10 cm deep test bed made of AC 6120 was found for an increase from 1 to 10 % in the NO₂ content of the carrier gas (air) (5).

Since the carrier gas in the off-gas section of the dissolver might be nitrogen in case of subsequent Kr removal by cryogenic distillation, the behavior of AC 6120/H₁ in N₂/NO_x mixtures was investigated in some laboratory tests. NO in pure nitrogen reduces to metallic silver the AgNO₃ impregnation of AC 6120/H₁. This results in a loss of removal efficiency. This reaction can be suppressed by the presence of NO₂.

XI. Design of Iodine Filters for a Large Reprocessing Plant

XI. 1 Layout

Fig. 1 is a flowsheet with the planned filter sections for a large reprocessing plant. The filter containing the AC 6120/H₁ iodine sorption material will be so designed that silver in the sorption material reacts as quantitatively

as possible with iodine. The number of filter stages required is determined by the iodine concentration gradient in the sorption material and by the necessity to use as completely as possible the sorption material to be discarded. The concentration gradient achievable is depending on the volumetric flow and the linear gas velocity, respectively. It is intended to use a 2-stage iodine filter whose first filter drum in the direction of flow is loaded by iodine until it becomes exhausted, while the second filter drum is loaded to a little extent only until breakthrough of the first drum occurs. After the filter drum loaded up to exhaustion has been withdrawn, the partially loaded filter drum is transferred into the first position in the direction of flow and loaded until exhaustion.

As an alternative a method is investigated which relies on fixed filter positions. A discontinuous migrating bed filter will be developed in case that the good ability to flow of the iodine sorption material at AC 6120/H₁ filters should be confirmed.

XI. 2 Requirement of Storage Space

If 100 % of throughput is attained in a large reprocessing plant, a filter must be replaced every 6 days. The filter elements directly fit into the iron-hooped drums used for radioactive waste. About 50 iron-hooped drums of 200 l capacity will be filled every year. This means that only little storage space is required. The behavior of iodine loaded AC 6120/H₁ in salt will be the subject of further investigations. In case that the requirements of leachability of fission product iodine will not be met in the ultimate storage facility, it is planned to cement into 400 l drums the 200 l iron-hooped drums containing AC 6120/H₁.

References:

- (1) E. Henrich et al., Jodbehandlung bei der Brennstoffauflösung, Reaktortagung 1976, Proceedings.
- (2) W.C. Schmidt, Treatment of Gaseous Effluents, TID-7534, p. 371 (1957).
- (3) K.C. Patil et al., The Silver Nitrate-Iodine Reaction: Iodine Nitrate as the Intermediate, J. Inorg. Nucl. Chem. 29, p. 407 (1967).
- (4) J.G. Wilhelm, H.G. Dillmann, K. Gerlach, H. Schüttelkopf, KFK 1565, p. 175 (1971).
- (5) J.G. Wilhelm, H. Schüttelkopf, An Inorganic Adsorber Material for Off-Gas Cleaning in Fuel Reprocessing Plants, CONF-720 823, p. 540 (1972).
- (6) M.J. Bell, ORNL Isotope Generation and Depletion Code, ORNL 4626 (1974).
- (7) Privat communication, H. Schüttelkopf, GfK.
- (8) J. Furrer, R. Kaempffer, Untersuchung der Reaktionen von organischen Jodverbindungen mit feinst auf amorpher Kieselsäure verteiltem Silbernitrat, Mh. Chem. Bd. 107/IV, p. 933-938 (1976).

Annex: Direct Measurement of ^{129}I with the Low Energy Photon Spectrometer

In the measurements performed to determine the decontamination factor of the WAK iodine sorption filter iodine-129 on the iodine samplers is measured in a non-destructive way by use of a Low Energy Photon Spectrometer (LEPS). After careful mixing of the filter material two 1 g samples each were taken from each filter bed, weighed into small glass flasks and analyzed. The mean value of the two single measurements was converted to the total bed weight and the result attributed to the respective filter bed. The direct measurement of ^{129}I in the filter material samples using LEPS is briefly described below.

Iodine-129 decays via β -decay with a maximum β -energy of 150 keV into an excited instable state of ^{129}Xe (Fig. 12). $T_{1/2}$ of ^{129}I is 1.6×10^7 a resulting in a correspondingly low specific activity of 0.176 mCi/g. The excited ^{129}Xe nucleus ($T_{1/2} = 10^{-9}$ s) deactivates into the stable ground state either spontaneously while emitting a 39.6 keV γ -quantum with an absolute intensity of 7.5 % or by internal conversion. As a result of internal conversion the $^{129}\text{-Xe}$ atom emits its characteristic X-rays whose energies and absolute intensities related to ^{129}I decay are represented in Fig. 12 together with the data on γ -radiation.

For direct ^{129}I detection all the five lines traced in Fig. 12 are appropriate. It should be noted in this context that the X-ray lines are not only specific to ^{129}Xe and hence to ^{129}I but that they can be generated also by other active iodine isotopes with mass numbers greater than 127 by β -decay into Xe and subsequent stabilization by internal conversion (e.g. ^{131}I).

For application in reprocessing of irradiated fuels this fact, however, does not imply a limitation since any interfering iodine isotopes are short-lived and also their parents are not long-lived. The only exception is iodine-131 with a half-life of 8 days, which must be taken into account for extremely short cooling periods (< 180 days).

If disturbing ^{131}I amounts must be expected, it is recommended to make the detection by means of the 39.6 keV γ -line which is specific to ^{129}Xe and hence to ^{129}I .

However, it appears from Fig. 12 that detection by the two intensive X-ray lines ($K\alpha_1$ and $K\alpha_2$) is about 8 times more sensitive than detection by the γ -line since the two X-ray lines are measured together and thus yield a 57 % decay probability as against 7.5 % of the γ -line.

To satisfy the special requirements of ^{129}I analysis in reprocessing irradiated nuclear fuels, the following conditions should be fulfilled by the detector:

1. Very high response for γ -quanta with energies between 20 and 40 keV.
2. Very high sensitive area.
3. Resolution better than 500 eV.
4. The response of the detector should be negligible for quanta with energies above 100 keV so that the disturbing background by Compton scattering of higher energetic γ -quanta can be kept low.

14th ERDA AIR CLEANING CONFERENCE

For this reason Low Energy Photon Spectrometers with planar horizontal Ge(Li) detectors were used, with the following characteristics:

Sensitive area	500 mm ²
Sensitive depth	7 mm
Window	0.5 mm Al
Resolution	< 0.5 keV at 60 keV
Response at 30 keV	~ 100 %

For the absolute calibration of detectors an NBS ¹²⁹I standard solution (SRM 4949) was used as a primary standard (Fig. 13). The ¹²⁹I loaded AC 6120 was calibrated against the NBS standard indicated above by means of activation analysis. The calibration curves are linear from the experimental detection limit at $\sim 2 \times 10^{-12}$ up to more than 10^{-7} Ci ¹²⁹I per ml or g AC 6120, both for measurements at the 39.6 keV- γ -line and for the more intensive sum peak of the $K\alpha_1$ and $K\alpha_2$ X-ray lines of ¹²⁹Xe.

Fig. 14 shows the spectrum of an AC 6120 sample loaded with 6.3×10^{-7} Ci ¹²⁹I in the WAK dissolver off-gas.

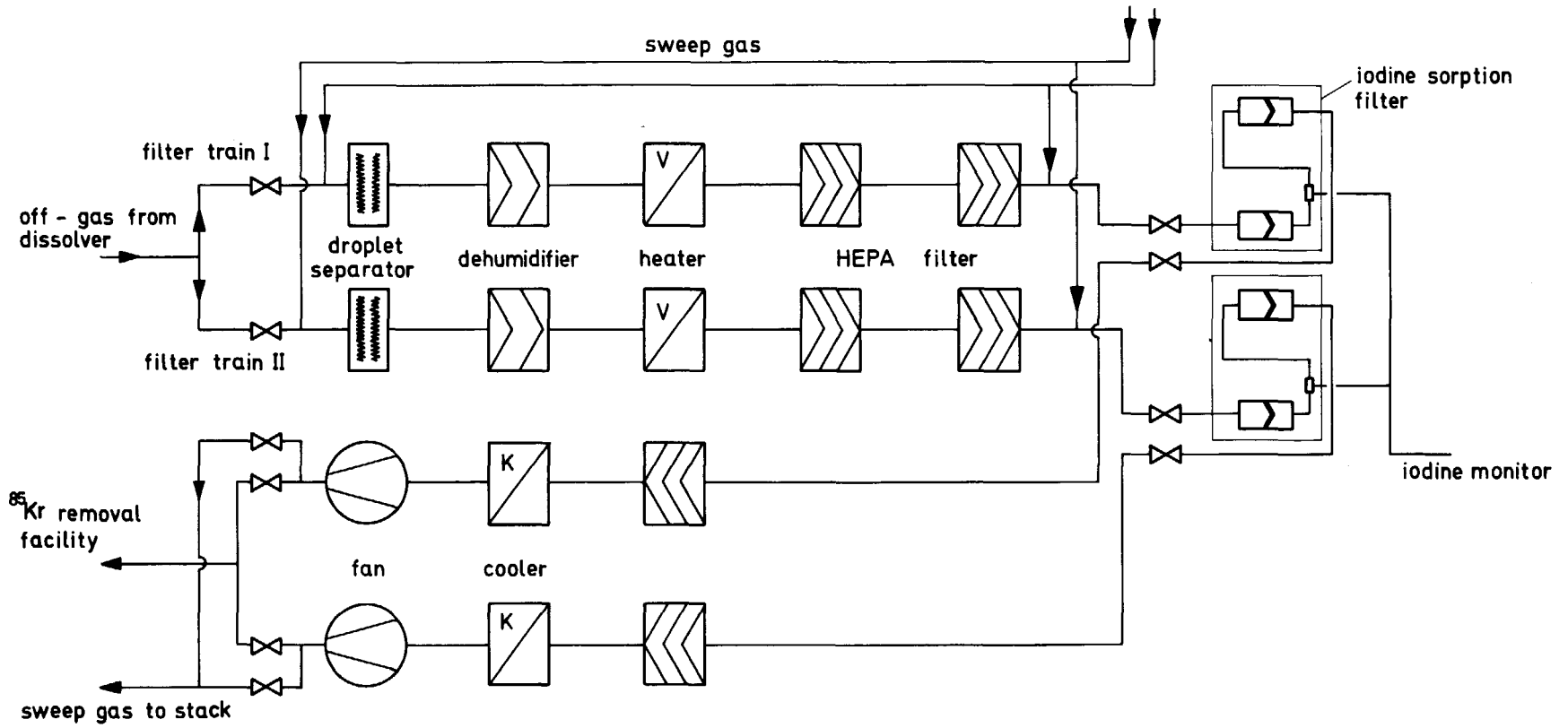


FIG. 1 Filter train for a large reprocessing plant

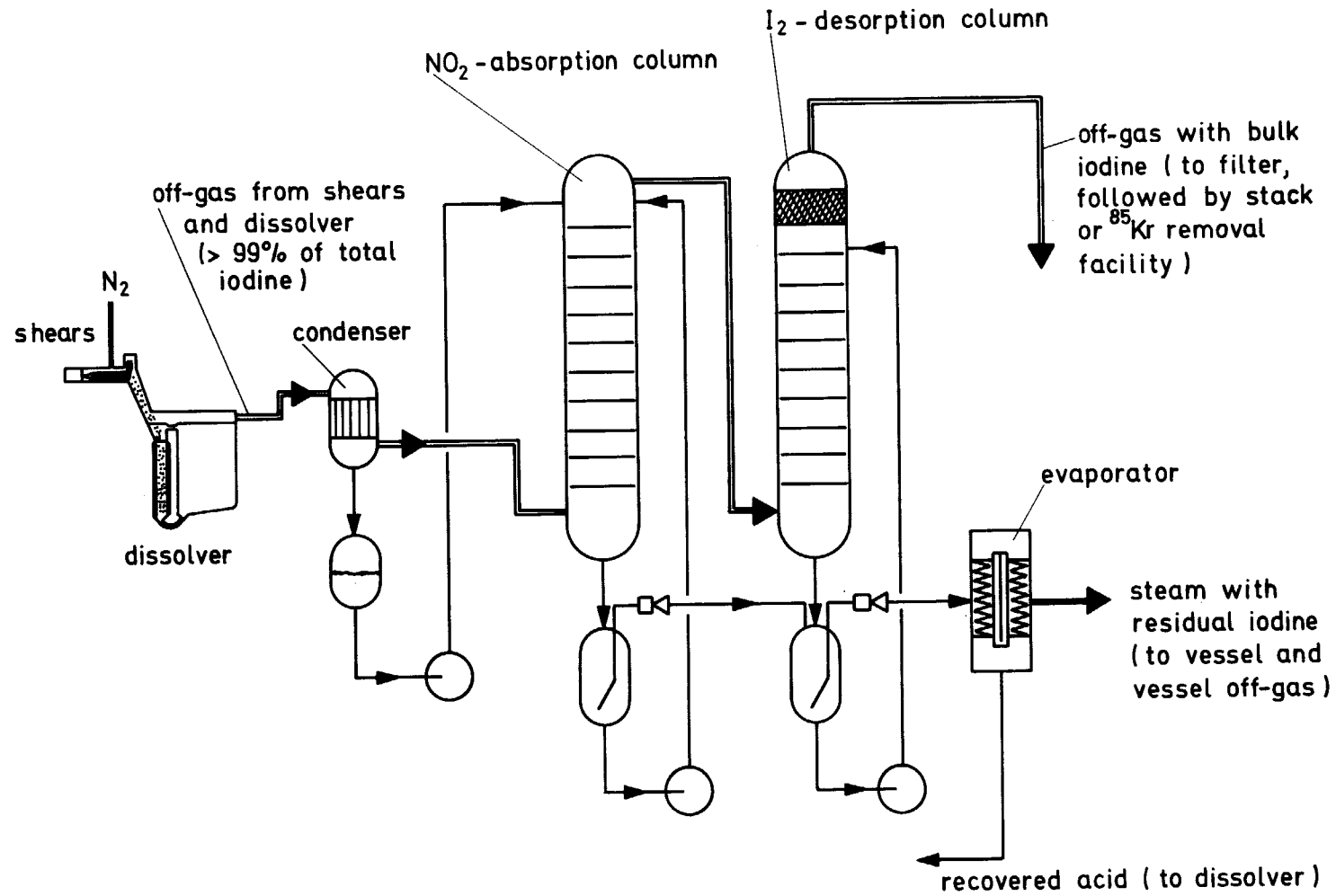


FIG. 2 Path of the fission product iodine in the head end of a reprocessing plant

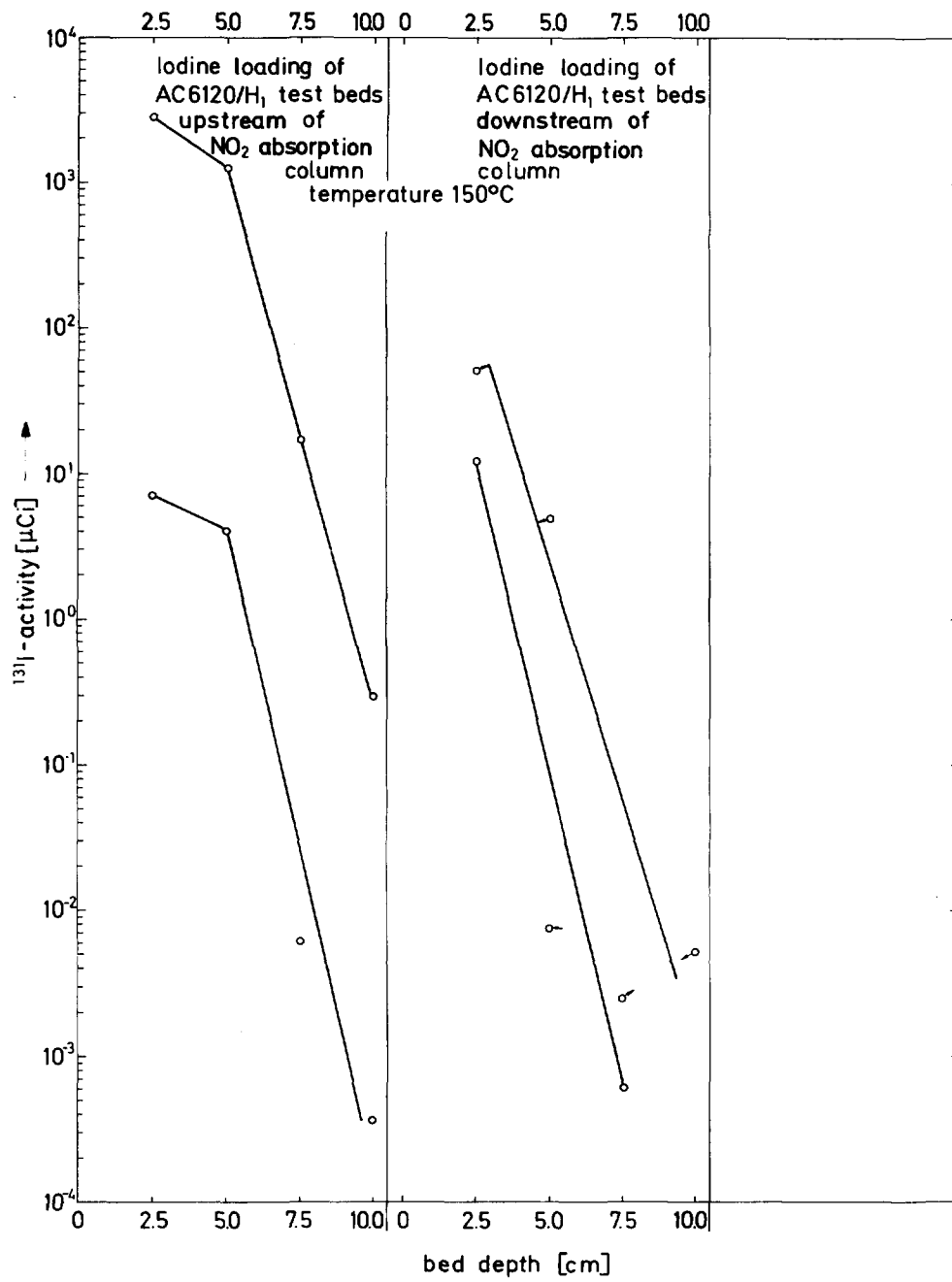


FIG. 3 iodine removal from dissolver off-gas by AC 6120/H₁

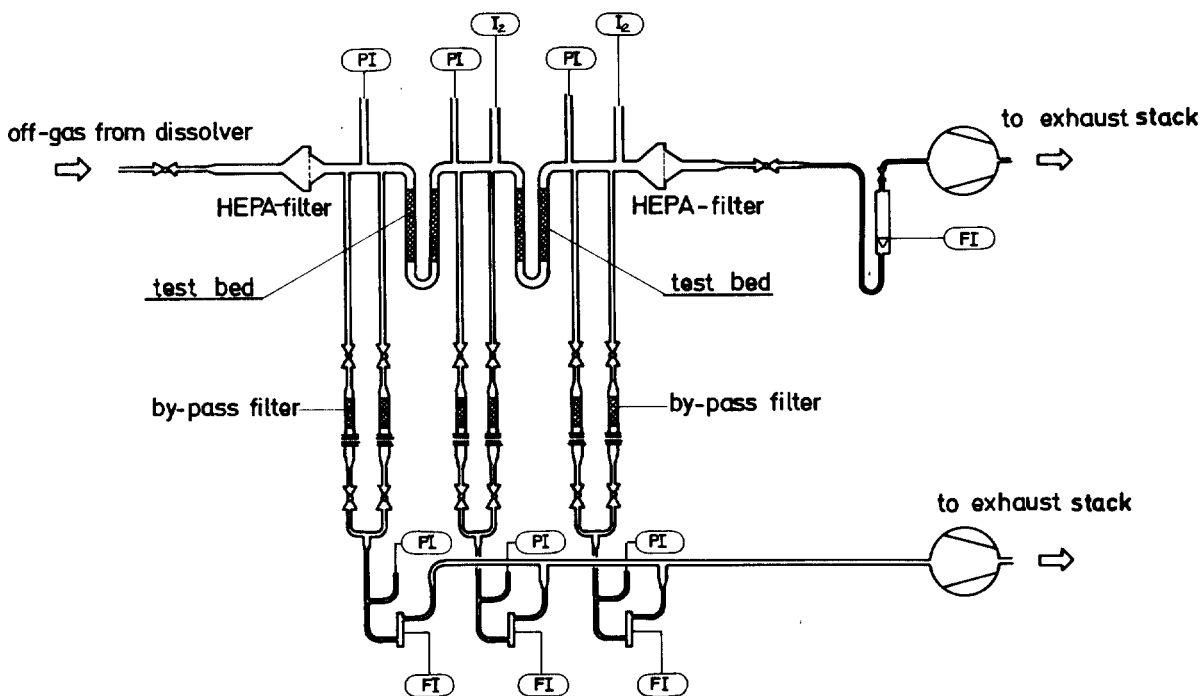


FIG. 4 Test rig for iodine sorption material in the dissolver off-gas of the Karlsruhe Reprocessing Plant (WAK).

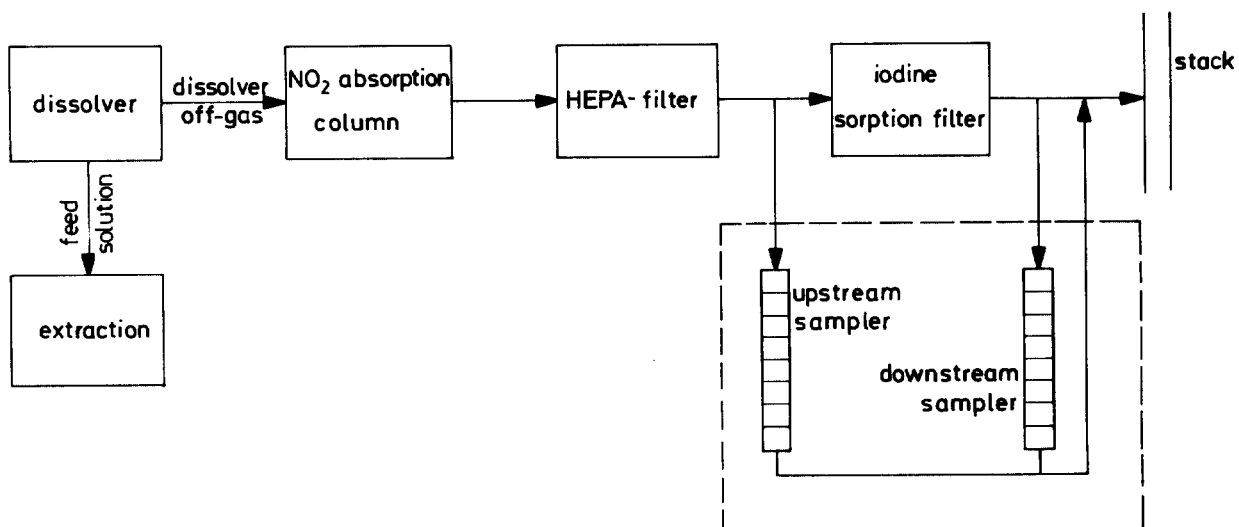


FIG. 5 Flow sheet of the WAK dissolver off-gas system

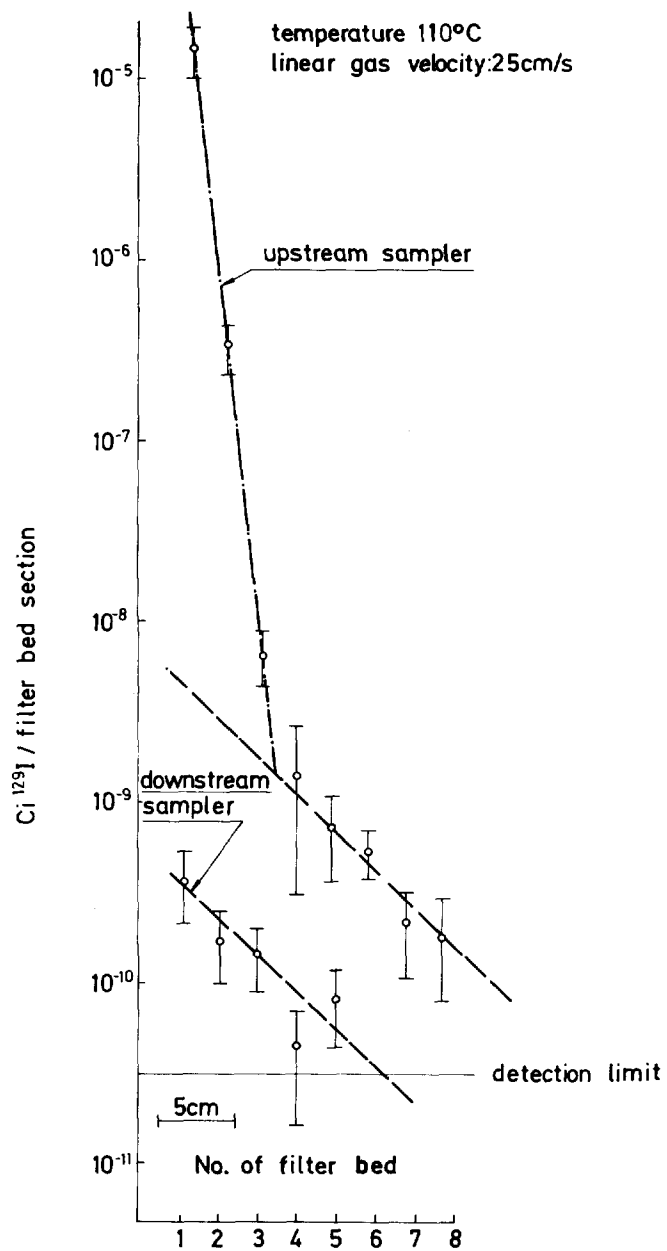


FIG. 6 Activity profile of ¹²⁹I in AC 6120 samplers upstream and downstream of the dissolver off-gas filter of WAK

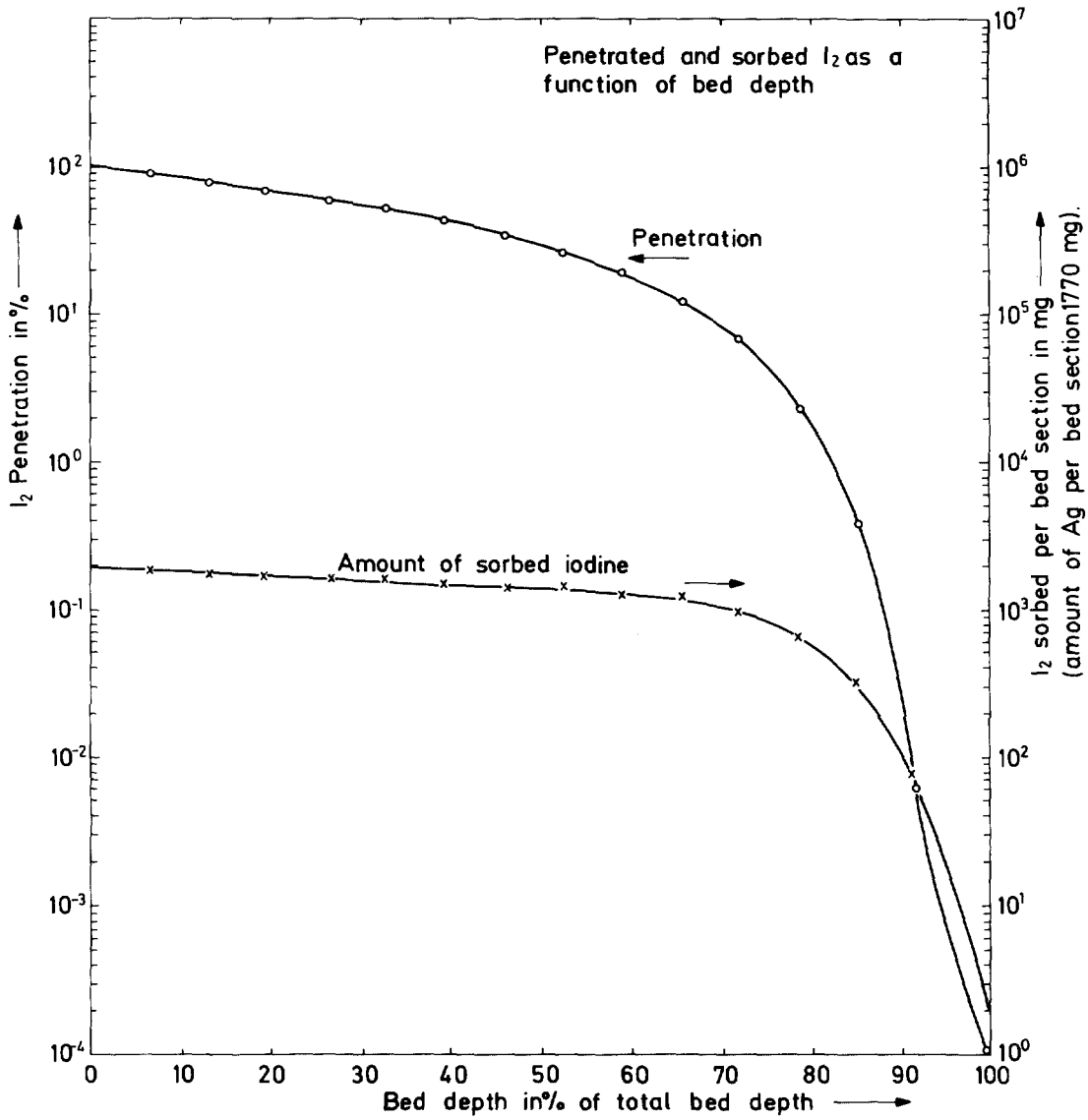


FIG. 7 Loading of AC 6120/H₁ test beds with large amounts of I₂

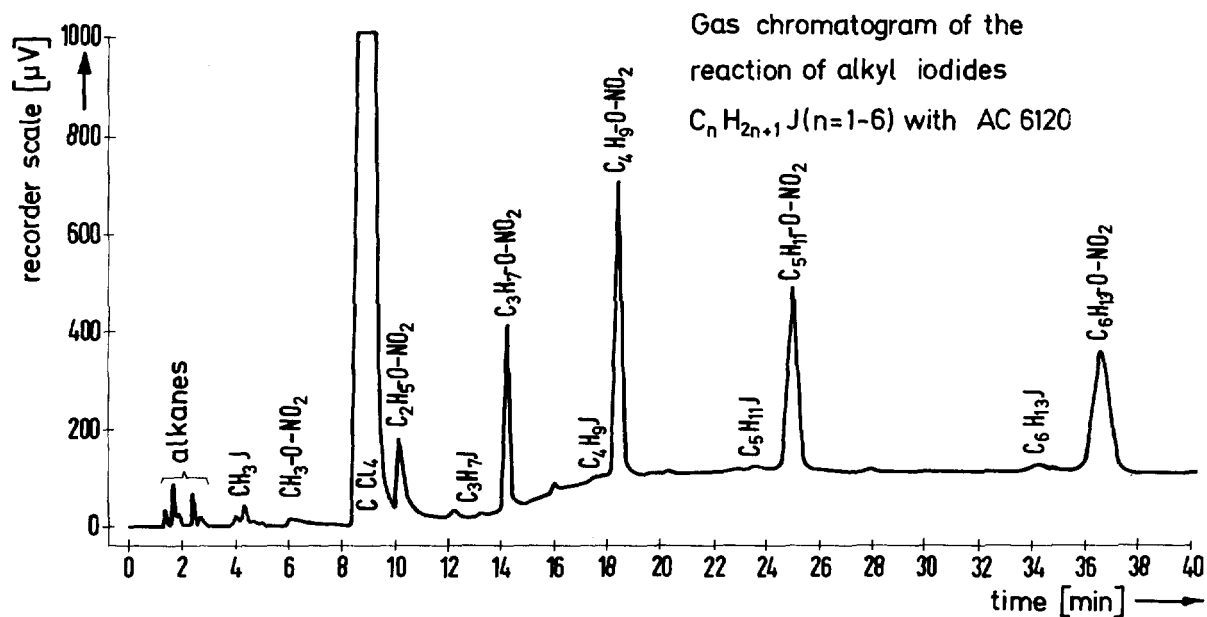
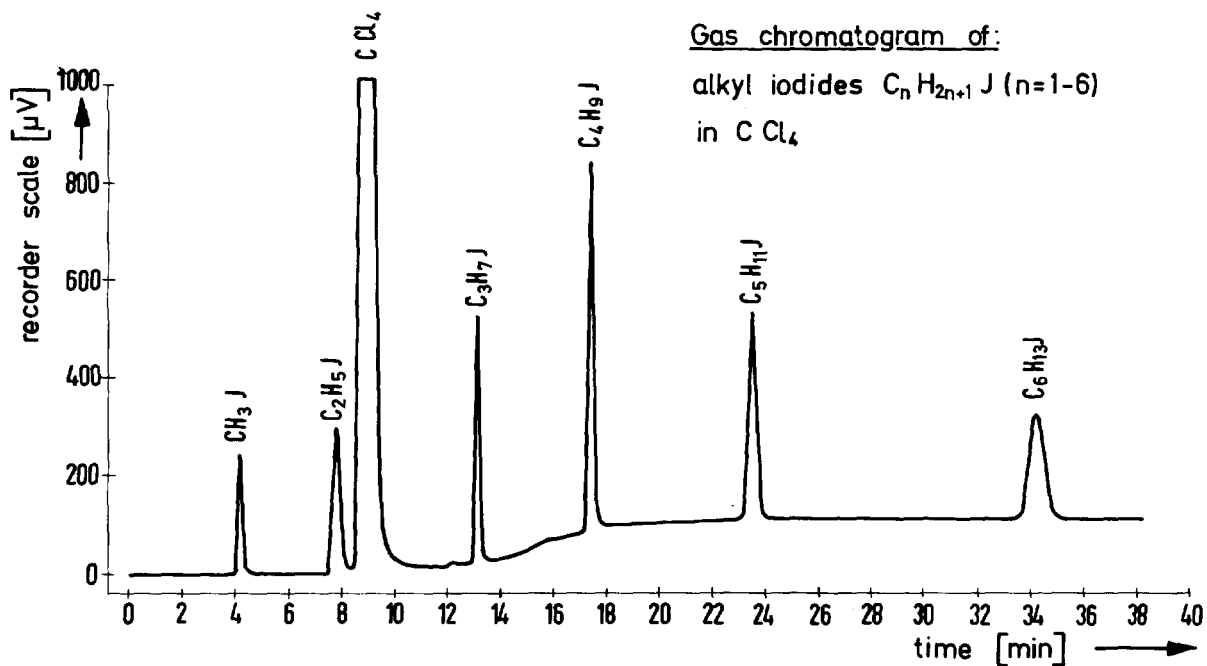


FIG. 8

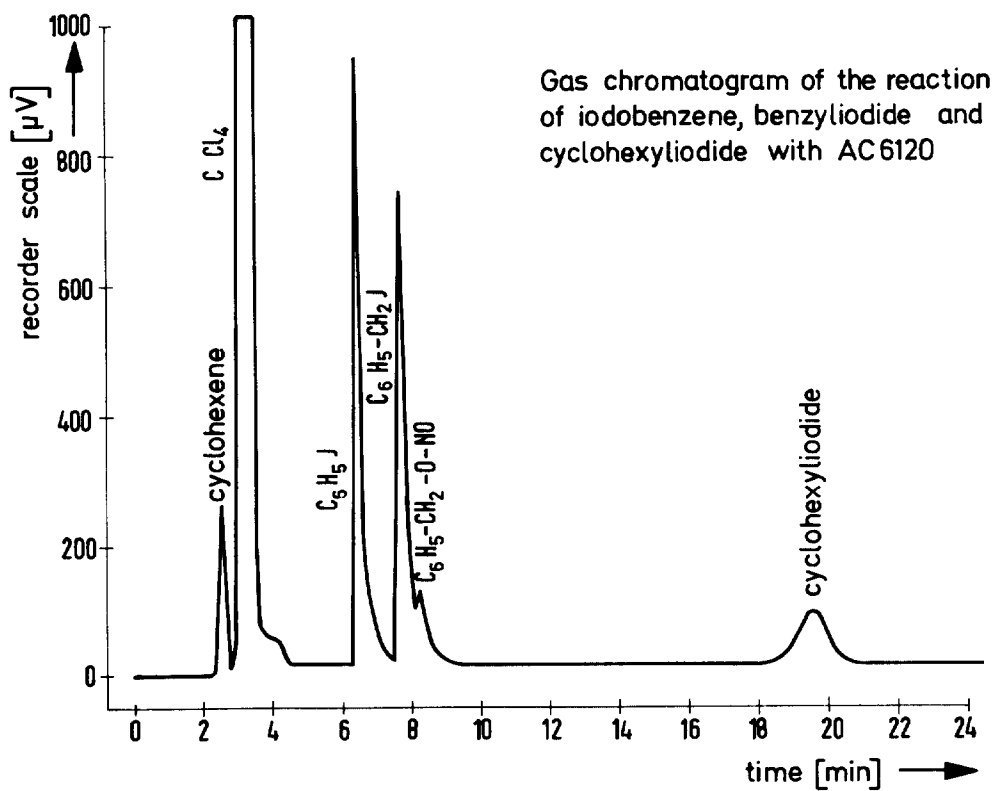
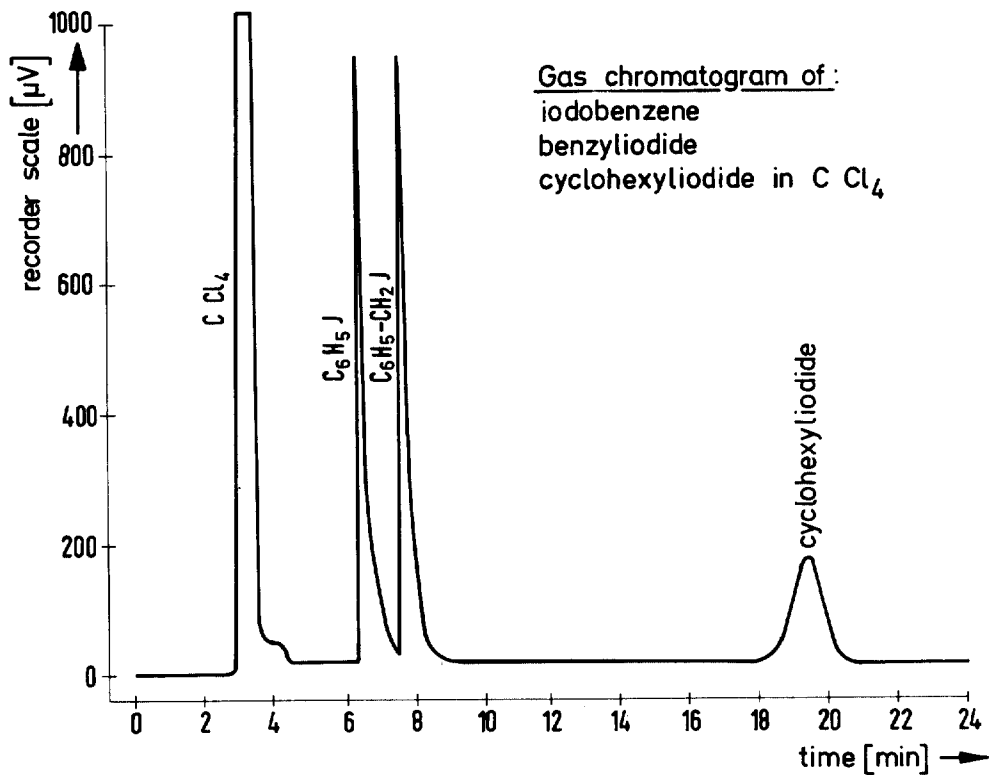


FIG. 9

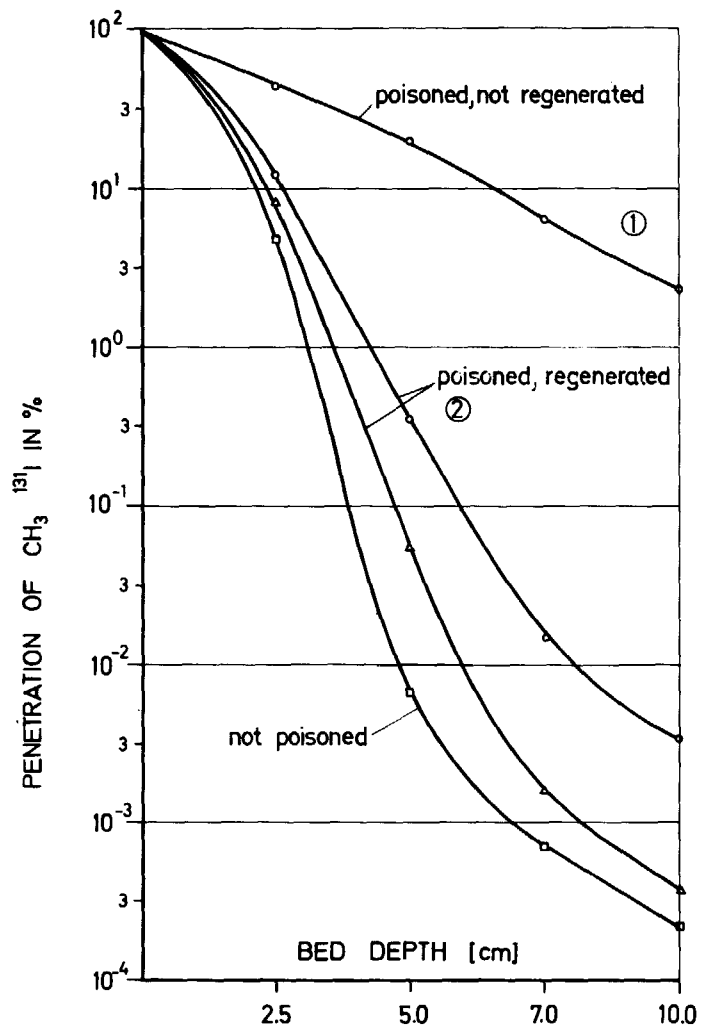


FIG. 10 Penetration of AC6120 test beds by $\text{CH}_3^{131}\text{I}$ after use in vessel off-gas and after regeneration with NO_2 .

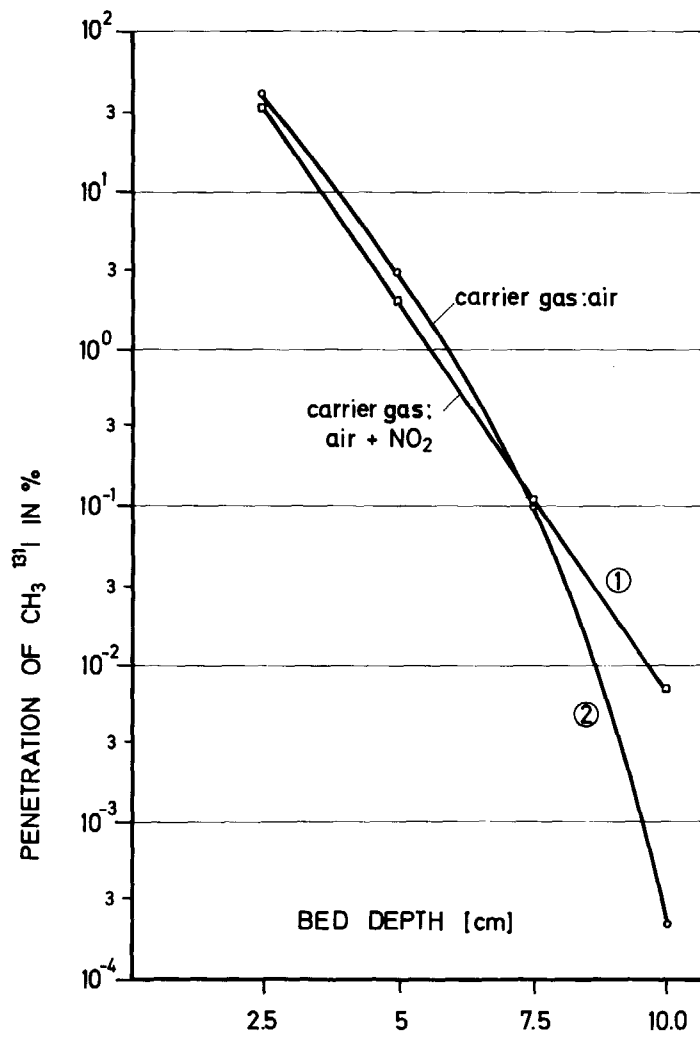
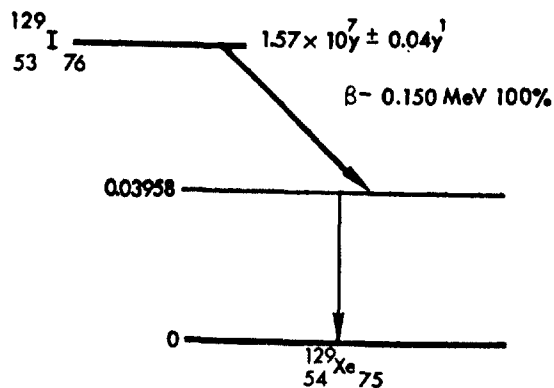


FIG. 11 Penetration of AC6120 test beds by $\text{CH}_3^{131}\text{I}$ after use in dissolver off-gas.

Notes on Iodine-129 (copied from NBS Certificate)

Decay Scheme



Radiation	Energy (MeV)	Intensity (%)	Relative Intensity to $K\alpha_1$	Conversion Coefficients	ω_K
γ	0.03958 ± 0.0003 (1)	7.52		α_K 10.5 $\alpha_{L.M}$ 1.8 α_T 12.3 (1)	
$x(K\alpha_1)$	0.02978	37.0	1		(4) 0.889 ± 0.020
$x(K\alpha_2)$	0.029458	19.9	0.537		
$x(K\beta_1^1)$	0.03360	10.8	0.292		
$x(K\beta_2^1)$	0.03442 (2)	2.4	0.064 (3)		
β^-	0.150 ± 0.005 (1)				

1. Nuclear Data Sheets, Vol. 8, No. 2, August, 1972.
2. NSRDS-NBS14: X-Ray Wavelengths and X-Ray Energy Levels.
3. Atomic Data, Nov., 1970.
4. Reviews of Modern Physics 44, 716, 1972.

FIG. 12

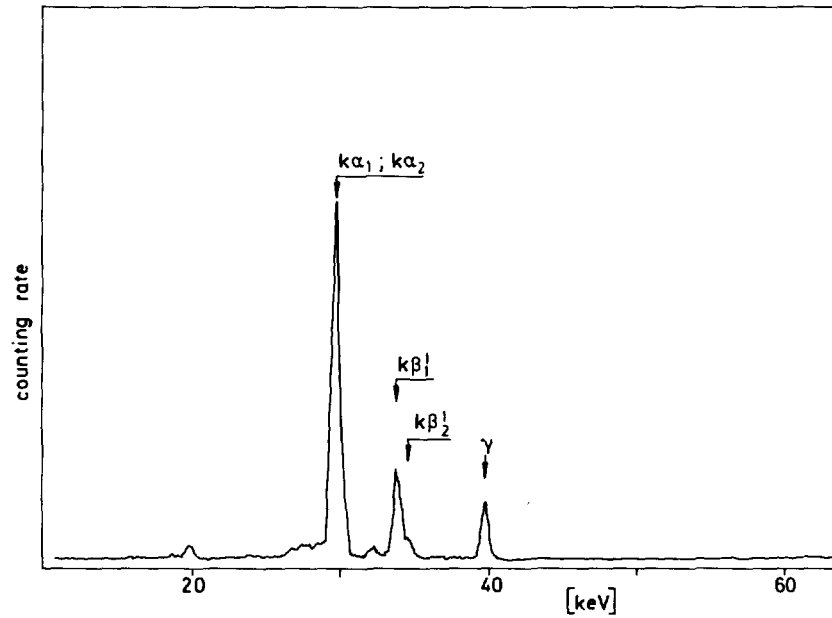


Fig. 13 γ /X-ray spectrum of 1 ml of NBS standard solution SRM 4949 with 2×10^{-8} Ci ^{129}I

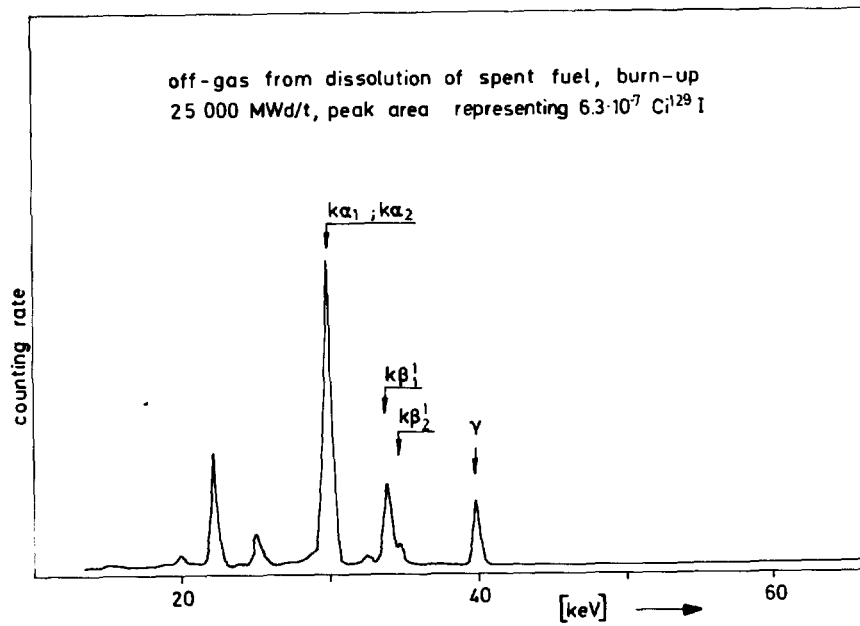


Fig. 14 γ /X-ray spectrum of an AC 6120 sample loaded with ^{129}I

14th ERDA AIR CLEANING CONFERENCE

Tab. I Removal of ^{131}I in form of $\text{CH}_3^{131}\text{I}$ by commercially produced AC 6120

Conditions:

Ag content of sorption material : 7 wt.%
 grain size : 1 - 2 mm
 Sweep gas : humid air, dew point: 30°C
 temperature of sweep gas and test bed: 150°C
 linear air velocity : 25 cm/s
 Loading : 1.1 mg $\text{CH}_3^{127}\text{I}$ + 6 μCi $\text{CH}_3^{131}\text{I}$ per g
 of AC 6120, loading period: 1 h

bed depth (cm)	2.5	5.0	7.5	10.0
residence time (s)	0.1	0.2	0.3	0.4
removal efficiency (%)	99.85	99.999	99.9995	99.9997

Tab. II Removal of ^{131}I in form of $\text{CH}_3^{131}\text{I}$ by commercially produced AC 6120/H₁

Conditions:

Ag content of sorption material : 12 wt.%
 grain size : 1 - 2 mm
 Sweep gas : humid air, dew point: 30°C
 temperature sweep gas and test bed: 150°C
 linear air velocity : 25 cm/s
 Loading : 1 mg $\text{CH}_3^{127}\text{I}$ + 5 μCi $\text{CH}_3^{131}\text{I}$ per g
 of AC 6120, loading period: 1 h

bed depth (cm)	2.5	5.0	7.5	10.0
residence time (s)	0.1	0.2	0.3	0.4
removal efficiency (%)	99.975	99.9956	99.9989	99.9998

14th ERDA AIR CLEANING CONFERENCE

Tab. III Removal of iodine from dissolver off-gas of SAP Marcoule by use of AC 6120/H₁

Bed depth: 35 cm, Temperature of off-gas and test bed: 150°C, residence time: 1.6 s.
 Concentration of iodine in dissolver off-gas, averaged over period of dissolution: ~ 4.5 g/m³

No.	loading time [h]	off-gas volume [m ³]	K ¹²⁷ I spiking of feed solution [g]	Position of test bed relativ to NO ₂ -absorption column ²	¹³¹ I-removal efficiency [%]
1	2	3	44.5	downstream	99.998
2	7 (9.0) ^{**}	10.5	42	upstream	99.9992
3	6.5 (15.5)	9.75	52	upstream	99.994
4	6.25(21.75)	9.4	0	downstream	99.995
5	8.5	12.75	52	downstream	99.96
6	8.5 (17.0)	12.75	52	downstream	99.996
7	6.75(23.75)	10.1	52	upstream	99.999
8	7.0 (30.75)	10.5	52	downstream	99.994

**) bracketed values: cumulative loading time of successive loading periods

Tab. IV Removal of iodine by an AC 6120/H₁ test bed of proposed bed depth for a large reprocessing plant. Sweep gas: humid air + 1 % NO₂, 150°C

Grain size of iodine sorption material: 1 - 2 mm
 dew point of humid air : 30°C, preconditioning: 20 h, loading period: 4 h
 sweep gas continued for an additional : 4 h. Loading 18.1 g I₂
 mixed with : 1.04 mCi ¹³¹I

data for accumulated bed depth			data for single section of test bed			
% of total bed depth	¹³¹ I removal efficiency [%]	I ₂ loading [mg]	No. of test bed section	I ₂ loading [mg]	reacted amount of Ag [mg]	Ag reacted in % of Ag inventory
6.6	10.9	1970	1.	1970	1680	87.7
13.1	22.0	3980	2.	2010	1710	89.3
19.7	33.0	5970	3.	1990	1690	88.4
26.3	44.0	7960	4.	1990	1690	88.4
32.9	55.0	9950	5.	1990	1690	88.4
39.5	65.7	11890	6.	1940	1650	86.0
46.0	75.6	13680	7.	1790	1520	80.1
52.6	84.0	15200	8.	1520	1290	67.5
59.2	91.2	16510	9.	1310	1110	57.9
65.8	96.5	17469	10.	959	815	42.6
72.3	99.4	17994	11.	525	446	23.3
78.9	99.9964	18099	12.	105	92	4.8
85.5	99.9994	18100	13.	0.5	0.4	0.02
92.1	99.9995	-	14.	+))	+))	+))
100.0	99.9998	-	15.	+))	+))	+))

+) falling below detection limit

14th ERDA AIR CLEANING CONFERENCE

Tab. V Removal of iodine by an AC 6120/H₁ test bed of proposed bed depth for a large reprocessing plant. Sweep gas: humid air + 2,5% NO₂, 150°C

Grain size of iodine sorption material: 1 - 2 mm
 dew point of humid air : 30°C, preconditioning: 20 h, loading period: 5 h
 sweep gas continued for an additional : 12 h. Loading 18.1 g I₂
 mixed with : 0.55 mCi ¹³¹I

data for accumulated bed depth			data for single section of test bed			
% of total bed depth	¹³¹ I removal efficiency [%]	I ₂ loading [mg]	No. of test bed section	I ₂ loading [mg]	reacted amount of Ag [mg]	Ag reacted in % of Ag inventory
6.6	11.4	2070	1.	2070	1760	94.3
13.1	22.5	4080	2.	2010	1710	91.6
19.7	33.4	6050	3.	1970	1670	89.7
26.3	44.0	7970	4.	1920	1630	87.5
32.9	54.1	9790	5.	1820	1540	82.7
39.5	63.5	11490	6.	1700	1450	77.5
46.0	72.3	13090	7.	1600	1360	72.8
52.6	80.1	14490	8.	1400	1190	63.9
59.2	86.8	15710	9.	1220	1040	55.7
65.8	92.2	16684	10.	974	828	44.4
72.3	96.0	17366	11.	682	580	31.1
78.9	98.3	17782	12.	416	354	19.0
85.5	99.5	18003	13.	221	188	10.1
92.1	99.903	18080	14.	74	63	3.4
100.0	99.9987	18096	15.	16	14	0.8

Tab. VI Removal of iodine by an AC 6120/H₁ test bed of proposed bed depth for a large reprocessing plant. Sweep gas: humid air + 5% NO₂, 150°C

Grain size of iodine sorption material: 1 - 2 mm
 dew point of humid air : 30°C, preconditioning: 20 h, loading period: 5 h
 sweep gas continued for an additional : 4 h. Loading 18.1 g I₂
 mixed with : 1 mCi ¹³¹I

data for accumulated bed depth			data for single section of test bed			
% of total bed depth	¹³¹ I removal efficiency [%]	I ₂ loading [mg]	No. of test bed section	I ₂ loading [mg]	reacted amount of Ag [mg]	Ag reacted in % of Ag inventory
6.6	10.9	1960	1.	1960	1670	94.2
13.1	21.8	3940	2.	1980	1680	95.0
19.7	32.7	5910	3.	1970	1680	94.6
26.3	43.4	7850	4.	1940	1640	92.8
32.9	54.1	9790	5.	1940	1650	92.9
39.5	64.7	11720	6.	1930	1640	92.5
46.0	75.2	13610	7.	1890	1610	90.8
52.6	85.2	15420	8.	1810	1540	87.1
59.2	91.2	16500	9.	1080	917	51.7
65.8	95.5	17276	10.	776	660	32.2
72.3	98.3	17785	11.	509	433	24.4
78.9	99.7	18035	12.	250	213	12.0
85.5	99.9901	18091	13.	56	48	2.7
92.1	99.9990	18093	14.	2	2	0.1
100.0	99.9997	18094	15.	1	1	-

14th ERDA AIR CLEANING CONFERENCE

Tab. VII Removal of iodine by an AC 6120/H₁ test bed of proposed bed depth for a large reprocessing plant. Sweep gas: humid air 5 % NO₂, 120°C

Grain size of iodine sorption material: 1 - 2 mm
 dew point of humid air : 30°C, preconditioning: 20 h, loading period: 5 h
 sweep gas continued for an additional : 4 h. Loading 18.1 g I₂
 mixed with : 1.04 mCi ¹³¹I

data for accumulated bed depth			data for single section of test bed			
% of total bed depth	¹³¹ I removal efficiency [%]	I ₂ loading [mg]	No. of test bed section	I ₂ loading [mg]	reacted amount of Ag [mg]	Ag reacted in % of Ag inventory
6.6	10.5	1900	1.	1900	1620	91.4
13.1	20.6	3720	2.	1820	1550	87.5
19.7	30.5	5510	3.	1790	1520	86.0
26.3	40.0	7220	4.	1710	1450	82.1
32.9	49.1	8880	5.	1660	1410	80.0
39.5	57.8	10460	6.	1580	1340	75.8
46.0	66.0	11940	7.	1480	1260	71.1
52.6	74.1	13400	8.	1460	1240	69.9
59.2	81.5	14740	9.	1340	1140	64.5
65.8	88.4	16000	10.	1260	1070	60.3
72.3	94.0	17010	11.	1010	850	48.5
78.9	97.8	17692	12.	682	580	32.8
85.5	99.6	18012	13.	320	272	15.4
92.1	99.9936	18088	14.	76	65	3.7
100.0	99.9998	18090	15.	2	2	0.1

Tab. VIII Removal of iodine by a test bed out of molecular sieve type 13 X-Ag. Proposed bed depth for a large reprocessing plant, sweep gas: humid air + 5 % NO₂, 150°C

Grain size of iodine sorption material: 1 - 2 mm
 dew point humid air : 30°C, preconditioning: 20 h, loading period: 4 h
 sweep gas continued for an additional : 4 h. Loading: 18.1 g I₂
 mixed with : 1.57 mCi ¹³¹I

data for accumulated bed depth			data for single section of test bed			
% of total bed depth	¹³¹ I removal efficiency [%]	I ₂ loading [mg]	No. of test bed section	I ₂ loading [mg]	reacted amount of Ag [mg]	Ag reacted in % of Ag inventory
6.6	21.6	3910	1.	3910	3320	35.2
13.1	44.0	7970	2.	4060	3450	36.5
19.7	63.6	11520	3.	3550	3010	32.0
26.3	81.0	14660	4.	3140	2670	28.2
32.9	93.6	16950	5.	2290	1950	20.6
39.5	99.6	18030	6.	1080	920	9.7
46.0	99.9994	18100	7.	70	61	0.6
52.6	**> 99.999	-	8.	-	-	-
59.2	**> 99.999	-	9.	-	-	-

**> below detection limit

14th ERDA AIR CLEANING CONFERENCE

Tab. IX Removal of iodine by a test bed made of molecular sieve, type 13 X-Ag. Proposed bed depth for a large reprocessing plant, sweep gas: humid air, 150°C

Grain size of iodine sorption material: 1 - 2 mm
 dew point humid air : 30°C, preconditioning: 20 h, loading period: 4 h
 Sweep gas continued for an additional : 20 h. Loading 36.2 g I₂
 mixed with : 1.41 mCi ¹³¹I

data for accumulated bed depth			data for single section of test bed			
% of total bed depth	¹³¹ I removal efficiency [%]	I ₂ loading [mg]	No. of test bed section	I ₂ loading [mg]	reacted amount of Ag [mg]	Ag reacted in % of Ag inventory
6.6	17.3	6270	1.	6270	5330	56.4
13.1	33.6	12160	2.	5890	5010	53.0
19.7	48.8	17670	3.	5510	4680	49.5
26.3	62.9	22800	4.	5130	4370	46.2
32.9	75.6	27380	5.	4580	3890	41.1
39.5	86.5	31330	6.	3950	3360	35.5
46.0	94.7	34290	7.	2960	2520	26.7
52.6	99.1	35890	8.	1600	1360	14.4
59.2	99.9992	36200	9.	310	260	2.8
65.8	99.9999	36200	10.	0.3	0.3	3 · 10 ⁻³
72.3	**>99.9999	-	11.	-	-	-
78.9	**>99.9999	-	12.	-	-	-

**> below detection limit

Comparison of the silver utilization as a function of the bed depth for the iodine sorption materials AC 6120 and MS 13X-Ag

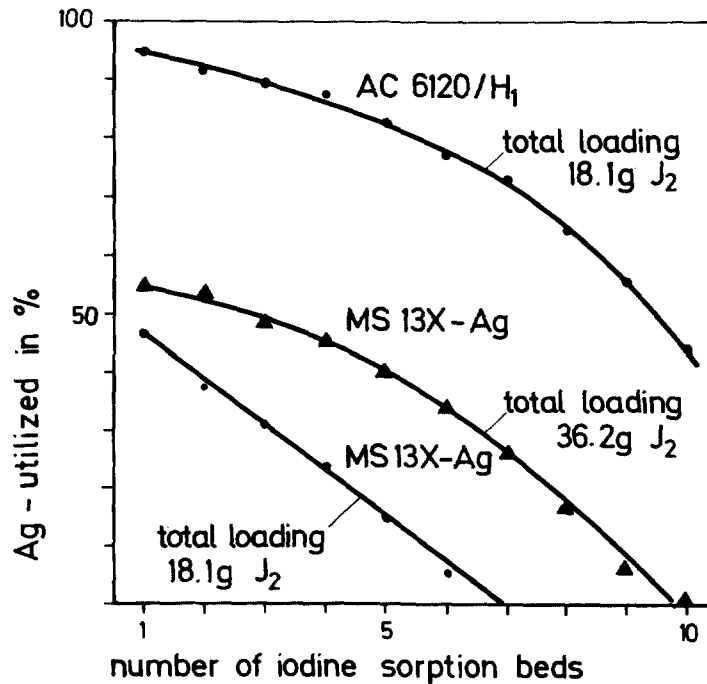
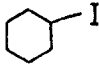
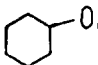
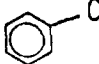
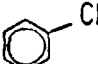
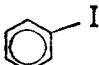


FIG. 15

Tab. X Reactions of AC 6120 with gaseous organic iodine compounds

Compound	Reaction products
CH ₃ I	AgI, CH ₃ ONO ₂ , alkanes
C ₂ H ₅ I	AgI, C ₂ H ₅ ONO ₂
:	:
:	:
C ₁₂ H ₂₅ I	AgI, C ₁₂ H ₂₅ ONO ₂
CH ₃ -CHI-CH ₂ -CH ₃	AgI, H ₃ C-CH=CH-CH ₃ , H ₂ C=CH-CH ₂ -CH ₃ , HNO ₃
(CH ₃) ₃ CI	AgI, (CH ₃) ₂ -C=CH ₂ , C _n H _{2n+1} I
	AgI,  , HNO ₃
	AgI, 
	no reaction up to 180°C

DISCUSSION

PARKER: Is the concentration of TBP in the air stream in the pilot plant representative of what you might find in reprocessing facilities, or are you just guessing?

WILHELM: The filters tested had been installed in an operating reprocessing plant. We obtained the iodine removal data with contaminants produced under operational conditions.

PARKER: Is it representative of what you might find in a full scale reprocessing plant?

WILHELM: I think so.

MURBACH: What is AC-6120?

WILHELM: It is amorphous silicic acid with a special pore structure, impregnated with 7% AgNO_3 by weight (12% for AC-6120/H1).

DEITZ: Have other impregnations than AgNO_3 been tested on AC-6120?

WILHELM: AC-6120 identifies an AgNO_3 impregnated material. The base material has been impregnated with other impregnants, but the results were not as good as with AgNO_3 .

SKOLRUD: During the AC-6120 regeneration step, do only the phosphate compounds (as contaminants) desorb?

WILHELM: The main regeneration effect is the transformation of elemental Ag and Ag_2O , which are the reaction products of reduction processes with organic compounds, to AgNO_3 . I do not know whether the Ag_3PO_4 reacts with NO_2 , but after regeneration, the performance of the material is so fully restored that apparently Ag_3PO_4 causes no difficulties.

SKOLRUD: What is the NO_2 content during regeneration?

WILHELM: We used 2.5% NO_2 in the process.

14th ERDA AIR CLEANING CONFERENCE

GOVERNMENT-INDUSTRY CONFERENCE ON ADSORBERS AND ADSORPTION MEDIA

C. A. Burchsted
Secretary, Government-Industry Conference

The Government-Industry Conference on Adsorbers and Adsorption Media met at Washington, D.C., on March 25, 1976, with M. W. First (HACL) presiding. Jack Dempsey, ERDA, gave the welcome and also outlined the program for the 14th ERDA Air Cleaning Conference to be held in Sun Valley, Idaho, in August.

V. R. Deitz, Naval Research Laboratory

Deitz reported on Phase III of the Domestic Carbon Program. This program was undertaken several years ago under the urging and direction of Humphrey Gilbert, USAEC, to identify suitable domestically available base materials for nuclear grade activated carbon. In Phase I, C. A. Burchsted, ORNL, surveyed the carbon industry and selected a number of promising materials for further investigation. In Phase II, the properties and ability to impregnate these materials were studied.* In Phase III, Deitz investigated the mechanisms involved in radioiodine trapping by adsorbents and the role of the base carbon. A two-stage impregnation procedure using salts of iodine oxyacids, I_2 , and/or KI in the first stage and hexamethyltetramine (HMTA), a high-flash-point tertiary amine, in the second, was developed. The results were comparable to the best TEDA-KI-impregnated coconut carbons, but with more favorable (higher) ignition temperature. It was found that the smaller iodine molecules must be put on the carbon first, then the larger HMTA molecules; the procedure cannot be reversed. Patents have been applied for by ERDA. Confirmatory tests were made by Evans (SRL) and Rivers (AAF).

Deitz described the chemistry of the new impregnation method and the mechanism of radioiodine trapping and retention. He believes that radioiodine trapping by adsorbents is a catalytic process (as opposed to the isotopic exchange and chemical reaction mechanisms currently in vogue) with CH_3I reacting with the reactive species placed on the carbon in a chain reaction. The carbon serves primarily as a catalyst support, although it is probably not completely inert in the reaction. The chain reaction can be killed by acidification, either by reaction products, poisons inherent in the carbon itself, or poisons collected from the air stream. The base carbon serves as a sink for the reaction products, but can become poisoned if they become excessive. Deitz found a dependence of radioiodine effectiveness on bed depth (to be reported at the 14th Air Cleaning Conference), velocity (at constant gas residence time), pH, and I_2 -to-KI content of the base carbon/impregnant complex. The spontaneous ignition and desorption temperatures of

* V. R. Deitz and C. A. Burchsted, *Survey of Domestic Charcoals for Iodine Retention*, NRL Memorandum Report 2960, Naval Research Lab.

the HMTA-impregnated carbons were greater than 430°C and 200°C, respectively, for all base materials. Base materials included coal, petroleum, wood, and nut carbons, in addition to coconut used as a "control." Deitz concluded that a satisfactory base material must:

- have a large surface area ($> 1000 \text{ m}^2/\text{g}$) to support the impregnants.
- support a high pH (water extract) to protect the impregnants.
- have an optimum particle size distribution and hardness.
- have sufficient macropore volume to transport radioiodine and reaction products to "active sites" on the surface.
- have sufficient excess surface area to accommodate contaminants expected under service conditions.
- have high ignition and impregnant-desorption temperatures.
- have with proper impregnation good radioiodine effectiveness at high RH.

A. G. Evans, Savannah River Laboratory

Evans reported on the application of the new impregnation method to a variety of base materials. He found it possible to successfully impregnate any satisfactory base material by adjusting the HMTA, iodine, and flame-retardent contents of the impregnant. Reproducibility of the two-stage impregnation was good when the base carbon was consistent from lot to lot, and radiolytic iodine desorption of the better combinations were comparable to those of the best current carbons. Evans found that there must be sufficient excess alkalinity in the impregnant and/or natural alkalinity of the base carbon to maintain proper pH. It was also found that the iodine/potassium ratio is critical to the formation of oxyiodine salts that can be retained by the carbon.

Work at SRL verifies that close control of particle size and particle size distribution in original purchase is essential for satisfactory performance and good service life. With respect to service aging and weathering, smaller particles were superior from the standpoints of both CH_3I and radiation penetration over a period of service and suffer less breakdown in service. (Note: the importance of close control over particle size and particle size distribution was discussed by Evans and Dr. Wilhelm at the last meeting of the Government-Industry Conference.)

Studies of used carbons from the Savannah River confinement systems showed a dramatic drop in pH of water extract after exposure to service conditions (from a pH of 9 to 10 new to a pH of 5-6 over a period of 12 to 20 months). It is possible that monitoring of the pH of the water extract may be a means of monitoring the useful life of the carbon. The drop in pH results from poisoning due to contaminants removed from the air. Evans noted a

continuous increase in chloride content, probably due to chlorinated compounds, but the effect of this on pH is unknown. It is known that SO₂ and NO_x reduces pH and poisons the carbon. There is also a decrease in ignition temperature with aging. Dr. Wilhelm noted that much of the solvents may result from the curing of paints in operating areas of the plant. Surface area also decreases with service aging. Although surface area is regenerable, pH, ignition temperature, and poisoning effects are not reversible.

J. T. Collins, R. R. Bellamy, U. S. Nuclear Regulatory Commission

Collins discussed the philosophy of the NRC position, noting several criteria (Nos. 41, 42, and 43; and 19 and 51) of 10-CFR-50 Appendix A which deal with mitigation of the consequences of an accident and release under normal operation, that Appendix I provides numerical guides for implementation of ALARA, and that only Branch Technical Positions pertaining to air cleaning systems are available for guidance for non-ESF systems. Bellamy discussed NRC's Standard Review Plans and what is looked for in the review of Safety Analysis Reports. NRC recommends carbon adsorbers in ESF systems, in offgas and holdup systems, and in non-ESF normal ventilation systems. Copies of tables from Regulatory Guide 1.52 and the Branch Technical Position for non-ESF systems were passed out (see attachments). The BTP essentially downgrades the recommended requirements for carbon for non-ESF systems from that recommended for ESF systems. The new issue of Regulatory Guide 1.52 will be out this summer. Bellamy also noted that source term calculation procedures are given in Nuclear Regulatory Reports 75-0016 and -009. The new issue of Regulatory Guide 1.52 still recommends sampling and laboratory testing of carbons from ESF systems every 720 hours of filter system operation or annually, whichever is less. As noted by Evans, aging and weathering of carbon is a site-specific parameter, and the recommendation to test every 720 hours of system operation is considered conservative. Activated carbon is not actually required in ESF systems, and alternatives will be considered and can be approved by NRC. The 95% ball-pan hardness value is specified by NRC because of the substantial carbon attrition experienced in some adsorption systems. Kovach (Nuclear Consulting Services) noted that some of this attrition may result from inadequate filling of adsorber cells. A representative of Mine Safety Appliances Company questioned the validity of the 95% hardness specification.

Dr. Jurgen Wilhem, Karlsruhe, Germany

Wilhelm described a German adsorption system which has two stages of activated carbon. The first stage is loaded with an unimpregnated carbon and serves as a guard bed for the second stage of impregnated carbon. The first stage is unheated (heating of the first stage would simply drive the petroleum base and low boiling point compounds captured in it into the second stage). Provision is made for periodic heating of the second stage to drive off higher boiling point compounds (poisons) not caught in the first stage. The arrangement has been used successfully to restore the effectiveness of the second stage carbon after a period of use and to extend the useful life of the system.

14th ERDA AIR CLEANING CONFERENCE

Wilhelm discussed round-robin testing of carbons in Europe. The proposed European-U.S. round-robin program proposed after the Karlsruhe meeting in 1973 was inconclusive, but did indicate the need to test the laboratories rather than carbons *per se*. A subsequent round-robin in Europe employed uniform samples of Norit, Sutcliffe-Speakman, and a French carbon tested under the following conditions:

Temperature	30°C
Relative Humidity	95%
Bed Size	2.5 cm dia x 5 cm deep
CH ₃ I Concentration	50 µg CH ₃ I/gC
Airflow Velocity	25 cm/s
Preequilibration Period	16 h
Loading Period	60 m
Elution Period	1 - 2 h

A second test was made with RH = 98-100%. A face-to-face meeting of the participants was held before this second series with the results that test values of the various laboratories were close. Wilhelm stressed the need for face-to-face meetings if such round-robins are to be successful. The round-robin indicated that test bed diameter is not a significant parameter, but apparent density (AD) is. A final report of the European test program is at least two years away.

Germany bases acceptance of activated carbon on a K factor where:

$$K = \frac{\log DF}{\dagger}$$

where,

DF = decontamination factor.

† = gas-residence time = bulk volume divided by volume airflow.

A K value of 5, minimum, is considered acceptable. The K factor for the European round-robin tests showed variances that cannot be explained yet. Obviously, AD is important and must be very accurately determined.

J. L. Kovach, Nuclear Containment Systems

Kovach reported on NCS testing of new and used carbons. The tests show that used carbon samples should not be preequilibrated when making iodine and methyl iodide "efficiency" tests. Preequilibration of used carbon in effect regenerates them and gives incorrect test results. NCS found up to 160 different compounds coming off unimpregnated carbons even before they had been exposed to the service environment. Tests of coal-base carbons gave off substantial quantities of sulfur as SO₂; as much as 0.2% as sulfur in new carbons and 3.5% in aged carbons.

14th ERDA AIR CLEANING CONFERENCE

Kovach also commented on variation of carbon samplers used in current systems and stressed the need for greater uniformity of design. Results of iodine and methyl iodide "efficiency" tests of carbons from widely varying sampler and sampler-installation designs are difficult, if not impossible, to correlate.

NCS reports many instances of significant settling observed in carbon cells in operating adsorption systems. Kovach recommended that cells be vibrated at the natural frequency of the cells during filling to alleviate the problem. He noted that sampler cartridges are generally better packed than cells of the system, which results in iodine and methyl iodide test results that are not representative of the actual system. He recommended that any one adsorption system be filled with carbon from the same manufacturing batch; the use of several batches in the same system gives poor results. Also, there is a definite correlation between the amount of dusting from cells and the orientation of screen perforations. He recommended to cell manufacturers that the rough surfaces of screens (due to perforating operation) be on the outside of the beds.

For used carbon, Kovach recommended that a test temperature of 20°C with no preequilibration be used. This was noted by the ASTM D28 Committee members present.

F. R. Schwartz, North American Carbon Company

Schwartz reported on an investigation of carbon particle degradation. The current test methods (ball-pan, dust elutriation, T-bar stirring) do not measure degradation accurately and test results can seldom be correlated with field use. Schwartz gave the ASTM definitions of "abrasion resistance," "crushing strength," and "hardness" (see ASTM D2652) and showed that the forces involved in degradation are different than those actually measured by the currently recognized tests. NAC is currently developing new tests that will be made available to the industry, one that measures abrasion resistance, the other to measure crushing strength. The work to date on these tests indicates that both tests can distinguish between granular carbons with respect to their ability to resist abrasion and crushing forces and seem to be independent of particle size and geometry effects and appear to correlate with field experience. (Note: ASTM D-28 Committee at its annual meeting in Chicago in June 1976 decided against submitting any of the currently recognized tests as methods for measuring abrasion resistance at this time. The method for the ball-pan hardness test was submitted for ballot, but simply as a test for a measurable property of carbon for comparison purposes.)

C. A. Burchsted, Union Carbide Corporation, Oak Ridge, Tennessee

Burchsted summarized the status of current standards relating to activated carbon and adsorption systems:

ANSI N509	<i>Requirements for Nuclear Power Plant Air Cleaning Units and Components</i>	Will probably be issued in summer 1976
-----------	---	--

14th ERDA AIR CLEANING CONFERENCE

ANSI N510	<i>Testing of Nuclear Air Cleaning Systems</i>	Issued
AACC CS-8	<i>High-Efficiency Gas-Phase Adsorber Cells</i>	Revision in Progress
RDT M16-1	<i>Gas-Phase Adsorbents for Trapping Radioactive Iodine and Iodine Compounds</i>	Revision in Progress
ASTM D2652	<i>Definitions of Terms Relating to Activated Carbon</i>	Issued Reaffirmed
ASTM D2854	<i>Test for Apparent Density of Activated Carbon</i>	Issued Reaffirmed
ASTM D2862	<i>Test for Particle Size Distribution of Granulated Activated Carbon</i>	Issued Reaffirmed
ASTM D2866	<i>Test for Total Ash Content of Activated Carbon</i>	Issued Reaffirmed
ASTM D2867	<i>Test for Moisture in Activated Carbon</i>	Issued
ASTM D3466	<i>Test for Ignition Temperature of Activated Carbon</i>	Approved for Issue
ASTM D3467	<i>Test for Carbon Tetrachloride Activity of Activated Carbon</i>	To be issued summer 1976
ASTM D----	<i>Radioiodine Testing of Nuclear Grade Gas-Phase Adsorbents</i>	Committee Ballot July 1976

R. A. Lorenz, Oak Ridge National Laboratory

Lorenz summarized findings of the Oak Ridge work on auto-ignition of activated carbon due to fission-product heating. At low airflow velocity through the bed there is no "break away" temperature rise to indicate the occurrence of ignition, so ignition is defined as the temperature corresponding to a rate of rise of 20°C/m. This temperature corresponds to a heat release rate (primarily due to oxidation) of 15 cal/g of carbon/min. For air velocities below 2 fpm, the rate of oxidation heat release decreases following ignition and carbon-bed temperature stabilizes at about 400°C. An increase in airflow velocity results in higher heat-release rate and higher bed temperature. At low airflow velocities, significant iodine desorption did not result from bed heatup and ignition at any time during the ORNL tests; it is concluded, therefore, that time is available in the event of an adsorption system fire to carry out fire extinguishment operations if suitable fire extinguishing techniques can be developed.

The ORNL tests indicated that a highly penetrating form of radioiodine (HOI ?) is continuously formed and released from an adsorption system in a radiation field. The rate of formation

14th ERDA AIR CLEANING CONFERENCE

and release is apparently dependent on moisture and radiation intensity and is independent of carbon-bed temperature (between 70°C and 400°C), airflow velocity (between 2 and 28 fpm), carbon base material, impregnant, and adsorbed contaminants (paint fumes, etc). The partition coefficient of this penetrating species in water is less than 10, but higher in CCl₄. The collection efficiency of the species at 130°C is poor for activated carbon but about 20 to 50 times better for silver-exchanged zeolite. Collection on silver nitrate coated adsorbers at 130°C is also poor. The species will sorb on both activated carbon and silver-zeolite at - 78°C.

The ORNL work also confirms the finding, reported at previous G-I Conference meetings, that sorption of radioiodine as CH₃I is a function of airflow velocity through the bed with constant gas residence time. A comparison of work by Ackley (ORNL) and Underhill (HACL) using ⁸⁵Kr indicates that there is a minimum collection efficiency at about 0.2 to 0.8 cm/sec.

J. F. Fish, American Air Filter Company

Fish, who is chairman of the ASME Committee on Nuclear Air and Gas Treatment (CONAGT) presented the case for qualification of field testing personnel. CONAGT has made provision for a subcommittee on qualification of field test personnel in view of the proliferation of testing agencies, some of whom appear to have limited competence in the field. It was proposed that Harvard Air Cleaning Laboratory might conduct the qualification activity for ERDA or NRC. Fish also recommended the qualification of testing laboratories and proposed that any such laboratory be sanctioned by NRC. Such laboratories would be required to periodically requalify by making tests on standardized samples prepared by NRL or an ERDA facility such as ORNL or SRL. One sample would be new, unused material, another would be taken from a system in which it had been exposed to service environment. Comparison of test results would indicate problems with respect to procedure, technique, and other laboratory-sensitive conditions. Fish pointed out that there is a precedent for such action in the HEPA filter Quality Assurance program operated by ERDA at Oak Ridge, Hanford, and Rocky Flats. Such a program approaches Government licensing and in some respects functions as a "Bureau of Standards" for this area. The benefit would be the assurance to NRC and plant operators that the data developed to verify the efficacy of on-line systems is valid under the test conditions imposed.

14th ERDA AIR CLEANING CONFERENCE

TABLE 2

FROM PROPOSED REGULATORY GUIDE

SUMMARY TABLE OF NEW ACTIVATED CARBON PHYSICAL PROPERTIES
Batch Tests to be Performed on Finished Adsorbent
(Recommendations for Out-Of-Containment Systems)

TEST	ACCEPTABLE TEST METHOD	ACCEPTABLE RESULTS
1. Particle Size Distribution	ASTM D2862 (Ref. 28)	Retained on #6 ASTM E11 (Ref. 29) Sieve: 0.0% Retained on #8 ASTM E11 (Ref. 29) Sieve: 5.0% Maximum Through #8, retained on #12 Sieve: 40% to 60% Through #12, retained on #16 Sieve: 40% to 60% Through #16 ASTM E11 (Ref. 29) Sieve: 5.0% max. Through #18 ASTM E11 (Ref. 29) Sieve: 1.0% max.
2. Hardness Number	RDT M16-1T, Appendix C (Ref. 30)	95 minimum
3. Ignition Temperature	RDT M16-1T, Appendix C (Ref. 30)	330°C minimum at 100 fpm
4. Activity	CCl ₄ Activity, RDT M16-1T, Appendix C (Ref. 30)	60 minimum
5. Radioiodine Removal Efficiency		
a. Methyl Iodide, 25°C and 95% Relative Humidity	RDT M16-1T (Ref. 30), para. 4.5.3, except 95% relative humidity air is required.	99%
b. Methyl Iodide, 80°C and 95% Relative Humidity	RDT M16-1T, (Ref. 30), para 4.5.3, except 80°C and 95% relative humidity air is required for test (pre- and post-loading sweep medium is 25°C)	99%
c. Methyl Iodide, in Containment	RDT M16-1T, (Ref. 30), para. 4.5.4, except duration is 2 hours at 3.7 atm. pressure	98%
Radioiodine Removal Efficiency (Cont'd)		
d. Elemental Iodine Retention	Savannah River Laboratory (Ref. 31)	99.9% loading 99% loading plus elution
6. Bulk Density	ASTM D2854 (Ref. 32)	0.38 gm/ml minimum
7. Impregnant Content	State Procedure	State type (not to exceed 5% by weight)

NOTES:

- (1) A batch test is defined as a test made on a production batch of product to establish suitability for a specific application. A batch of activated carbon is defined as that quantity of the same grade, type, and series of material which has been homogenized to exhibit, within reasonable tolerance, the same performance and physical characteristics; and for which the manufacturer can demonstrate by acceptable tests and quality control practices such uniformity. All material in the same batch shall be activated, impregnated, and otherwise treated under the same process conditions and procedures, in the same process equipment, and shall be produced under the same manufacturing release and instructions. Material produced in the same charge of batch-type equipment shall constitute a batch; material produced in different charges of the same batch-type equipment may be included in the same batch only if it can be homogenized as above. The maximum batch size shall be 350 cu. ft. of activated carbon.
- (2) Test 4 should be performed on base material.
- (3) Test 5a should be performed for qualification purposes. A qualification test is a test which establishes the suitability of a product for a general application, normally a one-time test reflecting historical typical performance of material.
- (4) Test 5c should be performed for qualification purposes on carbon to be installed in primary containment (recirculating) atmosphere cleanup systems.

14th ERDA AIR CLEANING CONFERENCE

CLOSING REMARKS OF SESSION CHAIRMAN: (R. D. Rivers)

This morning when Mr. W. H. Hannum stated the aims of this conference he said he hoped that we would actually be learning something. I think this session indicates that we are, but that the process of learning is never easy. We move from mere reporting of results and performance, from attempts to find something that somehow works, to far more detailed understandings of the processes and conditions under which things will operate.

I emphasize the word "detail". A fraction of a per cent of impregnant here, a sequence of impregnation there, a pattern of equilibration in test procedures, the exact sequence of adsorption media in a sampling train - all of these things influence our thinking, our results, the development of our materials and methods.

Jurgen Wilhelm in his introductory remarks has summarized the papers given, and I think there have been no surprises. I will confine these remarks to the controversies that arose, and try to summarize where this set of papers places us.

A recurrent theme here has been: How do we determine the present condition of a bank of carbon that has been in service, and what will its remaining life be? Strauss and Deckers both found problems in the first step to answer this question: obtaining a sample representative of the full-scale system being examined. Their questioners seemed to say problems were exaggerated, and that explanations-and cures - could be found for the anomalies Strauss and Deckers observed. Assuming these problems can be overcome, we must decide how to test a given sample. Hunt's observations of the regenerative effects of equilibration of aged carbon was not challenged, though Deitz promises to give some contradictory data for new carbons in Session 9; possibly the two effects counter each other at some point. The data reported by Evans on used carbons shows very high

14th ERDA AIR CLEANING CONFERENCE

penetration values, in spite of 16-hour equilibration before testing. It is possible that penetrations would have been greater if Evans had not pre-equilibrated. Parrish described a procedure for relating the ultimate life of a carbon bed to data obtained early in its life. The strength of the correlations he showed were indeed remarkable, considering the wide variation in ambient contaminants observed around nuclear plants. If this technique can be shown reliable in other locales than those which gave Parish's correlations, it will indeed be a useful method for it also allows life prediction for different bed depths.

Jonas delved into the same area from a more detailed, theoretical viewpoint, showing that the "rate constant" for radiomethyl iodide capture by several impregnated carbons is proportional to the square root of the superficial bed velocity. The dependence of this rate constant on particle size did not agree with earlier studies. Jonas' contention that the data indicate catalysis as the controlling surface phenomenon may well be true. The argument would be more persuasive if the observed rate constants (which, incidentally, include mass transfer effects) do not decline with long bed exposure. Deckers and Sigli offer a way to avoid prediction to some extent: measure current bed performance using radioiodine compounds. The concept has been reported before; their equipment shows admirable attention to safety and convenience. They admit, however, that they cannot by their test tell what an adsorber will do under accident conditions. Humidity and temperature have serious effects, and Lorenz documents still another, radiation. Heating and ignition were observed, and radiolytic generation of as yet uncharacterized radioiodine compounds. The data is welcome, though it may herald troubles. Staples reported performance of various metal exchanged zeolites, and a procedure for

14th ERDA AIR CLEANING CONFERENCE

regenerating silver zeolite. Critique of his paper centered around economics: The process appears technically sound, but is it really worth the bother? There may be simpler means to make use of the potential inherent in zeolites or other inorganic chemisorbers.

Deitz and Evans gave data on a new variety of impregnated activated carbon. The material appears promising; it can be made from more readily obtainable coal base carbon. It is disappointing that this new material does not have the kind of order-of-magnitude performance improvement that zeolites represent (though at great cost, and same environmental sensitivity).

To overcome these problems, we need adsorption materials which provide penetrations one-tenth to one-hundredth allowable levels, with reliability over the entire range of operating and accident conditions. The materials now available meet regulatory goals, but at the price of painful quality control and monitoring. As we struggle to find how current materials respond to the environments they face, and how to keep them operating at allowable performance levels, we should reserve some effort for materials which advance performance by orders of magnitude, not fractions of a percent.

SESSION V

SAMPLING AND MONITORING

Tuesday, August 3, 1976

CHAIRMAN: H. Etinger

SELECTIVE SAMPLING OF HYPOIODOUS ACID

M. J. Kabat

AN ANALYSIS FORMAT AND EVALUATION METHODS FOR EFFLUENT PARTICLE SAMPLING SYSTEMS IN NUCLEAR FACILITIES

L. C. Schwendiman, J. A. Glissmeyer

THE USE OF A SINGLE PARTICLE INTRA-CAVITY LASER PARTICLE SPECTROMETER FOR MEASUREMENTS OF HEPA FILTERS AND FILTER SYSTEMS

B. G. Schuster, D. J. Osetek

OPENING REMARKS OF SESSION CHAIRMAN:

Most of the other sessions of this conference are concerned with the design and performance of control systems for nuclear facilities. The three papers this morning will consider different aspects of monitoring or evaluating the performance of some of these controls. As such, they constitute the documentation that these controls perform as advertised over the normal operating cycle, or during non-standard operating conditions; satisfy existing regulatory requirements; and satisfy public concerns, which, as Dr. First pointed out, is becoming more and more critical regarding potential health and environmental effects. These three papers are quite important to the overall air cleaning systems used in nuclear facilities.

The first paper will consider another aspect of the iodine problem which we heard a lot about yesterday. It describes a sampling system to distinguish between hypoiodous acid from other forms of iodine, since their effects are different. The second paper will detail a systematic approach to evaluating air sampling systems for nuclear facilities. This can be used to optimize design of new air sampling systems, as well as evaluating the limitation of existing systems. Since air sampling is one of the cornerstones of monitoring proper, for safe performance of these facilities, this is a very important topic. The last paper details a new technique and new instrumentation for in-place HEPA filter testing; especially when multiple HEPA filters are involved, or multiple layers of filter media are used. Since new emission restrictions and redundancy requirements are making the use of multiple HEPA filter banks more and more common, this subject has significant importance in terms of possible capital plant and operational cost savings.

14th ERDA AIR CLEANING CONFERENCE

SELECTIVE SAMPLING OF HYPOIODOUS ACID

M.J. Kabat
Ontario Hydro
Central Health Physics Services
Pickering Generating Station
Box 160
Pickering, Ontario, Canada.

Abstract

A new material has been developed which efficiently separates hypoiodous acid from a mixture of penetrative species of airborne radioiodine. This selective absorbent has high absorption and retention efficiency for hypoiodous acid under conditions of high relative humidity and short residence time for an extended sampling period. Very low absorption of methyl iodide in this absorbent has been measured under the same conditions.

A sampler, components of which selectively absorb particulate iodine, elemental iodine, hypoiodous acid and organic iodides, has been assembled and successfully applied for airborne radioiodine sampling in an operational field.

The method and equipment used for laboratory testing of the HOI absorbent and for field sampling of iodine species are described herein. Experimental results are also presented and discussed in this paper.

I. Introduction

It has been proven in many previous reports and publications that airborne radioiodine occurs in nuclear power station areas and effluents in three chemical forms: elemental iodine vapour, an inorganic compound - hypoiodous acid and organic forms - mostly as methyl iodide. These iodine species are of greatly different radiobiological significance, particularly for population exposure (via a food chain) evaluation. The deposition rate of elemental iodine on vegetation is reported to be approximately one thousand times greater than the deposition rate of methyl iodide. Hypoiodous acid deposition has not yet been measured because of difficulties experienced in its selective measurement under the practical range of atmospheric conditions and long time sampling. For the above reasons, a considerable effort has been made in our laboratory to develop an adequate system for selective sampling of the above airborne iodine chemical species.

II. Origin and Behaviour of HOI

A theoretical analysis of HOI chemistry and experimental investigation of its sorption on commercially available iodine absorbents was provided in the Central Health Physics laboratory and published in 1974⁽¹⁾. It was concluded in this paper that:

14th ERDA AIR CLEANING CONFERENCE

1. Iodine concentrations in all operational systems of CANDU nuclear power stations are extremely low, even when the radioiodine activity is close to the maximum permissible operational limits.

2. High yield of HOI is obtained from hydrolysis of I_2 in aqueous solutions of very low iodine concentrations ($\leq 10^{-8}$ M).

3. Besides elemental iodine, which is slightly volatile, HOI is the only inorganic iodine compound formed in water solutions under specified conditions which is considered to be highly volatile.

4. Hypoiodous acid has a low chemical reactivity in neutral aqueous solutions (probably because of low dissociation rate).

5. Charcoal is an efficient absorbent for airborne HOI.

6. The existing non-charcoal iodine absorbents are not as efficient for HOI removal, particularly at high humidity.

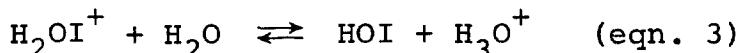
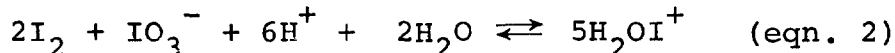
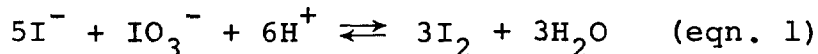
A method was developed, and it is being used in CANDU power stations, which eliminates the formation of HOI in the spent fuel storage bay (by addition of hydrazine to bay water).

Theoretical assumptions of HOI deposition on vegetation were derived from our theoretical and experimental studies on HOI chemistry, and were discussed at the 1975 annual meeting of ANS (2). These assumptions have now been confirmed by experiment, the results of which will be published in the near future.

III. Method of HOI Generation

The method described in (1) was used for short-term generation of HOI containing a minimum amount of organic species of iodine.

A long-term continuous supply of HOI was needed for the testing of selective HOI absorbents. Oxidation of $^{131}I^-$ with IO_3^- was applied for this purpose which provided a continuous supply of airborne HOI for a period of several days. The involved reactions can be expressed by the following chemical equations:



Practically all $^{131}I^-$ is transferred to H_2OI^+ through reactions (eqn. 1) and (eqn. 2) under conditions of low pH (pH ~ 2.0) and high excess of IO_3^- ($\sim 3 \times 10^{-4}$ M). The dissociation equilibrium in reaction (eqn. 3) forms HOI which is continuously stripped with a He-stream from the solution. Because of good stability of H_2OI^+ under the above conditions, HOI can be

continuously generated at a slowly declining rate through a period of several days.

Description of Testing Apparatus

The apparatus used for testing the selective HOI absorbents is illustrated in Figure 1.

HOI Generator. Hypoiodous acid formed in generator G through the above reactions was stripped with a He-stream (50 ml/min). The solution droplets were removed with a glass fibre filter F and dry helium (50 ml/min) added to reduce the relative humidity of the He-HOI stream. This was done in order to achieve efficient removal of elemental iodine with Cu screens. The He-HOI stream was then mixed with the air stream from the air supply system described below. The HOI generator is shown in Figure 2.

Air Supply System. Laboratory air was continuously saturated with steam in the heated drum humidifier DH. Partial condensation of the excessive water vapour was provided in condenser C1. The dew point of the air sample was controlled with condenser C2. Condensate was collected in a thermostatically cooled container. The air temperature (= dew point) was measured with thermometer T1 and the air stream carried into a heating coil HC, the temperature of which was kept constant with a thermostatically controlled bath TB2.

The relative humidity of air downstream of T2 was calculated from its dew point (= T1 reading) and its higher temperature at T2. The relative humidity was also continuously measured with monitor RH (Electro-Hygrometer, Lab-Line Instrument Inc., Model No. 2210) which was being recalibrated at regular intervals with an Abbeon Certified Hygrometer, Model ABl67B. A photograph of the air supply system is shown in Figure 3.

Absorbent Testing Columns. Column A1: Five rings (each 46 mm diameter x 10 mm deep) in series were filled with the tested absorbent. At the challenge gas flow of 25 lpm, its residence time in a 50 mm deep column of the HOI absorbent was 0.2 sec.

An additional ring with 25 mm of fresh HOI absorbent was applied in the cases when greater than 1% of HOI penetration through the original, 50 mm deep, absorbent bed was expected (i.e., during the absorbent aging experiments).

Column A2: Two rings (46 mm diameter x 10 mm deep and 46 mm diameter x 25 mm deep) in series, filled with a fresh TEDA impregnated charcoal, were used for absorption of organic species of iodine penetrating through the HOI absorbent.

Glass Fibre Filter: A glass fibre filter F2 was installed (on several occasions) downstream of column A1 in order to remove and measure particles of the HOI absorbent eventually stripped from column A1 with the challenge gas stream. No measureable ¹³¹I was ever identified on this filter. A disassembled set of testing columns is shown in Figure 4.

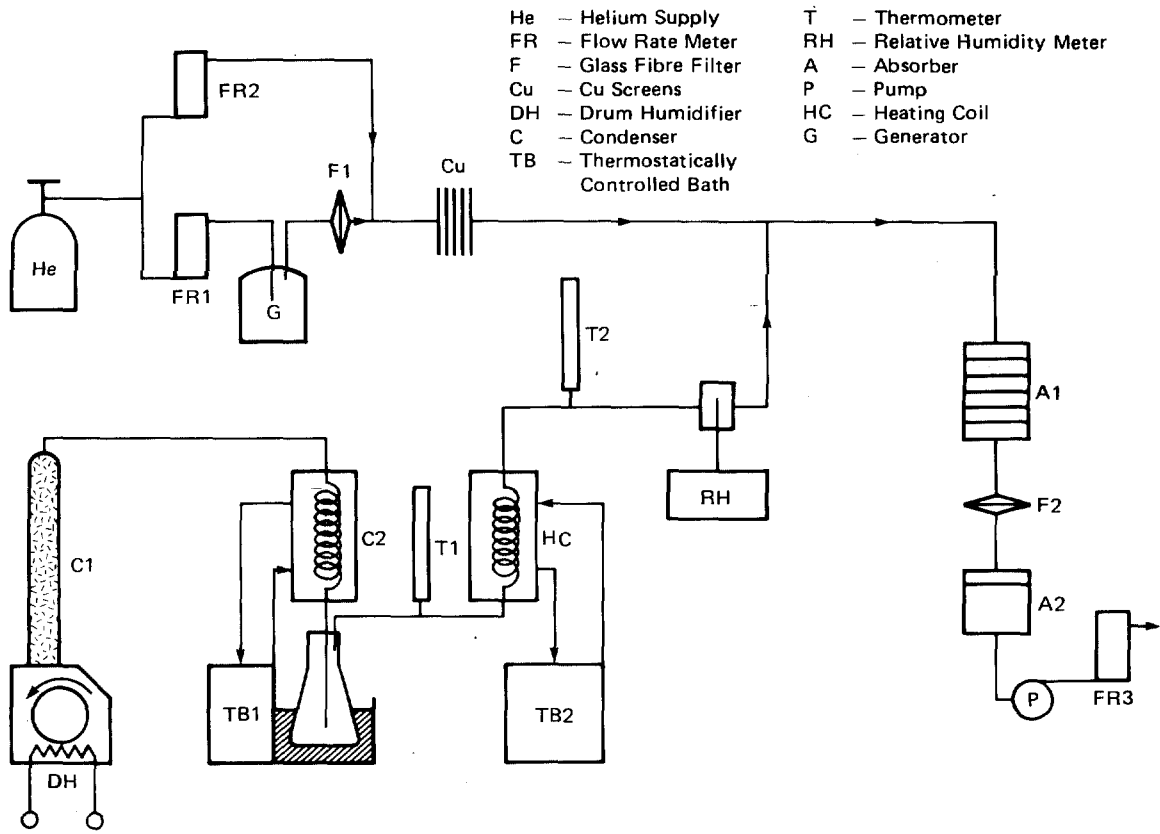


Figure 1 Test setup.

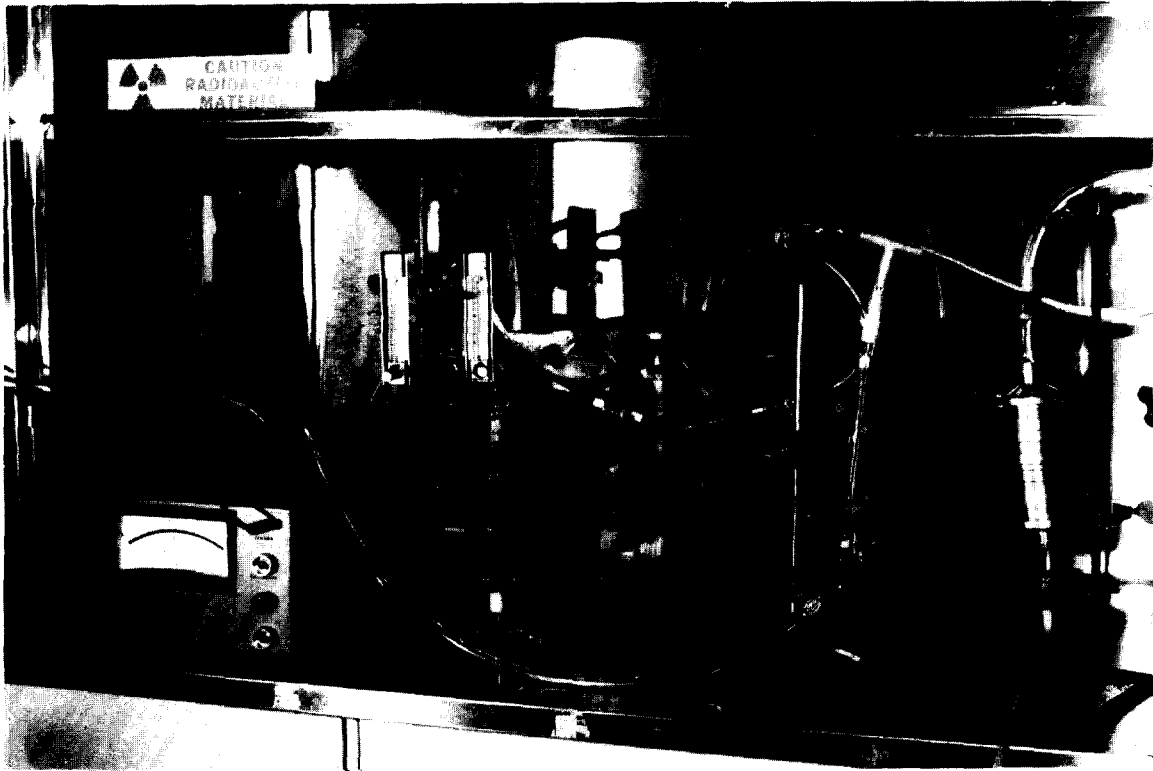


Figure 2 HOI generator.

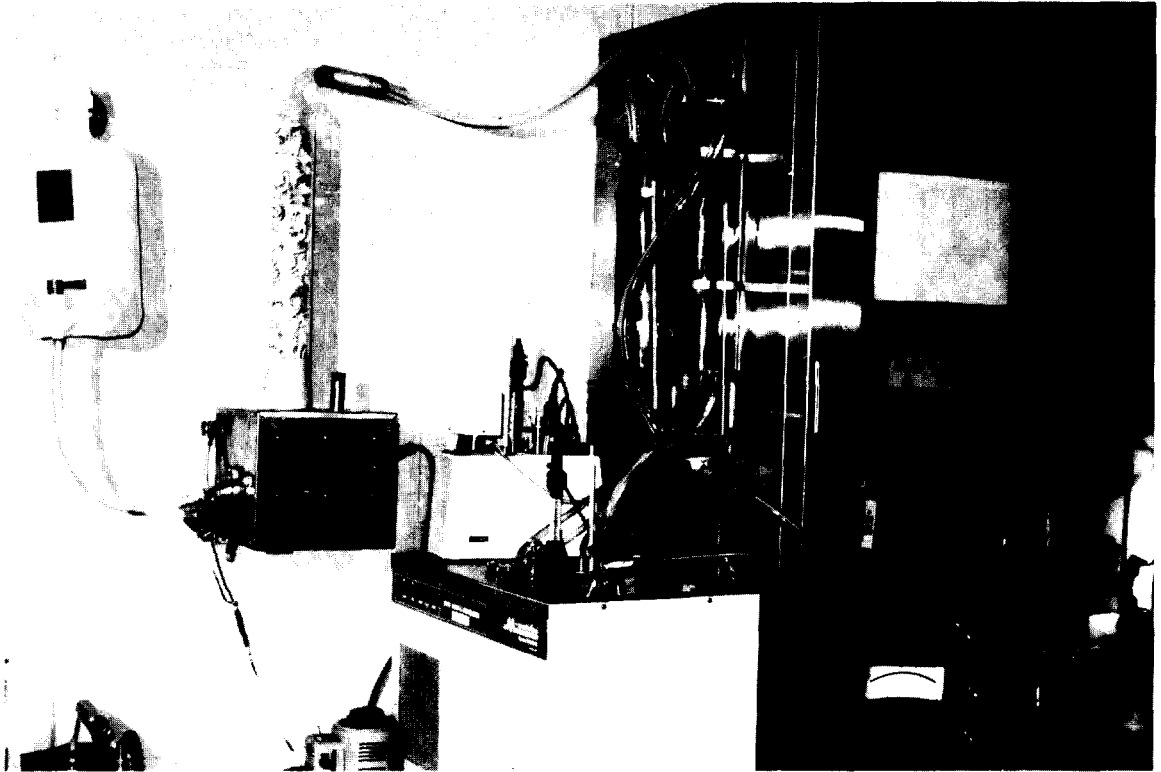


Figure 3 Air supply system.

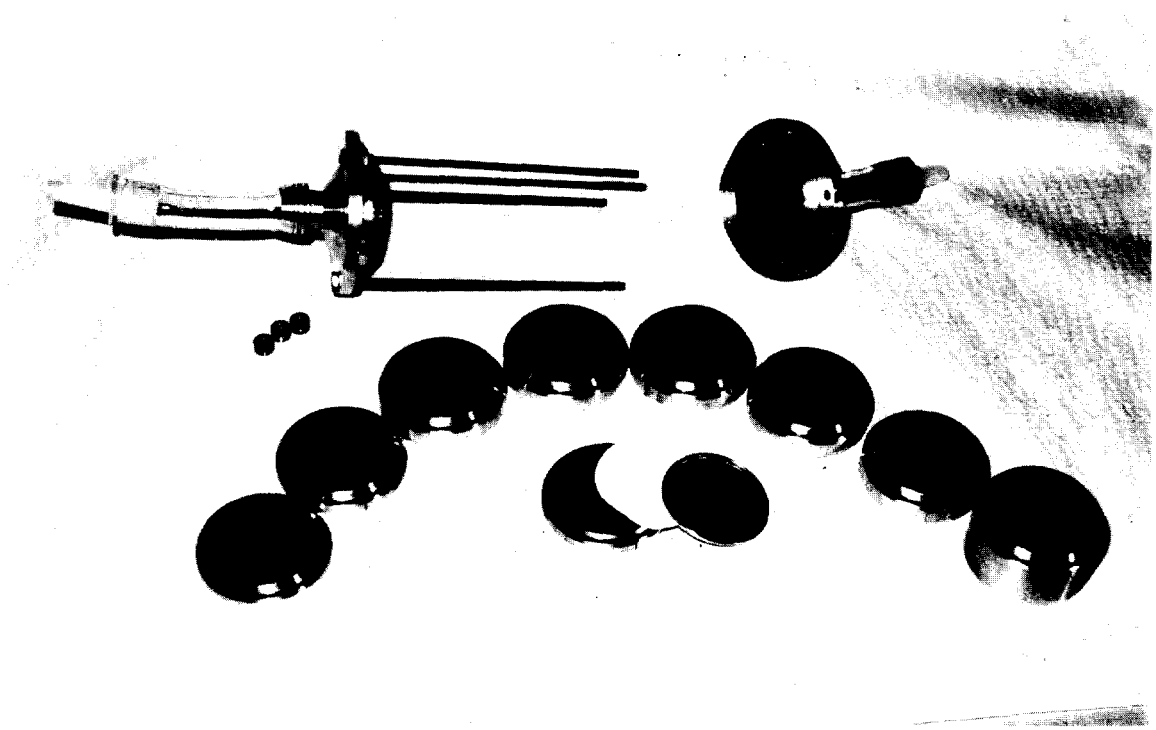


Figure 4 Disassembled set of testing columns.

IV. Experimental Evaluation of the Selective HOI Absorbent Performance

Several materials were tested for HOI absorption efficiency and reported in (1). All of the tested absorbents had high efficiency for CH_3I removal, therefore none of them were suitable for selective HOI sampling. A number of other solid and liquid absorbents (absorbents, metals, 4-iodophenol, solutions, oil) were tested subsequently which absorbed HOI efficiently and selectively, but their performance in long-term sampling at $\text{RH} > 70\%$ did not fulfill our requirements.

Finally, summarizing the practical experience from the HOI generation and absorption experiments, the physicochemical model of selective HOI absorption was established and an absorbent developed (a carbon based material) which gives optimum performance. The HOI absorption model and technical details on this absorbent will be published after submitting an application for a patent on the absorbent.

Absorption properties of the HOI absorbent are discussed below.

Experimental Conditions

The challenge gas (air + HO^{131}I with $< 1\%$ He) was passed through the adsorbent in columns A1 and A2 and each ring was separately measured with a calibrated Ge - Li detector coupled to a Canberra Multichannel Gamma Analyzer, Model 8180. Sufficiently long counting time was applied in measurement of the downstream side of the A1 column in order to reduce the statistical counting error below $\pm 10\%$ at 95% confidence level.

In experiments where the time interval between activity measurement on identical samples was longer than approximately five hours, the measured ^{131}I activity was corrected for decay and the integrated ^{131}I total in the columns was compared with the initial total from the first measurement in the set. This method was particularly useful in long-term desorption measurements.

The depth of the A1 column (HOI absorbent) was applied in all measurements that HOI penetration did not exceed 1% . Therefore, all ^{131}I identified in the A2 absorbent (TEDA impregnated charcoal) was considered to be an organic compound of iodine.

The amount of organic iodides varied within a range of 1% to 15% of the total ^{131}I absorbed in the columns. Low content of organic forms (1% to 3%) was present in HOI generated from freshly supplied ^{131}I solutions, and it was then continuously increased with the solution storage time up to approximately 15% after five weeks of storage.

14th ERDA AIR CLEANING CONFERENCE

A histogram of the typical absorption profile through the depth of the columns A1 and A2 is illustrated in Figure 5.

Absorption of HOI

The basic, non-treated carbon had high efficiency for HOI absorption at low humidity through short sampling intervals. It also absorbed a significant portion of CH_3I and retention of HOI was not satisfactory. The graph in Figure 6 indicates that a significant desorption of HOI with passing air occurs within a few hours.

Treated carbon (of the identical batch) was slightly less efficient for HOI absorption, but both CH_3I absorption and HOI desorption rates were substantially reduced. Figure 7 shows HOI absorption and desorption characteristics, measured under the same conditions as applied in the non-treated carbon testing (40% RH, 22°C).

The HOI absorbent was slightly less efficient at 98% RH as illustrated in Figure 8. Iodine retention in the absorbent was still very good under these conditions.

No concentration dependence in absorption of HOI in this material was determined as illustrated in Figure 9.

Dependence of HOI absorption efficiency on the challenge gas flow rate illustrated in Figure 10 indicates that the rate of HOI absorption was not constant when a different face velocity of the challenge gas was applied.

The HOI absorption rate is expressed by a quality factor K,

$$K = \frac{\ln D}{\Delta t}$$

where, D = Decontamination factor
 Δt = Residence time.

Then at $\Delta t = 0.1$ sec,

<u>Sample Flow (lpm)</u>	<u>K</u>	<u>Depth of Absorbent that Removes 99% of HOI (mm)</u>
12	31.6	18
25	43.8	26
50	56.5	40

Then, the penetration P (%) after the challenge gas residence time Δt (seconds) can be calculated from,

$$P = e^{-K\Delta t} \times 100$$

497

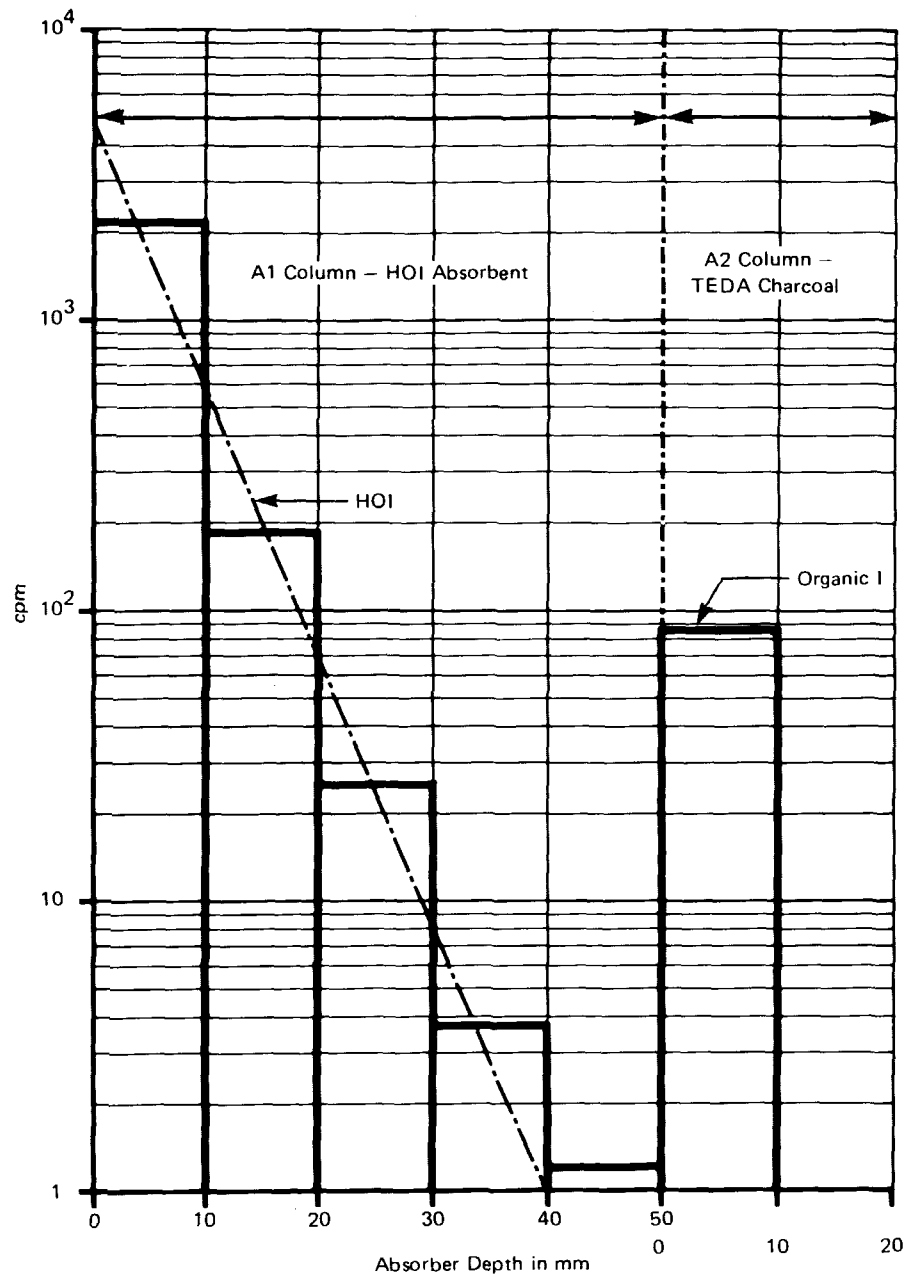


Figure 5 Typical ^{131}I profile through absorption columns.

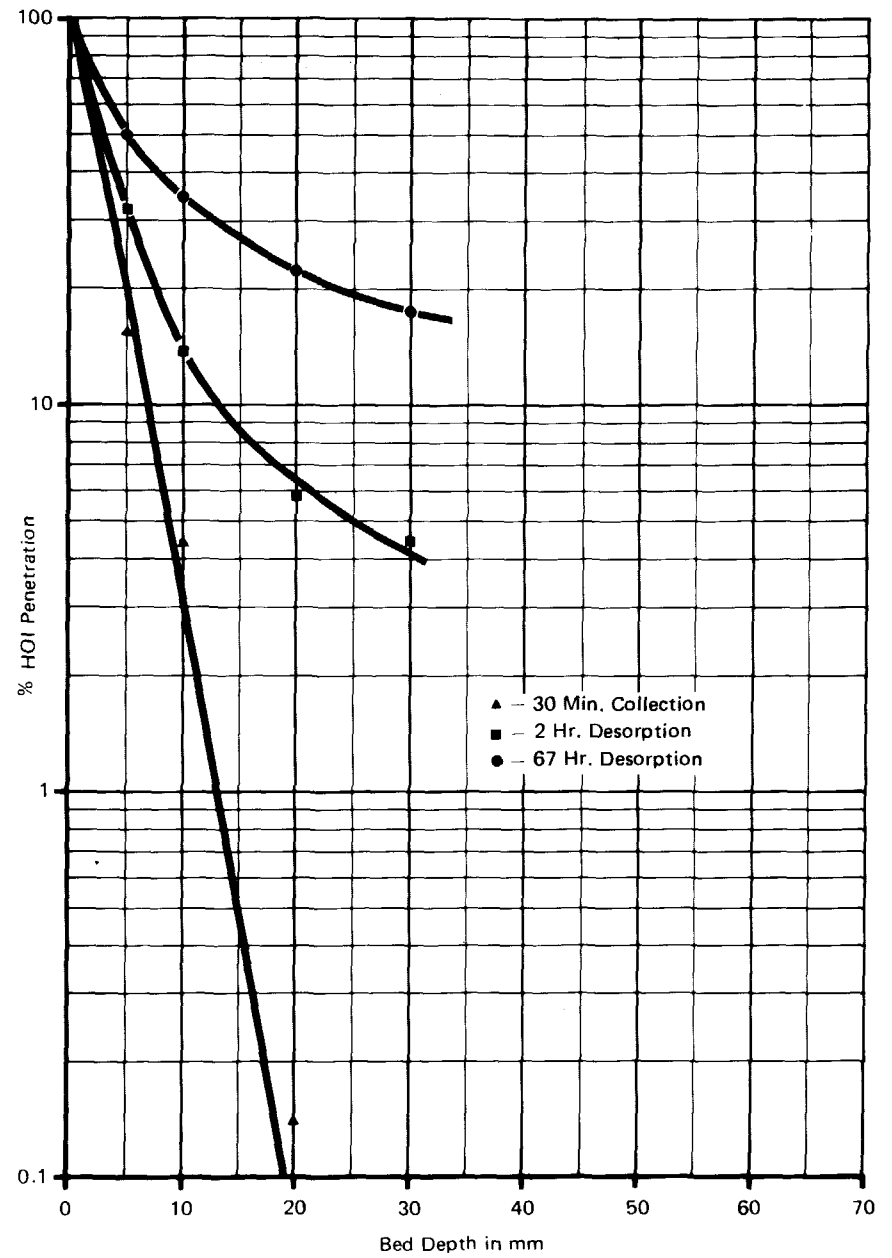


Figure 6 Absorption of HOI in a non-treated carbon; 40% RH, 22°C.

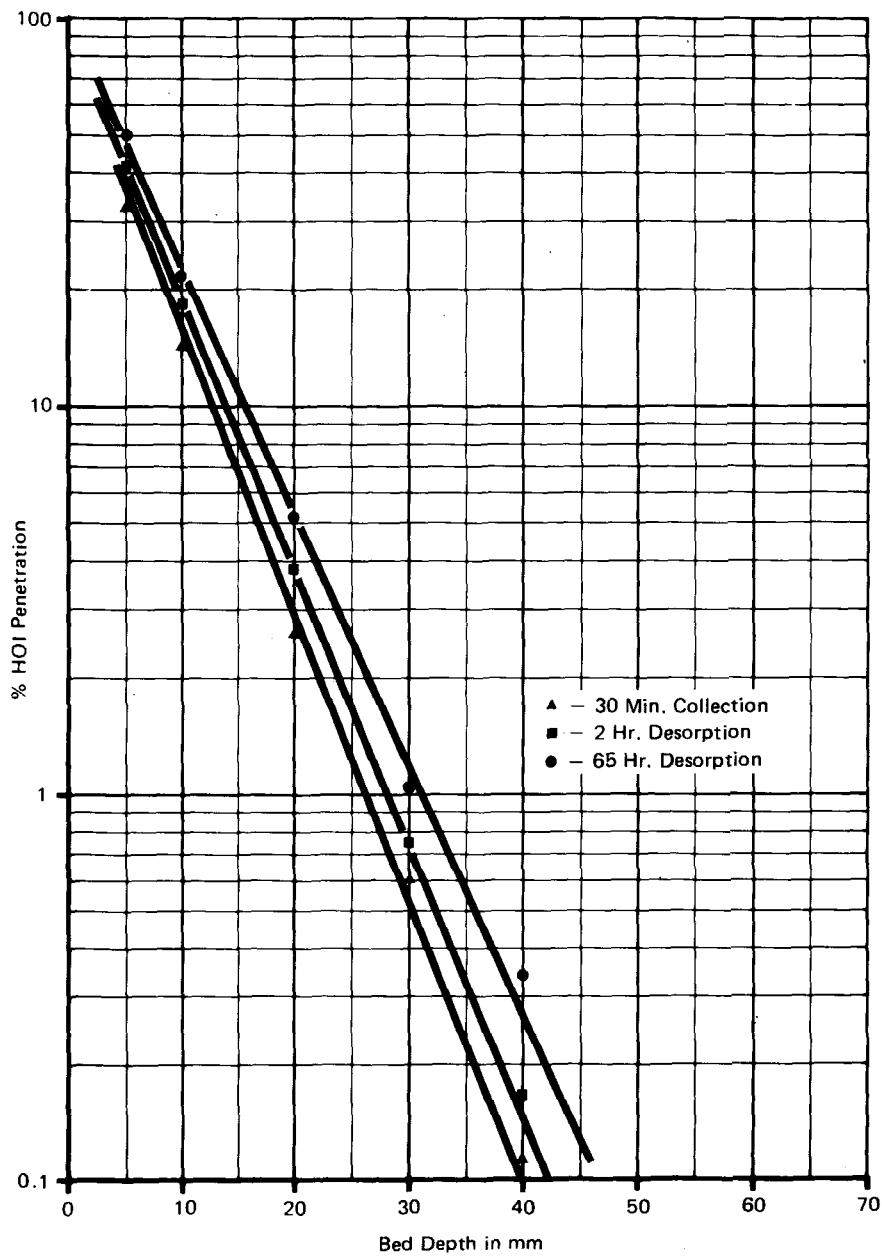


Figure 7 HOI absorbent; 40% RH, 22°C.

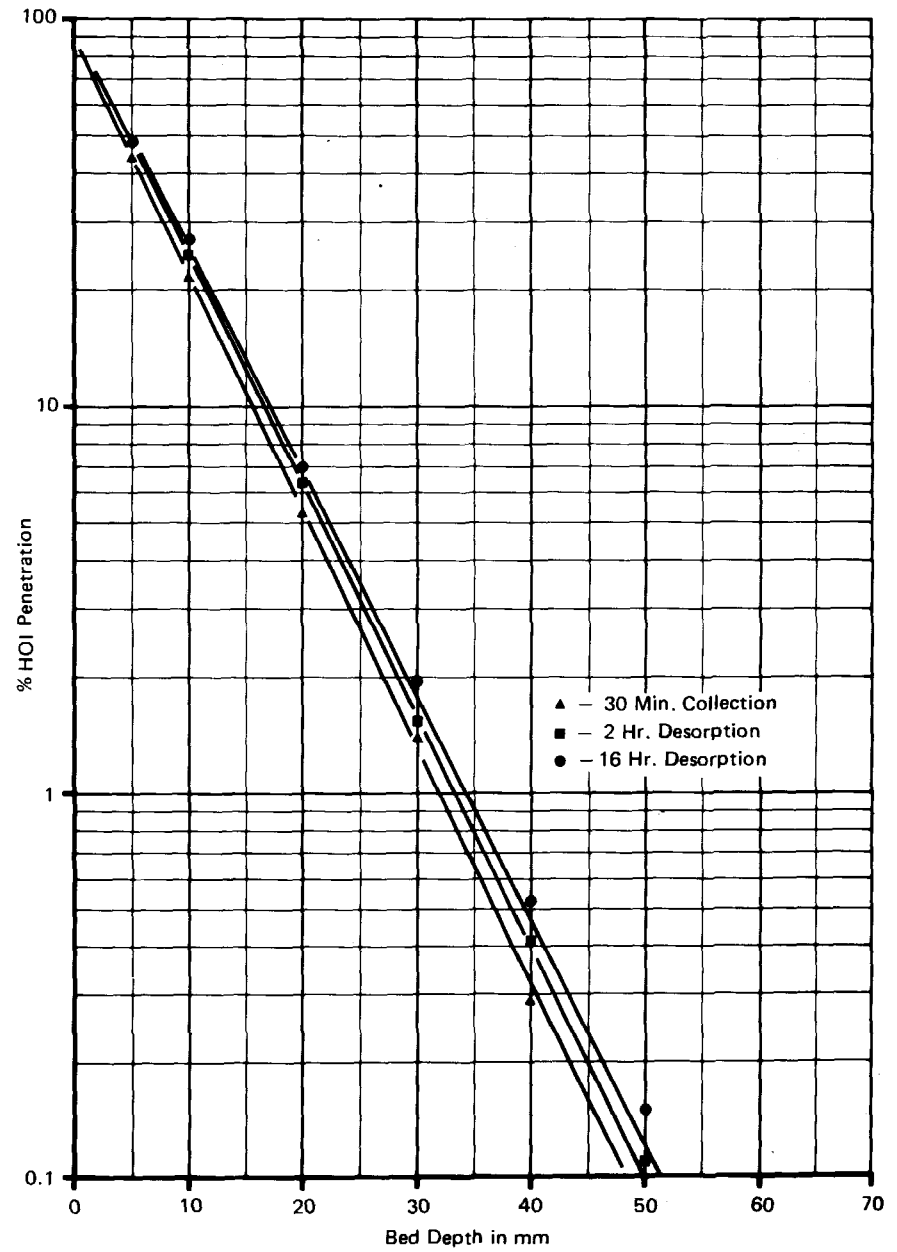


Figure 8 HOI absorbent; 98% RH, 22°C.

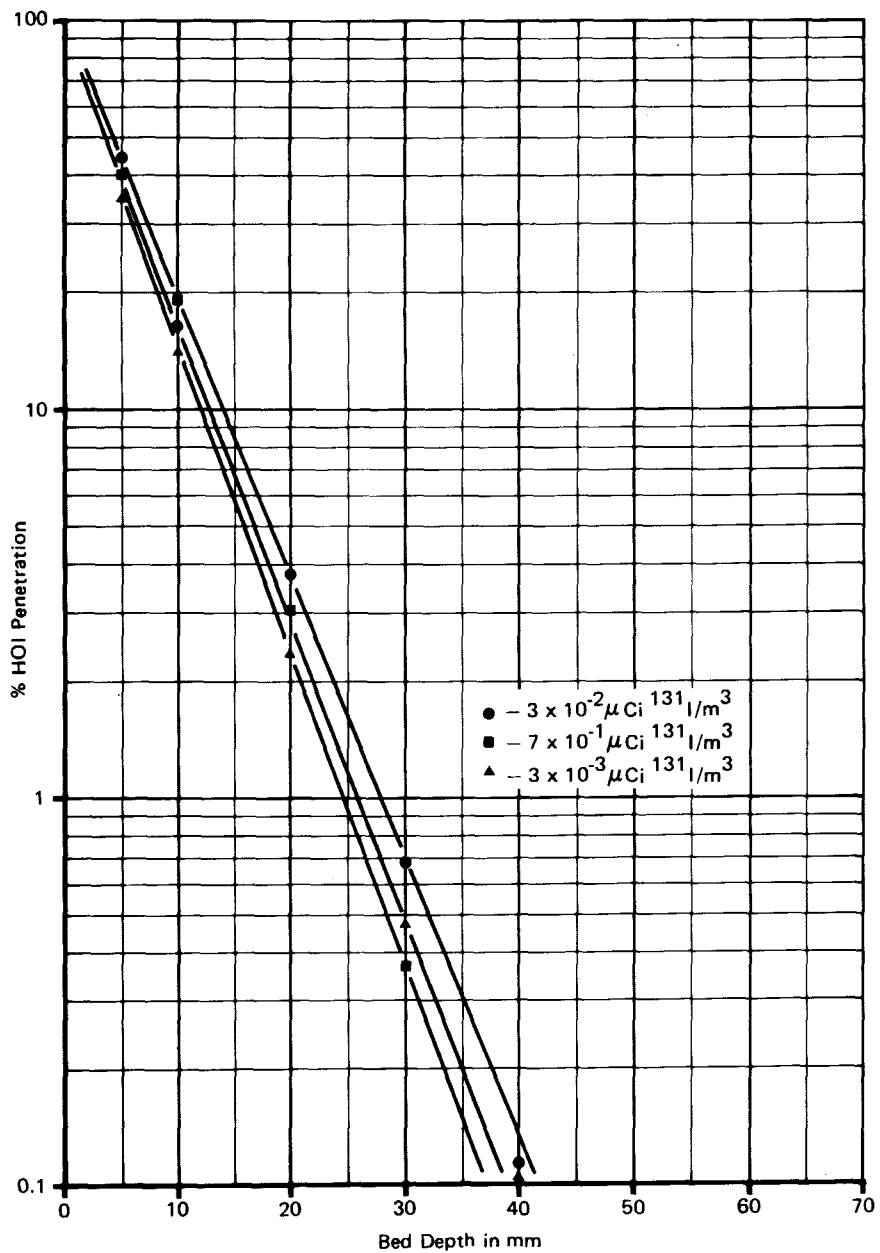


Figure 9 HOI absorption at different airborne concentrations; 40% RH, 22°C.

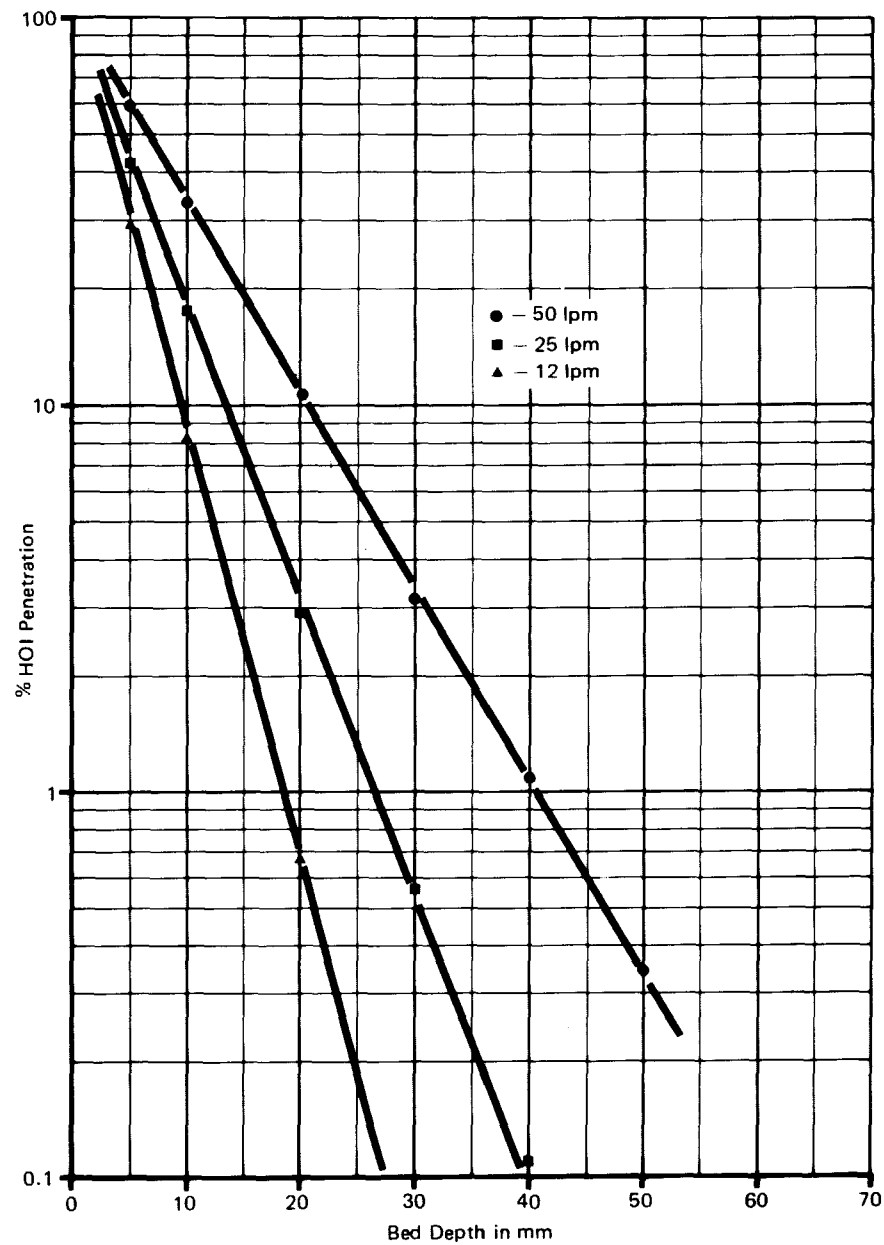


Figure 10 Dependence of HOI absorption efficiency on the sample flow; 40% RH, 22°C.

The practical implication of this observation was that the sampling column depth did not increase proportionally with the sampling flow increase at the same decontamination factor. This is an advantageous feature of the HOI adsorbent for its use in high volume sampling applications.

Further, the HOI adsorbent was tested under long-term sampling conditions. The adsorbent column A1 was exposed to a continuous air flow under the most common sampling conditions (50% RH, 22°C), and its efficiency for HOI absorption was measured after six days and twenty-one days of continuous aging.

Graphical results in Figure 11 show that the adsorbent retained its good efficiency (in ≥ 50 mm deep bed) for a period of one week under these conditions. After three weeks of aging, the efficiency was reduced to approximately 80% with low desorption rate, which can be classified as good under the applied conditions.

The adsorbent efficiency for HOI was reduced more drastically (as expected) during the high humidity aging process. Figure 12 shows that good absorption efficiency remained after four days of continuous aging at 98% RH, 22°C conditions.

Results of the adsorbent testing under extreme conditions, illustrated in Figure 13, indicate that the adsorbent can be used for HOI sampling under fog conditions when water condensation occurs in the adsorbent column. The suggested factor for sampling efficiency correction is approximately 1.4, if the sampling or aging interval does not exceed twenty-four hours under these conditions. The graph also shows that retention of the absorbed iodine is still very good under such extreme conditions.

Absorption of I_2 and CH_3I in the HOI Adsorbent

The HOI adsorbent was highly efficient for elemental iodine absorption. Therefore, when iodine species were to be sampled selectively, I_2 had to be absorbed in a preceding adsorbent which had a minimum affinity to HOI and CH_3I .

Absorption of CH_3I on the HOI adsorbent was measured under 30%, 50%, 60% and 98% RH conditions. The results presented in Figure 14 show that the fraction of the absorbed CH_3I varied with the relative humidity of the challenge gas from about 4%/25 mm at low humidity to only 1%/25 mm at 98% RH.

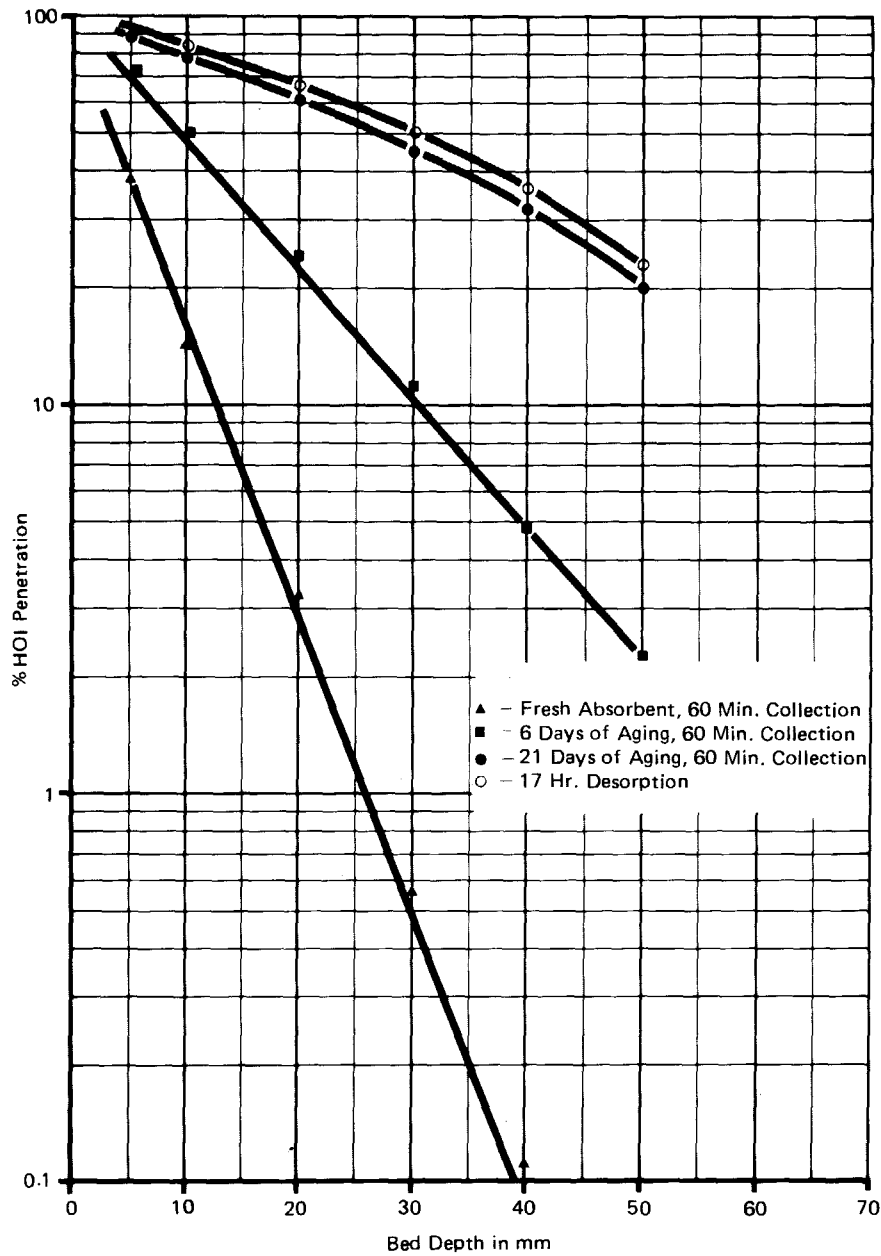


Figure 11 HOI absorbent aging at 50% RH, 22°C.

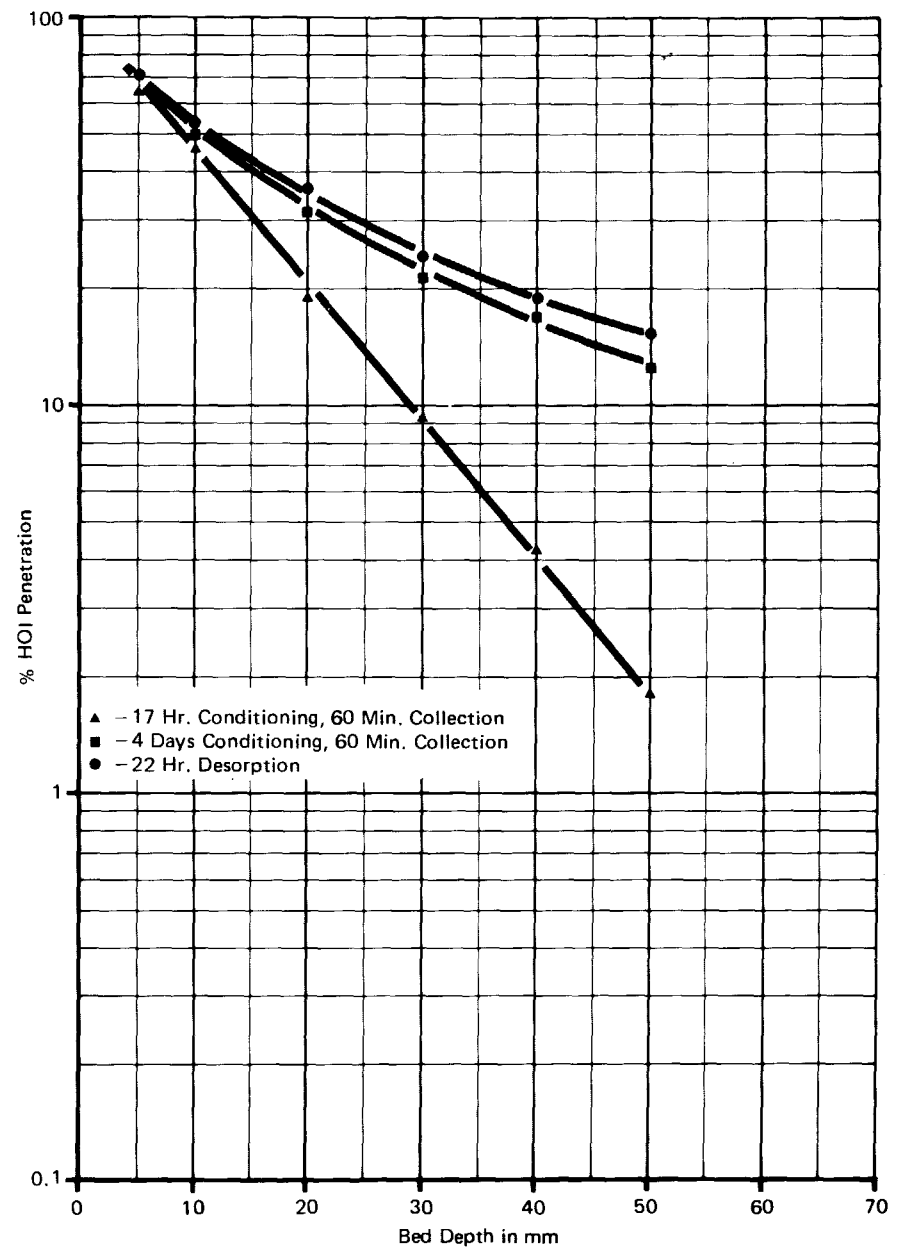


Figure 12 HOI absorbent aging at 95% RH, 22°C.

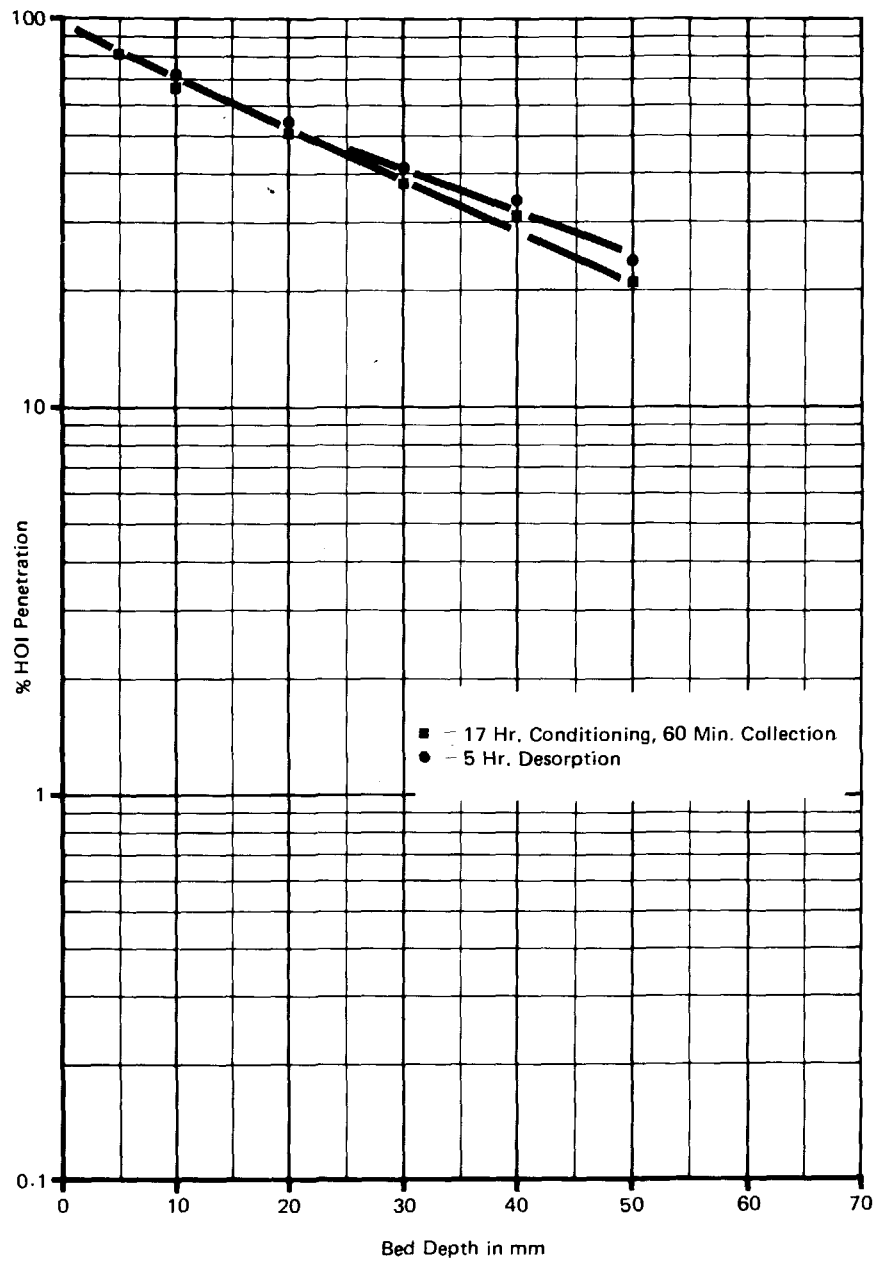


Figure 13 HOI absorbent aging; slight condensation, 22°C.

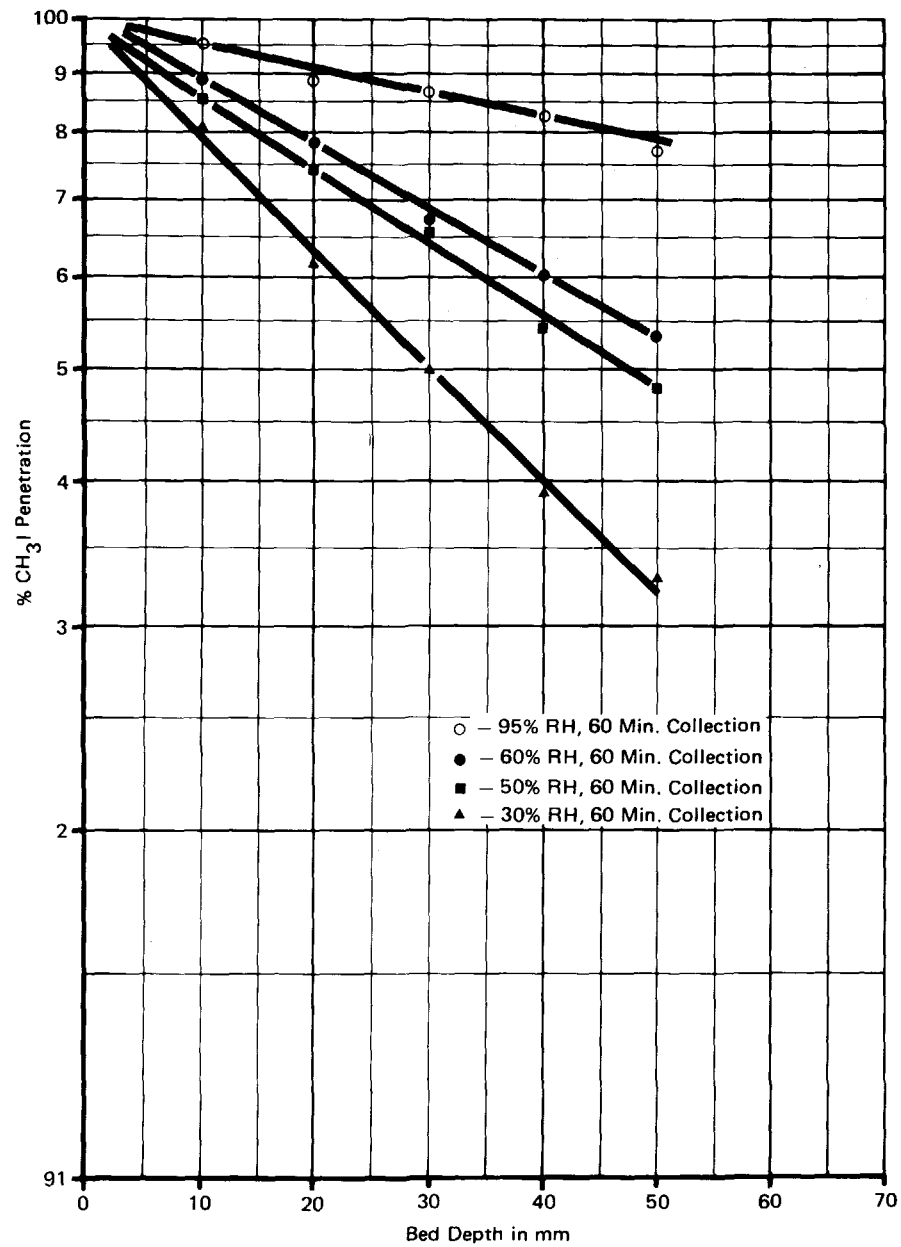


Figure 14 CH₃I absorption in HOI absorbent.

V. Selective Sampling of Airborne Iodine Speciessampling Equipment

A RadēCo H809V Sampler with a modified head, as illustrated in Figure 15, was used for the sampling of iodine species in the CANDU station areas.

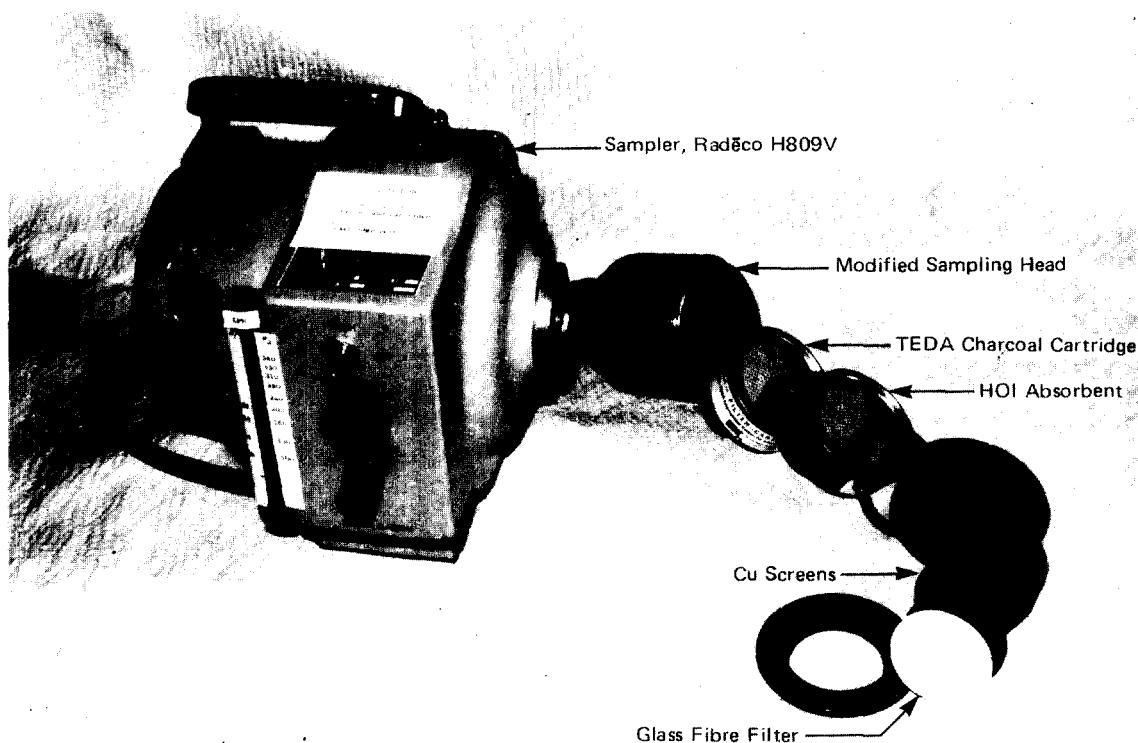


Figure 15 Sampling equipment.

The function of the sampler is as follows:

- Particles are removed from the passing air sample with a Gellman A filter (pure glass fibre, diameter 50 mm).
- Elemental iodine is absorbed in Cu screens (approximately 10 screens, mesh 100, 50 mm diameter).
- HOI is absorbed in a metal cartridge filled with HOI absorbent.
- Organic compounds of iodine are absorbed in a Scott No. 4235-TA cartridge (filled with TEDA impregnated charcoal).

Cuprum screens were the only components in the samplig system which were suitable only for short-term I_2 sampling (maximum of thirty minutes at 30 lpm [~ 1 cfm] air flow). After this time their efficiency for I_2 absorption started to decline. Further, Cu

screens must be etched with HI just before their use. The etching procedure is given in ⁽³⁾.

In spite of the above complications, Cu screens are being used in our laboratory for specific sampling of I₂ and its removal from gas streams, because of the high efficiency for I₂ absorption and the minimum absorption of HOI (<5%) under the applied conditions. All of the other tested I₂ absorbents absorbed significant portions of HOI; iodine retention was not satisfactory.

Procedure for Selective Sampling and Evaluation of Airborne Radioiodine Species

A sampling flow rate of 30 lpm (~1 cfm) corresponds to the residence time of 0.1 seconds in both the HOI and organic I absorbents. This gives ≥97% absorption efficiency for all three iodine components at 98% RH. Absorption of both HOI on Cu screens and CH₃I in the HOI absorbent does not exceed 5% within the RH range of 30%³ to 98%. A sampling time of up to thirty minutes can be applied when I₂ concentration is to be selectively measured.

It is recommended that in long-term HOI and organic I sampling, two or more HOI absorbent cartridges be applied in series, or the air sampling flow be adequately reduced.

The last cartridge (TEDA charcoal) remains at >98% efficiency for a period of several weeks under the above conditions.

When a dry air (<30% RH) sample is taken, which contains a major portion of organic I, its estimated amount (5%) may be subtracted from iodine activity measured in the HOI absorbent and coincidentally added to the TEDA cartridge results as follows:

$$\text{cpm (org. I)} = \text{cpm (TEDA cartridge)} + 5\%$$

$$\text{cpm (HOI)} = \text{cpm (HOI absorbent)} - 5\% \text{ of cpm (TEDA)}$$

In most practical situations this correction can be neglected.

VI. Conclusions

1. The new absorbent described above has high efficiency for selective HOI absorption within a wide range of sampling conditions. The absorbent retains its good efficiency for a period of several weeks in a continuous sampling regime.

2. The described assembly provides selective sampling for particulate forms of iodine, elemental iodine vapour, hypoiodous acid and organic species of radioiodine.

3. The sampler was successfully applied in identifying the ratio of HOI to organic iodine species in the Pickering NGS spent fuel transfer room atmosphere, after a significant release of fission products had occurred from a defective fuel bundle.

4. For long-term sampling of all radioiodine species in nuclear stations stack effluents and in the environment, an adequate elemental iodine absorbent still has to be developed.

Acknowledgement

The author wishes to express his appreciation to Mr. J. Hartwell for his contribution to the experimental program.

VII. References

1. M. Kabat. "Testing and evaluation of absorbers for gaseous penetrative forms of Radioiodine." Paper presented at the 13th AEC Air Cleaning Conference, San Francisco, August 1974, Proceedings pp.765-800.

2. Panel discussion: "Atmospheric dispersion and nuclear power plant dose assessment - II." ANS annual meeting, New Orleans, June 1975, p.524.

3. P.J. Barry. "Sampling of airborne radioiodine by copper screens." Health Physics, 15, pp.243-250. (1968)

DISCUSSION

LORENZ: I have two questions. (1) Will your adsorber work at higher temperatures, such as 125°C, in either steam and air or dry steam? (2) Have you tried silver plated screens to see if they are specific for elemental iodine?

KABAT: The sampler can be used under the same conditions as other carbons. The impregnant is not volatile. I tested silver plated screens for both elemental iodine and HOI. Silver is very efficient for elemental iodine but absorbs a significant fraction of HOI.

DIETZ: Can the HOI adsorbent be regenerated by heating?

KABAT: Yes, this material can be regenerated, but it is not practical because of its low cost.

WILHELM: What is the chemical reaction that traps HOI?

KABAT: I am sorry, I cannot release this information now. I am going to apply for a patent on the HOI absorbent. The physiochemical model of the selective absorption process and detailed information on this material will be published after submitting the patent application.

KABAT: The limit on sampling time is related to the limited lifetime of the copper screen which is used in the sampler for elemental iodine. The other components, HOI and methyl iodide absorbents, have a much longer life; at least one week, as discussed in more detail in the paper. HOI is analyzed on the adsorber by radiometric evaluation of the column components to determine the amount of radioiodine absorbed in the HOI and methyl iodide absorbents.

14th ERDA AIR CLEANING CONFERENCE

AN ANALYSIS FORMAT AND EVALUATION METHODS FOR EFFLUENT PARTICLE SAMPLING SYSTEMS IN NUCLEAR FACILITIES*

L. C. Schwendiman, J. A. Glissmeyer

Battelle, Pacific Northwest Laboratories
Richland, Washington

Abstract

Airborne effluent sampling systems for nuclear facilities are frequently designed, installed, and operated without a systematic approach which discloses and takes into account all the circumstances and conditions which would affect the validity and adequacy of the sample. Without a comprehensive check list or something similar, the designer of the system may not be given the important information needed to provide a good design. In like manner, an already operating system may be better appraised. Furthermore, the discipline of a more formal approach may compel the one who will use the system to make sure he knows what he wants and can thus give the designer the needed information. An important consideration is the criteria to be applied to the samples to be taken. This analysis format consists of a listing of questions and statements calling forth the necessary information required to analyze a sampling system. With this information developed, one can proceed with an evaluation, the methodology of which is also discussed in the paper. Errors in probe placement, failure to sample at the proper rate, delivery line losses, and others are evaluated using mathematical models and empirically derived relationships. Experimental methods are also described for demonstrating that quality sampling will be achieved. The experiments include using a temporary, simple, but optimal sample collection system to evaluate the more complex systems. The use of tracer particles injected into the stream is also discussed. The samples obtained with the existing system are compared with those obtained by the temporary, optimal system.

Introduction

Compliance with Nuclear Regulatory Commission, Environmental Protection Agency requirements, and state regulatory limits on the release of airborne radioactive particles and gases mandates that airborne effluents discharged to the atmosphere be sampled and measured. Although information is available to assist the specification and design of samplers and monitors for particles in an effluent stream, there is no comprehensive analysis format which can be used to assure that a sampler design will achieve its stated objective. Similarly, the evaluation of a system already installed against a stated performance criteria can be accomplished efficiently only when such an analysis format or required data sheet is available. Once the criteria are stated, and the analysis has been

* Work performed under U.S. ERDA Contract E(45-1)-1830.

14th ERDA AIR CLEANING CONFERENCE

completed, using the questions of the analysis format, a sampling installation can be designed, or one already installed can be evaluated.

The evaluation and validation process may require field measurements and demonstrations to support the theoretical evaluation, depending upon the degree of compromise made with good sampling practices.

Objective

The objectives of this paper are: (1) to present an analysis format for a nuclear facility particulate effluent sampling system and (2) to describe some methods for the evaluation of such a system against performance criteria.

Establishing the Sampling and Monitoring Criteria

Those responsible for reporting effluent concentrations to demonstrate compliance with regulatory requirements must determine exactly what the sampling and monitoring system is to accomplish. At first glance this may seem a trivial requirement, but what is required may be a very simple system or a very complex one. The sample may be an inventory sample which will integrate over a 24-hour or a one-week period. On the other hand, the sample may be a monitor-type sample for unusual releases and require a much larger or smaller sampling rate than the inventory-type sample. Are both types needed? The question of the range of particle sizes to be sampled in a representative way should be decided. Even though effluents from nuclear facilities are efficiently filtered, over long periods of operation, the ducts downstream of the filters may accumulate contaminated dust which may have entirely different characteristics than the primary released materials. The question of particle sizes present during a malfunction in the system yielding off-standard conditions must likewise be addressed. The sensitivity of the radiochemical analysis methods for the sample must be carefully considered taking into account the length of time available for analysis and counting the sample for the required accuracy.

Following is a list of statements which taken together will establish the criteria for which a sampling system can be designed or against which an installed sampling and radiochemical analysis system can be evaluated:

1. Name the isotopes to be sampled and measured. (Specific or general such as gross beta, gross alpha emitters.)
2. State the purpose of the sampler installation.
 - a. To obtain an integrated release of radioactivity associated with particles.
 - b. To obtain a sample for continuous monitoring by a detector "looking" at the collected material.

3. State the minimum quantity (μCi) of the isotope(s) in question which must be measured to a given \pm on a stated confidence interval, in a stated period of time. For example:

"The inventory sampler must provide a ^{239}Pu sample over a 24-hour period such that $0.01 \mu\text{Ci}$ can be measured by direct counting a filter in a 10-minute count to $\pm 25\%$ at the 90% confidence level. Detector efficiency is 0.40."

or

"The monitor sample must be withdrawn in a representative way at such a rate that $1 \times 10^{-12} \mu\text{Ci/cc}$ of ^{239}Pu will trip an alarm within 15 minutes."

The statement of sensitivity and accuracy must be consistent and realistic with:

- The total stack flow of effluent and the release limit in terms of curies per day or per week, etc.
- The efficiency of the detector to be used.
- The background counting rate, taking into account energy discrimination in the system, and naturally occurring interferences.
- The counting statistical reliability within the time constraints imposed.

4. State overall accuracy required of sample extraction and delivery to the collector. This statement would cover the acceptable deviation from complete representativeness of the sample extraction and any distortion resulting from line losses, etc. The accuracy may be related to the fraction of the release limit experienced during the sampling period. For example:

at 10% of permitted release, Accuracy: $\pm 100\%$
 at 80% of permitted release, Accuracy: $\pm 20\%$

Compliance under these criteria statements would be determined only after the sampling. A system designed for $\pm 20\%$ at the outset would not fall short even when very low emission levels were experienced.

5. State the range of particle sizes for which the system is to be designed. (Comment: This statement may permit all or some fraction of particles above a certain size to be very poorly sampled. A statement such as "At least 95% of particles $\leq 5 \mu\text{m}$ AED to be extracted and 75% of particles $\leq 10 \mu\text{m}$ and $\geq 5 \mu\text{m}$." Since many sampling systems' efficiencies are highly dependent on particle size, it is necessary to set down a particle size criteria.)

14th ERDA AIR CLEANING CONFERENCE

6. State whether the inventory sample is also to be the continuous monitor sample which would be analyzed in a laboratory after the fact.
7. State the upper limit of the range of the monitoring system. This will help define the electronics of the system to prevent overloading during release incidents.
8. State the emergency electrical back-up system required to assure continuity during power failure.
9. State the requirements for "fail safe" monitoring. Malfunction of sampler air mover, detector failure, etc., should activate an alarm.
10. State required detector calibration frequency and methods.

The Analysis Format and Check List

With the sampling and monitoring criteria established, the design of a new system, or evaluation of an existing sampling system can be undertaken. In either situation, the same information is required. In the case of the new designs the designer has flexibility and many options to adjust the system parameters to meet the design criteria. The format and check list developed below is one to be applied to the evaluation of an already-installed system. It is the purpose of the analysis format and check list to acquire the needed data to insure that the system can be designed or evaluated properly.

Sampler Location and Physical Description

- A. Building number and name, sampler designation.
- B. Ventilation component or exhaust to be sampled. State anticipated radionuclides in exhaust.
- C. Description. Brief description with good, understandable sketch of ventilation system and sampler. Current engineering drawings. (Insure that actual system conforms to drawings.)
- D. Specific information needed.
 1. Air flow rate in stream sampled.
 2. Velocity distribution at section sampled.
 3. Dimensions of duct.
 4. Location of sample withdrawal point(s) with respect to nearest fan, bend, transition, breeching, air filter.
 5. Sampling system materials in direct contact with sampled air.
 6. Inlet sample probe dimensions.
 7. Bends in lines between probe inlet and collector media.

14th ERDA AIR CLEANING CONFERENCE

8. Horizontal delivery lines - lengths, dimensions.
9. Vertical lines - lengths, dimensions.
10. Design sampler flow rate. Velocity in the sampling probe inlet.
11. Is a manifold and secondary sample probe used? Describe.
12. Location and description of sample flow measuring device and recorder, if used. Calibration, or other confirmation of flow rate accuracy taking into account humidity, temperature, and pressure.
13. Provision for eliminating moisture condensation in sampling line.
14. Sample temperature measurement.
15. Measurement or knowledge of temperature and humidity of effluent exhaust air.
16. Description and location of sample pump or aspirator.
17. Are there any provisions for measuring radioactivity associated with different particle sizes? If so, describe.

Sampler Collector Media and Support

- A. Media - glass fiber filters, cellulose, membrane, etc.
- B. Dimensions of filter.
- C. Design face velocity.
- D. Assumed filter efficiency, references.
- E. Description of filter holder.

Sampler Operation

- A. Provide written procedure for start-up and operation of sampler.
- B. Provide written procedure for shut-down and collector removal.
- C. How are collectors protected in transport to counting room?
- D. State sampling time.
- E. Are checks made of equipment and flowmeter during the run? Describe. Are alarms or indicators showing pump failure incorporated in the system? How soon can corrective action be carried out? Is emergency power available in case of power failure?
- F. Is visual appearance of collector recorded, such as color, wet, dry, torn, sound, etc.?
- G. How is filter or other collector identified?

Measurement of Radioactive Constituents on Collector Media (Sample Assayed After Collection)

- A. Sample removal processing.
 1. Collector media sectioned?
 2. Chemical processing, leaching, extraction?
- B. Describe detector system used.
 1. Alpha particle counter, beta particle counter, gamma detector, other? Describe.

14th ERDA AIR CLEANING CONFERENCE

2. Geometrical arrangement for counting radioactivity on collectors.
- C. Describe counter operation.
 1. Give time-length of count, or other index such as total counts taken.
 2. State statistical quality controls on counting system. Describe calibration procedures for specific isotopes and total α , β , and γ counting.
 3. Show how error and confidence limit of sample count are calculated and expressed, taking into account the background of the counter, and length of count. State how "minimum detectable" quantity is determined.
- D. Calculation of 24-hour release to the environment, or other reporting basis.
 1. Define elements of calculation, and the formula used.
 2. Show error estimate for each term in calculation and how determined.
 3. Is an error range determined for the 24-hour release of radionuclides? If so, how is it determined, and what confidence level is used? For example, is the error based on the most significant error in the several elements of the determination, or is the error estimated taking into account propagation of errors in separate, several elements of the calculation?
 4. State the minimum "detectable" 24-hour release, and state the confidence interval with such statements as "...There is only 1 chance in 10 that a release twice this value will go undetected." Convert the release limit into equivalent concentration in the effluent stream sampled in $\mu\text{Ci/cc}$. Explain how the detection limit is determined (Anticipated statistical fluctuations in the background count will provide one reference point for estimating detection sensitivity.)

Records

- A. State how sample results are entered into the official record of released radioactive materials, and the procedure for maintaining this record.
- B. Describe format of this record.

The following section is the analysis format for the monitoring function of the sampling system. In general, the above sections are applicable to the constant monitoring function of a sampling system. Frequently, but not necessarily, the sampler fills a dual role of an inventory of the 24-hour release and a monitor. A detector is located in close proximity to the collector, and the counting rate or accumulated count is recorded at a point in a control room, or other frequently occupied space. Appropriate alarms are provided.

Monitoring Function

- A. Description -- Describe the collector-detector installed in the system.

14th ERDA AIR CLEANING CONFERENCE

1. Geometrical arrangement of collector and detector.
 2. Written and graphic description of pathway of gas and particles through the system. Drawings, sketches, etc.
 3. Describe radioactivity detectors. (Whether α , β , or γ , solid state, GM counters, sodium iodide, etc.) Is discrimination provided to permit only selected radio-nuclides to be sensed?
 4. Flow rate, if not included in section titled "Measurement of Radioactive Constituents on Collector Media (Samples Assayed After Collection)."
 5. Describe signal generated and how displayed. (Count rate instrument, scaler, other integrating system. Is background automatically subtracted, etc.)
- B. Response to radionuclides for which system is designed.
1. State whether total alpha particle, total beta, total gamma, photon detector, or whether discrimination is provided for radiation type and energy.
 2. State method for detector calibration.
 - a. Source used - certification, standardization.
 - b. Frequency (built-in checks, etc.).
 - c. Adjustment to predetermined limits? Discriminator setting, etc.
 - d. Linearity at "high" levels of release. Calibration under this circumstance.
 3. State dynamic range of the instrumentation.
 - a. Anticipated maximum rate of release during accident or other inadvertent releases.
 - b. System response at important action levels. Describe the release levels prompting various actions. State how and how often the monitor is functionally tested at the various levels of concern.
 4. State sensitivity of the system. Provide statement of minimum radioactivity detectable and support the statement in a discussion of background routinely experienced, the detector-collector geometry and intrinsic detection efficiency of the radiation sensor, the sample flow rate and the time required to reach a stated level above background. State the results in terms of the release in μCi , which would be detected above background with a 90% probability. For the design sampling time between filter or other collector replacement, state the minimum detectable release rate and equivalent concentration $\mu\text{Ci}/\text{cc}$ in the effluent stream sampled.

Reliability

- A. State whether a redundant monitor is provided.
- B. Describe provisions for insuring that failure of any critical feature will be signaled.
 1. Sample flow.
 2. Detector components.
 3. Charts.
 4. Alarm circuits.

14th ERDA AIR CLEANING CONFERENCE

- C. Describe availability of emergency power and time sequence to activate.
- D. Describe the time sequence of actions to correct a monitor malfunction. Is the time required to restore the monitor to normal operation consistent with technical specifications or other licensing requirement for operating the facility with continuous monitoring of effluents? Explain the rationale leading to current operating practice.
- E. Describe preventive maintenance procedures which assure reliability.
 - 1. Component functional tests.
 - 2. Parts replacement program.
 - 3. Spare parts and components availability.
 - 4. Other.

Evaluation of Particle Sampling and Monitoring Systems

With the Sampling Criteria defined and with the data supplied from the Analysis Format and Check List, one can proceed to evaluate the system as designed or as it exists. The compliance with many of the sampling criteria can be assessed by simple inspection; however, determining the compliance with criteria governing performance and representativeness requires more detailed attention. In this section are discussed the elements of theoretical and experimental evaluation procedures which will lead to decisions regarding compliance with sampling criteria.

Theoretical Evaluation

With the complete data about the configuration and operation of a sampling system one can proceed with a theoretical (or paper study) evaluation of the system's compliance with the performance and sample representativeness requirements of the sampling criteria. Topics that can be addressed in a paper study include: (1) sample aliquot sizes as regards monitor sensitivity and inventory sample analysis accuracy; (2) extraction caused sample bias; (3) fractional delivery of particulates to the collector; (4) collection efficiency; and (5) the combining of these factors to determine if the samples collected are likely to be representative* of the particulate effluent.

Aliquot Size - Inventory Sample Accuracy. The size of the sample aliquot is an important element to consider when evaluating ability to determine integrated releases with a given accuracy. Some of the factors which determine a minimum sample aliquot (assuming representative samples are collected) are:

* A representative sample is one withdrawn from the bulk stream and delivered to the collector in such a way that the collected sample will have the same radioactivity (particulate) per unit volume sampled as exists in the bulk stream. The degree to which the sample may fail to be representative should be defined in the criteria.

14th ERDA AIR CLEANING CONFERENCE

1. Radionuclides of concern.
2. Minimum concentration of isotope which must be measurable.
3. Time interval over which the concentration is to be averaged.
4. Desired accuracy for the analysis of the collected sample at the minimum required concentration.
5. Analytical techniques.

The requirements of the first four factors are usually specified in the sampling criteria and the last is defined by existing laboratory techniques. A common equation relating many of these factors is:

$$\frac{\mu\text{Ci}}{\text{cc}_{\text{effluent}}} = (\text{net c/min})_{\text{sample}} \times \frac{1}{\text{eff}} \times \frac{1}{\text{sample flowrate, ft}^3/\text{min}} \times \frac{\text{ft}^3}{28,320 \text{ cc}} \times \frac{1}{\Delta t, \text{min}} \times \frac{\mu\text{Ci} \cdot \text{min}}{2.22(10^6)\text{d}} \quad (1)$$

where eff is the counting efficiency in count/disintegration and Δt is the sample collection period. The equation is easily rearranged to express the sample flowrate as a function of the other parameters.

A common equation which relates analysis accuracy to the net counting rate is

$$\text{95\% Confidence Interval Limit} = 1.96 \sqrt{\frac{\text{net c/min} + \text{background c/min}}{\text{sample counting time}} + \frac{\text{background c/min}}{\text{background counting time}}} \quad (2)$$

Given a desired \pm accuracy at the 95% confidence level and knowing the details of the analytical technique, the required net count rate for that accuracy and technique can be calculated. The required net count rate can then be inserted into the rearranged equation (1), along with the collection period, minimum measurable concentration and counting efficiency to calculate a minimum required sample flow rate.

To illustrate the use of these equations an example case will be considered with the following assumptions and specifications:

1. Principal isotope present in particulate form and of concern is ^{239}Pu .
2. Minimum measurable concentration is $6 \times 10^{-14} \mu\text{Ci/cc}$.
3. Sample collection time is 24 hours.
4. Detector counting efficiency is 0.40 c/d.
5. Sample counting time is 15 minutes, and background counting time is 5 minutes.
6. Normal background for detector is 0.2 c/min.
7. Desired count accuracy for measuring the above release is $\pm 10\%$, 95% confidence level.

14th ERDA AIR CLEANING CONFERENCE

Taking the last three assumptions and substituting into equation (2) it can be shown that a net count rate of 27 c/min is needed to achieve the desired counting accuracy. Rearranging equation (1) and substituting in the first four assumptions, the minimum required sample flow rate is:

$$\begin{aligned} \text{Sample flow rate} &= 27 \text{ net c/min} \times d/0.4 \text{ c} \times \frac{1}{1440 \text{ min}} \\ &\times \frac{\text{cc}}{6 \times 10^{-14} \text{ } \mu\text{Ci}} \times \frac{\text{ } \mu\text{Ci min}}{2.22 (10^6)d} \times \frac{\text{ft}^3}{28,320 \text{ cc}} \quad (3) \\ &= 12.4 \text{ ft}^3/\text{min} \end{aligned}$$

The existing sample flow rate or the design sample flow rate can then be compared to the calculated flow rate. In some cases, the required flow rate is impractical, this indicates that the specifications of the sampling criteria need to be reconsidered or improvement in the analytical technique needs to be sought. It should be remembered that the calculated sample flow rate is a minimum value because only counting errors are considered and the collected samples are assumed to be representative.

Aliquot Size - Monitor Sample Sensitivity. Many of the factors which affect the monitor sensitivity are the same as those which affect the inventory sample accuracy. They are:

1. Radionuclides of concern,
2. Minimum concentration which must be detected,
3. Time interval within which the minimum concentration must be detected,
4. Counting time (if not continuous),
5. Background level at monitor,
6. Monitor counting efficiency,
7. Sample aliquot size.

Again, the first three factors are usually specified in the sampling criteria and the second three are usually dictated by the available monitoring equipment. Thus, the size of the sample aliquot again becomes an important element in monitor sensitivity and is dependent on the other six factors. With the assumption that ideally representative samples are collected, a minimum required sample flow rate can be calculated once the other factors are specified. The existing sample flow rate or proposed flow rate can then be compared to the calculated minimum.

To give an example of such a calculation the following assumptions will be made:

1. The radionuclide to be monitored is ^{239}Pu .
2. A minimum average concentration of $10^{-13} \text{ } \mu\text{Ci/cc}$ must be detectable above background within a 24-hour collection period.
3. The monitor functions continuously and uses energy discrimination to analyze for ^{239}Pu .

4. The monitor counting efficiency is 0.1 c/d, the background level is 1 c/min, and the detectable response above background is 5 c/m.

The required sample flowrate is then calculated as follows:

$$\begin{aligned} \text{Sample Flowrate} &= \frac{\text{cc}}{10^{-13} \mu\text{Ci}} \times \frac{\text{ft}^3}{28,320 \text{ cc}} \times \frac{\mu\text{Ci min}}{2.22(10^6)\text{d}} \times \frac{\text{d}}{0.1 \text{ c}} \\ &\times \frac{1}{1440 \text{ min}} \times 5 \text{ c/min} = 5.5 \text{ ft}^3/\text{min}. \end{aligned} \quad (4)$$

Again, if in some cases the required minimum flow rate is impractical to achieve, then the specifications of the criteria and the monitoring instrumentation need to be reconsidered.

Extraction-Caused Sample Bias. A bias in collected particulate samples can be caused by the process of sample extraction.* The magnitude of the bias is dependent upon the different sampling conditions, effluent conditions, and particle sizes. Extraction-caused bias can be the result of nonisokinetic extraction or a poor choice of extraction location(s).

Nonisokinetic Extraction Bias. Because particulates do not exactly follow the flow of the gas, it is desirable to minimize flow disturbances and direction changes caused by extraction nozzles. Sample bias caused by the sample gas velocity being different from the approaching gas velocity has been observed by several workers.^[1,2,3,4] Matching the sample airstream velocity at the nozzle to the approaching airstream velocity is known as isokinetic sampling. Several models have been developed to correlate bias, degree of isokinesis, and particle size.^[2,5] The following model by Davies^[4] relates the bias or ratio of sample particle concentration to approach particle concentration, C/C_a , with a function of velocities and particle characteristics,

$$\frac{C}{C_a} = 1 + \left[\frac{V_a}{V_s} - 1 \right] \left[\frac{2 \text{ Stk}}{1 + 2 \text{ Stk}} \right]. \quad (5)$$

In this equation:

- C = concentration in the sample,
- C_a = actual concentration in the stream,
- V_a = gas velocity approaching the nozzle,
- V_s = velocity in the inlet of the sample probe,
- Stk = Stokes' number, the ratio of twice the stopping distance to the nozzle inlet diameter.

* Extraction is herein defined to be the process of separating the sample aliquot from the effluent.

Stokes' number is calculated from the expression:

$$\text{Stk} = \frac{v_a d_p^2 \rho_p}{9 \mu d_o} \quad (6)$$

in which

- d_p = diameter of the particle in cm,
- ρ_p = density of particle in g/cm³,
- μ = viscosity of air in poise,
- d_o = diameter of inlet nozzle in cm.

It can be shown from the above equations and for a given extraction configuration that the bias becomes more significant as the particle size increases.

Location Caused Extraction Bias. The magnitude of location caused extraction bias is not predicted by calculations or theoretical considerations; however, guidelines exist which can indicate whether or not representative samples can be extracted from a given location.^[6] In general the ideal sampling location in a stack or duct is in a vertical run 10 duct diameters and 5 duct diameters from the nearest significant upstream and downstream flow disturbances respectively. It is theoretically possible to obtain a representative sample from a single location; however, it is difficult to find that location, especially if the velocity profile is at all complicated. Instead of finding a single ideal location it is recommended to make up the total sample from samples extracted at various points on the location cross section^[5], or to use some sort of moving probe.

Fractional Delivery of Particles to the Collector. The concentration of sampled particulates is further altered by the deposition and possible later resuspension of particulates in the piping and fittings through which the sample passes before reaching the collection point. The effects of particulate deposition in fittings, valves, transitions, cavities, and later particulate resuspension upon the sample representativeness cannot be predicted by present models. However, there are some models that can be used to estimate the magnitude of concentration modification in smooth horizontal and vertical tubes and in bends. With these models one can find indications, at least, of portions of sample delivery systems where sample modification occurs. The following are some of the available models to aid in the evaluation. (The reader is referred to the references cited for the detailed development of the models.) It can be shown with all the following models that the concentration modification is strongly dependent on the particle sizes that are being considered.

14th ERDA AIR CLEANING CONFERENCE

Gravity Settling in Laminar Flow. The following model was developed [7, 8] for calculating the fractional penetration (or concentration modification) of aerosols in laminar flow in horizontal tubes.

$$C/C_a = 1 - \frac{2}{\pi} \left[2Z\sqrt{1 - Z^2/3} + \arcsin (Z^{1/3}) - Z^{1/3}\sqrt{1 - Z^2/3} \right] \quad (7)$$

$$Z = 0.75 \frac{V_{gs} L}{V_a D} \quad (\text{dimensionless}) \quad (8)$$

V_{gs} = terminal gravitational settling velocity

V_a = velocity in tube (laminar flow conditions)

L = length of duct

D = diameter of duct,

and

$$V_{gs} = \frac{g d_p^2 (\rho_p - \rho)}{18\mu} \quad (9)$$

g = acceleration due to gravity

d_p = particle diameter

ρ_p = particle density

ρ = gas density

μ = gas viscosity.

When $Z \leq 0.2$, equation (6) is approximated within 2% by: [10]

$$C/C_a = e^{-1.7Z}. \quad (10)$$

Bend Losses in Laminar Flow. A model for predicting impaction efficiency of aerosols in laminar flow in bends has been proposed by Cheng and Wang. [9] Adapting the model for the calculation of particulate concentration modification for aerosols with Stokes' Number < 0.1 yields;

$$C/C_a \approx 1 - \left(1 + \frac{\pi}{2R_o} + \frac{2}{3R_o^2} \right) Stk, \quad (11)$$

where R_o is the radius of curvature of the bend divided by the tube radius.

14th ERDA AIR CLEANING CONFERENCE

Gravity Settling-Turbulent Flow. The models for calculating the concentration modification in turbulent flow and for various particle sizes are of the general form^[10]

$$C/C_a = e^{-AL^*} \quad (12)$$

where A is a dimensionless loss factor and L* is the dimensionless tube length. Generally, the dimensionless loss factor is a ratio of settling velocity and gas velocity. For the gravity settling problem

$$A_g = \frac{4}{\pi} \frac{V_{gs}}{V_a}, \quad (13)$$

where V_{gs} is the settling velocity which can be calculated by equation (9).

The dimensionless tube length, L*, is given by

$$L^* = L/D \quad (14)$$

Turbulent Impaction. Turbulent impaction is generally taken into account for turbulent flow in both horizontal and vertical tubes. From the empirical correlation proposed by Sehmel^[11] the following equation for the dimensionless loss factor is derived^[10]:

$$A_t = 1.169 \times 10^{-16} \text{ sp.gr.}_p^{1.01} \text{ Re}^{2.9} R^{2.10} \quad (15)$$

Again, the concentration modification is calculated by equations (12) and (14).

For horizontal tubes the gravity settling and turbulent impaction models are combined to calculate the concentration modification. The two models are simply combined as follows:

$$A_{\text{total}} = A_t + A_g \quad (16)$$

and

$$C/C_{a(\text{combined})} = e^{-A_{\text{total}}L^*} \quad (17)$$

For vertical tubes the turbulent impaction model alone is used to calculate a concentration modification.

Bend Losses in Turbulent Flow. For the case of turbulent flow through bends the following simple model is proposed to give an indication of concentration modification.^[10] The model is essentially similar to that for the gravity settling problem. The dimensionless loss parameter is defined as:

$$A_b = \frac{4}{A} \frac{V_{cs}}{V_a} = \frac{2}{9} \frac{\rho_p d_p^2 V_a}{\mu R_b}, \quad (18)$$

where V_{cs} is the centrifugal settling velocity. The centrifugal settling velocity is similar to that for gravity settling except that the acceleration of gravity is replaced by the centrifugal acceleration which is approximated by V_a^2/R_b .

Again the concentration modification is calculated by equation (12) where,

$$L^* = \frac{\pi}{180^\circ} \frac{\theta R_b}{D} \quad (19)$$

Sample Collection Efficiency. The efficiency of the collection filter is an important factor to be considered in the evaluation of sample representativeness. Included in the consideration of efficiency is the effect of self absorption of the filter material upon the counting efficiency. Unfortunately, the collection efficiency and self absorption have to be determined experimentally; however, the collection efficiencies for several filters and particle sizes have been reported in the literature, and can be factored into the theoretical evaluation.

Combining Concentration Modifications. Many sample delivery systems include one or more bends and horizontal and vertical runs of tubing. The calculated concentration modifications for each segment of the system plus the nonisokinetic extraction bias can be combined in most cases (except when extraction occurs more than once) by a simple calculation. The total system concentration modification can be calculated as follows:

$$C/C_a \text{ (total system)} = \prod_{i=1}^{n \text{ segments}} (C/C_a)_i \quad (20)$$

The combined concentration modification can indicate whether or not the samples collected by an existing or proposed system will be representative of the particulate effluent to the extent desired.

Experimental Methods for Evaluation of Sampling Systems

A second approach to the evaluation of an existing sampling system is to conduct a series of experiments to demonstrate the representativeness of the collected samples. A reasonable way to do this is to collect samples of the effluent with a standard sampling device while at the same time samples are being collected with the existing system. The concentration data from the standard and routine samples can then be compared to give an indication of the representativeness of the samples collected with the existing system. The following discussions will address some of the preparations necessary to collect the standard samples and offer some suggestions as to what can be done with the samples to allow comparisons of the data.

Preparations for Obtaining Standard Samples. One of the major preparations for standard sampling is to choose as ideal a sampling location as possible. The guidelines mentioned earlier under the heading "Location Caused Extraction Bias", can be helpful in finding a satisfactory location. The access at the chosen location must be large enough for the insertion of sampling probe and/or filter support.

Once the location is chosen, it is necessary to learn as much as possible about the condition of the effluent at that location. A complete velocity profile of the duct cross section is necessary and a temperature and pressure profile will be helpful as well (for determining mass flux). It is also valuable to determine the effluent humidity and dewpoint so steps can be taken to avoid moisture condensation in sampling lines and on the collected samples.

After the above information is obtained, it is necessary to determine the concentration profile of the particulate effluents in the available cross section. This can be found by simultaneously collecting samples from several points in the cross section. With the data from several sets of simultaneous samples, significant differences from point to point may be determined by constructing a two-way classification analysis of variance table. Then one or more "standard" sampling points can be selected.

The sampling configuration for the concentration profile experiment and for the following comparison experiments should be as simple as possible. Each sample can be collected by fixing a tapered nozzle to the front of a filter holder and suspending the assembly in the duct. The inside and outside tapers of the nozzle should be no more than 15° to minimize the airflow disturbance and particle deposition on the inside wall. The filter should be chosen to have a high collection efficiency for the particulate sizes expected and to permit a sufficient sample flow rate. The vacuum pumps and flow control equipment can be located exterior to the duct. The flow rate and nozzle inlet size should be adjusted so each sample can be extracted isokinetically for the

velocity at each sampling point. Prior to analyzing the concentration profile data the data must be normalized for differences in sample flow rate and any other differences at each location.

Information about the size distribution of the particulates of interest is also helpful for interpreting the results of the comparison tests because the performance of a sampling system is highly dependent upon the sizes of the particles it is expected to sample. Particle size data can be obtained with the use of light scattering devices for particle sizing, microscopic analysis of particles collected on filters, or cascade impactors. The cascade impactor is the preferred device because the aerosol size fractions are collected on separate samples which can then be analyzed for the element, compound, or radionuclide of interest. The particle sizing samples should be extracted from the same location as the standard samples.

Comparison of Sampling Data. Once a location is found and equipment assembled to obtain the standard samples the performance of the existing sampling equipment can be tested. The collection intervals for the standard samples should be the same as for the sampling system being tested. Also, the samples collected by both systems should be analyzed for the particulates of concern in the same laboratory and with the same procedure, and the data should be normalized for differences in sample flow rates.

There are several ways the two sets of data can be analyzed and the sampling criteria that are being used will influence the choice of method. One method is to perform a linear regression on the data to see if a constant or percent bias exists. If the regression line does not pass through the origin, a constant bias exists between the routine and "standard" samplings. If the regression line passes through the origin, but with a slope other than one, then a percent bias is indicated. A second method is to calculate the difference in each sample pair and then calculate the mean difference. Hypotheses on the mean difference can then be tested. Another possibility is to perform statistical manipulation on the ratios of each sample pair if the ratios can be shown to be normally distributed. Methods other than these three may also be appropriate to test if the samples collected with an existing system comply with the chosen sampling criteria.

Use of Tracer Aerosols. As is common for the effluents of some nuclear industry facilities, the concentrations of the particulates of concern are too low to permit the collection of samples and the completion of such an experimental program as the above in a reasonable length of time. In such instances a tracer aerosol injected into the effluent may help to expedite the experiments. Some of the desirable characteristics of the tracer aerosol are:

1. Nontoxic in the quantities used,
2. Inert to the effluent and sampling system environments,
3. Not already present in the effluent or collection media to any appreciable extent,

14th ERDA AIR CLEANING CONFERENCE

4. Same particle size distribution upon generation as the particulates of concern or of the same size which corresponds to the requirements of the sampling criteria,
5. Easy to analyze on collected samples with an available technique.

The tracer aerosol should be injected into the effluent stream at a point far enough upstream of both the existing and standard sampling systems to allow for thorough mixing of the tracer with the effluent.

Also, it is important that the device used to generate the aerosol can be used in the field and can generate the required amount and required rate reproducibly.

Summary and Conclusions

An evaluation of an existing or proposed particulate effluent sampling system includes the following elements.

- It is essential to decide what function the sampler is to perform and what defines successful performance of that function.
- Information must be gathered concerning all the factors affecting sampler performance. Some of the factors mentioned in the paper are: sampler location, sampler environment, sample collection medium, sampler construction, and sample analysis and monitoring.
- The evaluation then proceeds as either or both a theoretical or experimental study. In the theoretical study the effects of aliquot size, extraction bias, particle deposition, and other factors upon both the representativeness of collected samples and accuracy of sample analysis or monitoring can be estimated. In the experimental study the samples collected with the existing system are compared with simultaneously collected standard samples to estimate the performance of the existing system. Tracer aerosols have been found to be a useful tool in the experimental study because of the cleanliness of nuclear facility effluents.

Many of these elements of the evaluation method can also be useful to the designer of sampling systems because the effects of design upon the sampler performance can be predicted.

Nomenclature

- A = dimensionless loss factor
- A_b = dimensionless loss factor for bends
- A_g = gravity settling dimensionless loss factor
- A_t = turbulent deposition dimensionless loss factor

14th ERDA AIR CLEANING CONFERENCE

C = aerosol concentration
C_a = original aerosol concentration
D = tube inside diameter
L = length
L* = dimensionless length
R = ratio of particle size in microns to tube diameter in centimeters
R_b = bend radius
R_o = ratio of bend radius to tube inside diameter
Re = tube Reynolds' Number
Stk = particle Stokes' Number
V_a = average gas velocity
V_{cs} = particle settling velocity in bends for centrifugal acceleration.
V_{gs} = particle terminal settling velocity
V_s = sample airstream velocity inside nozzle orifice
Z = dimensionless settling factor for laminar flow
c = counts
cc = cubic centimeter
d = disintegration
d_p = particle diameter
d_o = probe nozzle orifice diameter
eff = counting efficiency, c/d
ft³ = cubic feet
g = acceleration due to gravity
min = minute
sp.gr._p = particle specific gravity
Δt = elapsed sample collection time

14th ERDA AIR CLEANING CONFERENCE

θ = angle of bend, degrees

μ = gas viscosity

μCi = microcurie

ρ = gas density

ρ_p = particle density

14th ERDA AIR CLEANING CONFERENCE

References

- [1] S. Badzioch, "Collection of Gas-Borne Dust Particles by Means of an Aspirated Sampling Nozzle," British Journal of Applied Physics, Vol. 10, January 1959.
- [2] H. H. Watson, "Errors Due to Anisokinetic Sampling of Aerosols," American Industrial Hygiene Association Quarterly, Vol. 15, March 1954, pp. 21-25.
- [3] S. P. Belyayev and L. M. Levin, "An Experimental Investigation of Aerosol Aspiration," translated by J. Findlay from Izv. Akad. Nauk. Ser., Atmospheric and Oceanic Physics, Vol. 6, No. 11, 1970, p. 1137.
- [4] G. A. Sehmel, "Particle Sampling Bias Introduced by Anisokinetic Sampling and Deposition Within the Sampling Lines," American Industrial Hygiene Assoc. Journ., Vol. 31, Nov.-Dec., 1970, pp. 758-771.
- [5] C. N. Davies, "The Entry of Aerosols into Sampling Tubes and Heads," Brit. J. Applied Physics, Ser. 2, 1 p. 921-932.
- [6] American National Standards - ANSI N13.1-1969, Guide to Sampling Airborne Radioactive Materials in Nuclear Facilities, American National Standards Institute, New York, NY, (1969).
- [7] G. Natanson, Quoted by N. A. Fuchs, The Mechanics of Aerosols, Pergamon Press, Oxford, England, 1964, p. 112.
- [8] J. W. Thomas, "Gravity Settling of Particles in a Horizontal Tube," J. Air Pollution Control Association, Vol. 8, pp. 32-34, 1958.
- [9] Yung-Sung Cheng and Chiu-Sen Wang, "Inertial Deposition of Particles in a Bend," Aerosol Science, Vol. 6, pp. 139-145, 1975.
- [10] L. C. Schwendiman, G. E. Stegen, and J. A. Glissmeyer, "Methods and Aids for Assessing Particle Losses in Sampling Lines," presented at the American Industrial Hygiene Association Meeting, Minneapolis, Minnesota, 1975. BNWL-SA-5138, Battelle-Northwest, Richland, Washington, 1975.
- [11] G. A. Sehmel, "Particle Deposition from Turbulent Air Flow," Journal of Geophysical Research, Vol. 75, No. 9, pp. 1766-1781, 1970.

14th ERDA AIR CLEANING CONFERENCE

THE USE OF A SINGLE PARTICLE INTRA-CAVITY LASER PARTICLE SPECTROMETER FOR MEASUREMENTS OF HEPA FILTERS AND FILTER SYSTEMS*

B.G. Schuster and D.J. Osetek
Los Alamos Scientific Laboratory
University of California
Los Alamos, New Mexico 87545

Abstract

Current tests of HEPA filters and/or filter installations using DOP aerosols and conventional forward light-scatter photometers are limited to measuring protection factors of 10^4 to 10^5 . In addition, forward light-scattering photometers have markedly decreased sensitivity to $<0.3 \mu\text{m}$ particles and basically measure only a scattering signal which is not uniquely related to any given concentration or size distribution of scatterers. These limitations require that high efficiency systems, such as multiple stage HEPA filters, be evaluated one stage at a time, a procedure which is quite often impractical for many existing air cleaning systems and which may be in error.

In order to obviate these difficulties, a single particle intra-cavity laser particle spectrometer has been used to measure protection factors of up to 2.4×10^8 for multiple HEPA systems and individual double ply HEPA filters. Because of the instrumental size resolution, protection factor as a function of particle size can be determined from $.06 \mu\text{m}$ to $2.9 \mu\text{m}$. The lack of background enables single counts to be statistically significant. Since coincidence errors occur at particle concentration $>10^6/\text{liter}$, a known dilution must be introduced to measure challenge concentrations greater than this. The dilution measurement may be accomplished with the aid of a forward light-scattering photometer.

I. Introduction

Test methods for HEPA filter installations currently consist of testing individual stages of multi-stage systems. The method currently in use consists of introducing a challenge aerosol of DOP upstream of the stage to be measured and making light-scattering measurements with a forward light-scattering photometer upstream and downstream of the filter bank. The ratio of the two scattering signals is then used to determine the protection factor (PF) or penetration of the stage. Light-scattering photometers currently in use have an effective dynamic range limited, primarily by sensitivity, to 10^4 , hence limiting the measurable PF to this range. The PFs thus measured are simply a ratio of light-scattering signals which are not uniquely related to either the concentration or size distribution of the population of scatters. Since the filtration process changes the size distribution, the PFs determined in the above fashion are strictly

*Work supported by the U.S. Energy Research and Development Administration.

14th ERDA AIR CLEANING CONFERENCE

valid only for monodisperse aerosols, and then only if size changes due to coagulation and/or evaporation do not occur. High efficiency systems such as multi-stage installations can at best be evaluated only on a single stage basis, a procedure, which, because of some present designs as well as new design criteria,¹ is quite often impractical and may result in defining an incorrect PF.

A method for accurate testing of PFs to 10^8 , e.g., two-stage systems, would obviate the above difficulties and in addition decrease operational downtime and worker exposure. The design of new facilities, e.g., installations using doubleply HEPA filters, should also become simpler and less expensive. The following results, on a laboratory scale, show the feasibility of one such method.

II. Design Criteria and Apparatus

The design criteria for the laboratory scale experiment were predicated on the method to be used for measurement of downstream aerosol concentration. Considering the protection factor desired an initial challenge of 10^9 particles/liter would be attenuated, after passage through 2 HEPA filters, to as little as one particle/liter. Greater challenge concentrations (of approximately $0.3 \mu\text{m}$ CMD) would load the first filter so excessively that the testing procedure would be destructive. A conventional forward light-scattering photometer² is incapable of measuring the low concentrations anticipated downstream of two HEPA filters. Filter sampling, even with a tracer aerosol such as uranine, would require impractically long sampling periods to obtain a detectable concentration. The required sensitivity dictated a device capable of counting and measuring single particles.

A sensitive, laser operated, optical single particle counter and spectrometer was chosen as the detector. This device relies on the scattering of laser light at 633 nm within the optical cavity of a He-Ne laser. The He-Ne laser, being a low gain device, has an intracavity radiation field some 500 times as great as the rated output power. It is the scattering³ of this intense field by a particle, which is detected and measured. The detector signals are sorted and stored in a 16-channel multi-channel analyzer. By use of a range selection switch, a size spectrum from $.06 \mu\text{m}$ to $2.9 \mu\text{m}$ may be measured in concentrations as high as 10^7 /liter with less than 1% coincidence error.

A laboratory wind tunnel was constructed for testing two $20.3 \text{ cm} \times 20.3 \text{ cm} \times 10.2 \text{ cm}$ (8" x 8" x 4") HEPA filters in tandem (Fig. 1). This system is simply a scaled-down version of a typical HEPA industrial system, the flow volume per unit filter surface area being the same in both cases. In this manner, the feasibility of the measurement could be verified without the necessity of first building a high volume challenge aerosol generator. Clean air was provided by filtration of room air through a $30.5 \text{ cm} \times 30.5 \text{ cm} \times 15.3 \text{ cm}$ (12"x12"x6") filter. The design airflow was 25 cfm and appropriate orifice plates for flow measurements, isokinetic probes for sampling, and pressure gauges at each filter station were incorporated into the system. In order to enable measurements of the challenge concentration upstream of the first filter, a diluter stage consisting of a second wind tunnel was also constructed so that 0.2% of the challenge aerosol could be sampled by the diluter and measured by the optical

single particle counter. The dilution ratio is variable and is confirmed by either filter sampling or photometer sampling of the challenge and diluted aerosol. A six stem (24 jet) Collison type aerosol generator was constructed to provide the challenge aerosol.

III. Challenge Aerosol Characteristics

Two different aerosols have been characterized for their use in laboratory experiments. Both of these were generated by the six stem Collison generator described above. The solid aerosol was produced from a 5% solution of NaCl in water. Its characteristic spectrum (Fig. 2) is quite different than would be expected from a log-normal distribution; in particular, the low end of the spectrum shows no tendency to return to zero, i.e., the distribution is monotonically decreasing.

The spectral characteristics (Fig 3) of an aerosol generated from a 5% DOP in ethyl alcohol solution are very similar to those produced by the NaCl solution. Both distributions may be quite well approximated by the function

$$\frac{\ln N(D)}{\ln N(D_0)} = \exp \{-k(D-D_0)\} \quad \text{where,} \quad (1)$$

$N(D_0)$ is the count at smallest size D_0 , and $N(D)$ is the count at some other diameter, D . The constant, k , may be obtained from fitting the curve, and in the case of the DOP aerosol, is equal to 3.21.

These distributions are different from those measured with an earlier model spectrometer. This discrepancy is presumably due to the much higher resolution and sensitivity of the present detector, which does not decrease at the small end of the spectrum.

The aerosol generator design figure of approximately 10^9 particles/liter was verified with the single particle spectrometer.

IV. Single HEPA Filter Characteristics

Sodium Chloride Aerosol

One of the problems anticipated in challenging HEPA filter systems with extremely high challenge aerosol concentrations was destruction of the performance of the first filter due to loading, particularly with a solid aerosol. In order to determine HEPA performance under these conditions, a filter with DOP quality control protection factor of 8.3×10^3 was monitored for 11 sequential 2-min periods, for a total of 22 min, using the aerosol spectrometer. The penetration of this filter decayed exponentially with a half-life of 4.5 min. This same penetration decay was consistent for all size ranges, i.e., penetration was not size dependent for particles between 0.1 and 1.0 μm (Fig. 4). Extrapolation to zero time sampling yielded a count protection factor of 9.8×10^4 , an order of magnitude greater than determined by DOP quality control testing.

A similar experiment was conducted with a second filter with a DOP quality control determined protection factor of 7.1×10^3 . The

penetration for this filter remained constant for 8 min and then assumed an exponential decay with half-life of 1.9 min as shown in Fig. 5. Spectral decomposition of the decay rates indicated some variation as a function of size, but probably within the figure of merit associated with the data. The initial constant penetration was probably due to a leak which finally was plugged by the challenge aerosol. Even so, the measured protection factor was 1.1×10^5 , more than an order of magnitude greater than the DOP figure. Eight sets of filter decay data provide widely scattered penetration decay rates with a range of half-lives of 1.6 min to 13.5 min, with an average of about 4 min.

While performing these and subsequent tests, substantial leaks were discovered in the cases of several of the test filters. A coating of RTV cement was sufficient to stop the leaks.

One area of interest in multiple filter test studies is the variation of efficiency with size of the challenge aerosol. If such a variation exists, a challenge aerosol distribution will be modified so that the least efficiently collected part of the aerosol spectrum will be the challenge for the second filter in a tandem configuration. Hence, if a gross measurement of PF is made for each of two filters separately (as is now the case), the product of these measurements will overestimate the system PF.

Four individual filters were challenged with the aerosol distributions displayed in Figs. 2 and 3. The quality control penetration data for these four filters were within a factor of two of each other. Three of the filters were challenged with NaCl aerosol, and one with DOP aerosol. Protection factors per unit size interval were obtained by dividing the challenge aerosol count/unit time/size channel by a similar count in the downstream flow. The results of these measurements are plotted as PF against size (Fig.6.). It is immediately manifest that these filters are extremely efficient for particles less than $0.10 \mu\text{m}$. Protection factor reaches a minimum at about $0.19 \mu\text{m}$ and begins to increase again beyond $.23 \mu\text{m}$. These results are in consonance with theoretical arguments which predict enhanced collection of very small particles and large particles due to Brownian diffusion and direct impaction respectively. The inference to be drawn from these results is that for test results to be at least grossly reliable, a substantial portion of the test aerosol must be in the range $0.1 \mu\text{m}$ to $0.23 \mu\text{m}$ for particle count/size measurements. For nonsize discriminating instruments such as a forward light-scattering photometer, where the signal may be proportional to the second or third moment of the diameter, the challenge aerosol should not exceed $0.23 \mu\text{m}$ and preferably should be within the limits of $0.1 \mu\text{m}$ to $0.23 \mu\text{m}$.

DOP Aerosol

Similar HEPA filter performance experiments were conducted using the DOP spectrum illustrated in Fig. 3. The loading characteristics of these filters challenged by DOP are very much different than for the NaCl aerosol. Referring to Figs. 7 and 8, penetration initially drops, then slowly climbs to near its starting value. The system is flushed with clean air for 30 min before DOP is re-introduced, at which time the penetration increases. It was

14th ERDA AIR CLEANING CONFERENCE

initially thought that liquid DOP, blown off the backside of the filter was responsible for the first increase in penetration. However, the subsequent drying period (DOP vapor pressure is 8% that of H₂O at STP) and further increase of penetration discounts this supposition. Examination of the filter media under high magnification before and after exposure to DOP indicated no obvious change in structure.

The variation of protection factor with size is displayed in Fig. 9. The performance against DOP is very similar to that of NaCl, with the minimum occurring for the same size. The minimum value is again approximately that given by the quality control test.

V. Multi-Ply HEPA Filter Tests

Several filters constructed with a multi-ply HEPA filter medium were supplied for evaluation. The utility of these filters would appear to be in their use in compact filtration systems, in reducing down time for changes (fewer filters), reducing potential personnel exposure (fewer changes), and decreasing total number of potential leaks. A problem would exist with conventional testing since the PF for two plies would be expected to be approximately equal to the product of the PFs per individual ply, i.e., in excess of 10⁶, and this could not be quantitated with existing test techniques.

The filters were tested with NaCl or DOP aerosols. Loading of the filter, particularly by NaCl, changes the characteristics of the filter sufficiently so that a subsequent test with DOP would not be meaningful.

The test results for the filters are summarized in the first two rows of Table I.

TABLE I
PENETRATIONS OF SELECTED FILTERS

Filter No.	Pressure Initial	Drop Final	Tested Penetration (50 CFM) .3 μm QC(DOP)	Measured Penetration @LASL (25CFM)
A452698	.6" H ₂ O	.8" H ₂ O	.002%	(.000011 ± .000003)% (NaCl)
A452696	1.39" H ₂ O	1.40" H ₂ O	.004%	(.0000014 ± .0000005)% (DOP)
34652	.72" H ₂ O	.76" H ₂ O	.008%	(.0031 ± .0002)% (DOP)

The initial and final pressure drops indicate the loading effects of the aerosol over the 15 min test period. The loading is substantial for NaCl. For comparison purposes, the data for a conventional single ply filter tested with DOP is shown in the third row of Table I.

The gross discrepancy between these results and the QC test results are principally due to the lack of sensitivity of the forward scattering photometer used in the DOP QC test. Readings of 10⁻⁵% simply get lost in the noise of the forward scattering photometer.

14th ERDA AIR CLEANING CONFERENCE

VI. Tandem HEPA Filter Tests

A series of measurements was performed on two stage HEPA filter configurations using both 5% NaCl in water and 5% DOP in alcohol to generate the challenge aerosols. The procedure used is as follows. Background counts downstream of each filter section were made with the aerosol spectrometer and external leaks sealed until the count rate was less than 1 per 10-min interval. This was done with a 25 cfm airflow with no aerosol generation. With the generator turned on, a 1-min sample was taken downstream of the first filter. A subsequent 10-min sample was then taken downstream of the second filter. Samples were then obtained downstream of the first filter for 10 more 1-min sample periods so that an interpolated (back to time zero) penetration decay curve could be obtained. A 1-min sample was taken at the diluter stage and the dilution factor was determined by photometer and/or filter samples obtained between the diluter and the main wind tunnel.

Table II summarizes the results of the 6 sets of filters measured.

P is the protection factor, the subscripts refer to the position of the filter (1, 2 or 2 + 1), and whether this is a DOP quality control determined (s) or measured (m) value. The values of P_{21m} are actual measured operational values integrated over a 10-min interval and have not been corrected for the penetration decay of the first filter. Such a correction would decrease P_{1m} and would be applied to P_{21m} hence decreasing it. The values of P_{2m} are derived from the ratio of P_{21m}/P_{1m} . To reiterate, P_{1m} is the zero-time first filter protection factor, and P_{21m} is the overall factor for a 10-min period during which the penetration of the first filter is constantly decreasing. The product of P_{1s} and P_{2s} yields P_{21s} . During an 11-min period of testing, the pressure drop across the first filter increases by about 15%. This loading makes it mandatory that, at least with a NaCl challenge aerosol, the testing period be kept as short as possible. It may be that a DOP challenge aerosol will not present this problem. This hypothesis will be checked.

These measurements indicate that overall protection factors as high as 2.5×10^8 can be measured during a 10-min integration period. A physically less dense aerosol coupled with a spectrometer sensitive to $0.05 \mu\text{m}$ particles may extend the measurements to 1×10^9 .

Testing of similar configurations with DOP provided more information because the tests could be run for a longer period of time due to the different loading characteristics produced by DOP. Table III provides histories of the PF as a function of time. Unlike the systems tested with NaCl, where the loading on the first filter continually increased the PF to a value greater than would be expected from the quality control data, the DOP tested systems usually display a PF an order of magnitude less than inferred from the quality control data. The variation with time is not monotonic. The figure of merit associated with the counts determining P_{21m} in both tables are typically $\approx 25\%$. Note the value of 3.03×10^7 in the fourth row.

14th ERDA AIR CLEANING CONFERENCE

TABLE II

TANDEM PROTECTION FACTORS (NaCl)

<u>Quality Control (0.3 μm DOP)</u>	<u>Measured (NaCl)</u>
I	
P _{1s} 7.2 x 10 ³	P _{1m} 1.1x 10 ⁵
P _{2s} 1.3 x 10 ⁴	P _{2m} 1.5 x 10 ³
P _{21s} 9.4 x 10 ⁷	P _{21m} 1.6 x 10 ⁸
II	
P _{1s} 1.3 x 10 ⁴	P _{1m} 1.7 x 10 ⁴
P _{2s} 1.0 x 10 ⁴	P _{2m} 8.2 x 10 ²
P _{21s} 1.3 x 10 ⁸	P _{21m} 1.4 x 10 ⁷
III	
P _{1s} 1.0 x 10 ⁴	P _{1m} 3.2 x 10 ⁴
P _{2s} 4.2 x 10 ³	P _{2m} 6.6 x 10 ³
P _{21s} 4.2 x 10 ⁷	P _{21m} 2.1 x 10 ⁸
IV	
P _{1s} 1.3 x 10 ⁴	P _{1m} 2.8 x 10 ⁵
P _{2s} 4.2 x 10 ³	P _{2m} 1.5 x 10 ²
P _{21s} 5.5 x 10 ⁷	P _{21m} 4.1 x 10 ⁷
V	
P _{1s} 8.3 x 10 ³	P _{1m} 4.7 x 10 ⁴
P _{2s} 4.2 x 10 ³	P _{2m} 5.1 x 10 ³
P _{21s} 3.5 x 10 ⁷	P _{21m} 2.4 x 10 ⁸
VI	
P _{1s} 1.3 x 10 ⁴	P ₂₁ >1.3 x 10 ⁵
P _{2s} 4.2 x 10 ³	P _{2m} >1.8 x 10 ³
P _{21s} 5.5 x 10 ⁷	P _{21m} >2.4 x 10 ⁸

14th ERDA AIR CLEANING CONFERENCE

Under conditions in which long integration times are required to obtain a statistically significant count downstream of a tandem system, DOP appears to be a better challenging agent than NaCl in that it produces less of a change in the system during the duration of the test and also provides more conservative test data. The initial pressure drop of about .75 inches H₂O across the first filter would rise to a maximum of 1.23 but then decrease to 1.00 after a short period of clean air flushing. This was not true with filters challenged by NaCl. The excessive upstream concentrations required give rise to a concern over agglomeration processes that may occur for either aerosol between the upstream measurement point and the first filter face.

Of additional concern, in the case of DOP, is a possible change in size distribution due to evaporation between the two measurement stations. The severity of such a process would depend on the time in transit and DOP vapor supersaturation. The smallest droplets observable are still too large to be greatly influenced by the Thompson effect⁴ so that the loss would manifest itself in the large particle part of the spectrum as the entire observable spectrum uniformly evaporates.

VII Field Tests

One single stage 20,000 CFM system has been tested using the single particle laser spectrometer and a cloud maker thermal DOP generator. This test yields a P.F. of $5 \times 10^4 \pm 16\%$ for a 30 second integration time. A forward light scattering photometer usually used for this test was unable to provide a reading out of the background noise. Extrapolating the requirements for a similar two stage system results in 3 aerosol generators, 20 min. integration time and on accuracy of $\pm 40\%$. A 200,000 CFM single stage system would require only that the integration time be extended to 5 min to provide the same accuracy as for the 20,000 CFM stage system. Measurements of both two stage and large single stage systems will be made in the near future.

VIII. Conclusion

The use of a single particle laser particle spectrometer has proven to be remarkably successful in the characterization of HEPA filter performance against NaCl and DOP aerosols. Single particle counting statistics and total absence of detector background noise make it possible to detect and measure particle concentrations below the detection level of other detectors. Total counts as low as 4 are significant and yield a figure of merit of $\pm 50\%$.

TABLE III

TANDEM PROTECTION FACTORS (DOP)

QUALITY CONTROL	MEASURED (DOP)			
	PERIOD #1	PERIOD #2	PERIOD #3	PERIOD #4
	1 - 13 minutes	13 - 36 minutes	37 - 62 minutes	63 - 96 minutes
P_{1s} 2.50×10^4	P_{1m} 8.21×10^3	1.27×10^4	1.01×10^4	2.84×10^3
P_{2s} 2.50×10^4	P_{2m} 2.24×10^3	3.73×10^3	9.71×10^4	1.10×10^4
P_{21s} 6.25×10^8	P_{21m} 1.84×10^7	4.74×10^7	9.81×10^7	3.12×10^7
	1 - 11 minutes	12 - 17 minutes	18 - 23 minutes	24 - 27 minutes
P_{1s} 2.50×10^4	P_{1m} 5.80×10^3	6.80×10^3	5.05×10^3	4.24×10^3
P_{2s} 2.50×10^4	P_{2m} 4.35×10^3	7.42×10^3	5.56×10^3	4.76×10^3
P_{21s} 6.25×10^8	P_{21m} 2.53×10^7	5.05×10^7	2.81×10^7	2.02×10^7
	0 - 1 minute	2 - 11 minutes	12 - 23 minutes	24 - 60 minutes
P_{1s} 2.50×10^4	P_{1m} 2.87×10^3	2.87×10^3	2.87×10^3	2.87×10^3
P_{2s} 2.5×10^4	P_{2m} 7.58×10^3	3.52×10^4	7.58×10^3	8.44×10^3
P_{21s} 6.25×10^8	P_{21m} 2.18×10^7	1.01×10^8	2.18×10^7	2.42×10^7
	4 - 9 minutes	10 - 40 minutes	41 - 45 minutes	46 - 50 minutes
P_{1s} 5.00×10^4	P_{1m} 2.44×10^4	6.29×10^4	3.14×10^3	5.22×10^3
P_{2s} 5.00×10^4	P_{2m} 2.07×10^4	4.82×10^4	1.79×10^4	2.42×10^4
P_{21s} 2.50×10^9	P_{21m} 5.05×10^8	3.03×10^9	5.02×10^7	1.26×10^8
	0 - 5 minutes	6 - 10 minutes	11 - 15 minutes	16 - 20 minutes
P_{1s} 1.67×10^4	P_{1m} 3.22×10^3	7.86×10^3	5.09×10^3	5.59×10^3
P_{2s} 5.00×10^4	P_{2m} 1.57×10^4	6.42×10^3	2.48×10^4	9.03×10^4
P_{21s} 8.33×10^8	P_{21m} 5.05×10^7	5.05×10^7	1.26×10^8	5.05×10^8

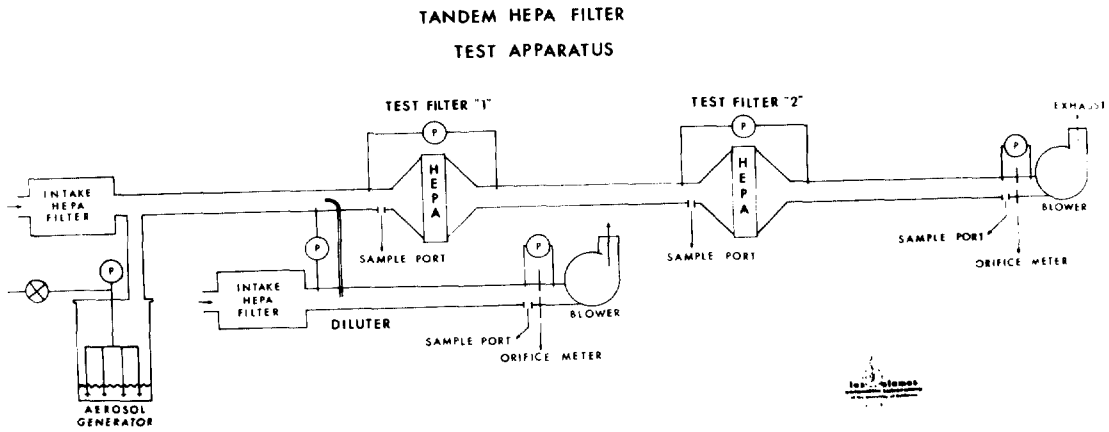


Fig. 1.
HEPA Filter Test Apparatus.

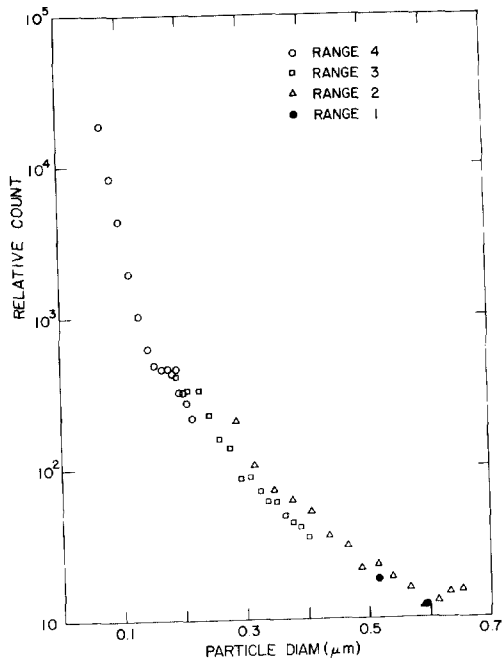


Fig. 2.
Size Spectrum of
NaCl in H₂O.

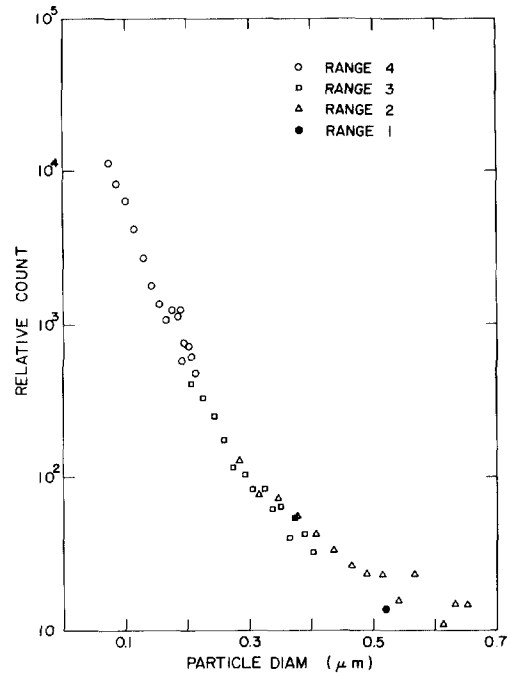


Fig. 3.
Size Spectrum of
5% DOP in alcohol.

NaCl TEST RESULTS

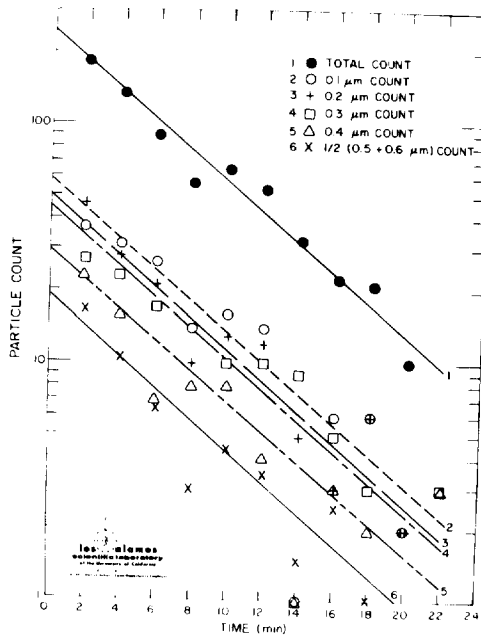


Fig. 4.

Size Dependence of Penetration Decay, NaCl Challenge.

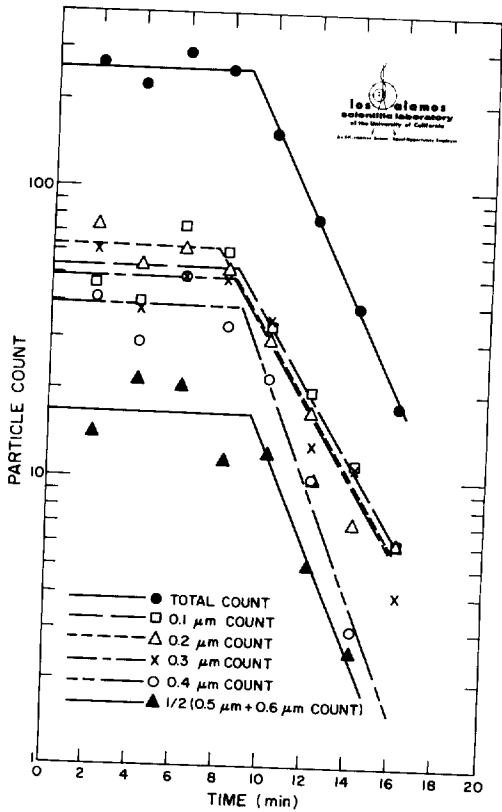


Fig. 5.

Size Dependence of Penetration Decay, NaCl Challenge.

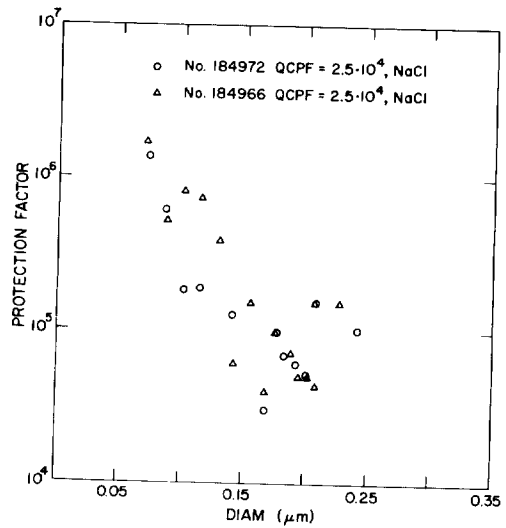


Fig. 6.

Protection Factor as a Function of Particle Size.

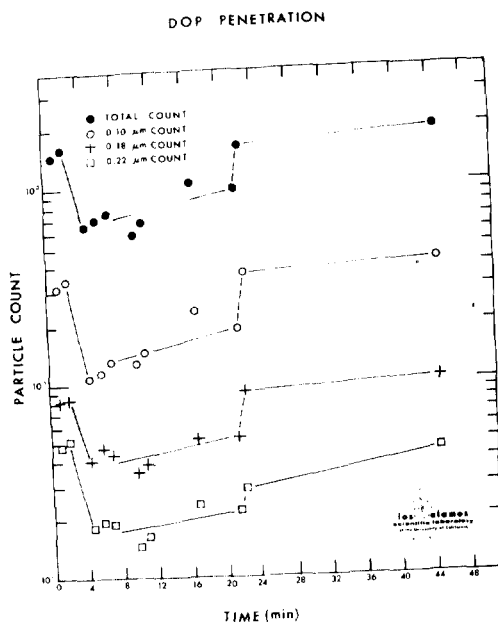


Fig. 7.
Size Dependence of Penetration Decay, DOP Challenge.

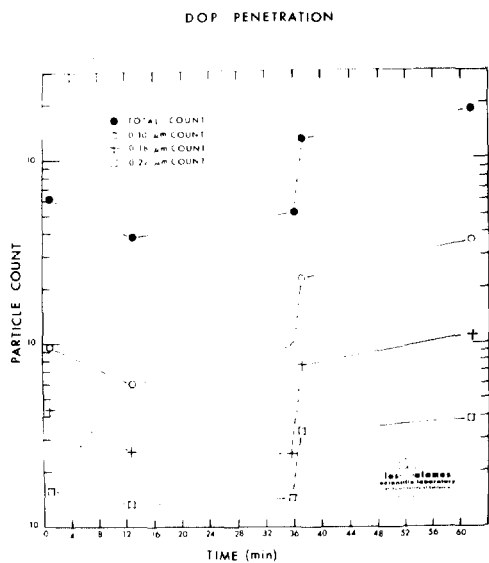


Fig. 8.
Size Dependence of Penetration decay, DOP Challenge.

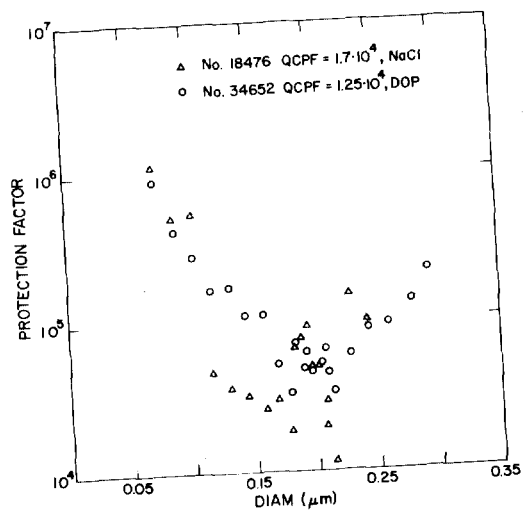


Fig. 9.
Protection Factor as a Function of Particle Size.

14th ERDA AIR CLEANING CONFERENCE

References - HEPA Paper

1. A.E.C. Division of Operational Safety and Division of Engineering Construction, "HEPA filtration guidelines (draft)" (1971).
2. R. Hiebert, R. Stafford, and L. Pollat, "Improved light-scattering photometer for air filtration studies", Los Alamos Scientific Laboratory Report LA-4627-MS (1971).
3. B.G. Schuster and R. Knollenberg, "Detection and sizing of small particles in an open cavity gas laser", Appl. Optics, II, No. 7 PP 1515-1520, (1972).
4. J. Frenkel, Kinetic Theory of Liquids, Dover Publications, Inc., New York, 1955, P366.

DISCUSSION

SCHURR: Is your laser spectrometer applicable to on-line particle size analysis of general particle composition?

SCHUSTER: No. We have used polystyrene latex but the instrument certainly has been used for collecting all sorts of atmospheric dust. The gentleman who now builds this instrument is an atmospheric scientist and has a wide variety of these instruments. He has them on aircraft and has measured a wide variety of atmospheric dust as well as some of the industrial dusts.

CHEEVER: Are there plans to make the laser particle spectrometer commercially available?

SCHUSTER: It is already commercially available.

RIVERS: Your Figures 4 and 5 show a very rapid improvement in particle penetration over a period of about 20 minutes exposure to the sodium chloride aerosol. In both cases, regardless of particle size, penetration declined by a factor of about 200 with this exposure. Table 1 shows that pressure drop increases for these exposures were in the order of 0.1 in. W.G., or even less. The concentration, by my calculations, was about 31 mg/m³, in contrast to the usual DOP concentration of about 80 mg/m³. We have never observed or read about such improvements using either DOP smoke, NaCl, or ambient dusts. Do you think the effect could be due to your measurement technique? If the effect is real, and sustained, we probably ought to treat every filter bank with a 20-minute dose of NaCl smoke.

SCHUSTER: The single filter test displayed in Table I is for a DOP challenge and so cannot be correlated with Figures 4 and 5 which illustrate NaCl penetration. I'm curious as to how you arrived at your figure for mass challenge concentration since there is not sufficient information in the paper to make such a computation. I would not advocate filter bank pre-treatment with a 20 minute challenge of NaCl smoke.